1 December 2006 | $10

Science

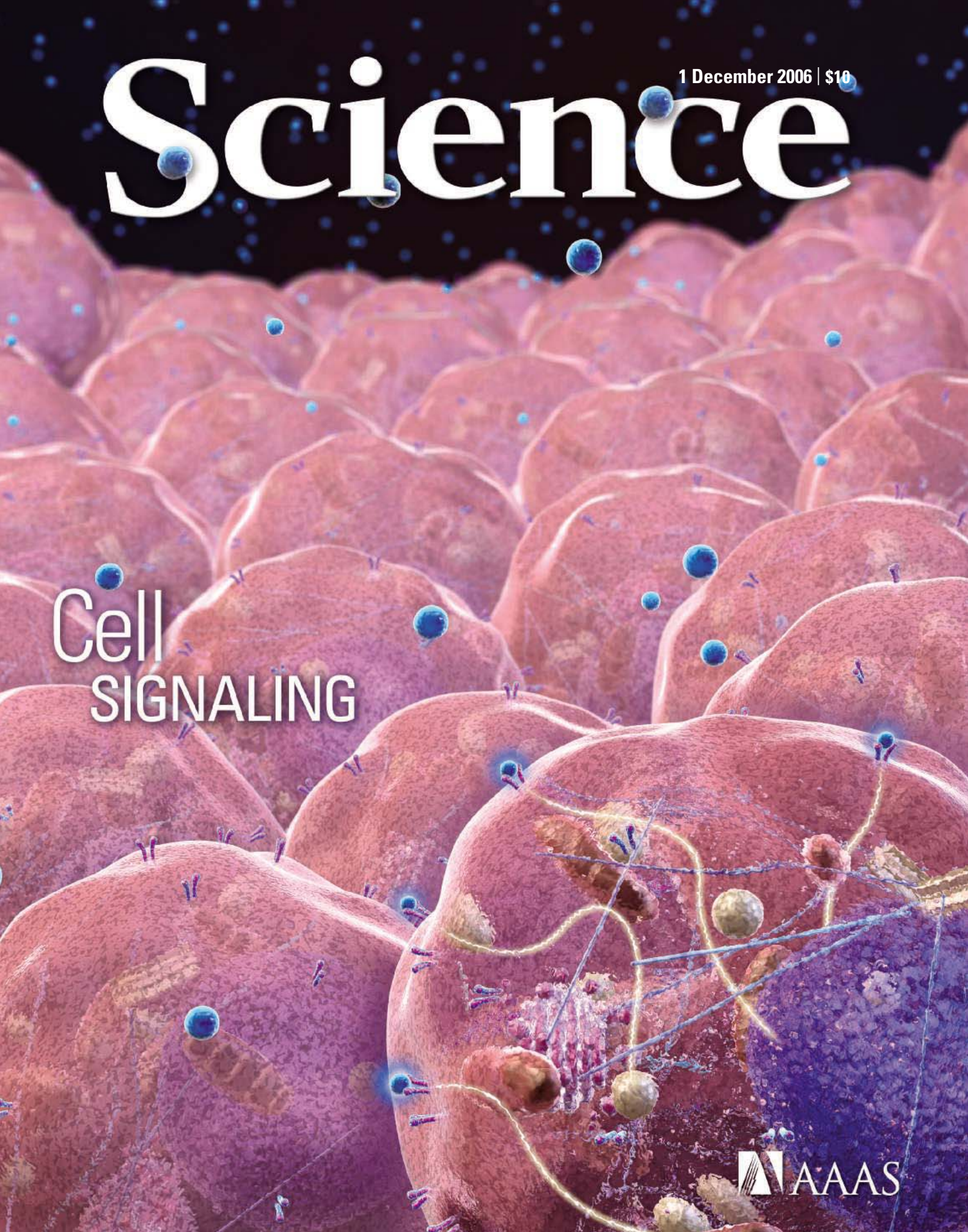

Cell SIGNALING

AAAS

* this drug knows everything about Mr. Holliday.

It's tailor-made for his DNA. IBM and IBM Business Partners are working to support research that is making personalized medicine a reality. From data-mining algorithms and vast supercomputing power to secure genomic information warehouses, we're helping pharma and biotech companies shorten drug development cycles, streamline clinical trials, and bring new targeted treatments to market. Want innovation for growth? Talk to the innovator's innovator. Call on IBM. To learn more, visit ibm.com/healthcare/personalized

what makes you special?

IBM

How much is 5¢ really worth?

Find out with our new thermostable Paq5000™ DNA Polymerase for PCR.

Our new Paq5000™ DNA Polymerase* is an economic alternative to *Taq* that costs only 5 cents per unit.** This new enzyme provides improved PCR yield with reduced cycling time and is ideal for routine end-point PCR on targets up to 6 kb (genomic). Furthermore, the Paq5000 DNA polymerase is derived from a *Pyrococcus* species and comes with an optimized 10X buffer. Switch from *Taq* to Paq5000 DNA polymerase today!

Obtain Equal or Better Yield than *Taq* DNA Polymerase

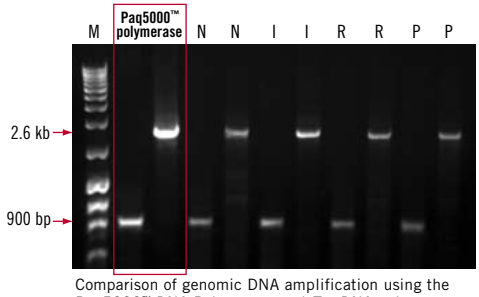

Comparison of genomic DNA amplification using the Paq5000™ DNA Polymerase and *Taq* DNA polymerase from various suppliers (competitors N, I, R, P) using standard conditions.

Need More Information? Give Us A Call:

Stratagene US and Canada
Order: 800-424-5444 x3
Technical Service: 800-894-1304 x2

Stratagene Japan K.K.
Order: 3-5821-8077
Technical Service: 3-5821-8076

Stratagene Europe
Order: 00800-7000-7000
Technical Service: 00800-7400-7400

www.stratagene.com

Ask us about these great products:

Paq5000™ DNA Polymerase	**500 units**	**600680**
	1000 units	**600682**
	5000 units	**600684**

Call for special pricing on large orders and custom/bulk packaging.

* US Patent Nos. 7,045,328, 6,734,293, 6,489,150, 6,444,428, 6,183,997, and 5,489,523. Purchase of this product conveys to the purchaser the non-transferable right under these patents to use the product for research use only.

** Pricing in US Dollars. Pricing valid in US only. For pricing in other countries, please contact your Stratagene sales representative or your local distributor.

STRATAGENE®

GE Healthcare

ÄKTA™

100,000 scientists working with proteins believe in ÄKTA, UNICORN and wizards.

To 100,000 scientists worldwide, ÄKTA™ sets the standard in protein purification. All systems in the ÄKTAdesign™ family work with intelligent UNICORN™ software, which makes it easy to control every stage of your purification process. But we're never content to stand still. The result is products like ÄKTAxpress™, which can solve low expression and double-tagged protein purification challenges, and ÄKTApurifier™, a time-saving automated protein purification system that can be configured to suit your personal application and workflow needs.

By continually developing technology that can turn your scientific ideas into reality, we're bringing science to life and helping transform healthcare.

We call it Protein Separations Re-imagined.

Discover the legendary purification power of UNICORN and ÄKTA, visit www.gehealthcare.com/akta

imagination at work

GE09-06

Volume 314, Issue 5804

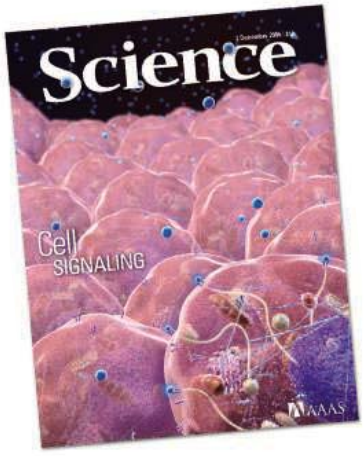

COVER

Artist's representation of communication pathways initiated by cell surface receptors that influence cell physiology and organelle function. This joint special issue between *Science* and *Science*'s STKE highlights new insights into signaling mechanisms that control development and reproduction (see page 1409).

Image: Christopher Bickel

See also related STKE material on page 1347 or at www.sciencemag.org/sciext/cellsignaling06/

DEPARTMENTS

EDITORIAL

SPECIAL SECTION

Cell Signaling

INTRODUCTION

PERSPECTIVES

CONNECTIONS MAPS

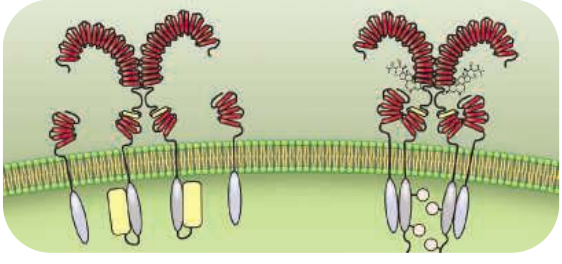

1410

1374

NEWS OF THE WEEK

NEWS FOCUS

CONTENTS continued >>

Systems Biology — RNAi

FlexiPlate siRNA — your customized RNAi solution

New

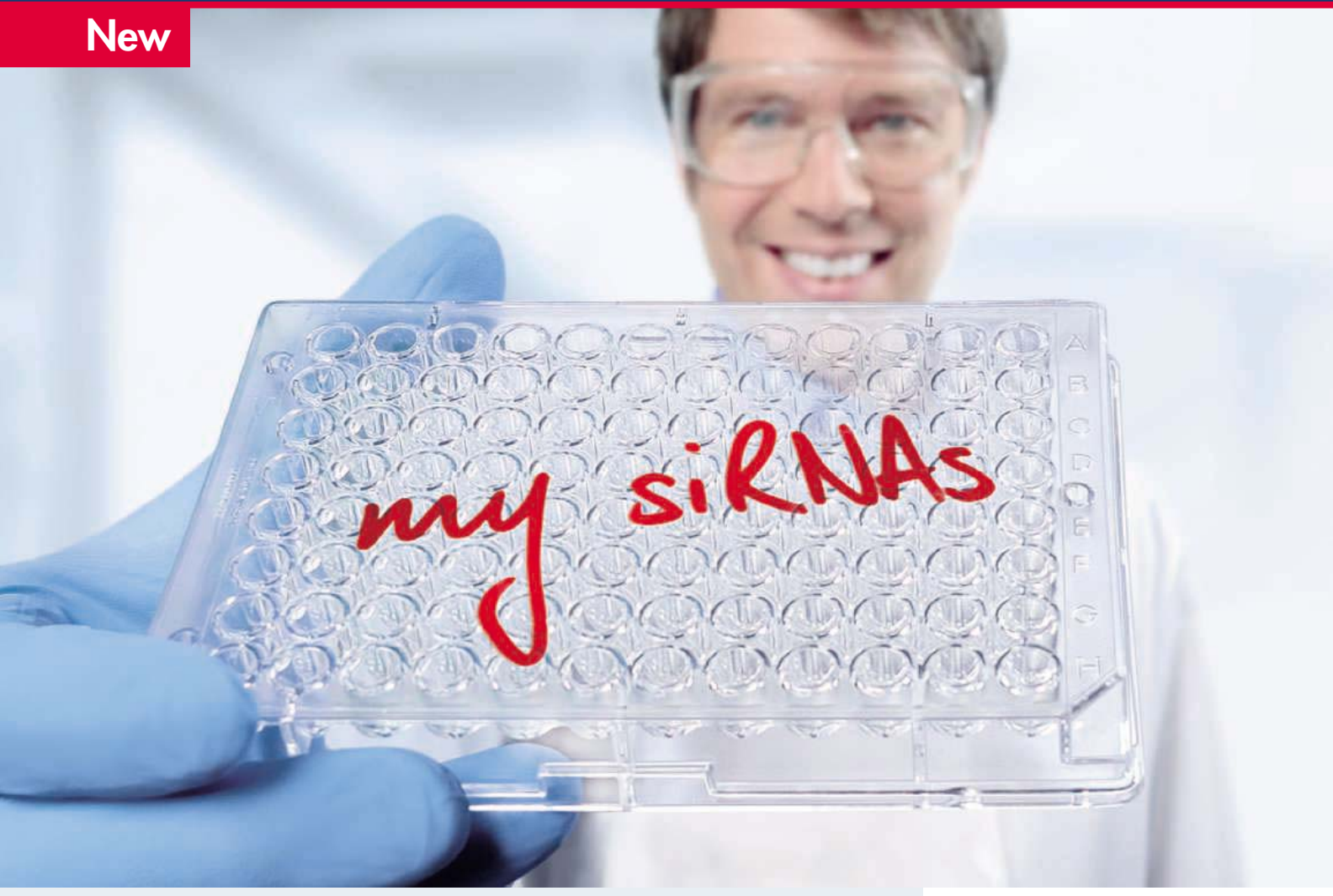

FlexiPlate siRNA from QIAGEN is a giant leap forward for more flexible, cost-effective RNAi screening!

- Maximum flexibility to select siRNAs for human and mouse genes, controls, scales, and 96-well plate layout
- Economical options allow screening of more target genes within budget
- Cutting-edge siRNA design minimizes off-target effects and maximizes potency
- Fast and easy access via QIAGEN's GeneGlobe™ Web portal

Experience maximum flexibility at www.qiagen.com/GeneGlobe !

QIAGEN

WWW.QIAGEN.COM

Science

SCIENCE EXPRESS

www.sciencexpress.org

LETTERS

BOOKS *ET AL.*

POLICY FORUM

PERSPECTIVES

TECHNICAL COMMENT ABSTRACTS

BREVIA

RESEARCH ARTICLE

REPORTS

CONTENTS continued **>>**

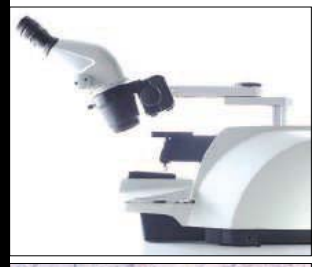

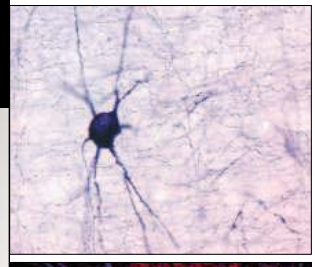

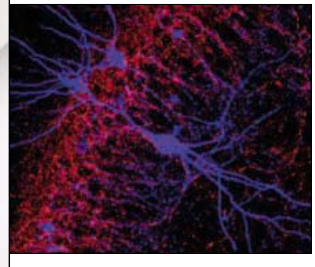

Good Vibrations... Great Sections!

"Ideally, a tissue slicer should generate large-amplitude and high-frequency movements of the cutting blade in a horizontal axis, with minimal vibrations in the vertical axis." *(According to Prof. P. Jonas, Institute of Physiology, University of Freiburg, Germany).

Leica translated this into the Leica VT1200 and the Leica VT1200 S Vibrating Blade Microtome for cutting fresh and fixed tissues.

Designed with **You** in Mind!

* Ref: Pflügers Arch - Eur. J. Physiol. (2002) 443:491-501
Patch-clamp recording in brain slices with improved slicer technology

*J.R.P. Geiger - J. Bischofberger - I. Vida - U. Fröbe
S. Pfitzinger - H.J. Weber - K. Haverkampf - P. Jonas

www.leica-microsystems.com/VT1200 S

Leica
MICROSYSTEMS

Science

REPORTS *CONTINUED...*

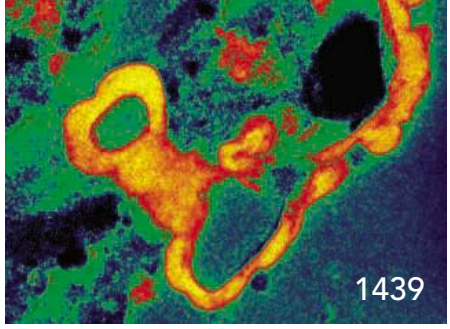

AAAS
ADVANCING SCIENCE, SERVING SOCIETY

SCIENCE (ISSN 0036-8075) is published weekly on Friday, except the last week in December, by the American Association for the Advancement of Science, 1200 New York Avenue, NW, Washington, DC 20005. Periodicals Mail postage (publication No. 484460) paid at Washington, DC, and additional mailing offices. Domestic individual membership and subscription (51 issues): $139 ($74 allocated to subscription). Domestic institutional subscription (51 issues): $650; Foreign postage extra: Mexico, Caribbean (surface mail) $55; other countries (air assist delivery) $85. First class, airmail, student, and emeritus rates on request. Canadian rates with GST available upon request, GST #1254 88122. Publications Mail Agreement Number 1069624. **Printed in the U.S.A.**

Change of address: Allow 4 weeks, giving old and new addresses and 8-digit account number. **Postmaster:** Send change of address to AAAS, P.O. Box 96178, Washington, DC 20090–6178. **Single-copy sales:** $10.00 current issue, $15.00 back issue prepaid includes surface postage; bulk rates on request. The identification code for *Science* is 0036-8075. *Science* is indexed in the *Reader's Guide to Periodical Literature* and in several specialized indexes.

CONTENTS continued **>>**

Setting New Heights

Elevate your research with Bio-Rad's wide range of high-quality protein standards for electrophoresis and blotting applications.

- Recombinant protein standards offer 10 sharp, nonshifting bands for MW determination on gels and blots
- Natural protein standards are available in high, low, and broad ranges to monitor transfer efficiency and for MW estimation on gels and blots
- IEF standards allow reproducible, dependable pI calibration in native polyacrylamide and agarose IEF gels
- 2-D SDS-PAGE standards provide calibrated references for the pI and MW of proteins in 2-D SDS-PAGE applications

For more information on our wide selection of standards, visit us on the Web at **www.bio-rad.com/ad/proteinstandards/**

Precision Plus Protein™
Standards Family

Visit us on the Web at **discover.bio-rad.com**
Call toll free at 1-800-4BIORAD (1-800-424-6723);
outside the US, contact your local sales office.

BIO-RAD

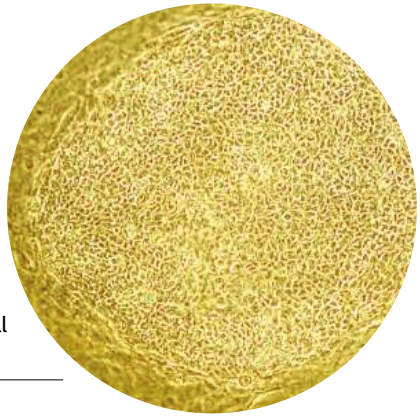

Adapting to stem cell research policies.

SCIENCE CAREERS

www.sciencecareers.org

CAREER RESOURCES FOR SCIENTISTS

EUROPE: Navigating the Stem Cell Research Maze
S. Webb and E. Pain
Building a stem cell research career in Europe means navigating the policy maze in each country.

US: It Ain't Over Till It's Over
B. Benderly
A bureaucratic snag has stalled California's postdoc unionization drive.

CANADA: Winning the HHMI International Research Award
A. Fazekas
A young biomedical researcher explains how career choices translated into professional success.

GRANTSNET: December 2006 Funding News
J. Fernandez
Read about the latest in research funding, scholarships, fellowships, and internships for postdocs and students.

Fit for consumption.

SCIENCENOW

www.sciencenow.org DAILY NEWS COVERAGE

Taking the Toxin out of Cotton
Engineered plants have edible seeds, providing a possible new source of cheap protein.

Clocking Cosmic Eyewalls
Scientists measure the speed of a spinning black hole.

Chimps Go Ape Over Older Females
Findings give clues to evolution of human mate preference.

CREDIT (*SCIENCE CAREERS*): NIH

SPECIAL SECTION

Cell Signaling

SCIENCE'S STKE

www.stke.org

SIGNAL TRANSDUCTION KNOWLEDGE ENVIRONMENT

EDITORIAL GUIDE: Signal Reception and Transmission
N. R. Gough
New pathways and updates to the Database of Cell Signaling highlight how signals received at the surface are transmitted into the cell to mediate complex cellular responses.

Separate individual or institutional subscriptions to these products may be required for full-text access.

Bibliographies made tra easy.

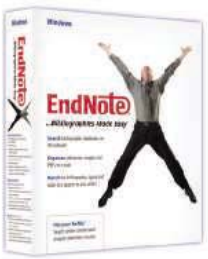

For over two decades, EndNote® has been the industry standard software tool for creating and managing bibliographies. With EndNote X, we're creating a new standard for ease-of-use. And that has students, researchers, writers and librarians jumping for joy.

Expanded PDF management lets you drag and drop PDF files for auto-linking and storage. An enhanced reference list display lets you see more information. More options make it easier to search EndNote libraries. And increased flexibility gives you more ways to enter and edit references—and create bibliographies in over 2,300 publishing styles.

EndNote X is compatible with Microsoft® Word for Windows® and Mac® OS X, and EndNote libraries can easily be shared across platforms. That makes it not only Xtra easy to use, but also Xtra easy to work with throughout your organization—and all over the world.

Download your Free demo or buy online today. www.endnote.com

EndNote®
...Bibliographies Made Easy™

THOMSON™

800-722-1227 • 760-438-5526
rs.info@thomson.com

Discover RefViz®
Search online content and analyze references visually

EDITED BY STELLA HURTLEY AND PHIL SZUROMI

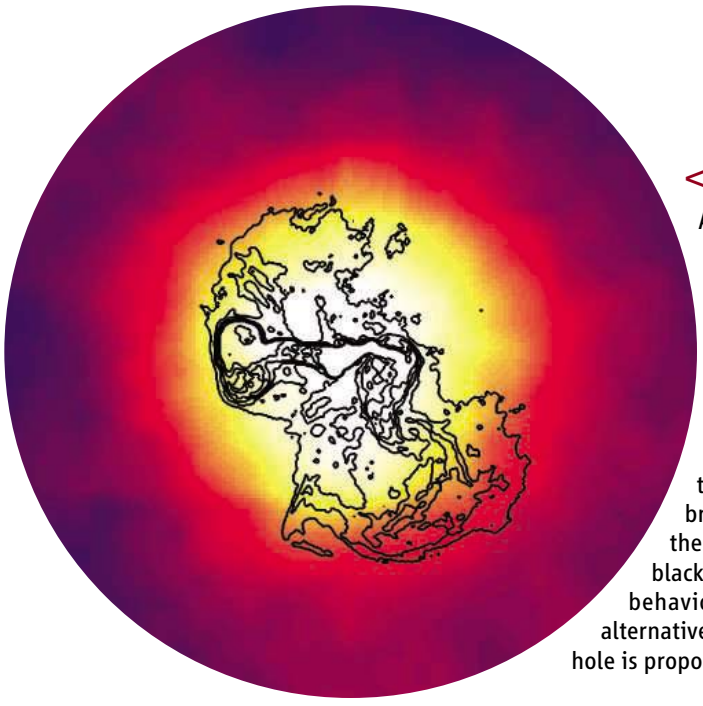

<< Fast Flickering

Among the very few known extragalactic emitters of very high energy tera–electron volt (TeV) γ rays are blazars, which are galaxies with relativistic particle jets that point toward Earth. It has been suggested that the TeV γ rays originate in those jets. By monitoring the nearby radio galaxy M87, whose twin jets are oriented in the plane of the sky rather than pointed at us, **Aharonian *et al.*** (p. 1424, published online 26 October; see the Perspective by **Fabian**) show that γ rays in active galaxies are actually produced near the central black hole. M87 is bright in γ rays up to 10 TeV, and its brightness varies daily. Such fast variations imply the source of the γ rays lies near the Schwarzschild radius of the supermassive black hole that lies at the heart of the M87 galaxy. Although this behavior may fit some leptonic models for γ-ray production, an alternative mechanism of proton curvature radiation near to the black hole is proposed.

Phytoplankton Clouds

Phytoplankton produce compounds that can become aerosols, which suggests that biological productivity might exert an important control on cloudiness over the ocean if these aerosols act as cloud condensation nuclei. **Meskhidze and Nenes** (p. 1419, published online 2 November) combine satellite observations of surface ocean chlorophyll a content and cloud cover to show that biological productivity can have a significant effect on shallow marine clouds. Cloud droplet number concentrations over a phytoplankton bloom in the Southern Ocean doubled, and cloud effective radius was reduced by 30%, which led to a large change in the short-wave radiative flux at the top of the atmosphere.

In Tune for a Second

High-resolution spectroscopy generally requires a trade-off between the size of the ensemble being probed and the coherence of that sample during the course of the measurement, so that increasing the sample size to raise signal strength often broadens the signal of interest. **Boyd *et al.*** (p. 1430) have used an optical trap to inhibit the random motion of strontium atoms in order to maintain coherence of the photoexcited sample for ~1 second. By careful frequency stabilization of the probe laser, an absorption line at ~10^{14} hertz could be measured with a corresponding width of ~1 hertz. The attained ratio of frequency to linewidth, or quality factor, exceeds previous values by an order of magnitude. Such capabilities facilitate high-precision unit standardization and enhanced measures of fundamental physical constants.

Monsoon Violence

Most climate models have predicted that extreme rainfall events will become more common as air temperature rises, but observational evidence of this trend has been hard to find. **Goswami *et al.*** (p. 1442) used a daily rainfall data set for central India to show that there was an increase in the frequency and intensity of heavy rain events, and a decrease in the frequency of light to moderate rain events, for the monsoon seasons from 1951 to 2000. The mean rainfall did not show a significant trend because the increasing contribution from heavy events was offset by a decreasing one from light ones. These findings suggest that severe rain events over India will become more common if global warming continues as expected.

Controlled Coupling of Qubits

Performing logical operations on quantum computers will require the coupling and decoupling of qubits so that individual qubits can be prepared in a given quantum state, allowed to interact, and be read out once the final state is achieved. **Hime *et al.*** (p. 1427) demonstrate on-and-off control on a pair of superconducting-flux qubits coupled through their mutual inductance. With both qubits also coupled to a nearby superconducting quantum interference device (SQUID), their mutual inductance and the extent of the coupling strength could be controlled by varying the working parameters of the SQUID.

Lining Up at the Front

Self-assembly of molecules can create nanoscale features on flat surfaces, but the maximum extent of a single domain is usually on the order of tens of micrometers. **Van Hameren *et al.*** (p. 1433) show that disk-like molecules, in which three porphyrin groups bearing long alkyl groups assemble around a central core, form very long aligned chains over areas of several square millimeters through a dewetting process. On mica, single-column stacks form lines parallel to the evaporation front of smaller droplets, whereas for larger droplets, longer evaporation times cause larger lines of aggregates to grow normal to the evaporation front. Patterns formed on rougher glass surfaces were less regular but could still be used to align liquid crystal molecules.

Continued on page 1351

CREDITS (TOP TO BOTTOM): AHARONIAN *ET AL.*; GOSWAMI *ET AL.*

Open to anything

The Agilent DNA Microarray Platform enables research on your own terms

As a genomics researcher, you need tools that empower rather than impede. Whether you're searching for low-abundance gene expression targets, performing genome-wide scans on whole blood samples or adopting emerging applications such as oligo array CGH or ChIP-on-chip, you need a microarray platform that has the flexibility, sensitivity and genome coverage that your research requires. A platform that will keep your research moving forward, wherever it takes you.

To hear from researchers who are charting their own course in Genomics **visit www.OpenGenomics.com**

Agilent Technologies

Continued from page 1349

More Boys Preferred

Biases in sex ratio at birth have led to the suggestion that females may manipulate the sex of their offspring. **Gomendio *et al.*** (p. 1445) now show that males may also influence offspring sex ratio. In red deer, more fertile males tend to produce proportionally more sons who are likely to inherit high fertility rates. Sperm collected during the rut from males living in natural populations was used for artificial insemination to minimize known female effects on sex ratio. Such male contributions to biases in offspring sex ratio suggest an evolutionary scenario in which conflicts of interest between males and females in relation to the sex of their offspring may play an important role.

Turing Patterning in the Mouse Hairs

More than 50 years ago, Alan Turing provided a theoretical explanation of biological pattern formation through a hypothesis of reaction-diffusion, whereby patterns, such as that for hair follicles or feather distribution, can form as a result of positive and negative feedback regulation of an inhibitor and activator. Turing models have since been used to account for patterns in many chemical systems, but have not been successful in explaining biological pattering in developmental model systems such as the fly. **Sick *et al.*** (p. 1447, published online 2 November; see the Perspective by **Maini *et al.***) have now examined hair follicle arrangements in mice that arise through the WNT activator protein and its inhibitor DKK and show through computation modeling that reaction-diffusion can account for the patterning observed.

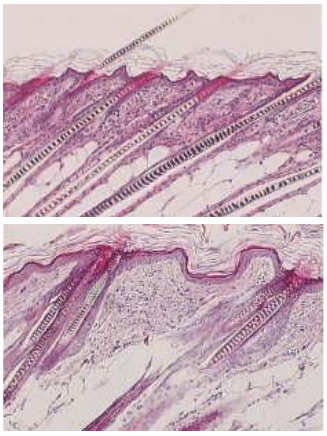

CREDIT: PFINGSTEN *ET AL.*

Not Lost in Translation

The canonical mechanism for initiation of protein synthesis in eukaryotes involves a nucleotide cap on messenger RNA (mRNA) that is recognized by an initiation protein factor. However, a variety of pathogenic viruses and cellular mRNAs bypass the canonical mechanism by using structured RNA sequences, called internal ribosomal entry sites (IRESs), to initiate translation. **Pfingsten *et al.*** (p. 1450) have determined the structure of the ribosome-binding domain of an IRES at 3.1 angstrom resolution. The RNA prefolds to create a specific ribosome-binding structure. By docking the structure onto cryoelectron microscopic reconstructions of an IRES-ribosome complex, contacts were identified that drive binding and induce conformational change in the ribosome.

Of Genes and Gut Reactions

Inflammatory bowel diseases (IBDs) such as Crohn's disease and ulcerative colitis are thought to be caused by an inappropriate immune response to commensal intestinal bacteria. There is strong evidence that these disorders have a genetic component; for example, individuals carrying specific sequence variants of the *NOD2/CARD15* gene are at increased risk. Now, in a genome-wide association study, **Duerr *et al.*** (p. 1461, published online 26 October; see the Perspective by **Cardon**) find that a rare sequence variant of the gene encoding the receptor for interleukin-23 (*IL23R*) significantly lowers an individual's risk of developing IBDs. Interleukin-23 is a cytokine that has attracted increasing attention because of its role in a wide range of chronic inflammatory diseases in mouse models, including IBDs, multiple sclerosis, and arthritis.

Progesterone and Breast Cancer

Mutations in the breast cancer susceptibility gene *BRCA1* greatly increase a woman's risk of developing breast and ovarian cancers. Why do these mutations predominantly affect hormone-responsive tissues when the mutant gene is widely expressed throughout the body? **Poole *et al.*** (p. 1467; see the news story by **Marx**) suggest that this tissue specificity is caused in part by BRCA1-mediated effects on signaling by the hormone progesterone. Mammary epithelial cells (MECs) of *Brca1/p53*-deficient mice accumulated high levels of progesterone receptors, probably through defective degradation by the proteasome, and developed aberrant proliferation of the MECs. Treatment with the progesterone antagonist mifepristone (RU 486) prevented or delayed mammary tumor development in the mice.

Donald Kennedy is the Editor-in-Chief of *Science*.

Responding to Fraud

Our journal—as well as science with a small "s"—went through a disappointing and troubling experience with the two stem cell papers from the South Korean research group led by Dr. Woo Suk Hwang. As a result of an investigation by a committee from Seoul National University, the first paper from this group, *Science* **303**, 1669 (2004), was found to be fraudulent and was subsequently retracted by *Science*. A second paper, *Science* **308**, 1777 (2005), published a year later, was retracted for the same reasons.

What *Science* did then entailed two steps. First, we compiled a chronological anthology of the editorial review process for both papers; it included all submissions; correspondence among editors, our Board of Reviewing Editors, peer reviewers, authors, and agencies responsible for regulatory oversight in South Korea; and notes on telephone conversations. This material was reviewed by an internal review committee of six in-house editors. This archive and their comments were then sent to an outside committee consisting of three members of our external Senior Editorial Board (John Brauman, George Whitesides, and Linda Partridge), a former *Science* senior editor who is now the U.S. Executive Editor at *Nature* (Linda Miller), and two distinguished biologists who work in the stem cell community (Doug Melton and John Gearhart). The committee was asked to make a thorough and unsparing analysis of *Science*'s handling of both papers and to make recommendations for changes in procedure that might protect both the journal and the scientific community from further unfortunate outcomes of this kind.

"The report sends us some tough messages about what *Science* should do to confront a present reality and prepare for a more challenging future."

The report, and a short response from *Science*, are available at www.sciencemag.org/cgi/content/full/314/5804/1353/DC1. The report is notable for its thoroughness, insight, and candor. It reaches several conclusions; some of these apply to our journal and to those of us who edit and publish it, and others are relevant for the larger community of scientists. The good news for *Science* is that its editors and peer reviewers not only followed the procedures in place here and at other top-tier journals, but made a substantially greater effort than for most papers to ensure that the science was sound. The not-so-good news is that the report sends us some tough messages about what *Science* should do to confront a present reality and prepare for a more challenging future. It points out forcefully that the environment for science now presents increased incentives for the production of work that is intentionally misleading or distorted by self-interest. It urges us to give special attention to a relatively small number of papers that are likely to be especially visible or influential.

We are now formulating ways to respond to this advice. The report recommends developing a risk assessment template. We have been conducting discussions among ourselves and with committee members to develop criteria for deciding which papers deserve particularly careful editorial scrutiny. Papers that are of substantial public interest, present results that are unexpected and/or counterintuitive, or touch on areas of high political controversy may fall into this category. We are also considering the kinds of special attention that might be given to these high-risk papers. These might include higher standards for including primary data, demands for clearer specification of the roles of all authors, and more intensive evaluation of the treatment of digital images. The report makes no bones about the fact that for some papers that meet the higher risk standard, the experience will be time-consuming and expensive for the journal and "may lead to conflict with authors."

This is not the first time that scientific journals have had to adapt their procedures to new realities in the world they live in. After 9/11 and the subsequent anthrax releases in the United States, journals developed guidelines for recognizing and dealing with papers that might present international security problems. As we did then, we will be looking for ways to meet a new challenge, while maintaining the integrity of the review process and minimizing damage to the expectations of our authors and the speed of our publication process. We invite your comments and plan to keep you informed as we develop particular policies in response to these recommendations.

– Donald Kennedy

10.1126/science.1137840

TaKaRa

The Future of High Fidelity PCR

PrimeSTAR™

Introducing Two New Additions to the PrimeSTAR™ *Family*

PrimeSTAR™ with GC Buffer

PrimeSTAR™ Premix

✔ *Superior Accuracy*

✔ *Excellent Efficiency*

Takara Bio Introduces:

PrimeSTAR™ HS DNA Polymerase, a novel new high fidelity PCR enzyme which provides maximum fidelity as well as extended product length (8.5 kb for human genomic DNA; 22 kb for λ DNA). Targeted for demanding cloning (i.e. amplification of cDNA libraries) and sequencing applications, PrimeSTAR™ HS offers extremely high accuracy, excellent amplification efficiency and shortened reaction times.

PrimeSTAR™ HS offers:

- **High Accuracy:** A strong exonuclease activity results in an extremely low error rate, with only 12 errors per 250,000 bp as determined by DNA sequence analysis.
- **High Efficiency:** Higher than *Taq* Polymerase.
- **Robust Amplification:** A single PCR cycling protocol can be used to amplify products of varying sizes.
- **GC-Rich Targets:** Robust performance even with GC-rich templates.

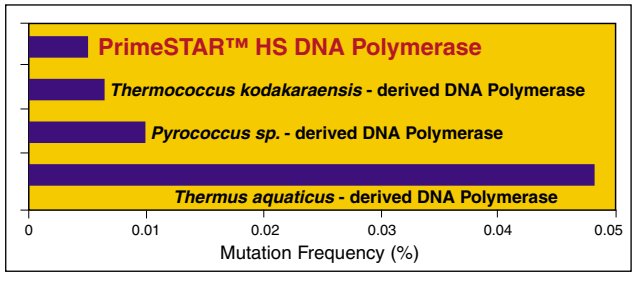

PrimeSTAR™ Fidelity Comparison with Other DNA Polymerases and *Taq*.

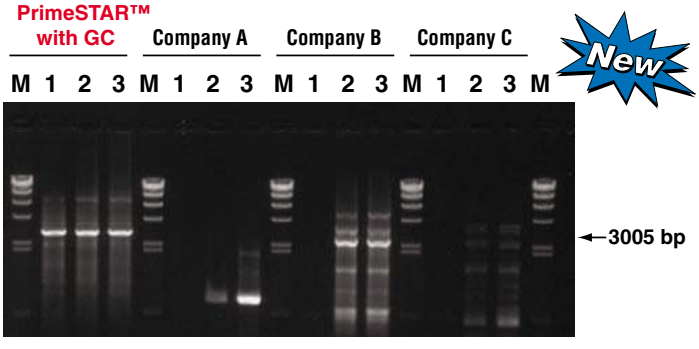

Amplification of a 3005 bp high-GC (73.2%) TthHB8 genomic DNA template. The performance of high fidelity, high-GC enzymes from Companies A, B, and C was compared with PrimeSTAR™ HS DNA Polymerase with GC Buffer. Lanes 1, 2, and 3: 100 pg, 1 ng, 10 ng human genomic DNA template.

TAKARA BIO INC.
The Biotechnology Company™

Otsu, Shiga, Japan
Phone: +81 77-543-7247
Fax: +81 77-543-9254

USA: Takara Mirus Bio Inc. Phone: 888-251-6618 • www.takaramirusbio.com
Europe: Takara Bio Europe S.A.S. Phone: +33 1 3904 6880 • www.takara-bio.eu
Korea: Takara Korea Biomedical Inc. Phone: +82 31 739 3300 • www.takara.co.kr
China: Takara Biotechnology (Dalian) Co., Ltd. Phone: +86 411 8764 1681 • www.takara.com.cn

For more information and a list of Takara distributors worldwide, please visit our website today!

www.takara-bio.com

Dingo (top), rat-kangaroo (right).

ECOLOGY/EVOLUTION

Going to the Dingoes

In the past 200 years, since the arrival of Europeans in Australia, 18 of the continent's mammal species have become extinct. These extinctions have been chiefly attributed to introduced, non-native predators, especially foxes and cats. Johnson *et al*. present evidence that the success of these medium-sized introduced predators has been the direct result of persecution by humans of Australia's native large predator, the dingo. In areas where dingoes have been left alone, foxes and cat populations are kept at bay, and the diversity and abundance of native marsupials are greater. Thus, top predators can maintain biodiversity at middle trophic levels and may help ecosystems to resist invasion by alien species. By allowing dingo populations to recover in regions where they have been persecuted, it might be possible to insure remaining small marsupials against further decline and extinction. — AMS

Proc. R. Soc. London Ser. B 10.1098/rspb.2006.3711 (2006).

CELL BIOLOGY

Toward the Chaperome

The expression of misfolded or aberrant proteins on the cell surface could wreak havoc with the immune system. Cells have therefore developed an efficient quality-control system, which diverts misfolded membrane and secretory proteins from the secretory pathway by retaining and degrading them at the entry portal to the secretory pathway, the endoplasmic reticulum (ER). One well-studied example of quality control involves the cystic fibrosis transmembrane conductance regulator (CFTR), misfolding of which is responsible for disease in a large proportion of sufferers. However, sometimes quality control is too stringent, and functional, though mutant, proteins are retained. Wang *et al*. used a systematic approach to examine the folding pathway and protein interaction partners of CFTR and the common disease variant CFTR ΔF508, which, even though functional, is retained in the ER. A variety of chaperone proteins, which help to promote protein folding, are present in the ER, and a chaperome of over 30 proteins involved in CFTR folding and transport was identified from among more than 200 interacting proteins. In particular, Aha1, a Hsp90 co-chaperone ATPase regulator, was found to be important in retaining mutant CFTR. When levels of Aha1 were reduced, mutant CFTR managed to escape from the ER and reached the plasma membrane. Interfering with CFTR-specific chaperone mechanisms may thus be a useful strategy to correct disease, and other protein misfolding diseases might be similarly amenable to equivalent interventions. — SMH

Cell **127**, 803 (2006).

GEOLOGY

Sediment Sources

The Nile River drains much of northeast Africa, and its sediments reflect erosion across the continent. Dams such as the Aswan have caused efficient collection of these sediments in the human-made lakes that form behind them. Garzanti *et al.* examined the mineralogy and amount of sand dumped by the Nile into these lakes and found that ~200 million metric tons of sediment are transported per year, several times the quantities estimated previously. The sand is mainly composed of basaltic rock or feldspar and metamorphic minerals, indicative of the Ethiopian highlands, an area of abundant deforestation and farming that receives monsoon rainfall during summer. Thus, a relatively small area of the Nile drainage, greatly affected by humans, supplies most of the sediments carried by the river to artificial lakes. — BH

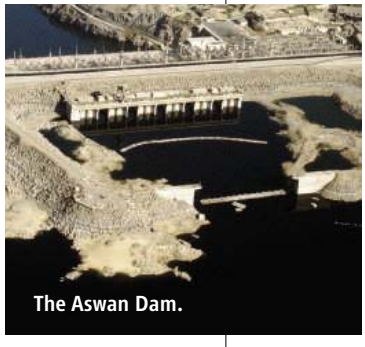

The Aswan Dam.

Earth Planet. Sci. Lett. 10.1016/j.epsl.2006.10.001 (2006).

CHEMISTRY

Catalyst Compatibility

The isolation and purification procedures that follow synthetic chemical reactions often produce substantial quantities of waste material. Research has thus increasingly focused on methods for carrying out multiple reaction steps in a single vessel. However, the mutual incompatibility of many catalysts, in particular Lewis acids and bases, presents a major challenge to this approach.

Poe *et al.* present an encapsulation technique that allows the mixing of a polymeric amine catalyst with a nickel-centered Lewis acid while avoiding the complexation reaction that would deactivate both. The poly(ethyleneimine) base is treated with a cross-linking agent in a methanol/cyclohexane emulsion, yielding a microcapsule morphology that conserves catalytic activity in the condensation reaction of benzaldehyde and nitromethane. Addition of a bis(diamino)nickel catalyst to the reaction mixture promotes a Michael addition of dimethyl malonate to the dehydrated product in ~80% yield. Moreover, the compatibility of the two catalysts is a boon to selectivity as well as efficiency; the nickel complex staves off a side pathway that would lead to a double nitromethane adduct. — JSY

J. Am. Chem. Soc. **128**, 10.1021/ja066476l (2006).

Continued on page 1357

Vinton G. Cerf
Vice President and Chief Internet Evangelist
Google

Amy Wu
Computer Science Student
Stanford University

Benjamin Mako Hill
Research Assistant
MIT Media Laboratory

Maria Klawe
President
Harvey Mudd College

ACM: KNOWLEDGE, COLLABORATION & INNOVATION IN COMPUTING

Uniting the world's computing professionals, researchers and educators to inspire dialogue, share resources and address the computing field's challenges in the 21st Century.

Association for Computing Machinery
Advancing Computing as a Science & Profession
www.acm.org/learnmore

Continued from page 1355

IMMUNOLOGY

Trekking Lymph Node Tracks

Lymph nodes are crucial staging posts from which immune responses are launched throughout the body. To achieve this, naïve lymphocytes must locate and respond to their specific antigens, which are relatively scarce. The active migratory tendency of lymphocytes helps to achieve this, and the structural organization of the lymph node itself also improves the chances of antigen encounter. Bajenoff *et al*. now find that organized networks of stromal cells provide trackways for lymphocytes to travel around lymph nodes. With a combination of microscopy and real-time intravital imaging, T cells were seen to enter the lymph node paracortex by interacting with fibroblastic

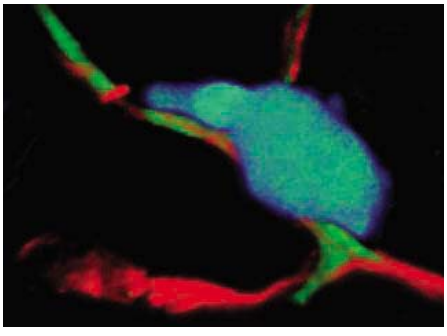

T cell (blue) on the FRC network (red and green).

reticular cells (FRCs). Inside the lymph node, the FRC formed a three-dimensional network along which a large proportion of T cells could crawl. Antigen-presenting dendritic cells also associated with the FRC network, which is consistent with the idea that this would optimize the rate of encounter between the two types of cell. B cells were also seen to move along the FRC tracks within the paracortex, transferring to a similar network of dendritic cells once they had entered the lymph node follicle. It will now be interesting to elucidate the molecular cues that govern migration along these cellular highways and byways. — SJS

Immunity **25** 10.1016/j.immuni.2006.10.011 (2006).

PHYSICS

Fast Track for Fusion

The search for controlled nuclear fusion for energy production has been hindered by substantial engineering and fundamental physical challenges. One approach has been to confine a hot plasma with magnetic fields in a device called a Tokamak and then to heat the plasma until nuclear reactions become self-sustaining. As the plasma is heated, however, the highest-velocity ions can drive wave motions and instabilities that disrupt its integrity. Worse yet, the fast ions can escape with their energy rather than contributing to the heating process. Bindslev *et al.* report a diagnostic technique in which beams of electromagnetic waves at frequencies of ~110 GHz are scattered off the ions in the TEXTOR (Tokamak Experiment for Technology-Oriented Research) reactor in Germany. The energy spectrum of the scattered photons from this collective Thomson scattering process reveals the velocity distribution of the fast ions. By acquiring spectra at different times during the heating of the plasma, the authors can uncover the evolution of the fast ion dynamics. Diagnostic tools such as this are expected to be especially important when ITER (the International Thermonuclear Experimental Reactor) commences operation in 2016. — DV

Phys. Rev. Lett. **97**, 205005 (2006).

Science STKE AAAS

www.stke.org

<< Shedding Light on Immunosuppression

Ultraviolet (UV) radiation from sunlight has been implicated in skin cancer and—perhaps not coincidentally—suppresses the immune response. UV-dependent immune suppression depends on its absorption by an epidermal photoreceptor. *Trans*-urocanic acid (UCA) isomerizes to *cis*-UCA in response to UV exposure, and epidermal UCA acts as a UV photoreceptor that can mediate immune suppression. The mechanism whereby *cis*-UCA affects the immune response, however, has been unclear. *Cis*-UCA forms a ring-like structure in solution, and Walterscheid *et al*., who serendipitously observed that the serotonin receptor antagonist ketanserin blocked UV- and *cis*-UCA–mediated immune suppression, now find that *cis*-UCA can bind to human serotonin receptors. *Cis*-UCA stimulated calcium mobilization in cells that express the serotonin receptor, and this calcium mobilization was blocked by ketanserin. UV- or *cis*-UCA–induced immune suppression in mice was blocked by antibodies directed against serotonin (as well as by antibodies directed against *cis*-UCA) and by serotonin receptor antagonists. Thus, the ability of *cis*-UCA to suppress the immune response—and that of UV radiation—are mediated through the serotonin receptor. — EMA

Proc. Natl. Acad. Sci. U.S.A. **103**, 17420 (2006).

CREDITS: BAJENOFF *ET AL.*, *IMMUNITY* **25** 10.1016/J.IMMUNI.2006.10.011 (2006)

Give Knowledge

It's not too late to order —
Say Happy Holidays all year. Give *Science* each week.

Special Gift Subscription Rate*
Professional $99 Postdoc/Student $50

Give 51 issues of *Science* along with the same yearlong benefits of AAAS membership that you enjoy.

You'll give colleagues a career boost and students an academic leg-up. You'll intrigue and enlighten friends; educate and entertain family members. And you'll add new supporters for the AAAS international, public policy, education, and career programs that advance science and serve society.

Make your holiday shopping list today—go to:

promo.aaas.org/giftnov
or call 1-866-434-AAAS (2227)

When you give *Science*, you receive our popular AAAS shirt.

Science
AAAS

*New members only. International orders will receive *Science* digital edition — to place an order outside the U.S., go to promo.aaas.org/giftn.

2 months from submission to publication?

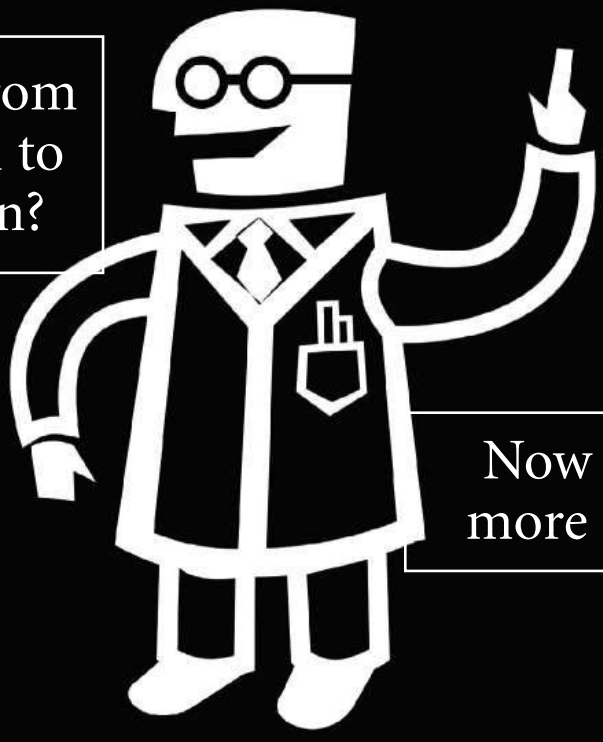

Now that's more like it.

Introducing *T-BME Letters*.

IEEE Engineering in Medicine and Biology Society announces a new publication format for reports of high quality, novel and high impact biomedical engineering science and methodologies with a prompt publication turn around time. T-BME Letters combines the rapid dissemination of electronic journals with the archival value of in-print publications. Peer review, decision and electronic posting of accepted manuscripts in IEEEXplore take place within two months, after which accepted papers can be downloaded by the research community and can be referenced as "in Press" until printing.

Get the Recognition you deserve.

T-BME Letters is a publication of the 8,000 member IEEE Engineering in Medicine and Biology Society and is managed as part of the prestigious and oldest biomedical engineering journal, the IEEE Transactions on Biomedical Engineering. It's the source engineers, biomedical researchers and professionals turn to for up-to-date and informative research on important advances in biomedical engineering and applied biophysics.

Submitting a manuscript is easy.

Manuscripts are to be short (4 pages), complete, accurate and clear as all manuscripts are either accepted "as is" (with only very minor modifications possible), or rejected. They may be submitted to the T-BME Manuscript Central website at http://embs-ieee.manuscriptcentral.com

Put our fast-track publishing guarantee to the test.

See for yourself what instant gratification feels like. Submit your original manuscript to T-BME Letters and we promise you'll hear from us immediately. **In fact, we guarantee it.**

T-BME Letters is indexed by Medline/PubMed For full submission details, please consult the journal website at http://bme.cnel.ufl.edu

MEDLINE
U.S. National Library of Medicine

EMB | IEEE

www.sciencemag.org

Science

1200 New York Avenue, NW
Washington, DC 20005
Editorial: 202-326-6550, FAX 202-289-7562
News: 202-326-6500, FAX 202-371-9227

Bateman House, 82-88 Hills Road
Cambridge, UK CB2 1LQ
+44 (0) 1223 326500, FAX +44 (0) 1223 326501

Subscription Services For change of address, missing issues, new orders and renewals, and payment questions: 866-434-AAAS (2227) or 202-326-6417, FAX 202-842-1065. Mailing addresses: AAAS, P.O. Box 96178, Washington, DC 20090-6178 or AAAS Member Services, 1200 New York Avenue, NW, Washington, DC 20005

Institutional Site Licenses please call 202-326-6755 for any questions or information

Reprints: Author Inquiries 800-635-7181
Commercial Inquiries 803-359-4578
Corrections 202-326-6501

Permissions 202-326-7074, FAX 202-682-0816

Member Benefits Bookstore: AAAS/BarnesandNoble.com bookstore www.aaas.org/bn; Car purchase discount: Subaru VIP Program 202-326-6417; Credit Card: MBNA 800-847-7378; Car Rentals: Hertz 800-654-2200 CDP#343457, Dollar 800-800-4000 #AA1115; AAAS Travels: Betchart Expeditions 800-252-4910; Life Insurance: Seabury & Smith 800-424-9883; Other Benefits: AAAS Member Services 202-326-6417 or www.aaasmember.org.

science_editors@aaas.org	(for general editorial queries)
science_letters@aaas.org	(for queries about letters)
science_reviews@aaas.org	(for returning manuscript reviews)
science_bookrevs@aaas.org	(for book review queries)

Published by the American Association for the Advancement of Science (AAAS), *Science* serves its readers as a forum for the presentation and discussion of important issues related to the advancement of science, including the presentation of minority or conflicting points of view, rather than by publishing only material on which a consensus has been reached. Accordingly, all articles published in *Science*—including editorials, news and comment, and book reviews—are signed and reflect the individual views of the authors and not official points of view adopted by the AAAS or the institutions with which the authors are affiliated.

AAAS was founded in 1848 and incorporated in 1874. Its mission is to advance science and innovation throughout the world for the benefit of all people. The goals of the association are to: foster communication among scientists, engineers and the public; enhance international cooperation in science and its applications; promote the responsible conduct and use of science and technology; foster education in science and technology for everyone; enhance the science and technology workforce and infrastructure; increase public understanding and appreciation of science and technology; and strengthen support for the science and technology enterprise.

Information for Contributors

See pages 102 and 103 of the 6 January 2006 issue or access www.sciencemag.org/feature/contribinfo/home.shtml

EDITOR-IN-CHIEF **Donald Kennedy**
EXECUTIVE EDITOR **Monica M. Bradford**
DEPUTY EDITORS **R. Brooks Hanson, Barbara R. Jasny, Katrina L. Kelner**
NEWS EDITOR **Colin Norman**

Editorial supervisory senior editor Phillip D. Szuromi; **senior editor/perspectives** Lisa D. Chong; **senior editors** Gilbert J. Chin, Pamela J. Hines, Paula A. Kiberstis (Boston), Marc S. Lavine (Toronto), Beverly A. Purnell, L. Bryan Ray, Guy Riddihough, H. Jesse Smith, Valda Vinson, David Voss; **associate editors** Jake S. Yeston, Laura M. Zahn; **online editor** Stewart Wills; **associate online editor** Tara S. Marathe; **book review editor** Sherman J. Suter; **associate letters editor** Etta Kavanagh; **information specialist** Janet Kegg; **editorial manager** Cara Tate; **senior copy editors** Jeffrey E. Cook, Cynthia Howe, Harry Jach, Barbara P. Ordway, Jennifer Sills, Trista Wagoner; **copy editors** Lauren Kmec, Peter Mooreside; **editorial coordinators** Carolyn Kyle, Beverly Shields; **publication assistants** Ramatoulaye Diop, Chris Filiatreau, Joi S. Granger, Jeffrey Hearn, Lisa Johnson, Scott Miller, Jerry Richardson, Brian White, Anita Wynn; **editorial assistants** Maris M. Bish, Emily Guise, Patricia M. Moore; **executive assistant** Sylvia S. Kihara; **administrative support** Maryrose Police

News senior correspondent Jean Marx; **deputy news editors** Robert Coontz, Jeffrey Mervis, Leslie Roberts, John Travis; **contributing editors** Elizabeth Culotta, Polly Shulman; **news writers** Yudhijit Bhattacharjee, Adrian Cho, Jennifer Couzin, David Grimm, Constance Holden, Jocelyn Kaiser, Richard A. Kerr, Eli Kintisch, Andrew Lawler (New England), Greg Miller, Elizabeth Pennisi, Robert F. Service (Pacific NW), Erik Stokstad; Rhituparna Chatterjee (intern); **contributing correspondents** Barry A. Cipra, Jon Cohen (San Diego, CA), Daniel Ferber, Ann Gibbons, Robert Irion, Mitch Leslie, Charles C. Mann, Evelyn Strauss, Gary Taubes, Ingrid Wickelgren; **copy editors** Linda B. Felaco, Rachel Curran, Sean Richardson; **administrative support** Scherraine Mack, Fannie Groom **bureaus:** Berkeley, CA: 510-652-0302, FAX 510-652-1867, New England: 207-549-7755, San Diego, CA: 760-942-3252, FAX 760-942-4979, Pacific Northwest: 503-963-1940

Production director James Landry; **senior manager** Wendy K. Shank; **assistant manager** Rebecca Doshi; **senior specialists** Jay Covert, Chris Redwood; **specialist** Steve Forrester **Preflight director** David M. Tompkins; **manager** Marcus Spiegler; **specialist** Jessie Mudjitaba

Art director Kelly Buckheit Krause; **illustrators** Chris Bickel, Katharine Sutliff; **senior art associates** Holly Bishop, Laura Creveling, Preston Huey; **associate** Nayomi Kevitiyagala; **photo editor** Leslie Blizard

***Science* International**

Europe (science@science-int.co.uk) **editorial: international managing editor** Andrew M. Sugden; **senior editor/perspectives** Julia Fahrenkamp-Uppenbrink; **senior editors** Caroline Ash (Geneva: +41 (0) 222 346 3106), Stella M. Hurtley, Ian S. Osborne, Stephen J. Simpson, Peter Stern; **associate editor** Joanne Baker **editorial support** Alice Whaley; Deborah Dennison **administrative support** Janet Clements, Phil Marlow, Jill White; **news: international news editor** Eliot Marshall **deputy news editor** Daniel Clery; **correspondent** Gretchen Vogel (Berlin: +49 (0) 30 2809 3902, FAX +49 (0) 30 2809 8365); **contributing correspondents** Michael Balter (Paris), Martin Enserink (Amsterdam and Paris), John Bohannon (Vienna)

Asia Japan Office: Asca Corporation, Eiko Ishioka, Fusako Tamura, 1-8-13, Hirano-cho, Chuo-ku, Osaka-shi, Osaka, 541-0046 Japan; +81 (0) 6 6202 6272, FAX +81 (0) 6 6202 6271; asca@os.gulf.or.jp; **asia news editor** Richard Stone +66 2 662 5818 (rstone@aaas.org) **japan news bureau** Dennis Normile (contributing correspondent, +81 (0) 3 3391 0630, FAX 81 (0) 3 5936 3531; dnormile@gol.com); **china representative** Hao Xin, + 86 (0) 10 6307 4439 or 6307 3676, FAX +86 (0) 10 6307 4358; cindyhao@gmail.com; **south asia** Pallava Bagla (contributing correspondent +91 (0) 11 2271 2896; pbagla@vsnl.com)

Africa Robert Koenig (contributing correspondent, rob.koenig@gmail.com)

EXECUTIVE PUBLISHER **Alan I. Leshner**
PUBLISHER **Beth Rosner**

Fulfillment & Membership Services (membership@aaas.org) **director** Marlene Zendell; **manager** Waylon Butler; **systems specialist** Andrew Vargo; **customer service supervisor** Pat Butler; **specialists** Laurie Baker, Tamara Alfson, Karena Smith, Vicki Linton, Latoya Casteel; **circulation associate** Christopher Refice; **data entry supervisor** Cynthia Johnson; **specialists** Tomeka Diggs, Tarrika Hill, Erin Layne

Business Operations and Administration director Deborah Rivera-Wienhold; **business manager** Randy Yi; **senior business analyst** Lisa Donovan; **business analyst** Jessica Tierney; **financial analyst** Michael LoBue, Farida Yeasmin; **rights and permissions: administrator** Emilie David; **associate** Elizabeth Sandler; **marketing: director** John Meyers; **marketing managers** Darryl Walter, Allison Pritchard; **marketing associates** Julianne Wielga, Mary Ellen Crowley, Catherine Featherston, Alison Chandler, Lauren Lamoureux; **international marketing manager** Wendy Sturley; **marketing/member services executive:** Linda Rusk; **japan sales** Jason Hannaford; **site license sales: director** Tom Ryan; **sales and customer service** Mehan Dossani, Kiki Forsythe, Catherine Holland, Wendy Wise; **electronic media: manager** Lizabeth Harman; **assistant manager** Lisa Stanford **production associates** Nichele Johnston, Kimberly Oster

Advertising director worldwide ad sales Bill Moran

Product (science_advertising@aaas.org); **midwest** Rick Bongiovanni: 330-405-7080, FAX 330-405-7081 • **west coast/w. canada** Teola Young: 650-964-2266 **east coast/e. canada** Christopher Breslin: 443-512-0330, FAX 443-512-0331 • **uk/europe/asia** Julie Skeet: +44 (0) 1223-326-524, FAX +44 (0) 1223-325-532 **japan** Mashy Yoshikawa: +81 (0) 33235 5961, FAX +81 (0) 33235 5852 **traffic manager** Carol Maddox; **sales coordinator** Deiandra Simms

Commercial Editor Sean Sanders: 202-326-6430

Classified (advertise@sciencecareers.org); **u.s.: recruitment sales manager** Ian King: 202-326-6528, FAX 202-289-6742; **u.s./industry:** Darrell Bryant: 202-326-6533; **midwest/canada:** Daryl Anderson: 202-326-6543; **northeast:** Allison Millar: 202-326-6572; **southeast:** Fernando Junco: 202-326-6740; **west:** Katie Putney: 202-326-6577; **sales coordinators** Erika Bryant; Rohan Edmonson, Shirley Young; **international: sales manager** Tracy Holmes: +44 (0) 1223 326525, FAX +44 (0) 1223 326532; **sales** Christina Harrison, Svitlana Barnes; **sales assistant** Kellie Jones; **japan:** Jason Hannaford: +81 (0) 52 757 5360, FAX +81 (0) 52 757 5361; **advertising production operations manager** Deborah Tompkins; **associates** Christine Hall; Amy Hardcastle; **publications assistants** Robert Buck; Mary Lagnaoui

AAAS Board of Directors retiring president, chair Gilbert S. Omenn; **president** John P. Holdren; **president-elect** David Baltimore; **treasurer** David E. Shaw; **chief executive officer** Alan I. Leshner; **board** Rosina M. Bierbaum; John E. Dowling; Lynn W. Enquist; Susan M. Fitzpatrick; Alice Gast; Thomas Pollard; Peter J. Stang; Kathryn D. Sullivan

AAAS
ADVANCING SCIENCE, SERVING SOCIETY

Be More Specific.

TaqMan MicroRNA Assays—the miRNA quantitation solution.

TaqMan® MicroRNA Assays are exactly what's needed for high-quality gene expression quantitation results in miRNA research. Whether profiling miRNA or monitoring specific miRNA genes, you'll get the gold standard in sensitivity, specificity, and ease of use that only real-time PCR TaqMan® assays can provide. The TaqMan MicroRNA Assay specifically measures the biologically active mature form—not the inactive precursor miRNA transcript. And since the assays are functionally validated, you can be confident they will work for your target of interest. TaqMan® chemistry provides the single-base specificity to differentiate between closely related sequences, and unparalleled sensitivity to help conserve your precious samples.

The rapidly growing TaqMan® MicroRNA Assays portfolio includes assays for human, mouse, rat, *C. elegans*, *Drosophila*, and *Arabidopsis*.

Get all the specifics at mirna.appliedbiosystems.com

Applied Biosystems

25 YEARS ADVANCING SCIENCE

new!

The power of small²

NanoDrop introduces a Fluorospectrometer

1 µl samples ▪ No cuvettes ▪ 10-second measurements ▪ Broad spectral output

Small footprint. Revolutionary technology. The NanoDrop® ND-3300 Fluorospectrometer is a powerful new tool for fluorescence spectrometry. Choose from many pre-defined methods or configure your own.

- **Nucleic acids:** Determine concentration of dsDNA using PicoGreen® assay (2 pg), Quant-iT™ DNA assay or Hoechst 33258 dye; RNA using RiboGreen® dye
- **Proteins:** Determine concentration using Quant-iT™ protein assay
- **More:** FITC (fluorescein), Cy-Alexa Fluor dyes, B-Phycoerythrin, Quinine Sulfate, Sulforhodamine and 4-MU

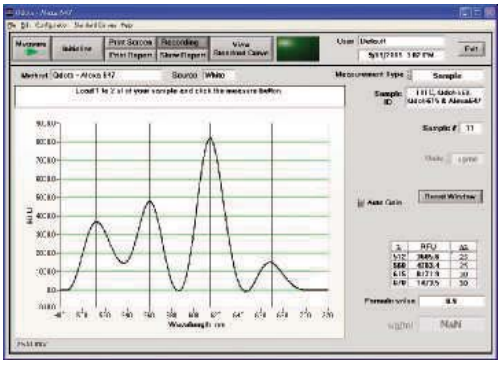

Measurement is as easy as pipette and read, requiring only 1-2 µl of sample. No cuvettes are necessary — simply wipe the optical surfaces and you're ready for your next sample. A broad excitation range is achieved using UV, blue and white LED sources. The uniquely clean optics of the patented retention system, combined with proprietary white LED signal processing, enables measurements across a wide range of wavelengths without the need for filter changes. The ND-3300 is small, simple and powerful enough for your most challenging and precious samples.

And for the power of small in absorbance measurement, the NanoDrop® ND-1000 UV/Vis Spectrophotometer can detect down to 2ng/µl and up to 3700 ng/µl of dsDNA without dilutions.

Ready to experience the power of small? Contact us today and try the ND-3300 or ND-1000 in your own lab.

FREE one week evaluation

Call for details **(302)479-7707** **www.nanodrop.com**

NanoDrop

ANOTHER PHYSICS DEPARTMENT DOWN

Reading University last week became the 21st British university to announce the closure of its physics department since 1997. Despite protests from staff and students and a petition from more than 2000 researchers around the world, the university council voted on 20 November to accept no more physics students. The department will close in 2010.

U.K. universities are largely government-funded, with the amounts determined by numbers of students and quality of research. Reading Vice-Chancellor Gordon Marshall said in an open letter that the physics department is losing about $1 million a year because it is not getting enough new students—28 this year against a target of 50—or enough research income.

The closure of science and math departments (*Science*, 4 February 2005, p. 668) prompted the U.K. government last month to announce $140 million to help key departments over the next 3 years. But it won't be enough to help Reading, Marshall says. Philip Diamond of the Institute of Physics in London says economics favors big departments these days; a half-dozen now account for half of all U.K. physics students, and "small ones are just vulnerable."

WELL-WIRED WHALES >>


Humpback whale.

Some whales have a specialized brain cell that hitherto has been seen only in humans and great apes—leading some scientists to suggest that cetaceans evolved their relatively advanced brains before primates did.

Humans, chimps, and gorillas share a type of cortical nerve cell—called a spindle neuron—that is lacking in all other primates. The cells appear to connect regions implicated in higher cognitive functions to other parts of the brain.

Neuroscientist Patrick Hof and neuroendocrinologist Estel Van der Gucht of Mount Sinai School of Medicine in New York City have now discovered spindle neurons, in areas homologous to their location in human brains, in several large-brained cetaceans including humpback and fin whales. The researchers estimate that bigger-brained whales evolved spindle neurons 22 million to 30 million years ago. Because the common ancestor of great apes only dates to about 15 million years ago, the pair concludes that these cells must have evolved independently in apes and whales. Reporting online this week in *The Anatomical Record*, they speculate that whale talents such as the formation of social groups as well as singing and other communicative skills are linked to the enhanced connectivity provided by spindle neurons.

Clever but smaller-brained dolphins don't have spindle neurons. John Allman, a neurobiologist at the California Institute of Technology in Pasadena, says the neurons are probably "adaptations that support fast communication … in very large brains." Allman says his group is looking to see whether elephants also have the cells.

Keeping Book on Baby

Baby books, those little pamphlets that record baby's first steps and first words, now interest more than doting relatives. Scholars are finding the books a new source of close-up information on the early lives of infants from different times.

Last month, the University of California, Los Angeles (UCLA), Louise M. Darling Biomedical Library held a reception to introduce its collection of more than 500 baby books dating back to 1884. It's a historical treasure trove that charts shifting attitudes about public health and parenthood, says archivist Russell Johnson. "A space for the father to make entries doesn't show up until around World War II," he notes.

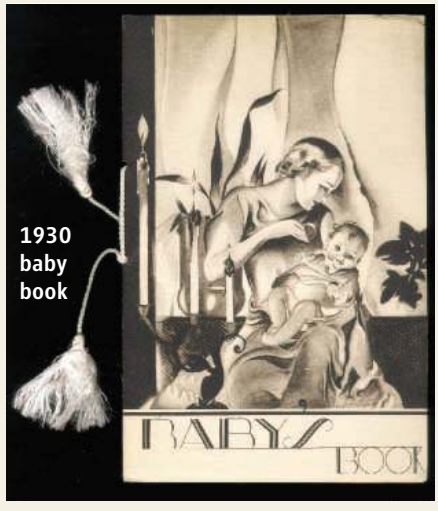

1930 baby book

The books may have emerged as part of a late–19th century public health campaign to "Save the Babies," according to Jacqueline H. Wolf, a medical historian at Ohio University in Athens. "Baby books represented a change in cultural thinking," she says. "Infants were not weak and susceptible, as people had long argued. Rather, infant death was preventable."

Russell says UCLA welcomes donations from all eras, especially because the library often battles collectors of famous children's book illustrators when copies come up on eBay.

NETWATCH >>

Diseases on the Move

Visitors to the new site HEALTHmap can pinpoint the latest outbreaks of more than 50 human and animal illnesses, from avian influenza to chikungunya fever, a mosquito-spread disease of Asia and Africa. Created by epidemiologist John Brownstein of Harvard Medical School in Boston and software developer Clark Freifeld of Children's Hospital Boston, the site automatically picks up and charts fresh case reports and other data from sources such as the World Health Organization, Google News, and the disease alert Web site ProMed-Mail. You can sort the information by disease and country and click on the world map to summon the original report or article. >>
www.healthmap.org

Up Next

THE FIRST PODSTER. There you are, standing by your poster at the big annual meeting, when the Big Kahuna in your field walks up. If only you had some multimedia to make a quick impression. Next time, try attaching some video iPods to your poster, says graduate student Pascal Wallisch of the University of Chicago in Illinois, who unveiled what may be the world's first "Podster" at October's meeting of the Society for Neuroscience in Atlanta, Georgia.

Wallisch got the idea after a poster session at the 2005 neuroscience meeting in which he used his laptop to show videos of his research on the primate visual system. Reaching around to point at the screen was awkward, however, and the batteries ran out. So this year, he replaced the laptop with two iPods, each loaded with videos to explain different features of his experiment. It gave visitors a more interactive experience, he says, and left his hands free.

Passers-by loved the concept, says Wallisch, as did two Apple Computer reps from a nearby booth—until they found out he'd used a Microsoft product to create the poster's text and graphics. "Then they just left," Wallisch says.

ON CAMPUS

CLEVERNESS CONTROVERSY. A Danish IQ researcher who was suspended after his research suggested that men have slightly higher IQs than women has been found guilty of "official misconduct" but reinstated in his job.

Psychologist Helmuth Nyborg, 69, of the University of Aarhus was suspended last spring following criticism of a report from a longitudinal study called the Skanderborg project. Nyborg reported in a June 2005 paper in the *Journal of Personality and Individual Differences* that when IQ test scores of 62 Danes he has been following since the 1970s are properly analyzed, they reveal a roughly four-point advantage for males.

Although Nyborg is not alone in reporting such a sex difference, some scholars criticized the research on methodological grounds. University officials set up a committee to investigate, and in July, it reported that there was no evidence of fraud. In September, the university declared that Nyborg had demonstrated "grossly negligent behavior" and issued him a "severe reprimand" before revoking his suspension. Colleagues from around the world have rallied to his defense, accusing the university of having political motives and claiming that the errors in his research were trivial.

POLITICS

U.K. SCIENCE MINISTER. An educator turned politician is the new U.K. minister for science and innovation. Malcolm Wicks, 59, succeeds David Sainsbury, who stepped down last month after 8 years marked by a doubling of U.K. spending on research.

The son of a Labour Member of Parliament and a Labour MP himself since 1992, Wicks most recently guided a strategic plan for a dramatic shift to low-CO_2-emitting power sources as energy minister in the Blair government.

Slowing the buildup of greenhouse gases, he said, is the "world's most pressing challenge." Wicks has called the United Kingdom's and the world's failure to address nuclear waste "an absolute disgrace," although he has also said that nuclear power could be a clean alternative to fossil fuels. Wicks attended the London School of Economics but has no formal training in science.

Rising Stars >>

IN TANDEM. Sometimes a little sibling rivalry can be a good thing. Last week, Kevin Shenderov, a 19-year-old senior at New York University, followed the footsteps of his brother Eugene by winning a Rhodes Scholarship. Kevin (left) intends to pursue a doctorate in immunology at Oxford University—just as Eugene (center) is now doing.

The brothers credit their parents, Peter, a medical physicist, and Faina, who is completing a doctorate in pharmacy, for inculcating a love of science. Both worked at Memorial Sloan-Kettering Cancer Center in New York City when the boys were growing up, and "the dinner conversation pretty much always centered around what was going on at the hospital," says Eugene, 23, who won a Rhodes 2 years ago. "Science was the family's bread and butter."

Peter says the brothers have pushed each other but remain close. "This kind of competition is pulling them together," he says. "The accomplishment is the icing on the cake."

Got a tip for this page? E-mail people@aaas.org

CREDITS (TOP TO BOTTOM): BEN SCOTT; COURTESY OF MALCOLM WICKS; KLAUS GOTTFREDSON; PETER SHENDEROV

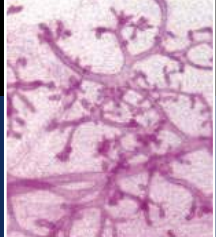

Progesterone and breast cancer 1370

A new way to engineer flies 1371

SCIENTIFIC CONDUCT

China's Fraud Buster Hit by Libel Judgments; Defenders Rally Round

BEIJING—China's self-appointed science cop, Fang Shi-min, was dealt a pair of setbacks last week in his high-profile crusade against academic misconduct. Two Chinese courts handed down libel judgments against Fang, known by his nom de guerre Fang Zhouzi, and the newspapers and Internet sites that have featured his writings on pseudoscience and fraud. Fang's revelations have cost several scientists their jobs and reputations.

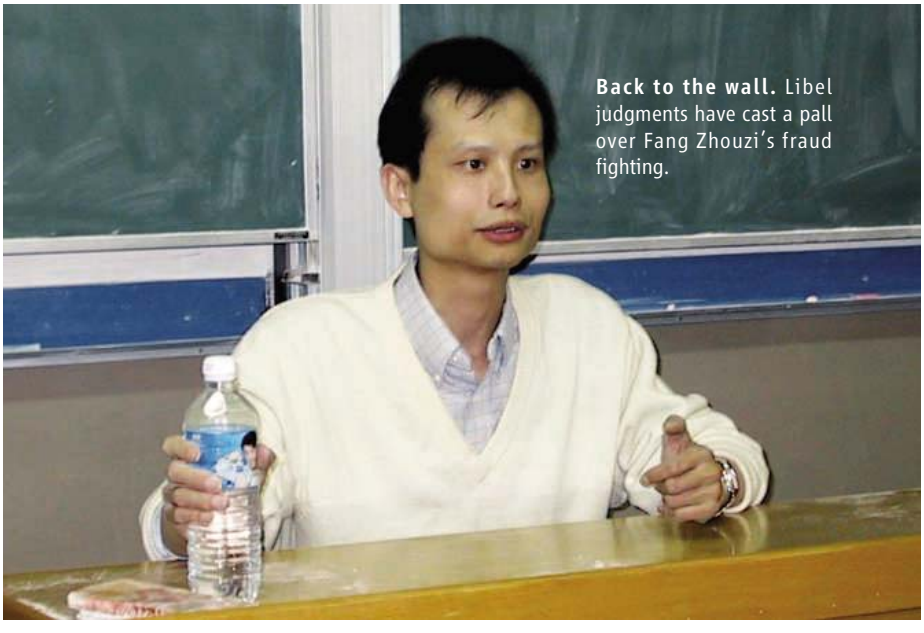

Back to the wall. Libel judgments have cast a pall over Fang Zhouzi's fraud fighting.

With Fang now on the defensive, his backers are setting up two funds to help foot the costs of litigation. "If you strike false science, false science [makers] will strike you," says Guo Zhengyi, a science writer and a co-organizer of one foundation. Guo and others say they hope that, by drawing attention to what they call "absurd" court rulings, they may force the government to crack down on corruption.

Fang received a Ph.D. in biochemistry and did a postdoc in the United States before becoming a science essayist. He got fired up about fraud in 2001, after reading dubious claims in the Chinese media about "nucleotide supplements." Fang then started using his Web site, *Xin Yu Si* ("New Threads"), to debunk pseudoscience and expose alleged misconduct, from résumé padding to data fabrication (*Science*, 10 August 2001, p. 1039).

By Fang's tally, New Threads has aired allegations against more than 500 individuals. Fang uncovered some cases himself, but most were e-mailed to him by others. Few exposures have led to official investigations, and fewer still have resulted in punishment—the most notable being the dismissals earlier this year of an assistant dean of Qinghua University's medical school in Beijing and a dean at Tongji University in Shanghai, both for having falsified their résumés and exaggerated achievements.

The anonymous allegations published on New Threads trouble some people, who liken them to *dazibao*, or posters, used during the Cultural Revolution to denounce "class enemies." Fang and his supporters contend there's a big difference: The Web postings are individual actions not directed by the state. The Chinese government takes an ambiguous stance: It blocks access in China to New Threads' U.S.–based site, www.xys.org, but allows access to mirror sites.

Fang's recent setbacks came on consecutive days. On 21 November, a Beijing intermediate court ruled that an article Fang wrote in 2005 defamed the late Liu Zihua, a Sichuan provincial government employee. In a dissertation written in France in the 1930s, Liu presented calculations based on the eight trigrams of an ancient divination text, *I Ching* (*Book of Changes*), predicting the existence of a 10th major planet in the solar system. Liu's prognostication was resurrected after last year's announced discovery of 2003UB313 (now officially a dwarf planet named Eris). A Sichuan newspaper ran a story extolling Liu's prophecy.

In an essay, Fang labeled Liu's prediction "pseudoscience" and noted that a Chinese astronomer discredited it in the 1940s. Liu's widow and son sued Fang and several newspapers and Internet content providers for libel. The court judged Fang's words "insulting" to Liu and ordered him to apologize publicly and pay Liu's family $2500 plus legal fees. The family did not respond to an interview request.

Then on 22 November, a court in Xi'an slapped another libel judgment on Fang, ordering him and *Beijing Keji Bao* (*Beijing Sci-Tech Report*) to pay Xi'an Fanyi University $18,750 and its president Ding Zuyi $1250 in damages plus legal fees. In 2004, Chinese newspapers ran stories citing a "report" in the *Los Angeles Times* lauding Ding as one of China's most respected university presidents and his private college for training translators as the 10th-ranked university in China. In a 2005 article in *Beijing Sci-Tech Report*, Fang quoted an education ministry spokesperson, who stated that investigations showed the report to be "a self-paid advertisement." Ding sued Fang for libel. Ding could not be reached for comment.

Fang is appealing another libel verdict by a Wuhan court last July. In this case, Xiao Chuan-guo, a urology professor at Huazhong University of Science and Technology in Wuhan and a clinical associate professor at New York University School of Medicine, sued after Fang accused him in an

CREDIT: R. STONE/*SCIENCE*

Pruning science in the classroom 1374

South Africa's turnaround on HIV 1378

Saving the saola 1380

essay last year of counting conference abstracts as publications in international journals to inflate his achievements. Fang also challenged Xiao's claim that a surgical procedure he invented is recognized internationally and has won neurourology's "highest award." The presiding judge ruled that Fang's criticisms "seriously lacked facts" and ordered him to apologize publicly and pay Xiao $3750 in compensation. A final ruling is expected in early December.

Xiao told *Science* that the accusations are groundless and that Fang "intentionally confused" Xiao's urology awards. Xiao says he supported Fang until 2002, after which he concluded that Fang had begun to "misguide the public" with less-than-solid accusations.

In response to the Wuhan ruling, Zhang Feng, a Florida-based financial analyst and college classmate of Fang's, along with eight other expatriates, last month established the Organization for Scientific and Academic Integrity in China to raise money for Fang and other anticorruption campaigners. So far, the nonprofit has received more than $10,000 in donations. And in China, Guo and others are creating a separate science fraud-fighting fund. Fang's lawyer, Peng Jian, hopes the foundations will raise money to "implement systematic investigations into some individual cases or organize seminars to discuss legal punishments against proved misconduct makers."

Fang vows to continue "using sharp-tongued criticism" to expose misconduct and folly. But he doubts that his freelance fraud busting can play a "decisive role" in cleaning up Chinese academia. To be more effective, he says, he intends to report future allegations, when appropriate, to a new disciplinary office at China's Ministry of Science and Technology and wait for a response before posting them online.

–JIA HEPENG AND HAO XIN

Jia Hepeng is a writer in Beijing.

DEVELOPMENTAL BIOLOGY

Fraud Investigation Clouds Paper on Early Cell Fate

A surprising report in a contentious area of developmental biology has sparked a scientific misconduct investigation at the University of Missouri, Columbia. Until that inquiry is complete, the results of the implicated paper, published in *Science* earlier this year, remain in limbo.

Contrary to prevailing dogma, the report claimed that mouse embryo cells have distinct fates from the time of the very first cell division. If true, those findings would dramatically change the current understanding of mammalian embryo development—and could also play a role in ongoing political and ethical debates over cloning and stem cells.

But the senior author of the paper now says the results are not trustworthy and predicts that the paper will be retracted as soon as the university completes its investigation. The paper, which was accepted as *Science* editors were embroiled in the scandal surrounding Woo Suk Hwang's human cloning papers in early 2006 (see Editorial on p. 1353), again raises questions about the limitations of the peer-review process in detecting fraud.

Published in the 17 February issue of *Science* (p. 992), the paper caused an immediate stir. It is well known that embryonic cells of insects and amphibians have distinct fates from the first cell divisions, but the picture for mammalian embryos has been far murkier (*Science*, 6 May 2005, p. 782). Experiments in which mouse embryos are teased apart and cells transplanted from one embryo to another have suggested that until about a week after fertilization, mammalian embryo cells are quite interchangeable. There is an ongoing debate, however, over whether very early embryo cells—when the embryo is at the four- or eight-cell stage—might have a tendency toward one fate or another, although they are not yet committed. The results published in February indicated a much earlier differentiation than anyone else in the field had suggested.

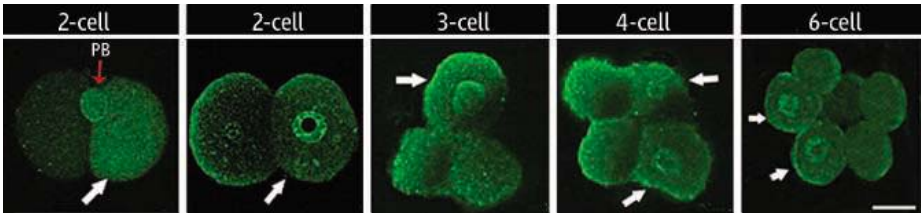

Surprisingly clear. The paper reported finding the Cdx2 protein (green) concentrated in just one of the cells in two-cell mouse embryos.

CREDIT: R. M. ROBERTS *ET AL.* (2006)

The corresponding author, R. Michael Roberts, is an expert in bovine embryology and until this year had not been involved in the debate. In the paper, Roberts, with postdoctoral fellows Kaushik Deb and Hwan Yul Yong and microscope technician Mayandi Sivaguru, claimed that in most mouse embryos there was a distinct difference between cells from the first cell division on. One cell had strong expression of a gene called *Cdx2*, the paper claimed, and eventually went on to give rise to the placental tissues. The other, which had less *Cdx2* expression, went on to form the eventual fetus. The scientists argued that their observations might help explain why cloning in mammals is so inefficient. If *Cdx2* expression is disrupted by cloning, they speculated, then embryos might have a hard time developing further.

Proponents of so-called alternative nuclear transfer were also excited by the results. This technique has gained some support among people otherwise opposed to stem cell research and human nuclear transfer because it hypothetically offers a way to derive stem cells without destroying an embryo. If scientists use egg cells or somatic cells lacking *Cdx2* for their nuclear transfer, the reasoning goes, the resulting cells would be unable to form a true embryo.

The Roberts results seemed to help the supporters' case: If the gene is so crucial from the very beginning, then that would strengthen the argument that cells lacking it could not be called an embryo. ▶

K. lactis Protein Expression Kit from New England Biolabs

YEAST PROTEIN EXPRESSION MADE EASY

The *K. lactis* Protein Expression Kit provides a simple method to clone and express your gene of interest in the yeast *Kluyveromyces lactis*. This system offers many advantages over bacterial systems and eliminates the methanol containing medium and antibiotic requirements of *Pichia pastoris*. With easy-to-use protocols and highly competent *K. lactis* cells included, this system can take you from bench top to large scale production with ease.

Advantages:

- High yield protein expression
- Rapid high cell density growth
- Methanol-free growth media
- Plasmid integration enhances stability
- Acetamide selection enriches for multi-copy integrants, enhancing yield
- Tight control of gene expression enables expression of toxic genes
- Access to eukaryotic protein folding and glycosylation machinery
- Simultaneous expression of multiple proteins
- Ease-of-use for those inexperienced with yeast systems
- Yeast competent cells included
- No license required for research use

***K. lactis* Protein Expression Kit** **E1000**

Kit components sold separately

***K. lactis* GG799 Competent Cells** **C1001**

pKLAC1 Vector **N3740**

	K. lactis	*P. pastoris*
High yield expression	✓	✓
Rapid high cell density growth	✓	✓
Yeast Competent Cells Included	✓	
Methanol-free growth media	✓	
Antibiotic-free Selection	✓	
Enhanced multi-copy integration	✓	
Protein folding and glycosylation	✓	✓
Expression of genes toxic to *E. coli*	✓	✓

Quick comparison of *K. lactis* and *P. pastoris* expression systems.

For more information and international distribution network, please visit www.neb.com

- **New England Biolabs Inc.** 240 County Road, Ipswich, MA 01938 USA 1-800-NEB-LABS Tel. (978) 927-5054 Fax (978) 921-1350 info@neb.com
- **Canada** Tel. (800) 387-1095 info@ca.neb.com
- **Germany** Tel. 0800/246 5227 info@de.neb.com
- **UK** Tel. (0800) 318486 info@uk.neb.com
- **China** Tel. 010-82378266 beijing@neb-china.com

NEW ENGLAND BioLabs® Inc.
the leader in enzyme technology

The results, however, "were so drastically different from any of the results obtained by any other group" that most people viewed them skeptically from the start, says Magdalena Zernicka-Goetz of the University of Cambridge, U.K. However, it wasn't immediately clear why the results were so different, she says. A different strain of mice or a different labeling technique might have been the cause, she says.

Others in the field were less willing to suspend their disbelief. Within weeks of the paper's publication, Roberts says, several scientists wrote to *Science*, to Roberts, and to the University of Missouri, pointing out problems with the data. Some of the images seemed suspiciously similar to each other, they said. In others, the staining didn't seem to line up exactly with the cells. By late April, Roberts says, the university had started an investigation.

It was soon clear that there was reason to worry about the data's veracity, Roberts says. "In my view, there are a number of questionable images," he says. But until the university investigation is complete, he says, the team will not be able to explain the details of what is wrong or retract the paper. Roberts says the university is being very cautious about assigning any blame before the investigation is complete. All the co-authors have since left the university. Two have found other jobs, and a third has apparently dropped out of contact. In the meantime, *Science* issued an "Editorial Expression of Concern" to alert the community that it should not trust the published results (*Science*, 27 October, p. 592).

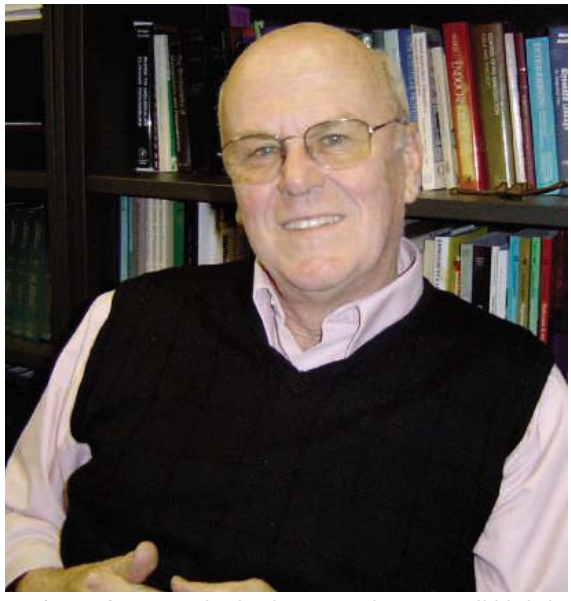

Senior author. R. Michael Roberts says the paper will likely be retracted as soon as the University of Missouri finishes its investigation.

CREDIT: NORMA MCCORMACK/UNIVERSITY OF MISSOURI, COLUMBIA

Some critics question why the paper was published in the first place or why image-analysis techniques—which *Science* editors said they put in place at the beginning of the year—didn't spot the apparent problems. Davor Solter of the Max Planck Institute for Immunobiology in Freiburg, Germany, one of the scientists who wrote to *Science*, contends that the review process was flawed. *Science* editors declined to discuss the specifics of the review process, which is confidential, but Katrina Kelner, deputy editor for biology, says, "*Science* published the paper based on feedback we got from the field."

Solter speculates that leading scientists in the field did not review the paper, noting that if they had, they likely would have caught the problems. But Richard Behringer of M. D. Anderson Cancer Center in Houston, Texas, is not sure the problems could have been spotted ahead of time. Although Behringer now says he can see the evidence of duplicated images, he says at first reading the paper seemed solid, if surprising. "I can understand why referees would say OK," he says.

Kelner and *Science* Editor-in-Chief Donald Kennedy add that even if the data are found to have been manipulated, the new image-analysis techniques would not have picked it up. Those techniques can flag unmatched pixels that are signs of deletions or cut-and-paste manipulations. But duplicated images—like those in the Hwang paper—are harder to spot, Kelner says.

In retrospect, Roberts says he wishes he had been more cautious with the results his lab members presented to him. "I didn't go into this with preconceived ideas. I got into it by happenstance," he says. The research was aimed at determining whether *Cdx2* was involved in turning on another gene in bovine embryos, he explains, and the mouse embryos were used as controls to analyze *Cdx2* expression. "But the results looked so beautiful, you couldn't come to any other conclusion." Since questions about the paper were raised, he says, "I've obviously questioned myself and my judgment. I haven't had a good night's sleep since February."

The University of Missouri is expected to finish its investigation later this month.

–GRETCHEN VOGEL

Party Animals

AMSTERDAM—The Dutch Party for Animals gained two seats in the 150-member Second Chamber of Parliament last week after drawing 1.9% of the votes nationwide. The group, one of whose goals is the eventual elimination of animal experimentation, appears to be the first political party devoted to animal welfare. Its platform includes a ban on transgenic animals, better oversight of animal experiments, including better housing and daily checks by independent vets, and more research on alternatives.

–MARTIN ENSERINK

Dawkins Versus the Gods

After scanning the titles in a local bookshop, Oxford University geneticist Richard Dawkins discovered that "real science" was "outnumbered three to one by pseudoscience." Concerned that "the enlightenment is under threat," the author of *The God Delusion* has created and will help fund the Richard Dawkins Foundation for Science and Reason. The new charity, with U.S. and U.K. branches, will support research on "the psychological basis of unreason," produce videos and books, and run a Web site (richarddawkins.net/foundation). Another goal, "to oppose … well-financed efforts to teach creationism in science classes," will put it up against the U.K.–based Truth in Science, which recently sent "intelligent design" promotional packs to 5700 British secondary schools. Truth in Science claims it received 59 positive responses.

–ELIOT MARSHALL

Hope for German GM crops

BERLIN—In a move to support plant researchers, the German agriculture minister has apparently agreed to ease rules controlling the planting of genetically modified (GM) crops. German media reported last week that the minister, Horst Seehofer, will propose allowing the government to pay for damages resulting from any gene-altered pollen that escapes from government-funded research plots. Under current rules, the farmers or researchers who plant GM seeds are liable for any pollen that might contaminate a neighbor's field, preventing it from being sold as GM-free. The proposal, contained in a measure that could be presented to legislators early next year, would also restrict public access to information about where GM crops are planted. Despite overwhelming public opposition to GM foods, research minister Annette Schavan has been pushing for such rules.

–GRETCHEN VOGEL

MEDICINE

Squelching Progesterone's Signal May Prevent Breast Cancer

A woman who carries a mutated *BRCA1* gene faces a daunting decision: She can opt for constant monitoring hoping to catch any cancer early, while it's still curable, or she can elect to have her breasts or ovaries removed to prevent cancer from developing in the first place. Results described on page 1467 now suggest that one day there may be a third option: using drugs rather than surgery to prevent *BRCA1*-mediated breast cancers.

BRCA1 is a so-called tumor suppressor, a gene that in its normal form protects against cancer. One way it does this is by helping cells repair DNA damage that might otherwise result in cancer-causing mutations. The new work, which comes from Eva Lee and her colleagues at the University of California, Irvine, points to another cancer-preventing role for *BRCA1*. By aiding in the degradation of the receptor through which progesterone exerts its effects, the gene's protein product apparently checks the hormone's growth-promoting action on breast tissue.

Lee's team also showed that mifepristone, a drug that induces abortions by inhibiting the progesterone receptor, blocks the development of mammary tumors in mice that have had the rodent version of *BRCA1* inactivated in their mammary glands. "The paper has a mechanism [of *BRCA1* activity] and has clinical implications. It's potentially important," says Eliot Rosen of Georgetown University School of Medicine in Washington, D.C., who is also studying the interaction between *BRCA1* and progesterone.

Previous work had raised suspicions that progesterone fosters breast cancer development. For example, women taking both estrogen and progesterone to treat menopausal symptoms have a higher risk of developing breast cancer than women who take estrogen only. And working with human breast cancer cells in lab cultures, Rosen's team found that normal *BRCA1* inhibits the action of the progesterone receptor, although how has been unclear.

In the current work, Lee and her colleagues created mice that lacked functioning copies of the rodent versions of both *BRCA1* and *p53*, another tumor suppressor that is frequently mutated in breast cancers. Although the female mice had never been mated, their mammary tissue showed increased cell proliferation—much as the breasts of pregnant woman do when high progesterone levels prepare the mammary glands for lactation. What's more, all the rodents developed mammary cancers by the age of 8 months. Mice treated with mifepristone, however, were still tumor-free at 12 months of age.

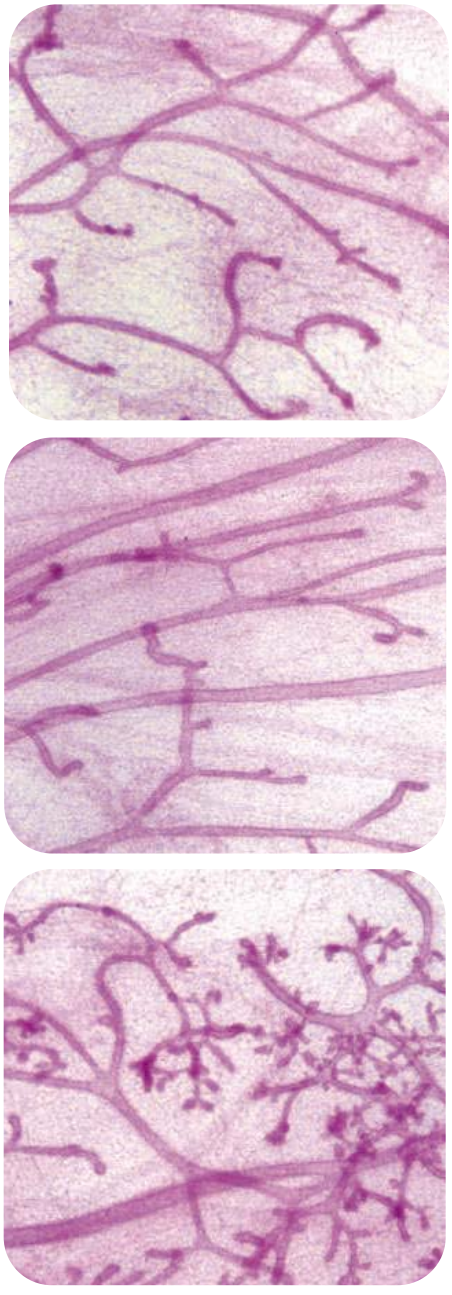

Releasing the brakes. The ducts from mouse mammary tissue in which both the *p53* and *BRCA1* genes have been inactivated (*bottom*) show increased growth and branching compared to ducts from either normal mice (*top*) or animals in which only *p53* is inactive (*middle*).

CREDIT: A. J. POOLE *ET AL./ SCIENCE*

Lee and her colleagues then took a closer look at the epithelial cells that give rise to breast cancer. "A lot more cells" from the double-mutant mice had progesterone receptors, she says, than did cells from normal animals or from animals in which only the *p53* gene had been knocked out.

Further work on cultured mouse and human cells revealed that the progesterone receptor is broken down less readily when BRCA1 activity is missing. As a result, "the [hormone's] signal goes on much longer," Lee says. The excessive cell growth this produces provides extra chances for cancer-promoting DNA mutations to occur, especially because *BRCA1* loss also handicaps the cell's DNA repair machinery. The participation of the progesterone receptor in *BRCA1*-mediated breast cancer could help explain why tumors occur specifically in the breast and ovaries even though the gene is mutated in cells throughout the body. Those other cells don't carry progesterone receptors.

Lee points out that mifepristone itself may not be suitable for long-term use in cancer prevention because it acts on steroid receptors besides the one for progesterone. It might therefore cause unacceptable side effects such as immune suppression. Other more specific progesterone blockers are under development, Lee notes.

There is uncertainty about how accurately the new mouse model reflects human breast cancer. Lee cites findings by Jeff Boyd's team at Memorial Sloan-Kettering Cancer Center in New York City that tissue adjacent to human breast tumors with *BRCA1* mutations shows elevated progesterone expression compared to tissue from normal breast. However, Christine Clarke and her colleagues at the University of Sydney at Westmead Millennium Institute in Westmead, Australia, actually saw a decrease in progesterone receptors in tissue removed by mastectomy from *BRCA1* carriers.

The two situations aren't quite comparable. "The status of tissue around tumors is different from that of tissue taken from normal breast," Clarke says. But that issue, and likely many others, needs to be resolved before cancer prevention trials of progesterone inhibitors can begin.

–JEAN MARX

MOLECULAR BIOLOGY

Three Methods Add Up to One New Way to Genetically Engineer Fruit Flies

When Koen Venken began a Ph.D. project on fruit fly genetics at Baylor College of Medicine in Houston, Texas, 4 years ago, he quickly became frustrated by limitations of the standard techniques for genetically engineering the insects. So he turned his attention to developing a novel procedure. The result, described in a paper published online by *Science* this week (www.sciencemag.org/cgi/content/abstract/1134426), appears to be a powerful new way of making transgenic flies, one that will likely make it easier to study fruit fly genes that were previously too large to work with and to compare the behavior of similar genes belonging to different fly species.

BAC-ed up. A new method allows researchers to insert lots of DNA into fruit flies.

CREDIT: GETTY IMAGES

The work eases two roadblocks that have long troubled the fly community: inserting genes longer than about 20,000 DNA bases—which make up more than 5% of the insect's genes—and controlling where in the genome those genes land, which impacts how they get expressed. "The real advantage here is that it's a way of putting in really big bits of DNA" into the fly, says Michael Ashburner, a fly geneticist at the University of Cambridge, United Kingdom.

Traditionally, geneticists create transgenic flies with help from a piece of fly DNA called the P element. Roughly 2 decades ago Gerald Rubin, now director of the Howard Hughes Medical Institute's (HHMI's) Janelia Farm in Loudoun County, Virginia, and his colleagues spliced a stretch of DNA into a portion of a P element and found that the new DNA was easily incorporated into the fly's genome. The P element, however, can't integrate long stretches of DNA like the ones Venken wanted to work with when he joined the Baylor lab of geneticist and HHMI investigator Hugo Bellen.

So Venken took components of the P element, including ones that allow it to integrate DNA into the fly genome, and added them to loops of bacterial DNA called plasmids. These bacterial artificial chromosomes (BACs) can more stably retain larger amounts of foreign DNA than a P element alone. To add into those BACs the DNA he wanted to insert into the flies, Venken next turned to a technique called recombineering, which was developed about 8 years ago. Recombineering involves allowing a BAC to recombine with an intended transgene within bacteria, isolating that BAC, and then using other bacteria to make multiple copies of it.

Finally, Venken used a third existing technique to control where in the fly genome the BAC-ferried gene would land. When he injected the BACs into fruit fly embryos, Venken also injected messenger RNA that encodes an enyzme made by a bacterial virus called a phage. This enzyme normally inserts a phage's DNA into specific sites on a bacterial genome, but in these circumstances, it integrates the BAC-carried gene at similar DNA sequences engineered into the fly genome.

Using this combination of methods, Venken, Bellen, and their colleagues have inserted DNA stretches as long as 133,000 bases into the fly genome. "It's now not clear what the upper limit is," says Daniel Barbash, a geneticist at Cornell University. Bellen's lab is now assembling a library of fly DNA in the novel BACs for interested researchers.

The new approach "is a significant technical advance," says Rubin. It "allows us to do certain things we couldn't do before," such as study the effects of whole gene complexes, like the homeotic genes that affect early development. And several scientists note that this blended approach might work to genetically modify other organisms. "The potential to export this system to … other animals is quite high," says Barbash.

–JENNIFER COUZIN

EPA, Berkeley Think Small

The U.S. Environmental Protection Agency (EPA) has decided to regulate silver ions, the bacteria-killing nanoparticles used in products as diverse as shoe liners and food storage containers. The agency will require Samsung, which sells an ion-emitting device in a washing machine, to spell out possible environmental impacts under rules that apply to pesticides, even though the agency does not yet know whether the device involves nanomaterials. "The fact that EPA seems to be addressing this is a good thing," says physicist Andrew Maynard of the Woodrow Wilson International Center for Scholars in Washington, D.C. The upcoming federal notice could clarify whether the decision heralds broader federal limits on nanotechnology.

Meanwhile, scientists in Berkeley, California, say their work will not be affected by a proposed city rule, the first of its kind in the United States, that would require the registration of nanoparticles. The council is expected to discuss the measure next week.

–ELI KINTISCH

South Korean Flu Mystery

An outbreak of the H5N1 strain of bird flu in South Korea may reignite debate over how the disease is spread. Researchers had long argued about whether the H5N1 strain, which has killed 258 humans since it started sweeping through Asia in 2003, is spread by wild birds or the movement of infected poultry and contaminated crates and vehicles.

Last week, the South Korean government confirmed H5N1 as the culprit behind the deaths of 6000 chickens on a farm in Iksan, south of Seoul, the first known H5N1 outbreak in Korea since 2003. The route of infection in that incident has never been proven, although South Korea's Ministry of Agriculture & Forestry has since warned on its Web site about the potential for H5N1 transmission from migratory birds to domestic chickens to people.

Casting the blame on migratory fowl "could lead to the vilification of wild birds" and attempts to slaughter them or disturb their habitat, warns ornithologist Nial Moores of Birds Korea, a conservation group. "The real danger comes from poultry infecting wild birds and not the other way around," Moores says. He's particularly worried about major wintering grounds at the mouth of the Geum River, 5 kilometers from Iksan, currently home to the world's largest concentration of Baikal teal. "If avian influenza gets transmitted into this flock, it could be devastating," Moores says.

–DENNIS NORMILE

- Refrigerated versions also available

- Fixed-angle rotor F-35-6-30

- Fixed-angle rotor FA-45-30-11

- Swing bucket rotor for vessels and plates

Choose up to 11 different rotors

One size spins all!

Our 5804/5810 Series benchtop Centrifuges satisfy your application needs by offering remarkable throughput, high capacity and flexibility for a wide range of sample containers.

Your 3-in-1 Centrifuges. Versatile, high speed micro-centrifuges; large-capacity tube and 16-place capacity microplate centrifuges; all in one space-saving unit.

Eppendorf 5804/5810 Series benchtop Centrifuges

- Model 5804
- Refrigerated Model 5804 R
- Model 5810
- Refrigerated Model 5810 R

For more information visit **www.eppendorf.com**

eppendorf

In touch with life

Your local distributor: www.eppendorf.com/worldwide · Application Support: +49 180-3 66 67 89
Eppendorf AG · Germany · +49 40 538 01-0 • Eppendorf North America, Inc. 800-645-3050

DRUG RESEARCH

WHO Panel Weighs Radical Ideas

Lifesaving antiretroviral drugs have been available for a decade in wealthy countries, yet millions of HIV-infected people south of the equator still can't get them. The medicine cupboard is equally bare for people afflicted by tropical illnesses such as visceral leishmaniasis, sleeping sickness, and Chagas disease, for which there are no truly good therapies. Western medical science has not done well by the world's poor, and some critics blame this on its reverence for intellectual property (IP). Is it time to overhaul the IP protection system? A new working group hosted by the World Health Organization (WHO) will consider that question in a series of meetings beginning next week in Geneva, Switzerland.

Critics of the current IP protection system hope that WHO's Intergovernmental Working Group (IGWG) on Public Health, Innovation and Intellectual Property will reform—or even hack down—the still-expanding worldwide patent system. They say it puts lifesaving new drugs beyond the reach of poor patients and hampers development of new medicines for tropical diseases. But others, including the pharmaceutical industry, argue that the IP protection system isn't the real problem and that the talks in Geneva risk distracting people from practical solutions. The IGWG—whose members will include representatives of governments as well as nongovernmental organizations—appears "motivated by anticapitalism rather than logical thinking about how to get drugs to patients," says Trevor Jones, a former director of research and development at the Wellcome Foundation.

Patents are designed to spur the invention of new products. But they also allow companies to charge high prices, putting people without purchasing power at a disadvantage. Many critics say it is not enough to help the poor get access to drugs; the system's incentives must be changed. To produce new drugs for neglected diseases, they say, the world needs a new R&D system that rewards not market sales but the potential to save lives and improve health.

One such framework, which the IGWG may consider, is a hotly debated proposal for an international treaty to open up drug discovery, championed since 2002 by James Love, director of the Consumer Project on Technology in Washington, D.C. Under Love's "R&D Treaty," countries would agree to spend a minimum percentage of gross domestic product on medical research, including a portion for neglected diseases. In addition, the treaty would promote open access to research findings and possibly add R&D incentives. For instance, governments could award big monetary prizes for those who invent important new medicines. Manufacturers would then be free to produce and market them cheaply.

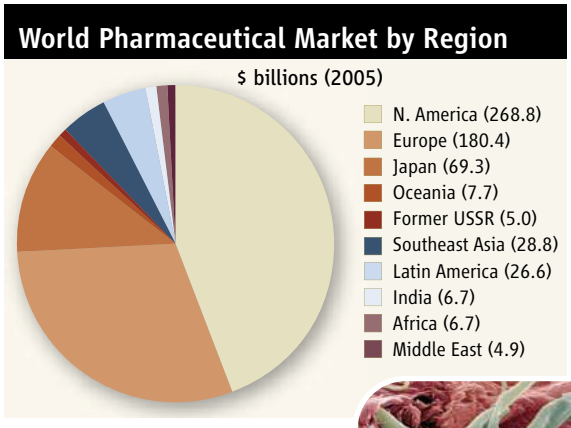

SOURCE: CIPIH; IMS HEALTH; PHOTO: GETTY IMAGES

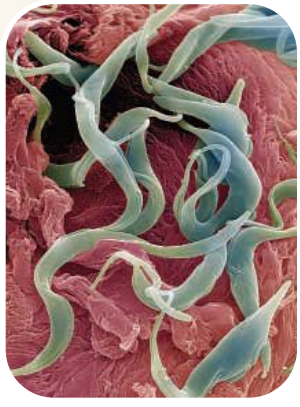

No profit? A minuscule pharmaceutical market in developing countries limits R&D on drugs against trypanosomes, which cause African sleeping sickness and Chagas disease.

The treaty, recommended in a letter to the World Health Assembly by 162 scientists, health experts, and others last year, "is widely seen as the end of the pharmaceutical industry as we know it," says Anne-Laure Ropars, a researcher at the George Institute for International Health in London.

No wonder the industry is vehemently opposed. The treaty would create an "extremely complicated international bureaucracy," says Eric Noehrenberg of the International Federation of Pharmaceutical Manufacturers and Associations in Geneva, adding that the award system would never work. Instead, Noehrenberg offers a different idea: The world should create markets where they currently don't exist. For instance, companies could be enticed with research grants from a "Global Tropical Disease Fund" or the promise of guaranteed sales should they develop an effective new drug.

The industry also contributes through a model called the public-private partnership (PPP). Over the past 10 years, more than two dozen PPPs have sprung up to tackle diseases of the poor. Enlisting industry, academia, governments, and foundations, these partnerships, such as the TB Alliance and the Medicines for Malaria Venture (MMV), have produced many new candidate drugs (*Science*, 13 January, p. 167). And the IP protection regime has not been an obstacle, says MMV president Chris Hentschel: "If people spent less time thinking about IP and more about other things, we would make more progress."

But others point out that health PPPs have a narrow base: 60% of their funding comes from a single source, the Bill and Melinda Gates Foundation; governments contribute very little. Moreover, industry tends to help PPPs that work on diseases that affect both the poor and people from rich countries, such as malaria and TB, says Els Torreele, project manager at the Drugs for Neglected Diseases Initiative. Given the scope of the problem, something more radical is needed, she says.

Whether the IGWG can deliver a solution remains to be seen. The group's predecessor at WHO, the Commission on Public Health, Innovation, and Intellectual Property Rights, issued a raft of recommendations in April—such as increasing contributions to PPPs and building clinical trial capacity—but could not agree on some key patent issues. Some predict that when the IGWG issues its final report to the World Health Assembly in May 2008, it may propose ways to implement the less controversial parts from the April review rather than a radical reform.

But Love thinks the world may be ready for a change. He notes that, although the U.S. government has generally aligned itself with the pharmaceutical industry, it strongly supported increased access to HIV drugs in Africa. It also unexpectedly voted for the resolution introduced by Kenya and Brazil that called the IGWG into existence. (The drug companies and the European Commission opposed the plan.) Love is hoping for another surprise.

–MARTIN ENSERINK

Many U.S. educators think that a streamlined science curriculum with fewer topics per grade is a necessary first step toward boosting student achievement

Doing More With Less

WHAT DO SCHOOLCHILDREN NEED TO know to be scientifically literate? Scientists and educators keep coming up with new answers to that deceptively simple question. As states gear up for two nationwide assessments of student achievement in science, many educators think that the time is ripe to take another hard look at what children should be taught. But others worry that reviving debate on that contentious topic may divert attention and resources from the bigger challenge of actually improving student performance in science.

Everybody agrees that current practices aren't good enough. "It is the height of national folly to think that America can maintain any competitive edge in science the way we are now teaching and testing it," asserts Michael Casserly, executive director of the Council of the Great City Schools in Washington, D.C., after urban schools last month reported low performance in science. There's also consensus that the curriculum is a big part of the problem. A September report by a panel of experts assembled by the National Academies' National Research Council (NRC) deplores curricula that "contain too many disconnected topics that are given equal priority, with too little attention to how … [knowledge] is enhanced from grade to grade." The result, says the panel in *Taking Science to School* (nap.edu), is that students receive a "fragile foundation" in science. That fragile foundation is exposed in both national assessments of what students know and in international comparisons with their peers.

Those poor performances are fueling a campaign by the National Science Teachers Association (NSTA) to develop a national consensus around what NSTA Executive Director Gerald Wheeler calls "science anchors": a small number of concepts that educators agree are essential for students to understand at any particular grade level. "There are way too many things in the standards," Wheeler says, "and too much divergence in what's being taught across the country." He sees the anchors as a de facto core curriculum drawn from topics that most schools are already teaching, "like Newton's law of gravity, or evolution and natural selection."

Wheeler hopes to influence two testing regimens that dominate U.S. elementary and secondary school education. The first, the 2001 federal No Child Left Behind Act (NCLB), requires states to test students in grades 3 through 8 each year in reading and mathematics. Its importance derives from the sanctions facing schools whose students do not make sufficient progress each year. Next year, science will be added to that lineup, although the law doesn't hold schools accountable for student achievement in that subject. The second is the National Assessment of Educational Progress (NAEP), a nonbinding, quadrennial federal assessment of student achievement in grades 4, 8, and 12 across several subjects. Although called the nation's report card, its results are not broken out by schools and districts, and there are no penalties for poor performance.

One big sticking point is that, thanks to the country's 200-year history of local control over education, there isn't a national curriculum. Casserly and many educators would like to see voluntary national standards that would reduce variations among the 50 states and 15,000 local school districts. Two Senate bills introduced earlier this year would move the country in that direction by asking expert panels to identify common ground among state curricula and standards. One bill (S. 3790), from Senator Hillary Clinton (D–NY), would even develop a model math and science curriculum and sample assessment questions. The other (S. 2357), by Senator Edward "Ted" Kennedy (D–MA), would help states align their curricula and standards to national benchmarks. Neither bill attracted much attention this year, but that's likely to change next year, when Kennedy takes over as chair of the Senate panel with jurisdiction over federal education efforts.

CREDIT: AAAS PROJECT 2061

Clear on the concept. AAAS's Ted Willard leads a teachers' workshop on using the *Atlas of Science Literacy*.

Do it again

Standards-based instruction is not a new idea. And this is not the first time the concept is being invoked to help raise student achievement in science. In the early 1990s, scientists and educators rallied around the idea of describing the important concepts in biology, chemistry, physics, and the earth sciences that all U.S. elementary and secondary school students need to master, as well as the nature of scientific thought. The movement crested with the appearance of two acclaimed documents: the 1993 *Science Benchmarks for All Americans* from AAAS (which publishes *Science*), and the National Academies' 1996 *National Science Education Standards*. Educators hoped the standards would ensure not only that teachers covered the most important topics but also that there would be a seamless transition from one grade to the next—and, in a highly mobile society, that children wouldn't be shortchanged if they moved from one district to another.

So far, so good. "Before the standards, teachers pretty much taught whatever they wanted to," says Megan Lewis, who teaches physical sciences, chemistry, and physics to high school students in the rural Glen Lake, Michigan, school district. But because many officials see standards as a threat to local control over education, they are no more than voluntary yardsticks that states are free to adopt, modify, or ignore. Over the past decade, state and local education authorities have used those documents as a starting point for compiling their own standards. Unfortunately, the results have been less than ideal.

Take Lewis's home state. Michigan was one of the pioneers in the standards movement, adopting science guidelines in 1991. In 2000, the document was revamped and renamed the Michigan Curriculum Framework. Since then, it's undergone another metamorphosis, emerging this summer as the Michigan Merit Curriculum. The current version, which describes what students should know at each grade level, is linked to tougher statewide graduation requirements that, for the first time, mandate 3 years of high school science.

Lewis is very supportive of the state's attempt to upgrade science instruction. But she wonders why her state has just adopted its third set of science standards since she began teaching 14 years ago. "Why are we doing this again?" she asks. "Science is science."

Hydra-headed science

If only it were that simple. For one thing, most experts agree that the nationwide standards that came out in the 1990s weren't really a bare-bones version of what students needed to master. "We pared down by 40% the amount of material that was being taught, we estimated," says George "Pinkie" Nelson, former director of AAAS's Project 2061, which developed *Benchmarks* and another AAAS product, called the *Atlas of Science Literacy*, that presents the concepts in *Benchmarks* as a cluster of interlocking maps to help teachers prepare lessons on any particular topic. "But there was still way too much material." Sally Goetz Shuler, executive director of the National Science Resources Center, a joint effort of the National Academies and the Smithsonian Institution in Washington, D.C., calls them "a good first effort. … They were a lot better than the mile-wide, inch-deep" curriculum most states were offering at the time. "But they were still way too complicated," she adds, "especially beyond the fifth grade."

One problem in developing science standards is the multiple fields that must be included. "Remember, it's the sciences, not science," says Janice Earle, a senior program director for elementary and secondary education at the National Science Foundation (NSF), which funded the recent NRC report and supported the creation of both 1990s standards documents. One consequence is what Shuler calls "the science wars," in which experts lobby to make sure their specialty is adequately represented in any standards document.

That effect is magnified as each state (Iowa is the lone exception) develops its own standards, says Nelson, who runs a science, math, and technology education program at Western Washington University in Bellingham. "It's easier to put things in than to take them out," he notes. Expanding the standards, in turn, has led to ever-larger textbooks, as publishers scramble to make sure their materials cover all the topics state and local school districts had crammed into their standards.

But despite their heft, those textbooks often fail to capture the idea that science is, in the words of the recent NRC report, "not only a body of knowledge, but also a way of knowing" about the world. That approach includes formulating and testing hypotheses, adjusting one's understanding to fit the data, and then blending that new information with what the student already knows to come up with a better understanding of any particular phenomenon. It's a process that doesn't fit neatly into a lecture, or even an experiment, the report points out. And it's something that few students have a chance to experience at any level.

"My students have a hard time figuring out how things really work," says Thomas Lord, a plant biologist and science educator at Indiana University of Pennsylvania in Indiana, Pennsylvania. "When I teach the water cycle, for example, I ask them about the role that plants play in the process. Not one kid mentions photosynthesis. And these are science majors." Lord worries that any standards, especially something concise such as science anchors, could simplify the curriculum to the point of squeezing out the real science students need to learn.

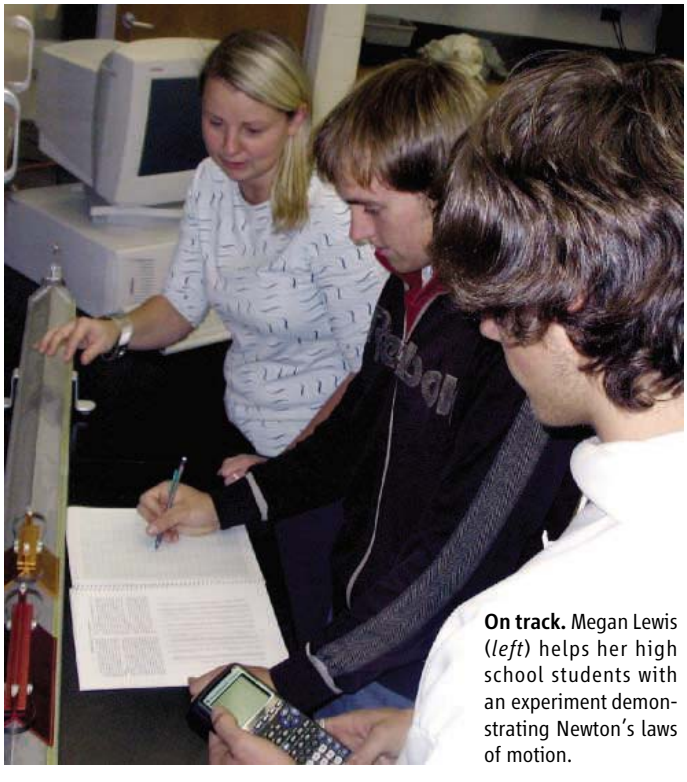

On track. Megan Lewis (*left*) helps her high school students with an experiment demonstrating Newton's laws of motion.

CREDIT: PROVIDED BY MEGAN LEWIS

From zero to 10

To be sure, the standards are just one element in reforming science education, an effort that includes improved teacher training and professional development and stronger ties between

school districts and university science faculty. "Gerry's idea of putting together some big ideas is an important one," says Nelson. "And new standards are fine. But I think that it's zero on a 10-point scale of improving U.S. science education."

Wheeler agrees that science anchors won't suddenly make students smarter or give teachers a better understanding of fundamental scientific concepts that they never learned adequately before entering the classroom. But he thinks that the anchors might be attractive to states preparing for two upcoming major assessments. "It's a way of identifying the low-hanging fruit. It's a marketing technique," he admits. "Once people buy into the concept, then maybe we can get them to develop better assessment items, and professional development, around them. If that happens, then I think we will be moving in the right direction."

The science component of NCLB begins in 2007–'08, for students in one grade at each of three levels: elementary, middle, and high school. But the results won't be counted as part of the law's requirement that students show adequate yearly progress (AYP). "Not being part of AYP means that science may remain on the back burner," Wheeler fears. A more promising target may be NAEP, which will be given next in 2009. Earlier this year, an expert panel (Wheeler chaired its steering committee) sketched out a new "framework" of what the test should cover, as well as new ways to measure that knowledge.

The draft NAEP framework (nagb.org) drew explicitly from the two 1990s documents, says Senta Raizen of the National Center for Improving Science Education run by WestEd, a California-based nonprofit with a contract from NAEP's oversight body to revise the assessment. "Our hypothesis was, if it's in both documents that it's in," says Raizen, who co-chaired the project's planning committee. "If only one, then we'll think about it. So there's nothing fundamentally new about the content." Raizen emphasizes that NAEP isn't trying to tell states what to teach—"we don't have a national curriculum in this country"—and that NAEP provides only "a snapshot" of what students have learned. But she agrees that it can "serve as a model" for the upcoming NCLB assessments that states must devise.

Anchors aweigh. NSTA's Gerry Wheeler (*center*) talks with Wendy Benz (*left*) and Chad Sechrist at a regional teachers' conference in Baltimore, Maryland.

A matter of time

NSF's Earle thinks there are valid reasons to be optimistic about the latest efforts to clarify what students need to know in science. "I'm sensing that maybe it is time to think about taking the next step," Earle opines. "The standards have been out there for a decade or so, and it takes people a while to digest them." But don't expect anything to happen quickly, she counsels: "U.S. education is not efficient, by definition. We have a very decentralized system."

Michigan's Lewis doesn't have the luxury of time. As a classroom teacher, she's responsible for making sure her students understand the subject matter and can pass the high-stakes tests. As a result, she suggests, only partly in jest, that some of the money being used to rework science standards might be better spent on her students. "With $10,000, I could buy enough [PASCO] probes for every kid in my class," she says, referring to equipment that allows experimental data on temperature, acceleration, and other features of the physical world to be collected and analyzed.

Wheeler agrees that the interaction of student and teacher is paramount to improving how schoolchildren learn science. "A clear set of standards aligned to the state assessment is a key first step," he reiterates. "But unfortunately, we have to take about four first steps," he adds, ticking off the need for better materials, improved professional development, and higher teacher retention rates. "Otherwise, there's going to be a lot of finger-pointing at the fourth grade teacher whose students didn't do well enough on the science assessment. And that doesn't help anybody."

–JEFFREY MERVIS

ASTROPHYSICS

Burst-Hunter's Rich Data Harvest Yields a Cosmic Enigma

The 2-year-old Swift gamma ray satellite has delighted astrophysicists with its versatility—and surprised them with observations that don't fit the models

SAN FRANCISCO, CALIFORNIA—In the quest for the secrets of cosmic explosions known as gamma ray bursts (GRBs), no satellite has been more successful than Swift.

Launched 2 years ago in November, Swift has outperformed expectations, providing NASA with a steady stream of news to report. Swift not only has been recording its predicted budget of bursts (about 100 a year) but also has gathered abundant data on other astrophysical phenomena, from nearby black holes in active galaxies to the most energetic magnetic flare ever detected on a star. "Swift has been a scientific bonanza," says high-energy astrophysicist Ilana Harrus of NASA's Goddard Space Flight Center in Greenbelt, Maryland. "It's the satellite that keeps on giving."

Now, Swift has given astrophysicists a major surprise. Its observation of a GRB earlier this year has challenged the standard classification system for such bursts.

GRBs are intense pulses of extremely high-frequency radiation emanating from distant space. Such bursts were first detected almost 4 decades ago by satellites designed to seek signs of nuclear weapons tests. When gamma radiation arrived from space instead of the ground, baffled astrophysicists groped for explanations. Among the more speculative suggestions was that the bursts signaled the demise of faraway civilizations that had annihilated themselves in nuclear wars.

In the 1990s, however, observations from the orbiting Compton Gamma Ray Observatory provided enough information to pin down

CREDIT: NSTA

key details, eventually establishing that some bursts were associated with supernova explosions. Others seemed to result from cosmic collisions, perhaps between neutron stars, the small, dense spheres left behind by supernovae.

Bursts believed to be associated with neutron stars were typically short—lasting less than 2 seconds. "Long" bursts lasted from seconds to minutes and were generally "softer"—meaning lower in energy—than the short, "hard" higher-energy bursts. Long bursts have been clearly linked to supernovae, but the short bursts' link to neutron stars is more speculative. "Short bursts lack a smoking gun," says Joshua Bloom, a GRB investigator at the University of California, Berkeley.

In June, Swift further blurred the line between short and long by finding a long, soft burst with no apparent connection to a supernova, several astrophysicists reported at a recent meeting here.* That new burst and other Swift observations challenge the standard two-category scheme and raise questions about the nature of GRB progenitors.

"I see a growing crisis of classification," said Bloom. "We don't just have long bursts and short bursts anymore that map directly to these progenitors. We actually have counterexamples in both cases that are really throwing a monkey [wrench] in the works."

The prime culprit behind the category crisis is a burst recorded on 14 June that lasted 103 seconds, far into the range generally regarded as long. Observers eagerly awaited the appearance of stellar brightening signaling the supernova explosion responsible for the burst. But the supernova never showed.

Further observations suggested that the 14 June event was not a typical long burst in other ways. The initial pulse was high in energy but was then followed by a softer afterglow.

"That was kind of reminiscent of other short bursts we've seen," Swift principal investigator Neil Gehrels of NASA Goddard said at the astrophysics meeting, suggesting that it belonged in the "short" category. "Short isn't the right word," Gehrels said, but in many respects "it appears to group with the short bursts, and that could explain the lack of a supernova."

In a paper posted online, Gehrels and collaborators argue that the 14 June burst requires a new categorization system. "This combination of a long-duration event without an accompanying supernova … opens the door on a new gamma ray burst classification scheme that straddles both long and short bursts," the Swift scientists wrote.

In another online paper, Johan Fynbo of the Niels Bohr Institute in Copenhagen, Denmark, and an international team of collaborators including Berkeley's Bloom suggest that the 14 June burst implies a new type of explosive star death, producing a GRB but no supernova. If so, the burst represents the first of a whole new category of GRBs. Gehrels's and Fynbo's papers have both been accepted for publication in *Nature*.

Other astrophysicists, however, say it's too soon to junk the two-category system or invent new stellar death processes. "These guys are going off and making claims that you have a whole new class of [GRB] population never before seen," says Bradley Schaefer of Louisiana State University (LSU), Baton Rouge. For such an extraordinary claim, he says, "you ought to have at least good evidence."

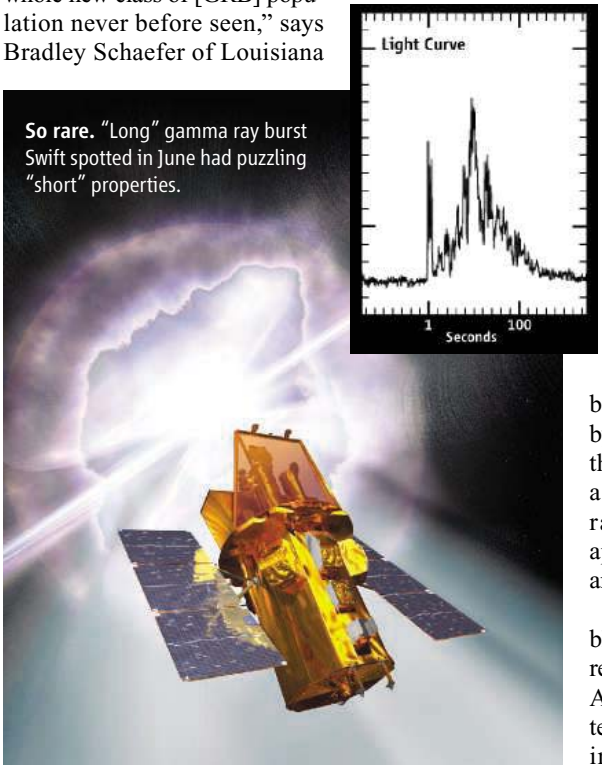

So rare. "Long" gamma ray burst Swift spotted in June had puzzling "short" properties.

In fact, Schaefer says, the mystery of the missing supernova could have a simple solution: The burst may have occurred far enough away to make the stellar explosion too dim to notice. Lack of a supernova seems mysterious only because the burst was estimated to be at a redshift of 0.125, relatively nearby in cosmic terms. But in a paper posted on the online astrophysics preprint archive (astro-ph/0608441), Schaefer and LSU collaborator Limin Xiao point out that that distance estimate is based solely on the measured redshift of the nearest galaxy along the line of sight to the burst. Perhaps that galaxy was not actually the burst's host and the burst was much farther away, too far for the supernova associated with it to be visible.

Data from Swift and other instruments can be used to estimate the intrinsic brightness of the burst, Schaefer and Xiao point out. Comparing the intrinsic brightness with the observed brightness gives a good measure of distance. Various indicators all suggest a high brightness for the burst, leading Schaefer and Xiao to assign it a redshift of about 2, far enough away to explain the lack of a supernova sighting. They calculate the odds of such a lineup of a galaxy with a more distant burst to be 1 in 125; because Swift has recorded more than 190 bursts, finding one such alignment is not surprising. "It's fully consistent with chance coincidence," Schaefer says.

A similar conclusion appeared in a paper published 10 November in *Astrophysical Journal Letters*. B. E. Cobb and colleagues at Yale University determined the likelihood of lineup coincidence to be from about 1 in 50 to 1 in 200. Consequently, from one to four such coincidences would be expected in the bursts observed by Swift so far. "The conclusion that [the 14 June burst] requires a 'new paradigm' for gamma ray burst formation should be approached with caution," Cobb and colleagues wrote.

Actually, a second such possible coincidence had already been recorded before the 14 June event. A burst detected in May also was technically "long"—at 4 seconds in duration—with no sign of a supernova. But that event was fainter and poorly observed, Schaefer and Xiao noted, and the burst might also have originated far behind the presumed host galaxy.

In any case, Swift's findings have surely complicated the older views of GRBs, providing much precise data that astrophysicists will have to digest to get a clearer understanding of the sources and properties of those cosmic flashes.

"Our real goal here is to attempt to uncover the progenitors of gamma ray bursts, whether they be long-duration gamma ray bursts or short-duration gamma ray bursts," says Bloom. "We're trying to understand the diversity of the phenomenon. And because of Swift and other satellites, we're now in the position to really ask these questions in detail."

–TOM SIEGFRIED

Tom Siegfried is a writer in Los Angeles, California.

* High Energy Astrophysics Division of the American Astronomical Society, 4–7 October.

CREDITS: SPECTRUM ASTRO; (INSET) ADAPTED FROM SWIFT/SONOMA

South Africa Bolsters HIV/AIDS Plan, but Obstacles Remain

Ridicule at the Toronto AIDS Conference spurred South Africa's Cabinet to order a new plan to battle the epidemic

PRETORIA AND SOWETO, SOUTH AFRICA—When small baskets of garlic, lemons, and beets highlighted the South African exhibit at the XVI International AIDS Conference in Toronto last summer, many delegates were outraged. They viewed the display—intended to show the importance of nutrition in bolstering immune systems—as trivializing the response to the epidemic that now infects 5.5 million South Africans and kills an estimated 800 of them a day. As the meeting ended, Stephen Lewis, the United Nations special envoy for HIV/AIDS in Africa, lashed out at aspects of South Africa's AIDS policies as "wrong, immoral, [and] indefensible."

The ridicule in Toronto was followed by a sharply critical letter to President Thabo Mbeki from 82 prominent international scientists, including Nobelist David Baltimore, virologist Robert Gallo, and 11 South African researchers. Arguing that garlic and lemons "are not alternatives to effective medications," the researchers warned that "many people are … dying unnecessarily" in South Africa because they do not have access to antiretroviral (ARV) drugs to slow the progression of the disease. Although the country has the world's largest ARV program, it now reaches only about a quarter of the South Africans who are estimated to need the drugs.

Under fire. South Africa's embattled health minister, Manto Tshabalala-Msimang, has been the target of protesters who called for her dismissal.

Reflecting the outcry, some of South Africa's leading newspapers called in September for the resignation of the garlic-promoting health minister, Manto Tshabalala-Msimang. At about the same time, South Africa's ruling Cabinet, unhappy to again be the focus of international scientific scorn, decided to revive the near-moribund South African National AIDS Council. It named Deputy President Phumzile Mlambo-Ngcuka—rather than the controversial health minister—as the nation's point person for developing a more effective HIV/AIDS strategic plan for the next 5 years.

The deputy president planned to outline the framework of that new plan on 1 December, World AIDS Day. A draft of the wide-ranging plan, obtained by *Science*, features commitments to bolster prevention programs to sharply reduce the number of people being infected with HIV; better coordinate the government's often-fragmented response to the epidemic; support AIDS vaccine and antimicrobial research; and significantly expand ARV treatment—although the exact ARV target numbers were still being developed.

Many South African scientists, clinicians, and activists welcomed the long-overdue initiative to revamp HIV/AIDS programs. "For years, we had been confronted with obfuscation and confusion and a lack of leadership on HIV/AIDS," says Francois Venter, who heads the Southern African HIV Clinicians Society. But he and others cautioned that the devil is in the details, some of which were not available as *Science* went to press. And no one was expecting that the announcement of a new action plan would end the debate on South Africa's HIV/AIDS policies.

The need for more effective government programs is clear. Although a draft of the plan cited evidence that "HIV incidence has started to decrease," a November report by the Joint United Nations Programme on HIV/AIDS and the World Health Organization says that HIV prevalence—at nearly 19% of South Africa's adult population in 2005—"has not yet reached a plateau." The nation's 5.5 million infected people include a quarter of a million children under age 15, the report said. It also warned of "a continuing, rising trend in HIV infection levels" among pregnant women using prenatal clinics.

A history of controversy

International dissatisfaction with the country's HIV/AIDS policy is rooted in a series of government controversies and miscues over the past decade. In 1997, an attempt to fast-track clinical trials of a drug called Virodene ended in disgrace when a review panel found that the substance was toxic and had been prematurely tested on humans. Three years later, in early 2000, Mbeki sent a letter to the White House and to the U.N. Secretary-General suggesting that factors other than HIV could cause AIDS and asserting that it would be a "criminal betrayal" to "mimic foreign approaches to treating HIV/AIDS."

Later that year, delegates to the International AIDS Conference in Durban were stunned that Mbeki and his health minister continued to question the connection between HIV and AIDS and failed to support ARV therapy. "The government took a strange position opposed by well-established science," recalls the chair of the Durban meeting, pediatric AIDS researcher Hoosen Coovadia of the University of KwaZulu-Natal.

Meanwhile, as the epidemic worsened, the government came under increasing pressure to take decisive action. In 2002, Mbeki began to distance himself from the denialists and endorsed the concept of making ARVs available to pregnant women and rape survivors. Late in 2003, a panel developed an ARV roll-out plan, which went into effect the following spring and now covers about 214,000 persons. Noting that the South African ARV program reaches more people than that of any other country, Medical Research Council

(MRC) President Anthony MBewu contends that South Africa's recent initiatives on HIV/AIDS treatment and prevention have begun to blunt the epidemic.

Trying to rehabilitate the government's international image on HIV/AIDS policy, Cabinet officials are avoiding any public expression of AIDS denialism. Government spokesperson Themba J. Maseko told *Science* that "the position of the government is based on the understanding that HIV causes AIDS." Even South Africa's most outspoken AIDS activist, Zackie Achmat, credits the ruling African National Congress party with exerting pressure to suppress AIDS denialism within its ranks. Although Mbeki has not made a definitive statement of his own position, Maseko says the president fully supports the Cabinet's recent HIV/AIDS decisions on developing a new action plan.

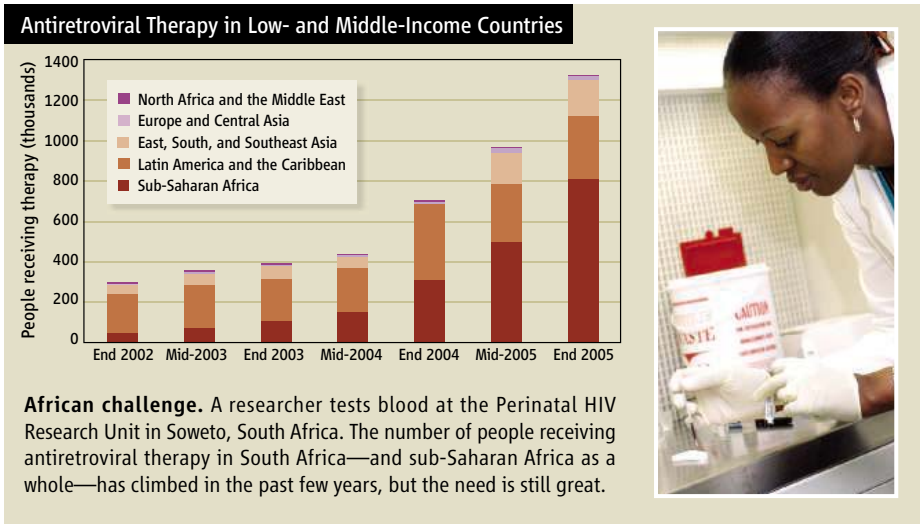

African challenge. A researcher tests blood at the Perinatal HIV Research Unit in Soweto, South Africa. The number of people receiving antiretroviral therapy in South Africa—and sub-Saharan Africa as a whole—has climbed in the past few years, but the need is still great.

A targeted approach

After the Toronto AIDS meeting, with the health minister hospitalized with a respiratory ailment, the Cabinet asked Deputy President Mlambo-Ngcuka to try to mend fences with interest groups and develop a stronger HIV/AIDS plan. Declaring that the nation's AIDS policy debate was at "a critical point," she held meetings this fall with leading clinicians, scientists, and activists to try to resolve "difficulties and misunderstandings" and forge a consensus.

The most difficult single issue in reaching such an agreement has been setting targets for ARV treatments. (The government bears most of the costs of ARV drugs at public clinics, but international organizations and donors pay for ARV costs at many private or religious facilities, and medical insurance covers other individuals.) The government originally planned to announce specific ARV targets on World AIDS Day as part of the new plan. Indeed, one draft listed a goal of tripling the current ARV numbers, to 650,000 adults and 100,000 children, by 2011. But as soon as the plan's early drafts began circulating, AIDS activists and clinician groups began lobbying for much higher numbers, and they persuaded the deputy president to delay announcing specific targets until a compromise could be worked out, probably early next year.

Four influential AIDS groups that sought the delay—the Southern African HIV Clinicians Society, the activist Treatment Action Campaign, the AIDS Law Project, and the University of the Witwatersrand's Reproductive Health and HIV Research Unit—delivered a 28-page critique in November of an early draft of the action plan. That response, obtained by *Science*, argued that the proposed ARV targets "represent approximately 20 percent of those requiring treatment, and should be revised upwards. All epidemiologic data suggests that there are approximately 800,000 people who need ARVs at the moment … and that an additional 500,000 people will require treatment annually going forward."

The critique also argues that the nation's research facilities are "largely uncoordinated when it comes to research on HIV" and recommends that a national health supervisory council find ways to improve coordination.

The draft HIV/AIDS plan did not address the coordination issue, but it confirmed that basic and clinical research into the epidemic were national priorities. Although shy on details, the draft specifically called for boosting research into microbicides and AIDS vaccines, a research strength of the country. MRC President MBewu told *Science* that "HIV/AIDS is the nation's top research priority."

Action plan. Deputy President Phumzile Mlambo-Ngcuka is South Africa's new point person in bolstering the nation's HIV/AIDS action plan.

Uphill battle

Although generally heartened by plans to boost HIV/AIDS prevention and treatment programs, South African scientists and activists caution that obstacles remain. For some, the chief problem is the recuperating health minister, Tshabalala-Msimang, who remains responsible for implementing the new HIV/AIDS plan. In November, she issued a statement lashing out at her critics and reaffirming her commitment to nutrition and traditional medicine in HIV/AIDS treatment.

University of Cape Town economist Nicoli Nattrass, an expert on the impact of the epidemic on South Africa, believes that HIV/AIDS activists "have won an important ideological battle," but—with the health minister still involved in implementation—"the counterinsurgency remains strong."

Clinicians and researchers are eager to see evidence that the government will back up its new HIV/AIDS commitments with more funding and improvements in health facilities. "Setting ambitious targets is good, but you have to have the resources and plans to meet those targets," says researcher Coovadia.

Complicating the challenge, tuberculosis is rife among South Africans infected with HIV, and new drug-resistant strains are threatening to spread rapidly. "We've got two epidemics clashing in a dangerous way. We can't carry on with business as usual," says immunologist Linda-Gail Bekker, co-director of the Desmond Tutu HIV Center in Cape Town.

Clinician Venter agrees that "a lot more needs to be done to get control of this epidemic." Still, he says, "it helps to have support at the top." **–ROBERT KOENIG**

CREDITS (TOP, LEFT TO RIGHT): WHO/UNAIDS (2005); PERINATAL HIV RESEARCH UNIT, SOWETO; (BOTTOM) LERATO MADUNA/REUTERS

Vanishing breed. A young captive saola shortly before its death in Hanoi in 1993.

WILDLIFE CONSERVATION

The Saola's Last Stand

Wildlife experts say the rare Southeast Asian ungulate may soon disappear; a Vietnamese lab is undertaking a controversial attempt to clone it

PU MAT NATURE RESERVE, VIETNAM—Do Tuoc climbs a steep riverbank, entering the realm of the elusive saola. The creature, a cousin of cows, goats, and antelopes, is so rare that even Tuoc, who discovered the species in 1992, has never spied one in the wild. The forest ecologist finds safe footing on the slick slope and grabs a handful of broad, dark-green Araceae leaves. "Saola like to eat these," Tuoc says. "At least, we have seen bite marks."

A decade ago, the saola made headlines as the first large mammal new to science in more than half a century. Recent sleuthing suggests that the exotic ungulate is sliding toward extinction. At most, 250 saola are thought to roam the Annamites (called the Truong Son Mountains in Vietnam) of central Vietnam and Laos.

Now scientists are embarking on a last-ditch effort to save the critically endangered species. Vietnam's National Saola Conservation Action Plan, expected to be approved by the government later this month, prescribes measures, including a hunting ban, that are deemed essential for the saola's survival. Meanwhile, a Vietnamese team is pursuing a conservation option of last resort: an attempt to clone the saola. But somatic cloning is supremely difficult even in the best-studied mammals—and "we know almost nothing about the saola," says zoologist Nguyen Xuan Dang of the Institute of Ecology and Biological Resources in Hanoi.

More is at stake than one obscure relict species. The ecosystem that shelters the saola is home to an array of creatures, including at least two kinds of muntjac deer found nowhere else in the world. Saving this unique menagerie "would be a success story for other countries to follow," says Barney Long, a conservation biologist with the World Wide Fund for Nature (WWF) who is working with local scientists and officials to protect the saola in central Vietnam.

On the track of unknown animals. Ecologist Do Tuoc, Araceae in hand, at the Pu Mat Nature Reserve.

The odds are against Long and company. "Foundations can easily raise funds for primates, tigers, elephants, rhinos," says Dang. "For the saola, we can't even get money to educate the public, to tell people to stop hunting it." As Vietnam's action plan notes starkly, "resources and attention afforded to the saola are currently insufficient to protect it from extinction in the immediate future."

Trophy hunting

Whereas biologists are captivated by the saola's unicornlike mystique, villagers in Truong Huong, on the edge of the Pu Mat Nature Reserve, are blasé about the beast. Few in this ethnic Thai community have seen a saola, and when they do, the outcome for the demure herbivore is almost invariably bad.

In a wooden house built on stilts, Lo Van Tinh, a farmer, sits cross-legged with four generations of family huddled around him and describes how, one day 10 years ago, he was hunting turtles in a mountain river. His dog spotted a saola mother and calf upstream and gave chase. The mother escaped, but her calf was cornered and assumed a defensive posture. Although a saola in captivity betrays no fear of humans, at the sight of a dog it snorts and hunkers head down, brandishing its long, straight horns, says saola expert William Robichaud, a zoologist with the Nakai-Nam Theun National Protected Area in Laos. That renders the saola easy to shoot, and for a juvenile, easy to grab. "I caught it with my hands," says Tinh. The saola did not survive the 2-day hike back to Truong Huong, so Tinh and his family ate it. It was like beef, although not as tasty, he says.

In a home in nearby Truong Chinh village, a pair of saola horns hangs in a place of honor next to a poster of a smiling Vietnamese model. The dark-brown horns, about 40 centimeters in length, are more than twice as long as the head, which has short, coarse, chestnut-brown hair. To local people, the slightly diverging horns resemble the parallel wooden posts that support a spinning wheel (hence the name: *Sao* means "post," and *la* means "spinning wheel"). Streaks of white hair above the eyes look like garish mascara.

It was in a home just like this that Tuoc discovered the saola. In May 1992, he was part of a team dispatched by the Ministry of Forestry, with WWF support, to Vu Quang forest, roughly 100 kilometers southeast of Pu Mat, to survey biodiversity in advance of Vu Quang's designation as a nature reserve.

CREDITS (TOP TO BOTTOM): WWF-CANON/DAVID HULSE; MUTSUMI STONE

Tuoc, schmoozing with the local villagers, wangled an invitation to a young hunter's home, where the team was shown a peculiar skull and horns. "I immediately thought it was a new species of antelope," Tuoc says. But it was puzzling, as antelope prefer dry areas, and much of the Truong Son range is soaked by seasonal monsoons. Excited by the find, he asked local hunters to look for other specimens. Two more pairs of horns soon materialized, convincing the scientists that they had indeed found a new species, which they anointed the "Vu Quang ox."

WWF funded a follow-up survey that November that turned up about two dozen pairs of horns and an intact saola skin. DNA analysis of the mitochondrial cytochrome b gene revealed a new bovid genus, and a paper in *Nature* in 1993 unveiled *Pseudoryx nghetinhensis*. (Subsequent DNA analyses suggest that cattle are its closest cousins.) The animal was confirmed in Laos through villager sightings and trophy horns in 1993. The species name is an amalgamation of the two Vietnamese provinces where specimens were first uncovered. The common name Vu Quang ox soon gave way to saola, a less parochial designation and one with historical roots. The first known written reference to the species is in an early 20th century Lao-French dictionary, which defines saola as an "antelope of the rocks," says Robichaud.

The saola was the first large mammal discovery since the kouprey, a wild ox in Southeast Asia, in 1937. As an encore, Tuoc and colleagues first described the large-antlered (formerly giant) muntjac in 1994 and the diminutive Truong Son muntjac in 1997. (Both were discovered simultaneously in Laos.) With three mammal species under his belt, Tuoc has become a legend in cryptozoology, the study of previously unknown, presumed, or mythical creatures. "I've been very lucky," he says.

Zoological riddle

Ever since the saola's appearance, its biology, like the animal itself, has remained an enigma. In June 1993, Tuoc and colleagues at the Forest Inventory and Planning Institute in Hanoi took custody of two young saola that had been captured in Vu Quang. The animals ate several dozen kinds of plants and put on weight fast, Tuoc says. But after 2 months, they succumbed to infections. In all, 20-odd saola have been captured in Vietnam and Laos. All but two that were released into the wild died quickly in captivity.

The saola's fragility is no big surprise. "Certain animals in captivity, especially ungulates, are highly sensitive to stress," says David Wildt, head of the Center for Species Survival at the Smithsonian's Conservation and Research Center near Front Royal, Virginia. Or the problem could be as simple as an "inappropriate" diet, says Wildt, whose team has pioneered techniques for breeding delicate creatures such as the Elds deer and the black-footed ferret. "A careful examination of why these animals die after capture is really needed," he says.

What little is known about the saola has been gleaned primarily from the short-lived captives. In the mid-1990s, Cheng Syavong, a Lao general, offered a reward for the capture of a saola for his Lak Xao Zoo. In January 1996, Cheng procured an adult female. "I had the good fortune to observe her daily," says Robichaud. The saola, he says, marked territory by flaring open a fleshy flap covering her maxillary glands on either side of the snout and stroking the underside across rocks, depositing a pungent, musky paste. The massive scent glands are thought to be the largest of any living mammal.

"Her most striking and endearing aspect," Robichaud says, "was her utter calmness in the presence of humans." Soon after arriving at Lak Xao, the saola allowed people to stroke her and fed from their hands. "She was tamer and more approachable than any domestic livestock I'd ever been around," he says. But after a mere 18 days in captivity, the saola died suddenly, and no autopsy was performed—although she was found to be bearing a male fetus.

Saola are so rarely seen in the wild that it wasn't until 1998 that one was first caught on film in its habitat, by a camera trap near a mineral-rich spring in Pu Mat. Robichaud and Robert Timmons, an independent conservation biologist in Southeast Asia, have suggested that the survivors are descendents of a Pleistocene bottleneck, when their wet evergreen forests receded during cool, dry ice ages. "The current distribution of saola may reflect where these ice age refugia were," says Robichaud.

Humans now have the saola on the ropes. In 1992, scientists pegged the population at 500 to 1000 in Vietnam, says Long. The estimate in Vietnam's action plan—"probably" fewer than 200—could be a large under- or overestimate, he says. But Long says a decline is evident "from the amount of hunted trophies that we see" and the lack of sightings in areas where the saola once roamed. Saola are also killed in snares set for more lucrative game such as bears, which fetch a high price for their gall bladders. Vietnam's action plan would ban snares in saola territory.

Habitat fragmentation further endangers the species. The action plan notes that the

Museum piece. A saola head in a hunter's home near Pu Mat. Saola sightings in Laos and Vietnam are dwindling.

CREDIT (TOP): MUTSUMI STONE

A click of your mouse delivers over ~~1000~~ 1500 of ours.

Instant access to over 1,500 knockout mouse lines.

Taconic, one of the world's leading breeders of laboratory mice, and Lexicon Genetics, a pioneer in knockout mouse technologies, team up to bring you immediate access to an ever-expanding database of over 1,500 mouse models. Concentrated in the "druggable" gene classes, most knockout models already exist as live mice and can be delivered within weeks. Result? Readily available, immensely valuable research tools that accelerate the drug discovery and development process—and give you a serious competitive advantage.

The search ends here.

Visit our website **http://taconic.lexgen.com** to download the entire portfolio or search for a gene of interest.

Taconic

nearly completed Ho Chi Minh Highway, which will link northern and southern Vietnam, "must be viewed as the single largest threat to the connectivity of Saola populations and their habitat." With support from the World Bank, the Dutch Development Organization, and the U.S. Agency for International Development, WWF is working with Vietnamese authorities to protect forests in two provinces, Thua Thien Hue and Quang Nam, where the largest saola subpopulation, approximately 50 individuals, is found. This "Saola Conservation Landscape" abuts forests in Laos, providing contiguous habitat for some of the few dozen saola thought to live across the border.

As an additional safeguard, Vietnam's national action plan would forbid keeping saola in captivity until 2010, unless one is confiscated from a hunter or liberated from a snare and is too injured to be released into the wild. To Wildt, this is a risky strategy. "I don't go along with the philosophy of leave them only in the wild and hope for the best," he says. He suggests that saola experts convene a workshop that would take a hard look at captive breeding. "It's not like this has never been done before," he says.

A genetic "Hail Mary"

Long and others argue that without a robust effort to shield the saola from hunters and preserve its habitat, the animal is doomed. For all they know, the species may already have passed the point of no return.

That possibility is the main justification for a controversial, high-tech bid to keep the species on life support. On the tree-lined grounds of the Vietnamese Academy of Science and Technology in central Hanoi, a team at the Institute of Biotechnology led by Bui Xuan Nguyen is trying to clone the saola.

Nguyen knows the project is a long shot. But his lab has a chance at succeeding: He and his staff have been collaborating with top reproductive biologists in France, Japan, and elsewhere for 30 years and have racked up achievements in embryo transfer and in vitro fertilization in animals such as cows and rabbits. Nguyen is also credited with having developed a technique for rapidly freezing eggs and sperm that is particularly handy for preserving samples in the field. Building on this work, Nguyen is spearheading an effort to set up a lab network in Southeast Asia next year to "cryobank" frozen germ cells of rare species.

Soon after the cloning of the sheep Dolly in 1997, Nguyen says, he thought the revolutionary technique might be applicable to endangered species conservation. By then, the saola had become an icon in Vietnam. Nguyen struck up a collaboration with Tuoc's forest institute. "When someone finds a saola, the institute calls us and we immediately go take tissue samples," Nguyen says. They have samples from one male and two females, including 30 immature eggs from one of the females that died.

Eleventh-hour heroics? Bui Xuan Nguyen hopes to clone a saola. So far, his team's early saola embryos have failed to develop.

They've held on to most of the eggs in the event that, someday, they might be able to attempt in vitro fertilization. But Nguyen has decided that "we cannot wait for a live female." Working with Patrick Chesné from the lab of Jean-Paul Renard of the National Institute for Agricultural Research in Paris, Nguyen has used nuclear transfer to inject saola DNA into cow, goat, and swamp buffalo eggs. They have obtained early embryos—blastocysts—but these fail to develop. "We don't have any idea how to get past this stage," Nguyen says. A fundamental hurdle is the dearth of knowledge about saola biology. "We have no information on the reproductive cycle, no idea how long pregnancy lasts," he says.

Nguyen and his collaborators have filled in some gaps. For instance, they've established that the saola has 50 chromosomes. (Cows have 60, buffalo 84.) Nguyen now hopes to unravel how saola nuclei are reprogrammed. During reprogramming, an egg turns back the clock on an adult nucleus by removing chemical signatures of development, which returns it to an embryonic state—an essential step in somatic cloning. "We're interested in early molecular events in saola and closely related species," says Renard.

When all the problems of interspecies cloning—such as different chromosome numbers and different mitochondrial DNA—are solved, then "cloning the saola will be possible," predicts Takashi Nagai, a reproductive biologist at the National Institute of Livestock and Grassland Science in Tsukuba, Japan, who is working with Nguyen to conserve the genetic line of Vietnamese miniature pigs. Nguyen says he will persevere: "I'm a patient man."

Some biologists, however, deem the effort hasty—or misguided. "Cloning is a tool for last-ditch heroics," says Wildt. "It's too premature to consider it" for the saola, he says. "I don't see any conservation benefit from cloning the saola," adds Long. "The money … would be much better spent trying to protect the species in the wild." (Nguyen says his funding is "modest.") To Long, the battle must be fought in the Truong Son Mountains. "If we lose the saola," he says, "it will be a symbol of our failure to protect this unique ecosystem."

That could jeopardize unknown species. "In Vietnam, there is still a lot of terrain not yet surveyed," says Dang. Only in 2005, the kha-nyou, a bizarre, smallish rodent, was described from a specimen found in a Lao market; an expedition brought back the first live specimen last May. "There are small and medium-sized animals waiting to be discovered," Dang says.

Optimists about the saola's fate are about as rare as the animal itself—but Tuoc is one of them. Natural enemies like the dhole are becoming scarcer, he says. Provided that snares are removed and vital habitat is preserved, the saola should be able to rebound, Tuoc says. "Maybe I'll never see one in the wild," admits the cryptozoologist extraordinaire. "But I think—no, I hope—it will survive." For the saola, survival will mean vanishing back into the misty sanctuary that hid it so well until humans came along.

–RICHARD STONE

CREDITS (TOP TO BOTTOM): MUTSUMI STONE; BUI XUAN NGUYEN

CellTiter-Glo® – The Perfect Assay.

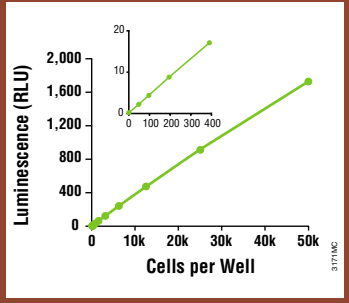

Dynamic range from less than 10 cells to over 10,000 cells.

Measure as few as 10 cells in less than 10 minutes—with a single-step protocol for quantifying intracellular ATP. From basic research to high-throughput drug screening, the CellTiter-Glo Assay is judged the best. It enables you to easily estimate cell number, measure cell viability or quantitate cytotoxic effects. Discriminating scientific minds agree; CellTiter-Glo is the perfect assay. See for yourself. For a **FREE SAMPLE** visit: **www.promega.com/celltiterglo**

PROMEGA CORPORATION • www.promega.com

Promega

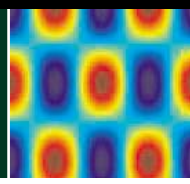

LETTERS

edited by Etta Kavanagh

Balancing Communication and Safety

DEMOCRATIC SOCIETIES ARE NOW ENGAGED AGAINST TERRORIST ACTIVITIES. In such an environment, there is tension between the desire to withhold scientific information from those who would use it for ill and the need to not stifle fundamental research in the life sciences or the open communication of results. To inhibit the pursuit of science may suggest safety from those prepared to use science for harmful purposes, but any sense of security is false. Freedom for research and communication is more necessary than ever, and the best defense against those who would employ science as a weapon is scientific excellence. There will inevitably be worldwide communication of the results of scientific studies, but open communication is vital to peer review and an independent evaluation of research, including oversight by the executive and legislative branches of government as well as the public. Open communication is also essential for public-health and public-safety planning, for the robust growth of business and technology, and for research that will be beneficial for society. Such openness is additionally necessary for the development of countermeasures against sinister applications of science. Preventing publication, even if that could be accomplished, will not prevent the misuse of science because sanctions will not deter those who have a malevolent intent. Secrecy instead poses the danger of enforced ignorance.

"Freedom for research and communication is more necessary than ever…"
—Ehrlich

The life-sciences community has generally garnered public trust. To ensure the continued success of the scientific enterprise, it is critical to maintain and further that trust against the possibility of public misunderstanding, particularly in an ever-changing scientific and political environment. To preserve their credibility, members of the scientific community must remain sensitive to the potential that information could be misused by individuals and communities to endanger public safety and health or otherwise jeopardize national security; continuing education and responsible engagement in the wider body politic are required.

Life scientists enjoy a virtually unrestricted exchange of information; shared information has been a safeguard and a cornerstone. But legitimate threats to our national security necessitate that there be appropriate oversight of scientific research and publication. Restraints of the kind set forth by President Reagan in National Security Decision Directive (NSDD) 189 (*1*) are fit. However, perfect regulation is impossible because it assumes perfect compliance. While the scientific community continues to accept responsibility for principled research and communication, and regulation as a management tool, the public and the government must recognize that true national security requires scientific accomplishment and that scientific excellence requires the open communication of research and results. **SUSAN A. EHRLICH***

Judge, Arizona Court of Appeals, 1501 West Washington Street, Phoenix, AZ 85007, USA, and a member of the National Science Advisory Board on Biosecurity.

*The views expressed are the author's alone.

Reference

1. Available at www.fas.org/irp/offdocs/nsdd/nsdd-189.htm.

Glossing Over the Complexity of Water

ALTHOUGH WE APPLAUD THE RECOGNITION GIVEN BY *Science* to Freshwater Resources, the recent Special Section (25 Aug., pp. 1067–1090) missed an opportunity to highlight the multifaceted nature of water resources research. Framing "the" water problem as a search to quench a universal thirst ("A thirsty world") glosses over critical differences in the causes of, and thus the solutions to, water problems across regions. It forces the discussion into the domains of supply augmentation and engineering and marginalizes underlying drivers of "thirst" such as rapid urbanization, economic transitions, geopolitical factors, or poverty.

Lack of access to water in many African countries, for example, is less the outcome of a first-order water scarcity than of a second-order scarcity of social resources (*1*). As the News story "Running out of water—and time" (J. Bohannon, p. 1085) suggests, Gaza suffers at least as much from geopolitical factors that inhibit access to money and nearby water as from the "environmental problem" of "running out of water." Water transfers or desalination help overcome local/regional scarcity, but with important environmental, social, and economic costs ("Going against the flow," R. Stone, H. Jia, News Focus, p. 1034; "Desalination freshens up," R. F. Service, News, p. 1088). For example, Israel's water management is becoming "sustainable" ("Seeking sustainability: Israel's evolving water management strategy," A. Tal, Perspective, p. 1081) only from a narrow technical perspective that treats as exogenous the growth in its arid south and neglects the environmental and third-party impacts of overexploiting the Jordan River. First-order scarcity metrics ("Global hydrological cycles and world water resources," T. Oki, S. Kanae, Review, p. 1068), especially global ones, overlook such specificities and are of limited policy use.

The interdisciplinary water research community has shifted its attention to context-specific and proactive approaches such as watershed management, ecological engineering, demand management, reallocation, and collaborative/adaptive planning (*2*). We understand that the Special Section was not meant to be an exhaustive review of freshwater issues. But institutional, political, and economic options deserve more than cursory mention in *Science*, since it is primarily these, rather than technical fixes alone, that "offer a measure of hope for the future" ("A thirsty world," J. Yeston *et al.*, p. 1067).

GIORGOS KALLIS, MICHAEL KIPARSKY, ANITA MILMAN, ISHA RAY

Energy and Resources Group (ERG), University of California at Berkeley, Berkeley, CA 94720–3050, USA. E-mail: gkallis@berkeley.edu

References

1. J. Lundqvist, M. Falkenmark, C. Folke, L. Gordon, L. Ohlsson, *New Dimensions in Water Security* (FAO AGL/MISC/25/2000, UN Food and Agriculture Organization, Rome, 2000).
2. P. H. Gleick, *Water Int.* **25**, 127 (2000).
3. The Letter was written with input from the ERG Water Group.

Mitochondrial DNA and Population Size

IN THEIR REPORT "POPULATION SIZE DOES NOT influence mitochondrial genetic diversity in animals" (28 Apr., p. 570), E. Bazin *et al.* present compelling evidence that selective sweeps occur in animal mitochondrial DNA (mtDNA) and reduce genetic diversity below the level expected at mutation-drift equilibrium in some taxa. They also assert that this evidence implies that mtDNA has limited relevance to biodiversity and conservation studies. I contest this claim on two fronts.

First, the selective sweeps that they detect occur at very deep phylogenetic levels (phyla to class), which translate into deep evolutionary time (hundreds of millions of years). It is rare that conservation biologists are interested in how mtDNA diversity is distributed at such a level. Rather, it is standard practice that genetic diversity is interpreted in the context of a relevant, almost always closely related, control group (*1*). This practice is designed to account as best as possible for the potentially confounding historical, demographic, mutational, and selective variables that influence genetic diversity.

Second, it is well established that the geographical distribution of mtDNA diversity as determined by lineage-sorting, and not just diversity per se, is informative with respect to biodiversity conservation (*2*–*4*). Use of this criterion is recognized to address the very differences in accumulation or maintenance of genetic diversity within different taxa described by Bazin *et al.*—otherwise known as the "how much divergence is enough" question (*3*).

Clearly, conservation biologists should not ignore selective sweeps; they do occur, and sometimes rapidly (*5*). However, mtDNA diversity is abundant at the population, species, and genus level of animals (*2*), and it is here that it can be, and is, most relevant and routinely exploited for conservation purposes. This would not be the case if selective sweeps were as dominant a force as implied by Bazin *et al.* Despite their claims, Bazin *et al.*'s results have limited relevance to most standard applications of mtDNA in conservation.

OLIVER F. BERRY

School of Animal Biology, University of Western Australia, Stirling Highway, Crawley, Western Australia 6009, Australia.

References

1. J. L. Bouzat, *Genetica* **110**, 109 (2000).
2. J. C. Avise, *Phylogeography: The History and Formation of Species* (Harvard Univ. Press, Cambridge, MA, 2000).
3. C. Moritz, *Trends Ecol. Evol.* **9**, 373 (1994).
4. P. D. N. Hebert, A. Cywinska, S. L. Ball, J. R. deWaard, *Proc. R. Soc. London B* **270**, 313 (2002).
5. M. Turelli, A. A. Hoffmann, *Nature* **353**, 440 (1991).

IN A META-ANALYSIS OF GENETIC POLYmorphism, E. Bazin *et al.* suggest that mitochondrial DNA (mtDNA) is more profoundly affected by nonneutral evolution than nuclear loci ("Population size does not influence mitochondrial genetic diversity in animals," Reports, 28 Apr., p. 570). This interpretation has already led some to conclude that mtDNA is of little utility in studies of evolution and conservation. It is well known

that multiple evolutionary processes must be considered in interpreting patterns of genetic diversity at any gene region (*1*, *2*). However, dismissing mtDNA as a more biased analytical tool is neither necessary nor justified (*3*).

First, it is inappropriate to approximate effective population size (N_e) from census size, as is implied by Bazin *et al.*'s "intuitive" predictions. Bottlenecks, fluctuating population size, reproductive strategies, and geographic structure, none of which can be inferred reliably from present census size, profoundly impact N_e and genetic diversity (*4*). Indeed, invertebrate taxa and fish generally have greater census size than tetrapods, but there is also greater diversity in life history and reproductive strategies, traits that alter patterns of sequence divergence within and among taxa.

Second, the neutrality index (NI) may be inappropriate for distantly related taxa because the high substitution rate and site heterogeneity of mtDNA often lead to mutational saturation in protein-coding genes (see figure). This saturation biases the NI toward values <1 as species divergence increases. The smaller number of invertebrate mtDNA genomes currently available tends to force more distant outgroup comparisons.

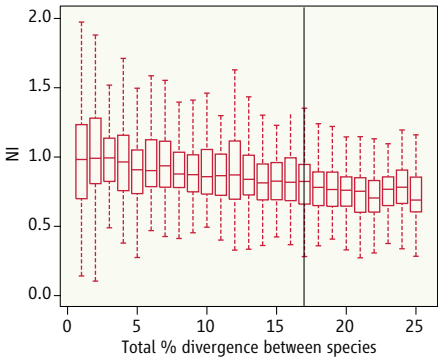

◀ Neutrality indices simulated for a single nonrecombining 1 kb coding region. For each interspecific distance class, 100 coalescent simulations were performed comparing an ingroup taxon of $n = 10$ and expected within-species pairwise divergence of 2% to a single outgroup taxon. Simulations assume a transition:transversion ratio of 2 and a relative substitution rate of 2:1:20 for the first, second, and third codon positions, respectively. Thick horizontal bars indicate medians, and boxes include 50% of the distributions. The vertical line indicates the cutoff point used by Bazin *et al.* in their meta-analysis.

Bazin *et al.* rightfully emphasize the necessity of adequately testing for deviation from the neutral model for mtDNA, as with all loci. Further, the meta-analytical tools developed by Bazin *et al.* and others can help assess the time scale of selective sweeps relative to demographic events commonly considered by evolutionary biologists (e.g., effects of glaciation, high variance in reproductive success, and recent/incipient speciation). All genetic data come with complications, but we argue that it is inappropriate and unnecessary to dismiss the contribution that mtDNA sequence data—still one of the most powerful universal sources of genetic variation for nonmodel animals—can make to studies of conservation, taxonomy, and historical demography.

JOHN P. WARES,[1] PAUL H. BARBER,[2]
JEFFREY ROSS-IBARRA,[1] ERIK E. SOTKA,[3]
ROBERT J. TOONEN[4]

[1]Department of Genetics, University of Georgia, Athens, GA 30606, USA. [2]Department of Biology, Boston University, Boston, MA 02215, USA. [3]Grice Marine Laboratory, College of Charleston, Charleston, SC 29412, USA. [4]Hawai'i Institute of Marine Biology, University of Hawai'i at Manoa, Kane'ohe, HI 96744, USA.

References

1. S. Y. W. Ho, M. J. Phillips, A. Cooper, A. J. Drummond, *Mol. Biol. Evol.* **22**, 1561 (2005).
2. A. S. Gerber, R. Loggins, S. Kumar, T. E. Dowling, *Annu. Rev. Genet.* **35**, 539 (2001).
3. D. Rubinoff, B. S. Holland, *Syst. Biol.* **54**, 952 (2005).
4. R. Frankham, *Genet. Res.* **66**, 95 (1995).

Letters to the Editor

Letters (~300 words) discuss material published in *Science* in the previous 6 months or issues of general interest. They can be submitted through the Web (www.submit2science.org) or by regular mail (1200 New York Ave., NW, Washington, DC 20005, USA). Letters are not acknowledged upon receipt, nor are authors generally consulted before publication. Whether published in full or in part, letters are subject to editing for clarity and space.

Response

Berry and Wares *et al.* independently comment on our conclusion that mtDNA might not be a reliable marker of species population size and diversity. They introduce four arguments: (i) age of selective sweeps, (ii) census size versus effective size, (iii) distance to outgroup, and (iv) the usefulness of mtDNA despite selective sweeps.

1) Despite the fact that our study is based on comparisons between distantly related taxa, the selective sweeps we think have contributed to decreased mtDNA diversity in large populations must be recent ones, because they have influenced the level of polymorphism observable within species.

2) We agree that effective population size can be very different from census population size, to an extent largely variable between species. Our analysis, however, recovers a positive relationship between nuclear genetic diversity and indicators of species abundance, indicating that effective and census populations sizes are correlated. The lack of relationship with mtDNA markers can therefore hardly be due to the census versus effective size problem, especially given the much larger data set analyzed.

3) It is true that very distant outgroups can bias the NI analysis because of saturation of the synonymous divergence (d_s), as neatly demonstrated by Wares' simulations. Our data set does not show strong variation of mitochondrial d_S across taxa: the average d_S is 0.262 in invertebrates versus 0.266 in vertebrates.

4) We do not mean to argue that mtDNA markers should be abandoned; there are many practical reasons why they can be useful. We strongly caution mtDNA users, however, that within-species mtDNA variations are likely to be influenced by natural selection, especially in invertebrate species, where adaptation might be the rule. The age of the most recent mtDNA ancestor, in particular, should not be connected to any climatic, geologic, or biotic event unless confirmation is obtained from nuclear markers.

E. BAZIN, S. GLÉMIN, N. GALTIER
CNRS UMR 5171–Génome, Populations, Interactions, Adaptation–Université Montpellier 2, 34095 Montpellier Cedex 5, France.

TECHNICAL COMMENT ABSTRACT

Comment on "Population Size Does Not Influence Mitochondrial Genetic Diversity in Animals"

Connie J. Mulligan, Andrew Kitchen, Michael M. Miyamoto

Bazin *et al.* (Reports, 28 April 2006, p. 570) found no relationship between mitochondrial DNA (mtDNA) diversity and population size when comparing across large groups of animals. We show empirically that species with smaller populations, as represented by eutherian mammals, exhibit a positive correlation between mtDNA and allozyme variation, suggesting that mtDNA diversity may correlate with population size in these animals.

Full text at
www.sciencemag.org/cgi/content/full/314/5804/1390a

EVOLUTION

A Subaltern View of Eusociality

Raghavendra Gadagkar

In the early 1980s, a group of scholars consisting largely of Indian historians set up the Subaltern Studies Group and persuaded Oxford University Press, New Delhi, to launch a new publication series, *Subaltern Studies: Writings of South Asian History and Society*. Inspired and led by their chief mentor, Ranajit Guha, many, now well-known, historians (among them Gyan Prakash, Gayatri Chakravorty Spivak, Partha Chaterjee, Shahid Amin, and Gyanendra Pandey) pursued a relatively new brand of historiography (*1*). The principal novelty of their approach was to focus on ordinary people—the masses, the peasants, and other marginalized groups. They created a history from "below" rather than the usual narrative of the kings, leaders, and other elites. Two decades and ten volumes later, it is clear that the subaltern studies have yielded a valuable new perspective on history, one perhaps especially useful for understanding and managing present-day social and cultural problems.

In his 1971 book *The Insect Societies*, Edward O. Wilson (*2*) picked "eusociality"—a term coined by Suzanne Batra (*3*) and given a second lease on life by Charles Michener (*4*)—to describe the most organized of animal societies, those in which group members share a composite nest and exhibit cooperative brood care, overlap of generations, and reproductive castes. Wilson vested eusociality with such an elite status that, overnight, students of ants, bees, wasps, and termites felt they belonged to a privileged new community of entomologists ideally poised to solve the Darwinian paradox of altruism. They (I should say, we) have done well: Hundreds of species of eusocial insects have been studied in depth, and we now have a reasonably sophisticated understanding of the forces that mold the evolution of insect societies. Nevertheless, no one would claim that the problems concerning the evolution of sociality and altruism are entirely solved.

The reviewer is at the Centre for Ecological Sciences, Indian Institute of Science, Bangalore, 560012, India. E-mail: ragh@ces.iisc.ernet.in

CREDIT: E. KUNHIKRISHNAN

What should we do next? It often helps to start from a new perspective. To this end, some are offering bold new theoretical approaches (*5*–*8*). But perhaps we also need fresh data from previously neglected kinds of insect societies. This is the approach James T. Costa offers in *The Other Insect Societies*. Costa (the director of the Highlands Biological Station, North Carolina, and a professor at Western Carolina University) launches the entomological equivalent of subaltern studies, focusing deliberately on species that have failed to make it to Wilson's elite grade of eusociality.

The Other Insect Societies

by James T. Costa

Harvard University Press, Cambridge, MA, 2006. 811 pp. $59.95, £38.95, €55.30. ISBN 0-674-02163-0.

Readers will find in the book a fascinating wealth of information about the obscure social lives of earwigs, grasshoppers, crickets, mantids, cockroaches, aphids, treehoppers, bugs, thrips, beetles, caterpillars, sawflies, and even some non-insect arthropods (spiders, centipedes, millipedes, and crustaceans). Costa's book will inevitably be compared with *The Evolution of Social Behavior in Insects and Arachnids*, edited by Jae C. Choe and Bernard Crespi (*9*)—Wilson and Burt Hölldobler both mention that work in their introductory comments on the book. In my review of the Choe and Crespi volume, I likened it to Aladdin's magic lamp and the index to a genie who can "take you to wonderful, unheard-of and even amorous worlds" (*10*). *The Other Insect Societies* is a new avatar of the magic lamp, complete with a high-power genie. It provides over 1000 entries in its subject index and over 2000 in both the taxonomic and author indices. And in contrast to the contributors to the Choe and Crespi volume, Costa tells readers a great deal about the source of his facts—who did what, when, why, where, and how.

I doubt that many people would read the book from cover to cover or benefit from doing so. It is more likely that readers who are already wedded to specific taxa will devour the chapters on their favorites with pleasure and profit. I am rather optimistic that, paralleling the effects of the subaltern studies of Indian historians, a focus on other insect societies will provide valuable fresh perspectives useful even for understanding present-day eusocial species.

Although I found much to praise in the book, if I were to write a 100-page review—and one could envision such a review; after all, it's a 700-page book—I would probably devote 90 pages to extol its virtues and some 10 pages to criticize and disagree with the author. I would dispute some of his interpretations, regret his failure to cite certain papers, question some of his assignments of priority, and reject his calls to abandon less entrenched terms (e.g., subsocial, communal) while retaining eusociality. Costa proceeds at an unduly leisurely pace, which is made more problematic by the absence of summaries at the end of individual chapters. A thematic, rather than taxonomic, treatment of the subject matter probably would have been more enticing and easier to follow; it might also have allowed Costa to weave the

Gathering together to gather. In mud puddling, males gather from wet soil supplementary nutrients needed by the females to produce more eggs. This aggregation of common albatross butterfly (*Appias albina*) was photographed at the Chinnar Wildlife Sanctuary, Kerala, India.

chapters together into a more unified account. I would not endorse the claim that the "hope for a universal ecological explanation of cooperative breeding may be doomed." Although I have now used my quota of 100 words of criticism and disagreement proportionate with the length of this review, I cannot ignore the author's most remarkable statement. After criticizing S. Mukerji, for not knowing in 1927 that the position of the spinning apparatus and the mechanism of spinning in embiids (webspinners) had already been discovered and published by M. Rimsky-Korsakov in 1910, Costa incredibly goes on to say that "Perhaps we should not be surprised at such errors; after all, these inconspicuous insects long remained out of reach for most temperate-zone entomologists." It seems mind-boggling that such an invidious statement was written in the first place, let alone that it passed the scrutiny of referees and editors.

I would not claim that what is already known about the non-eusocial insect societies, as painstakingly and thoroughly detailed in Costa's book, makes us substantially wiser about the evolution of insect social behavior. Instead, I suspect that the book will draw attention to these other insect societies and make their study fashionable and feasible. A few hours with Costa's book will bring any beginner up to date with a century's worth of scattered literature on almost everything that is known about any of the many obscure groups of insects discussed. One could reasonably expect a new graduate student to read the appropriate chapter in the book and embark on a study of the corresponding group for her dissertation.

There is also an altogether different reason why I am delighted to see *The Other Insect Societies* in print. If an early-career academic like James Costa can write a 700-page account that covers relatively little of his own research, there is still some hope that we can bring the reading and writing of books back into fashion among younger biologists.

References

1. D. Ludden, Ed., *Reading Subaltern Studies: Critical History, Contested Meaning, and the Globalisation of South Asia* (Permanent Black, Delhi, 2005).
2. E. O. Wilson, *The Insect Societies* (Harvard Univ. Press, Cambridge, MA, 1971).
3. S. W. T. Batra, *Indian J. Entomol.* **28**, 375 (1966).
4. C. D. Michener, *Annu. Rev. Entomol.* **14**, 299 (1969).
5. E. O. Wilson, B.Hölldobler, *Proc. Natl. Acad. Sci. U.S.A.* **102**, 13367 (2005).
6. D. L. Cassill, *J. Bioecon.* **200**, 1 (2006).
7. P. Nonacs, K. M. Kapheim, *Proc. XV Congr. Int. Union Study Soc. Insects, Washington, DC,* p. 28 (2006); http://iussi.confex.com/iussi/2006/techprogram/P1602.HTM.
8. J. H. Hunt, *The Evolution of Social Wasps* (Oxford Univ. Press, Oxford, forthcoming).
9. J. C. Choe, B. J. Crespi, Eds., *The Evolution of Social Behavior in Insects and Arachnids* (Cambridge Univ. Press, Cambridge, 1997).
10. R. Gadagkar, *Trends Ecol. Evol.* **13**, 122 (1998).

10.1126/science.1135094

ENVIRONMENT AND RELIGION

Hoping to Establish Common Ground for Saving Biodiversity

Steven Bouma-Prediger

Edward O. Wilson is no stranger to readers of *Science* or the general public. One of the most famous scientists living today, Wilson is the author of more than 20 books, two of which have won the Pulitzer Prize for nonfiction. In his 40 years as a faculty member at Harvard University, he has put forward important scientific theories (including island biogeography and sociobiology) and coined novel terms (such as biophilia). Through it all, Wilson has been an articulate and passionate advocate for the conservation of the natural world.

Though now retired, Wilson's influence is still considerable. So any book from him is noteworthy. But his *The Creation: An Appeal to Save Life on Earth* is certain to draw added attention, not least because the book is written as a personal letter to a hypothetical Baptist pastor. Although raised in Alabama as a Southern Baptist, Wilson long ago gave up that faith; he is now and has long been a self-proclaimed "secular humanist." Nonetheless, given the scope and pace of ecological degradation, Wilson suggests that Christians and secularists "set aside our differences in order to save the Creation." His new book is, as it were, an olive branch extended to Christians, especially conservative Christians in North America, to make common cause in the effort to preserve biodiversity.

The Creation
An Appeal to Save Life on Earth
by Edward O. Wilson
Norton, New York, 2006. 185 pp. $21.95, C$27.50. ISBN 0-393-06217-1.

Wilson's argument, in essence, is this. His first premise is that "the Creation—living Nature—is in deep trouble"; indeed, we are facing a "biological catastrophe." Evidence for this claim runs throughout the book, from a discussion of alien species in 16th-century Hispaniola to the current "pauperization of Earth" evident in tropical rainforests. We face a stark choice: either "conserve Earth's natural heritage, or let future generations adjust to a biologically impoverished world."

The second premise, and the reason for this particular book, is Wilson's belief that "religion and science are the two most powerful forces in the world today," and thus "if religion and science could be united on the common ground of biological conservation, the problem [of biological catastrophe] would soon be solved." So writing to his imagined Baptist pastor, Wilson acknowledges that "you have the power to help solve a great problem about which I care deeply."

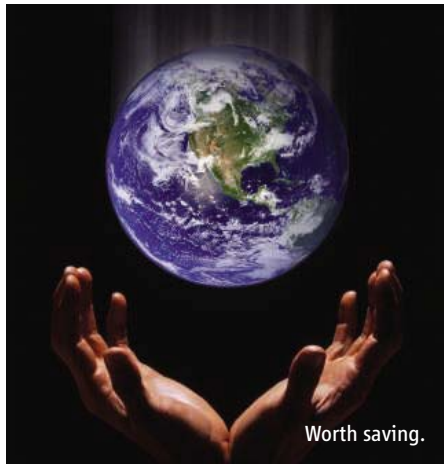
Worth saving.

CREDITS: NASA, JUPITER PHOTOS

Wilson devotes most of the book to an attempt to persuade his reader to care for the planet and its biota. For example, he argues that because we humans are inextricably dependent on a plethora of other species for our very survival, "even the most recalcitrant people must come to view conservation as simple prudence in the management of Earth's natural economy." In addition to self-interest, however, Wilson insists that each species is "a masterpiece of biology, and well worth saving." He further argues that many organisms, such as the pitchfork ant, evoke wonder and that such wonder motivates care. Moving still farther beyond prudence, Wilson

The reviewer is at the Department of Religion, Hope College, 126 East 10th Street, Holland, MI 49423, USA. E-mail: boumapred@webmail.hope.edu

NOTA BENE: EXHIBITS

Delightful Digital Diversions

From Space War! to Nintendo DS Lite, computer and video gaming is now venerable enough to have an entire exhibition devoted to its history (Game On)—which is a bit of a shock in itself. The first game in the exhibition at London's Science Museum, Space War!, was designed by Steve Russell and friends at the Massachusetts Institute of Technology in the distant days of 1962. The equipment required to play that game (see photograph) is arresting: The computer alone (a PDP-1, donated to MIT by the Digital Equipment Corporation in the hope that the students would "use it productively") occupies the space of several wardrobes, there is a cumbersome monitor with a 2-foot tube, and it's all hooked up to an electric typewriter. This bulky construction is the only true anachronism in the show.

Game On

curated by Conrad Bodman and Lucian King for the Barbican Art Gallery

Science Museum, London, through 25 February 2007. www.sciencemuseum.org.uk/exhibitions/gameon/

Three of us—one from the pre-gaming generation and two 12-year-old connoisseurs of the hand-held console—went to review almost half a century of computer game evolution. The exhibition, sponsored by Nintendo, is displayed in a series of rooms in roughly chronological order, and it beeps, buzzes, and flashes like an arcade. Most of the exhibits are fully operational, allowing the visitor hands-on experience. (The exception, frustratingly, is the hand-held equipment, much of which is displayed beneath a glass dome.)

From the PDP-1, one rapidly moves into more familiar territory. The next phase of miniaturization was accomplished within little more than a decade. The game machines of the 1970s, housed in the fruit-machine cabinets and knee-high tables of arcades and bar rooms, have been the stock in trade of the industry ever since. Despite minimal instructions, our two 21st-century gamers had no trouble familiarizing themselves with the games of that decade. And, it was gratifying to the oldest member of the team to discover his Space Invaders technique intact after a quarter century of abstinence and to achieve rare tactical superiority over the next generation.

As the hardware continued on the path to increasing portability and invaded the home, games themselves diversified in several directions—action, puzzle, simulation—and evolved into the vast array on today's market. Because of the limits of space, Game On samples this diversification sparingly, but nonetheless instructively. Even though some old favorites are inevitably missing, the narrative provided by the generous graphics fills in the gaps. The artwork is by the British illustrator Jon Burgerman; its centerpiece is a giant timeline charting the history of gaming in the form of a fantastical segmented creature spread along the entire wall of the first hall.

The exhibition is perhaps not as much about the science of computer gaming as about how technology and design, graphic arts and characterization have interacted to give life to one of the major social phenomena and wealth generators of the post-industrial world. In the United Kingdom alone, more than half the population (with an almost even gender split) regularly uses electronic games. The enhancement of 3D skills and the hand-eye-brain coordination that these games allegedly offer have put gaming on the compulsory training schedules of pilots in some air forces. The pervasive influence of computer games and debates on their possible wider social effects (e.g., violence, loss of social skills, sexism, and ethnicism) are tentatively explored in two sections of the exhibition devoted to games culture in the United States, Europe, and Japan.

Where next? The exhibition ends with questions on the future of computer gaming. In the coming months a number of ancillary events and talks, some by games pioneers, are scheduled at the Science Museum, to explore and develop these and other themes of the exhibition.

–Andrew M. Sugden, Hugh A. Russell, Rowan M. A. Sugden

10.1126/science.1137012

CREDIT: ANDREW SUGDEN

also asserts that "the Creation, whether you believe it was placed on this planet by a single act of God or accept the scientific evidence that it evolved autonomously during billions of years, is the greatest heritage, other than the reasoning mind itself, ever provided to humanity." This heritage, he insists, we humans are duty-bound to preserve.

There is much to admire in this book. Wilson is at his best when describing the natural world in all its wondrous detail. The expertise of this world-class biologist is evident. Wilson is also persuasive in communicating a sense of urgency about the looming ecological crisis. His feel for the biological vital signs of our home planet rings tellingly true. Lastly, Wilson honestly confronts what he calls "the ignorance and self-absorption" of humanity. He dismantles the claims of those, both secular and religious, who either see no harm in ecological degradation or believe that zoos, aquariums, and botanical gardens can suffice to save biodiversity. In this regard Wilson perceptively criticizes a naïve faith in technology as the supposed savior of all that ails us.

The book, however, has some serious shortcomings. First, the term "the Creation" is a religious term that logically implies a Creator. In his use of this term, does Wilson intend to imply the existence of God? Also, Wilson seems to use "the Creation" interchangeably with "living Nature" and "Earth," but it is far from clear that these all mean the same thing. Furthermore, Wilson speaks often of "religion and science" when what he means is Christianity and biology. Few would hold that religion can be reduced to Christianity or natural science reduced to biology. In addition, Wilson's conceptions of science, religion, and their interrelationship are problematic. Is it really the case that "without science there had to be religion"? Lastly, at the end of the book, one wonders whether the arguments Wilson puts forward will persuade his Baptist (and other Christian) readers to care for Earth. Absent any more explicitly religious arguments, I'm not at all sure his hypothetical reader will be convinced.

Notwithstanding the above criticisms, *The Creation* is an important book. At a time when there is much evidence that Christians are taking their biblical call to be earthkeepers more seriously, Wilson offers an irenic invitation to form "an alliance for life." Christians have every good reason to join with Wilson and meet on common ground—both the beliefs we share and the Earth we are called to serve and protect (Genesis 2:15). At a time when "life on this planet can stand no more plundering," may we so meet.

References

1. E. O. Wilson, *On Human Nature* (Harvard Univ. Press, Cambridge, MA, 1978).
2. B. Hölldobler, E. O. Wilson, *The Ants* (Harvard Univ. Press, Cambridge, MA, 1990).

10.1126/science.1135704

SCIENCE AND LAW

When Patents Threaten Science

Patents should not be used to protect laws of nature, products of nature, or mathematical formulas.

Lori Andrews,[1]* Jordan Paradise,[2] Timothy Holbrook,[1] Danielle Bochneak[1]

What if each generation of scientists was forbidden to use—or even think about—the theorems, principles, and natural phenomena that had been discovered or proven by the previous generation of scientists? Researchers may soon find themselves in that position as the U.S. Patent and Trademark Office (USPTO) comes dangerously close to issuing patents on the basic building blocks of science itself. A U.S. Supreme Court decision in June 2006, *Laboratory Corporation* v. *Metabolite Laboratories* (*1*), and a solicitation by the USPTO in July 2006 for comments on proposed guidelines for patent examiners (*2*–*4*) have raised questions about the delicate balance between a common body of knowledge and the exclusive rights over scientific information embodied in a patent.

The patent at issue in the *Metabolite* case covered the following process: Use any test (whether patented or unpatented) to measure the level of the amino acid homocysteine in a body fluid and then, if the level is elevated above the norm, conclude that vitamin B deficiency is likely. The Court of Appeals for the Federal Circuit held that LabCorp induced infringement of that patent (and thus was liable for over $2 million in damages) based on the publication to physicians of a law of nature—the relation between levels of homocysteine and vitamin deficiency (*5*). Astonishingly, the Federal Circuit also held that physicians (or researchers) would infringe the patent merely by thinking about the relation between homocysteine and vitamin deficiency when they analyzed an alternative homocysteine test (*5*).

As the Supreme Court contemplated the merits of the *Metabolite* case, legal scholars wrote commentaries (*6*, *7*), and major newspapers ran editorials (*8, 9*) addressing the problems in the current interpretation of patentable subject matter by the USPTO and federal courts. In June 2006, the Supreme Court dismissed the appeal for procedural reasons (*1*), which allowed this patent on a biological fact to stay in effect.

[1]Institute for Science, Law, and Technology, Chicago-Kent College of Law, Chicago, IL 60661, USA. [2]Consortium on Law and Values in Health, Environment, and the Life Sciences, University of Minnesota Law School, Minneapolis, MN 55455, USA.

*Author for correspondence. E-mail: landrews@kentlaw.edu

Patents on Scientific Building Blocks and Processes

The USPTO has issued various patents that could interfere with the work of basic scientists, social scientists, and engineers. These range from correlation patents, such as the one in the *Metabolite* case, to patents on certain ways of analyzing data. Patents can chill research if the patent holder forbids other researchers from using the scientific fact or natural phenomenon, or charges an excessive fee for access to that knowledge.

One patent claims the use of a computer to derive a solution to any optimization algorithm. Optimization problems have traditionally been expressed in terms of the hypothetical traveling salesman who has to travel his route with the minimum expenditure of time and money. Commentators expressed the opinion that no one would ever attempt to patent such an obvious and important method of problem-solving (*10*). But in 2005, a patent was issued for the process of solving the traveling salesman problem with a computer program that used a standard statistical algorithm outputting a set of optimal data points given certain inputs and constants (*11*). Although the inventor includes superficial language referencing a machine, what is actually claimed is the first step to solving any optimization or linear programming problem. The patent holder can, until the patent expires in 2021, demand a royalty from any industrial engineer, facilities planner, telecommunications analyst, or other researcher who uses this algorithm with computer assistance.

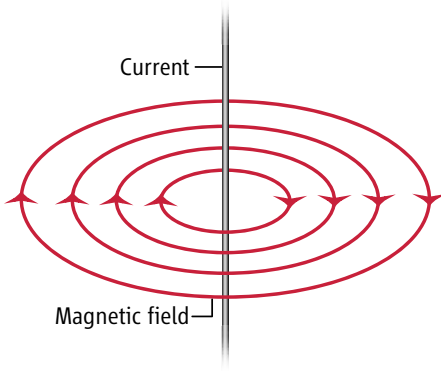

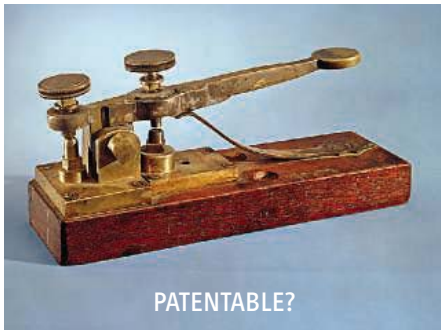

What can be patented? (**Top**) Natural relationship between magnetic field and electrical current. (**Bottom**) Samuel Morse's telegraph machine.

Another patent claims "a method of psychological testing of a person, comprising: (a) instructing the person to produce a drawing which includes at least one pictorial representation of each of at least a majority of the following items: a hand, an eye, a tree, a fish, a star, a spiral; a half-circle, and a zigzag; and (b) subjecting to psychological interpretation the drawing produced in response to step (a)" (*12*). Although the patent mentions specific pictures, a cognitive science researcher who substitutes his own drawings may be found liable of infringement under the doctrine of equivalents (*13*). The patent thus covers a basic psychological research evaluation technique.

The patent entitled "[d]atabase and system for storing, comparing and displaying genomic information" encompasses the very manner in which a computer user may access genomic libraries for viewing (*14*). Included in the claims is the "method of comparing genetic complements of different types of organisms" by means of electronic sequence libraries (*14*). Such a broad patent may restrict meaningful access to and analysis of genetic sequence information that would otherwise be freely available to researchers who wish to compare, for example, the genes of mice to the genes of humans.

Patents that claim the correlation between the existence of a genetic mutation and the predisposition to a disorder are also problematic (*15*). One patent claims the process of assessing a patient's risk of developing certain neurological or neuropsychiatric disorders based on the presence of specific polymorphisms (*16*). However, mutations are natural occurrences and, if patients have the mutation,

they necessarily have the predisposition. Similar to the patent at issue in *Metabolite*, a patent covering a natural correlation could apply to researchers who study the mutation and its effects, or who design tests aimed at targeting the mutation, or who even think about this relation.

Ignoring Supreme Court Precedent

A close look at patent policy and U.S. Supreme Court jurisprudence—as well as an understanding of the nature of the scientific enterprise—provides a foundation for assuring that the laws of nature and products of nature remain freely available to all. Not every discovery or innovation is entitled to patent protection. U.S. patent law dictates that patent applicants must satisfy a number of requirements in order to be issued a patent by the USPTO. An invention must be of eligible subject matter (*17*).

In the 1854 *O'Reilly* v. *Morse* case, the U.S. Supreme Court expressed its concern that granting Samuel Morse broad rights to a law of nature, beyond its particular application (the telegraph), would afford Morse the right to exclude others from making new innovations that Morse himself did not invent or even contemplate. Accordingly, the Court stated that Morse's claim to "a monopoly in [electro-magnetism's] use, however developed, for the purpose of printing at a distance" was "too broad, and not warranted by law" (*18*). The Court explained that patent law did not support overly broad patent rights to scientific principles because such monopolies "would be unjust to the public…and defeat the manifest object of the law" (*18*).

The Supreme Court continued to police the line between invention and scientific principle in *Parker* v. *Flook*, rejecting a patent that claimed a method for calculating updates in the catalytic conversion process as merely a mathematical formula (*19*). The Court reasoned that such a scientific principle, though useful, simply "reveals a relationship that has always existed" (*19*). Likewise, the Supreme Court in *Gottschalk* v. *Benson* held that a claim to the conversion of numerical data into binary code in any type of general-purpose digital computer was unpatentable because it was "so abstract and sweeping" that it was an attempt at patenting an idea rather than an inventive process (*20*).

In 1980 the Supreme Court handed down a seminal decision in *Diamond* v. *Chakrabarty* (*21*). Often mischaracterized as opening the door for patents claiming isolated and purified versions of naturally occurring products, including human genetic material, the Court actually distinguished between a product of nature and a patentable genetically modified bacterium cell that did not exist in nature. The Court reiterated that "a new mineral discovered in the earth or a new plant found in the wild is not patentable…. Likewise, Einstein could not patent his celebrated law that $E = mc^2$; nor could Newton have patented the law of gravity. Such discoveries are 'manifestations of . . . nature, free to all men'" (*21*).

Even if a patent applicant exercised considerable innovation discovering a law of nature or product of nature, neither is patentable under existing Supreme Court precedent. A person might expend money and creativity building a telescope, but he should not be able to patent the new planet he discovers through the telescope.

Justices Breyer, Stevens, and Souter, dissenting in the *Metabolite* case, said: "The justification for the principle does not lie in any claim that 'laws of nature' are obvious, or that their discovery is easy, or that they are not useful. To the contrary, research into such matters may be costly and time-consuming; monetary incentives may matter; and the fruits of those incentives and that research may prove of great benefit to the human race. Rather, the reason for the exclusion is that sometimes *too much* patent protection can impede rather than 'promote the Progress of Science and useful Arts,' the constitutional objective of patent and copyright protection" (*1*).

The idea that a patent could block future innovation, to the detriment of the public, is pertinent because the USPTO is granting patents that could block scientific inquiry. Although the discoveries of natural phenomenon may be necessary precursors to invention, improperly tying up these discoveries with patent rights will only drive up the costs of such subsequent innovations, if not thwart them altogether.

The USPTO and lower courts are responsible for granting and enforcing patent rights that run contrary to U.S. Supreme Court precedent (*22*). Merging the U.S. Court of Claims and the U.S. Court of Customs and Patent Appeals to create the Federal Circuit in 1982 seems to have accelerated this expansion by creating a specialized, arguably pro-patent court.

Patent applicants who seek to patent laws of nature often point to a Federal Circuit opinion, *State Street Bank & Trust Co.* v. *Signature Financial Group*, which suggests that a law of nature is patentable if it produces a "useful, concrete, and tangible result" (*23*). However, this is clearly overinclusive and in direct conflict with existing Supreme Court precedent (*1*). To be patentable, there must be something more—a human invention that produces a result beyond the law of nature or product of nature itself.

Conclusion

Scientists may not have paid sufficient attention to the privatization of common knowledge because, in the past, they felt that research activities did not require approval from patent holders. The 2002 *Madey* v. *Duke* decision put an end to such protection (*24*). Scientists can be influential by helping policy-makers understand that open access to basic laws of nature, products of nature, and mathematical formulae is necessary for scientists to explore and innovate. The U.S. Supreme Court has recognized that fact, but, increasingly, the USPTO in granting such patents and the Federal Circuit in upholding them seem to have forgotten it.

References and Notes

1. 126 S. Ct. 2921 (2006).
2. "Request for comments on interim guidelines for examination of patent applications for patent subject matter eligibility," *Fed. Reg.* **70**, 75451 (2006).
3. *Fed. Reg.* **71**, 34307 (2006).
4. See also "Interim guidelines for examination of patent applications for patent subject matter eligibility," *Off. Gaz. Pat. Office* **1300**, 142 (15 November 2005).
5. *Metabolite Labs., Inc.* v. *Lab. Corp. of Am. Holdings,* 370 F. 3d 1354 (Fed. Cir. 2004).
6. R. S. Eisenberg, *Nat. Biotechnol.* **24**, 317 (2006).
7. L. Andrews, *Chron. Higher Educ.* **52**, (24), B20 (17 February 2006).
8. *Wall Street Journal*, 1 March 2006, p. A14.
9. *New York Times*, 22 March 2006, p. A24.
10. B. Klemens, *Math You Can't Use* (Brookings Institution Press, Washington, DC, 2006), pp. 46–61.
11. U.S. Patent 6,904,421 (2005).
12. U.S. Patent 5,190,458 (1993).
13. *Graver Tank & Mfg. Co.* v. *Linde Air Products Co.*, 339 U.S. 605, 609 (1950).
14. U.S. Patent 5,966,712 (1999).
15. J. Paradise *et al.*, *Science* **307**, 1566 (2005).
16. U.S. Patent 6,660,476 (1999).
17. 35 U.S.Code § 101.
18. *O'Reilly* v. *Morse*, 56 U.S. 62 (1854).
19. *Parker* v. *Flook*, 437 U.S. 584 (1978).
20. *Gottschalk* v. *Benson*, 409 U.S. 63, 68 (1972).
21. *Diamond* v. *Chakrabarty*, 447 U.S. 303 (1980).
22. S. Merrill *et al.*, Eds., *A Patent System for the 21st Century* (National Research Council, National Academies Press, Washington, DC, 2004), pp. 25–27.
23. *State Street Bank & Trust Co.* v. *Signature Fin. Group* 149 F. 3d 1368, 1373 (Fed. Cir. 1998), *cert. denied* 525 U.S. 1093 (1999).
24. *Madey* v. *Duke University*, 307 F. 3d 1351, 1362 (Fed. Cir. 2002).

25. Funded by the Robert Wood Johnson Foundation Investigator Awards in Health Policy Research Program; the Office of Science, U.S. Department of Energy under award number DE-FG02-06ER64276; and an NSF grant, SES 0508321.

10.1126/science.1135872

DEVELOPMENTAL BIOLOGY

The Turing Model Comes of Molecular Age

Molecular analyses of hair follicle formation provide evidence to support the most well-known mathematical model for biological pattern formation.

Philip K. Maini, Ruth E. Baker, Cheng-Ming Chuong

What are the underlying mechanisms that give rise to complex patterns in biology? Despite recent advances in biotechnology and mathematical modeling, this still remains a largely open question. As reported on page 1447 of this issue, Sick *et al.* have made a major advance toward answering this question by identifying key molecular players in hair follicle growth and by confirming the validity of perhaps the best-known mathematical model for biological pattern formation (*1*).

In a seminal paper, Alan Turing proposed that spatial patterns result from a phenomenon he termed "diffusion-driven instability" (*2*). He showed mathematically that small spatial fluctuations in an otherwise well-mixed system of reacting and diffusing chemicals could become unstable, and that amplification of these fluctuations could lead to a spatial pattern of chemicals that he termed morphogens (i.e., substances that stimulate the development of form or structure in an organism). He proposed that this spatial arrangement could serve as a prepattern for development. Turing's work was groundbreaking because the mathematical nature of the resulting patterns is wholly counterintuitive; since their discovery, they have motivated much mathematical research. However, the model has been the subject of controversy because it has been deemed too simplistic and the search for real biological examples has been neglected. Moreover, although diffusion-driven instability has been shown to be present in chemistry, there is substantial evidence in the fruit fly *Drosophila* to refute the model for biology (*3*). The report by Sick *et al.*, by providing the first compelling biological evidence for the Turing model, is thus a landmark publication.

The formation of skin appendages (hairs, feathers, etc.) is an excellent paradigm for patterning because these systems are amenable to experimental manipulation. Nagorcka was the first to propose the Turing model to explain hair pattern formation (*4*), but at that stage the molecular biology was lagging behind the theory. It was only in 1998 that Jung *et al.* made the first efforts to link known molecular morphogens with a reaction-diffusion mechanism for feather germ formation (*5*). They showed how the size, number, and distribution of appendages could be modulated by altering morphogen concentrations (*6*).

Sick *et al.* investigated the regulation of hair follicle patterning in developing murine skin. They propose that the protein WNT and its inhibitor DKK are morphogens in the Turing sense. Expression of the protein Dkk1, which inhibits WNT, is actually controlled by secreted WNTs, and both WNTs and DKKs are secreted into the extracellular space where they diffuse, thereby acting over longer distances. Given that the WNT proteins are substantially larger than the DKKs, one would expect a large difference in their rates of diffusion. This makes possible the classical "short-range activation, long-range inhibition" phenomenon that underlies diffusion-driven instability (*7*).

Because hair follicle patterning occurs in waves, the authors used a reaction-diffusion model to set up an initial pattern of follicles. Then, along the same lines as Mooney and Nagorcka (*8*), they assumed these follicles to be chemical sources giving rise to a second wave of hair follicle formation on a larger domain (due to the growth of skin). The model predicts that moderate overexpression of activator (WNT) increases follicular density, whereas moderate overexpression of inhibitor (DKK) during the initial inductive wave increases the interfollicular spacing. Sick *et al.* have verified these predictions experimentally, providing strong evidence for a genetic underpinning of a Turing reaction-diffusion model.

Together the papers of Jung *et al.* and Sick *et al.* show that the skin progenitors are stem cells, in that they are multipotent and may assume appendage or interappendage fates depending on the local chemical environment at the time of specification. In this sense, the molecular components identified by these experiments appear to be acting as morphogens in the true Turing sense.

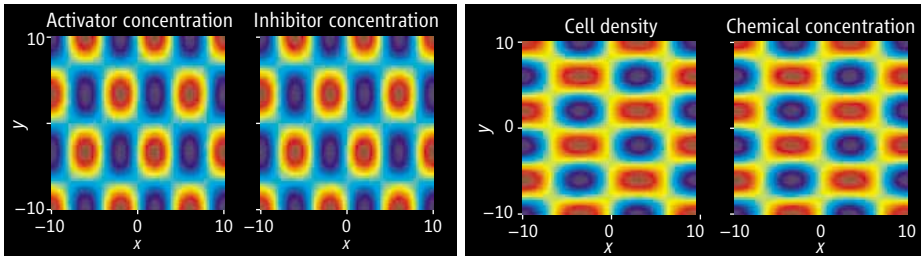

Biological pattern formation. Two mechanisms can show similar results. (**Left**) Outcome of a reaction-diffusion model (*7*) in which activator and inhibitor react and diffuse. Small random fluctuations in the initial field lead to coinciding spatial patterns of activator and inhibitor concentration. (**Right**) Results of a cell chemotaxis model (*9*) in which cells and chemical both diffuse, with cells also moving up gradients in chemical concentration. Again, small random fluctuations in the initial field lead to coinciding spatial patterns in cell density and chemical concentration. Blue indicates low concentration levels; red indicates high levels.

In principle, a reaction-diffusion model can set up a chemical prepattern before we can visualize changes in cell distribution. That is, it determines sites at which cells will cluster: Regions of high cell density coincide with those of increased morphogen concentration—although the model does not specify how this rearrangement occurs. On the other hand, it is possible for cellular aggregations to form without such a prepattern via simple chemotactic movement in response to gradients in chemical concentration. By way of illustration, the patterns formed by these two different mechanisms are shown in the figure. It is immediately obvious how similar such patterns are.

This highlights one of the difficulties in mathematical modeling: determining which

P. K. Maini is at the Center for Mathematical Biology, University of Oxford, Oxford OX1 3LB, UK, and the Oxford Center for Integrative Systems Biology, University of Oxford, Oxford OX1 3QU, UK. R. E. Baker is at the Center for Mathematical Biology, University of Oxford, Oxford OX1 3LB, UK. C.-M. Chuong is in the Department of Pathology, University of Southern California, Los Angeles, CA 90033, USA. E-mail: maini@maths.ox.ac.uk

is the "correct" model. Now that WNT and DKK have been identified as possible morphogens, this issue can be addressed experimentally. The key requirement, then, is that the results of such experiments are used to test and refine models, ruling some out if the data allow us to do so. The WNT-DKK interaction does appear to be qualitatively of the form necessary for a Turing-type system, but it is now imperative that we try to overcome the experimental challenges in measuring key parameters (rates of production, decay, diffusion coefficients, etc.) so that quantitative tests can be performed to determine whether the system actually is of Turing type. This would then be the first definitive example of the Turing model in biology.

Turing models have been proposed to describe other types of patterns observed in developmental biology. Two applications currently receiving much attention from experimentalists are pigmentation patterning in fish and skeletal development in the mouse limb. Although the evidence for a Turing diffusion-driven instability in these systems is not as strong as that presented by Sick *et al*., their report should stimulate further work in biological pattern formation.

References and Notes

1. S. Sick, S. Reinker, J. Timmer, T. Schlake, *Science* **314**, 1447 (2006); published online 2 November 2006 (10.1126/science.1130088).
2. A. M. Turing, *Philos. Trans. R. Soc. London Ser. B* **237**, 37 (1952).
3. M. Akam, *Nature* **341**, 282 (1989).
4. B. N. Nagorcka, *Biosystems* **16**, 323 (1983–1984).
5. H.-S. Jung *et al*., *Dev. Biol.* **196**, 11 (1998).
6. T.-X. Jiang, H.-S. Jung, R. B. Widelitz, C.-M. Chuong, *Development* **126**, 4997 (1999).
7. A. Gierer, H. Meinhardt, *Kybernetik* **12**, 30 (1972).
8. J. R. Mooney, B. N. Nagorcka, *J. Theor. Biol.* **115**, 299 (1985).
9. M. R. Myerscough, P. K. Maini, J. D. Murray, K. H. Winters, in *Dynamics of Complex Interconnected Biological Systems*, T. L. Vincent, A. I. Mees, L. S. Jennings, Eds. (Birkhäuser, Boston, MA, 1990), pp. 65–83.
10. Supported by Research Councils UK, Lloyds Tercentenary, Microsoft Corporation, and St. Hugh's College, Oxford (R.E.B.) and by NIH (C.-M.C.).

10.116/science.1136396

ASTRONOMY

Variable High-Energy γ Rays from the Elliptical Galaxy M87

High-energy γ rays emanating from intense jets of matter that are associated with certain galaxies provide clues to jet formation.

A. C. Fabian

Almost 90 years ago, astronomer Heber Curtis recorded the presence of a "curious straight ray" connected to the nucleus of the giant elliptical galaxy M87. Since then, researchers have acquired high-resolution images of this famous jet at wavelengths from the radio to x-ray bands (see the figure). In these images, the jet appears on only one side of the galaxy nucleus because it is moving in our direction at very close to the speed of light; the side pointed away from us is so dim as to be invisible. Rapid motion of nearby gas and stars reveals that the central engine in this energetic nucleus is a massive black hole. On page 1424 of this issue, Aharonian *et al*. now report observations of M87 at the highest energies of the γ-ray band, which may reveal new details of how the emissions from this galaxy are powered and how the jet is created (*1*).

The first hints of highly energetic teraelectron-volt (TeV) emission from M87 were reported by the High Energy Gamma Ray Astronomy (HEGRA) collaboration in 1998 (*2*). Since 2003, regular observations of M87 have been made by the High Energy Stereoscopic System (H.E.S.S.), sited in Namibia (*3*). Aharonian *et al.* now find evidence of fast variations in the TeV γ emission from the source in H.E.S.S. observations made during a bright phase of the jet in 2005.

The high-energy γ emission varies on a time scale of about 1 day, which is comparable to the time it takes light to cross the black hole and is therefore the shortest natural time scale of the system. This is about 10 times as fast as variations seen from M87 at any other wavelength, which points to an origin for the γ rays close to the black hole. In the optical images, there is a peculiar knot about 100 pc (1 pc = 3.26 light years) along the jet (see right panel of the figure) where some slow variations have been seen, but this is unlikely to be the source of the TeV photons because it would require the jet to be unreasonably tightly collimated there.

Variable TeV γ emission has been seen from other galactic nuclei with jets known as blazars. In these objects, we are looking more or less straight down the jet, which relativistically boosts both the energy of the emission and its observed intensity. For typical conditions, if the jet from M87 were a blazar we would have to be observing the jet within an angle of about 6°. However, the M87 jet is generally considered to be pointing at 30° to 40° or so away from our line of sight, which puts us out of the extreme blazar situation. Measuring the angle with confi-

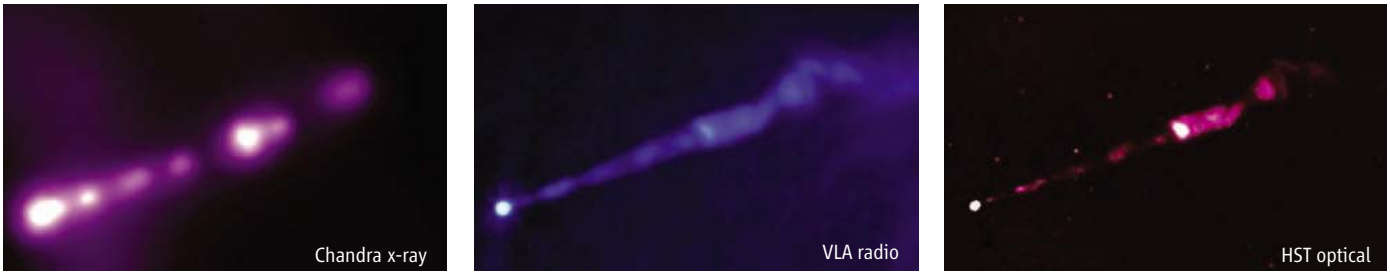

Energetic jet. The M87 jet imaged at x-ray wavelengths by the Chandra spacecraft (**left**), at radio wavelengths by the Very Large Array (**middle**), and at optical wavelengths by the Hubble Space Telescope (**right**). The view of each panel is 32 arc sec by 21 arc sec. Total length of the arc is 2000 pc.

The author is at the Institute of Astronomy, Madingley Road, Cambridge CB3 0HA, UK. E-mail: acf@ast.cam.ac.uk

dence is difficult, but evidence for apparent faster-than-light motion in the jet seen in Hubble Space Telescope images (*4*) does support a smaller value of <20°. However, the more the jet points directly at us the longer it must really be: We see a projected length of about 2 kpc, and if it is at 20° it must then be 6 kpc long. It would be surprising if one of the nearest powerful jets were pointed almost directly at us. All of this argues against M87 being a blazar.

What mechanism accelerates matter and the resulting radiation to TeV energies is not clear. Indeed, the details of how a relativistic jet is produced and accelerated remain a mystery, despite many years of study. Jet outflows are commonly found where matter accretes via a disc onto a central object, whether it be a star or a black hole. The speed of the outflow appears roughly proportional to the escape velocity from the object. The radio and optical emission in the M87 jet is polarized and is therefore synchrotron radiation that is produced when energetic electrons (or positrons) spiral around magnetic fields. Sufficiently energetic electrons then scatter the synchrotron photons up to TeV energies, particularly when highly beamed, as in a blazar. Whether such jets also contain substantial numbers of protons is uncertain, as is whether protons can produce the observed hard spectrum of high-energy γ rays observed from M87.

An exciting possibility is that the TeV emission comes from between the black hole and the inner end of the radio jet, that is, from the acceleration zone. The jet can be traced down to within a few hundreds of times the radius of the event horizon of the black hole in very-high-resolution radio images, meaning that the acceleration happens close to the black hole. It is often speculated that jets are accelerated and collimated by magnetic fields brought in with matter accreting onto the black hole. Close to the black hole, the jet may be completely dominated by magnetic fields. The particles necessary for us to see the jet are either created (as electron-positron pairs) or picked up further along the jet from the accretion flow and from the interstellar medium of the host galaxy. A black hole does not have an intrinsic magnetic field, but a rapidly spinning black hole surrounded by magnetic fields can drag the fields around with it (*5*) and, as in a pulsar, can in principle generate enormous electric fields (10^{17} V or more), which would have more than sufficient potential to create TeV photons (*6*). The accreting gas probably conducts too well and would short-circuit the generation of extreme electric fields, however.

In terms of energy output, the TeV emission in M87 is only a few times 10^{40} erg s^{-1}, whereas the jets probably have a mechanical power 100 to 1000 times as large, as indicated by the bubbles created by them in the surrounding hot gas (*7*). Therefore, TeV emission could be a minor energy loss from the jet, unless much more TeV power is beamed out of our line of sight. Even if it is minor in power, it may still be of great importance if it is our only direct probe of the acceleration region.

NASA's Gamma Ray Large Area Space Telescope (GLAST) should be launched in less than a year, detecting γ rays up to 0.3 TeV, which nicely complements the ground-based Cerenkov telescopes like H.E.S.S. that operate at higher energy. Blazars will be among the prime targets for these instruments, but objects such as M87 and other radio galaxies where the jet is not pointing directly our way will make for interesting observing. If all goes well, we shall understand how the jet in M87 operates before the centenary of its discovery takes place.

References

1. F. Aharonian *et al.*, *Science* **314**, 1424 (2006). Published online 26 October 2006; 10.1126/science.1134408.
2. M. Beilicke *et al.*, *New Astron. Rev.* **48**, 407 (2004).
3. F. Aharonian *et al.*, *Astron. Astrophys.* **403**, L1 (2003).
4. J. A. Biretta, W. B. Sparks, F. Macchetto, *Astrophys. J.* **520**, 621 (1999).
5. R. D. Blandford, R. L. Znajek, *Mon. Not. Roy. Astron. Soc.* **179**, 433 (1977).
6. R. L. Znajek, *Mon. Not. Roy. Astron. Soc.* **185**, 833 (1978).
7. A. J. Young, A. S. Wilson, C. G. Mundell, *Astrophys. J.* **579**, 560 (2002).

10.1126/science.1136199

ATMOSPHERE

When Dry Air Is Too Humid

Thomas Peter, Claudia Marcolli, Peter Spichtinger, Thierry Corti, Marcia B. Baker, Thomas Koop

Analyses of upper tropospheric humidity are forcing reassessment of how ice clouds form.

As moist air rises to colder regions in the atmosphere, the humidity rises above its equilibrium value over ice. To relax this metastability, the air releases its water vapor via ice cloud formation. Such atmospheric ice clouds form in two steps: First, ice nucleates in or on existing aerosol particles; second, these ice particles grow through condensation of supersaturated water vapor onto the ice surfaces. Recent field observations (*1*–*3*) call into question the basic principles underpinning the current understanding of ice cloud formation and alter the assessment of water distribution in the upper troposphere.

The governing quantity for nucleation and growth is the excess activity relative to the equilibrium humidity over ice, also called ice supersaturation (expressed as a percentage). The equilibrium humidity decreases strongly with falling temperature. Hence, when an ascending air mass cools, it can become supersaturated with respect to ice. Ice nucleation requires a supersaturation above a critical threshold value. Nucleation can occur homogeneously from aqueous solution droplets, or heterogeneously on particles known as ice nuclei. At upper-troposphere temperatures, homogeneous freezing sets in at a supersaturation of ~60% (*4*); lower supersaturations are sufficient for heterogeneous nucleation. After nucleation, vapor molecules condense onto the ice particles, causing them to grow and the gas phase to become depleted in water until equilibrium is reached (see the green curves in the figure).

Large-scale regions of persistent supersaturation up to 60% outside ice clouds are not unexpected in the absence of ice nuclei. Yet values even above 100% have been observed in cloud-free regions (*1*) (red curves in the figure). These values are far above the critical value for homogeneous ice nucleation (*5*) or cloud chamber data (*6*).

At least as puzzling are supersaturations of 30% reported to persist inside ice clouds and contrails (*2*) for at least 1 hour of aircraft measurement time (*3*) (orange curves in the figure). Such large supersaturations are expected to relax rapidly as a result of fast vapor condensation (*7*) unless continuous cooling remains sufficiently strong. To achieve such cooling, the clouds would have to rise by several kilometers in the measurement time, which contradicts the observations.

Th. Peter, C. Marcolli, P. Spichtinger, and T. Corti are at the Institute for Atmospheric and Climate Science, Eidgenössische Technische Hochschule (ETH) Zürich, 8092 Zürich, Switzerland. E-mail: thomas.peter@ethz.ch M. B. Baker is in the Department of Atmospheric Sciences, University of Washington, Seattle, WA 98195, USA. T. Koop is in the Department of Chemistry, Bielefeld University, D-33615 Bielefeld, Germany.

PICTURE YOURSELF AS A AAAS SCIENCE & TECHNOLOGY POLICY FELLOW!

Advance your career and serve society by plugging the power of science into public policy. Year-long Science & Technology Policy Fellowships offer opportunities in six thematic areas: Congressional • Diplomacy • Energy, Environment, Agriculture & Natural Resources • Global Stewardship • Health, Education, & Human Services • National Defense & Global Security.

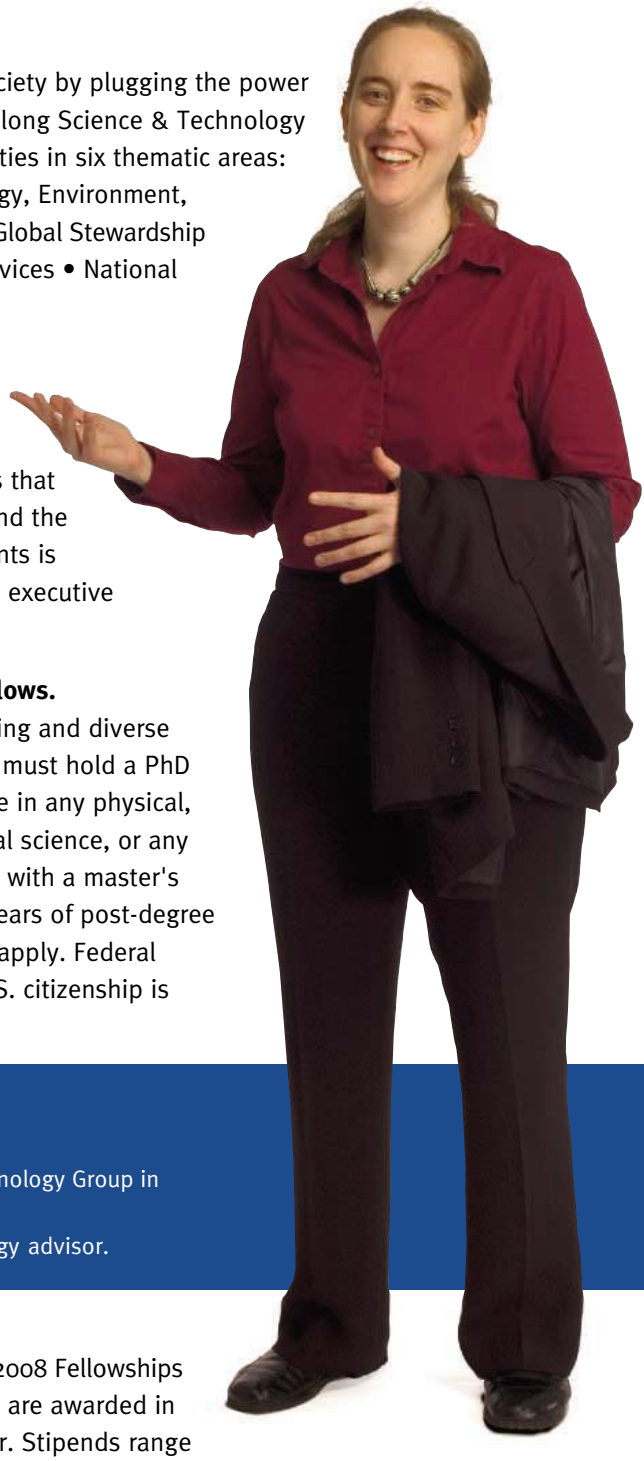

Work in Dynamic Washington, D.C.
Since 1973, AAAS Fellows have been applying their expertise to federal decision-making processes that affect people in the U.S. and around the world. A broad range of assignments is available in the U.S. Congress and executive branch agencies.

Join a Network of Nearly 2,000 Fellows.
AAAS Fellows benefit from a growing and diverse network of colleagues. Applicants must hold a PhD or equivalent doctoral-level degree in any physical, biological, medical/health, or social science, or any engineering discipline. Individuals with a master's degree in engineering and three years of post-degree professional experience also may apply. Federal employees are not eligible and U.S. citizenship is required.

Enhancing Public Policy, Advancing Science Careers

Kathy Kahn, PhD

Interdisciplinary Biological Sciences, University of Missouri.

2004-2006 AAAS Fellow at the U.S. Department of Agriculture, Biotechnology Group in the Foreign Agricultural Service.

Recently hired by her fellowship office as an agricultural biotechnology advisor.

Apply Now!
Application deadline for the 2007-2008 Fellowships is 20 December 2006. Fellowships are awarded in the spring and begin in September. Stipends range from $67,000 to $87,000, depending on experience.
To apply: fellowships.aaas.org

AAAS
ADVANCING SCIENCE, SERVING SOCIETY

Measuring water in the upper troposphere is difficult. A major international effort to assess water vapor measurements in the upper troposphere and stratosphere concluded that, on the basis of laboratory calibrations, typical mean accuracies of aircraft and balloon instruments were on the order of 10% (*8*). However, direct comparisons in the upper troposphere suggest that differences between various instruments on aircraft and balloons often exceed 25%, especially when temperatures are very low (*9*). Also, balloon-borne instruments appear to yield mostly lower supersaturations than do aircraft instruments (*10*). Nonetheless, large supersaturations were observed during all recent aircraft and balloon campaigns; these studies used a range of instruments based on different measurement principles (*11*). Hence, only a fraction of the observed supersaturations can be ascribed to instrumental inaccuracies.

The theoretical assumptions underlying modeling of ice cloud formation should also be reassessed. How can we explain ice nucleation in light of the extreme supersaturations observed in cloud-free regions, and ice growth in light of the persistent supersaturations observed within dense ice clouds?

Outside ice clouds, the supersaturation at which ice nucleation occurs depends on the equilibrium vapor pressure of supercooled water. Measured data only exist down to ~235 K and must be extrapolated to lower temperatures (*12*), possibly leading to errors of up to 20%. Moreover, although air masses appear to always contain sufficient numbers of aerosol particles for cloud formation, the composition of these aerosols might inhibit ice nucleation. The homogeneous ice nucleation threshold of 60% was established for atmospherically relevant salt solutions and sulfuric acid, but only for a few organic species. Cloud chamber data indicate that aerosols containing only organic and elemental carbon may be almost completely unable to nucleate ice (*13*). Alternatively, if water-rich aerosols were fully covered with organic surfactants, nucleation might be suppressed if it started preferentially at the surface (*14*). In field experiments, the presence of organic pollutants has indeed been associated with impeded ice particle formation (*15*). However, laboratory data of surface nucleation and field data on particle composition and surface morphology of upper tropospheric aerosols are too limited to allow any conclusions to be drawn.

Inside sufficiently dense ice clouds, condensation should rapidly reduce vapor pressures in excess of the equilibrium vapor pressure of ice. However, errors in this equilibrium value might lead to perceived supersaturation. Laboratory data show (*16*) that below 200 K, cubic ice (a metastable form of ice) nucleates first and might persist in clouds. The equilibrium vapor pressure for cubic ice is ~10% higher than that for stable hexagonal ice (*17*).

But even after an ice crystal has nucleated and transformed into hexagonal ice, surface effects might hinder its growth. It is usually assumed that most water molecules hitting the crystal are built into the lattice, but recent laboratory data indicate that this is the case for fewer than 10% (*18*) or even as few as 0.4% (*19*) of water molecules. Furthermore, gas-phase species such as nitric acid may selectively block the growth sites on ice crystals (*2*), although this hypothesis needs support from laboratory studies.

Further reasons for the observed supersaturations may be related not to the properties of individual ice particles, but to effects on larger scales. The presence of ice nuclei in cloud-free air may initiate ice nucleation below the homogeneous-nucleation threshold, leading to clouds with low ice particle number densities, in which supersaturations might be sustained for relatively long periods. Also, conditions within clouds might fluctuate faster than aircraft-borne instruments can resolve, causing apparent supersaturation by averaging over glaciated and ice-free supersaturated patches. Verification of such effects will have to await higher-resolution instrumentation.

None of these hypotheses is likely to be the sole explanation for the observed high supersaturations outside and inside ice clouds. The uncertainties in the expressions used to retrieve the supersaturation from the data must be resolved and their usage clarified (*12*). Uncertainties in the aircraft and balloon data must be determined accurately. In addition, mesoscale meteorological fluctuations must be characterized, theories of ice nucleation and growth must be reassessed, and state-of-the-art numerical models must be compared. Six years after a major effort to characterize the distribution of upper atmospheric water (*8*), the issue is again open, and, because of its climatic importance, more pressing than ever.

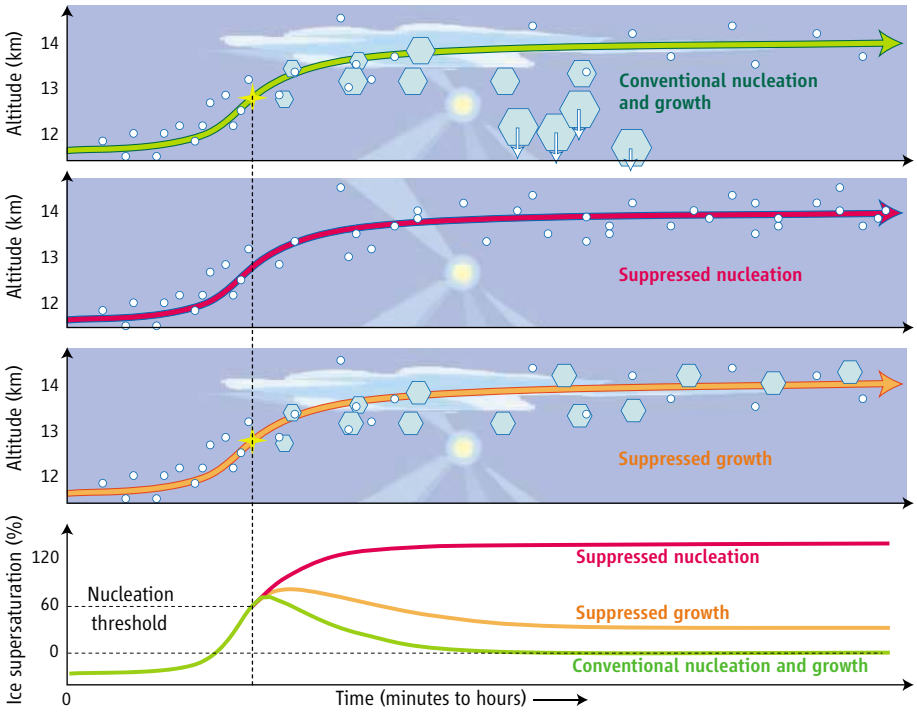

Rising air and ice cloud formation. The top three panels sketch three scenarios for the formation of ice clouds along an ascending air parcel trajectory; the bottom panel sketches the effect of these scenarios on supersaturation. According to conventional understanding, ice particles nucleate (star), grow, and reduce the supersaturation (green curves). Recent observations suggest suppressed nucleation (red curves) or suppressd growth (orange curves) in large parts of the atmosphere.

References and Notes

1. E. J. Jensen *et al.*, *Atmos. Chem. Phys.* **5**, 851 (2005).
2. R. S. Gao *et al.*, *Science* **303**, 516 (2004).
3. S. H. Lee *et al.*, *J. Geophys. Res.* **109**, D20209, 10.1029/2004JD005033 (2004).
4. T. Koop *et al.*, *Nature* **406**, 611 (2000).

5. In a cooling event, when aerosol particles are exposed to a supersaturation of 60%, the characteristic time for ice nucleation is ~1 min. This drops to <1 s for the atmospheric measurements described in (*1*).
6. J. P. D. Abbatt *et al.*, *Science* **313**, 1770 (2006); published online 30 August 2006 (10.1126/science.1129726).
7. The characteristic time to consume the supersaturation due to vapor condensation is determined by how rapidly gas-phase water molecules can diffuse to and accommodate on ice surfaces. For the ice clouds described in (*2*), this time should be ~1 min.
8. D. Kley, J. M. Russell III, C. Phillips, Eds., *SPARC Assessment of Upper Tropospheric and Stratospheric Water Vapour* (www.aero.jussieu.fr/~sparc/WAVASFINAL_000206/WWW_wavas/Cover.html).
9. H. Vömel, in *Report from the NDACC Meeting on Atmospheric Water Vapour Measurement*, G. Braathen, Ed. (Univ. of Bern, Bern, Switzerland, 2006); www.iapmw.unibe.ch/research/collaboration/ndsc-microwave/workshop2006).
10. H. Vömel *et al.*, *J. Geophys. Res.* **107**, 10.1029/2001JD000707 (2002).
11. A. Korolev, G. A. Isaac, *J. Atmos. Sci.* **63**, 2865 (2006).
12. D. M. Murphy, T. Koop, *Q. J. R. Meteorol. Soc.* **131**, 1539 (2005).
13. O. Möhler *et al.*, *Meteorol. Z.* **14**, 477 (2005).
14. A. Tabazadeh, Y. S. Djikaev, H. Reiss, *Proc. Natl. Acad. Sci. U.S.A.* **99**, 15873 (2002).
15. P. J. DeMott *et al.*, *Proc. Natl. Acad. Sci. U.S.A.* **100**, 14655 (2003).
16. B. J. Murray, D. A. Knopf, A. K. Bertram, *Nature* **434**, 202 (2005).
17. J. E. Shilling *et al.*, *Geophys. Res. Lett.* **33**, L17801, 10.1029/2006GL026671 (2006).
18. P. Pratte, H. van den Bergh, M. J. Rossi, *J. Phys. Chem. A* **110**, 3042 (2006).
19. N. Magee, A. M. Moyle, D. Lamb, *Geophys. Res. Lett.* **33**, L17813, 10.1029/2006GL026665 (2006).

10.1126/science.1135199

CELL BIOLOGY

Tools to Tamper with Phosphoinositides

Rapidly depleting or elevating specific phosphoinositide lipids in the plasma membrane reveals their role in controlling cellular processes.

Stuart McLaughlin

The lipid phosphatidylinositol 4,5-bisphosphate (PIP_2) both regulates many different processes at the cell's plasma membrane (*1*) and is the source of three "second messenger" molecules that transmit signals throughout the cell. This multiplicity of functions can make it difficult to sort out whether a particular regulatory activity of PIP_2—for example, activating an ion channel or anchoring a peripheral protein to the plasma membrane—is due to direct interaction or indirect effects related to the second messengers. Moreover, the toolbox for investigating the role of lipids in cell signaling is limited compared to that available for studying specific proteins. Two reports in this issue highlight the utility of a new tool that rapidly depletes the plasma membrane of PIP_2 without producing the three signaling molecules. On page 1454, Suh *et al.* (*2*) show that PIP_2 acts directly on a K^+ ion channel to modulate its activity in the plasma membrane, and on page 1458, Heo *et al.* (*3*) demonstrate that phosphoinositides probably target guanosine triphosphatases (GTPases) to the plasma membrane. This and related tools described in the papers open the door for new investigations of phosphoinositide function in living cells.

The ion channel report starts from the earlier observation that muscarinic receptor–triggered phospholipase C (PLC) activation closes KCNQ (Kv7) K^+ channels (*2*). PLC could directly induce closing of this channel by depleting the plasma membrane PIP_2, which binds to and activates the channel (see the figure). Alternatively, PLC-catalyzed hydrolysis of PIP_2 produces the second messengers inositol 1,4,5-trisphosphate (IP_3) and diacylglycerol (DAG) (see the figure). This leads to the activation of protein kinase C and Ca^{2+}-calmodulin, which also affect KCNQ channel activity. Suh *et al.* engineered a lipid phosphatase that, when bound to a rapamycin analog, can translocate rapidly from the cytoplasm to the plasma membrane, where it removes a 5′ phosphate from PIP_2 (see the figure). Depleting the PIP_2 causes the KCNQ current measured in cultured mammalian cells to fall promptly to zero, without changing Ca^{2+}, DAG, or IP_3 concentrations.

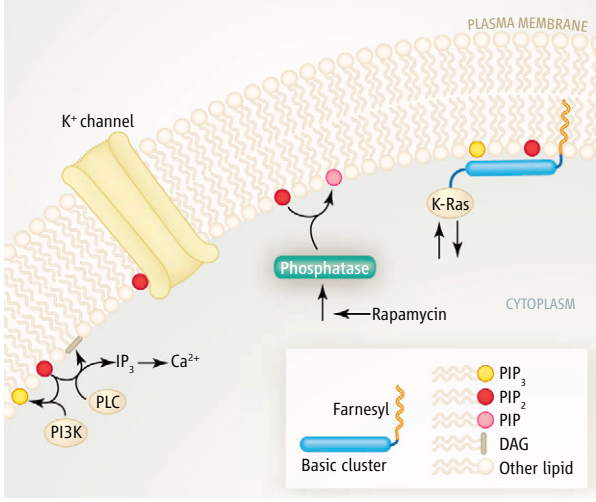

PIP_2, potassium channels, and peripheral proteins. Lipid phosphatase-based tools that manipulate the amount of phosphatidylinositol 4,5-bisphosphate (PIP_2) in the plasma membrane of living cells (by translocating to the membrane upon addition of rapamycin) reveal that this phosphoinositide regulates a potassium channel and helps anchor K-Ras and other GTPases to the plasma membrane. PIP_2 is also the source of three signaling molecules: Phosphorylation by phosphatidylinositol 3-kinase (PI3K) yields phosphatidylinositol 3,4,5-trisphosphate (PIP_3); hydrolysis by phospholipase C (PLC) yields diacylglycerol (DAG) and inositol 1,4,5-trisphosphate (IP_3). PIP, phosphatidylinositol 4-phosphate.

The second report focuses on the role of PIP_2 and phosphatidylinositol 3,4,5-trisphosphate (PIP_3) in binding members of the Ras, Rab, Arf, and Rho families of GTPases to the inner leaflet of the plasma membrane. Heo *et al.* imaged the subcellular location of 125 fluorescently tagged GTPases in cultured mammalian cells to survey plasma membrane–targeting mechanisms. One of their important observations is that of the 50 GTPases that localize to the plasma membrane, 40 contain a cluster of basic (positively charged) amino acids.

Unstructured clusters of basic residues target a wide variety of peripheral proteins to the plasma membrane—but how? Work from several laboratories, including those of Meyer (*3*) and Grinstein (*4*), established that a cluster of about eight positively charged lysine residues in the carboxyl terminus of the GTPase K-Ras, which acts in concert with a farnesyl lipid moiety, targets and anchors the protein to the inner leaflet of the plasma membrane (see the figure). Is this a general electrostatic effect mediated by the predominant acidic (negatively

The author is in the Department of Physiology, Stony Brook University, Stony Brook, NY 11794–8661, USA. E-mail smclaughlin@notes.cc.sunysb.edu

charged) phosphatidylserine lipids in the plasma membrane, or do the much less abundant phosphoinositides PIP_2 and PIP_3 play a key role in targeting?

Heo *et al*. used the same conjugated form of a constitutively active yeast lipid phosphatase to study the potential role of PIP_2 in GTPase–plasma membrane interactions. Using the phosphatase, rather than PLC, to deplete the plasma membrane of PIP_2 had little effect on the membrane association of the GTPases (PLC-mediated hydrolysis of PIP_2 leads to activation of protein kinase C and Ca^{2+}-calmodulin, both of which cause K-Ras to move off the membrane). This was not surprising, because previous work showed that K-Ras binds well to phospholipid vesicles with putative physiological levels (20%) of monovalent phosphatidylserine (*4*). The surprise came when cells were also treated with inhibitors of phosphatidylinositol 3-kinase to reduce both PIP_2 and PIP_3 in the membrane: K-Ras4B and the other GTPases with a cluster of basic residues translocated from the plasma membrane. The authors conclude that both phosphoinositide molecules target and anchor clusters of basic residues to the plasma membrane.

This conclusion may generate controversy for two reasons. First, it challenges the common wisdom that PIP_3 "is present in negligible amounts in resting cells" (*1*). Second, it challenges the hypothesis, first put forth by Silvius, that the cluster of basic residues on a GTPase associates with the plasma membrane because its inner leaflet may contain a higher mole fraction of phosphatidylserine than the cytoplasmic leaflets of intracellular organelle membranes, and thus has a more negative surface potential (*5*). However, data in Yeung *et al*. (*4*) support the conclusion that it is PIP_2 and PIP_3 (*3*), rather than phosphatidylserine, that likely target K-Ras to the plasma membrane.

Experiments on model phospholipid membranes and theoretical calculations explain why clusters of basic residues in proteins require neither structure nor specific sequences to laterally sequester polyvalent PIP_2 and PIP_3. These clusters produce a local positive electrostatic potential that extends about 1 nm from the region and acts as a deep "basin of attraction" for multivalent negatively charged phosphoinositides (*6*). Uncertainty about several factors—for example, the free concentration and lateral distribution of lipids in biological membranes or the proximity of acidic residues to the basic cluster—means that experiments on model membranes cannot be used to tease out the relative importance of phosphatidylserine or phosphoinositides in targeting or anchoring peripheral proteins with clusters of basic residues to the plasma membrane. The results on GTPases suggest that the phosphoinositides PIP_2 and PIP_3 may be more important (*3*).

The new lipid phosphatase (and kinase) tools should also prove useful for investigating the binding of other proteins with membrane-sticky clusters of basic residues [for example, the scaffolding protein gravin and the protein kinase Src] and the many other plasma membrane processes involving PIP_2 and PIP_3 (*1*). Indeed, a different group recently used essentially the same phosphatase tool to investigate how PIP_2 affects both endocytosis and the transient receptor potential melastatin 8 (TRPM8) Ca^{2+} conducting channel (*7*). If you are interested in the many functions of the phosphoinositides in the plasma membrane, and how the new tools can be used to investigate these functions, read these important reports (*2*, *3*, *7*).

References

1. G. Di Paolo, P. De Camilli, *Nature* **443**, 651 (2006).
2. B.-C. Suh, T. Inoue, T. Meyer, B. Hille, *Science* **314**, 1454 (2006); published online 21 September 2006 (10.1126/science.1131163).
3. W. D. Heo *et al. Science* **314**, 1458 (2006); published online 9 November 2006 (10.1126/science.1134389).
4. T. Yeung *et al*., *Science* **313**, 347 (2006).
5. W. Cho, R. V. Stahelin, *Annu Rev. Biophys. Biomol. Struct.* **34**, 119 (2005).
6. S. McLaughlin, D. Murray, *Nature* **438**, 605 (2005).
7. P. Varnai, B. Thyagarajan, T. Rohacs, T. Balla, *J. Cell Biol.* **175**, 377 (2006).

Published online 9 November 2006;
10.1126/science.1136314
Include this information when citing this paper.

GENETICS

Delivering New Disease Genes

Lon R. Cardon

Complex diseases represent an extraordinary challenge to geneticists, but recent results are revealing some successful strategies.

Since the human genome was sequenced, advances in human genetics research have steadily built momentum toward identifying genes that influence common human diseases. Validation of millions of genetic variants, rapid advances in genotyping technologies, and the ongoing establishment of repositories of large, population-based patient samples have created expectations of imminent discoveries of prized disease genes. Have these activities truly laid the foundation for gene identification? On page 1461 of this issue, Duerr *et al*. (*1*) demonstrate an association between variants in the *IL23R* gene and Crohn's disease, a common inflammatory condition of the gastrointestinal tract. Their results show that complex disease genes are finally yielding their secrets and provide crucial validation of the long journey to gene discovery.

Enhanced online at www.sciencemag.org/cgi/content/full/314/5804/1403

Duerr *et al*. used a genome-wide association approach premised on a simple idea: Assay genomic DNA from a sample of cases (diseased patients) and controls for a very large number of genetic variants, or single-nucleotide polymorphisms (SNPs); then, at each SNP site, compare the frequencies among cases and controls (Duerr *et al*. examined more than 300,000 SNPs). Sites that differ significantly between cases and controls are then validated in independent samples. In practice, of course, genome-wide association is more complicated. Individual differences in most common diseases are thought to arise from a relatively small number of genes (numbering in the tens to hundreds), most of which contribute only modestly to the overall disease risk (*2*). Therefore, in a large-scale association screen, most disease gene variants are expected to produce only a small "signal" that is difficult to detect among a large number of SNPs. One big question is how many (if any) of the signals will be large enough to separate from the "noise" (*3, 4*). The answer from the *IL23R* study is not many, but even a few may be enough to help uncover significant novel disease-associated variants.

The genome-wide association screen of Duerr *et al*. revealed three SNPs with evidence for disease association more than 100 times as large as that of the next most statistically significant SNP. In genome-wide association scans, such SNPs are usually either artifacts due to genotyping error, or rarely observed examples of variants with large

The author is at the Wellcome Trust Centre for Human Genetics, University of Oxford, Oxford OX3 7BN, UK, and Fred Hutchinson Cancer Research Center, Seattle, WA 98109, USA. E-mail: lon.cardon@well.ox.ac.uk

Thank you

to all of the sponsors and supporters of the 2007 AAAS Annual Meeting

SUBARU

Roche Pharmaceuticals

National Science Foundation

P&G beauty

L'ORÉAL

MERCK

The Science Channel

SUPPORTERS

Lawrence Livermore National Laboratory

European Commission

New Zealand Ministry of Research, Science, and Technology

Exploratorium

To become an exhibitor or sponsor of the meeting contact
Jill C. Perla
Manager of Marketing, Exhibits, and Sponsors
E-mail: jperla@aaas.org
Phone: 202-326-6736
Web site: http://www.aaasmeeting.org

In addition, generous funding for AAAS Awards was provided by Johnson & Johnson Pharmaceutical Research & Development L.L.C., GE Healthcare, and Affymetrix.

AAAS
ADVANCING SCIENCE, SERVING SOCIETY

phenotypic effects. Distinguishing these two outcomes is challenging because there is little statistical and experimental information to guide the process (*5*). Duerr *et al.* found that two of the three SNPs with the strongest evidence for association are in a well-known susceptibility gene (*CARD15*) for Crohn's disease (*6*, *7*), and the third is a nonsynonymous coding change in *IL23R*, a gene encoding a receptor for the proinflammatory cytokine interleukin-23. Thus, two of the top three hits validated the genome-wide association proof-of-principle, and the third was either an artifact or a true positive result.

Replication of genome-wide association findings is essential to distinguish these possibilities. Unfortunately, replication has not been an area of strength in genetic association studies (*4*). In this case, however, Duerr *et al*. replicated the *IL23R* finding unambiguously, revealing strong statistical support for the same SNP, with the same risk allele, and in the same specific phenotypes in larger independent samples of disease patient cases, controls, and families. Together with the recent identification of genes associated with age-related macular degeneration by similar techniques (*8*, *9*), the *IL23R* finding should help future studies, as researchers can better understand the statistical profiles of genuinely associated disease alleles.

The finding of an association between *IL23R* and Crohn's disease has already led to other discoveries. Duerr *et al*. examined the chromosomal locations of their remaining genome-wide association SNPs to see if others were in the same region as the *IL23R* gene. Many were, some of which had supportive but not striking statistical evidence for association. Replication studies and further statistical analysis suggest that several of these SNPs contribute independently to Crohn's disease. These loci of smaller effect were detectable because of the initial discovery of the highly significant variant (see the figure).

Should we be surprised that the genome-wide association revealed only one unambiguous novel SNP for the disease of interest? Probably not. The Crohn's disease sample size of 547 cases and 548 controls is small for such a study, having the statistical power to detect only large genetic effects, of which there are likely few in the genome. The problem of statistical power is especially salient when the associated variant occurs at low frequency, such as the *IL23R* variant studied by Duerr *et al*., which has a frequency of 2 to 3%. Larger sample sizes will be needed to identify more disease loci.

There are at least two important lessons in the strategy used to uncover *IL23R* and the macular degeneration genes. First, though the initial genome-wide association discoveries may uncover relatively few "low-hanging fruit"—especially with small sample sizes—they may lead to identifying more stubborn variants with smaller effect size (*10*–*12*). Second, every SNP counts. Had the one highly significant SNP not been included in the genome-wide association panel by Duerr *et al*., the entire discovery might have been delayed or even missed

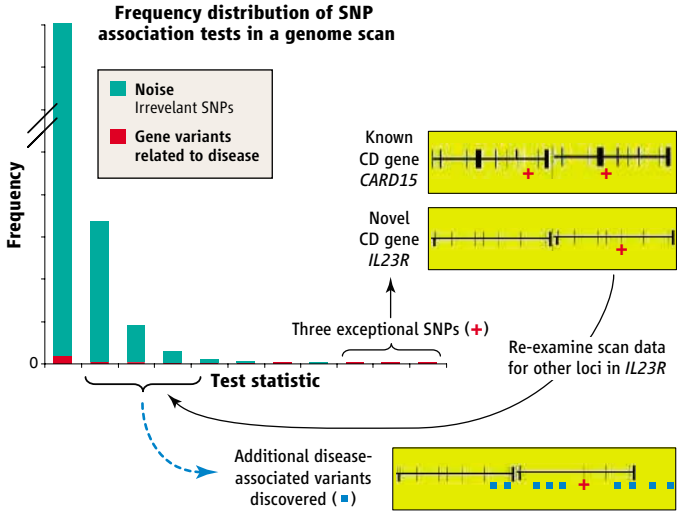

Cascade of discovery. Common human diseases are thought to have few disease loci (red) relative to the number of single-nucleotide polymorphisms (SNPs) tested (green), and most of the true loci will have a small effect. The greatest statistical power is thus attributed to loci that occur least frequently in the genome. Duerr *et al*. found three SNPs associated with Crohn's disease (CD), two in a known disease gene and one in the *IL23R* gene. This allowed them to extract other real SNP-disease associations embedded in the noise of the initial genome-wide scan.

Dozens of genome-wide association studies are under way, and many more are planned. So why have Crohn's disease and age-related macular degeneration been the particular traits to yield such striking results? One reason relates to phenotypic specificity. To reduce pathogenic and genetic heterogeneity, Duerr *et al*. focused initially on patients with a specific type of Crohn's disease and further conditioned on genetic backgrounds having known differences in Crohn's disease prevalence. Similarly, the findings on age-related macular degeneration resulted from a series of refined phenotypic classifications. This careful attention to phenotypes reduces a primary source of heterogeneity and is thus directly beneficial to genome-wide association studies.

The comulative effect of all of these aspects of the *IL23R* study is to lend confidence in the results, which is not always readily apparent in other designs. A recent study of association between the *KIBRA* gene and human memory (*13*) adopted an entirely different design, using pooled DNA samples in multistage genotyping, analyzing different memory measures in the primary and replication phases, and studying patient samples from different geographic locations, some with high levels of population substructure. These phenotypic and sampling differences may eventually support the generality of the reported finding, but they will complicate interpretations of external confirmation because the hypotheses generated may be difficult to falsify—negative results could reflect either measurement differences or lack of replication, whereas strictly positive associations would require firm concordance in phenotypes and sampling to demonstrate consistency.

Not all genome-wide association studies will be as successful as the *IL23R* finding. Sample size will be a key determinant of outcome, as will genetic, population, and phenotypic heterogeneity. In addition, it is increasingly important to present data and results for all analyses conducted, which is one of the few shortcomings of the Duerr *et al.* report. In any case, results from the current generation of genetic studies should help provide a foundation for the next set of problems, involving detection of rare genetic variants, leveraging the genetics to better understand environmental risk factors, and ultimately, using this hard-won information to improve public health.

References

1. R. H. Duerr *et al.*, *Science* **314**, 1461 (2006); published online 26 October 2006 (10.1126/science.1135245).
2. K. T. Zondervan, L. R. Cardon, *Nat. Rev. Genet.* **5**, 89 (2004).
3. W. Y. Wang, B. J. Barratt, D. G. Clayton, J. A. Todd, *Nat. Rev. Genet.* **6**, 109 (2005).
4. L. J. Palmer, L. R. Cardon, *Lancet* **366**, 1223 (2005).
5. D. G. Clayton *et al.*, *Nat. Genet.* **37**, 1243 (2005).
6. Y. Ogura *et al.*, *Nature* **411**, 603 (2001).
7. J. P. Hugot *et al.*, *Nature* **411**, 599 (2001).
8. R. J. Klein *et al.*, *Science* **308**, 385 (2005).
9. A. DeWan *et al.*, *Science* **314**, 989 (2006).
10. M. Li *et al.*, *Nat. Genet.* **38**, 1049 (2006).
11. B. Gold *et al.*, *Nat. Genet.* **38**, 458 (2006).
12. J. Maller *et al.*, *Nat. Genet.* **38**, 1055 (2006).
13. A. Papassotiropoulos *et al.*, *Science* **314**, 475 (2006).

10.1126/science.1136668

RETROSPECTIVE

Edward I. Stiefel (1942–2006)

François M. M. Morel and John T. Groves

E. I. Stiefel was a bioinorganic chemist whose insights into the roles of metals in living systems have led to practical applications and new research ideas.

Edward I. Stiefel, an unusual chemist who bridged industry and academia, pure chemistry and applications, and bioinorganic and environmental chemistry, died on 4 September 2006 in Robert Wood Johnson Hospital, New Brunswick, New Jersey. His insights into the functions of metals in living systems led to a new understanding of key biological processes, new technological applications, and a better appreciation of the interactions among the cycles of trace and major elements on Earth, both today and in the past.

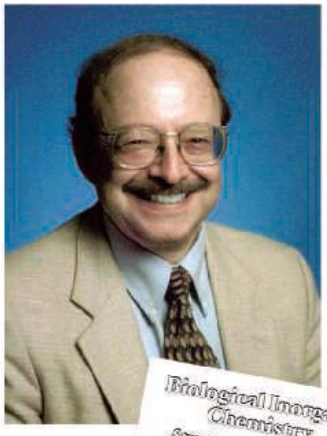

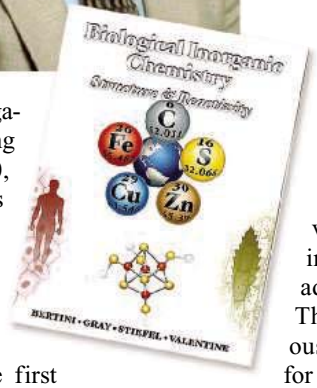

Ed grew up in Brooklyn, New York. He received his Ph.D. with Harry Gray at Columbia University in 1967 and then served on the faculty at the State University of New York at Stony Brook, before becoming a senior investigator at the Charles F. Kettering Research Laboratory. In 1980, he joined the Catalytic Materials Group at Exxon's Corporate Strategic Research Center in Annandale, New Jersey. Following his retirement from ExxonMobil in 2001, Ed accepted a position at Princeton University as the first holder of the Ralph W. Dornte Chair, a distinguished visiting lecturer position with the rank of professor.

Ed's research interests involved the bioinorganic, coordination, and environmental chemistry of transition-metal ions, particularly iron and molybdenum. While at Kettering, he codiscovered bacterioferritin, the iron storage protein of prokaryotes (*1*), and made pioneering advances in our understanding of nitrogenase enzymes, illuminating the role of molybdenum in catalyzing the conversion of atmospheric nitrogen to ammonia.

His arrival at Exxon made an immediate impact on the company, vastly increasing the interdisciplinary research by the company's Catalytic Materials Group. He initiated discussions concerning the active centers of nitrogenase and other molybdenum enzymes that bridged "industrial" and "biological" catalysis. This new insight led him to wonder whether tungsten-associated enzymes might exist that would be analogous to known molybdenum enzymes. Stiefel predicted the existence of such enzymes before their discovery in *Pyrococcus furiosus*, a microbe that thrives in the boiling waters of hot springs (*2*).

> "In every problem he tackled, he had **a phenomenal ability to see the big picture.**"
>
> —Harry Gray

While at Exxon, Ed developed many new molybdenum compounds that have proven useful as catalysts and lubricating oil additives. For example, he was the principal inventor of the commercially important "thiomolybdate" additive for lubricating oils. This compound had previously been used as a catalyst for the desulfurization of crude oil and was found to make the oil more slippery and less prone to oxidize.

His knowledge of the bioinorganic chemistry and biology of metalloenzymes proved to be invaluable when he became one of the principal architects of the cleanup after the *Exxon Valdez* oil spill in Alaska in 1989. This massive effort successfully applied the principles of bioinorganic chemistry and microbiology to a very-large-scale environmental remediation project. Ed's interdisciplinary interests also shaped the science agenda and recruitment strategies of Exxon's Corporate Strategic Research Center. Ed's genius lay in his ability to understand complex chemical issues over a wide range of scales, from molecular to cellular to global.

At Princeton, Ed was instrumental in developing three very popular courses: a freshman seminar entitled "Elements of Life"; a graduate-level course on "Metals in Biology" (jointly with J. T. Groves); and, in collaboration with colleagues, an innovative multidepartmental course on "Life in the Universe," which was instrumental in doubling the number of chemistry majors. Students in Ed's courses revered him. The evening freshman seminars kept students on the edge of their seats and often went on well into the night.

Ed held 30 U.S. patents and published more than 150 scientific articles. His review article on "The Coordination and Bioinorganic Chemistry of Molybdenum" has been cited in more than 800 publications. And his contributions to science and his inspiration to students and colleagues are continuing. He is the coauthor of several articles that are in various stages of publication, some of which bring together the various strands of his multifaceted career. One upcoming article deals with the function of iron storage proteins in ocean regions where life is limited by the availability of iron (*3*). He is a coeditor of the book *Biological Inorganic Chemistry: Structure and Reactivity*, which has just been published (*4*) and is destined to become a classic.

Ed Stiefel was a joyful man, a compassionate friend, an inspiring teacher, and a generous colleague. At a recent colloquium at Princeton, his close friend and early mentor Harry Gray most concisely described what it meant to have Ed Stiefel as a colleague: "A discussion of a research problem with Ed was really special. He understood the roles metals play in living systems better than anyone. In every problem he tackled, he had a phenomenal ability to see the big picture. He was a scholar's scholar." He is survived by his wife Jeannette, a frequent visitor and friend of the Princeton Chemistry Department, and their daughter Karen.

The authors are in the Department of Geosciences and Chemistry, Princeton University, Princeton, NJ 08544, USA. E-mail: morel@princeton.edu; jtgroves@princeton.edu

References

1. E. I. Stiefel, G. D. Watt, *Nature* **279**, 81 (1979).
2. S. Mukund, M. W. W. Adams, *J. Biol. Chem.* **265**, 11508 (1990).
3. M. Castruita *et al.*, in preparation.
4. I. Bertini, H. B. Gray, E. I. Stiefel, J. S. Valentine, Eds., *Biological Inorganic Chemistry: Structure and Reactivity* (University Science Books, Sausalito, CA 2006).

10.1126/science.1136957

CREDITS: EXXONMOBIL

ALA
Association for Laboratory Automation

Be Part Of It!
LabAutomation2007

The premier conference and exhibition on emerging and merging laboratory technologies, offering a compelling educational program featuring five tracks:

- Detection and Separation
- Micro- and Nanotechnologies
- High-Throughput Technologies
- Informatics
- Emerging Areas in Laboratory Automation

What's New?

- The Laboratory of the Future – Peter Grandsard Ph.D., Director of Research, Amgen
- Innovation Ave*NEW* – an exhibition of the world's leading start-up companies serving the laboratory automation community
- A New and Expanded ALA Career Fair – featuring practical sessions and one-to-one consultations
- Late Night With LRIG – A Rapid-Fire Exchange on Innovative Products & Services
- The ALA Medal of Excellence Award Sponsored by Symyx Technologies, Inc.
- More than 100 podium presentations, and 19 hands-on and engaging short courses

Short Courses: January 27-28
Conference: January 28-31
Exhibition: January 28-30

Palm Springs Convention Center
Palm Springs, California

LabAutomation 2007

Where laboratory technologies emerge and merge

Register Today!

Visit **labautomation.org/LA/LA07** for more information, including travel and housing information.

ALA is a non-profit association committed to driving progress in laboratory technologies through high-quality education that benefits the global scientific community, including its membership of scientists, academicians, and industry thought leaders.

Science & Engineering Visualization Challenge

Call for Entries

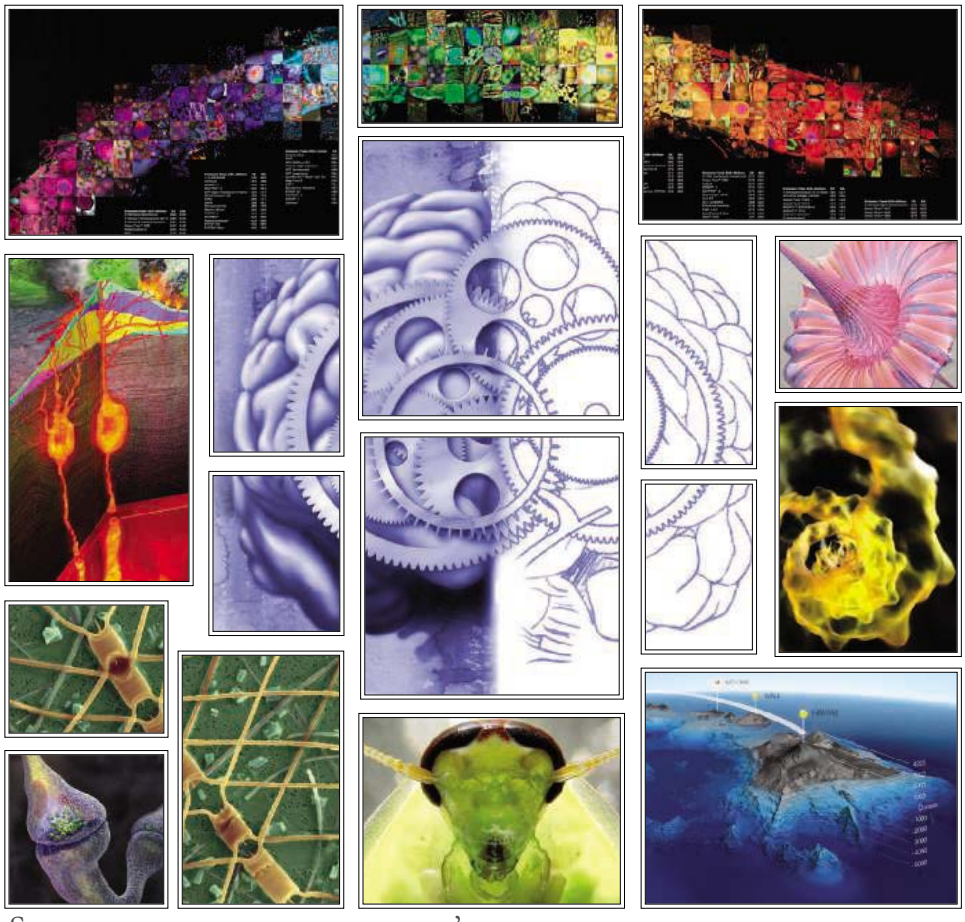

Science and engineering's most powerful statements are not made from words alone

Entry Deadline: May 31, 2007

When the left brain collaborates with the right brain, science emerges with art to enhance communication and understanding of research results—illustrating concepts, depicting phenomena and drawing conclusions.

The National Science Foundation (NSF) and the journal *Science*, published by the American Association for the Advancement of Science, invite you to participate in the fifth annual Science and Engineering Visualization Challenge. The competition recognizes scientists, engineers, visualization specialists and artists for producing or commissioning innovative work in visual communication.

Winners in each category will be published in the Sept. 28, 2007 issue of *Science* and *Science* Online, and will be displayed on the NSF Web site.

Award Categories:

Illustrations,
Informational Graphics,
Interactive Media,
Non-Interactive Media,
Photographs

Complete Entry Information: www.nsf.gov/news/special_reports/scivis/

NSF

Science AAAS

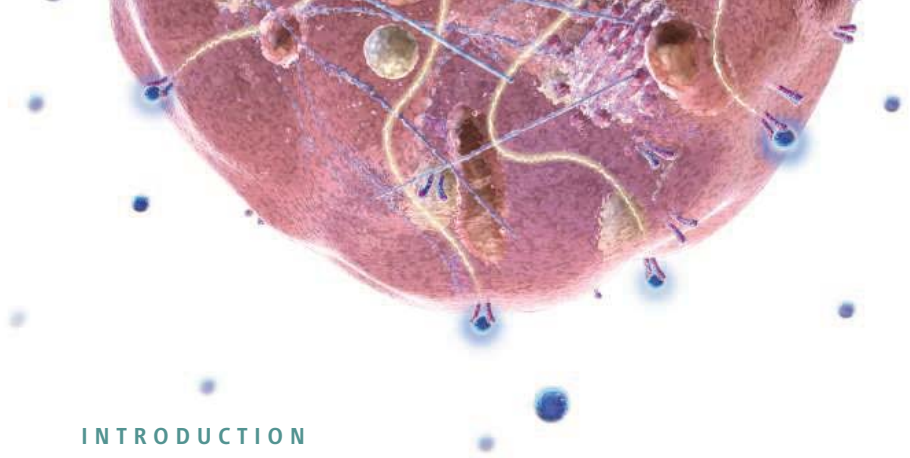

INTRODUCTION

Size, Mates, and Fates

THE *SCIENCE* PERSPECTIVES AND ASSOCIATED CONNECTIONS MAPS IN THE Database of Cell Signaling at *Science*'s Signal Transduction Knowledge Environment (www.sciencemag.org/sciext/cellsignaling06/) highlight pathways initiated by three different types of receptors: brassinosteroid receptors that control plant size, G protein–coupled receptors that control mating responses in yeast, and Notch receptors that control cell fate in animals.

Brassinosteroids are plant hormones that contribute to cell growth and division, differentiation, and reproductive development. As Belkhadir and Chory (p. 1410) describe, the brassinosteroid receptor BR1 is a plasma membrane–localized leucine-rich–repeat receptor kinase that initiates a kinase cascade, ultimately controlling gene expression. Experiments in *Arabidopsis thaliana* have revealed that the active receptor complex is a serine-threonine kinase that initiates a process that inactivates BIN2, the plant homolog of glycogen synthase kinase 3 (GSK-3). *Arabidopsis* BIN2 is localized to the nucleus, whereas in animals, GSK-3 is cytosolic. BIM, which resembles the animal transcription factor Myc, interacts with the brassinosteroid response factor BES to enhance its activity. Thus, at each step of the brassinosteroid pathway—from the steroid hormone–like ligands to the transcription factors in the nucleus—there are similarities with animal pathways; however, no known pathway in animals assembles this cast of characters in quite the same way.

Even well-characterized pathways continue to reveal new secrets. The yeast mating response is an extensively studied G protein–coupled receptor pathway, in which the Gβγ subunits have been in the spotlight as the subunits that activate the mitogen-activated protein kinase cascade. Now, Slessareva and Dohlman (p. 1412) describe how the Gα subunit participates in transmitting the mating signal by interacting with the phosphoinositide 3-kinase (PI3K) at the endosome to stimulate the production of phosphoinositide 3-phosphate. Not only was this a previously unknown function and location for Gα in the yeast mating response, but the regulatory subunit of PI3K appears to serve as a noncanonical Gβ subunit for the endosomally located Gα, a discovery that will undoubtedly stimulate a search for similar types of interactions in other systems.

The Notch signaling pathway is crucial to animal development, and aberrant activity of this pathway is associated with certain types of leukemia. Ehebauer *et al.* (p. 1414) explain how the transmembrane Notch receptor interacts with the transmembrane ligand on adjacent cells, which leads to cleavage and release of the Notch intracellular domain (NICD) that translocates to the nucleus and regulates gene expression. The cleavage of Notch remains an open area of research, with various candidates for the protease that performs the first cleavage in the extracellular domain and questions surrounding whether the second cleavage event occurs at the plasma membrane or after internalization. Notch acts in concert with other morphogenic signals to control cell fate; thus, understanding Notch signaling within the more complex signaling network remains a critical avenue of investigation. This knowledge may not only yield insight into animal development but also open the doors to new therapeutic opportunities in cases where the loss of differentiation contributes to disease.

– NANCY R. GOUGH, ELIZABETH M. ADLER, L. BRYAN RAY

CREDIT: C. BICKEL/*SCIENCE*

Cell Signaling

CONTENTS

Perspectives

Connections Maps

See also related STKE material on page 1347 or at www.sciencemag.org/sciext/cellsignaling06/

Science

PERSPECTIVE

Brassinosteroid Signaling: A Paradigm for Steroid Hormone Signaling from the Cell Surface

Youssef Belkhadir and Joanne Chory*

Plants use the coordinated action of several small-molecule hormones to grow and develop optimally in response to a changing environment. Among these hormones are the brassinosteroids (BRs), the polyhydroxylated steroid hormones of plants. BRs bind a small family of leucine-rich repeat receptor kinases at the cell surface, thereby initiating an intracellular signal transduction cascade that results in the altered expression of hundreds of genes.

Brassinosteroids (BRs) are small growth-promoting molecules found at low concentrations throughout the plant kingdom. In a technical tour de force, researchers in the late 1970s purified a bioactive steroid from *Brassica napus* bee-collected pollen. The most active BR was identified by single-crystal x-ray analysis as a steroidal lactone and was named brassinolide (BL) (*1*). The role of BRs as plant hormones was clarified in the mid-1990s with the discovery of *Arabidopsis thaliana* mutants that were deficient in BR biosynthesis. BR-deficient mutants are extremely dwarfed with very small curled leaves; the mutants can be rescued to wild-type stature by exogenous application of BL (*2*, *3*) (Fig. 1). Analysis of these mutants showed that BRs play a role in cell expansion and division, differentiation, and reproductive development. The regulation of these processes by BRs allows plants to develop a body plan that is optimal for their ambient environment and may confer increased adaptation to various stresses. The ease of analysis of the BR-deficient phenotype allowed the identification of the plasma membrane–localized BR receptor and much of the intracellular signaling pathway that regulates BR-responsive gene expression (*4*–*6*). However, key open questions remain with respect to how the BR signaling pathway contributes to the adaptive plasticity of plant growth.

BRs have structures similar to those of animal steroid hormones. BR biosynthesis enzymes share sequence identity with mammalian steroid biosynthetic enzymes (e.g., DET2 is a plant ortholog of mammalian steroid 5α-reductases, and most of the other biosynthetic genes are cytochrome P450s) (*7*). The major branch of the biosynthetic pathway, from campesterol to BL, was determined using a combination of *Arabidopsis* genetics and feeding experiments with BR biosynthetic intermediates.

Plant Biology Laboratory and Howard Hughes Medical Institute, Salk Institute for Biological Studies, La Jolla, CA 92037, USA.

*To whom correspondence should be addressed. E-mail: chory@salk.edu

Forward genetic screens for dwarf mutants that were not rescued by exogenous addition of BL led to the identification of multiple mutant alleles of a single locus, *BRI1* (*brassinosteroid insensitive 1*) (*8*, *9*) (Fig. 1). BRI1 is a leucine-rich repeat receptor kinase (LRR-RK) that has an extracellular domain with an N-terminal signal peptide followed by 24 imperfect leucine-rich repeats (LRRs), a single transmembrane domain, and an intracellular serine-threonine kinase domain followed by a short C-terminal tail. BRI1 is the major BR-binding activity of *Arabidopsis*. The minimal BR-binding domain is a 94–amino acid subdomain that includes the 70–amino acid "island" just proximal to LRR20 and the atypical LRR, LRR21 (Fig. 1) (*10*). As such, the signaling pathway defined by BRI1 represents a paradigm for steroid perception at the cell surface and may have implications for the understanding of the growing field of plasma membrane steroid signaling in metazoans.

In the absence of steroid, the kinase activity of BRI1 is inhibited by both cis and trans mechanisms. BKI1 (BRI1 kinase inhibitor 1) is a plasma membrane–associated phosphoprotein that interacts directly with the kinase domain of BRI1 (*6*, *11*). Binding of BRs to preformed BRI1 homo-oligomers triggers the rapid dissociation of BKI1 from the plasma membrane (*11*). In vitro, BKI1 interferes with the interaction of BRI1 with its signaling partner, a second plasma membrane–localized LRR-RK called BAK1 [BRI1-associated receptor kinase 1, also known as SERK3 (somatic embryogenesis receptor kinase 3)] (*12*).

Although the precise sequence of events is not clear, BR binding also allows autophosphorylation of critical serine and threonine residues located in the activation loop of the kinase domain of BRI1 (*13*, *14*). This, in turn, alleviates the autoinhibitory effect of the C-terminal tail on kinase activity and allows further autophosphorylation of the receptor, which increases the affinity of BRI1 for BAK1 (*13*). BAK1 has a short extracellular domain comprising five LRRs. Although BR binding to BRI1 is independent of BAK1, a BRI1-BAK1 hetero-oligomer may be the active signaling complex. SERK1, a BAK1 homolog, also interacts with BRI1, and genetic experiments have implicated this protein in the signaling pathway (*12*). In addition to the plasma membrane, a signaling-competent BRI1-BAK1 hetero-oligomer was detected in bona fide endocytic compartments of plant protoplasts (*12*). Furthermore, overexpression of BAK1 appears to augment the internalization of BRI1 in heterologous cell cultures. Thus, the function of the SERK family in BR signaling may be to facilitate the entry of BRI1 into these intracellular compartments. The physiological role of an endosome-localized BRI1-BAK1 hetero-oligomer is not currently known.

Only the *BRI1* locus was defined by loss-of-function mutations that caused BR-resistant dwarfism; however, several additional components of the pathway were identified by analysis of gain-of-function phenotypes or plants with increased sensitivity to BRs. A *bin2* (*brassinosteroid insensitive 2*) dwarf mutant phenotype results from a semi-dominant mutation. BIN2 is one member of an *Arabidopsis* subfamily of glycogen synthase kinase 3 (GSK3, also known as Shaggy-like kinases). Although single loss-of-function alleles revealed no effect on BR signaling (*6*, *15*), reduced expression of the entire subfamily results in plants with enhanced BR responses, supporting a role for these three kinases as negative regulators of BR signaling (*15*). BIN2 localizes to multiple subcellular compartments but appears to exert its largest effects on BR signaling when it is retained in the nucleus.

BSU1 (*BRI1 suppressor 1*) was identified as a dominant suppressor of a weak *bri1* mutant (*4*, *6*). *BSU1* overexpression substantially suppresses the dwarf phenotypes associated with either the *bri1* or *bin2* mutations, which suggests that BSU1 is a positive regulator of BR signaling that acts on the same process or downstream of BIN2. *BSU1* encodes a nuclear-localized serine-threonine phosphatase with an N-terminal domain comprising Kelch repeats. Loss of *BSU1* function has no effect on *Arabidopsis*, but when the expression of *BSU1* and three related genes is reduced by RNA interference, the resulting plant is dwarfed (*16*, *17*). The substrates of BIN2 and BSU1 are likely to be a family of plant-specific transcription factors. The founding members of this family, BES1 (bri1 ems 1) and BZR1 (brassinazole resistant 1), are 89% identical and contain multiple predicted GSK3 phosphorylation sites (*4*, *15*). Recent models propose that the balanced activities of BIN2 and BSU1 directly control the phosphorylation state of BES1 and BZR1. BIN2-induced phosphorylation of BES1 inhibits its transcriptional activity through impaired multimerization and DNA binding activity at BR-responsive target promoters. In contrast, in the presence of BRs, BES1 and BZR1 are dephosphorylated by the combined inactivation of BIN2 and the phosphatase activity of BSU1,

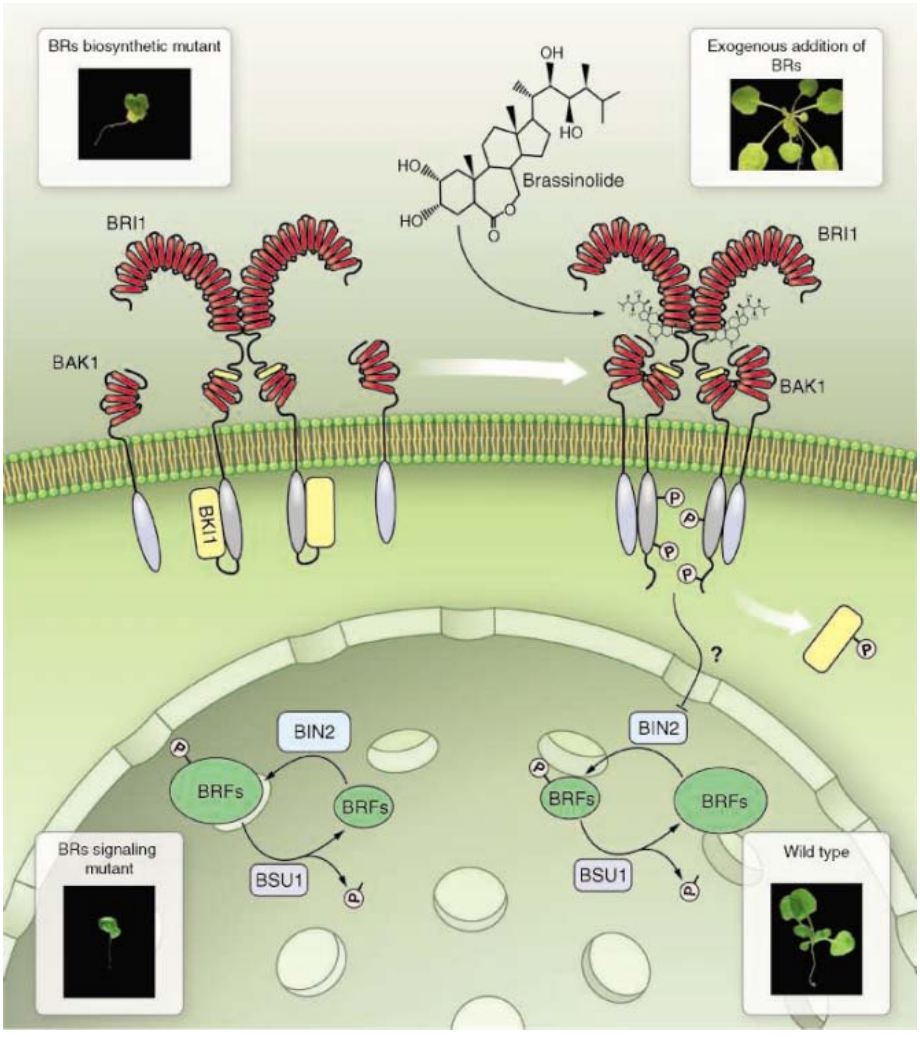

Fig. 1. A model of BR control of *Arabidopsis* size. *Arabidopsis* biosynthetic mutants that do not produce brassinolide (BL) are dwarf (upper left photo) but can be rescued to full stature by exogenous application of BL (upper right photo). BR signaling mutants (lower left photo) cannot be rescued by exogenous BL. In the absence of BRs, the kinase domains of the BRI1 homodimer are inhibited by both their own C-terminal domain and by an interaction with BKI1. This allows the GSK3 homolog, BIN2, to phosphorylate and inactivate the brassinosteroid response transcription factors (BRFs), including BES1 and BZR1. Direct binding of BL to BRI1 homodimers results in conformational changes of the kinase domain, leading to the phosphorylation of the C-terminal domain of BRI1 and phosphorylation of BKI1, which causes displacement of BKI1 from the plasma membrane and the release of autoinhibition of BRI1. These events lead to BRI1's association with BAK1 and consequent activation of the receptor. The active signaling receptor complex inhibits the activity of BIN2 by an unknown mechanism, allowing dephosphorylation of the BRFs by BSU1 and activation or repression of their target genes and optimal plant growth (lower right photo). The horseshoe-shaped representations of BRI1 and BAK1 LRR domains, as well as the putative LRR (red domains) interactions, are inferred from structural models of LRR-containing proteins. The atypical LRR21 is represented by a yellow domain. The BL docking into the binding site is speculative. Phosphorylation events are indicated by a circled P.

which allows them to homo- or heterodimerize and bind more efficiently to the BR-responsive elements to either positively or negatively regulate BR-responsive target genes (*15*, *18*).

Despite tremendous progress in understanding the molecular and cellular effects of BRs, key issues remain unanswered. First, details of the receptor activation mechanism need to be clarified and the physiological role of the endosomal BRI1-BAK1 hetero-oligomer needs to be determined. Second, a major gap exists in the pathway between events at the plasma membrane and in the nucleus. Understanding how BIN2 is inactivated and how its subcellular localization may be altered in response to BRs may help fill in this gap. A third area of investigation revolves around the pleiotropic actions of BRs on plant tolerance to temperature, salt, and pathogens. Although the signaling pathway defined by BRI1 is known mostly for controlling the rapid increase in tissue mass, it remains possible that the other effects of BRs are mediated by different signaling pathways. Finally, every signaling component, from BRI1 to the regulated transcription factors, is redundantly encoded in the genome. Perhaps redundancy in BR signaling could increase the robustness of the pathway to mutations; alternatively, partial redundancy due to overlapping expression patterns of signaling components may help to fine-tune the pleiotropic BR response. A systematic analysis of the function and expression patterns of family members will help to unravel these questions.

Ultimately, the goal of this work is to understand how plant size is controlled and to be able to manipulate plant growth for human benefit. BRs play an important role in the processes that control plant size, but other small-molecule hormones also contribute to cell expansion and division. Although there is redundancy within a given hormonal pathway, loss of response to any one plant hormone cannot be compensated for by the action of another hormone. To add another level of complexity, the entire program can be altered by changes in the environment's ambient light or temperature. Plants provide an accessible model for answering questions of organ or organismal size because the number of cell types and different organs is small, organ size is easily manipulated by environment, and many of the individual signaling pathways are known. Questions that can be addressed include how the levels of plant hormones change throughout development and in response to an ever-changing environment, and how these different pathways interact within individual cells. Ultimately, we may answer the age-old question of how the size of an organism is determined.

References and Notes

1. M. D. Grove *et al.*, *Nature* **281**, 216 (1979).
2. J. Li *et al.*, *Science* **272**, 398 (1996).
3. M. Szekeres *et al.*, *Cell* **85**, 171 (1996).
4. G. Vert *et al.*, *Annu. Rev. Cell Dev. Biol.* **21**, 177 (2005).
5. Y. Belkhadir *et al.*, Brassinosteroid Signaling Pathway, *Sci. STKE* (Connections Map, as seen October 2006) (http://stke.sciencemag.org/cgi/cm/stkecm;CMP_19131).
6. Y. Belkhadir *et al.*, *Arabidopsis* Brassinosteroid Signaling Pathway, *Sci. STKE* (Connections Map, as seen October 2006) (http://stke.sciencemag.org/cgi/cm/stkecm;CMP_19349).
7. S. Fujioka, T. Yokota, *Annu. Rev. Plant Biol.* **54**, 137 (2003).
8. J. Li, J. Chory, *Cell* **90**, 929 (1997).
9. S. D. Clouse *et al.*, *Plant Physiol.* **111**, 671 (1996).
10. T. Kinoshita *et al.*, *Nature* **433**, 167 (2005).
11. X. Wang, J. Chory, *Science* **313**, 1118 (2006).
12. R. Karlova, S. C. De Vries, *Sci. STKE* **2006**, pe36 (2006).
13. X. Wang *et al.*, *Dev. Cell* **8**, 855 (2005).
14. X. Wang *et al.*, *Plant Cell* **17**, 1685 (2005).
15. G. Vert, J. Chory, *Nature* **441**, 96 (2006).
16. Z. Y. Wang *et al.*, *Dev. Cell* **2**, 505 (2002).
17. Y. Yin *et al.*, *Cell* **109**, 181 (2002).
18. L. Li, X. W. Deng, *Trends Plant Sci.* **10**, 266 (2005).
19. Supported by USDA and NSF grants (J.C.) and by the Howard Hughes Medical Institute. Y.B. is a Howard Hughes Medical Institute Fellow of the Life Sciences Research Foundation. We thank S. Savaldi-Goldstein for *Arabidopsis* pictures.

10.1126/science.1134040

PERSPECTIVE

G Protein Signaling in Yeast: New Components, New Connections, New Compartments

Janna E. Slessareva and Henrik G. Dohlman*

Signaling by cell surface receptors and heterotrimeric guanine nucleotide–binding proteins (G proteins) is one of the most exhaustively studied processes in the cell but remains a major focus of molecular pharmacology research. The pheromone-response system in yeast (see the Connections Map at *Science*'s Signal Transduction Knowledge Environment) has provided numerous major advances in our understanding of G protein signaling and regulation. However, the basic features of this prototypical pathway have remained largely unchanged since the mid-1990s. New tools available in yeast are beginning to uncover new pathway components and interactions and have revealed signaling in unexpected locations within the cell.

Many extracellular signals are detected by cell surface receptors and further transmitted inside the cell by G proteins, which serve as molecular switches (*1*). Activated receptors promote exchange of guanosine triphosphate (GTP) for guanosine diphosphate (GDP) bound to G protein α subunits, triggering the dissociation of the G protein α and βγ subunits and thus allowing them to signal. In yeast, mating pheromones activate a G protein and protein kinase cascade that includes Fus3 and Kss1, two members of the mitogen-activated protein (MAP) kinase family (*2*). G protein activation is eventually terminated by the intrinsic guanine triphosphatase (GTPase) activity of Gα subunits, a process that is accelerated by proteins known as regulators of G protein signaling (or RGS proteins) (*1*). Thus, the intensity of the signal depends on the opposing actions of receptors and RGS proteins. Proper functioning of G protein–mediated signal transduction mechanisms is extremely important, because defects in these pathways are implicated in a wide variety of diseases (*3*). Correspondingly, a substantial fraction of all pharmaceuticals act directly or indirectly on G protein–coupled receptors (*4*). Thus, it is possible that a new generation of drugs will act on RGS proteins and other newly discovered regulators of G protein activity (*5*).

The yeast *Saccharomyces cerevisiae* represents an attractive and appropriate model for investigating basic mechanisms of G protein and MAP kinase signaling (*2*) and in particular for finding new pathway regulators. Yeast is also emerging as a versatile model for systems-level analysis of complex signaling networks. The yeast genome was the first among eukaryotes to be sequenced. There exist comprehensive microarrays for transcription analysis, gene deletion arrays for genome-scale phenotypic analysis, and gene fusion arrays for systematic protein purification and in situ localization studies. The existence of these resources has profoundly transformed our approach to the identification and functional characterization of cell signaling regulators. Indeed, yeast is the only experimental system where it is possible to track the expression, localization, and activity of nearly every component of the G protein signaling pathway, from the cell surface to the nucleus (Fig. 1).

In the pheromone response pathway, the Gβγ subunits (Ste4 and Ste18) were long regarded as the sole signal-transmitting component of the G protein heterotrimer. The Gα subunit (Gpa1) was thought to regulate the amounts of free Gβγ: releasing Gβγ when in the activated GTP-bound form and sequestering Gβγ when in the inactivated GDP-bound form. Evidence of a positive signaling role for Gpa1 came from studies showing that GTPase-deficient (and thus constitutively active) Gpa1 mutants, including $Gpa1^{Q323L}$, activate mating-specific gene transcription and morphological changes in the absence of added pheromone (*6*).

However, the question still remained: How does activated Gα transmit its signal and contribute to the mating response pathway? A study published this year brings us closer to answering this question (*7*). A systematic analysis of nearly 5000 gene deletion strains revealed seven genes

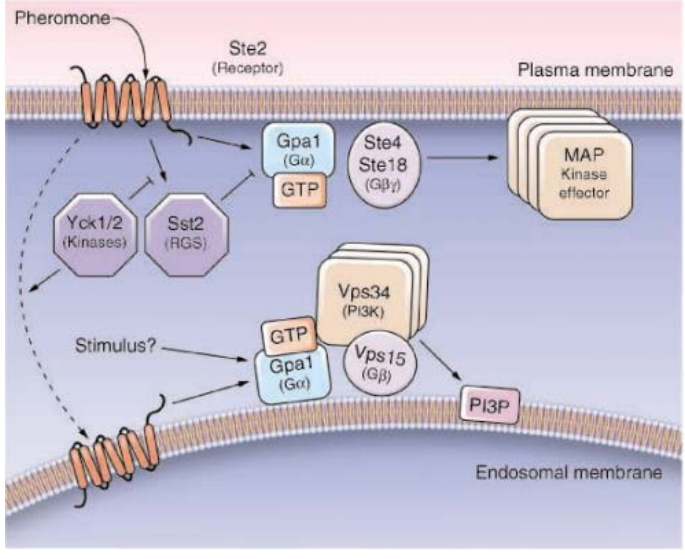

Fig. 1. New features of RGS and G protein signaling in yeast. (Top) Activation of the receptor (Ste2) by mating pheromone leads to GTP binding and dissociation of the G protein α subunit (Gpa1) from the Gβγ subunits (Ste4 and Ste18). Gβγ activates multiple effectors at the plasma membrane, including components of a MAP kinase signaling cascade. The RGS protein Sst2 binds to the receptor and accelerates Gpa1 GTP hydrolysis. Casein kinase I (Yck1 and Yck2) phosphorylates the receptor, displacing Sst2 and promoting receptor endocytosis. (Bottom) Gpa1 is also present at the endosome. Activation by endocytosed receptor or another unknown factor may lead to GTP binding and dissociation of Gpa1 from the Gβ-like protein Vps15. Activated Gpa1-GTP then binds directly to the phosphoinositide 3-kinase (PI3K) Vps34. Elevated PI3P recruits proteins containing FYVE domains and PX domains to the endosome. Note that Vps15 and Vps34 are part of a multiprotein complex that also includes Vps30 and Vps38 or Atg14.

Department of Biochemistry and Biophysics, University of North Carolina, Chapel Hill, NC 27599–7260, USA.

*To whom correspondence should be addressed. E-mail: hdohlman@med.unc.edu

required for Gpa1^{Q323L}-mediated responses. Two of the genes, *VPS34* and *VPS15*, encode the catalytic and regulatory subunits, respectively, of the sole phosphatidylinositol 3-kinase in yeast. Surprisingly, Vps34 and Vps15 are found at intracellular compartments, such as endosomes and Golgi, rather than at the plasma membrane where receptors and G proteins are normally thought to reside. Activated Gα localizes along with Vps34 at the endosome, binds to Vps34 directly, and triggers increased production of the Vps34 product, phosphatidylinositol 3-phosphate (PI3P). These observations suggest that Vps34 is a bona fide Gα effector capable of generating a second messenger. The regulatory subunit Vps15 has a seven WD40 domain repeat structure and binds directly to the inactive GDP-bound form of Gpa1, both hallmark features of known Gβ subunits. These findings imply that Vps15 functions as an alternate Gβ, but one acting at the endosome instead of at the plasma membrane. In further support of this model, it was shown that Vps15 is needed to target Gα to the endosome, whereas the canonical Gβ subunit Ste4 targets Gα to the plasma membrane (*7*).

Although it is widely accepted that G proteins signal at the plasma membrane, it has long been recognized that they are also present at intracellular compartments (*8*). Previous studies have implicated these intracellular G proteins in the regulation of membrane traffic (*9*). It has also become increasingly evident that membrane trafficking and signal transduction events are closely linked and that G protein signals can originate from intracellular compartments as well as from the plasma membrane (*10*, *11*). Consequently, endosomes should be considered not only as a site of membrane sorting but also as a site of cell signaling (*12*).

How is the internal pool of G proteins regulated? One possibility is that Gα is initially activated by receptors at the plasma membrane and is then delivered to intracellular compartments. Another possibility is that the agonist-bound receptor transits to the endosome and activates Gα directly. Yet a third possibility is that Gα is activated by a distinct guanine nucleotide exchange factor located at the endosome. In fact, in other organisms a number of nonreceptor accessory proteins have been shown to activate Gα in vitro; of these a physiological role has been demonstrated for mammalian Ric-8A, which activates Gα proteins during cell division (*1*, *8*, *13*).

Why would having segregated pools of Gα be physiologically important? Signaling by Gpa1^{Q323L} may provide some clues. Although it mimics most aspects of pheromone binding at the cell surface, Gpa1^{Q323L} at the endosome preferentially activates just one of the two mating-specific MAP kinases and fails to trigger the cell division arrest that normally precedes mating. Thus, whereas Gα signaling at the plasma membrane is clearly important for the early steps of the pheromone response, Gα signaling at the endosome appears to convey a fundamentally different signal.

How does segregation of Gpa1 to two distinct membrane compartments relate to observed functional differences? As mentioned above, there could be differences in the activation step. Alternatively, there could be differences in how the two pools of G protein are inactivated. For example, it is possible that the internal pool of G protein is no longer attenuated by RGS proteins. Alternatively, both mechanisms might contribute. Recent studies in a variety of organisms suggest coordination between the receptors that activate the signal and the RGS proteins that inactivate the signal. RGS proteins show selectivity for particular Gα subunits, but some RGS proteins can physically interact with the receptors (*14*). One particularly intriguing example of receptor-RGS cooperation is provided by the plant protein AtRGS1, which has both RGS- and receptor-like domains, suggesting that it functions both as a G protein activator and inactivator (*15*). More recent findings reveal that the yeast RGS protein Sst2 can bind directly to the pheromone receptor Ste2 at the plasma membrane (*16*). Presumably Sst2 interaction with its cognate receptor ensures that pathway regulation is both rapid and receptor-specific. Regulation is receptor-specific because of selective binding to Sst2. Regulation is rapid, because receptor binding positions the RGS domain of Sst2 in close proximity to its substrate, Gpa1. In this scenario, RGS positioning close to Gα sets the threshold for pheromone response, preventing signaling at low pheromone concentrations. As signaling at the plasma membrane wanes, endocytosed receptors might continue to signal from the endosome or other internal compartments, as reported for other receptors (*10*). Phosphorylation of the receptor promotes endocytosis and also results in dissociation of the RGS protein, suggesting that the RGS protein does not follow the receptor as it undergoes endocytosis. Thus, one way that endosomal signaling may differ from plasma membrane signaling is if the RGS protein is no longer in close proximity to the G protein.

Lastly, there may be as yet undiscovered pathway regulators acting at the endosome, perhaps in response to PI3P production. Unlike many other second messengers, however, PI3P cannot diffuse freely and remains bound to membranes at the site of synthesis. Therefore, PI3P might serve to recruit proteins with PI3P-binding domains to the endosome (*17*). Such protein recruitment may allow assembly of signaling complexes that are distinct from those known to exist at the plasma membrane. In support of this model, Gpa1^{Q323L} promotes translocation of the PI3P-binding protein Bem1 to the endosome (*7*). Bem1 functions as an adaptor protein that promotes activation of other signaling components, including the small GTPase Cdc42 and the MAP kinase Fus3 (*18*). The adaptor protein Ste5 serves a similar role in transmitting the Gβγ signal at the plasma membrane (*19*).

If history is any guide, lessons learned in yeast will prove applicable to signaling events in more complex organisms. The identification of Sst2 and other RGS family members in the mid-1990s led to a dramatic rethinking of how G protein signaling pathways are organized and regulated. This view has now been further refined with the realization that receptors and RGS proteins cooperate to modulate G protein activity. Moreover, the old dogma of G protein–mediated signaling only at the plasma membrane must now be modified to include signaling from internal compartments. These discoveries benefited from the development of powerful genome-scale proteomic and genomic tools available in yeast. Our ability to fully exploit these tools is still evolving, but we can be confident that they will eventually provide us with a truly global or systems-level understanding of how cells respond to changes in their environment.

References and Notes

1. C. R. McCudden, M. D. Hains, R. J. Kimple, D. P. Siderovski, F. S. Willard, *Cell. Mol. Life Sci.* **62**, 551 (2005).
2. Y. Wang, H. G. Dohlman, *Science* **306**, 1508 (2004).
3. Z. Farfel, H. R. Bourne, T. Iiri, *N. Engl. J. Med.* **340**, 1012 (1999).
4. A. Wise, K. Gearing, S. Rees, *Drug Discov. Today* **7**, 235 (2002).
5. D. L. Roman *et al.*, *Mol. Pharmacol.* **71**, 169 (2006).
6. M. Guo *et al.*, *Mol. Cell* **12**, 517 (2003).
7. J. E. Slessareva, S. M. Routt, B. Temple, V. A. Bankaitis, H. G. Dohlman, *Cell* **126**, 191 (2006).
8. M. Sato, J. B. Blumer, V. Simon, S. M. Lanier, *Annu. Rev. Pharmacol. Toxicol.* **46**, 151 (2006).
9. J. B. Helms, *FEBS Lett.* **369**, 84 (1995).
10. A. Sorkin, M. Von Zastrow, *Nat. Rev. Mol. Cell Biol.* **3**, 600 (2002).
11. A. Mor, M. R. Philips, *Annu. Rev. Immunol.* **24**, 771 (2006).
12. M. Miaczynska, L. Pelkmans, M. Zerial, *Curr. Opin. Cell Biol.* **16**, 400 (2004).
13. G. G. Tall, A. M. Krumins, A. G. Gilman, *J. Biol. Chem.* **278**, 8356 (2003).
14. M. Abramow-Newerly, A. A. Roy, C. Nunn, P. Chidiac, *Cell. Signal.* **18**, 579 (2006).
15. J.-G. Chen *et al.*, *Science* **301**, 1728 (2003).
16. D. R. Ballon *et al.*, *Cell* **126**, 1079 (2006).
17. S. Misra, G. J. Miller, J. H. Hurley, *Cell* **107**, 559 (2001).
18. D. M. Lyons, S. K. Mahanty, K. Y. Choi, M. Manandhar, E. A. Elion, *Mol. Cell. Biol.* **16**, 4095 (1996).
19. E. A. Elion, *J. Cell Sci.* **114**, 3967 (2001).

20. Supported by NIH grant P01-GM065533.

10.1126/science.1134041

PERSPECTIVE

Notch, a Universal Arbiter of Cell Fate Decisions

Matthias Ehebauer,[1] Penelope Hayward,[2] Alfonso Martinez Arias[2]*

Members of the Notch family of receptors act as membrane-tethered transcription factors that are tightly associated with binary cell fate decisions. Notch signaling acts as a molecular gate that allows cells to adopt or forfeit a particular fate. Interaction of Notch with ligands triggers a sequence of proteolytic cleavages that release the intracellular domain to the nucleus; this mechanism is a target of therapies for leukemias associated with Notch activation. Although the molecular mechanism of Notch activation is well characterized, further analysis in an appropriate cellular context will provide new insight into Notch signaling.

The formation of an organism relies on the generation of diverse cell types that provide the bricks for creating tissues and organs. Observations initially made during studies of insect nervous system development highlight two simple and linked strategies that underlie cell fate determination: (i) Cells attain their fates through binary choices, and (ii) initially, all cells in a given population can adopt an alternative fate, but only some maintain this new fate stably, whereas others revert to the default fate (Fig. 1A). The population of cells involved in making this binary choice is called an equivalence group, and the process of cell fate pruning usually involves lateral inhibition, in which the cell that adopts the alternative fate blocks this choice in its neighbors (*1*). These strategies for cell fate determination occur in numerous developmental processes in different cell types. Signaling by Notch receptors is intimately associated with these events and may provide a universal mechanism for cell fate determination (*2*).

The central elements of Notch signaling are featured in an STKE Connections Map (*3*). The Notch receptors encompass a cohort of transmembrane proteins with an extracellular domain composed of tandemly arranged epidermal growth factor (EGF)–like repeats (36 in the canonical form of Notch); a membrane-proximal set of specific cysteine-rich repeats, the Lin12-Notch (LN) repeats; and an intracellular moiety that contains seven conserved ankyrin repeats, which mediate much of the function of the receptor (Fig. 1B) (*2*). Notch receptors are membrane-tethered transcription factors that are released into the nucleus upon activation by the ligand (*2*, *4*). The Notch ligands, collectively known as Delta, Serrate, and Lag2 (DSL) (*3*), are also transmembrane proteins with extracellular arrays of EGF-like repeats (*2*–*4*). Notch signaling is deceptively simple (Fig. 1C). The interaction of Notch with DSL proteins induces a cleavage (S2) within the Notch extracellular domain near the transmembrane region, generating a substrate for a ligand-independent cleavage (S3) catalyzed within the transmembrane domain by the Presenilin complex. The S3 cleavage frees the intracellular domain of Notch (NICD) to enter the nucleus (*5*), where it interacts with members of the CBF1, Su(H), and Lag1 (CSL) family of transcription factors (*3*). CSL proteins are transcriptional repressors that are turned into activators through interaction with NICD (*3*, *6*). The CSL-NICD complex recruits other proteins, which regulate the stability of the complex, ensuring a tight control over the signaling event. The CSL-NICD complex modulates the transcription of different targets, but its activity is frequently linked to the expression of members of the Enhancer of Split, Hairy/Enhancer of Split–related, Hairy and Enhancer of Split [E(spl)/HER/HES] family of transcriptional regulators, which act as a core extension of the pathway (*3*). There is increasing evidence that Notch can signal in a CSL-independent manner and that this also plays a role in development and disease (*7*).

Detailed observations of receptors and ligands raise some questions that challenge the apparent simplicity of the pathway. For example, although a Notch receptor found in insects and higher eukaryotes has 36 EGF-like repeats and a conserved intracellular domain, the nematode receptor and two of the mammalian forms (Notch 3 and Notch 4) have fewer repeats and smaller intracellular domains. The functional consequences of these differences are not yet clear. Moreover, the DSL ligands fall into two structurally different classes, Delta-like and Serrate, which appear to mediate different interactions with Notch. The STKE Connections Map (*3*) might serve as a framework to guide research into such questions.

Mutations that lead to Notch malfunction have been associated with various diseases (*8*), including cancer (*9*). Of particular interest are dominant, ligand-independent activating mutations of *Notch1* that require the S3 cleavage and are associated with T cell acute lymphoblastic leukemias (*10*). These mutations provide a clear link between a signaling event and a specific disease but also serve as a basis to test therapies that target the γ-secretase activity of the Presenilin complex. In other instances, the normal activity of Notch provides a means for tampering with cancers. For example, Wnt signaling–mediated colorectal tumors can be curbed by inhibiting Notch signaling to induce the differentiation of these tumors (*11*).

Genetic analysis has demonstrated the universality of Notch signaling as an arbiter of cell fate. In this process, Notch acts in a permissive manner: It does not determine the fate of a cell but rather whether a given fate is adopted (*2*, *4*). In addition to this signature function, there is evidence that Notch plays other roles in development. For example, it is a central element of a molecular oscillator that establishes segmentation in vertebrates (*12*) and, probably, in other segmented organisms (*13*). In this task, it appears that Notch also acts permissively through a mechanism similar to that involved in cell fate decisions, coordinating more than determining the activity of different cells. The notion that Notch has mostly a modulatory role has recently been elegantly shown in the differentiation of mouse embryonic stem cells (*14*). In a few instances, Notch has also been shown to act in an instructive fashion (*15*).

We understand in detail how NICD is released from the membrane and how it interacts with DNA binding effectors. What else is there to be learned? One avenue of research will be to determine how this functional cassette is plugged in to normal and pathological cell specification networks. Also, increasing evidence suggests that endocytosis and trafficking of ligands and receptors play central roles in Notch activation (Fig. 1C) (*16*, *17*). Notably, endocytosis of DSL ligands is a prerequisite for their functional interaction with the receptor, and the S3 cleavage of Notch requires both endocytosis and trafficking to an internal compartment. Furthermore, studies of *Drosophila* mutants suggest that endocytosis is used in two different manners to regulate Notch signaling: It ensures that there is no ligand-independent signaling, and it regulates ligand-dependent activity. In the next few years, trafficking will probably emerge as a central element in the biology of Notch and its therapeutic potential in Notch-dependent diseases. Finally, an important area of future research will involve interactions of Notch with other signaling pathways, in particular with Wnt (*18*, *19*).

It is likely that in the near future, placing Notch signaling in an appropriate cellular context elucidating its interactions with other signaling pathways will not simply add detail to the

[1]Department of Biochemistry, University of Cambridge, Cambridge CB2 1GA, UK. [2]Department of Genetics, University of Cambridge, Cambridge CB2 3EH, UK.

*To whom correspondence should be addressed. E-mail: ama11@hermes.cam.ac.uk

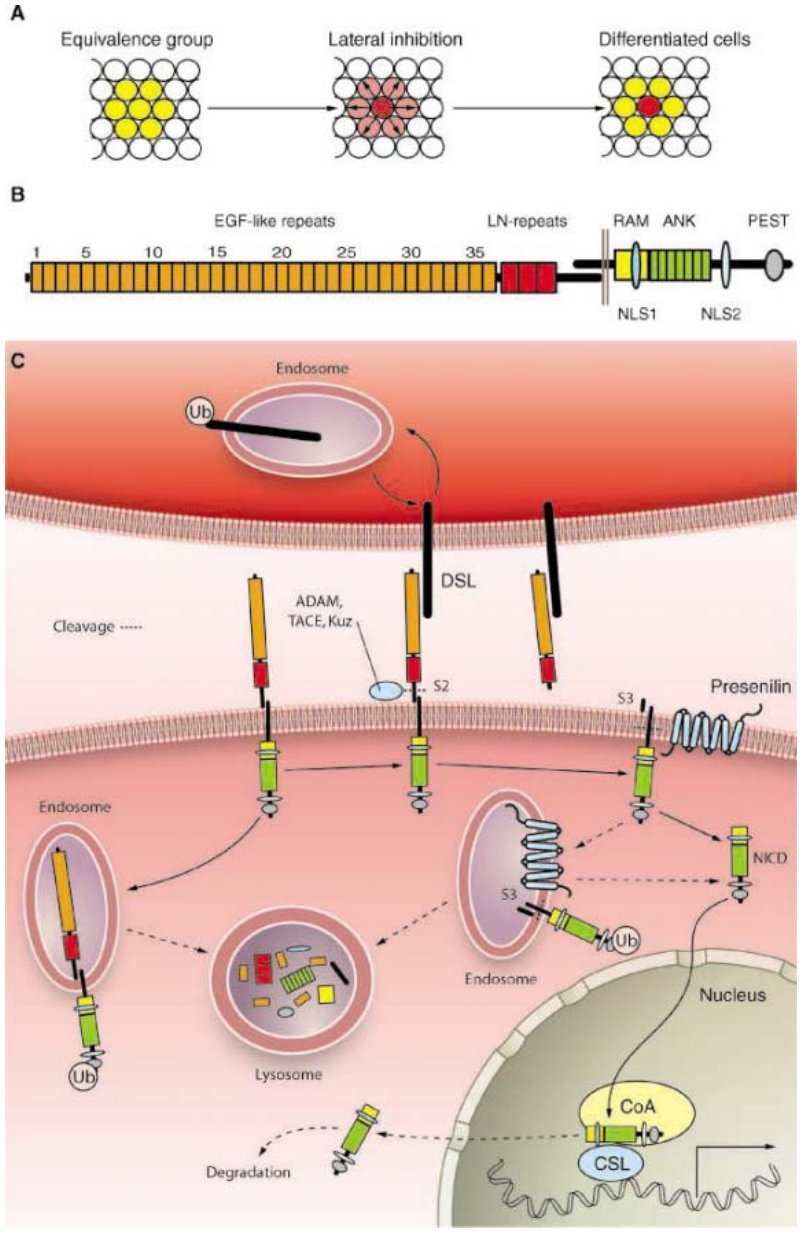

Fig. 1. Notch receptor signaling and architecture. (**A**) All cells within an equivalence group are in a particular state (yellow) and possess similar amounts of Notch and Delta. A combination of intrinsic and extrinsic signals induces a new cell state (light red) and breaks this balance by increasing the abundance of Delta in one or a few cells (dark red). Consequently, Notch signaling is activated in neighboring cells, suppressing the alternative fate and reverting these neighboring cells to their original fate through lateral inhibition. (**B**) Domain architecture of the Notch receptor family. The organization of human Notch1 is shown as an example. All Notch receptors consist of two polypeptides at the cell surface, except *Drosophila*, in which a linear form of the receptor might exist at the cell surface. RAM, recombination signal-binding protein for J-κ (RBPJκ)–associated molecule region; ANK, ankyrin; NLS, nuclear localization sequence; Pro-Glu-Ser-Thr (PEST), degradation motif. (**C**) Ligand binding to the Notch receptor triggers signaling through successive proteolytic cleavages. The ligand (DSL) binds to the EGF repeats (orange) in the extracellular domain of the Notch receptor. A protease cleaves Notch at the S2 site, removing the bulk of the extracellular domain. The identity of this protease is not clear; it may be a disintegrin and metalloprotease protein (ADAM), tumor necrosis factor–α converting enzyme (TACE), or Kuzbanian (Kuz). The membrane-tethered intracellular domain is then cleaved by the Presenilin complex at site S3, either in the plasma membrane or after endocytosis, freeing the NICD. NICD then moves to the nucleus, where it forms a binary complex with CSL, which recruits coactivators (CoA) to form the transcription-activating complex. Notch signaling can be regulated by endocytosis. NICD becomes monoubiquitylated (Ub), targeting the receptor to the lysosome for degradation. NICD in the nucleus is degraded in a proteasome-dependent manner, although the location of degradation is not clear. Solid arrows indicate demonstrated routes; dashed arrows indicate routes tentatively inferred from data.

molecular outline we have at the moment (*3*) but rather reveal new vistas of this central signaling pathway. The focus so far has been on the elements of a linear cascade and their interactions, but further consideration would suggest that it takes more than a collection of biochemical reactions to get cells to make functioning organisms.

References and Notes

1. P. Simpson, *Development* **109**, 509 (1990).
2. F. Schweisguth, *Curr. Biol.* **14**, R129 (2004).
3. M. Ehebauer, P. Hayward, A. Martinez-Arias, Notch signaling pathway. *Science's STKE* (Connections Map, as seen August 2006) (http://stke.sciencemag.org/cgi/cm/stkecm;CMP_19043).
4. R. Kopan, *J. Cell Sci.* **115**, 1095 (2002).
5. E. H. Schroeter, J. A. Kisslinger, R. Kopan, *Nature* **393**, 382 (1998).
6. E. C. Lai, *EMBO Rep.* **3**, 840 (2002).
7. A. Martinez Arias, V. Zecchini, K. Brennan, *Curr. Opin. Gen. Dev.* **12**, 524 (2002).
8. T. Gridley, *Hum. Mol. Genet.* **12**, R9 (2003).
9. F. Radtke, K. Raj, *Nat. Rev. Cancer* **3**, 756 (2003).
10. A. P. Weng *et al.*, *Science* **306**, 269 (2004).
11. J. H. van Es *et al.*, *Nature* **435**, 959 (2005).
12. P. C. Rida, N. Le Minh, Y. J. Jiang, *Dev. Biol.* **265**, 2 (2004).
13. A. Stollewerk, M. Schoppmeier, W. G. Damen, *Nature* **423**, 863 (2003).
14. S. Lowell, A. Benchoua, B. Heavey, A. G. Smith, *PLoS Biol.* **4**, e121 (2006).
15. S. Bray, *Semin. Cell Dev. Biol.* **9**, 591 (1998).
16. R. Le Borgne, A. Bardin, F. Schweisguth, *Development* **132**, 1751 (2005).
17. R. Le Borgne, *Curr. Opin. Cell Biol.* **18**, 213 (2006).
18. A. W. Duncan *et al.*, *Nat. Immunol.* **6**, 314 (2005).
19. P. Hayward *et al.*, *Development* **132**, 1819 (2005).

20. Our research is supported by the Wellcome Trust.

10.1126/science.1134042

For news and research with impact, turn to *Science*

There's only one source for news and research with the greatest impact – *Science*. With over 700,000 weekly print readers, and millions more online, *Science* ranks as one of the most highly read multidisciplinary journals in the world. And for impact, *Science* can't be beat. According to the recently released Thomson ISI Journal Citation Report 2005, *Science* ranked as the No. 1 most-cited multidisciplinary journal with a citation factor of 31. Founded in 1880 by inventor Thomas Edison, and published by the nonprofit AAAS, *Science*'s reputation as the leading source for news, research, and leading edge presentation of content continues to grow. Looking for news and research that will impact the world tomorrow? Then look in *Science*.

www.sciencemag.org

To join AAAS and receive your own personal copy of *Science* every week go to **www.aaas.org/join**

Science
AAAS

Old-Growth Forests Can Accumulate Carbon in Soils

Guoyi Zhou,[1]*† Shuguang Liu,[2]* Zhian Li,[1] Deqiang Zhang,[1] Xuli Tang,[1] Chuanyan Zhou,[1] Junhua Yan,[1] Jiangming Mo[1]

Old-growth forests have traditionally been considered negligible as carbon sinks because carbon uptake has been thought to be balanced by respiration (*1*). We show that soils in the top 20-cm soil layer in preserved old-growth forests in southern China accumulated atmospheric carbon at an unexpectedly high rate from 1979 to 2003. This phenomenon indicates the need for future research on the complex responses and adaptation of belowground processes to global environmental change.

Understanding the locations and driving forces of carbon sources and sinks at plot-to-global scales is critical for the prediction and management of the global carbon cycle and ultimately the behavior of the Earth's climate system (*2*). Major uncertainties remain in the geospatial distribution of terrestrial carbon sources and sinks and the mechanisms that drive the distribution and its change. Research efforts have largely been focused on the investigation and quantification of the impacts of climate variability and land use activities on the carbon cycle at various spatial and temporal scales. The soil carbon balance of old-growth forests has received little attention. It is generally accepted that soil organic carbon (SOC) levels in old-growth forests are in a steady state (*1*). To our knowledge, the long-term dynamics of SOC in old-growth forests and the validity of the above perception have not been tested.

We conducted a study to measure the long-term dynamics (1979 to 2003) of SOC stock in old-growth forests [age > 400 years (*3*)] at the Dinghushan Biosphere Reserve (23°09′21″N to 23°11′30″N and 112°30′39″E to 112°33′41″E) in Guangdong Province, China. The estimation of SOC stock change requires a series of measurements of SOC concentration, bulk density, and soil thickness taken at different points in time (*4*, *5*). In this study, we observed long-term changes in SOC concentration and bulk density but did not measure changes in soil thickness in the old-growth forests. Although soil thickness dynamics were not monitored, their possible contribution to the uncertainty in the results was analyzed and quantified by using upper and lower bounds of possible SOC change (Materials and Methods).

Results show that SOC concentration in the top 20-cm soil layer increased between 1979 and 2003 from about 1.4% to 2.35% at an average rate of 0.035% each year, which was significantly different from 0 at $\alpha = 0.05$. At the same time, the mean bulk density of the top 20-cm soil layer decreased significantly ($\alpha = 0.05$), with an average rate of 0.0032 g cm^{-3} $year^{-1}$. Measurements on a total of 230 composite soil samples collected between 1979 and 2003 suggested that SOC stock in the top 20-cm soil layer increased significantly during that time ($P < 0.0001$), with an average rate of 0.61 Mg C ha^{-1} $year^{-1}$ (Fig. 1). The lower and upper bounds of this average rate were 0.54 and 0.68 Mg C ha^{-1} $year^{-1}$, after considering the uncertainty introduced by the lack of thickness-change monitoring. We took more than enough samples to detect the observed SOC change. In fact, statistical analysis shows that 20 samples taken every 8 to 10 years of sampling interval (or 100 samples every 5 years) would be sufficient to detect the observed SOC change rate in these forests at a 95% confidence level. More samples would be required at shorter sampling intervals to detect the observed change, given the observed spatial variability of SOC concentration and bulk density.

The driving forces for this observed high rate of SOC increase in the old-growth forests are not clear at present and deserve further study. This study suggests that the carbon cycle processes in the belowground system of these forests are changing in response to the changing environment. This result directly challenges the prevailing belief in ecosystem ecology regarding carbon budget in old-growth forests (*1*) and supports the establishment of a new, non-equilibrium conceptual framework to study soil carbon dynamics. Our study further highlights the need to focus on the complexity of the belowground processes, as advocated in previous research (*6*, *7*), and the importance of establishing long-term observation studies on the responses of belowground processes to global change.

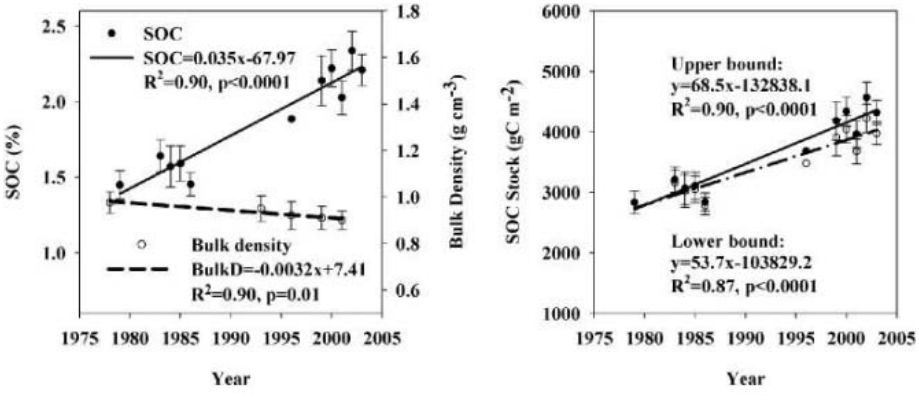

Fig. 1. Temporal changes of (**left**) soil organic carbon concentration, bulk density, and (**right**) soil organic carbon stock in the top 20-cm soil layer in broadleaved old-growth forests in Dinghushan Nature Reserve. Upper and lower bounds contain the uncertainty introduced by the lack of monitoring of soil thickness during the study period. Error bars indicate standard deviation.

References and Notes

1. E. P. Odum, *Science* **164**, 262 (1969).
2. Intergovernmental Panel on Climate Change, *Climate Change 2001: The Scientific Basis* (Cambridge Univ. Press, Cambridge, 2001).
3. C. D. Shen *et al.*, *Chin. Sci. Bull.* **44**, 251 (1999).
4. W. M. Post, R. C. Izaurralde, L. K. Mann, N. Bliss, *Clim. Change* **51**, 73 (2001).
5. F. Conen, M. V. Yakutin, A. D. Sambuu, *Glob. Change Biol.* **9**, 1515 (2003).
6. R. Lal, *Science* **304**, 1623 (2004).
7. C. A. Johnston *et al.*, *Front. Ecol. Environ.* **2**, 522 (2004).
8. G.Z. acknowledges support from the Chinese Ecosystem Research Network (CERN), the Chinese Academy of Science (project KSCX2-SW-120), and the Natural Science Foundation of China (project 30470306). S.L.'s work was supported by the USGS Geographic Analysis and Monitoring Program and the Earth Surface Dynamics Program. Work was performed under USGS contract 03CRCN0001.

Supporting Online Material

www.sciencemag.org/cgi/content/full/314/5804/1417/DC1
Materials and Methods
References

18 May 2006; accepted 13 September 2006
10.1126/science.1130168

[1]South China Botanical Garden, Chinese Academy of Sciences, Guangzhou, 510650, China. [2]SAIC, U.S. Geological Survey (USGS) Center for Earth Resources Observation and Science, Sioux Falls, SD 57198, USA.

*These authors contribute equally to this work.
†To whom correspondence should be addressed. E-mail: gyzhou@scib.ac.cn

From life on Mars to life sciences

For careers in science, turn to *Science*

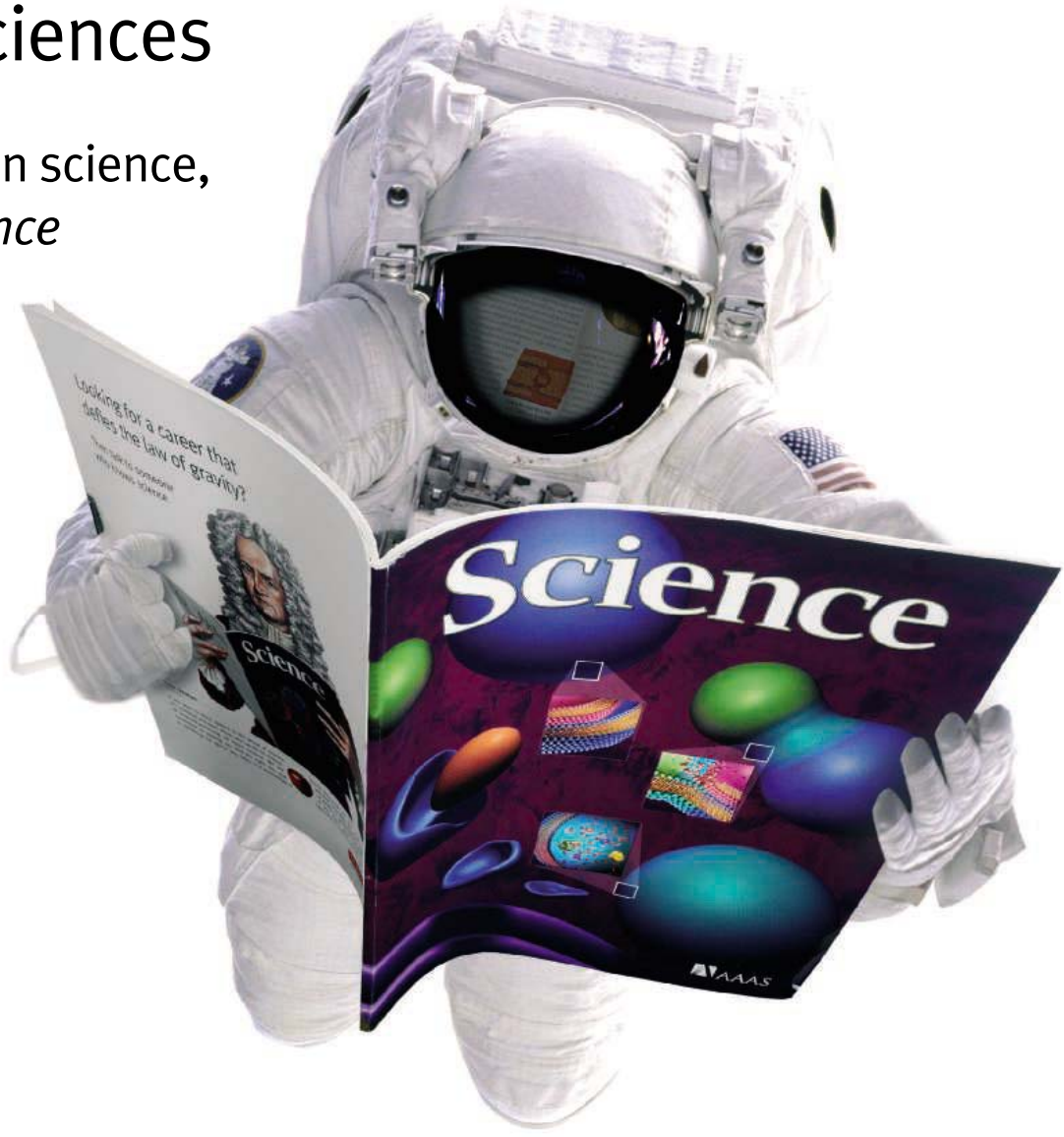

If you want your career to skyrocket, visit ScienceCareers.org. We know science. We are committed to helping you find the right job, and to delivering the useful advice you need. Our knowledge is firmly founded on the expertise of *Science*, the premier scientific journal, and the long experience of AAAS in advancing science around the world. ScienceCareers.org is the natural selection.

www.sciencecareers.org

Features include:

- Thousands of job postings
- Career tools from Next Wave
- Grant information
- Resume/CV Database
- Career Forum

ScienceCareers.org

We know science AAAS

Phytoplankton and Cloudiness in the Southern Ocean

Nicholas Meskhidze[1]*† and Athanasios Nenes[1,2]

The effect of ocean biological productivity on marine clouds is explored over a large phytoplankton bloom in the Southern Ocean with the use of remotely sensed data. Cloud droplet number concentration over the bloom was twice what it was away from the bloom, and cloud effective radius was reduced by 30%. The resulting change in the short-wave radiative flux at the top of the atmosphere was −15 watts per square meter, comparable to the aerosol indirect effect over highly polluted regions. This observed impact of phytoplankton on clouds is attributed to changes in the size distribution and chemical composition of cloud condensation nuclei. We propose that secondary organic aerosol, formed from the oxidation of phytoplankton-produced isoprene, can affect chemical composition of marine cloud condensation nuclei and influence cloud droplet number. Model simulations support this hypothesis, indicating that 100% of the observed changes in cloud properties can be attributed to the isoprene secondary organic aerosol.

Marine aerosols strongly affect properties and lifetime of stratiform clouds, influencing Earth's radiation budget and climate. The role of oceanic biota in modifying chemical composition and size distribution of marine cloud condensation nuclei (CCN) has been one of the most intriguing questions in climate studies. Production of sulfate from the oxidation of dimethylsulfide (DMS), proposed by Shaw (*1*) and explored by Charlson *et al*. (*2*) [the CLAW hypothesis, named after the authors of the paper, Charlson, Lovelock, Andreae, and Warren (*2*)] and primary emissions of biogenic organic matter from wave breaking (*3*, *4*) have been suggested as possible mechanisms by which phytoplankton can modulate properties of marine clouds. In this work, remotely sensed data from the Moderate Resolution Imaging Spectroradiometer (MODIS) and Sea-viewing Wide Field-of-view Sensor (SeaWiFS) were combined with the National Center for Environmental Prediction (NCEP)–generated meteorological fields to examine the effects of ocean productivity on cloud microphysical and radiative properties and explore an alternative pathway by which phytoplankton may affect marine CCN. The data analysis is carried out in the Southern Ocean (SO) near South Georgia Island. Because of its unique spatial location and topography, waters near the island are a natural laboratory for investigating the effects of marine productivity on clouds. Waters in this area can support massive phytoplankton blooms (*5*, *6*), with chlorophyll a concentrations ([Chl a]) more than an order of magnitude higher than the background (*7*, *8*). Because the surface [Chl a] in this area can be used as a reliable proxy for the primary production (*5*, *9*), satellite retrievals can provide the link between ocean productivity and clouds. Strong and persistent westerlies (*10*) make it possible to examine cloud properties upwind and downwind of the bloom, and the periodic nature of the bloom is ideal for exploring the temporal relationship between ocean productivity and regional clouds.

Temporal correlation between [Chl a] and R_{eff}. We restrict our analysis to liquid-water clouds. Figure 1 shows surface [Chl a] and effective radius (R_{eff}) in the SO for the 6 years of available data. Figure 1A demonstrates that the observed enhancement of primary productivity near South Georgia Island is a localized phenomenon that typically occurs between September and February. Despite its regularity, Fig. 1 shows substantial annual variations in the bloom's temporal appearance, spatial extent, and strength, with strong anticorrelation between [Chl a] and R_{eff}. In 2001 and 2002, the smallest R_{eff} coincided with the largest enhancement in [Chl a], whereas the largest summertime R_{eff} was observed during the austral summer of 2000 and 2001 with negligible phytoplankton levels. Such systematically significant temporal anticorrelation of [Chl a] and R_{eff} suggests a link between ocean biological productivity and marine cloud properties; however, the results shown in Fig. 1 alone cannot be used to ascertain a causal relationship, given that other factors such as variation in background aerosol size distribution and cloud dynamics may also affect R_{eff}. Phytoplankton productivity and clouds could also be influenced by large-scale atmospheric circulation; such a mechanism, if it exists, would exhibit a high correlation between [Chl a] and regional cloud properties even if ocean productivity had no effect on clouds.

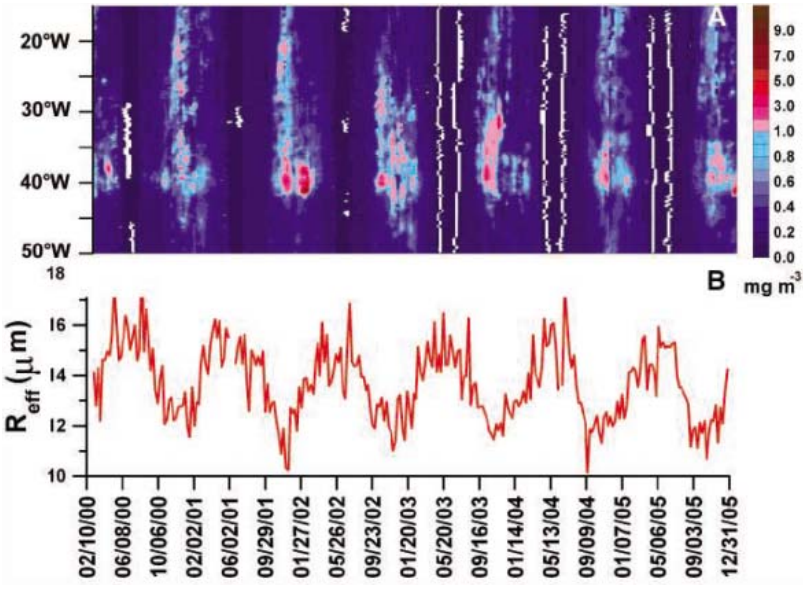

Fig. 1. The 8-day averaged (**A**) SeaWiFS-observed chlorophyll *a* and (**B**) MODIS-retrieved cloud effective radius. Data for [Chl a] is gridded at a resolution of 9 by 9 km and zonally averaged between 49°S and 54°S; data for R_{eff} is gridded at a resolution of 1° by 1° and averaged in the area of 49° to 54°S and 35° to 41°W. White areas in (A) indicate missing data.

[1]School of Earth and Atmospheric Sciences, Georgia Institute of Technology, Atlanta, GA 30332, USA. [2]School of Chemical and Biomolecular Engineering, Georgia Institute of Technology, Atlanta, GA 30332, USA.

*Present address: Department of Marine, Earth, and Atmospheric Sciences, North Carolina State University, Raleigh, NC 27695, USA.

†To whom correspondence should be addressed. E-mail: nmeskhidze@ncsu.edu

Effect of phytoplankton on clouds. To constrain the effect of phytoplankton on clouds, we adopt an approach similar to Chylek *et al*. (*11*). A rectangular geographical area was selected in the SO from 55°W to 21°W and 42°S to 60°S, then divided into 153 cells of 2° by 2°. The background colors in Fig. 2A correspond to the monthly averaged surface [Chl a] for the year with the largest bloom on record (Fig. 1). Increasing grid box number on Fig. 2B traverses through a row of cells in an eastward direction. Sharply increased [Chl a] between 48°S and 56°S indicates enhanced marine productivity near South Georgia Island.

Figure 2B suggests that average R_{eff} for background clouds in this area is ~14 μm, with a sharp decrease (~10 μm) in the vicinity of the bloom. Although MODIS-retrieved R_{eff} may be biased to larger sizes compared with in situ measurements, it is reasonable to expect that errors in observed relative changes of R_{eff} are small (*12*). This figure demonstrates that, on average, water clouds near the bloom region have effective droplet radii 30% smaller than those of background clouds over the SO.

Cloud droplet number concentration (CNDC) can be used as a direct microphysical link between the biology and cloud properties. From the remote sensing data, CNDC (cm^{-3}) can be estimated as (*13*, *14*):

$$\mathrm{CDNC} = \frac{3LWC}{4\pi\rho_w R_{eff}^3 k} = \frac{\tau}{2\pi k R_{eff}^2} \times \frac{1}{H} \quad (1)$$

where LWC is cloud liquid water content; ρ_w is the density of liquid water; H is the cloud thickness; τ and R_{eff} are MODIS-observed cloud optical depth and effective droplet radius, respectively; and k is the constant ~0.8 (*14*). H was estimated as the distance between the cloud lifting condensation level, z_{LCL} (used as a cloud base proxy), and the cloud-top height. The z_{LCL} is a strong function of relative humidity and temperature and is calculated using NCEP reanalysis surface data (*15*). Cloud-top height was computed by matching adiabatic liquid water path (LWP) with the MODIS-observed LWP. Because the average R_{eff} in the study area was typically less than the threshold effective radius for precipitation (~14 to 15 μm) (*16*), we assumed that precipitation did not cause substantial deviation of observed LWP from the adiabatic value. The calculated liquid water cloud thickness was between 250 and 400 m, consistent with observations (*17*, *18*). The uncertainty in H does not contribute considerably to the R_{eff} variability.

Figure 2B shows that the calculated monthly averaged CDNC outside the bloom area is ~55 cm^{-3}, whereas in the bloom region, CDNC increases sharply approaching twice the background level. Comparison of these values with the average summertime CDNCs for the Southern Ocean Cloud Experiment (SOCEX) shows that the estimated CDNC outside the bloom area compares well with 57 cm^{-3} reported for the SOCEX baseline conditions, whereas calculated CDNCs over the bloom are close to ones reported for the clouds affected by anthropogenic emissions (109 cm^{-3}) (*19*). This comparison suggests that the magnitude of variation of the SO marine cloud microphysics over the bloom may be comparable to anthropogenic indirect aerosol effects.

Other factors that may potentially affect CDNCs near the bloom are long-range transported Patagonian dust and sea salt. Because winds in the SO typically flow eastward (*10*), the presence of mineral dust will be manifested by noticeable decrease in aerosol optical thickness (AOT) from west to the east. Figure 2B shows that this is not the case. The enhanced productivity near South Georgia Island is primarily controlled by ocean upwelling, not by dust-Fe fertilization (*5*, *6*, *9*). Therefore, dust is not responsible for changes in either ocean productivity or R_{eff}. An increase in submicrometer-sized sea-salt particles can certainly affect CDNC, but this must be accompanied by an increase in surface wind speed over the bloom, which we did not observe (Fig. 2B). Although the general trend of increase in CDNC between 42°S and 54°S and decrease further southward can be associated with the variation in the surface wind speed (Fig. 2B), there is no clear relationship between the two near the bloom region.

Analysis of Fig. 2 indicates strong coupling between observed changes in marine biological productivity and microphysical properties of warm clouds over the bloom. We examined the possibility that both processes are driven by the same large-scale influence.

Role of meteorology. Strong winds (associated with cyclonic circulation) can cause vertical mixing and upwelling of nutrient-rich waters from below the mixed-layer depth, fueling photosynthesis and causing

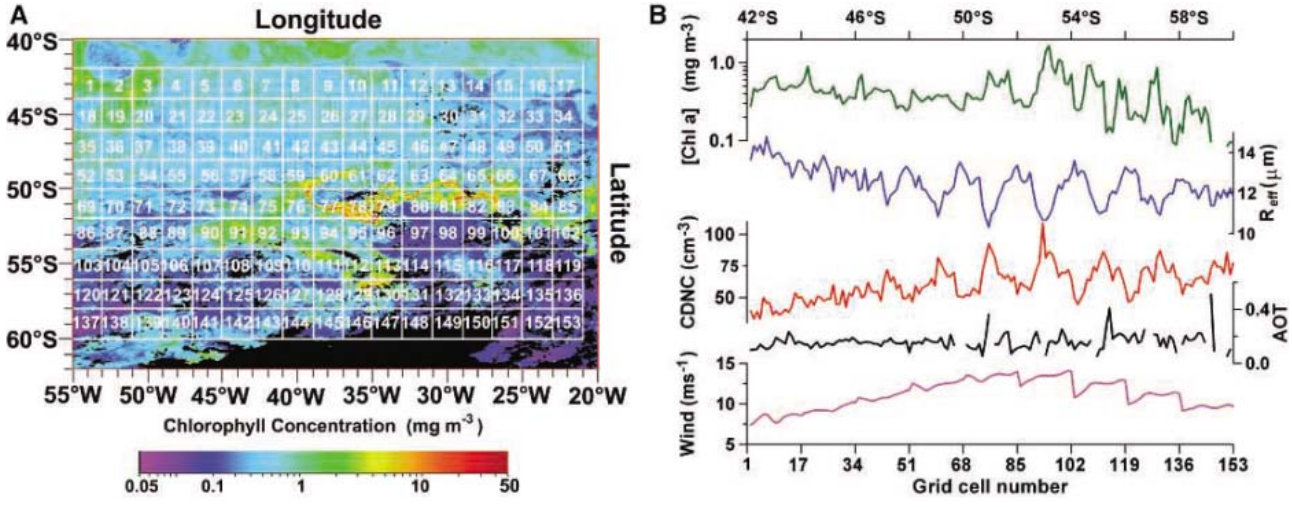

Fig. 2. (**A**) Monthly averaged (11 December 2001 to 8 January 2002) 4-km resolution SeaWiFS-observed surface [Chl a]. The black color over the ocean denotes the missing data due to clouds. The South Georgia Island boundary (54.3° to 55.0°S, 35.3° to 38.3°W) is located between cells 111 and 112. (**B**) The 2° by 2° square monthly averaged SeaWiFS surface chlorophyll concentration (green), MODIS cloud-top effective radius of liquid droplets (blue), estimated cloud droplet number concentration (red), aerosol optical thickness (black), and NCEP reanalysis–generated surface wind speed (purple) as a function of the grid cell number. Tick markers at every 17 cells correspond to the starting point of the next west-to-east row in (A). Broken line indicates the missing data.

large-scale phytoplankton blooms. Such deep water entrainments may also be associated with a depression in sea-surface temperatures (SST) (*20*, *21*) that may last up to 2 weeks and considerably influence properties of marine stratocumulus clouds (*22*). Cyclones would therefore generate a correlation (but no causality) between [Chl a] and cloud properties. The results of linear multiple regression analysis of satellite-retrieved and model-generated parameters shown in Table 1 suggest that cloud properties over the bloom are not influenced by cyclonic winds. To quantify the possible influence of phytoplankton on clouds, the analysis was carried out separately for the region with enhanced productivity (48°S to 56°S) near South Georgia Island and the areas with relatively low [Chl a] (42°S to 48°S and 56°S to 60°S), hereafter referred to as the inside and outside regions, respectively.

The analysis addresses two main questions: (i) Do meteorological parameters and [Chl a] affect R_{eff} differently in the inside and the outside regions? Table 1 shows a strong difference in the relationship of meteorological parameters and [Chl a] with R_{eff} in the inside and outside regions. Outside, R_{eff} is mainly controlled by large-scale atmospheric parameters (i.e., column precipitable water vapor, SST, surface wind speed, and AOT), and correlation between R_{eff} and [Chl a] is minor. The relationship between [Chl a] and R_{eff} in the inside region is markedly different from that of the outside region; inside, the effect of [Chl a] on R_{eff} has by far the strongest impact of all parameters examined. (ii) Can changes in meteorological parameters affect R_{eff} while changing [Chl a]? Linear multiple regression analysis suggests that in the outside region, the change in R_{eff} is primarily associated with variability in meteorological parameters, whereas in the inside region, [Chl a] is the single most important parameter controlling the R_{eff} (Table 1).

As a result of this analysis, we concluded that over the bloom, the relationship between the ocean productivity and R_{eff} of warm clouds is unique to these two variables and does not extend to large-scale meteorological parameters—i.e., biological productivity is the prime cause for changes in cloud microphysical and radiative parameters.

Radiative forcing. The perturbation in short-wave radiation (ΔF) at the top-of-the atmosphere (TOA) within our study area is estimated as (*23*)

$$\Delta F = -\frac{1}{3} F_{in} A_c R_c (1 - R_c) \Delta \ln N_{db} \quad (2)$$

where F_{in} is the monthly averaged solar flux at the top of marine liquid clouds calculated with the NASA Global Modeling Initiative (GMI) with implemented short-wave radiative transfer code (*24*); R_c and A_c are monthly averaged MODIS-observed cloud albedo and cloud fraction, respectively; and $\Delta \ln N_{db}$ is relative change in calculated CDNC [$\Delta \ln N_{db} = (N_d - N_b)/N_d$], where N_d and N_b are average droplet numbers over the bloom and in the background air, respectively. Because of variability of background CDNC in zonal direction (Fig. 2B), N_b was estimated separately for each longitude using a linear fit between the locations farthest from the bloom (square numbers 1 and 17, 18 and 34, and so on, in Fig. 2A).

Figure 3 shows considerable variation in TOA mean short-wave forcing in the study area resulting from changes in properties of liquid clouds. However, the remarkable feature of Fig. 3 is the very strong cooling near the bloom, reaching ~–15 W m^{-2}. Such a large change in TOA short-wave radiation is comparable in magnitude with the aerosol indirect effect in highly polluted regions (*24*–*26*), highlighting the need for improved quantification of interactions between marine biota, aerosols, clouds, and climate. Clearly, the link between ocean productivity and change in cloud properties is in the modification of CCN. We next examined whether production of secondary organic aerosol (SOA) from the oxidation of phytoplankton-produced isoprene can lead to considerable changes in marine CCN.

Phytoplankton isoprene SOA and its effect on CCN. Although organosulfur emissions and the transfer of surface active organic matter from the oceanic surface layer to the atmosphere have been studied in detail, little is known about the effect of phytoplankton-produced nonmethane hydrocarbons (NMHC) on marine aerosol. Oceans are known to be a potential source of NMHC and particularly

Table 1. The influence of meteorological parameters and [Chl a] on the R_{eff} in the Study area of the Southern Ocean. Meteorological parameters used as independent variables were selected according to Kaufman *et al.* (*56*). We analyzed dependence of R_{eff} on (i) MODIS-retrieved AOT, SST, cloud-top temperature (indicator of cloud height), and total precipitable water vapor (indicator of convergence); (ii) SeaWiFS-observed [Chl a]; and (iii) NCEP and National Center for Atmospheric Research (NCAR) reanalysis–generated surface wind speed, equivalent potential temperature difference between 500 and 925 hPa, and the broad-scale vertical motion at 850 hPa. The logarithm of the AOT is used to reduce nonlinearity in the regression (*56*). The parameters are ranked by order of importance based on the correlation with R_{eff} in the outside region. Columns to the right of correlation coefficients show the change in R_{eff} associated by the multiple regression with the changes in meteorological parameters and [Chl a]. To compare multiple regression coefficients of variables of different magnitudes and dispersions, we standardized all variables by subtracting the mean and dividing the result by the standard deviation. Therefore, coefficients given in the "Change in R_{eff}" columns show the average amount of change in R_{eff} when each meteorological parameter and [Chl a] change by one standard deviation, while keeping others constant. The range around the sample regression coefficients was determined for 95% confidence interval.

	Outside the bloom area (42°S to 48°S and 56°S to 60°S)		Inside the bloom area (48°S to 56°S)	
	Correlation to R_{eff}	Change in R_{eff}	Correlation to R_{eff}	Change in R_{eff}
Total column precipitable water vapor	0.67 ± 0.08	0.48 ± 0.10	–0.02 ± 0.12	–0.02 ± 0.10
Sea-surface temperature	0.65 ± 0.08	0.63 ± 0.09	0.01 ± 0.12	0.01 ± 0.11
Surface wind speed	–0.52 ± 0.09	–0.50 ± 0.11	–0.14 ± 0.12	–0.15 ± 0.10
ln(AOT)	–0.43 ± 0.10	–0.41 ± 0.09	–0.01 ± 0.12	–0.01 ± 0.13
Potential temperature difference	0.34 ± 0.10	–0.40 ± 0.11	–0.09 ± 0.12	–0.08 ± 0.11
Vertical velocity	–0.27 ± 0.10	0.23 ± 0.09	–0.10 ± 0.12	–0.12 ± 0.10
Eastern wind at 850 hPa	0.22 ± 0.10	0.27 ± 0.12	0.10 ± 0.12	0.01 ± 0.11
Cloud-top temperature	–0.02 ± 0.11	–0.01 ± 0.09	–0.02 ± 0.12	–0.02 ± 0.11
[Chl a]	0.18 ± 0.14	0.19 ± 0.10	–0.48 ± 0.11	–0.49 ± 0.09

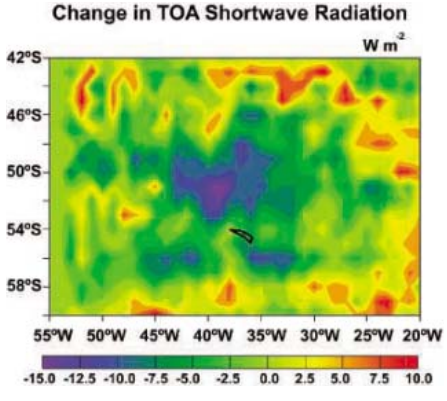

Fig. 3. Change in TOA short-wave radiation. The radiative effect was evaluated for the change in albedo of warm marine clouds. Calculations are carried out using monthly averaged MODIS-observed data at 1° by 1° resolution and the GMI-supplied monthly averaged solar flux at 4° by 5° resolution.

isoprene (*27*–*29*); observed atmospheric concentrations of isoprene in remote SO are high (~0.25 parts per billion by volume) (*30*)—about one-fifth the amount of typical boundary-layer isoprene concentration over the Amazon (*31*). Atmospheric oxidation of isoprene may lead to formation of SOA (*32*–*34*). Because SOA concentrations in remote marine regions are very small (*35*), ocean-emitted isoprene could contribute considerably to the organic fraction of marine CCN. We propose that isoprene SOA can affect CCN composition and contribute to the observed changes in cloud properties. To evaluate the plausibility of this hypothesis, we estimated atmospheric concentrations of isoprene, the resulting SOA, and its subsequent effect on CCN. Table 2 summarizes [Chl a] inside the bloom, estimated sea-air fluxes, and concentrations of isoprene in the marine boundary layer (MBL). Seawater-dissolved isoprene in the bloom region (C_w^A) was estimated with the approach of Palmer and Shaw (*36*).

For comparison, in Table 2 we include observed [Chl a] and dissolved isoprene concentrations for the iron-enriched North Patch of the Southern Ocean Iron Enrichment Experiment (SOFeX-N) (*37*). The average surface ocean [Chl a] measured for SOFeX-N and for the bloom in our study area are comparable (Table 2), yet SOFeX-N isoprene concentration was more than three orders of magnitude higher than estimated for the bloom. The chlorophyll content of seawater, as sensed by the satellite, is related to the rate of isoprene production (*38*). Given that both blooms had similar average [Chl a], were located in the SO at comparable latitudes, had similar SSTs and mixed-layer depths, and occurred in the same season, such large discrepancies in dissolved isoprene concentrations could arise from the difference in phytoplankton species. Laboratory studies show that isoprene production rates between diatoms, dinoflagellates, and coccolithophores can vary over orders of magnitude (*28*, *39*, *40*). Production rates suggested in (*36*) and used in Table 2 for C_w^A are applicable to species typical for the oligotrophic oceans (cyanobacteria, picoeucariotes, and coccolithophores) and are likely not representative of the blooms in the SO where microphytoplankton typically contributes >70% of total cell counts, followed by nano- and picophytoplankton (*41*–*43*). Inside the bloom, diatoms were five times more abundant than the next contributor, dinoflagellates; species measured (in order of their abundance) were *Thallasiosira* sp. 1, *Nitzschia* spp., and *Chaetoceros* spp. (*41*). In the absence of any local data and good similarity with SOFeX-N (*42*), dissolved isoprene in the bloom was estimated with SOFeX-N measured isoprene concentration and scaled with [Chl a]. Estimated sea-air fluxes of isoprene are orders of magnitude higher than the monthly averaged fluxes (0.4×10^8 to 8×10^8 molecules cm^{-2} s^{-1}) suggested for the SO (*36*), indicating that the global marine isoprene flux of ~0.1 Tg C $year^{-1}$ (*36*) should be viewed as the low-end estimate. In Table 2, we also include estimated MBL isoprene and SOA concentrations over the bloom.

To evaluate the role of this potentially important organic aerosol source on cloud microphysics, we calculated CDNC using a cloud parcel model (*44*). The simulations were performed for different concentrations of organic aerosol, non–sea-salt (nss) sulfate, and updraft velocities. The range of SOA concentrations examined (0 to 250 ng m^{-3}) corresponds to the estimated SOA over the background air and at the center of the bloom (Table 2). In all simulations, aerosol number remains constant; therefore, addition of SOA corresponds to the condensation growth and aging of marine aerosols (*44*). Ambient measurements and chamber experiments showed that 2-methyltetrols and C_5 alkene triols are some of the main particulate-phase oxidation products of isoprene under low-NO_x conditions (*32*, *45*–*48*). Because the reaction pathways leading to production of isoprene SOA and chemical properties of the oligomers with high molecular weight remain little understood (*45*), we assumed that ~20% of organic particulate mass is water soluble with chemical properties corresponding to 2-methyltetrols (*44*). Cloud-base updraft velocity is constrained by estimated CDNCs outside the bloom region. The background CDNC (the low left corner on Fig. 4, A and B) is well represented by trimodal marine aerosol size distribution and chemical composition (*44*) with updraft velocities between 0.35 to 0.5 ms^{-1}, typical of marine stratiform clouds (*15*, *49*). Figure 4 shows that the excess amount of organic mass increases CDNC; modification of the ambient size and CCN activity of marine aerosols due to addition of organic mass can explain up to 60% of the droplet number concentration over the bloom.

In addition to enhanced concentration of dissolved isoprene, ocean waters in blooms have commonly been characterized by elevated levels of DMS, atmospheric oxidation of which is a major source of nss sulfate in remote marine air. Model simulations show (left side of Fig. 4) that for the range of nss sulfate measured over the SO (*50*) sea-salt CCN and nss CCN may account for the enhanced CDNC over the bloom. However, Fig. 4 also shows that when mixed with SOA, even the minimal concentration of nss sulfate can fully account for the observed enhancement of CDNC. This is important, considering that regions with high isoprene productivity may not coincide with elevated levels of DMS (*30*) or under conditions with biological net DMS consumption in a bloom (*51*).

Our model results suggest that phytoplankton isoprene emissions could contribute to the organic fraction of marine CCN and be a viable mechanism by which ocean biota

Table 2. Ocean chlorophyll *a*, fluxes, and atmospheric concentrations of isoprene. [Chl a] inside the bloom is based on SeaWiFS observed chlorophyll *a* data retrieved at 9-km resolution. Maximum and minimum concentrations correspond to the middle and the edge of the bloom. C_w^A was estimated according to Palmer and Shaw (*36*). The isoprene production rate was calculated by multiplying suggested rates of 1.8 ± 0.7 μmol isoprene produced (grams phytoplankton chlorophyll a)$^{-1}$ day^{-1} by SeaWiFS [Chl a]. The range of dissolved isoprene is from Wingenter (*57*). C_w^B was estimated using SOFeX-N measured surface values and scaled with SeaWiFS [Chl a]. The sea-air isoprene flux F was parameterized as $F = k_l(C_{sw} - C_{BL}/H)$, where k_l is the piston velocity, C_{sw} is the estimated seawater concentration of isoprene in the bloom, C_{BL} is marine boundary layer isoprene concentration, and H is the Henry's law constant for isoprene (*58*). For the typical range of atmospheric and oceanic isoprene concentrations, the second term in the equation is at least an order of magnitude smaller (*38*) and therefore is ignored here. The $k_l = 0.39U_{10}^2(Sc/660)^{-0.5}$ (*59*), where U_{10} is NCEP reanalysis–generated monthly averaged wind speed at 10-m height, and Sc is the Schmidt number calculated using isoprene molar volume and MODIS-observed ocean temperatures. Amazon fluxes are the median fluxes over the tropical forest site of the Peruvian Amazon (*31*). Assuming that isoprene oxidation had no significant impact on OH levels in the MBL (*60*), the average MBL isoprene concentration above the bloom was calculated with the use of *FB*, the average isoprene lifetime of 2 hours and boundary layer height of 600 to 1000 m. The SOA concentration was estimated with the use of global isoprene SOA yield of 3% (*35*, *46*).

	[Chl a] (mg m^{-3})		Dissolved isoprene concentration (nM)			Isoprene flux (10^8 molecules cm^{-2} s^{-1})			Estimated MBL concentration (ng m^{-3})	
	Bloom	SOFeX	C_w^A	SOFeX	C_w^B	F_A	F_B	Amazon	Isoprene	SOA
Average	3.0	2.4	0.03	31.4	36.3	1.8	2370	18200	1920	50
Max	12.7	2.6	0.13	>40	145	8.6	9470	20000	7700	230
Min	0.1	0.1	0.003	<10	6.1	0.2	395	7000	320	5

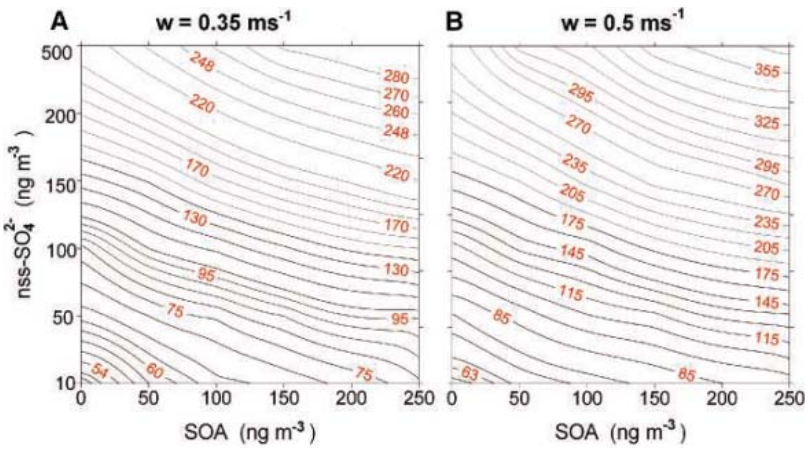

Fig. 4. (**A** and **B**) Contours of cloud droplet number concentration (cm^{-3}) as a function of chemical composition and updraft velocity.

may affect properties of shallow marine clouds. We propose that SOA of marine origin can act synergistically with the established mechanisms (*1*–*4*) and lead to changes in marine CCN chemical composition and number concentration.

Discussion and conclusions. Analysis of remotely sensed data indicates that over the enhanced biological productivity region of the SO, cloud droplet number was doubled and the effective radius was decreased by more than 30%. Analysis of data revealed that changes in the properties of warm clouds over the bloom were primarily associated with the enhanced ocean biological productivity. These changes can lead to a TOA short-wave radiative forcing of –15 W m^{-2}, comparable to the aerosol indirect effect over highly polluted regions of the globe. We propose that SOA formed from the oxidation of ocean-emitted isoprene can account for the observed change in properties of shallow marine clouds over the bloom. Model simulations presented support this hypothesis, making ocean isoprene emissions a viable mechanism by which marine biota may affect properties of shallow clouds. Considering that isoprene SOA can be an important source of marine aerosol organic mass, this unaccounted SOA may partly reconcile the large organic aerosol source missing from current global models (*52*). Cooperative efforts of researchers from different fields are required to provide accurate estimates of sea-air fluxes of biogenic volatile organic compounds (VOCs) in different parts of the ocean. Work is also needed to constrain the chemical composition of SOA in marine environments and its effect on aerosol activation. Future campaigns may provide the evidence for the importance of this new source of organics in the SO and the viability of the proposed mechanism. Given that the evolution of microalgae can be affected by anthropogenic air pollutants (*53*, *54*) and environmental changes (*55*), the proposed mechanism of SOA formation in remote marine air may need to be included in global models. Because the average concentration of [Chl a] in the bloom was similar to that of SOFeX-N, which is thought to be representative of the glacial era concentrations of Fe in the SO (*37*), we propose that SOA from phytoplankton-produced isoprene may have played a considerable role in climate transition, perhaps amplifying the negative feedback loop suggested by the CLAW hypothesis.

References and Notes

1. G. E. Shaw, *Clim. Change* **5**, 297 (1983).
2. R. J. Charlson, J. E. Lovelock, M. O. Andreae, S. G. Warren, *Nature* **326**, 655 (1987).
3. A. M. Middlebrook, D. M. Murphy, D. S. Thomson, *J. Geophys. Res.* **103**, 16475 (1998).
4. C. D. O'Dowd *et al.*, *Nature* **431**, 676 (2004).
5. R. E. Korb, M. Whitehouse, *Deep-Sea Res. I* **51**, 721 (2004).
6. N. Meskhidze, A. Nenes, W. L. Chameides, C. Luo, N. Mahowald, unpublished data.
7. J. H. Martin, S. E. Fitzwater, *Nature* **331**, 341 (1988).
8. P. W. Boyd *et al.*, *Nature* **407**, 695 (2000).
9. M. P. Meredith *et al.*, *Geophys. Res. Lett.* **30**, 2061 (2003).
10. S. T. Gille, *Ocean. Technol.* **22**, 1353 (2005).
11. P. Chylek *et al.*, *Geophys. Res. Lett.* **33**, L06806 (2006).
12. T. Nakajima, M. D. King, J. D. Spinhirne, L. F. Radke, *J. Atmos. Sci.* **48**, 728 (1991).
13. A. Slingo, *J. Atmos. Sci.* **46**, 1419 (1989).
14. G. M. Martin, D. W. Johnson, A. Spice, *J. Atmos. Sci.* **51**, 1823 (1994).
15. M. G. Lawrence, *Bull. Am. Meteorol. Soc.* **86**, 225 (2005).
16. H. Shao, G. Liu, *J. Geophys. Res.* **109**, D07205 (2004).
17. C. S. Bretherton *et al.*, *Bull. Am. Meteorol. Soc.* **85**, 967 (2004).
18. N. Meskhidze, A. Nenes, W. C. Conant, J. H. Seinfeld, *J. Geophys. Res.* **110**, D16202 (2005).
19. S. S. Yum, J. G. Hudson, *J. Geophys. Res.* **109**, D06204 (2004).
20. I. Lin *et al.*, *Geophys. Res. Lett.* **30**, 1718 (2003).
21. S. Son, T. Platt, H. Bouman, D. Lee, S. Sathyendranath, *Geophys. Res. Lett.* **33**, L05607 (2006).
22. D. A. Hegg, P. A. Durkee, H. H. Jonsson, K. Nielsen, D. S. Covert, *Geophys. Res. Lett.* **31**, L06113 (2004).
23. R. J. Charlson *et al.*, *Science* **255**, 423 (1992).
24. H. Bian, M. J. Prather, *J. Atmos. Chem.* **41**, 281 (2002).
25. A. Jones, D. L. Roberts, A. Slingo, *Nature* **370**, 450 (1994).
26. S. Menon, A. D. Del Genio, D. Koch, G. Tselioudis, *J. Atmos. Sci.* **59**, 692 (2002).
27. B. Bonsang, C. Polle, G. Lambert, *Geophys. Res. Lett.* **19**, 1129 (1992).
28. P. J. Milne, D. D. Riemer, R. G. Zika, L. E. Brand, *Mar. Chem.* **48**, 237 (1995).
29. W. J. Broadgate, P. S. Liss, S. A. Penkett, *Geophys. Res. Lett.* **24**, 2675 (1997).
30. Y. Yokouchi, H. J. Li, T. Machida, S. Aoki, H. Akimoto, *J. Geophys. Res.* **104**, 8067 (1999).
31. D. Helmig *et al.*, *J. Geophys. Res.* **103**, 25519 (1998).
32. M. Claeys *et al.*, *Science* **303**, 1173 (2004).
33. H.-J. Lim, A. G. Carlton, B. J. Turpin, *Environ. Sci. Technol.* **39**, 4441 (2005).
34. S. N. Matsunaga *et al.*, *Atmos. Chem. Phys. Discuss.* **5**, 11143 (2005).
35. D. K. Henze, J. H. Seinfeld, *Geophys. Res. Lett.* **33**, L09812 (2006).
36. P. I. Palmer, S. L. Shaw, *Geophys. Res. Lett.* **32**, L09805 (2005).
37. O. W. Wingenter *et al.*, *Proc. Natl. Acad. Sci. U.S.A.* **101**, 8537 (2004).
38. A. Guenther *et al.*, *J. Geophys. Res.* **100**, 8873 (1995).
39. R. M. Moore, D. E. Oram, S. A. Penkett, *Geophys. Res. Lett.* **21**, 2507 (1994).
40. S. L. Shaw, S. W. Chisholmb, R. G. Prinna, *Mar. Chem.* **80**, 227 (2003).
41. P. Ward *et al.*, *Deep-Sea Res. I* **52**, 421 (2005).
42. K. H. Coale *et al.*, *Science* **304**, 408 (2004).
43. D. Kamykowski, S.-J. Zentara, J. M. Morrison, A. C. Switzer, *Global Biogeochem. Cycles* **16**, 1077 (2002).
44. Materials and methods are available as supporting material on *Science* Online.
45. J. D. Surratt *et al.*, *J. Phys. Chem. A* **110**, 9665 (2006).
46. N. L. Ng *et al.*, *Environ. Sci. Technol.* **40**, 2283 (2006).
47. S. Decesari *et al.*, *Atmos. Chem. Phys.* **6**, 375 (2006).
48. W. Wang *et al.*, *Rapid Commun. Mass Spectrom.* **19**, 1343 (2005).
49. K. T. Whitby, *Atmos. Environ.* **12**, 135 (1978).
50. M. O. Andreae, W. Elbert, Y. Cai, T. W. Andreae, *J. Geophys. Res.* **104**, 21695 (1999).
51. Y. Le Clainche *et al.*, *J. Geophys. Res.* **111**, C01011 (2006).
52. C. L. Heald *et al.*, *Geophys. Res. Lett.* **32**, L18809 (2005).
53. N. Meskhidze, W. L. Chameides, A. Nenes, G. Chen, *Geophys. Res. Lett.* **30**, 2085 (2003).
54. N. Meskhidze, W. L. Chameides, A. Nenes, *J. Geophys. Res.* **110**, D03301 (2005).
55. J. Beardall, J. A. Raven, *Phycologia* **43**, 26 (2004).
56. Y. J. Kaufman, I. Koren, L. A. Remer, D. Rosenfeld, Y. Rudich, *Proc. Natl. Acad. Sci. U.S.A.* **102**, 11207 (2005).
57. O. Wingenter, *SOLAS News Issue 1* (2005), p. 5 (www.uea.ac.uk/env/solas/News1/newsletter.html/).
58. R. Wanninkhof, *J. Geophys. Res.* **97**, 7373 (1992).
59. R. M. Moore, W. Groszko, *J. Geophys. Res.* **104**, 11,163 (1999).
60. A. A. P. Pszenny, R. G. Prinn, G. Kleiman, X. Shil, T. S. Bates, *J. Geophys. Res.* **104**, 21,785 (1999).

61. This work was supported by a NASA New Investigator Award, an NSF CAREER award and a Blanchard-Milliken Young Faculty Fellowship. N.M. acknowledges support from a NASA Goddard Visiting Fellowship. We also thank C. O'Dowd, M. C. Facchini, S. N. Pandis, and three anonymous reviewers for their thoughtful comments.

Supporting Online Material

www.sciencemag.org/cgi/content/full/1131779/DC1
Materials and Methods
References

26 June 2006; accepted 25 October 2006
Published online 2 November 2006;
10.1126/science.1131779
Include this information when citing this paper.

Fast Variability of Tera–Electron Volt γ Rays from the Radio Galaxy M87

F. Aharonian,[1] A. G. Akhperjanian,[2] A. R. Bazer-Bachi,[3] M. Beilicke,[4]* W. Benbow,[1] D. Berge,[1] K. Bernlöhr,[1,5] C. Boisson,[6] O. Bolz,[1] V. Borrel,[3] I. Braun,[1] A. M. Brown,[7] R. Bühler,[1] I. Büsching,[8] S. Carrigan,[1] P. M. Chadwick,[7] L.-M. Chounet,[9] G. Coignet,[10] R. Cornils,[4] L. Costamante,[1,23] B. Degrange,[9] H. J. Dickinson,[7] A. Djannati-Ataï,[11] L. O'C. Drury,[12] G. Dubus,[9] K. Egberts,[1] D. Emmanoulopoulos,[13] P. Espigat,[11] F. Feinstein,[14] E. Ferrero,[13] A. Fiasson,[14] G. Fontaine,[9] Seb. Funk,[5] S. Funk,[1] M. Füßling,[5] Y. A. Gallant,[14] B. Giebels,[9] J. F. Glicenstein,[15] P. Goret,[15] C. Hadjichristidis,[7] D. Hauser,[1] M. Hauser,[13] G. Heinzelmann,[4] G. Henri,[16] G. Hermann,[1] J. A. Hinton,[1,13] A. Hoffmann,[17] W. Hofmann,[1] M. Holleran,[8] S. Hoppe,[1] D. Horns,[17] A. Jacholkowska,[14] O. C. de Jager,[8] E. Kendziorra,[17] M. Kerschhaggl,[5] B. Khélifi,[9,1] Nu. Komin,[14] A. Konopelko,[5]† K. Kosack,[1] G. Lamanna,[10] I. J. Latham,[7] R. Le Gallou,[7] A. Lemière,[11] M. Lemoine-Goumard,[9] J.-P. Lenain,[6] T. Lohse,[5] J. M. Martin,[6] O. Martineau-Huynh,[18] A. Marcowith,[3] C. Masterson,[1,23] G. Maurin,[11] T. J. L. McComb,[7] E. Moulin,[14] M. de Naurois,[18] D. Nedbal,[19] S. J. Nolan,[7] A. Noutsos,[7] K. J. Orford,[7] J. L. Osborne,[7] M. Ouchrif,[18,23] M. Panter,[1] G. Pelletier,[16] S. Pita,[11] G. Pühlhofer,[13] M. Punch,[11] S. Ranchon,[10] B. C. Raubenheimer,[8] M. Raue,[4] S. M. Rayner,[7] A. Reimer,[20] J. Ripken,[4] L. Rob,[19] L. Rolland,[15] S. Rosier-Lees,[10] G. Rowell,[1] V. Sahakian,[2] A. Santangelo,[17] L. Saugé,[16] S. Schlenker,[5] R. Schlickeiser,[20] R. Schröder,[20] U. Schwanke,[5] S. Schwarzburg,[17] S. Schwemmer,[13] A. Shalchi,[20] H. Sol,[6] D. Spangler,[7] F. Spanier,[20] R. Steenkamp,[21] C. Stegmann,[22] G. Superina,[9] P. H. Tam,[13] J.-P. Tavernet,[18] R. Terrier,[11] M. Tluczykont,[9,23] C. van Eldik,[1] G. Vasileiadis,[14] C. Venter,[8] J. P. Vialle,[10] P. Vincent,[18] H. J. Völk,[1] S. J. Wagner,[13] M. Ward[7]

The detection of fast variations of the tera–electron volt (TeV) (10^{12} eV) γ-ray flux, on time scales of days, from the nearby radio galaxy M87 is reported. These variations are about 10 times as fast as those observed in any other wave band and imply a very compact emission region with a dimension similar to the Schwarzschild radius of the central black hole. We thus can exclude several other sites and processes of the γ-ray production. The observations confirm that TeV γ rays are emitted by extragalactic sources other than blazars, where jets are not relativistically beamed toward the observer.

So far, the only extragalactic objects known to emit γ radiation up to energies of Tera electron volts (1 TeV = 10^{12} eV) are blazars. These are active galactic nuclei (AGN) with a plasma jet emanating from the vicinity of the black hole and pointing close to the observer's line of sight. Because of the bulk relativistic motion of the plasma in the jet, the energy and luminosity of emitted photons are boosted by relativistic effects, making blazars detectable up to TeV energies.

The nearby radio galaxy M87 is located in the Virgo cluster of galaxies at a distance of ~16 Mpc ($z = 0.0043$) and hosts a central black hole of $(3.2 \pm 0.9) \times 10^9$ solar masses (*1*). The 2-kpc scale plasma jet (*2*) originating from the center of M87 is resolved at different wavelengths (radio, optical, and x-ray). The observed inclination of the jet, at an angle of ~30° relative to the observer's line of sight (*3*), demonstrates that M87 is not a blazar and hence would represent a new class of TeV γ-ray emitters. M87 has also been suggested as an accelerator of the enigmatic ultra-high-energy (10^{20} eV) cosmic rays (*4*, *5*). Previously, weak evidence for $E > 730$ GeV γ-ray emission from M87 in 1998 and 1999 with a statistical significance of 4.1 SDs was reported by the High Energy Gamma Ray Astronomy (HEGRA) collaboration (*6*). No emission above 400 GeV was observed by the Whipple collaboration (*7*) from 2000-2003.

The observations reported here were performed with the High Energy Stereoscopic System (H.E.S.S.) located in Namibia. H.E.S.S. is an array of four imaging atmospheric-Cherenkov telescopes used for the measurement of cosmic γ rays of energies between 100 GeV and several 10 TeV [see (*8*) for more details]. The observations of M87 were performed between 2003 and 2006, yielding a total of 89 hours of data after quality selection cuts. After calibration (*9*), the H.E.S.S. standard analysis was applied to the data using hard event selection cuts (*10*). More information about the standard analysis, as well as a more recent, alternative analysis technique (*11*) which gives consistent results, can be found in (*12*).

An excess of 243 γ-ray events is measured from the direction of M87 in the whole data set, corresponding to a statistical significance of 13 SDs, establishing M87 as a TeV γ-ray source (Fig. 1). The position of the excess (right ascension, α; declination, δ) was found to be $\alpha = 12^h30^m\ 47.2^s \pm 1.4^s$, $\delta = +12°23'51'' \pm 19''$ (J2000.0). This is, within the quoted statistical error and the systematic pointing uncertainty of the H.E.S.S. telescopes (~20″ in both the right ascension and declination directions) compatible with the nominal (radio) position (*13*) of the nucleus of M87 ($\alpha = 12^h30^m\ 49.4^s$, $\delta = +12°23'28''$). Considering the angular resolution of H.E.S.S., the source is consistent with a pointlike object with an upper limit for a Gaussian surface-brightness profile of 3 arc min (99.9% confidence level). At the distance of M87 (16 Mpc), this corresponds to a radial extension of 13.7 kpc, which can be compared with the large-scale structure of M87 as seen at radio wavelengths (Fig. 1). A constraint on the size of the TeV emission region that is ~10^6 times as strong is deduced from the observed short-term flux variability, as shown below.

The differential energy spectra obtained for the 2004 and 2005 data sets (Fig. 2) are both well fit by a power-law function $dN/dE \propto E^{-\Gamma}$. The spectrum measured in 2005 is found to be hard ($\Gamma \sim 2.2$) and reaches beyond 10 TeV, with

[1]Max-Planck-Institut für Kernphysik, Post Office Box 103980, D 69029 Heidelberg, Germany. [2]Yerevan Physics Institute, 2 Alikhanian Brothers Street, 375036 Yerevan, Armenia. [3]Centre d'Etude Spatiale des Rayonnements, CNRS/UPS, 9 avenue du Colonel Roche, BP 4346, F-31029 Toulouse Cedex 4, France. [4]Universität Hamburg, Institut für Experimentalphysik, Luruper Chaussee 149, D 22761 Hamburg, Germany. [5]Institut für Physik, Humboldt-Universität zu Berlin, Newtonstrasse 15, D 12489 Berlin, Germany. [6]Laboratoire Univers et Théories, UMR 8102 du CNRS, Observatoire de Paris, Section de Meudon, F-92195 Meudon Cedex, France. [7]University of Durham, Department of Physics, South Road, Durham DH1 3LE, UK. [8]Unit for Space Physics, North-West University, Potchefstroom 2520, South Africa. [9]Laboratoire Leprince-Ringuet, IN2P3/CNRS, Ecole Polytechnique, F-91128 Palaiseau, France. [10]Laboratoire d'Annecy-le-Vieux de Physique des Particules, IN2P3/CNRS, 9 Chemin de Bellevue, BP 110 F-74941 Annecy-le-Vieux Cedex, France. [11]Astro Particule et Cosmologie, UMR 7164 (Université Paris 7, CNRS, CEA, Observatoire de Paris), 10 rue Alice Domon et Léonie Duquet, 75025 Paris Cedex 13, France. [12]Dublin Institute for Advanced Studies, 5 Merrion Square, Dublin 2, Ireland. [13]Landessternwarte, Universität Heidelberg, Königstuhl, D 69117 Heidelberg, Germany. [14]Laboratoire de Physique Théorique et Astroparticules, IN2P3/CNRS, Université Montpellier II, CC 70, Place Eugène Bataillon, F-34095 Montpellier Cedex 5, France. [15]DAPNIA/DSM/CEA, CE Saclay, F-91191 Gif-sur-Yvette Cedex, France. [16]Laboratoire d'Astrophysique de Grenoble, Institut National des Sciences de l'Univers/CNRS, Université Joseph Fourier, BP 53, F-38041 Grenoble Cedex 9, France. [17]Institut für Astronomie und Astrophysik, Universität Tübingen, Sand 1, D 72076 Tübingen, Germany. [18]Laboratoire de Physique Nucléaire et de Hautes Energies, IN2P3/CNRS, Universités Paris VI and VII, 4 Place Jussieu, F-75252 Paris Cedex 5, France. [19]Institute of Particle and Nuclear Physics, Charles University, V Holesovickach 2, 180 00 Prague 8, Czech Republic. [20]Institut für Theoretische Physik, Lehrstuhl IV, Weltraum und Astrophysik, Ruhr-Universität Bochum, D 44780 Bochum, Germany. [21]University of Namibia, Private Bag 13301, Windhoek, Namibia. [22]Universität Erlangen-Nürnberg, Physikalisches Institut, Erwin-Rommel-Str. 1, D 91058 Erlangen, Germany. [23]European Associated Laboratory for Gamma-Ray Astronomy, jointly supported by CNRS and Max-Planck-Gesellschaft.

*To whom correspondence should be addressed. E-mail: matthias.beilicke@desy.de

†Present address: Purdue University, Department of Physics, 525 Northwestern Avenue, West Lafayette, IN 47907–2036, USA.

an average γ-ray flux of a factor of ~5 as high as in 2004.

The total γ-ray flux above 730 GeV (Fig. 3) for the individual years from 2003 to 2006 indicates variability on a yearly basis (*14*) corresponding to a statistical significance of 3.2 SDs, being derived from a χ^2 fit of a constant function. The variability is confirmed by a Kolmogorov test comparing the distribution of photon arrival times to the distribution of background arrival times, yielding a statistical significance for burst-like (nonconstant) behavior of the source of 4.5 SDs. Unexpectedly, variability on time scales of days (flux doubling) was found in the high-state data of 2005 (Fig. 3A), with a statistical significance of more than 4 SDs. This is the fastest variability observed in any wave band from M87 and strongly constrains the size of the emission region of the TeV γ radiation, which is further discussed below. No indications for short-term variability were found in the data of 2003, 2004, and 2006, which is not unexpected given the generally lower statistical significances of the γ-ray excesses in those years.

These observational results (location, spectrum, and variability) challenge most scenarios of very-high-energy γ-ray production in extragalactic sources. Although the luminosity ($\approx 3 \times 10^{40}$ erg/s) of TeV γ rays is quite modest and does not cause any problems with the global energy budget of the active galaxy M87, several models can be dismissed. The upper limit on the angular size of ~ 3 arc min (13.7 kpc $\approx 4.3 \times 10^{22}$ cm) centered on the M87 nucleus position already excludes the core of the Virgo cluster (*15*) and outer radio regions of M87 as TeV γ-ray emitting zones. Further, the observed variability on time scales of $\Delta t \sim 2$ days requires a very compact emission region because of the light-crossing time. The characteristic size is limited to $R \leq c \times \Delta t \times \delta \approx 5 \times 10^{15}\ \delta$ cm $\approx 5 \times \delta\ R_s$, where δ is the relativistic Doppler factor (*16*) of the source of TeV radiation and $R_s \approx 10^{15}$ cm is the Schwarzschild radius of the M87 supermassive black hole. For any reasonable value of the Doppler factor (i.e., $1 < \delta < 50$, as used in the modeling of TeV γ-ray blazars), this implies a drastic constraint on the size of the TeV γ-ray source, which immediately excludes several potential sites and hypotheses of γ-ray production. First of all this concerns the elliptical galaxy M87 (*15*) and the γ-ray production due to dark matter annihilation (*17*). The most obvious candidate for efficient particle acceleration (*18*), namely the entire extended kiloparsec jet, is also excluded. Although compatible with the TeV source position, even the brightest knot in the jet (knot A) appears excluded, with its typical size on the order of one arc sec (about 80 pc $\approx 2.5 \times 10^{20}$ cm) resolved in the x-ray range (*19*).

An interesting possibility would be the peculiar knot (HST-1) in the jet of M87 (see supporting online text and fig. S2), a region of many violent events, with x-ray flares exceeding the luminosity of the core emission (*20*) and superluminal blobs being detected downstream. Modeling the high-energy radiation properties of this region (by synchrotron and inverse-Compton scenarios), several authors favor sizes in the range of 0.1 to 1 pc (for moderate values of the Doppler factor ranging between 2 and 5) (*20*–*22*). Formally, though, there is no robust lower limit on the size of HST-1; therefore, we cannot exclude HST-1 as a source of TeV γ rays. However, it would be hard to realize the short-term variability of the TeV γ-ray emission in relation to HST-1, at least within the framework of current models. Because the size of the γ-ray production region does not exceed $R \leq 5 \times 10^{15}\delta$ cm, the location of HST-1 along the jet at 0.85 arc sec from the nucleus, which corresponds to $d \approx 65$ pc $\approx 2 \times 10^{20}$cm, implies that the energy would be channeled from the central object into the γ-ray production region within an unrealistically small opening angle $\sim R/d \approx 1.5 \times 10^{-3}\ \delta$ degree.

The only remaining and promising possibility is to conclude that the site of TeV γ-ray production is the nucleus of M87 itself (*23*). In contrast to the established TeV γ-ray blazars, the large-scale jet of M87 is seen at a relatively large jet angle ($\theta \sim 30°$), which suggests a quite modest Doppler boosting of its radiation. Nevertheless, because of the proximity of M87, both leptonic (*24*) and hadronic (*5*, *25*) models predicted detectable TeV γ-ray emission. How-

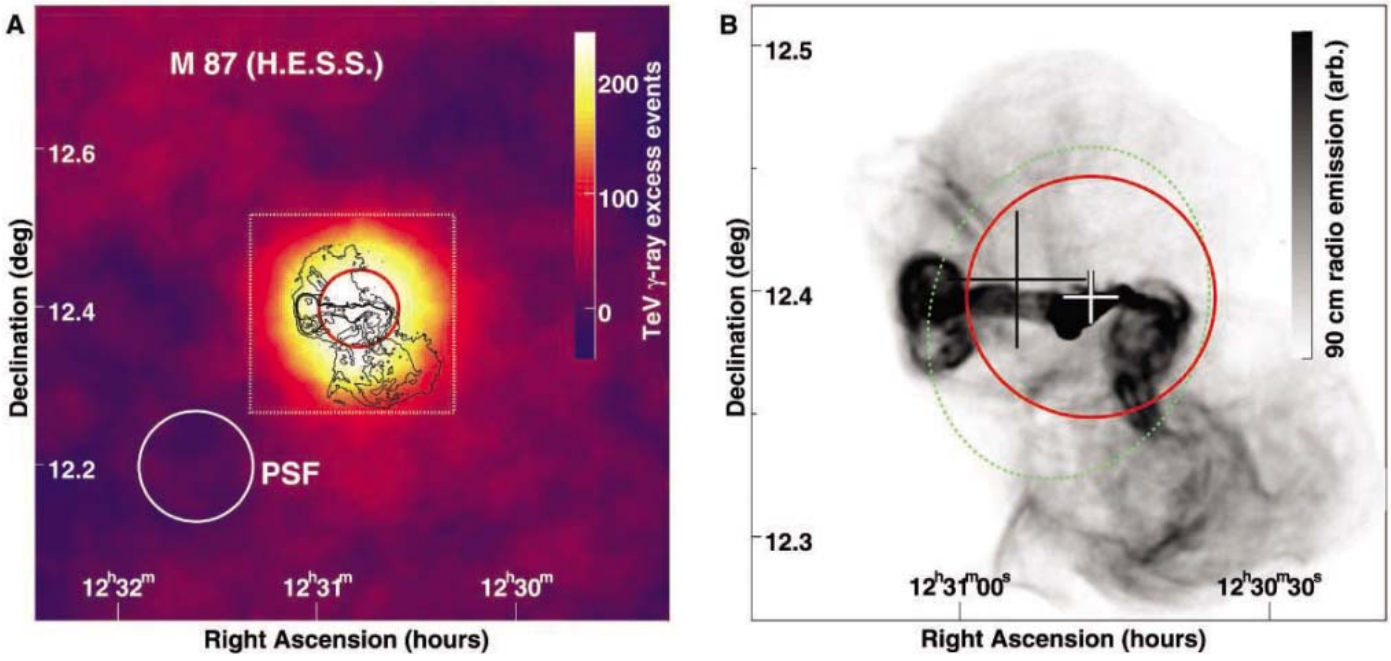

Fig. 1. Shown are the sky map as well as the position and extension limit of the TeV γ-ray emission from M87. (**A**) Smoothed TeV γ-ray excess map (color coded, 0.1° integration radius) as measured by H.E.S.S. The size (68% containment radius) of the H.E.S.S. point-spread function (PSF) is also indicated. The red circle indicates the intrinsic extension upper limit (99.9% confidence level) of 3 arc min of the TeV γ-ray excess corresponding to 13.7 kpc in M87. The contour lines show the 90-cm radio emission (*32*). The white box marks the cutout shown in (B). (**B**) The 90-cm radio data (*32*) measured with the Very Large Array, together with the TeV position with statistical and 20″ pointing uncertainty errors (white cross) and again the 99.9% confidence level extension upper limit (red circle). The size of the emission region deduced from the short-term variability is smaller by a factor of ~10^6. The black cross marks the position and statistical error of the γ-ray source reported by HEGRA. The green ellipse indicates the host galaxy seen in the optical wavelengths with an extension of 8.3 × 6.6 arc min in diameter.

ever, these scenarios typically produce a soft energy spectrum of TeV γ rays, clearly in contrast to the hard spectrum measured by H.E.S.S. Leptonic models can be adapted in various ways to match the new results. Within synchrotron self-Compton (SSC) scenarios (*26*), one method is to consider the possibility of differential Doppler-boosting in the jet near the core region, a phenomenon clearly expected in the jet formation zone, which extends over <0.1 pc from the nucleus (*27*). Emitting plasma blobs of small sizes with Doppler factors between 5 and 30 and magnetic fields well below equipartition can account for the observed TeV γ-ray emission. An additional flux contribution from inverse-Compton scattering of background photons, coming from scattered disk emission or from dust, can further reduce the range of Doppler factors toward moderate values.

The TeV γ-ray photons (independent of their production mechanism) might be absorbed by the pair-absorption process $\gamma_{TeV} + \gamma_{IR} \rightarrow e^+ e^-$ on the local infrared (IR) radiation field in the TeV γ-ray emission region. Because no signature for an absorption can be identified in the energy spectrum up to 10 TeV, one can derive an upper limit on the luminosity of the infrared radiation field at 0.1 eV (corresponding to a wavelength of ~10 μm, most relevant for absorption of 10 TeV γ rays) to be $L(0.1\ \mathrm{eV}) \leq 3.6 \times 10^{38}\ (R/10^{15}\ \mathrm{cm})$ erg/s, where R is the size of the TeV γ-ray emission region. Such a low central IR radiation luminosity supports the hypothesis of an advection-dominated accretion disk (i.e., an accretion disk with low radiative efficiency) in M87 (*28*) and generally excludes a strong contribution of external inverse-Compton emission on IR light to the TeV γ-ray flux.

If one accepts the hypothesis that protons can be accelerated as high as 10^{20} eV in jets of radio galaxies, then (hadronic) proton synchrotron models (*5*, *25*) cannot be excluded, considering the presented data. An alternative γ-ray production mechanism is curvature radiation of ultra-high-energy protons in the immediate vicinity of the supermassive black hole. This novel mechanism can simultaneously explain both the hard spectrum and fast variability of the observed TeV γ-ray emission. Rapidly rotating black holes embedded in externally supported magnetic fields can generate electric fields and accelerate protons to energies up to 10^{20} eV (*29*–*31*). Assuming that acceleration of protons takes place effectively within 3 Schwarzschild radii R_s, and if the horizon threading magnetic field is not much below 10^4 G, one should expect γ-ray radiation due to proton curvature radiation extending to at least 10 TeV. (The electron curvature radiation is less likely because of severe energy losses even in a tiny component of an irregular magnetic field.) No correlation with fluxes at other wavelengths is expected in this model. Although the size of the γ-ray production region, $R \sim 3\ R_s \sim 3 \times 10^{15}$ cm, perfectly matches the observed variability scale, and the model allows extension of the γ-ray spectrum to 10 TeV without any significant correlation at other wavelengths, the main problem of the model is the suggested magnetic field. It is orders of magnitude larger than the B field expected from the accretion process, given the very low accretion rate as it follows from the bolometric luminosity of the core as well as the estimates of the power of the jet in M87.

The time scale of the short-term variability of the TeV γ rays is on the order of the light-crossing time of the black hole (located at the center of M87), which is a natural time scale of the object. Therefore, the results reported here give clear evidence for the production of TeV γ rays in the immediate vicinity of the black hole of M87.

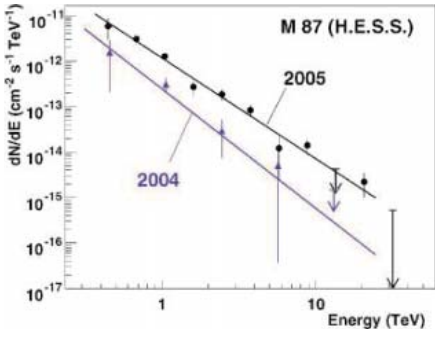

Fig. 2. The differential energy spectrum of M87 obtained from the 2004 and the 2005 data [using standard event selection cuts (*10*)], covering a range of ~400 GeV to ~10 TeV. Spectra for the 2003 and 2006 data sets could not be derived because of limited event statistics. Flux points with a statistical significance less than 1.5 SDs are given as upper limits (99.9% confidence level). The corresponding fits of a power-law function $dN/dE = I_0 \times (E/1\ \mathrm{TeV})^{-\Gamma}$ are indicated as lines. The photon indices are $\Gamma = 2.62 \pm 0.35$ (2004 data) and $\Gamma = 2.22 \pm 0.15$ (2005 data). Aside from the difference in the flux normalization by a factor of ~5 [$I_0 = (2.43 \pm 0.75) \times 10^{-13}$ cm^{-2} s^{-1} TeV^{-1} in 2004 and $I_0 = (11.7 \pm 1.6) \times 10^{-13}$ cm^{-2} s^{-1} TeV^{-1} in 2005], no variation in spectral shape is found within errors. The systematic error on the photon index and flux normalization are estimated to be $\Delta\Gamma = 0.1$ and $\Delta I_0/I_0 = 0.2$, respectively.

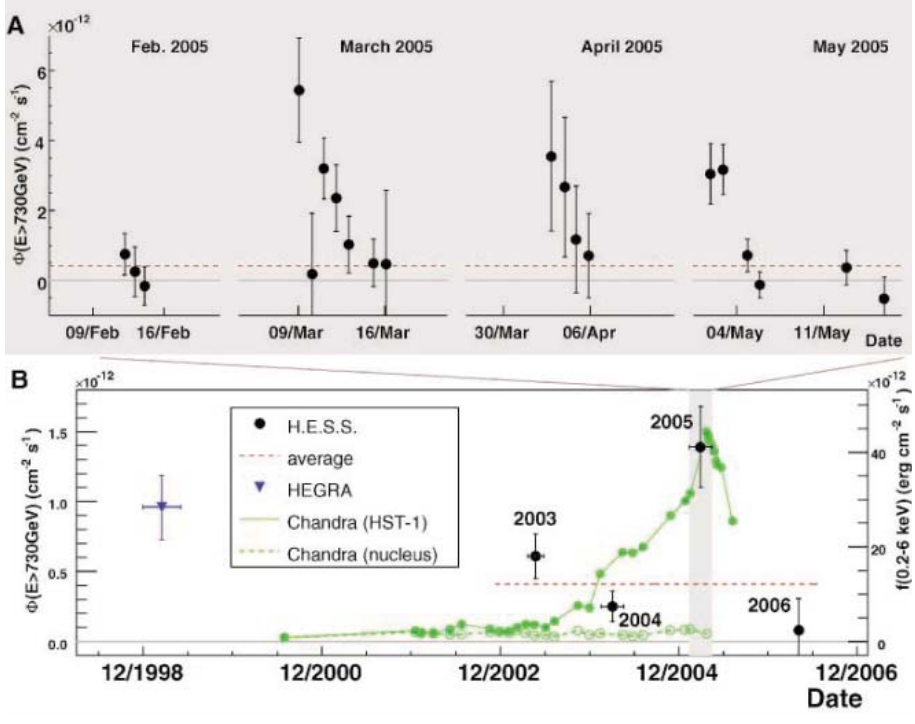

Fig. 3. Gamma-ray flux above an energy of 730 GeV as a function of time. The given error bars correspond to 1 SD statistical errors. (**B**) The average flux values for the years 2003 to 2006 as measured with H.E.S.S., together with a fit of a constant function (red line). The flux reported by HEGRA is also drawn (a systematic error must be taken into account when comparing results from the two instruments). (**A**) The night-by-night fluxes for the four individual months (February to May) of the high-state measurements in 2005, with significant variability on (flux doubling) time scales of ~2 days. The green points in (B) correspond to the 0.2 – 6 keV x-ray flux of the knot HST-1 [solid, (*20*)] and the nucleus [dashed, (*33*)] as measured by Chandra; the lines are linear interpolations of the flux points. No unambiguous correlation between the flux of x rays and TeV γ rays can be identified (the x-ray/TeV data were not gathered simultaneously).

References and Notes

1. F. Macchetto *et al.*, *Astrophys. J.* **489**, 579 (1997).
2. H. L. Marshall *et al.*, *Astrophys. J.* **564**, 683 (2002).

3. G. V. Bicknell, M. C. Begelman, *Astrophys. J.* **467**, 597 (1996).
4. P. L. Biermann *et al.*, *Nucl. Phys. B Proc. Suppl.* **87**, 417 (2000).
5. R. J. Protheroe *et al.*, *Astropart. Phys.* **19**, 559 (2003).
6. F. Aharonian *et al.*, HEGRA collaboration, *Astron. Astrophys.* **403**, L1 (2003).
7. S. Le Bohec *et al.*, *Astrophys. J.* **610**, 156 (2004).
8. W. Hofmann, *Proc. 29th Int. Cosmic Ray Conf. (Pune)*, **10**, 97 (2005).
9. F. Aharonian *et al.*, H.E.S.S. collaboration, *Astropart. Phys.* **22**, 109 (2004).
10. W. Benbow, *Proceedings: Towards a Network of Atmospheric Cherenkov Detectors VII (Palaiseau)*, 163 (2005).
11. M. de Naurois, *Proceedings: Towards a Network of Atmospheric Cherenkov Detectors VII (Palaiseau)*, 149 (2005); http://arxiv.org/abs/astro-ph/0607247.
12. Materials and methods are available as supporting online material on *Science* Online.
13. C. Ma *et al.*, *Astronom. J.* **116**, 516 (1998).
14. M. Beilicke *et al.*, *Proc. of TEXAS Symposium on Relativistic Astrophysics* (Stanford University), Paper #2403 (2004), see http://arxiv.org/abs/astro-ph/0504395.
15. C. Pfrommer, T. A. Enßlin, *Astron. Astrophys.* **407**, L73 (2003).
16. Emission from a region that is moving with a relativistic speed $\beta = v/c$ (c is the speed of light) is boosted along the direction of movement (relativistic beaming). The boost is a function of the observation angle θ relative to this direction and is described by the Doppler factor $\delta = [\Gamma(1 - \beta\cos\theta)]^{-1}$, where $\Gamma = (1 - \beta^2)^{-1/2}$ is the Lorentz factor of the emission region.
17. E. A. Baltz *et al.*, *Phys. Rev. D* **61**, 3514 (2000).
18. L. Stawarz *et al.*, *Astrophys. J.* **626**, 120 (2005).
19. E. S. Perlman, A. S. Wilson, *Astrophys. J.* **627**, 140 (2005).
20. D. E. Harris *et al.*, *Astrophys. J.* **640**, 211 (2006).
21. D. E. Harris *et al.*, *Astrophys. J.* **586**, L41 (2003).
22. L. Stawarz *et al.*, *Mon. Not. R. Astron. Soc.* **370**, 981 (2006).
23. W. Forman *et al.*, *Astrophys. J.* **635**, 894 (2005).
24. M. Georganopoulos *et al.*, *Astrophys. J.* **634**, L33 (2005).
25. A. Reimer *et al.*, *Astron. Astrophys.* **419**, 89 (2004).
26. D. L. Band, J. E. Grindlay, *Astrophys. J.* **308**, 576 (1986).
27. W. Junor, J. A. Biretta, M. Livio, *Nature* **401**, 891 (1999).
28. C. S. Reynolds, T. di Matteo, A. C. Fabian, U. Hwang, C. R. Canizares, *Mon. Not. R. Astron. Soc.* **283**, L111 (1996).
29. A. Levinson, *Phys. Rev. Lett.* **85**, 912 (2000).
30. E. Boldt, M. Loewenstein, *Mon. Not. R. Astron. Soc.* **316**, 29 (2000).
31. F. A. Aharonian, A. A. Belyanin, E. V. Derishev, V. V. Kocharovsky, Vl. V. Kocharovsky, *Phys. Rev. D* **66**, 023005 (2002).
32. F. N. Owen *et al.*, *Proceedings of The Universe at Low Radio Frequencies, ASP Conf. Ser.*, 199 (2000); http://xxx.lanl.gov/abs/astro-ph/0006152.
33. Provided by D. Harris, private communication.

34. The support of the Namibian authorities and of the University of Namibia in facilitating the construction and operation of H.E.S.S. is gratefully acknowledged, as is the support by the German Ministry for Education and Research (BMBF), the Max Planck Society, the French Ministry for Research, the CNRS-IN2P3, and the Astroparticle Interdisciplinary Programme of the CNRS, the UK Particle Physics and Astronomy Research Council (PPARC), the Institute of Particle and Nuclear Physics of the Charles University, the South African Department of Science and Technology and National Research Foundation, and the University of Namibia. We thank D. Harris for providing the Chandra x-ray light curve of the M87 nucleus.

Supporting Online Material

www.sciencemag.org/cgi/content/full/1134408/DC1
Materials and Methods
SOM Text
Figs. S1 and S2
Table S1
References

28 August 2006; accepted 11 October 2006
Published online 26 October 2006;
10.1126/science.1134408
Include this information when citing this paper.

Solid-State Qubits with Current-Controlled Coupling

T. Hime,[1] P. A. Reichardt,[1] B. L. T. Plourde,[1,2] T. L. Robertson,[1]* C.-E. Wu,[1]† A. V. Ustinov,[1]‡ John Clarke[1]§

The ability to switch the coupling between quantum bits (qubits) on and off is essential for implementing many quantum-computing algorithms. We demonstrated such control with two flux qubits coupled together through their mutual inductances and through the dc superconducting quantum interference device (SQUID) that reads out their magnetic flux states. A bias current applied to the SQUID in the zero-voltage state induced a change in the dynamic inductance, reducing the coupling energy controllably to zero and reversing its sign.

The past few years have seen major advances in the field of superconducting quantum bits (qubits). This family includes those based on electrical charge (*1*), magnetic flux (*2–4*), charge and phase (*5*), and the phase difference across a Josephson junction (*6*). Arbitrary superpositions of the single-qubit states can be prepared and manipulated by microwaves to produce Rabi oscillations, Ramsey fringes, and echoes long-familiar in atomic physics and nuclear magnetic resonance (*7*). The prepared quantum states remain coherent for times up to several microseconds (*8*). Coupling two or more qubits together results in entangled states (*9–15*) with energy spectra that exhibit the avoided crossings (anticrossings) predicted by quantum mechanics (*16*). In addition to studying quantum coherence in many-body systems, there is considerable interest in arrays of qubits for quantum computing. Because quantum computation requires both the manipulation of single qubits and the entanglement of many qubits, the ability to switch the coupling (*17–21*) between qubits on and off in a scalable architecture would enable many quantum-computing algorithms.

We conducted experiments on two flux qubits biased at the same frequency. In this regime, the antiferromagnetic interaction between the qubits produces an anticrossing and thus a splitting in the energy spectrum of the first and second excited states. By varying the bias current in the zero-voltage state of the superconducting quantum interference device (SQUID) used to read out the flux states of the coupled qubits, we reduced the coupling energy and hence the splitting of the two energy levels of the excited states to zero. Indeed, as predicted, we can even change the interaction from antiferromagnetic to ferromagnetic. Furthermore, we showed that the transition probability from the symmetric ground state to an antisymmetric excited state vanishes at the anticrossing, in qualitative agreement with calculations.

Each flux qubit consists of a superconducting loop interrupted by three Josephson tunnel junctions (*2*). When the applied magnetic flux Φ_q is at the degeneracy point $(n + \frac{1}{2})\Phi_0$ (where n is an integer such that $|\Phi_q - n\Phi_0| \leq \Phi_0/2$, $\Phi_0 \equiv h/2e$ is the flux quantum, h is the Planck constant, and e is the electron charge), a screening current I_q can flow around the loop in either direction, represented by the states $|\uparrow\rangle$ and $|\downarrow\rangle$. The ground and first excited states of the qubit correspond to symmetric and antisymmetric superpositions of the two current states and are separated by an energy Δ. When $\Phi_q \neq (n + \frac{1}{2})\Phi_0$, the energy difference increases to $\nu = (\Delta^2 + \varepsilon^2)^{1/2}$, where $\varepsilon = 2I_q[\Phi_q - (n + \frac{1}{2})\Phi_0]$. The state of the qubit is measured by coupling the flux generated by I_q to a dc SQUID. Two flux qubits are coupled through their mutual inductances to each other and to the SQUID. The interaction of two pairs of states produces four new states: a ground state $|0\rangle$ and three excited states $|1\rangle$, $|2\rangle$, and $|3\rangle$. Each of these states consists of a linear superposition of four basis states (*22*): the symmetric triplet $|\uparrow\uparrow\rangle$, $|S\rangle = (|\uparrow\downarrow\rangle + |\downarrow\uparrow\rangle)/2^{1/2}$, and $|\downarrow\downarrow\rangle$ and the antisymmetric singlet $|A\rangle = (|\uparrow\downarrow\rangle - |\downarrow\uparrow\rangle)/2^{1/2}$.

The two qubits A and B and their readout dc SQUID are shown schematically in Fig. 1A. The qubits have loop inductances L_{qA} and L_{qB} and

[1]Department of Physics, University of California, Berkeley, CA 94720–7300, USA. [2]Department of Physics, Syracuse University, Syracuse, NY 13244–1130, USA.

*Present address: Proteus Biomedical, 750 Chesapeake Drive, Redwood City, CA 94063, USA.
†Present address: Department of Physics, National Tsinghua University, Hsinchu 300, Taiwan.
‡Permanent address: Physikalisches Institut III, Universität Erlangen-Nürnberg, Erwin-Rommel-Strasse 1, D-91058 Erlangen, Germany.
§To whom correspondence should be addressed. E-mail: jclarke@berkeley.edu

are coupled through a mutual inductance M_{qq}. The surrounding dc SQUID consists of a loop with inductance L_S and two Josephson junctions, each with critical current I_0. The SQUID is coupled to qubits A and B through mutual inductances M_{qAS} and M_{qBS}. We can pass a bias current I_b through the SQUID and bias the qubits with independent applied fluxes Φ_A and Φ_B; these determine the applied SQUID flux Φ_S. By varying the bias current through the SQUID in the zero-voltage state, we showed theoretically that one can control the coupling energy K between the two qubits (*19*). The energy $K = K_0 + K_S$ has two contributions: a fixed energy K_0 through the mutual inductance of the two qubits, and a controllable energy K_S through their mutual inductances to the SQUID. In the zero-voltage state of a SQUID with appropriate parameters, the inverse dynamic inductance $\mathcal{L}^{-1} = \mathrm{Re}(\partial J/\partial \Phi_S)_{I_b}$ is nonlinear and can be positive, negative, or zero, depending on the values of Φ_S and I_b; Re indicates the real part, and J is the current circulating in the SQUID loop. As a result, the sign of the flux change coupled to (for example) qubit B through the SQUID by a given flux change in qubit A can be chosen to be positive, negative, or zero. The coupling energy K takes the form (*19*)

$$K = K_0 + K_S = 2I_{qA}I_{qB} \times (-M_{qq} - M_{qAS}M_{qBS}/\mathcal{L}) \quad (1)$$

where I_{qA} and I_{qB} are the qubit screening currents.

Figure 1B shows our experimental realization of the two qubits and their common SQUID. Our qubits have much larger areas than the three-junction qubits that have been described by other groups (*3*, *12*), and consequently we must take into account their geometrical inductances in simulating their characteristics (*23*). These large areas, together with the on-chip flux lines, enable us to apply independent flux biases using modest currents (~0.3 mA/Φ_0). We deliberately gave the two qubits slightly different areas and mutual inductances to the SQUID so that we could distinguish their flux signals. We measured the SQUID critical current by applying current pulses (Fig. 1C). For each measurement, using 10^5 current pulses, we adjusted the height of the first plateau to obtain a 50% probability of switching out of the zero-voltage state. We applied a pulse of microwave flux to the qubits before each current pulse to drive transitions between quantum states of the individual or coupled qubits, producing peaks and dips in the SQUID switching probability; we plotted the microwave frequency versus the applied flux to obtain energy spectra.

In Fig. 2A, we show the joint frequency spectrum of the qubits. The two flux lines enable us to keep the total flux applied to the SQUID nearly constant by applying fluxes of opposite sign to the qubits (*24*). Each spectrum arises from transitions from the ground state to the first excited state. Except near their apparent intersection, the spectra are excellent fits (dashed lines) to the prediction $\nu = (\Delta^2 + \varepsilon^2)^{1/2}$, yielding $\Delta_A/h = 8.872 \pm 0.005$ GHz and $\Delta_B/h = 8.990 \pm 0.004$ GHz (where errors are SD). An expanded view of the spectra near their intersection at 11.25 GHz (Fig. 2B) reveals an avoided crossing. The lower and upper spectra correspond to transitions from the ground state |0> to the first excited state |1> and the second excited state |2>, respectively. We fitted a hyperbolic curve to each data set to find a splitting of 122.6 ± 0.8 MHz.

The peaks in the lower spectrum of Fig. 2B vanish near the anticrossing, implying that the matrix elements vanish for transitions from |0> to |1>. The origin of this effect lies in the symmetry of the eigenstates (fig. S1). For $K < 0$, the contribution of the antisymmetric singlet state at the anticrossing vanishes for |0>, |2>, and |3>, leaving only contributions from the symmetric triplet states, whereas the converse is true for the state |1>. Consequently, transitions from the symmetric ground state |0> to the antisymmetric excited state |1> are forbidden.

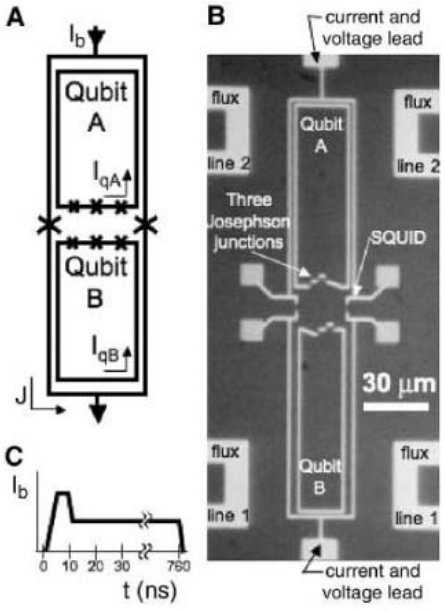

Fig. 1. Coupled flux qubits. (**A**) Two qubits, A and B, surrounded by the dc SQUID used to measure their magnetic flux states and control their inductive coupling. (**B**) The SQUID and the two qubits are fabricated on a Si chip from Al thin films in the same process, using two-angle evaporation; an intervening oxidation process forms the Josephson junctions. The SQUID junctions are 215 × 250 nm^2 and the qubit junctions are 180 × 205 nm^2 (two larger junctions) and 150 × 170 nm^2 (smaller junction). Film widths are 1 μm. Flux lines 1 and 2, connected (separately) in series, apply independent magnetic fluxes to the qubits and SQUID. The chip is enclosed in a superconducting box, and cooled to 50 mK in a dilution refrigerator. (**C**) Current pulse I_b used to determine the critical current.

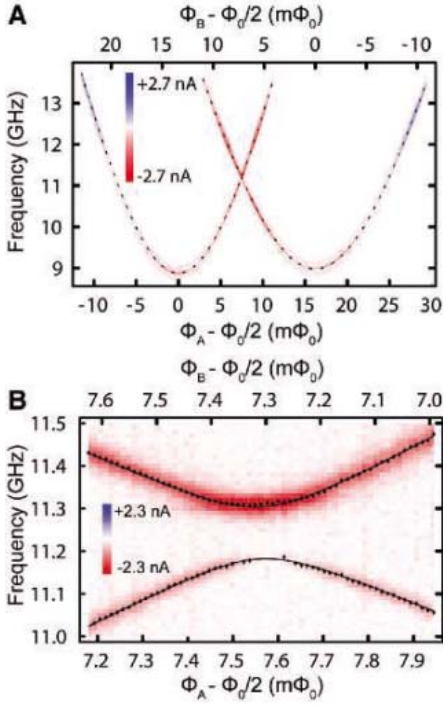

Fig. 2. Frequency versus flux for qubits. (**A**) Spectra of qubits A and B with their fluxes adjusted independently to separate their degeneracy points while keeping the flux applied to the SQUID nearly constant. Data were acquired in a 400-MHz bandwidth around the calculated peak centers. On this scale, the spectra appear to intersect at 11.25 GHz. Color bar indicates peak heights. (**B**) Spectrum shown in (A) expanded to reveal the anticrossing of the spectra of |1> and |2> of the coupled qubits; dots indicate the positions of maximum peak heights. Lower and upper spectra correspond to transitions from the ground state |0> to the excited states |1> and |2>, respectively. Frequency splitting at the anticrossing is 122.6 ± 0.8 MHz. Note the absence of data for |1> near the anticrossing.

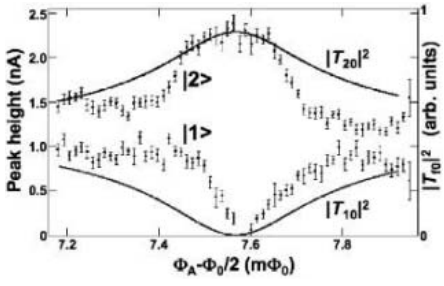

Fig. 3. Measured peak heights and calculated transition probabilities for transitions from the initial state |0> to the final states |1> and |2>. Flux dependence of measured peak heights taken from the spectra in Fig. 2B and of calculated square of matrix elements $|T_{10}|^2$ and $|T_{20}|^2$. $|T_{20}|^2$ is fitted to the peaks at the maximum peak height [measured in arbitrary (arb.) units].

This behavior is illustrated in Fig. 3, where we plot the measured peak heights taken from Fig. 2B. For the transitions from |0> to |1>, the amplitude of the peaks becomes vanishingly small at the anticrossing, whereas the peaks are enhanced for the transitions from |0> to |2>. Because the peak heights represent the probability of a transition for each measurement, we expected them to scale as the square of the matrix element $T_{f0} = \langle f|\sigma_z^{(A)} + \sigma_z^{(B)}|0\rangle$, where $f = 1,2$ is the final state and $\sigma_z^{(A)}$ and $\sigma_z^{(B)}$ are the Pauli spin operators, characterizing the coupling of the microwave excitation to the qubits. Figure 3 also shows the dependence of $|T_{10}|^2$ and $|T_{20}|^2$ on flux. There is a clear qualitative agreement between the peak heights and the transition probabilities.

In Fig. 4, A to C, at the slightly lower frequency of 10.75 GHz, we show our ability to control the coupling by applying a bias current to the SQUID. The bias current was switched on before the microwave pulse was applied (Fig. 4D, inset); this prebias current I_{pb} was low enough to ensure that the probability of the SQUID switching out of the zero-voltage state would be negligible. Within 10 ns of the microwaves being switched off, we increased the bias current to provide the readout pulse. We fitted hyperbolas to the data and corrected for the flux shift generated by the bias current in the SQUID during the measurement process [supporting online material (SOM) text]. We show our central result in Fig. 4D, where we plot the splitting versus I_{pb} for two different intersection frequencies. For both data sets, the splitting decreases smoothly as I_{pb} is increased. In the case of the data obtained at 10.75 GHz, the splitting goes almost to zero as I_{pb} is increased, and then increases. We believe that this result implies that the coupling was reduced to zero and subsequently changed sign as I_{pb} was increased. Higher values of I_{pb} caused the SQUID to switch prematurely. The two solid curves are the results of our simulations that used only the measured and calculated parameters listed in the caption to Fig. 4D. The calculated curves overestimate the splitting at zero bias current by about 28% and at the prebias current by about 15%. Given the many parameters in the theory and the uncertainties in some of them, we feel that the agreement with experiment is remarkably good. The dashed curves show fits to the data using common values of SQUID critical current and prebias current. The fits are excellent.

The ability to measure the quantum states of two qubits and to switch their coupling on and off with a single SQUID solely by means of its bias current represents an efficient architecture for a quantum computer. In particular, we have shown previously (*19*) that a quantum controlled-NOT logic gate can be implemented with this principle and would provide all the necessary ingredients to implement scalable universal quantum logic. Independent flux lines for the qubits are key to this scalable architecture; it is worth emphasizing, however, that these fluxes remain constant, and one needs only to switch a small current (~ 1 μA) in the SQUID to turn the interaction on and off.

Note added in proof: S. H. W. van der Ploeg *et al.* (preprint available at http://arxiv.org/abs/cond-mat/0605588) reported two flux qubits in which the coupling was controlled by means of a coupler loop and demonstrated that the sign of the ground state could be changed from antiferromagnetic to ferromagnetic. Spectroscopy of excited states was not described.

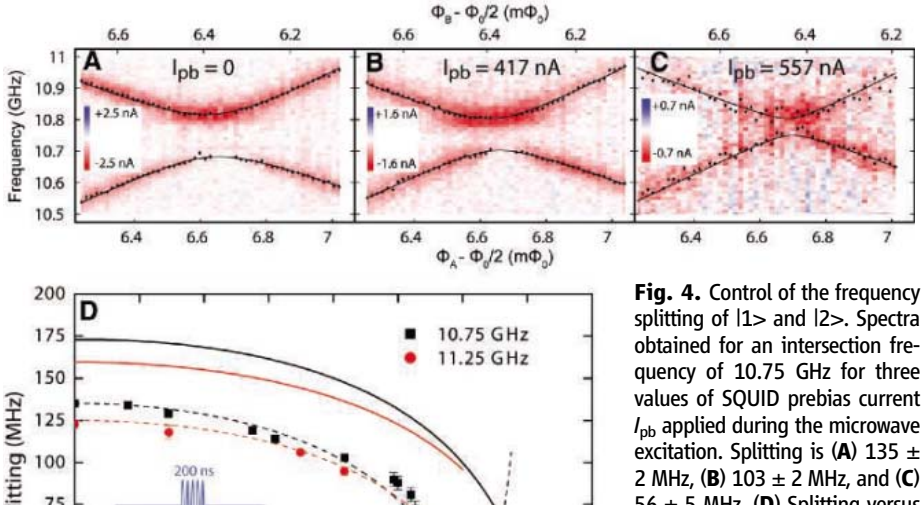

Fig. 4. Control of the frequency splitting of |1> and |2>. Spectra obtained for an intersection frequency of 10.75 GHz for three values of SQUID prebias current I_{pb} applied during the microwave excitation. Splitting is (**A**) 135 ± 2 MHz, (**B**) 103 ± 2 MHz, and (**C**) 56 ± 5 MHz. (**D**) Splitting versus I_{pb} for two intersection frequencies. Solid curves are predictions using the calculated (*25*) parameters M_{qq} = 0.75 picohenry (pH), M_{qAS} = 87.2 pH, M_{qBS} = 63.8 pH, L_S = 423 pH; measured parameters $I_{qA} = \frac{1}{2} d\varepsilon_A/d\Phi_{qA}$ = 146.0 ± 0.2 nA, $I_{qB} = \frac{1}{2} d\varepsilon_B/d\Phi_{qB}$ = 147.8 ± 0.2 nA, Φ_S(11.25 GHz) = 0.27 Φ_0, Φ_S(10.75 GHz) = 0.28 Φ_0; and the estimated maximum SQUID critical current $2I_0 = \pi\Delta_s/2eR_{NN}$ = 1.21 ± 0.054 μA, where Δ_s = 175 ± 5 μeV is the energy gap of Al, and R_{NN} = 228 ± 10 ohms is the resistance of the SQUID at voltages much greater than Δ_s/e. Uncertainties in the low-temperature impedances prevent precise determination of the currents, and we fitted the data using $2I_0$ = 0.844 μA and scaling the bias current by a factor of 0.767. Inset shows pulse sequence.

References and Notes

1. Y. Nakamura, Y. A. Pashkin, J. S. Tsai, *Nature* **398**, 786 (1999).
2. J. E. Mooij *et al.*, *Science* **285**, 1036 (1999).
3. C. H. van der Wal *et al.*, *Science* **290**, 773 (2000).
4. J. R. Friedman, V. Patel, W. Chen, S. K. Tolpygo, J. E. Lukens, *Nature* **406**, 43 (2000).
5. D. Vion *et al.*, *Science* **296**, 886 (2002).
6. J. M. Martinis, S. Nam, J. Aumentado, C. Urbina, *Phys. Rev. Lett.* **89**, 117901 (2002).
7. A. Abragam, *The Principles of Nuclear Magnetism* (Clarendon Press, Oxford, 1961).
8. P. Bertet *et al.*, *Phys. Rev. Lett.* **95**, 257002 (2005).
9. A. J. Berkley *et al.*, *Science* **300**, 1548 (2003).
10. T. Yamamoto, Yu. A. Pashkin, O. Astafiev, Y. Nakamura, J. S. Tsai, *Nature* **425**, 941 (2003).
11. Yu. A. Pashkin *et al.*, *Nature* **421**, 823 (2003).
12. A. Izmalkov *et al.*, *Phys. Rev. Lett.* **93**, 037003 (2004).
13. R. McDermott *et al.*, *Science* **307**, 1299 (2005).
14. J. B. Majer, F. G. Paauw, A. C. J. ter Haar, C. J. P. M. Harmans, J. E. Mooij, *Phys. Rev. Lett.* **94**, 090501 (2005).
15. M. Grajcar *et al.*, *Phys. Rev. Lett.* **96**, 047006 (2006).
16. J. Von Neumann, E. Wigner, *Z. Phys.* **30**, 467 (1929).
17. J. Q. You, J. S. Tsai, F. Nori, *Phys. Rev. Lett.* **89**, 197902 (2002).
18. D. V. Averin, C. Bruder, *Phys. Rev. Lett.* **91**, 057003 (2003).
19. B. L. T. Plourde *et al.*, *Phys. Rev. B* **70**, 140501(R) (2004).
20. P. Bertet, C. J. P. M. Harmans, J. E. Mooij, *Phys. Rev. B* **73**, 064512 (2006).
21. A. O. Niskanen, Y. Nakamura, J. S. Tsai, *Phys. Rev. B* **73**, 094506 (2006).
22. M. J. Storcz, F. K. Wilhelm, *Phys. Rev. A.* **67**, 042319 (2003).
23. T. L. Robertson *et al.*, *Phys. Rev. B* **73**, 174526 (2006).
24. B. L. T. Plourde *et al.*, *Phys. Rev. B* **72**, 060506(R) (2005).
25. M. Kamon, M. J. Tsuk, J. K. White, *IEEE Trans. Microw. Theory Tech.* **42**, 1750 (1994).

26. We thank F. Wilhelm for helpful discussions and I. Siddiqi for thoughtful comments on the manuscript. This work was supported by the NSF under grant EIA-020-5641, Air Force Office of Scientific Research under grant F49-620-02-1-0295, Army Research Office under grant DAAD-19-02-1-0187, Advanced Research and Development Activity, and Bavaria California Technology Center.

Supporting Online Material

www.sciencemag.org/cgi/content/full/314/5804/1427/DC1
SOM Text
Fig. S1

28 August 2006; accepted 18 October 2006
10.1126/science.1134388

Optical Atomic Coherence at the 1-Second Time Scale

Martin M. Boyd, Tanya Zelevinsky, Andrew D. Ludlow, Seth M. Foreman, Sebastian Blatt, Tetsuya Ido,* Jun Ye†

Highest-resolution laser spectroscopy has generally been limited to single trapped ion systems because of the rapid decoherence that plagues neutral atom ensembles. Precision spectroscopy of ultracold neutral atoms confined in a trapping potential now shows superior optical coherence without any deleterious effects from motional degrees of freedom, revealing optical resonance linewidths at the hertz level with a good signal-to-noise ratio. The resonance quality factor of 2.4×10^{14} is the highest ever recovered in any form of coherent spectroscopy. The spectral resolution permits direct observation of the breaking of nuclear spin degeneracy for the $^1S_0$ and $^3P_0$ optical clock states of ^{87}Sr under a small magnetic bias field. This optical approach for excitation of nuclear spin states allows an accurate measurement of the differential Landé g factor between $^1S_0$ and $^3P_0$. The optical atomic coherence demonstrated for collective excitation of a large number of atoms will have a strong impact on quantum measurement and precision frequency metrology.

The relative rates of coherent interaction and decoherence in a quantum system are of fundamental importance for both quantum information science (*1*) and precision metrology (*2*). Enhancing their ratio, which is equivalent to improving spectral resolving power, characterizes much of the recent progress in these fields. Trapped ions have so far provided the best platform for research in this direction, resulting in a number of seminal achievements (*3*–*8*). The principal advantage of the ion system lies in the clean separation between the internal atomic state and the external center-of-mass motion, leading to long coherence times associated with both internal and external degrees of freedom. A large ensemble of neutral atoms offers obvious benefits in the signal size and scalability of a quantum system (*9*, *10*). Multiatom collective effects can also dramatically enhance the coherent matter/field interaction strength (*11*). However, systems based on neutral atoms normally suffer from decoherence resulting from coupling between their internal and external degrees of freedom (*12*). In this article, we report a record-level spectral resolution in the optical domain based on a doubly forbidden transition in neutral atomic strontium. The atoms are confined in an optical trapping potential engineered for accurate separation between these degrees of freedom (*13*). The large number of quantum absorbers provides a dramatic enhancement in signal size for the recovered hertz-linewidth optical resonance profile.

The demonstrated neutral-atom coherence properties will affect a number of research fields, with some initial results reported here. Optical atomic clocks (*14*) benefit directly from the enhanced signal size and the high resonance quality factor Q. Tests of atomic theory can be performed with increased precision. The available spectral resolution also enables a direct optical manipulation of nuclear spins that are decoupled from the electronic angular momentum. Nuclear spins can have an exceedingly long relaxation time, making them a valuable alternative for quantum information processing and storage. Two ground-state nuclear spins can, for example, be entangled through dipolar interactions when photoassociation channels to high-lying electronic states (such as $^3P_1$) are excited (*15*). Combined with a quantum degenerate gas, the enhanced precision in measurement will further strengthen the prospects of using optical lattices to engineer condensed matter systems (for example, allowing massively parallel quantum measurements).

Much of the recent interest in alkaline earth atoms (and similar atoms and ions, such as Yb, Hg, In^+, and Al^+) arises from the study of the forbidden optical transitions, both for metrological applications and as a means for quantum control, with an important achievement being highly effective narrow line laser cooling (*16*–*18*). The spin-forbidden $^1S_0$-$^3P_1$ transition has been extensively studied as a potential optical frequency standard in Mg (*19*), Ca (*20*), and Sr (*21*, *22*) and has recently been explored as a tool for high-resolution molecular spectroscopy through photoassociation in ultracold Sr (*15*). The doubly forbidden $^1S_0$-$^3P_0$ transition is weakly allowed as a result of hyperfine-induced state mixing, yielding a linewidth of ~1 mHz for ^{87}Sr with a nuclear spin of $^9/_2$. This transition is a particularly attractive candidate for optical domain experiments, where long coherence times are desirable, and is currently being aggressively pursued for the realization of an optical atomic clock (*23*–*26*). Furthermore, because of the lack of electronic angular momentum, the level shifts of the two states can be matched with high accuracy in an optical trap (*13*), such that external motions do not decohere the superposition of the two states. Using optically cooled ^{87}Sr atoms in a zero-differential–Stark shift one-dimensional (1D) optical lattice and a cavity-stabilized probe laser with a sub-hertz spectral width, we have achieved probe-time–limited resonance linewidths of 1.8 Hz at the optical carrier frequency of 4.3×10^{14} Hz. The ratio of these frequencies, corresponding to a $Q \approx 2.4 \times 10^{14}$, is the highest obtained for any coherent spectral feature.

This ultrahigh spectral resolution allows us to perform experiments in the optical domain analogous to radio-frequency nuclear magnetic resonance (NMR) studies. Under a small magnetic bias field, we make direct observations of the magnetic sublevels associated with the nuclear spin. Furthermore, we have precisely determined the differential Landé g factor between $^1S_0$ and $^3P_0$ that arises from hyperfine mixing of $^3P_0$ with $^3P_1$ and $^1P_1$. This optical measurement approach uses only a small magnetic bias field, whereas traditional NMR experiments performed on a single state (either $^1S_0$ or $^3P_0$) would need large magnetic fields to induce splitting in the radio frequency range. Because the state mixing between $^3P_0$, $^3P_1$, and $^1P_1$ arises from both hyperfine interactions and external fields, the use of a small field permits an accurate, unperturbed measurement of mixing effects. Optical manipulation of nuclear spins shielded by two spin-paired valence electrons, performed with a superior spatial and atomic state selectivity, may provide an attractive choice for quantum information science.

Optical atomic clocks based on neutral atoms benefit directly from a large signal-to-noise ratio (S/N) and a superior line Q. Resolving nuclear sublevels with optical spectroscopy permits improved measurements of systematic errors associated with the nuclear spin, such as linear Zeeman shifts, and tensor polarizability that manifests itself as nuclear spin–dependent trap polarization sensitivity. Tensor polarizability of the $^3P_0$ state is one of the important potential systematic uncertainties for fermion-based clocks and is one of the primary motivations for recent proposals involving electromagnetically induced transparency resonances or dc magnetic field–induced state mixing in bosonic isotopes (*27*–*29*). The work reported here has permitted control of these systematic effects to $\sim 5 \times 10^{-16}$ (*30*). Given the superior S/N from the large number of quantum absorbers, we expect this system to be competitive among the best performing clocks in terms of stability. Accuracy is already approaching the level of the best atomic fountain clocks (*31*, *32*), and absolute frequency measurement is limited by the Cs clock–calibrated maser signal available to us by means of a fiber link (*33*). An all-optical clock comparison is necessary to reveal its greater potential.

To fully exploit the ultranarrow hyperfine-induced transition for high-precision spectrosco-

JILA, National Institute of Standards and Technology and University of Colorado, and Department of Physics, University of Colorado, Boulder, CO 80309–0440, USA.

*Present address: National Institute of Information and Communications Technology, Koganei, Tokyo, Japan.

†To whom correspondence should be addressed. E-mail: Ye@jila.colorado.edu

py, it is critical to minimize decoherence from both fundamental and technical origins. The ~100-s coherence time available from the ^{87}Sr atoms is not yet experimentally practical as a result of environmental perturbations to the probe laser phase at long time scales, but atomic coherence in the optical domain at 1 s can already greatly improve the current optical clock and quantum measurements. To achieve long atomic coherence times, we trap atoms in an optical lattice with a zero net ac Stark shift between the two clock states, enabling a large number of neutral atoms to be interrogated free of perturbations. The tight atomic confinement enables long probing times and permits spectroscopy free of broadening by atomic motion and photon recoil.

For the highest spectral resolution, it is necessary for the probe laser to have a narrow intrinsic linewidth and a stable center frequency. A cavity-stabilized 698-nm diode laser is used as the optical local oscillator for $^1S_0$-$^3P_0$ spectroscopy (*34*). The linewidth of this oscillator has been characterized by comparison with a second laser operating at 1064 nm via an optical frequency comb linking the two distant colors. A heterodyne optical beat signal between the two lasers, measured by the frequency comb, reveals a laser linewidth of <0.3 Hz (resolution-bandwidth–limited) at 1064 nm for a 3-s integration time. This result demonstrates the ability of the frequency comb to transfer optical phase coherence (~1 rad/s) across hundreds of terahertz. Our frequency comb is also referenced to a hydrogen maser calibrated by the National Institute of Standards and Technology (NIST) F1 Cs fountain clock (*31*), which allows us to accurately measure the probe laser frequency to 3×10^{-13} at 1 s. Additionally, the 698-nm laser has been compared with an independent laser system operating at the same wavelength, revealing a resolution-bandwidth–limited laser linewidth of 0.2 Hz, which increases to ~2 Hz for a 30-s integration time. After removing the linear drift, the stability of this local oscillator is $\sim 1 \times 10^{-15}$ from 1 to 1000 s, which is limited by the thermal noise of the cavity mirrors. Thus, the probe laser provides the optical coherence needed to perform experiments at the 1-s time scale.

^{87}Sr atoms are captured from an atomic beam and cooled to 1 mK by means of a magneto-optical trap (MOT) acting on the strong $^1S_0$-$^1P_1$ transition (Fig. 1A). This step is followed by a second-stage MOT with the use of the narrow $^1S_0$-$^3P_1$ intercombination line that cools the atoms to ~1.5 μK. During narrow line cooling, a nearly vertical 1D lattice is overlapped with the atom cloud for simultaneous cooling and trapping. The lattice is generated by a ~300-mW standing wave with a 60-μm beam waist at the wavelength of 813.428(1) nm, where the $^1S_0$ and $^3P_0$ ac Stark shifts from the trapping field are equal (*35*). The cooling and loading stages take ~0.7 s and result in a sample of 10^4 atoms, spread among ~100 lattice sites. The vacuum-limited lattice lifetime is >1 s. The atoms are confined in the Lamb-Dicke regime along the axis of the optical lattice. The Lamb-Dicke parameter, or the square root of the ratio of recoil frequency to trap oscillation frequency, is ~0.3. Both the axial and radial trap frequencies are much larger than the $^1S_0$-$^3P_0$ transition linewidth, leading to the spectral feature composed of a sharp optical carrier and two sets of resolved motional sidebands. One pair of sidebands is observed ±40 kHz away from the carrier, corresponding to the axial oscillation frequency in the lattice. The red-detuned sideband is strongly suppressed, indicating that nearly all atoms are in the motional ground state along the lattice axis. The second pair of sidebands at ±125 Hz from the carrier, with nearly equal amplitudes, corresponds to the trap oscillation frequency in the transverse plane.

With atoms confined in the lattice, the linearly polarized (parallel to the lattice polarization) 698-nm laser drives the π transitions (Fig. 1B) for probe times between 0.08 and 1 s, depending on the desired spectral resolution limited by the Fourier transform of the probe time. The effect of the probe laser is detected in two ways. First, after some atoms are excited to the long-lived $^3P_0$ state by the probe laser, the remaining $^1S_0$ population is measured by exciting the strong $^1S_0$-$^1P_1$ transition with a resonant pulse at 461 nm. The $^1S_0$-$^1P_1$ pulse scatters a large number of signal photons and heats the $^1S_0$ atoms out of the lattice, leaving only the $^3P_0$ atoms. Once the $^1S_0$ atoms have been removed, the $^3P_0$ population is determined by driving the $^3P_0$-$^3S_1$ and $^3P_2$-$^3S_1$

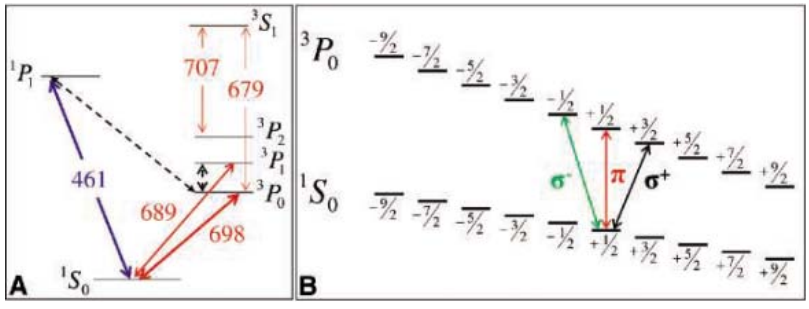

Fig. 1. (**A**) Partial ^{87}Sr energy-level diagram. Solid arrows show relevant electric dipole transitions with wavelengths in nanometers. Dashed arrows show the hyperfine interaction–induced state mixing between $^3P_0$ and $^3P_1$ and between $^3P_0$ and $^1P_1$, which provides the nonzero electric dipole moment for the doubly forbidden 698-nm transition. (**B**) The mixing alters the Landé *g* factor of the $^3P_0$ state such that it is ~50% larger than that of $^1S_0$, resulting in a linear Zeeman shift for the $^1S_0$-$^3P_0$ transition in the presence of a small magnetic field. The large nuclear spin of ^{87}Sr ($I = 9/2$) results in 10 sublevels for the $^1S_0$ and $^3P_0$ states, providing 28 possible transitions from the ground state.

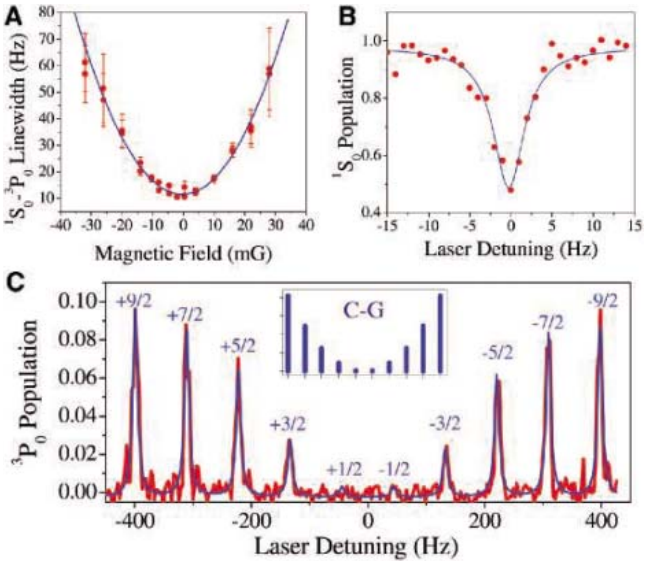

Fig. 2. Spectroscopy of the $^1S_0$-$^3P_0$ transition in ^{87}Sr. A pair of Helmholtz coils provides a variable field along the lattice (and probe) polarization axis, allowing a measurement of the field-dependent transition linewidth as shown in (**A**) where an 80-ms interrogation pulse is used, limiting the width to ~10 Hz. Error bars in (A) indicate measurement uncertainty in linewidth. (**B**) A representative spectrum when the ambient field is well controlled. Here, a longer probe time is used (~480 ms or a 1.8-Hz Fourier limit) but the linewidth is limited to 4.5 Hz by residual magnetic fields and possibly residual Stark shifts. (**C**) A field of 0.77 G is applied along the polarization axis, and the individual Fourier-limited (10 Hz) π transitions are easily resolved. Data are shown in red, and a fit of 10 evenly spaced transitions is shown in blue. The calculated transition probabilities based on Clebsch-Gordan (C-G) coefficients are included in the inset. In (B) and (C), the population is scaled by the total number of atoms available for spectroscopy (~10^4).

transitions (Fig. 1A), resulting in atomic decay to the ground state via $^3P_1$ for a second measurement with the use of the $^1S_0$-$^1P_1$ pulse. The second measurement provides superior *S*/*N* because only atoms initially excited by the 698-nm probe laser contribute to the fluorescence signal, and the zero background is not affected by shot-to-shot atom number fluctuations. Combining both approaches permits signal normalization against atom number fluctuations.

Although the $^3P_0$ and $^1S_0$ states are magnetically insensitive to first order, the hyperfine-induced state mixing, which allows the otherwise forbidden transition, modifies the $^3P_0$ nuclear *g* factor by ~50%. This effect results in a linear Zeeman shift in the $^1S_0$-$^3P_0$ transition of about –100 Hz/G per magnetic sublevel m_F (*36*, *37*), where we use the convention that the *g* factor and nuclear magnetic moment carry the same sign and 1 G = 10^{-4} T. This effect is shown schematically in Fig. 1B, where the 10 nuclear spin sublevels are resolved for the $^1S_0$ and $^3P_0$ states in the presence of a magnetic field. The linear Zeeman shift is an important issue for high-resolution spectroscopy, because the magnetic sensitivity can cause undesirable broadening of the transition, as well as line center shifts due to unbalanced population distribution among the sublevels. To achieve the narrowest resonance, the ambient magnetic field must be compensated with three orthogonal sets of Helmholtz coils. An example of this zeroing process is shown in Fig. 2A, where the transition linewidths are measured under various field strengths. After zeroing the field, narrow resonances as in Fig. 2B are routinely obtained. The displayed transition linewidth of 4.5 Hz [full width at half maximum (FWHM)] represents a resonance *Q* of ~10^{14}. The good *S*/*N* for the narrow line resonance achieved without any averaging or normalization arises from the contribution of 10^4 atoms. The ultrahigh spectral resolution has allowed a recent measurement of systematic effects for the optical clock transition at the 9 × 10^{-16} level (*30*).

The high-resolution spectroscopy enables direct measurement of the differential Landé *g* factor (Δg) between $^3P_0$ and $^1S_0$. To observe this state mixing effect, we applied a small magnetic field (<1 G) along the direction of the lattice polarization, and the probe laser polarization was again fixed along this quantization axis to drive π transitions. Figure 2C shows a direct observation of the hyperfine-induced state mixing in the form of 10 resolved transition components, with their relative amplitudes influenced by the Clebsch-Gordan coefficients. The narrow linewidth of the forbidden transition allows this nuclear-magnetic-resonance–like *g*-factor experiment to be performed optically at small magnetic fields. The magnitude of Δg can be measured by mapping out the line splitting versus magnetic field. Alternatively, 18 σ^+ and σ^- transitions (Fig. 1B) can be used to extract both the magnitude and sign [relative to the known $^1S_0$ *g* factor (*38*)] of Δg, without accurate calibration of the field. Using the latter approach, we find Δg = –108.8(4) Hz/G per m_F. The measured Δg permits determination of the $^3P_0$ lifetime of 140(40) s, in agreement with recent ab initio calculations (*39*, *40*). The uncertainty is largely dominated by inconsistencies among hyperfine mixing models (*36*, *37*).

The linewidth of each spectral feature in Fig. 2C is Fourier-limited by the 80-ms probe time to ~10 Hz. With the nuclear spin degeneracy removed by a small magnetic field, individual transition components allow exploration of the ultimate limit of our spectral resolution by eliminating any broadening mechanisms due to residual magnetic fields or light shifts, the likely limitation for data such as in Fig. 2B. To reduce the Fourier limit for the linewidth, we probed the spectra of a single resolved sublevel (m_F = $^5/_2$ in this case) using π polarization with the time window extended to 480 ms. Figure 3, A and B, shows some sample spectra of the isolated $^1S_0$ (m_F = $^5/_2$)–$^3P_0$ (m_F = $^5/_2$) transition with a Fourier-limited linewidth of 1.8 Hz, representing a line *Q* of ~ 2.4 × 10^{14}. This *Q* is reproduced reliably, as evidenced by the histogram of linewidths measured in the course of 1 hour (Fig. 3C). Typical linewidths are ~1 to 3 Hz, with the statistical scatter owing to residual probe laser noise at the 10-s time scale.

To further explore the limit of coherent atom-light interactions, we have also performed two-pulse optical Ramsey experiments on an isolated π transition. When a system is lifetime-limited, the Ramsey technique can achieve higher spectral resolution at the expense of *S*/*N*, leading to useful information on the decoherence process. By performing the experiment in the lattice, the Ramsey interrogation pulse can be prolonged, resulting in a markedly reduced Rabi pedestal width as compared to free-space spectroscopy. The reduced number of fringes greatly simplifies identification of the central fringe for applications such as frequency metrology. The fringe period (in Hz) is determined by the sum of the pulse interrogation time τ_R and the free-evolution time between pulses T_R and is given by $1/(\tau_R + T_R)$. Figure 3D shows a sample Ramsey spectrum, where τ_R = 20 ms and T_R = 25 ms, yielding a fringe pattern with a period of 20.8(3) Hz and fringe FWHM 10.4(2) Hz. For the same transition with τ_R raised to 80 ms and T_R to 200 ms (Fig. 3D, inset), the width of the Rabi pedestal is reduced to ~10 Hz, and the recorded fringe linewidth is 1.7(1) Hz.

This linewidth is recovered without substantial degradation of the fringe signal size, suggesting that the spectral resolution is limited by phase decoherence between light and atoms and not by effects such as trap lifetime. A limit of 1 to 2 Hz is consistent with our measurements of the probe laser noise integrated over the time scales used for spectroscopy. Other potential limitations to the spectral width include Doppler broadening resulting from the relative motion between the lattice and probe beams and broadening as a result of tunneling in the lattice. Future measurements will be improved by locking the probe laser to one of the resolved nuclear spin transitions to further suppress residual laser fluctuations. Although the *S*/*N* associated with a sublevel resonance is reduced when compared to a measurement involving all degenerate sublevels, >10^3 atoms still contribute to the signal, which allows measurement to proceed without averaging. Clearly, reaching the atom shot-noise limit and performing quantum state preparations will further enhance the *S*/*N*.

The line *Q* of ~2.4 × 10^{14} achieved here provides practical improvements in the fields of precision spectroscopy and quantum measurement. The neutral atom–based spectroscopic system now parallels the best ion systems in

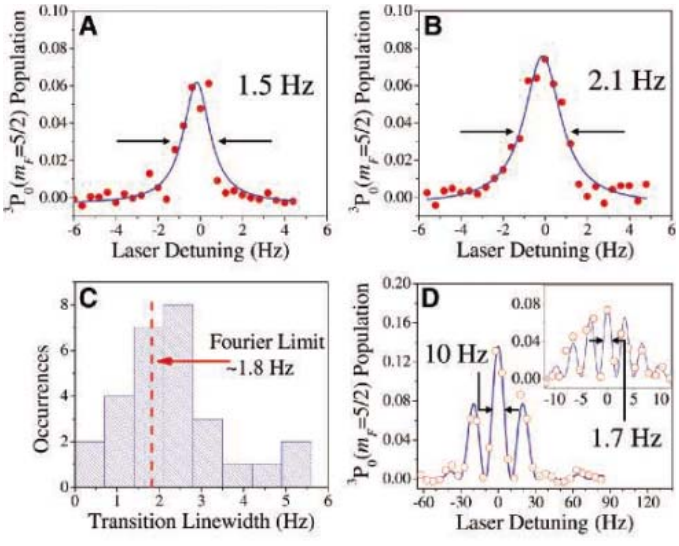

Fig. 3. Spectroscopy of the isolated $^1S_0$ (m_F = $^5/_2$)–$^3P_0$ (m_F = $^5/_2$) transition. Resolving individual sublevels allows spectroscopy without magnetic or Stark broadening. Spectra in (**A**) and (**B**) are taken under identical experimental conditions by means of a pulse time of 480 ms, and linewidths of 1.5(2) and 2.1(2) Hz are achieved. (**C**) A histogram of the linewidths of 28 traces obtained within ~1 hour. The average linewidth is near the 1.8-Hz Fourier limit (dashed red line). (**D**) Ramsey fringes with a 20.8(3)-Hz period and 10.4(2)-Hz fringe width, with data shown as open circles. Inset shows a Ramsey pattern with a 1.7(1)-Hz fringe FWHM.

terms of fractional resolution but greatly surpasses the latter in signal size. For optical frequency standards, the high resolution presented here has improved studies of systematic errors for the evaluation of clock accuracy. With these narrow resonances, clock instability below 10^{-16} at 100 s is anticipated in the near future. For quantum physics and engineering, this system opens the door to using neutral atoms for experiments in which long coherence times are necessary, motional and internal atomic quantum states must be controlled independently, and many parallel processors are desired.

References and Notes

1. D. Leibfried, R. Blatt, C. Monroe, D. Wineland, *Rev. Mod. Phys.* **75**, 281 (2003).
2. R. J. Rafac *et al.*, *Phys. Rev. Lett.* **85**, 2462 (2000).
3. P. O. Schmidt *et al.*, *Science* **309**, 749 (2005).
4. H. Häffner *et al.*, *Phys. Rev. Lett.* **90**, 143602 (2003).
5. H. Häffner *et al.*, *Nature* **438**, 643 (2005).
6. H. S. Margolis *et al.*, *Science* **306**, 1355 (2004).
7. T. Schneider, E. Peik, C. Tamm, *Phys. Rev. Lett.* **94**, 230801 (2005).
8. P. Dubé *et al.*, *Phys. Rev. Lett.* **95**, 033001 (2005).
9. D. L. Haycock, P. M. Alsing, I. H. Deutsch, J. Grondalski, P. S. Jessen, *Phys. Rev. Lett.* **85**, 3365 (2000).
10. I. Bloch, M. Greiner, in *Advances in Atomic Molecular and Optical Physics* (Academic Press, San Diego, CA, 2005), vol. 52, pp. 1–47.
11. A. T. Black, H. W. Chan, V. Vuletic, *Phys. Rev. Lett.* **91**, 203001 (2003).
12. J. Ye, D. W. Vernooy, H. J. Kimble, *Phys. Rev. Lett.* **83**, 4987 (1999).
13. H. Katori, M. Takamoto, V. G. Pal'chikov, V. D. Ovsiannikov, *Phys. Rev. Lett.* **91**, 173005 (2003).
14. See, for example, *Science* **306**, no. 5700 (2004).
15. T. Zelevinsky *et al.*, *Phys. Rev. Lett.* **96**, 203201 (2006).
16. T. Mukaiyama, H. Katori, T. Ido, Y. Li, M. Kuwata-Gonokami, *Phys. Rev. Lett.* **90**, 113002 (2003).
17. T. H. Loftus, T. Ido, A. D. Ludlow, M. M. Boyd, J. Ye, *Phys. Rev. Lett.* **93**, 073003 (2004).
18. T. H. Loftus, T. Ido, M. M. Boyd, A. D. Ludlow, J. Ye, *Phys. Rev. A* **70**, 063413 (2004).
19. F. Ruschewitz *et al.*, *Phys. Rev. Lett.* **80**, 3173 (1998).
20. U. Sterr *et al.*, *C. R. Phys.* **5**, 845 (2004).
21. T. Ido *et al.*, *Phys. Rev. Lett.* **94**, 153001 (2005).
22. G. Ferrari *et al.*, *Phys. Rev. Lett.* **91**, 243002 (2003).
23. I. Courtillot *et al.*, *Phys. Rev. A* **68**, 030501 (2003).
24. M. Takamoto, F. L. Hong, R. Higashi, H. Katori, *Nature* **435**, 321 (2005).
25. A. D. Ludlow *et al.*, *Phys. Rev. Lett.* **96**, 033003 (2006).
26. R. Le Targat, *Phys. Rev. Lett.* **97**, 130801 (2006).
27. R. Santra, E. Arimondo, T. Ido, C. H. Greene, J. Ye, *Phys. Rev. Lett.* **94**, 173002 (2005).
28. T. Hong, C. Cramer, W. Nagourney, E. N. Fortson, *Phys. Rev. Lett.* **94**, 050801 (2005).
29. Z. W. Barber *et al.*, *Phys. Rev. Lett.* **96**, 083002 (2006).
30. The magnetic field–induced frequency uncertainty is determined from the product of the measured residual magnetic field by means of the clock transition linewidth and experimentally determined frequency shifts versus given magnetic fields along three orthogonal directions. The total systematic uncertainty includes Stark shifts associated with the lattice and the probe beams, magnetic shift, density shift, and blackbody shift. For further details, see M. M. Boyd *et al.*; preprint available at http://arxiv.org/PS_cache/physics/pdf/0611/0611067.pdf.
31. T. P. Heavner, S. R. Jefferts, E. A. Donley, J. H. Shirley, T. E. Parker, *Metrologia* **42**, 411 (2005).
32. S. Bize *et al.*, *J. Phys. B Atom. Mol. Opt. Phys.* **38**, S449 (2005).
33. J. Ye *et al.*, *J. Opt. Soc. Am. B* **20**, 1459 (2003).
34. A. D. Ludlow *et al.*; preprint available at http://arvix.org/ftp/physics/papers/0610/0610274.pdf.
35. A. Brusch, R. Le Targat, X. Baillard, M. Fouche, P. Lemonde, *Phys. Rev. Lett.* **96**, 103003 (2006).
36. H. J. Kluge, H. Sauter, *Z. Phys.* **270**, 295 (1974).
37. A. Lurio, M. Mandel, R. Novick, *Phys. Rev.* **126**, 1758 (1962).
38. L. Olschewski, *Z. Phys. A* **249**, 205 (1972).
39. S. G. Porsev, A. Derevianko, *Phys. Rev. A* **69**, 042506 (2004).
40. R. Santra, K. V. Christ, C. H. Greene, *Phys. Rev. A* **69**, 042510 (2004).

41. We thank T. Parker and S. Diddams for providing the NIST hydrogen maser signal; J. C. Bergquist, I. H. Deutsch, C. H. Greene, J. L. Hall, and P. Julienne for helpful discussions; and X. Huang for technical assistance. The work at JILA is supported by the Office of Naval Research, NIST, and NSF. A.D.L. is supported by NSF–Interdisciplinary Graduate Education, Research and Training and the University of Colorado Optical Science and Engineering Program. T.Z. is a National Research Council postdoctoral fellow. T.I. acknowledges support from the Japan Science and Technology Agency.

10 August 2006; accepted 18 October 2006
10.1126/science.1133732

Macroscopic Hierarchical Surface Patterning of Porphyrin Trimers via Self-Assembly and Dewetting

Richard van Hameren,[1] Peter Schön,[1] Arend M. van Buul,[1] Johan Hoogboom,[2] Sergiy V. Lazarenko,[1] Jan W. Gerritsen,[1] Hans Engelkamp,[1] Peter C. M. Christianen,[1] Hans A. Heus,[1] Jan C. Maan,[1] Theo Rasing,[1] Sylvia Speller,[1] Alan E. Rowan,[1] Johannes A. A. W. Elemans,[1]* Roeland J. M. Nolte[1]

The use of bottom-up approaches to construct patterned surfaces for technological applications is appealing, but to date is applicable to only relatively small areas (~10 square micrometers). We constructed highly periodic patterns at macroscopic length scales, in the range of square millimeters, by combining self-assembly of disk-like porphyrin dyes with physical dewetting phenomena. The patterns consisted of equidistant 5-nanometer-wide lines spaced 0.5 to 1 micrometers apart, forming single porphyrin stacks containing millions of molecules, and were formed spontaneously upon drop-casting a solution of the molecules onto a mica surface. On glass, thicker lines are formed, which can be used to align liquid crystals in large domains of square millimeter size.

The formation of complex submicrometer patterns on surfaces that extend over macroscopic distances underlies the fabrication of integrated circuits and microelectromechanical devices (*1*–*3*). However, for many applications, such as detection arrays and optical elements, well-defined symmetrical patterns can be exploited, especially if the methods decrease the number of processing steps needed or avoid surface-invasive steps that scratch, rub, or etch the surface. Examples of complex pattern formation by noninvasive techniques are still few, usually require large polymeric molecules, and are often of small spatial extent (*4*–*12*). Self-assembly of molecules on a surface can be a simple, versatile, and less time-consuming approach and may lead to defect-free structures (*1*), especially if combined with physical processes such as dewetting and contact-line pinning. Here we report the spontaneous formation of periodic patterns of exceptionally long (up to 1 mm) columnar stacks of porphyrin dye molecules at a solid/liquid interface, with highly defined spatial and parallel ordering. These self-assembled patterns were then used to align liquid crystals (LCs) in domains measuring several square millimeters.

Porphyrin dye molecules can self-organize on a surface into small columnar stacks of submicrometer length (*13*, *14*). These architectures are generated as a result of combined self-assembly and dewetting, which take place simultaneously when a drop-casted solution of the porphyrin molecules is evaporated on a surface. In order to enhance the columnar stacking and hence the length of the assemblies, we have synthesized compound **1** (Fig. 1) (*15*), which consists of three porphyrin moieties that are linked via amide bonds to a central benzene core, a motif that is known to form extended hydrogen-bonded networks (*16*–*19*). Each porphyrin was equipped with three aliphatic hydrocarbon chains to increase the solubility of the stack in organic solvents.

The high tendency of **1** to form aggregates can be directly observed, in that at a concentration of 8 mg/ml, the chloroform solution formed a gel. This strong aggregation is highly dependent on the presence of the alkyl chains, because porphyrin trimers without these chains appeared not to gelate the solvent. In the proton nuclear magnetic resonance (NMR) spectrum of

[1]Institute for Molecules and Materials, Radboud University Nijmegen, Toernooiveld 1, 6525 ED, Nijmegen, Netherlands. [2]Department of Chemistry, Massachusetts Institute of Technology, 77 Massachusetts Avenue, Cambridge, MA 02139, USA.

*To whom correspondence should be addressed. E-mail: j.elemans@science.ru.nl

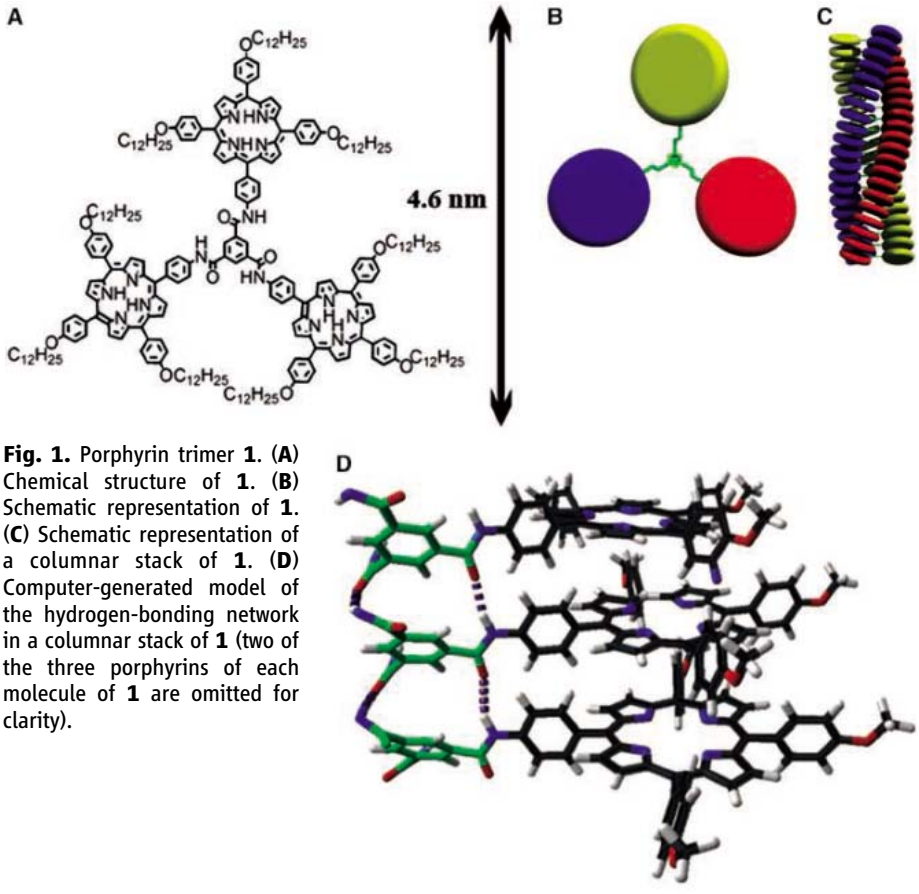

Fig. 1. Porphyrin trimer **1**. (**A**) Chemical structure of **1**. (**B**) Schematic representation of **1**. (**C**) Schematic representation of a columnar stack of **1**. (**D**) Computer-generated model of the hydrogen-bonding network in a columnar stack of **1** (two of the three porphyrins of each molecule of **1** are omitted for clarity).

1 in $CDCl_3$ ([**1**] = 10^{-4} M), very broad peaks were observed, suggesting large aggregate formation. The addition of d^6–dimethyl sulfoxide to this solution caused a sharpening of the NMR signals, which is the result of the solvent breaking up the hydrogen-bonding network (Fig. 1D) and dissolving the aggregates that are present in chloroform.

At the solid/liquid interface, the expected columnar stacking of **1** was confirmed by means of scanning tunneling microscopy (STM) (fig. S1). The aggregation behavior at a surface was further studied with atomic force microscopy (AFM). We drop-casted a diluted solution of **1** in chloroform ([**1**] = 4.8×10^{-6} M, 3-μl droplets) on mica. After evaporation, very large domains (up to ~3 mm^2) containing a highly ordered pattern of equidistant, nearly parallel, wire-like architectures were observed (Fig. 2, A and B). The height of the lines was 4.5 ± 0.4 nm (Fig. 2C), which corresponds remarkably well to the calculated diameter of **1**, indicating a pronounced shape persistence of the molecule. These observations indicate that the lines consisted of a columnar stack one molecule thick, with each of the lines containing millions of molecules. We will argue below that this self-organization of molecules on a macroscopic scale results from a hierarchical dewetting process.

Analysis of several samples revealed a narrow spatial distribution of the periodicity within one single domain [for example, 650 ± 40 nm in a domain with a size of 3 mm^2 (Fig. 2D)], but between several domains the value of the periodicity varied from 0.5 to 1 μm. The lines were oriented parallel with respect to the local solvent front, which can be deduced from the broader contact pinning lines on the sample (Fig. 2E). In addition, at the boundaries of these ordered domains, patterns more reminiscent of normal spinodal dewetting were observed (Fig. 2F). A clear correlation is seen between these two regions, because most columns in the periodic domain appear to grow out from the spinodal dewetting domain.

When larger droplets ([**1**] = 4.8×10^{-6} M, 10 μl in size) were deposited under similar conditions, the longer evaporation time formed porphyrin lines with different dimensions and orientations from those described above (Fig. 3A). A periodicity of 13.4 ± 0.7 μm and a line height of 55.4 ± 0.6 nm were observed. The latter value indicates that each line in this pattern consisted of a bundle of columnar stacks of **1**. Because of the larger dimensions, this pattern could be visualized via optical microscopy (Fig. 3B), which clearly demonstrated that the orientation of the lines, which were up to 0.8 mm long (fig. S3), was now orthogonal with respect to the solvent front. Scanning confocal fluorescence microscopy studies [Fig. 3C, excitation wavelength λ = 411 nm] confirmed that the lines consisted of molecules of **1**, and an emission spectrum characteristic of a porphyrin aggregate (*13*) was obtained (inset, Fig. 3C).

Because mica is birefringent, we could not study the assembly processes optically in real time. We could, however, visualize the line-formation process in real time on a glass surface ([**1**] = 4.8×10^{-5} M, 10-μl droplets), using an optical polarization microscope equipped with a charge-coupled device camera (movie S1). During the evaporation process, the front of the droplet was pinned several times, and upon its withdrawal, deposited material was observed (Fig. 3D). Simultaneously with the pinning, the formation of linear aggregates as a result of the self-assembly processes was already visible within the droplet, perpendicular to the front, before its withdrawal (fig. S2 and movie S1). However, the greater roughness of the glass substrate as compared to mica caused the pattern to be less well-defined.

The formation of the highly ordered line patterns is governed by a combination of molecular self-assembly and other physical processes (*13*). The strong self-assembly of **1**, which is governed by a balanced combination of hydrogen bonding and π–π stacking interactions, is essential for the growth of columnar stacks of almost millimeter length. No members of a wide family of porphyrin macrocycles (hexamers, dodecamers, and porphyrin trimers with ester instead of amide linkers) were able to form similar periodic patterns (*13*). The two primary physical processes that play a major role in pattern formation are contact-line pinning between the edge of a droplet and the surface (the so-called coffee-stain mechanism) and spinodal dewetting (*9*, *20*–*24*). The latter effect is observed when the surface of a thin film on a flat substrate (such as mica) is unstable and deforms spontaneously. Surfaces subject to this kind of dewetting are known to dewet via the formation of an undulating bicontinuous pattern (*24*). We postulate that this undulating pattern governs the spatial distribution of the linear aggregates (Fig. 3E). The small defects observed in Fig. 2A support this postulation, because their presence does not interrupt the periodicity of the patterns.

The initial physical phenomena, contact-line pinning and solvent evaporation, caused the molecules dissolved in the droplet to flow toward the contact line (*9*). In the case of the small droplets (3 μl), the contact line was pinned several times, leaving behind thin layers of deposited molecules of **1** at these positions (Fig. 2, E and G) (*9*). After repeated retractions of the solvent front, thin films remained between the pinned contact lines, which were then subject to spinodal dewetting. Combined with the propensity of **1** to form one-dimensional (1D) aggregates, this dewetting gave rise to the formation of the highly defined periodic patterns, with the contact pinning lines directing their orientation (Fig. 2G). Within each domain, the local spinodal

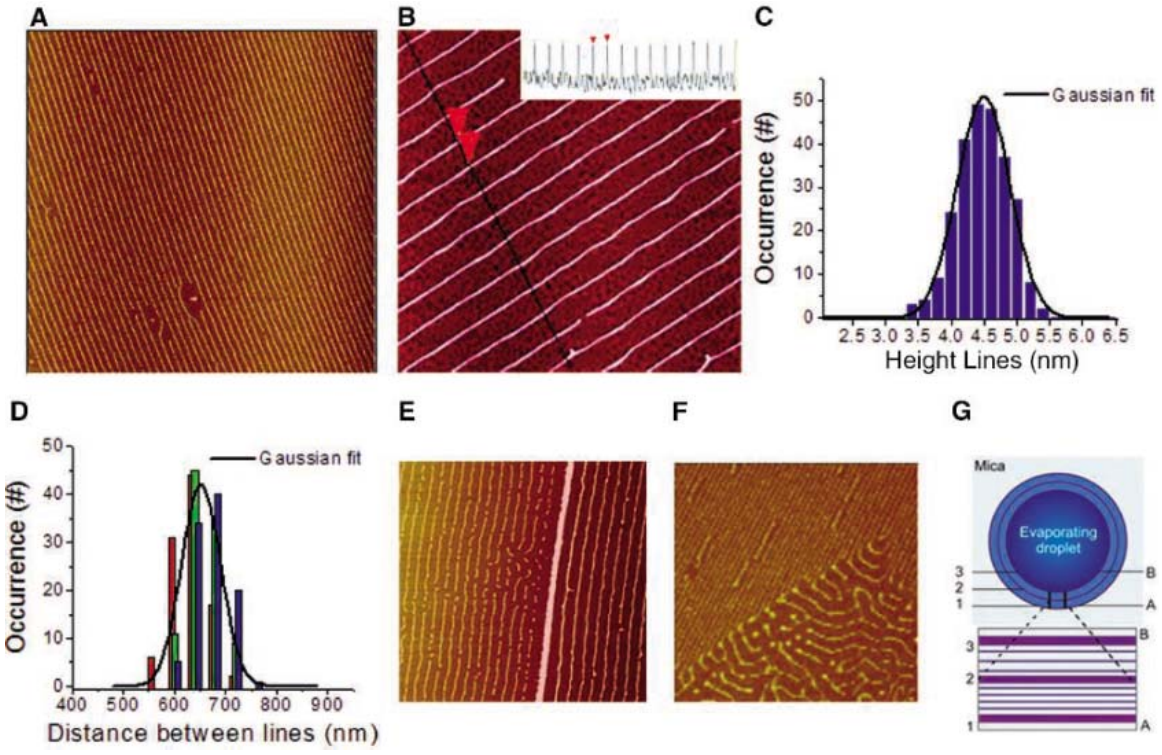

Fig. 2. Patterns formed on mica after the evaporation of 3-μl droplets of compound **1** in chloroform. (**A**) AFM image (scan size = 25 × 25 μm^2) of a pattern of highly ordered equidistant parallel lines. (**B**) AFM image (scan size = 10 × 10 μm^2), with the inset showing the cross section indicated in the AFM image. (**C**) Bar diagram showing the height distribution of the line pattern within a single domain, with the Gaussian fit demonstrating a line height of 4.5 nm, with standard deviation (σ) = 0.4 nm. (**D**) Bar diagram showing the spatial distribution of lines in a single domain (size = 3 mm^2). Each color represents a different position in a single domain. The Gaussian fit demonstrates that within this complete domain, the lines are 650 nm apart and σ = 40 nm. (**E**) AFM image (scan size = 14 × 14 μm^2) showing that the periodic pattern is parallel to the (bold) contact pinning line. (**F**) AFM image (scan size = 40 × 40 μm^2) of a domain transition between a highly ordered and a less ordered domain. (**G**) Mechanism of the formation of the patterned lines. During the evaporation of the droplet (A→B), the contact line is pinned several times, resulting in the formation of contact pinning lines (designated with 1, 2, and 3). After retraction of the solvent front, a thin film remains in which a pattern of thin lines is formed as a result of self-assembly and dewetting.

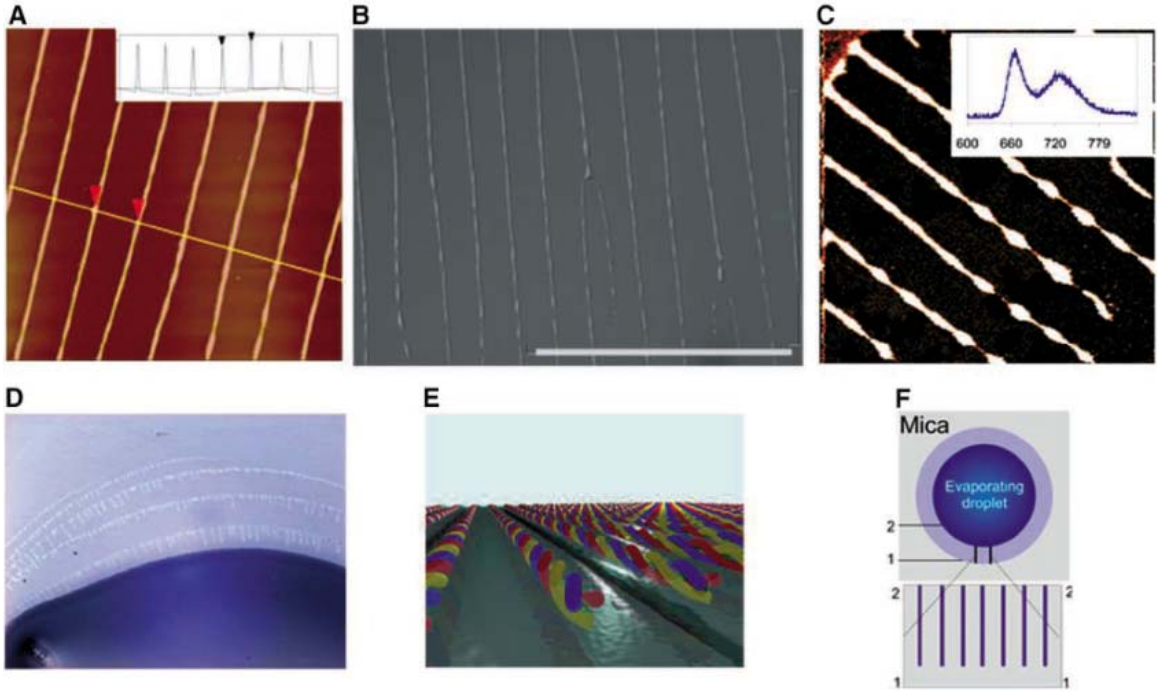

Fig. 3. Patterns formed after the evaporation of 10-μl droplets of compound **1** in chloroform. (**A**) AFM image (scan size = 95 × 95 μm^2) of a line pattern on mica. (**B**) Optical micrograph of the pattern formed on mica (scale bar, 100 μm). (**C**) Scanning confocal fluorescence microscopy image of the lines; the inset shows the characteristic fluorescence spectrum of a porphyrin aggregate, $\lambda_{max\ 1}$ = 665 nm and $\lambda_{max\ 2}$ = 726 nm. (**D**) Optical micrograph of the coffee-stain–like pattern formed during the evaporation of a solution of **1** in chloroform on glass ([**1**] = 4.8 × 10^{-5} M); the bottom part is still covered with solution (dark blue). The whitish stripes are the aggregates that remain after retraction of the droplet. (**E**) Proposed formation of periodic patterns on flat mica; spinodal dewetting causes an undulating pattern in the solvent, which governs the positioning of the aggregates and thus the spatial distribution of the lines. (**F**) Mechanism of the formation of the patterned lines. The presence of aggregates preformed in solution hinders the retraction of the solvent front from 1 to 2, causing partial pinning of the contact line. In combination with the molecular self-assembly, this partial pinning results in an orientation and growth of linear aggregates orthogonal to the local solvent front; contact pinning lines are not observed.

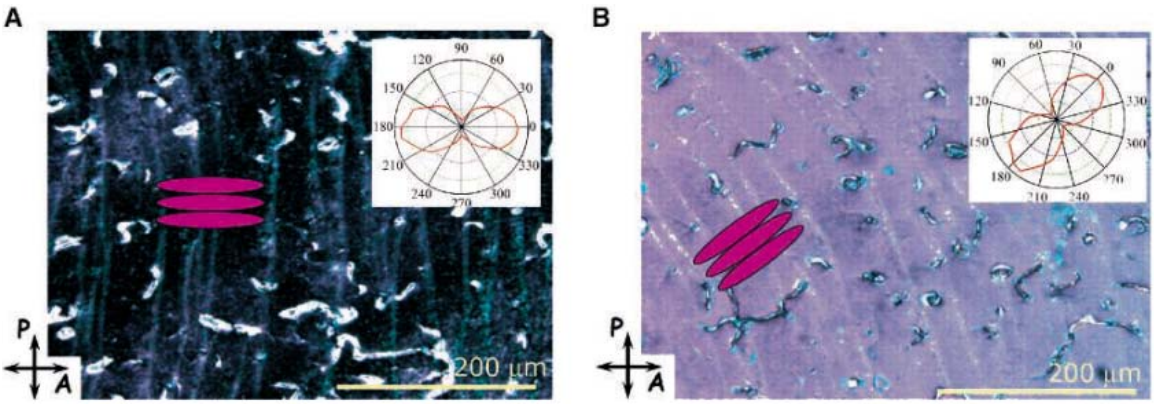

Fig. 4. Application of the patterns formed by **1** on a glass substrate as alignment layers for 5CB; polarizing microscopy images of a LC cell between crossed polarizers (denoted by P and A). (**A**) LC ordering parallel to the analyzer. (**B**) Texture after rotation of the sample over 45°. The local orientation of the 5CB molecules, deduced from the SHG rotational anisotropy patterns (insets), is depicted schematically in both images.

dewetting determined the periodicity, which in all cases was between 500 nm and 1 μm.

In the case of the larger droplets (10 μl), the evaporation of the solvent took longer and allowed the formation of larger aggregates already in solution, which were subsequently deposited (Fig. 3, A and B). Apparently, there was not enough material present at the contact line to completely pin it (*9*). The resulting partial pinning of the solvent front hindered the retraction of the contact line, and in contrast to the experiments with the smaller droplets, contact pinning lines were then not formed (Fig. 3F) (*9*). The partial pinning caused a flow of molecules toward and orthogonal to the contact line. The concomitant local increase in the concentration of molecules of **1** led to growth of the lines from a direction opposite to the molecular flow, resulting in an orthogonal orientation with respect to the solvent front. The combination of (i) the tendency of the molecules to form 1D aggregates, (ii) the occurrence or absence of contact line pinning, and (iii) spinodal dewetting effects resulted in the observed surface patterning in the two cases.

Previous reports have described organized assemblies of polymers (*25*), dendrimers (*3*, *26*, *27*), and block copolymers (*28*), leading to crystal-like domains on surfaces. In none of these cases, however, have 1D single molecular stacks spontaneously organized into periodic dissipative patterns been observed. Unlike our experiments, constructing such patterns requires invasive techniques such as lithography or sliding glass plates (*29*, *30*).

The line patterns obtained with the large droplets were investigated as possible LC alignment layers. LC cells, consisting of one glass plate covered with the aggregates and a non-rubbed counter-plate spin-coated with a commercially available polyimide, were prepared and filled with 4-cyano-4′-pentyl biphenyl (5CB) molecules in the isotropic phase to avoid flow alignment. Polarizing microscopy showed that the cells contained aligned LC domains of several square millimeters (Fig. 4) in the regions of the linear aggregates and no alignment in other areas. Closer inspection showed that the alignment was interrupted by concentric circles, which were the contact pinning lines (Fig. 3D).

The contact pinning lines themselves do not align the LC molecules but remain visible, which indicates that the formed aggregates are the ones that act as a command layer. Second harmonic generation (SHG) measurements confirmed that the mesogenic molecules were uniformly aligned parallel to the radially oriented stacks of **1** [that is, perpendicular to the contact lines, in exceptionally large domains (1 cm^2) (Fig. 4)]. As for most anisotropic surfaces that show LC alignment (*31*), the alignment was probably due to (i) a minimization of elastic energy and (ii) the presence of molecular interactions between the LC molecules and the oriented columnar stacks (*32*). In the case of the ordered porphyrin patterns, however, dipole-dipole interactions in particular are expected to have a large effect, because the head-to-tail orientation of the amide functions within the linear aggregates, as shown in Fig. 1D, creates a macroscopic dipole moment parallel to the stacking axis (*17*). The use of periodic patterns created by controlled self-organization may lead to a viable and cheap alternative to current methods of forming alignment layers.

The remaining challenge in exploiting this phenomenon will now be to further control the self-assembly in such a way that surface patterns can be oriented at will. Control over the periodic arrays might be accomplished by patterned heating of the surface with the use of laser gratings or by application of an electric field to align the high intrinsic dipole moments of the stacks. Extra stabilization of the patterns can be achieved by introducing cross-linkable groups (such as cinnamate, thiophene, or methacrylate units) in the alkyl chains, which would allow modification of the patterns after their deposition on the surface. The self-assembly/dewetting technique could also be applied in conjunction with conventional (photo-)lithographic or stamping methods.

References and Notes

1. H. O. Jacobs, A. R. Tao, A. Schwartz, D. H. Gracias, G. M. Whitesides, *Science* **296**, 323 (2002).
2. T. Verbiest *et al.*, *Science* **282**, 913 (1998).
3. V. Percec *et al.*, *Nature* **419**, 384 (2002).
4. R. D. Deegan *et al.*, *Nature* **389**, 827 (1997).
5. M. A. Ray, H. Kim, L. Jia, *Langmuir* **21**, 4786 (2005).
6. K. Mougin, H. Haidara, *Langmuir* **18**, 9566 (2002).
7. J. V. Barth *et al.*, *Angew. Chem. Int. Ed.* **39**, 1230 (2000).
8. M. A. Ray, H. Kim, L. Jia, *Langmuir* **21**, 4786 (2005).
9. R. D. Deegan, *Phys. Rev. E Stat. Phys. Plasmas Fluids Relat. Interdiscip. Topics* **61**, 475 (2000).
10. J. Huang, F. Kim, A. R. Tao, S. Conner, P. Yang, *Nat. Mater.* **4**, 896 (2005).
11. S. Vyawahare, K. M. Craig, A. Scherer, *Nano Lett.* **6**, 271 (2006).
12. I. I. Smalyukh *et al.*, *Phys. Rev. Lett.* **96**, 177801 (2006).
13. M. C. Lensen *et al.*, *Chem. Eur. J.* **10**, 831 (2004).
14. C. R. L. P. N. Jeukens *et al.*, *Nano Lett.* **4**, 1401 (2004).
15. Materials and methods are available as supporting material on *Science* Online.
16. S. Ranganathan *et al.*, *Chem. Commun.* **2001**, 2544 (2001).
17. M. L. Bushey, T. Q. Nguyen, W. Zhang, D. Horoszewski, C. Nuckolls, *Angew. Chem. Int. Ed.* **43**, 5446 (2004).
18. A. J. Wilson, M. Musada, R. P. Sijbesma, E. W. Meijer, *Angew. Chem. Int. Ed.* **44**, 2275 (2005).
19. M. P. Lightfoot, F. S. Mair, R. G. Pritchard, J. E. Warren, *Chem. Commun.* **1999**, 1945 (1999).
20. A. Sharma, R. Khanna, *Phys. Rev. Lett.* **81**, 3463 (1998).
21. A. Sharma, R. Khanna, *J. Chem. Phys.* **110**, 4929 (1999).
22. G. Reiter, *Science* **282**, 888 (1998).
23. A. M. Higgins, R. A. L. Jones, *Nature* **404**, 476 (2000).
24. A. Sharma, J. Mittal, R. Verma, *Langmuir* **18**, 10213 (2002).
25. M. H. Stenzel, C. Barner-Kowollik, T. P. Davis, *J. Polym. Sci. Part Polym. Chem.* **44**, 2363 (2006).
26. S. D. Hudson *et al.*, *Science* **278**, 449 (1997).
27. V. Percec *et al.*, *Nature* **430**, 764 (2004).
28. S. I. Stupp *et al.*, *Science* **276**, 384 (1997).
29. H. Yabu, M. Shimomura, *Adv. Funct. Mater.* **15**, 575 (2005).
30. Z. Lin, S. Granick, *J. Am. Chem. Soc.* **127**, 2816 (2005).
31. M. Behdani *et al.*, *Appl. Phys. Lett.* **80**, 4635 (2002).
32. T. Rasing, I. Musevic, *Surfaces and Interfaces of Liquid Crystals* (Springer, Heidelberg, 2004).
33. Supported by grants from the Netherlands Organization of Scientific Research (NWO) to R.J.M.N. (TOP grant), to J.A.A.W.E. (VENI grant), to P.S. (FOM/ALW), and to A.E.R. (VIDI grant); the National Research School Combination Catalysis (NRSC-C) to R. van H. and to R.J.M.N.; and the Royal Netherlands Academy of Science to R.J.M.N.

Supporting Online Material

www.sciencemag.org/cgi/content/full/314/5804/1433/DC1
Materials and Methods
Figs. S1 to S4
Reference
Movie S1

25 July 2006; accepted 28 September 2006
10.1126/science.1133004

Probing the Chiroptical Response of a Single Molecule

Ruthanne Hassey, Ellen J. Swain, Nathan I. Hammer, Dhandapani Venkataraman, Michael D. Barnes*

Chirally sensitive measurement techniques have generally been restricted to bulk samples. Here, we report the observation of fluorescence-detected circular dichroism (FDCD) from single (bridged-triarylamine) helicene molecules by using an excitation wavelength (457 nanometers) in the vicinity of an electronic transition that shows circular dichroism in bulk samples. The distributions of dissymmetry (*g*) parameters by analysis of signals from pure *M*- and *P*-type diastereomers are almost perfect mirror images of one another, each spanning a range of both positive and negative values. In addition, we observe a well-defined structure in the histogram of dissymmetry parameters suggestive of specific molecular orientations at the polymer interface. These single-molecule results highlight strong intrinsic circular dichroism responses that can be obscured by cancellation effects in ensemble measurements of a randomly oriented bulk sample.

Optical probes of chirality in organic systems are nearly as old as organic chemistry itself, tracing back to the early 1800s in initial studies of chiral natural products. Optical rotary dispersion and circular dichroism are now ubiquitous tools for characterizing and quantifying natural and synthetic chiral systems (*1*, *2*). More sophisticated gas- and condensed-phase probes have recently brought fresh insights to the role of solvation and local dielectric environment in the problem of light-matter interactions with chiral materials (*3*–*5*). However, because conventional techniques for probing chiroptical properties of molecular systems are based on scattering or absorption, they necessarily require extensive ensemble averaging, thus obscuring information on the specific chiroptical signature for an individual molecule as well as the heterogeneity of the response associated with a particular system. Here, we report observation of fluorescence-detected circular dichroism (FDCD) on individual helicene molecules deposited on the surface of a polymer film, and we show how the dichroic response is distributed for pure *P*- and *M*-type diastereomers. The measured distributions—each constructed from several hundred single-molecule measurements—are almost perfect mirror images of each other and are characterized by significantly larger average chiroptical response than observed in bulk solution. Surprisingly, the measured distributions span a range of dissymmetry parameters encompassing both positive and negative values. In addition, we find a well-defined structure in the histograms suggestive of specific molecular orientations at the polymer interface.

The chiroptical response of a molecular system is quantified by the dissymmetry parameter, *g*. In terms of fundamental molecular properties, *g* is defined as $4R/D$, where $R = \mathrm{Im}[\langle g|\boldsymbol{\mu}|e\rangle \langle e|\mathbf{m}|g\rangle]$, $|e\rangle$ and $|g\rangle$ are electronic states involved in the optical transition, $\boldsymbol{\mu}$ and $\mathbf{m}$ are the electric and magnetic dipole operators, and $D = |\langle g|\boldsymbol{\mu}|e\rangle|^2$ is the dipole oscillator strength, thus giving the range of possible *g* values of ±2 (*6*). Experimentally, *g* is determined by measured differential absorbance or luminescence intensity as $g = 2[\varepsilon_L - \varepsilon_R]/[\varepsilon_L + \varepsilon_R]$; typically, ensemble-averaged values of *g* are quite small (0.01 to 0.001). Recently, significantly higher average dissymmetry values have been observed in aggregates of conjugated polymers with chiral side chains (*7*, *8*), and experiments probing specific fine-structure components of $^5D_0 \rightarrow {}^7F_1$ transitions in Europium chelates have shown average *g* values between −0.7 and −1.8 (*9*). The latter result is particularly interesting in that such a large ensemble-averaged *g* value can be observed in such systems primarily because of the diminished sensitivity of inner-shell electronic transitions to environmental factors in rare earth ions. Thus, an important unresolved question is whether the generally weak chiroptical signature from molecular systems is a result of intrinsic molecular properties or the result of averaging over extrinsic heterogeneities such as molecular orientation or different local environments. Answers to these questions are vital to enhancing the purity of chiroptical response from a molecule of interest, thus potentially improving the practicability of such materials in device applications.

The power of single-molecule spectroscopy to disentangle heterogeneities in a complex physical system is well known (*10*–*12*). Many elegant published works on orientational dynamics (*13*), spectroscopy of conjugated polymers (*14*, *15*), and quantum dot systems (*16*), for example, have shown how a molecule-by-molecule approach can provide detailed information on the photophysics of complex systems. Recently, Venkataraman, Riehl, and co-workers demonstrated the synthesis and bulk chiroptical characterization of a new kind of helicene molecule based on a bridged triarylamine structure (Fig. 1B) in which the right (*P*)– or left (*M*)–handed helical structure is enforced by the presence of a camphanate group at the indicated position (*16*). This camphanate group serves only to maintain chirality and does not absorb or emit light at the wavelengths used and therefore is not expected to contribute to the chiroptical properties of the helicene molecules. A very small ensemble-averaged circular polarized luminescence ($\Delta\varepsilon/\varepsilon \approx 0.001$) was observed from solution-

Department of Chemistry, University of Massachusetts-Amherst, Amherst, MA 01003, USA.

*To whom correspondence should be addressed. E-mail: mdbarnes@chem.umass.edu

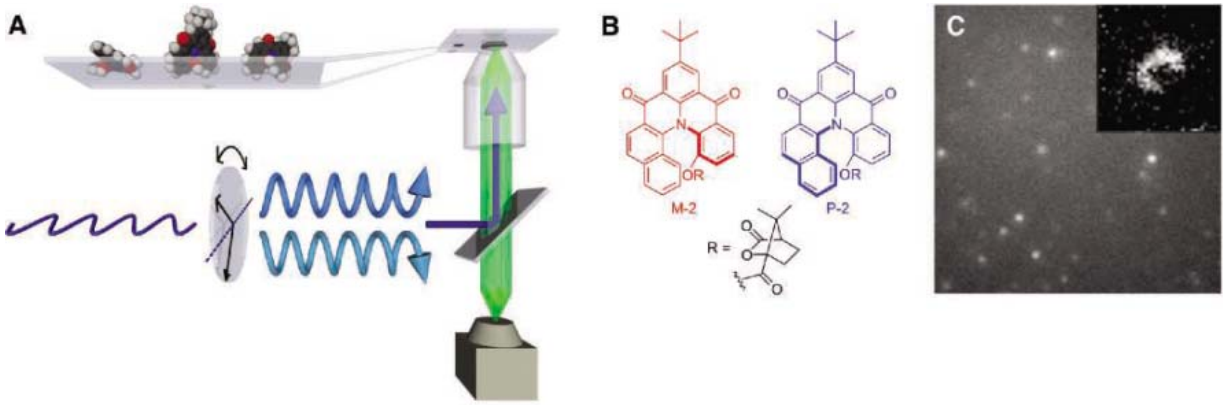

Fig. 1. (**A**) Experimental schematic. Linear-polarized laser radiation is periodically modulated between right- and left-handed circularly polarized light by rotation of a quarter waveplate. Fluorescence from single M2 or P2 molecules (**B**) was collected in an epi-configuration with a 1.4-NA oil objective and high-sensitivity CCD camera. (**C**) Typical (in-focus) fluorescence image and defocused image (inset) from a M2 sample.

phase samples of these species (*17*), similar in magnitude to the circular dichroism at the same excitation wavelengths. Our approach here was to use ultradilute solutions to immobilize single helicene molecules at the surface of a polymer film and image the fluorescence-detected circular dichroism by using single-molecule spectroscopy and imaging techniques.

Figure 1A shows a schematic of our experimental apparatus, which is similar in many regards to that described by Kahr and co-workers for imaging circular dichroism in inorganic crystals (*18*). Using an epi-illumination configuration on a Nikon TE300 microscope with 1.4–numerical aperture (NA) objective, we delivered right- or left-handed circularly polarized light from a CW Ar^+ ion laser (457 nm; ≈100 μW nominal power) to the sample by orienting a multi-order quarter waveplate (QWP) on a rotation stage at ±45° with respect to the (horizontal) input polarization axis, with 5 to 10 sequential charge-coupled device (CCD) camera exposures (Roper Scientific PhotonMax) for each QWP orientation (*19*). The molecules under study here were pure *M*- and *P*-type diastereomers of helicenes [as verified by ^{1}H–nuclear magnetic resonance (NMR)] derivatized with a camphanate moiety to enforce a specific chirality (Fig. 1B). Synthetic details are given elsewhere (*20*). For consistency in notation with respect to previously published work, we refer to the different diastereomers here simply as M2 and P2 (*17*). The 457-nm excitation wavelength excites transitions within the lowest electronic absorption band, where bulk solution and solid-film circular dichroism for these molecules are observed. Solutions of the two diastereomers were dissolved in semiconductor-grade methanol or cyclohexane and diluted to nominal concentrations of 10^{-11} M; film-based samples were prepared by drop-casting ≈200 μl of the ultradilute solution onto a thin polycylcoolefin (Zeonex) polymer film. We find that the photochemical stability of the helicenes is significantly enhanced by the use of a Zeonex supporting film over clean glass. In a typical fluorescence image obtained from such a sample, ~50 diffraction-limited fluorescent spots in a ≈300-μm^2 area are seen, which show temporal instabilities (blinking and discrete photobleaching) characteristic of single molecules (Fig. 1C). The defocused image shown in the inset of Fig. 1C illustrates the bidirectional nature of the transition moment in these chiral species. Similar in nature to defocused images observed in quantum dot systems (*21*), the spatial fluorescence intensity patterns for the single helicene molecules are distinctly different from well-known defocused images of single linear dipoles or multichromophoric systems (*22*).

Figure 2A shows representative fluorescence intensity traces from the M2 and P2 helicenes under excitation with right- and left-handed circularly polarized laser radiation. In these examples, the sample is illuminated with alternating right- and left-circular polarized laser radiation every 10 frames, with a 1-s integration time per frame. The dissymmetry factor, *g*, in the single-molecule FDCD signal was defined as $2[(I_L - I_R)/(I_L + I_R)]$, where I_R and I_L are the measured fluorescence intensities associated with right or left circularly polarized excitation, respectively (*23*, *24*). Single-molecule FDCD dissymmetry parameters were determined for each right and left circular polarization alternation cycle, and only fluorescent molecules with sufficient photochemical stability to follow intensity trajectories for at least 1.5 modulation cycles were used in the analysis. Although some variations in *g* are observed within a given single-molecule intensity trajectory, the gross value of *g* appears to be well defined for a given molecule during the measurement duration, suggesting that a particular single-molecule *g* factor is determined primarily by a predominantly static local environment.

Plotted as histograms (Fig. 2B), the distributions of the dissymmetry parameter, *g*, obtained from single M2 and P2 molecules are notable mirror images of one another and appear to be the sum of a broad symmetric (about $g = 0$) component spanning a range of $g \approx \pm 1.3$ and a much narrower component centered at $g \approx \pm 0.15$. Even though the compounds were isolated as pure diastereomers, we considered the possibility that the unexpected shape of the distributions could be associated with the opposite diastereomer formed by partial isomerization in methanol solution, or by reaction with condensed water vapor on the film during sample preparation. However, further experiments starting from pure M2 powder under strict anhydrous conditions with cyclohexane showed that the broad distribution persisted. Thus, we conclude that the symmetric component present in both M2 and P2 *g* distributions at 457-nm excitation is a photophysical property of the molecular system and not the result of sample degradation. Our experimental bias toward molecules with higher photostability might, however, bias the distribution of dissymmetry parameters to higher (absolute) values.

The structure of the histograms is intriguing and suggests a nonrandom distribution of chiral axes at the polymer-air interface. Differences between normalized *g* distributions for P2 cast from methanol versus cyclohexane solutions are subtle and limited to the wings of the two

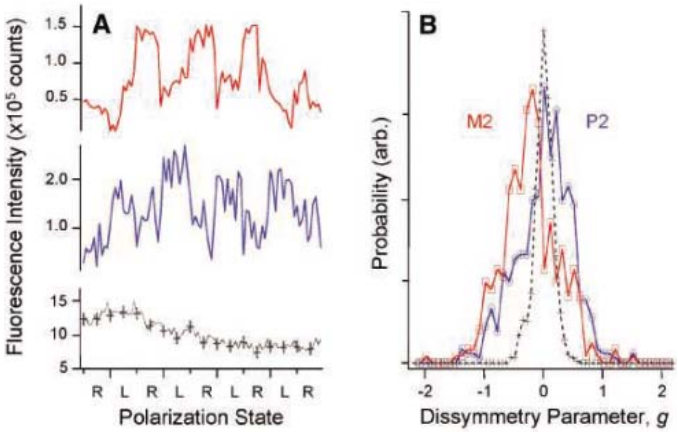

Fig. 2. (**A**) Representative fluorescence intensity traces as a function of excitation polarization state for dye-doped polymer nanosphere (black), single P2 molecule (blue), and single M2 molecule (red). The dissymmetry parameters extracted from the P2 and M2 traces shown here were 0.54 and –0.63, respectively. (**B**) Normalized histograms of FDCD dissymmetry parameters determined from single-molecule fluorescence measurements. The red curve with open squares represents data from M2, and the blue curve with open circles represents data from P2. For comparison, results from our control experiment with dye-doped 20-nm polymer nanospheres are shown (black curve with crosses). Data from ~500 single molecules were used in the construction of the histograms.

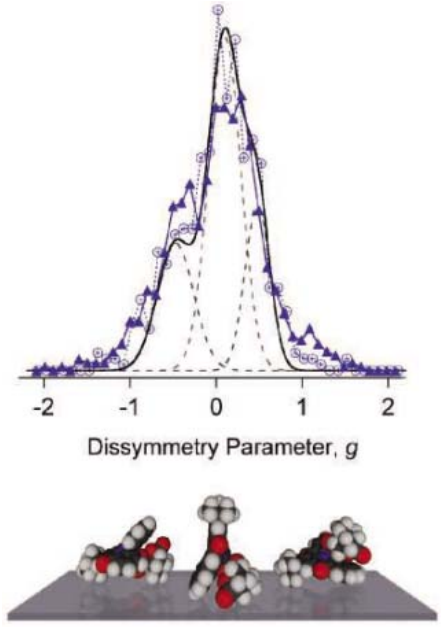

Fig. 3. Comparison of normalized dissymmetry parameter histograms for P2 dispersed from cyclohexane (dashed blue line and open circles) and methanol (solid blue line and triangles). The solid black curve is a fit to the P2/cyclohexane data with a three-component Gaussian fit. The lower graphic illustrates three different molecular orientations at the surface: camphanate-down, tripod, and camphanate-up.

distributions (Fig. 3) despite the solubility of Zeonex in the hydrocarbon but not the alcohol. Analysis of the M2 and P2 g distributions indicated three distinct components, with similar amplitudes but opposite signs for the two diastereomers. We propose that these three components are associated with three distinct stable molecular frame orientations at the surface shown in Fig. 3: camphanate down or up, and tripod (chiral axis perpendicular to the optical axis). These configurations correspond to the helicene frames parallel or perpendicular to the surface. We speculate that the opposite-handed component is associated with the "camphanate-up" orientation that places the helicene frame in direct contact with (or solvated by) the polymer film. Thus, the two in-plane orientations should be distinguishable from each other. Similar effects have been observed by Vaccaro and co-workers in cavity ringdown polarimetry measurements on (*S*)-(−)-propylene oxide, which show (for this particular system) that the specific rotation changes sign in the transition from the gas-phase to solvated molecule (*3*), illustrating the sensitivity of the chiroptical response to molecular environment. This effect is also analogous to the observation in crystals of tartaric acid of a variation in optical activity that is bisignate in nature (*25*). Here, we are restricted to molecular orientations induced by interactions with the substrate and as a result observe distinct contributions to the average g value. This result suggests that in solution phase, the measured g value represents a weighted average of all possible orientations and interactions with the solvent.

In summary, we observe that for a given bridged-triarylamine helicene diastereomer, there exists a significant probability of finding relatively large positive and negative g values whose distribution appears as a sum of three distinct components. We hope this result will spark further experimental and theoretical efforts in the study of individual chiral fluorophores. Our work demonstrates the feasibility of interrogating the fundamental nature of the interaction of light with chiral molecules at the single–quantum system level and provides valuable insights into the photophysics of chiral fluorophores. This result may also pave the way to the development of advanced new materials for efficient polarized light–emitting diodes (POLEDs) in next-generation display technologies (*26*).

References and Notes

1. M. Srinivasarao, *Chem. Rev.* **99**, 1935 (1999).
2. N. Berova, K. Nakanishi, R. W. Woody, Eds., *Circular Dichroism: Principles and Applications* (Wiley-VCH, New York, ed. 2, 2000).
3. T. Muller, K. B. Wiberg, P. H. Vaccaro, *J. Phys. Chem. A* **104**, 5959 (2000).
4. M. Y. Sfeir *et al.*, *Science* **312**, 554 (2006).
5. R. Fasel, M. Parschau, K. H. Ernst, *Nature* **439**, 449 (2006).
6 Contributions from electric dipole–electric quadrupole interactions that enter into the chiroptical response at the same order of perturbation theory as electric dipole–magnetic dipole interactions in the absence of ensemble averaging are expected to be small.
7. A. Satrijo, S. C. J. Meskers, T. M. Swager, *J. Am. Chem. Soc.* **128**, 9030 (2006).
8. J. N. Wilson *et al.*, *J. Am. Chem. Soc.* **124**, 6830 (2002).
9. R. W. Schwartz, H. G. Brittain, J. P. Riehl, W. Yeakel, F. S. Richardson, *Mol. Phys.* **34**, 361 (1977).
10. W. E. Moerner, *J. Phys. Chem. B* **106**, 910 (2002).
11. C. Bai, C. Wang, X. S. Xie, P. G. Wolynes, *Proc. Natl. Acad. Sci. U.S.A.* **96**, 11075 (1999).
12. S. Nie, R. N. Zare, *Annu. Rev. Biophys. Biomol. Struct.* **26**, 567 (1997).
13. A. P. Bartko, K. W. Xu, R. M. Dickson, *Phys. Rev. Lett.* **89**, 026101 (2002).
14. Z. H. Yu, P. F. Barbara, *J. Phys. Chem. B* **108**, 11321 (2004).
15. P. Kumar *et al.*, *J. Phys. Chem. B* **107**, 6252 (2003).
16. M. Nirmal *et al.*, *Nature* **383**, 802 (1996).
17. J. E. Field, G. Muller, J. P. Riehl, D. Venkataraman, *J. Am. Chem. Soc.* **125**, 11808 (2003).
18. K. Claborn, E. Puklin-Faucher, M. Kurimoto, W. Kaminsky, B. Kahr, *J. Am. Chem. Soc.* **125**, 14825 (2003).
19. The degree of circular polarization at the sample was determined to be >96%. Tests for artifactual FDCD performed on single DiI_{18} molecules randomly oriented in the *x-y* sample plane showed a distribution of dissymmetry parameters similar to that of the polymer nanosphere results.
20. J. E. Field, T. J. Hill, D. Venkataraman, *J. Org. Chem.* **68**, 6071 (2003).
21. X. Brokmann, L. Coolen, M. Dahan, J. P. Hermier, *Phys. Rev. Lett.* **93**, 107403 (2004).
22. A. P. Bartko, R. M. Dickson, *J. Phys. Chem. B* **103**, 11237 (1999).
23. J. P. Riehl, F. S. Richardson, *Chem. Rev.* **86**, 1 (1986).
24. F. S. Richardson, J. P. Riehl, *Chem. Rev.* **77**, 773 (1977).
25. D. Mucha, K. Stadnicka, W. Kaminsky, A. M. Glazer, *J. Phys. Condens. Matter* **9**, 10829 (1997).
26. S. H. Chen *et al.*, *Nature* **397**, 506 (1999).

27. Support from the U.S. Department of Energy Office of Basic Energy Sciences (grant 05ER15695), NSF-sponsored MRSEC, NSF CHE 0134287, and the Intelligence Community Postdoctoral Research Fellowship Program is gratefully acknowledged. E.J.S. acknowledges support from the Bates Summer Research Fellowship.

23 August 2006; accepted 16 October 2006
Published online 2 November 2006;
10.1126/science.1134231
Include this information when citing this paper.

Organic Globules in the Tagish Lake Meteorite: Remnants of the Protosolar Disk

Keiko Nakamura-Messenger,[1,2]* Scott Messenger,[1] Lindsay P. Keller,[1] Simon J. Clemett,[1,3] Michael E. Zolensky[1]

Coordinated transmission electron microscopy and isotopic measurements of organic globules in the Tagish Lake meteorite shows that they have elevated ratios of nitrogen-15 to nitrogen-14 (1.2 to 2 times terrestrial) and of deuterium to hydrogen (2.5 to 9 times terrestrial). These isotopic anomalies are indicative of mass fractionation during chemical reactions at extremely low temperatures (10 to 20 kelvin), characteristic of cold molecular clouds and the outer protosolar disk. The globules probably originated as organic ice coatings on preexisting grains that were photochemically processed into refractory organic matter. The globules resemble cometary carbon, hydrogen, oxygen, and nitrogen (CHON) particles, suggesting that such grains were important constituents of the solar system starting materials.

Carbonaceous chondrite meteorites contain rare micrometer-sized mineral grains from evolved stars (stardust) (*1*). These meteorites also contain remnants of interstellar organic matter, marked by anomalous H and N isotopic compositions. This material has undergone complex histories of processing, dilution, and isotopic exchange with solar system materials, obscuring its original chemical and physical state. Rare microscopic inclusions with highly anomalous H and N isotopic compositions occur in meteorites and interplanetary dust particles (IDPs), suggesting that some interstellar organic materials have survived intact (*2*–*4*). However, analytical limitations have left the nature of these materials poorly known.

Tagish Lake is a meteorite whose chemistry and mineralogy are intermediate between CI and CM2 carbonaceous chondrites (*5*). It was collected immediately after its fall was witnessed, minimizing terrestrial contamination (*5*). It has been linked to outer belt asteroids from its orbit, reflectance spectrum, hydrated mineralogy, and abundant carbonaceous matter, having 2.6 weight percent organic carbon (*5*–*7*). Tagish Lake organic matter often occurs as submicrometer, hollow globules (*8*). Similar objects were first observed in meteorite extracts in 1961 (*9*) and have recently been reported in several carbonaceous chondrites (*10*). However, owing to analytical

[1]Robert M. Walker Laboratory for Space Science, Astromaterials Research and Exploration Science Directorate, NASA Johnson Space Center, Houston, TX 77058, USA. [2]ESC Group/Jacobs Sverdrup, NASA Johnson Space Center, Houston, TX 77058, USA. [3]ESC Group/ERC Inc., NASA Johnson Space Center, Houston, TX 77058, USA.

*To whom correspondence should be addressed. E-mail: keiko.nakamura-1@nasa.gov

and sample limitations, the origins of these objects have not been well understood.

We performed coordinated in situ microstructural, chemical, and isotopic studies of Tagish Lake globules to establish whether their origins were products of chemical processes in the meteorite parent body, the solar nebula, a cold molecular cloud, or circumstellar environment. By determining their sources, the globules can provide direct probes of primordial chemical processes.

Fresh samples of Tagish Lake matrix were sectioned by ultramicrotomy in high-purity S into 50- to ~70-nm-thick sections (*11*). We observed numerous, mostly submicrometer, hollow organic globules in carbonate-free sections of the meteorite (Fig. 1). Although the average concentration was about one per 100 μm^2, aggregates of two to five globules are common. The globule diameters (140 to 1700 nm) vary significantly more than their wall thickness (100 to 200 nm). All but one of the globules appeared hollow in thin sections. High-resolution transmission electron microscopy (TEM) imaging and electron energy-loss spectroscopy (EELS) show that the globules consist of structurally amorphous C that lacks long-range order or development of graphite-like domains. The distribution of C, N, and O in the globules was obtained using energy-filtered TEM (EFTEM) imaging. The walls and cores of the organic globules are almost always free of other matrix materials.

Twenty-six of the globules identified by TEM and 1100 μm^2 of surrounding matrix material were subjected to C and N isotopic imaging with a NanoSIMS 50L ion microprobe [(*11*), table S1]. Remarkably, all of the globules had elevated $^{15}N/^{14}N$ ratios, with $\delta^{15}N$ values ranging from 200 to 1000‰, significantly exceeding bulk $^{15}N/^{14}N$ ratios of CI and CM2 chondrite meteorites (*7*, *12*) (Fig. 2) and Tagish Lake organic matter (77‰) (*7*). Although accounting for only ~1.5% of the area analyzed, the globules accounted for 80% of the highly ^{15}N-rich material ($\delta^{15}N > 400$‰). Eight of these globules were also measured for H isotopic compositions, and all were D-rich, with δD values ranging from 1800 to 8100‰. All globules are clearly spatially resolved in H and N isotopic images from the surrounding matrix material, with the exception of two globules that are adjacent to D-rich matrix material (Fig. 3). The C isotopic compositions of the globules had a narrower range ($\delta^{13}C \sim -77$ to +16‰), generally below the value of bulk Tagish Lake organic matter (–9‰)(*7*).

The fact that the globules all exhibited N and H isotopic anomalies that greatly exceeded the surrounding meteorite matrix rules out their possible formation in the Tagish Lake parent body. The globules have highly variable H and N isotopic ratios, even those within a few μm of each other (Fig. 3, C and D), making it unlikely that the isotopic variations resulted primarily from parent body processing. However, globules that are attached to each other have similar H and N isotopic compositions (Fig. 3, A and B), suggesting that the globules aggregated before incorporation into the Tagish Lake parent body.

The isotopic compositions of the globules are indicative of mass fractionation during chemical reactions at low temperatures (10 to 50 K). In cold molecular clouds, ion-molecule chemical reactions are promoted by cosmic ray ionization. Gas-phase molecules in cold interstellar clouds have D/H ratios enriched by factors of 10^2 to 10^5 relative to HD/H_2 (*13*). Grain surfaces are also predicted to become enriched in D/H via single-atom addition of D (*14*). D-enrichment may also have occurred in the protoplanetary disk in the region of the Kuiper Belt [>30 astronomical units (AU)], possibly reaching values of protostellar cores at distances of >100 AU (*15*). Nitrogen isotopic fractionation is expected at extremely low T (10 K), with $^{15}N/^{14}N$ ratios of poly-

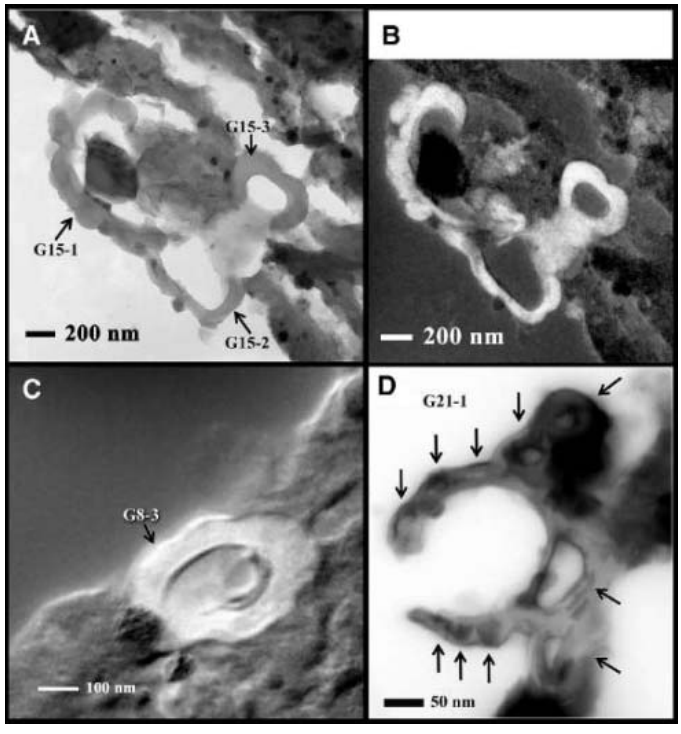

Fig. 1. EFTEM images of Tagish Lake organic globules. (**A**) Bright-field TEM image of three organic globules (G15-1 1.3 μm, G15-2 0.7 μm, and G15-3 0.55 μm) embedded in saponite matrix. (**B**) Carbon K-edge EFTEM image of the area shown in Fig. 3A, showing carbon-containing material in high contrast. Globule G15-1 (left) shows microstructure that may be subgrains within its wall. N and H isotopic images of these globules are shown in boxed areas of Fig. 3, A and B. (**C**) Carbon K-edge EFTEM image of globule G8-3 showing a typical hollow structure of an individual organic globule. N and H isotopic images of this globule are shown in boxed areas of Fig. 3, C and D. (**D**) This carbon postedge EFTEM image of globule aggregate G21-1 reveals its internal structure, indicating that it has incorporated several ~50-nm globules, shown by arrows.

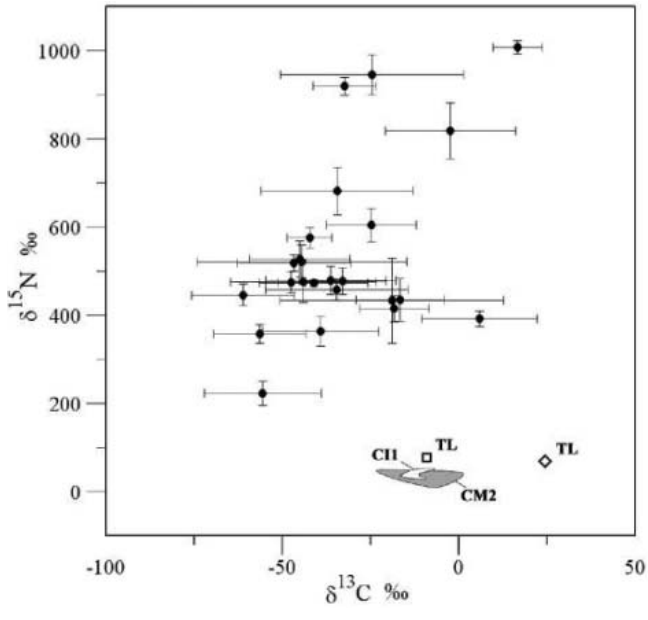

Fig. 2. Carbon and nitrogen isotopic compositions of Tagish Lake organic globules compared with ranges observed among whole-rock samples of CI1 ($\delta^{15}N = 31 - 52$‰), CM2 ($\delta^{15}N = 13 - 47$‰), whole rock Tagish Lake (diamond), and Tagish Lake organic matter (square) (*7*, *12*). The anomalous CM2 meteorite Bells has a bulk $\delta^{15}N$ value of 335‰ (*12*).

cyclic aromatic hydrocarbon (PAH) molecules and grain surfaces predicted to be enhanced by up to a factor of two (*16*). These conditions occur in cold molecular clouds and at the outermost regions of protoplanetary disks (>100 AU). The N isotopic anomalies in the globules likely resulted from chemical fractionation, not from nucleosynthesis, because they are enriched in both D/H and $^{15}N/^{14}N$ and also lack the large C isotopic anomalies characteristic of evolved stars. Their narrow range of $^{13}C/^{12}C$ ratios limits the degree of accompanying C isotopic fractionation to <50‰ (Fig. 2), consistent with expectations that significant C isotopic fractionation would not be preserved (*14*, *17*).

Carbonaceous chondrites contain a diversity of organic compounds, including hundreds of solvent extractable species and a dominant insoluble macromolecular material (*18*). These materials are moderately enriched in D and/or ^{15}N (typically δD <1000‰; $\delta^{15}N$ <200‰), with significant isotopic variations among different classes of organics and meteorites (*19*). In general, however these anomalies are well below those expected for cold molecular cloud materials, probably reflecting histories of alteration, mixing, and isotopic exchange of original interstellar organics with solar system materials.

Isotopic measurements of meteorites and IDPs at micrometer scales have revealed a much greater isotopic variability compared with values of bulk organic extracts, in some cases reaching values of cold molecular cloud molecules (δD = 50,000‰) (*3*, *4*). In several cases, D- and ^{15}N-rich "hotspots" were associated with carbonaceous materials (*4*, *20*, *21*). Here we show that in the Tagish Lake meteorite, the primary carriers of the most highly anomalous H and N are distinctive submicrometer organic globules.

Since forming, these globules experienced wide ranges of thermal and chemical conditions, ultimately residing in an aqueous solution that formed the phyllosilicates matrix of the Tagish Lake parent body (*5*). Hydrothermal alteration occurred among many carbonaceous chondrites, leaving variable imprints on their organic matter (*18*, *22*). Tagish Lake organic matter is unusually poor in soluble species that may have been lost by low-temperature chemical oxidation, resulting in the production of carbonate (*23*). Because the organic globules are only found in carbonate-free regions of Tagish Lake, this suggests that the globules are susceptible to chemical oxidation. Interestingly, two of the globules are adjacent to D-rich matrix material (Fig. 3, B and D) that may have originated from the globules. This is not observed in the N isotopic images, implying that the ^{15}N enrichments are carried by lower-solubility phases than the D-rich material, such as insoluble macromolecular material, PAHs, or amines. This would support the prediction that PAHs obtain the strongest ^{15}N enrichments in protostellar cores (*16*).

Ice grains in cold molecular clouds are either primarily H_2O-rich polar ices containing CO_2, CH_3OH, H_2CO, and NH_3, or nonpolar ices containing CO, CO_2, N_2, and O_2 (*24*, *25*). The globules are more likely to have formed by condensation of polar molecular ices, where abundant free H ($H/H_2 > 1$) was available to form hydrocarbons and deuterate molecules on grain surfaces. The isotopic variations of the globules may reflect the sensitivity of H and N isotopic fractionation to temperature, radiation environment, and chemical composition.

Interstellar ice analogs are readily converted into complex refractory organic compounds by exposure to ultraviolet (UV) radiation (*26*, *27*). The penetration depth of UV radiation is remarkably similar to the wall thickness of the organic globules (100 to 200 nm). The interiors of these objects may have been preexisting ice grains that were protected from radiation processing by the organic mantle. These cores remained more volatile than the coatings and would have volatilized at a later stage, leaving the organic globules with hollow cores.

Alternatively, the hollow structures of the globules may have resulted from asteroidal aqueous alteration. This is suggested by experimental production of hydrophobic, vesicle-rich materials from UV-irradiated interstellar ice analogs exposed to alkaline solutions, similar to conditions proposed for aqueous alteration of carbonaceous chondrites (*28*, *29*). However, these materials are generally much larger and weaker than the Tagish Lake organic globules.

Whatever their formation process, the organic globules very likely originated at the outer regions of the protosolar disk in the region of the Kuiper Belt or in the preceding cold molecular cloud, well beyond the influence of the Sun and the nascent planetary system. Consequently, similar organic globules should also have been incorporated into cometary parent bodies. Interestingly, many particles detected during the Giotto and Vega encounters with comet Halley were primarily composed of the elements C, H, O, and N (CHON particles) (*30*). The size range (40 to 2000 nm) and bulk compositions of CHON particles match the properties of the organic globules studied here, suggesting that such grains were prevalent throughout the protoplanetary disk. Microscopic organic globules may thus have been a common form of prebiotic organic matter delivered to the early

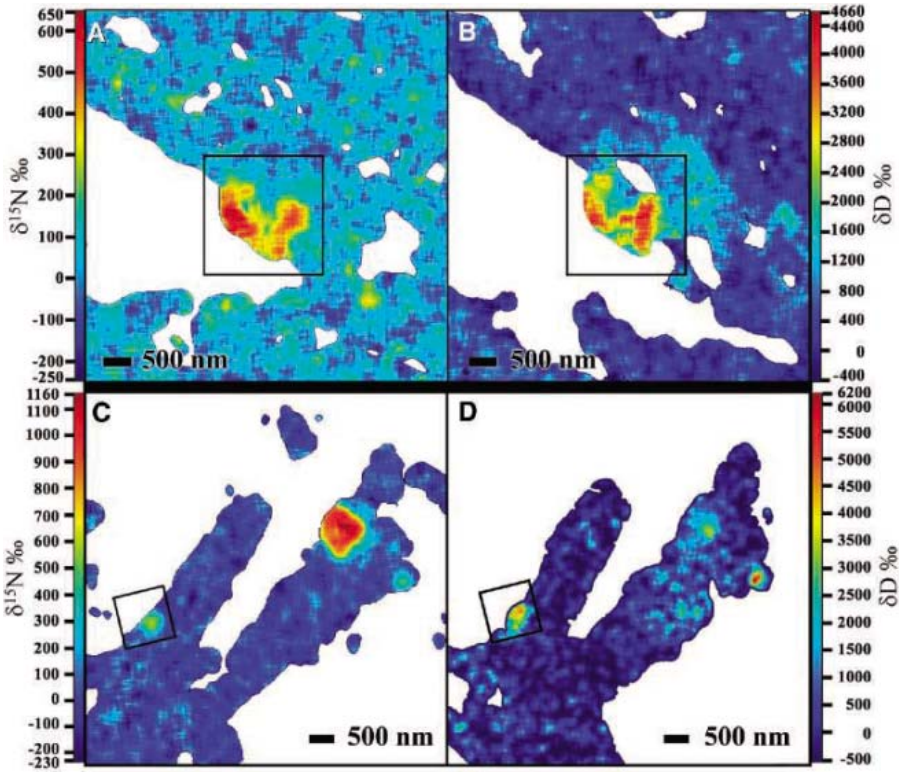

Fig. 3. (**A**) Nitrogen isotopic image of section G8-3 containing a uniformly ^{15}N-enriched globule aggregate. The box is the field of view of Fig. 1A. (**B**) Hydrogen isotopic image of the globule aggregate in Fig. 3A. The aggregate is uniformly enriched in D/H and is adjacent to D-rich matrix. (**C**) Nitrogen isotopic image of section G15 containing three globules with differing ^{15}N-enrichments. The boxes are fields of view of Fig. 1A and Fig. 1B. (**D**) Hydrogen isotopic image of the globules in Fig. 1C. All three globules are D-rich, but the magnitudes of the H and N isotopic anomalies are not correlated.

Earth by comets and meteorites. Further studies of these objects may elucidate whether their composition and membrane-like structures were important building blocks for the origin of life.

References and Notes

1. E. Zinner, in *Treatise on Geochemistry,* A. M. Davis, K. K. Turekian, H. D. Holland, Eds. (Elsevier, 2004), 1, p. 17.
2. S. Messenger, R. M. Walker, in *Astrophysical Implications of the Laboratory Study of Presolar Materials*, T. J. Bernatowicz, E. Zinner, Eds. (AIP Conference Proceedings 402, Woodbury, NY, 1997), p. 545.
3. S. Messenger, *Nature* **404**, 968 (2000).
4. H. Busemann *et al.*, *Science* **312**, 727 (2006).
5. P. G. Brown *et al.*, *Science* **290**, 320 (2000).
6. T. Hiroi, M. E. Zolensky, C. M. Pieters, *Science* **293**, 2234 (2001).
7. M. M. Grady, A. B. Verchovsky, I. A. Franchi, I. P. Wright, C. T. Pillinger, *Met. Planet. Sci.* **37**, 713 (2002).
8. K. Nakamura, M. E. Zolensky, S. Tomita, S. Nakashima, K. Tomeoka, *Int. J. Astrobiology* **1**, 179 (2002).
9. G. Claus, B. Nagy, *Nature* **192**, 594 (1961).
10. L. A. J. Garvie, P. R. Buseck, *Lunar Planet. Sci.* **37**, Abstract 1455 (2006).
11. Materials and methods are available as supporting online material on *Science* Online.
12. J. F. Kerridge, *Geochim. Cosmochim. Acta* **49**, 1707 (1985).
13. T. J. Millar, A. Bennett, E. Herbst, *Astrophys. J.* **340**, 906 (1989).
14. A. G. G. M. Tielens, in *Astrophysical Implications of the Laboratory Study of Presolar Materials,* T. J. Bernatowicz, E. Zinner, Eds. (AIP Conference Proceedings 402, Woodbury, NY, 1997), p. 523.
15. Y. Aikawa, E. Herbst, *Astrophys. J.* **526**, 314 (1999).
16. S. D. Rodgers, S. B. Charnley, *Mon. Not. R. Astron. Soc.* **352**, 600 (2004).
17. W. D. Langer, T. E. Graedel, *Astrophys. J. Suppl. Ser.* **69**, 241 (1989).
18. S. Pizzarello, G. W. Cooper, G. J. Flynn, in *Meteorites and the Early Solar System II*, D. S. Lauretta, H. Y. McSween, Eds. (Univ. Arizona Press, 2006), p. 625.
19. C. M. O'D. Alexander *et al.*, *Met. Planet. Sci.* **33**, 603 (1998).
20. L. P. Keller *et al.*, *Geochim. Cosmochim. Acta* **68**, 2577 (2004).
21. C. Floss *et al.*, *Science* **303**, 1355 (2004).
22. M. E. Zolensky, H. Y. McSween, in *Meteorites and the Early Solar System*, J. F. Kerridge, M. S. Matthews, Eds. (Univ. Arizona Press, 1988), pp. 114–143.
23. G. D. Cody, C. M. O'D. Alexander, *Geochim. Cosmochim. Acta* **69**, 1085 (2005).
24. J. H. Lacy, H. Faraji, S. A. Sandford, L. J. Allamandola, *Astrophys. J.* **501**, L105 (1998).
25. E. L. Gibb, D. C. B. Whittet, A. C. A. Boogert, A. G. G. M. Tielens, *Astrophys. J. Suppl. Ser.* **151**, 35 (2004).
26. A. Li, J. M. Greenberg, *Astron. Astrophys.* **323**, 566 (1997).
27. M. P. Bernstein *et al.*, *Astrophys. J.* **582**, L25 (2003).
28. J. P. Dworkin, D. W. Deamer, S. A. Sandford, L. J. Allamandola, *Proc. Natl. Acad. Sci. U.S.A.* **98**, 815 (2001).
29. M. E. Zolensky, W. L. Bourcier, J. L. Gooding, *Icarus* **78**, 411 (1989).
30. M. N. Fomenkova, *Space Sci. Rev.* **90**, 109 (1999).

31. We thank J. Brook, A. Hildebrand, P. Brown, and C. Roots for immediate and careful recovery of the Tagish Lake meteorite and for permitting its study. This research was supported by an NRC award to K.N.-M. and NASA Cosmochemistry grants to S.M., L.P.K., S.J.C., and M.E.Z. The JEOL 2500SE STEM and CAMECA NanoSIMS 50L were obtained with NASA Sample Return Laboratory Instrument Data Analysis Program grants to L.P.K. and S.M. This paper benefited from careful reviews by two anonymous reviewers. This is the inaugural paper from the newly established Robert M. Walker Laboratory for Space Science at Astromaterials Research and Exploration Science, NASA Johnson Space Center.

Supporting Online Material

www.sciencemag.org/cgi/content/full/314/5804/1439/DC1
Materials and Methods
Fig. S1
Table S1

6 July 2006; accepted 4 October 2006
10.1126/science.1132175

Increasing Trend of Extreme Rain Events Over India in a Warming Environment

B. N. Goswami,[1]* V. Venugopal,[2] D. Sengupta,[2] M. S. Madhusoodanan,[2] Prince K. Xavier[2]

Against a backdrop of rising global surface temperature, the stability of the Indian monsoon rainfall over the past century has been a puzzle. By using a daily rainfall data set, we show (i) significant rising trends in the frequency and the magnitude of extreme rain events and (ii) a significant decreasing trend in the frequency of moderate events over central India during the monsoon seasons from 1951 to 2000. The seasonal mean rainfall does not show a significant trend, because the contribution from increasing heavy events is offset by decreasing moderate events. A substantial increase in hazards related to heavy rain is expected over central India in the future.

Analysis of rain gauge data shows that Indian monsoon rainfall has remained stable over the past century even though the global mean surface temperature has risen steadily (*1*–*3*). Although the amount of summer monsoon rain [June to September (JJAS) seasonal mean all-India rainfall, AIR] has some interdecadal variability (*4*), it has no significant long-term trend (Fig. 1). Physical considerations and model studies indicate that tropospheric warming leads to an enhancement of moisture content of the atmosphere (*5*) and is associated with an increase in heavy rainfall events (*6*–*11*). Extreme rainfall results in landslides, flash floods, and crop damage that have major impacts on society, the economy, and the environment. Although prediction of such extreme weather events is still fraught with uncertainties, a proper assessment of likely future trends would help in setting up infrastructure for disaster preparedness.

The number of severe cyclonic storms over the north Indian Ocean (IO) has shown an increasing trend in the past 3 decades (*12*, *13*), consistent with similar findings over other basins (*12*). However, no coherent signal has emerged from investigations of the trend of daily station rainfall data over India (*13*–*16*), with some stations showing an increasing trend whereas others show a decreasing trend. The ambiguity in the existence of a trend in monsoon rainfall extremes may be partly related to the data and the methodologies used so far. Short-duration extreme rain events are a consequence of small-scale convective instabilities in a moist atmosphere. Although a fraction of extreme rain events is triggered in the background of synoptic disturbances (*17*) and is preferentially located around the tracks of monsoon lows and depressions, a large fraction arises from processes like severe thunderstorms and is more uniformly distributed in space and time. Even if the total number of extreme events over a homogeneous large-scale environment were to have an increasing trend, no significant trend may appear in data from a single station because of the inherently large variability and/or sampling issues (*18*–*23*). Therefore, we examined the trend of daily heavy and very heavy rain events over a relatively large region.

We used daily gridded rainfall data at 1°-by-1° resolution from the India Meteorological Department (IMD), based on 1803 stations (*24*, *25*) that have at least 90% data availability, for the period 1951–2000. The interannual variability of JJAS all-India rainfall (AIR2) from this data set (Fig. 1B) is similar to AIR, which is a long-term data set based on 306 stations (*26*). Daily anomalies of rainfall at each grid box were constructed as deviations of observed daily values from a smoothed climatological annual cycle (the sum of the mean and first three harmonics of the daily climatology). The climatological mean and variance of daily summer monsoon rainfall have large spatial variability across the country (Fig. 1A and fig. S1). However, over central India (CI, 74.5°E to 86.5°E and 16.5°N to 26.5°N, containing 143 grid boxes) the mean and the standard deviation are reasonably homogeneous (spatially

[1]Indian Institute of Tropical Meteorology, Doctor Homi Bhabha Road, Pashan, Pune 411 008, India. [2]Centre for Atmospheric and Oceanic Sciences, Indian Institute of Science, Bangalore, Karnataka 560 012, India.

*To whom correspondence should be addressed. E-mail: goswami@tropmet.res.in

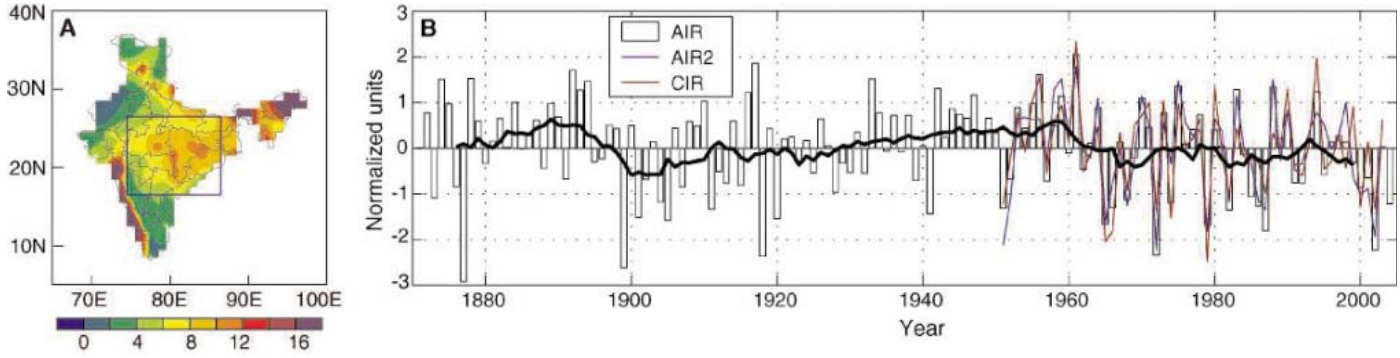

Fig. 1. (**A**) Climatological mean summer monsoon rainfall (mm/day). The box indicates the CI region used in our analysis. (**B**) Normalized (by the interannual standard deviation) JJAS AIR based on 306 stations (*26*) from 1871 to 2003 (bars). The mean is 84.9 cm, and the standard deviation is 8.4 cm. The solid black line represents an 11-year running mean indicating interdecadal variability but no trend. The AIR2 (blue) is the normalized seasonal mean AIR on the basis of the new gridded rainfall data (*24*). The seasonal mean and standard deviation are 94.0 cm and 9.1 cm, respectively. The CIR (red) is the normalized seasonal mean over CI on the basis of the gridded rainfall data set, the mean and the standard deviation of which are 69.5 cm and 11.2 cm, respectively.

uniform). Therefore, we select CI as the region to examine the trend of extreme rainfall over India.

The gridded daily data are smoother than the individual station data because of averaging over a 1°-by-1° box. The maximum 1-day rainfall during the summer monsoons of 1951 to 2003 in any box over CI is 58.2 cm. The seasonal mean over CI is 5.7 mm of rain in a day (mm/day), whereas the standard deviation of the daily anomalies is 11.5 mm/day. Although a fixed threshold for defining extreme events is not appropriate over regions where the mean climate has large spatial variability (*27*, *28*), a fixed threshold can be used to define extreme rain events over CI, where the seasonal mean climate as well as the daily variability is reasonably homogeneous (Fig. 1A and fig. S1). We used 100 mm/day in a 1°-by-1° box as a threshold to define a heavy rain event, whereas a threshold of 150 mm/day was used to define a very heavy event.

The temporal variance of daily rainfall anomalies averaged over CI shows a significant increasing trend (at 0.01 significance level) during 1951 to 2000 (Fig. 2A). The increasing trend of the coefficient of variability, defined as the ratio of the standard deviation to the mean, of daily monsoon rainfall (Fig. 2B) is a consequence of the absence of a trend in the seasonal mean (Fig. 1) and an increasing trend in the standard deviation. A trend in daily rainfall variance is related to a trend in large-scale moisture availability (*5*), which in turn is due to gradual warming of sea surface temperature (SST) (*7*). However, interannual changes in moisture content over CI can be influenced by regional-scale land surface processes as well as by atmospheric teleconnections associated with remote SST such as the El Niño and Southern Oscillation (ENSO). Although El Niño events are generally associated with positive SST anomaly over the tropical IO, they lead to drying of the atmosphere over CI through large-scale subsidence. As a result, daily CI rainfall variance and IO SST need not

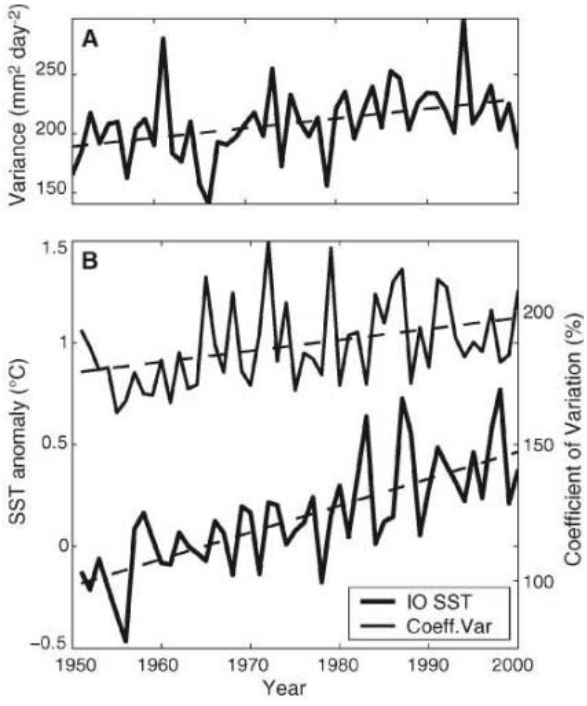

Fig. 2. (**A**) Temporal variation (1951 to 2000) in the variance of daily anomalies during summer monsoon seasons (June 1 to September 30), together with its linear trend (dashed line). (**B**) Coefficient of variability of daily precipitation during summer monsoon season and its trend (thin line) together with JJAS SST anomalies averaged over tropical IO and their trend (bold line). Statistically significant trends (0.01 significance level) are calculated on the basis of a *t* test, with a sample size of 50, under a null hypothesis of no trend.

be correlated on a year-to-year basis. The long-term increase of daily rainfall variance is likely due to the warming trend of tropical IO JJAS SST (Fig. 2) and the associated increase in water vapor (*5*).

The frequency histogram of daily rainfall at each 1° by 1° box (R) over CI during the summer monsoons of 1951 to 1970 and 1981 to 2000 was separately constructed (plotted as line curves in fig. S2) to assess the increase in variance in recent decades compared with those of the 1950s and 1960s. The tails of the histogram indicate a larger number of extreme events (≥100 mm/day of rain) during 1981–2000. On the other hand, the number of light to moderate events (≥5 mm/day but <100 mm/day) have decreased during 1981 to 2000 compared with 1951 to 1970. In fact, the frequency of heavy ($R \geq 100$ mm/day) and very heavy ($R \geq 150$ mm/day) events over CI shows clear and significant (at 0.01 significance level) increasing trends (Fig. 3) (*29*), whereas that of moderate events shows a significant (at 0.1 significance level) decreasing trend. There is a 10% increase per decade in the level of heavy rainfall activity since the early 1950s (Fig. 3A), whereas the number of very heavy events has more than doubled (Fig. 3B), indicating a large increase in disaster potential. These findings are in tune with model projections (*6*–*11*) and some observations (*30*) that indicate an increase in heavy rain events and a decrease in weak events under global warming scenarios.

In order to see whether the unambiguous increase in the frequency of heavy and very heavy events is also accompanied by an increase in the

intensity of heavy events, we examined the rain intensity between 99 and 99.99 percentiles (*31*) of summer monsoon rainfall (Fig. 4A). The rainfall intensity that contributed to the 99.75 percentile in the early 1950s seems to contribute to only the 99.5 percentile in the early 1990s, with events of higher intensity contributing to the higher percentiles. For instance, the average intensity of the heaviest four events in each monsoon season (Fig. 4B) shows an ~10% per decade increase over the 50-year period (18 to 26 cm), significant at 0.01 significance level.

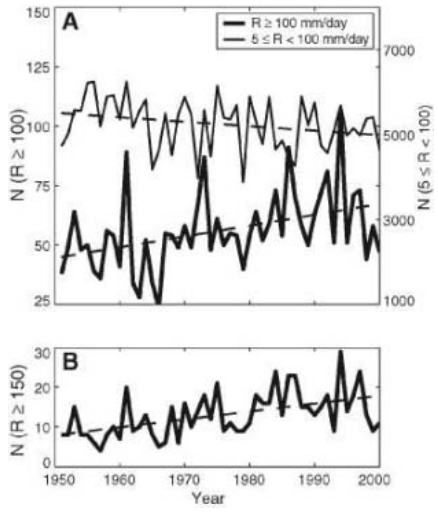

Fig. 3. Temporal variation (1951 to 2000) in the number (*N*) of (**A**) heavy ($R \geq 100$ mm/day, bold line) and moderate ($5 \leq R < 100$ mm/day, thin line) daily rain events and (**B**) very heavy events ($R \geq 150$ mm/day) during the summer monsoon season over CI. The statistical significance of the trends (dashed lines) was calculated as in Fig. 2.

Although the above results present strong evidence of an increase in the number of extreme monsoon weather events over India over the past half century, the Indian monsoon climate (seasonal mean monsoon rainfall) remains stable for the same period (Fig. 1). The findings in Fig. 3 help us piece this puzzle together. Note that although the frequency histograms for the two periods (1951 to 1970 and 1981 to 2000) have significant differences (fig. S2), the mean rainfall during these periods is nearly identical at 5.75 mm and 5.69 mm, respectively. The heavy events (≥100 mm/day of rain) contribute about 6.4% to the seasonal mean, whereas moderate events (from 5 mm/day to <100 mm/day) contribute about 85.8%. Although the relative contributions to the mean from these two classes do not balance in a given year, the contribution from the decreasing trend of moderate events is partially offset by that from increasing heavy rain events (*7*). Consequently, the seasonal total does not show any statistically significant change over longer time scales.

Previous attempts to detect trends in extreme rain events by using station data were inconclusive, probably because of the large year-to-year variability in Indian monsoon rainfall. To assess the role of sampling and variability, we examined the number of heavy rain events over regions of increasing size (fig. S3). We find that for regions smaller than about 800 km by 800 km, it is difficult to find significant trends in heavy rain events. On the other hand, the whole of India cannot be taken as one unit to investigate such trends. The northeast and the west coast are regions of high mean (Fig. 1A) and high variability (fig. S1), and local orography has a strong influence on the rainfall over both regions. Therefore, trends in extreme rainfall due to a warming environment are difficult to discern in these regions.

In spite of considerable year-to-year variability, there are significant increases in the frequency and the intensity of extreme monsoon rain events in central India over the past 50 years. Although desirable for applications, it is difficult to detect signals of climate change in extreme rain events at individual stations; instead, as we show, one needs a sufficiently large area to discern a trend reliably. The observed trends suggest enhanced risks associated with extreme rainfall over India in the coming decades.

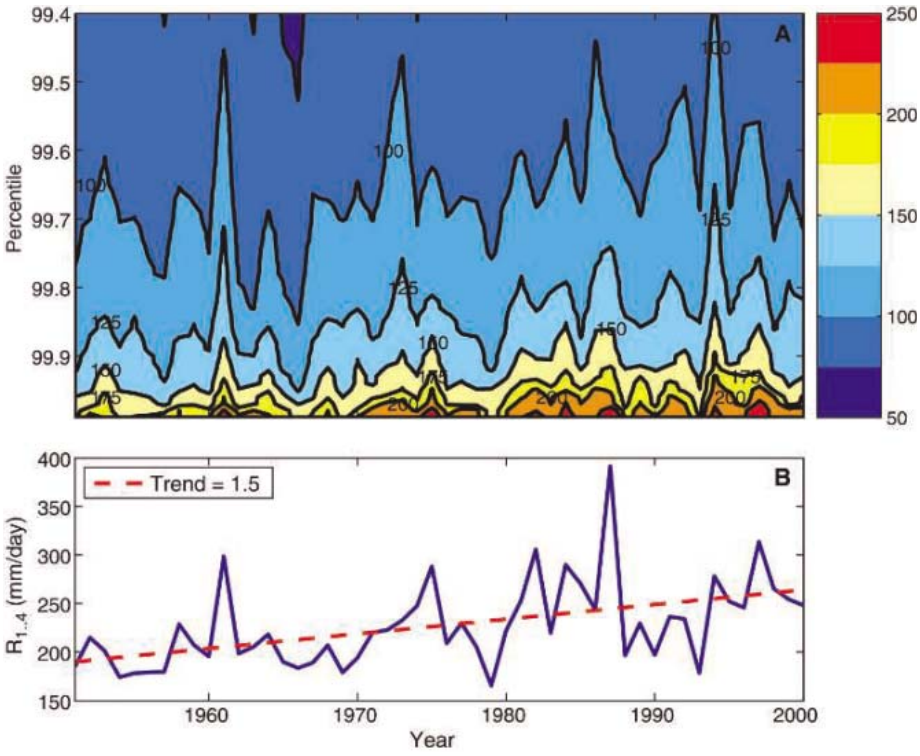

Fig. 4. Temporal variation (1951 to 2000) in (**A**) 99.4 to 99.99 percentiles of seasonal rainfall and (**B**) the mean rainfall of the four highest rain events every season ($R_{1..4}$). Color bar in (A) indicates rain intensity in mm/day. The statistical significance of the trend (dashed line) was calculated as in Fig. 2.

References and Notes

1. J. T. Houghton *et al.*, Eds., *Climate Change 2001: The Scientific Basis* (Cambridge Univ. Press, Cambridge, 2001).
2. A. N. Rayner *et al.*, *J. Geophys. Res.* **108**, 10.1029/2002]D002670 (2003).
3. M. E. Mann, R. S. Bradley, M. K. Hughes, *Geophys. Res. Lett.* **26**, 759 (1999).
4. B. N. Goswami, in *The Asian Monsoon*, B. Wang, Ed. (Praxis, Springer, Berlin, 2005), ch. 7, pp. 295–327.
5. K. E. Trenberth, J. Fasullo, L. Smith, *Clim. Dyn.* **24**, 741 (2005).
6. M. R. Allen, W. J. Ingram, *Nature* **419**, 224 (2002).
7. K. E. Trenberth, A. Dai, R. M. Rasmussen, D. B. Parsons, *Bull. Am. Meteor. Soc.* **84**, 1205 (2003).
8. K. J. Hennessy, J. M. Gregory, J. F. B. Mitchell, *Clim. Dyn.* **13**, 667 (1997).
9. H. B. Gordon, P. H. Whetton, A. B. Pittock, A. M. Fowler, M. R. Haylock, *Clim. Dyn.* **8**, 83 (1992).
10. A. G. Meehl *et al.*, *Bull. Am. Meteor. Soc.* **81**, 427 (2000).
11. V. A. Semenov, L. Bengtsson, *Clim. Dyn.* **19**, 123 (2002).
12. P. J. Webster, G. J. Holland, J. A. Curry, H.-R. Chang, *Science* **309**, 1844 (2005).
13. K. Rupa Kumar, K. Krishnakumar, R. G. Ashrit, S. K. Patwardhan, G. B. Pant, in *Climate Change and India*, P. R. Shukla *et al.*, Eds. (Tata McGraw Hill, New Delhi, 2002), pp. 24–75.
14. K. Krishnakumar *et al.*, paper presented at the Workshop on Indices and Indicators for Climate Extremes, National Climate Data Center, Ashville, NC, 3 to 6 June 1997.
15. S. Sen Roy, R. C. Balling Jr., *Int. J. Climatol.* **24**, 457 (2004).
16. L. V. Alexander *et al.*, *J. Geophys. Res.* **111**, 10.1029/2005]D006290 (2006).
17. P. A. Francis, S. Gadgil, *Meteorol. Atmos. Phys.* **94**, 27 10.1007/s00703-005-0167-2 (2006).
18. X. Zhang, W. D. Hogg, E. Mekis, *J. Clim.* **14**, 1923 (2001).
19. X. Zhang, F. W. Zwiers, G. Li, *J. Clim.* **17**, 1945 (2004).
20. D. A. Stone, A. J. Weaver, F. W. Zwiers, *Atmos. Ocean* **38**, 321 (2000).
21. C. Frei, C. Schär, *J. Clim.* **14**, 1568 (2001).
22. P. Frich *et al.*, *Clim. Res.* **19**, 193 (2002).
23. P. Ya. Groisman *et al.*, *J. Clim.* **18**, 1326 (2005).

24. M. Rajeevan, J. Bhate, J. D. Kale, B. Lal, *Curr. Sci.* **91**, 296 (2006).
25. Materials and methods are available on *Science* Online.
26. B. Parthasarathy, A. A. Munot, D. R. Kothawale, "Monthly and seasonal rainfall time series for all India, homogeneous divisions and meteorological subdivisions, 1871-1994" (Technical Report RR065, ISSN 025201075, Indian Institute of Tropical Meteorology, Pune, India, 1996).
27. M. Haylock, N. Nicholls, *Int. J. Climatol.* **20**, 1533 2000).
28. M. J. Manton, *Int. J. Climatol.* **21**, 269 (2001).
29. The frequency histogram of 1980 to 2000 rain is consistently above that of 1951 to 1970 rain for intensities greater than 70 mm/day (fig. S2B). The number of events larger than 70 mm/day shows a trend significant at the 0.1 significance level.
30. M. Brunetti, M. Colacino, M. Maugeri, T. Nanni, *Int. J. Climatol.* **21**, 299 (2001).
31. For each year, the calculation of percentiles is based on 122 days (monsoon season) and 143 grid points.
32. We thank the IMD for making the daily gridded rainfall data available, the Department of Ocean Development, Government of India, for partial support for this work, and J. Srinivasan for useful discussions.

Supporting Online Material
www.sciencemag.org/cgi/content/full/314/5804/1442/DC1
Materials and Methods
Figs. S1 to S3

3 July 2006; accepted 23 October 2006
10.1126/science.1132027

Male Fertility and Sex Ratio at Birth in Red Deer

Montserrat Gomendio,[1]* Aurelio F. Malo,[1] Ana J. Soler,[2] Maria R. Fernández-Santos,[2] Milagros C. Esteso,[2] Andrés J. García,[2] Eduardo R. S. Roldan,[1]*† Julian Garde[2]†

Efforts to test sex ratio theory have focused mostly on females. However, when males possess traits that could enhance the reproductive success of sons, males would also benefit from the manipulation of the offspring sex ratio. We tested the prediction that more-fertile red deer males produce more sons. Our findings reveal that male fertility is positively related to the proportion of male offspring. We also show that there is a positive correlation between the percentage of morphologically normal spermatozoa (a main determinant of male fertility) and the proportion of male offspring. Thus, males may contribute significantly to biases in sex ratio at birth among mammals, creating the potential for conflicts of interest between males and females.

The Trivers and Willard hypothesis (*1*) for sex allocation predicts that parents should increase the production of the sex with the higher fitness benefit. This hypothesis has been applied most often to mothers, who have a strong influence on offspring quality through maternal care. It can also apply to any trait that parents transmit to offspring that has a differential effect on the reproductive success of sons and daughters. Thus, among birds, offspring sex ratios may be adjusted in relation to the attractiveness of the father, because sons will inherit large sexual ornaments and will achieve high reproductive success (*2*). However, it is assumed that such manipulation is under female control, because in birds females are the heterogametic sex.

The possibility that males may also facultatively adjust sex ratio has seldom been considered. In haplodiploid insects, the offspring sex depends on whether the ovum is fertilized or not, and males may constrain sex ratios because males with poor-quality ejaculates fail to fertilize the ova (*3*). In mammals, males are the heterogametic sex, and offspring sex is determined by whether an X- or Y-chromosome–bearing spermatozoon fertilizes the ovum. Thus, mammalian males may have more control over the mechanisms of sex determination than they do in other taxa. In mammals, male fertility may have a great influence on the reproductive success of sons.

Ungulates are good models to test sex ratio theory because they are sexually dimorphic in body size, variance in reproductive success is greater among males, and the reproductive success of sons is more strongly influenced by maternal investment. Early studies on red deer (*Cervus elaphus*) found support for the prediction that high-quality mothers should produce sons (*4*), but subsequent studies have generated inconsistent results (*5*). Our previous studies have shown that in natural populations of red deer, males differ markedly in their fertility rates, and more-fertile males have faster swimming sperm and a greater proportion of normal spermatozoa (*6*). Thus, male reproductive success may not depend exclusively on body size, but also on the ability of males to fertilize females after copulation. Male fertility is advertised by antler size and complexity, so more-fertile males also have larger and more elaborate sexual characters, which may be inherited by their sons (*7*).

We tested the hypothesis that more-fertile red deer males produce more sons. The key challenge was to disentangle male and female effects by designing an experiment to retain the inter-male variation in fertility rates found in natural populations while minimizing differences between females (*8*). Thus, our experimental design was aimed at eliminating several female factors known to influence sex ratios: (i) We avoided the possibility that females may bias sex ratio in response to male quality by artificially inseminating females so that they had no direct experience with the males. (ii) We minimized differences in body condition by using a sample of females that were all in good physical condition, were kept under similar environmental conditions, and had access to an unlimited food supply. (iii) All females were inseminated at the same time in relation to ovulation, avoiding the confounding effects of insemination time. In contrast, by using sperm collected during the rut from males living in natural populations, we ensured a representative sample of the large degree of variation in male fertility previously described (*6*).

When the entire study sample is considered, a similar number of male and female offspring were produced (Table 1). However, among males, differences in fertility rates and in the proportion of male offspring were substantial. Male fertility rates ranged from 24 to 70%, and the proportion of male offspring ranged from 25 to 72% (Table 1).

Table 1. Descriptive statistics [mean, standard deviation (SD), and range] for male fertility rates, proportion of male offspring sired, percentage of normal sperm, sperm swimming-velocity parameters, and number of hinds inseminated per male (n = 14 red deer stags). VCL, curvilinear velocity; VSL, straight-line velocity; VAP, average path velocity.

Parameters	Mean	SD	Range min–max
Fertility rate (%)	50.39	13.06	24–70
Proportion of male offspring	0.50	0.14	0.25–0.72
Morphologically normal spermatozoa (%)	80.07	8.78	65–95
VCL (μm/s)	126.87	28.48	85–163
VSL (μm/s)	67.86	27.31	28–111
VAP (μm/s)	88.74	26.52	53–122
Hinds inseminated per male	24.57	16.00	11–69

[1]Reproductive Ecology and Biology Group, Department of Evolutionary Ecology, Museo Nacional de Ciencias Naturales [Consejo Superior de Investigaciones Científicas (CSIC)], 28006-Madrid, Spain. [2]Instituto de Investigación en Recursos Cinegéticos [CSIC-Universidad de Castilla-La Mancha–Junta de Communidades de Castilla-La Mancha (JCCM)], 02071-Albacete, Spain.

*To whom correspondence should be addressed. E-mail: montseg@mncn.csic.es (M.G.); roldane@mncn.csic.es (E.R.S.R.)
†These authors contributed equally to this work.

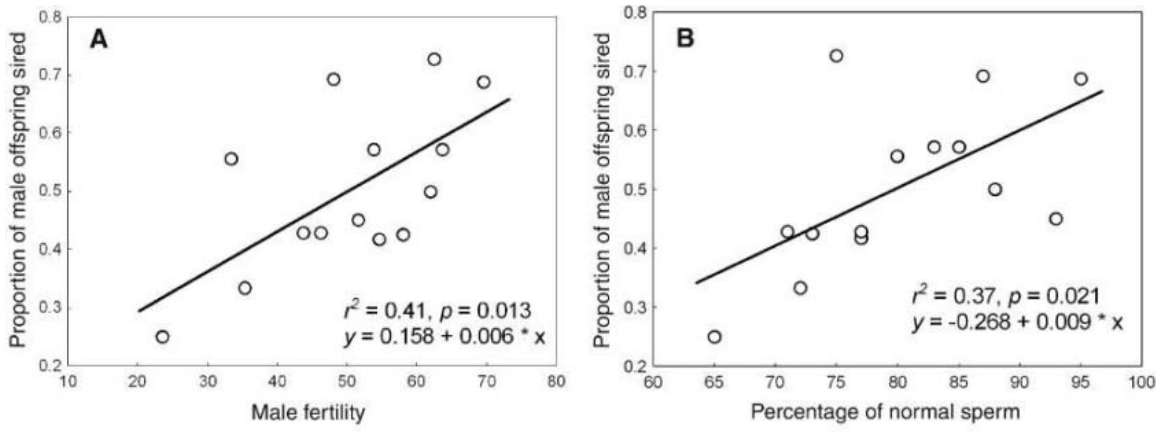

Fig. 1. (**A**) Relation between male fertility [(number of hinds pregnant/number of hinds inseminated) × 100] and proportion of male offspring sired. (**B**) Relation between percentage of normal spermatozoa and proportion of male offspring sired.

There was a significant relation between male fertility and the proportion of male offspring sired (squared correlation coefficient $r^2 = 0.41$, $P = 0.013$). More-fertile males sired a greater number of sons, and less-fertile males sired more daughters (Fig. 1A). There was also a significant relation between the percentage of morphologically normal spermatozoa and the proportion of male offspring sired per male ($r^2 = 0.37$, $P = 0.021$) (Fig. 1B). In contrast, no significant relation was found between sperm velocity parameters and the proportion of male offspring sired ($P > 0.05$).

Thus, of the two main determinants of male fertility—sperm swimming velocity and the proportion of normal spermatozoa (*6*)—the latter was found to be associated with sex ratio. This may be the case because the proportion of normal spermatozoa is more likely to be inherited by sons (*9*) than sperm swimming velocity, which may be influenced to a greater extent by environmental factors (*10*). Thus, males with a higher proportion of normal spermatozoa may benefit from producing sons who will inherit the trait that will increase their fertility, and they will thus achieve high reproductive success. In contrast, low-fertility males will benefit from producing daughters who will not inherit their father's poor ejaculate quality.

There are two possible mechanisms by which males may adjust sex ratio. First, although it is assumed that mammalian males produce equal numbers of X- and Y-bearing spermatozoa as a consequence of meiotic cell division, ejaculates may differ in the proportion of Y-bearing spermatozoa (*11*), resulting in biases in sex ratio at birth. Thus, high- and low-fertility males could differ in the proportion of Y-bearing spermatozoa in the ejaculate. Second, Y-bearing spermatozoa could be at an advantage in relation to X-bearing spermatozoa when produced by more-fertile males, whereas the opposite may occur among less-fertile males. Differences between males in the competitiveness of X- and Y-bearing spermatozoa could arise through differential expression of genes carried in the sex chromosomes (*12*). Such postmeiotic expression of germ line–specific X- or Y-linked genes has recently been demonstrated (*13*) and could influence sperm shape, size, and function. Furthermore, it has recently been shown that males with deletions in the Y chromosome produce Y-bearing spermatozoa with morphological abnormalities that are less efficient at fertilization, resulting in sex ratio biases toward females (*14*). Thus, red deer males with low fertility rates may have a lower proportion of morphologically normal spermatozoa as a consequence of genetic information on the Y chromosome, which would also impair the chances of fertilization of Y-bearing spermatozoa. On the contrary, males with high fertility rates may produce more-competitive Y-bearing spermatozoa. Alternatively, females could influence the fertilization success of X- and Y-bearing spermatozoa depending on the fertility of the male. This would require that females be able to assess ejaculate quality (and more specifically the proportion of normal spermatozoa) and bias sex ratio accordingly, given that in our experimental design females were prevented from evaluating male quality or copulatory behavior. This hypothesis assumes that differences in fertilization success between X- and Y-bearing spermatozoa are caused, not by differences in competitiveness between them (as proposed by the previous hypothesis), but by female selection in the reproductive tract.

Our experimental approach reveals unexpectedly large differences in fertility rates between males from natural populations when females are artificially inseminated. Are such differences in male fertility likely to occur in natural contexts? In the wild, low-fertility males could compensate by transferring more spermatozoa per ejaculation. This is unlikely to occur because in natural populations, low-fertility males have smaller testes that produce fewer spermatozoa (*6*), a trait that is known to have a major influence on fertility (*15*). Thus, the differences in fertility rates when all females are inseminated with equal sperm numbers are likely to be exacerbated when differences in sperm numbers come into play in natural contexts. Alternatively, low-fertility males could enhance their fertilization success by copulating more often with the same female, but the opportunities to do so may be limited. Because low-fertility males have smaller antlers (*7*), their ability to defend females for a long period of time may be constrained. Furthermore, in Mediterranean populations food is scarce during the mating season, and males either defend harems or establish territories where food resources are concentrated (*16*). Females move between territories and harems while searching for food; thus, repeated copulations with the same female may be rare. Finally, frequent copulations may lead to sperm depletion among low-fertility males given their limited sperm numbers; there is evidence that in natural populations, frequent copulation leads to sperm depletion and decreases male siring success (*17*). Thus, in natural populations, differences in fertility rates are likely to contribute substantially to differences between males in lifetime reproductive success.

Our findings suggest that mammalian males can manipulate the sex ratio of their offspring, thus creating an unforeseen evolutionary scenario that includes conflicts of interest between males and females. For instance, a fertile male may benefit from producing sons, but the costs of raising a male may be high for a female in poor physical condition (*18*). This level of conflict may improve our ability to explain biases in sex ratio at birth.

References and Notes

1. R. L. Trivers, D. E. Willard, *Science* **179**, 90 (1973).
2. H. Ellegren, L. Gustafsson, B. C. Sheldon, *Proc. Natl. Acad. Sci. U.S.A.* **93**, 11723 (1996).
3. H. J. Henter, *J. Evol. Biol.* **17**, 886 (2004).
4. T. H. Clutton-Brock, S. D. Albon, F. E. Guinness, *Nature* **308**, 358 (1984).
5. A. J. M. Hewison, J. M. Gaillard, *Trends Ecol. Evol.* **14**, 229 (1999).
6. A. F. Malo *et al.*, *Biol. Reprod.* **72**, 822 (2005).
7. A. F. Malo, E. R. S. Roldan, J. Garde, A. J. Soler, M. Gomendio, *Proc. R. Soc. London B Biol. Sci.* **272**, 149 (2005).
8. Materials and methods are available as supporting material on *Science* Online.
9. J. Smital, J. Wolf, L. L. De Sousa, *Anim. Reprod. Sci.* **86**, 119 (2005).
10. S. J. Kilgallon, L. W. Simmons, *Biol. Lett.* **1**, 253 (2005).
11. J. E. Chandler, A. M. Canal, J. B. Paul, E. B. Moser, *Theriogenology* **57**, 1327 (2002).
12. C. W. LaMunyon, S. Ward, *Proc. Natl. Acad. Sci. U.S.A.* **94**, 185 (1997).
13. P. J. Wang, D. C. Page, J. R. McCarrey, *Hum. Mol. Genet.* **14**, 2911 (2005).

14. M. A. Ward, P. S. Burgoyne, *Biol. Reprod.* **74**, 652 (2006).
15. M. Gomendio, A. H. Harcourt, E. R. S. Roldan, in *Sperm Competition and Sexual Selection*, T. R. Birkhead, A. P. Møller, Eds. (Academic Press, London, 1998).
16. J. Carranza, P. Fernandez-Llario, M. Gomendio, *Ethology* **102**, 793 (1996).
17. B. T. Preston, I. R. Stevenson, J. M. Pemberton, K. Wilson, *Nature* **409**, 681 (2001).
18. M. Gomendio, T. H. Clutton-Brock, S. D. Albon, F. E. Guinness, M. J. A. Simpson, *Nature* **343**, 261 (1990).
19. Empresa Medianilla allowed work at Finca Las Lomas. Funding was provided by Ministerio de Ciencia y Tecnologia, Ministerio de Educacion y Ciencia, European Regional Development Fund, and Instituto Nacional de Investigacion y Tecnologia Agraria. A.F.M. was supported by a studentship from MCYT, and A.J.S. and M.R.F.-S. received support from JCCM. We thank A. Cockburn, J. M. Cummins, C. LaMunyon, E. Martínez, and J. M. Vázquez for helpful discussions.

Supporting Online Material
www.sciencemag.org/cgi/content/full/314/5804/1445/DC1
Materials and Methods
References

26 July 2006; accepted 26 October 2006
10.1126/science.1133064

WNT and DKK Determine Hair Follicle Spacing Through a Reaction-Diffusion Mechanism

Stefanie Sick,[1] Stefan Reinker,[2]* Jens Timmer,[2] Thomas Schlake[1]†

Mathematical reaction-diffusion models have been suggested to describe formation of animal pigmentation patterns and distribution of epidermal appendages. However, the crucial signals and in vivo mechanisms are still elusive. Here we identify WNT and its inhibitor DKK as primary determinants of murine hair follicle spacing, using a combined experimental and computational modeling approach. Transgenic DKK overexpression reduces overall appendage density. Moderate suppression of endogenous WNT signaling forces follicles to form clusters during an otherwise normal morphogenetic program. These results confirm predictions of a WNT/DKK-specific mathematical model and provide in vivo corroboration of the reaction-diffusion mechanism for epidermal appendage formation.

The development of regularly arranged body parts has long fascinated experimental biologists and theoreticians alike. One area of long-standing debate has been the formation of epidermal appendages such as feathers and hairs. Theoretical models have provided seemingly simple solutions to complex developmental processes (*1*); in order to achieve regular patterns, the reaction-diffusion (RD) hypothesis of Alan Turing postulates a pair of activator and inhibitor with special characteristics (*2*) [supporting online material (SOM) text 1]. However, it remains largely unclear whether such predictions can be substantiated in molecular and mechanistic terms (*3*). Because canonical WNT signaling is essential for the induction of hair and feather follicles (*4, 5*) and forced stimulation of this pathway is sufficient to induce supernumerous appendages (*6, 7*), the pathway represents an appealing candidate for the primary signal that dictates follicle distribution. Here we set out to analyze its role in hair follicle arrangement by verifying predictions of a biologically adapted RD model.

The WNT pathway is active from the earliest stages of follicular development (*5, 8*) (Fig. 1A). Expression of the WNT inhibitor *Dkk1* is directly controlled by secreted WNTs (*9, 10*). Further aspects of this pathway and the RD mechanism are discussed in SOM text 2 and fig. S1. In developing murine skin, mesenchymal *Dkk1* expression is found adjacent to the early hair follicle bud (*5*) (Fig. 1B), whereas *Dkk4*, a further functional inhibitor of WNT signaling (*11, 12*), shows strong epithelial expression at discrete loci before hair placode formation (Fig. 1C). Weak expression in the early hair follicle bud indicates that *Dkk4* expression marks the forming follicle (Fig. 1C). Five LEF/TCF consensus binding motifs are found within 700 base pairs (bp) upstream of the transcriptional start site of *Dkk4*, and regulation of the promoter by the canonical WNT signaling pathway was suggested by transfection studies (Fig. 1D). Hence, the available data support the role of WNT and DKK as primary determinants of hair follicle spacing patterns.

If WNTs and WNT inhibitor(s) represent the two components required by the RD hypothesis, it should be possible to derive, from a WNT/DKK-specific RD model (SOM text 3), predictions about the outcome of experimental alterations of activating and inhibitory functions.

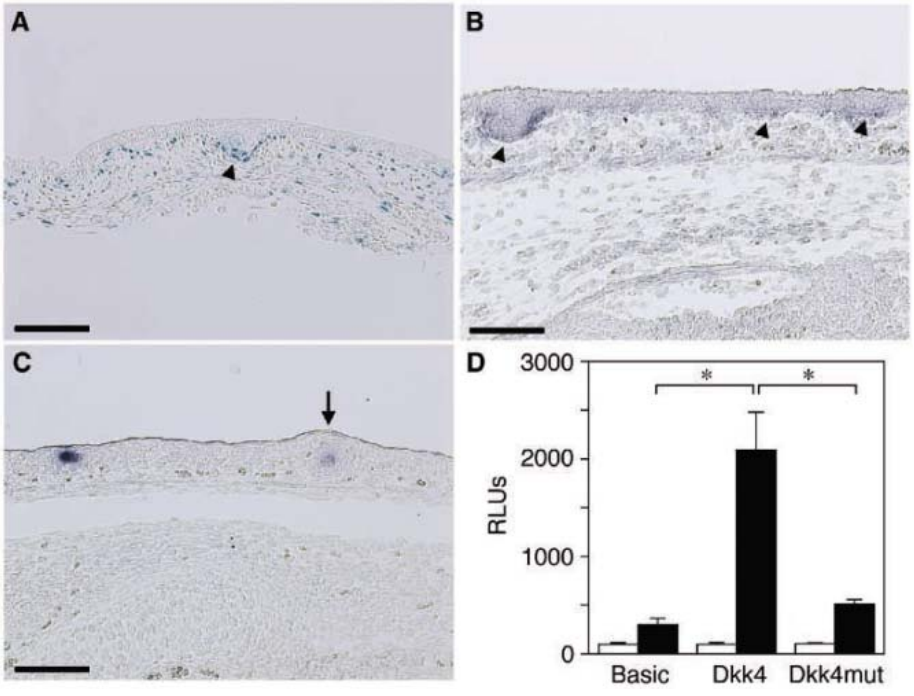

Fig. 1. WNT signaling and expression of *Dkk* genes are associated with hair follicle formation. (**A**) WNT signaling in mesenchymal cells is associated with developing hair follicles (arrowhead). BATgal mice harboring a WNT-responsive *lacZ* gene were used as a reporter. (**B**) Mesenchymal *Dkk1* expression adjacent to epithelial placodes and buds (arrowheads). (**C**) Strong epithelial *Dkk4* expression at discrete loci prior to hair placode formation. Expression rapidly declines after follicle budding (arrow). (A to C) Scale bars, 100 μm. (**D**) Reporter gene expression [relative light units (RLUs) ± SEM] after endogenous (white) and stimulated (black) canonical WNT signaling. *$P < 0.0001$ (*t* test) for stimulated WNT signaling (black columns).

[1]Max-Planck Institute of Immunobiology, Stuebeweg 51, 79108 Freiburg, Germany. [2]Institut für Physik, Universität Freiburg, Hermann-Herder-Strasse 3, 79104 Freiburg, Germany.

*Present address: Novartis Institutes for Biomedical Research, Basel, Switzerland.

†To whom correspondence should be addressed. E-mail: schlake@immunbio.mpg.de

Our computational modeling showed that moderate overexpression of activator during either the initial or a subsequent inductive wave increases follicular density (Fig. 2, A and B). By contrast, strong overexpression of activator completely disrupts the patterning process. Moderate overexpression of inhibitor during the initial inductive wave increases the interfollicular spacing (Fig. 2A). In line with the prediction of defective pattern formation after further enhancement of inhibitor expression, hair and feather follicle induction is indeed blocked in the presence of strong *Dkk1* expression (*4, 5*); however, the role of WNTs in appendage formation and patterning is still contentious. During a subsequent inductive wave, increased inhibitor expression blocks the development of new follicles in the interfollicular space (Fig. 2B). In addition, excess inhibitor gives rise to ringlike zones of high activator levels around preexisting appendages (Fig. 2B). If levels of activator above a threshold

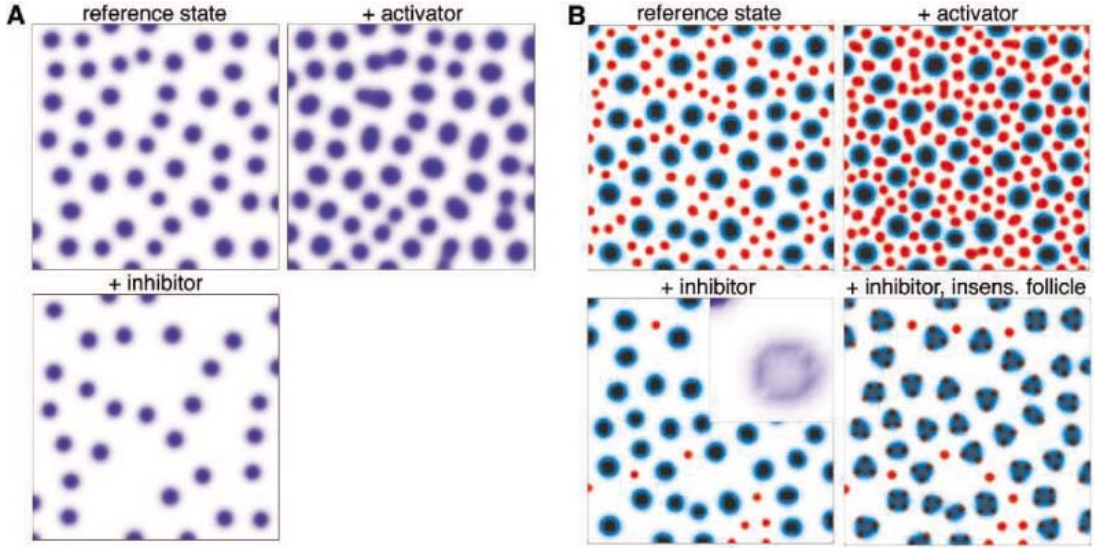

Fig. 2. A WNT/DKK-specific model of a reaction-diffusion system predicts changes in epidermal appendage distribution after transgenic interference with endogenous signaling. Diagrams for excess activator or inhibitor production correspond to moderate overexpression that was restricted to the forming appendages. (**A**) Modeling of the first inductive wave. The calculated distribution of activator is shown for a 100 × 100 area (arbitrary units). (**B**) Modeling of a subsequent inductive wave. The first wave is shown in blue, the second in red. The calculated distribution of activator is depicted for a 200 × 200 area. The inset reflects the difference in activator distribution between second and first inductive wave for a first wave follicle. An activator and inhibitor insensitivity of first wave follicles might reflect the in vivo situation most closely.

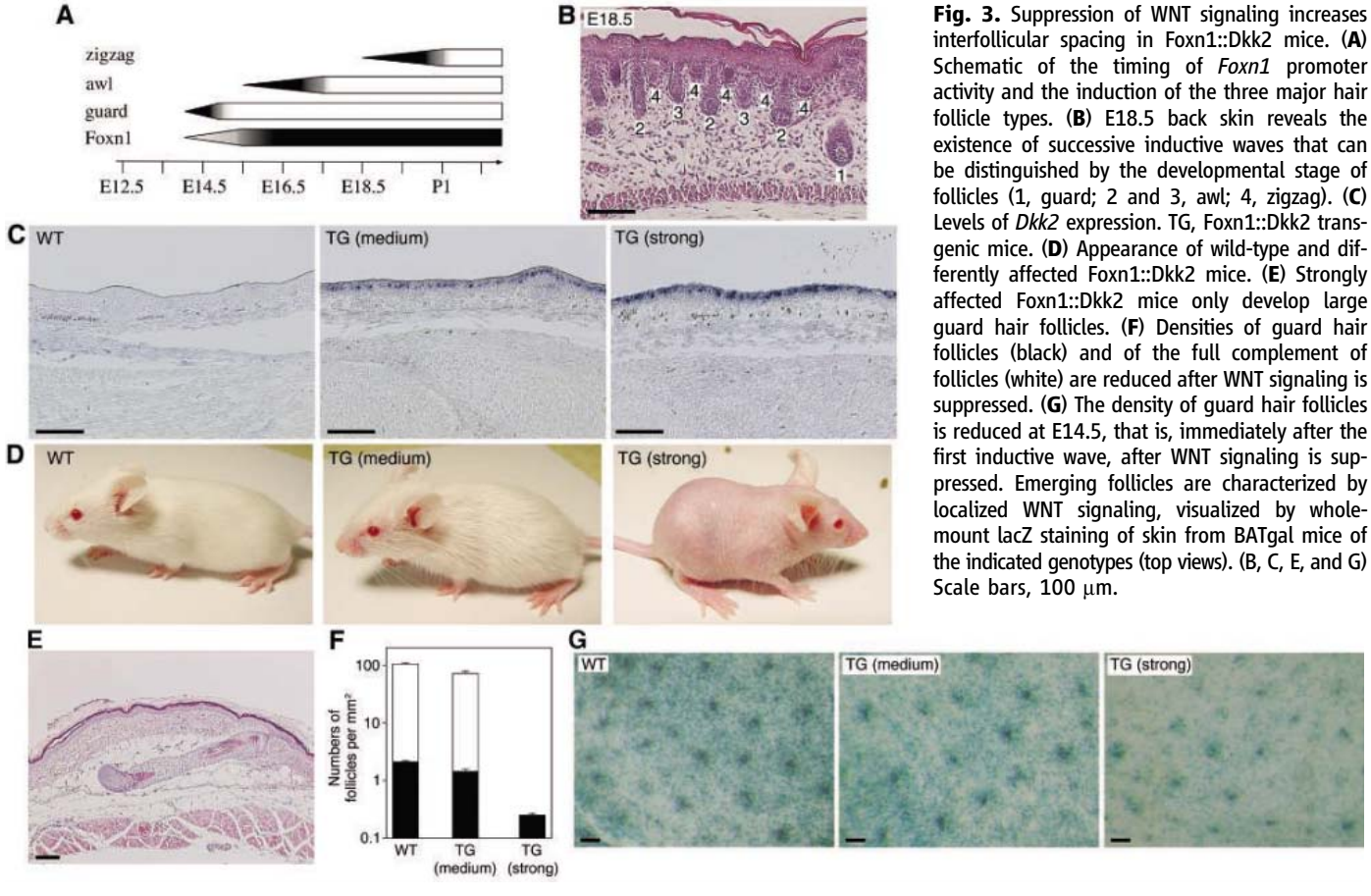

Fig. 3. Suppression of WNT signaling increases interfollicular spacing in Foxn1::Dkk2 mice. (**A**) Schematic of the timing of *Foxn1* promoter activity and the induction of the three major hair follicle types. (**B**) E18.5 back skin reveals the existence of successive inductive waves that can be distinguished by the developmental stage of follicles (1, guard; 2 and 3, awl; 4, zigzag). (**C**) Levels of *Dkk2* expression. TG, Foxn1::Dkk2 transgenic mice. (**D**) Appearance of wild-type and differently affected Foxn1::Dkk2 mice. (**E**) Strongly affected Foxn1::Dkk2 mice only develop large guard hair follicles. (**F**) Densities of guard hair follicles (black) and of the full complement of follicles (white) are reduced after WNT signaling is suppressed. (**G**) The density of guard hair follicles is reduced at E14.5, that is, immediately after the first inductive wave, after WNT signaling is suppressed. Emerging follicles are characterized by localized WNT signaling, visualized by whole-mount lacZ staining of skin from BATgal mice of the indicated genotypes (top views). (B, C, E, and G) Scale bars, 100 μm.

determine where appendages form, this suggests the possibility of follicle cluster formation. The ringlike zones of high activator levels are converted to discrete spots (Fig. 2B) if preexisting follicles become insensitive to activator and inhibitor (SOM text 4). Thus, moderate overexpression of inhibitor by the appendages predicts a quantitative as well as a qualitative read-out: The number of follicles is reduced, and their distribution is changed.

We used transgenic expression of inhibitor during hair follicle formation to experimentally test these theoretical predictions (Fig. 3 and SOM text 5 and fig. S2). In mouse, temporally well defined successive waves of induction during embryogenesis and early postnatal life give rise to three major hair follicle types (designated guard, awl, and zigzag) (*13*) (Fig. 3A). In compliance with the model, new follicles are initiated in between previously induced appendages (Fig. 3B). We analyzed four Foxn1::Dkk2 mouse lines in detail, and their phenotype was correlated to the level of transgene expression (Fig. 3, C and D). At high levels of ectopic *Dkk2* mRNA, mice appeared almost hairless; at lower levels, the hair coat is present but structurally abnormal (Fig. 3D). Suppression of hair follicle formation at high levels of *Dkk2* expression is consistent with previous results for *Dkk1* (*5*) and conforms to the prediction of our computational modeling. However, guard hair follicle induction still took place even in severely affected mice (Fig. 3, D and E) because of the delayed onset of *Foxn1* promoter activation relative to guard hair follicle induction (Fig. 3A and fig. S2).

The number of follicles per square millimeter is reduced by about 30% in adult Foxn1::Dkk2 (medium) mice (Fig. 3F). Regarding the first inductive wave that gives rise to guard hair follicles, a similar reduction is evident (Fig. 3F). In Foxn1::Dkk2 (strong) mice, which only develop guard hair follicles, the density is further reduced (Fig. 3F). The emergence of hair follicle buds is accompanied by localized WNT signaling in mesenchymal cells of the prospective dermal papilla (Fig. 1A). As expected, the density of these cell clusters is reduced in Foxn1::Dkk2 transgenic mice (Fig. 3G). However, we could not detect any difference between mice with high and medium mRNA levels. Thus, the significant decrease of guard hair follicle density in Foxn1::Dkk2 (strong) as compared with Foxn1::Dkk2 (medium) mice suggests the existence of more than one inductive wave for guard hair follicles; apparently, all but the first wave are blocked by strong transgene expression. For the first inductive wave, the results confirm the predictions of our model with respect to the quantitative effects of inhibitor overexpression.

As suggested by our simulations, WNT and DKK proteins may control the natural increase of follicle density during subsequent inductive waves (Fig. 2B and SOM text 6 and figs. S3 and S4). In order to investigate inhibitor effects on these waves, we next examined transgenic mice with an abnormal hair coat in more detail. These mice are characterized by a misdistribution of hair shafts. Whereas emerging hair shafts are almost evenly distributed over the skin surface in wild-type mice, bundles of hair shafts are separated by large areas of interfollicular epidermis in Foxn1::Dkk2 mice (Fig. 4A). Histological sections confirmed that usually more than three follicles are tightly clustered in transgenic mice (Fig. 4B); all follicles within a cluster gave rise to bona fide hair shafts. By contrast, follicles are clearly separated from each other in wild-type skin (Fig. 4B). Strong follicle clustering was also observed in Foxn1::Dkk1 mice (fig. S5), which corroborated its independence of the inhibitor's identity. A ringlike pattern of WNT signal-receiving cells around preexisting follicles confirms the model's prediction for activator distribution and indicates an initiation of cluster formation at about embryonic day 17.5 (E17.5) (Fig. 4C). Unequivocal morphological indications of hair follicle cluster formation were observed at E18.5 and postnatal

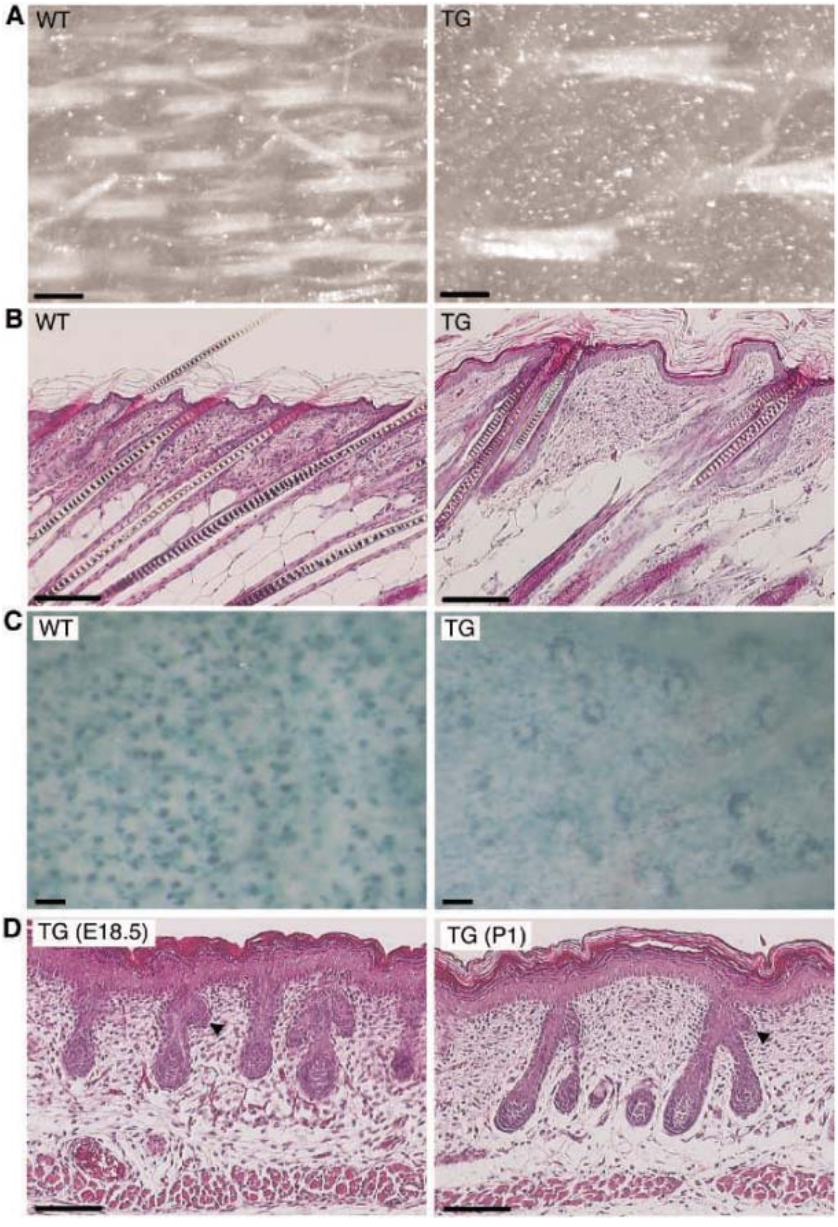

Fig. 4. A normal sequence of inductive waves gives rise to hair follicle clusters after moderate suppression of WNT signaling. (**A**) Hair distribution on the back of wild-type and Foxn1::Dkk2 mice. (**B**) Hair follicle distribution in the back skin of 10-day-old wild-type and Foxn1::Dkk2 animals. (**C**) Aberrant distribution of WNT signal–receiving cells in Foxn1::Dkk2 mice at E17.5. Canonical WNT signaling is visualized by whole-mount lacZ staining of back skin from BATgal mice of the indicated genotypes (top views). (**D**) New follicles (arrowheads) emerge at E18.5 and P1 in Foxn1::Dkk2 mice. All scale bars, 100 μm.

day 1 (P1) (Fig. 4D and fig. S6). Thus, hair follicle clusters in Foxn1::Dkk2 mice form during a normal inductive program by misdistribution of the normal complement of epidermal appendages (Fig. 4D and SOM text 7 and fig. S6).

We note that further signaling pathways are involved in interfollicular patterning. Studies on feather development demonstrated that fibroblast growth factors (FGFs) promote follicle formation, whereas BMP and EGF signaling confers interfollicular fate (*14, 15*). Because these pathways appear to be downstream of WNT signaling and exert feedback control (*5, 14, 16–19*), we propose that they mainly mediate and modulate WNT signals, thereby contributing to the stabilization and refinement of the patterning process. Indeed, ablation of the BMP receptor IA appears to have no major impact on hair follicle induction and distribution (*20*). However, suppression of BMP signaling that may reduce *Dkk1* expression (*19*) causes an increase in hair follicle density (*21*), consistent with our simulations (fig. S3C). Given that LEF1 plays an important role in WNT signaling, which controls ectodysplasin signals (*5, 22*), our results may also explain the misdistribution of follicles in *EdaA1* and *Lef1* transgenic mice (*23, 24*). However, a more sophisticated systems biology approach will be needed in the future to include the full complexity and dynamics of the WNT signaling pathway (*25*) in a model of interfollicular patterning. In conclusion, our combined experimental and computer modeling approach presents compelling evidence for WNT signaling and a reaction-diffusion mechanism as key determinants of hair follicle spacing patterns.

References and Notes

1. K. Amonlirdviman *et al.*, *Science* **307**, 423 (2005).
2. A. Turing, *Philos. Trans. R. Soc. London B Biol. Sci.* **237**, 37 (1952).
3. S. Kondo, R. Asai, *Nature* **376**, 765 (1995).
4. C. H. Chang *et al.*, *Mech. Dev.* **121**, 157 (2004).
5. T. Andl, S. T. Reddy, T. Gaddapara, S. E. Millar, *Dev. Cell* **2**, 643 (2002).
6. S. Nonchev *et al.*, *Development* **122**, 543 (1996).
7. U. Gat, R. DasGupta, L. Degenstein, E. Fuchs, *Cell* **95**, 605 (1998).
8. S. Reddy *et al.*, *Mech. Dev.* **107**, 69 (2001).
9. A. Niida *et al.*, *Oncogene* **23**, 8520 (2004).
10. M. N. Chamorro *et al.*, *EMBO J.* **24**, 73 (2005).
11. V. E. Krupnik *et al.*, *Gene* **238**, 301 (1999).
12. B. Mao, C. Niehrs, *Gene* **302**, 179 (2003).
13. F. W. Dry, *J. Genet.* **16**, 287 (1926).
14. H. S. Jung *et al.*, *Dev. Biol.* **196**, 11 (1998).
15. R. Atit, R. A. Conlon, L. Niswander, *Dev. Cell* **4**, 231 (2003).
16. K. Kratochwil, J. Galceran, S. Tontsch, W. Roth, R. Grosschedl, *Genes Dev.* **16**, 3173 (2002).
17. K. Kratochwil, M. Dull, I. Farinas, J. Galceran, R. Grosschedl, *Genes Dev.* **10**, 1382 (1996).
18. C. Jamora, R. DasGupta, P. Kocieniewski, E. Fuchs, *Nature* **422**, 317 (2003).
19. L. Grotewold, U. Ruther, *EMBO J.* **21**, 966 (2002).
20. K. Kobielak, H. A. Pasolli, L. Alonso, L. Polak, E. Fuchs, *J. Cell Biol.* **163**, 609 (2003).
21. M. Plikus *et al.*, *Am. J. Pathol.* **164**, 1099 (2004).
22. J. Behrens *et al.*, *Nature* **382**, 638 (1996).
23. T. Mustonen *et al.*, *Dev. Biol.* **259**, 123 (2003).
24. P. Zhou, C. Byrne, J. Jacobs, E. Fuchs, *Genes Dev.* **9**, 700 (1995).
25. R. DasGupta, A. Kaykas, R. T. Moon, N. Perrimon, *Science* **308**, 826 (2005).

56. We thank B. Hammerschmidt for her excellent technical help; B. Kanzler, E. Huber, and J. Wersing for producing transgenic mice; C. Bleul and T. Boehm for the *Foxn1* promoter construct; C. Niehrs for murine *Dkk1* cDNA; R. Kemler for *Lef1* and β-catenin expression plasmids; and T. Boehm for helpful discussions and comments on the manuscript.

Supporting Online Material

www.sciencemag.org/cgi/content/full/1130088/DC1
Materials and Methods
SOM Text
Figs. S1 to S6
References

5 May 2006; accepted 18 October 2006
Published online 2 November 2006;
10.1126/science.1130088
Include this information when citing this paper.

Structural Basis for Ribosome Recruitment and Manipulation by a Viral IRES RNA

Jennifer S. Pfingsten, David A. Costantino, Jeffrey S. Kieft*

Canonical cap-dependent translation initiation requires a large number of protein factors that act in a stepwise assembly process. In contrast, internal ribosomal entry sites (IRESs) are *cis*-acting RNAs that in some cases completely supplant these factors by recruiting and activating the ribosome using a single structured RNA. Here we present the crystal structures of the ribosome-binding domain from a Dicistroviridae intergenic region IRES at 3.1 angstrom resolution, providing a view of the prefolded architecture of an all-RNA translation initiation apparatus. Docking of the structure into cryo–electron microscopy reconstructions of an IRES-ribosome complex suggests a model for ribosome manipulation by a dynamic IRES RNA.

In eukaryotes, there are two known mechanisms for the initiation of protein synthesis (Fig. 1A). The canonical mechanism requires a modified nucleotide cap on the 5′ end of the mRNA, which is recognized by an initiation factor protein (eIF4E). This protein recruits other factors that assemble the ribosome on the mRNA in a stepwise process (*1*). In contrast, internal initiation of translation does not require a cap or recognition of the mRNA 5′ end. Rather, structured RNA sequences called internal ribosomal entry sites (IRESs) recruit and activate the translation machinery, functionally replacing many protein factors (*2*). IRESs are essential for infection by many medically and economically important viruses such as hepatitis C (HCV), hepatitis A, polio, foot-and-mouth disease, rhinovirus, coxsackievirus-B3, and HIV-1 (*3*). IRESs also drive the translation of eukaryotic mRNAs, encoding factors involved in development, growth regulation, apoptosis, transcription, translation, and other important cellular processes (*3*). The molecular rules underlying this RNA structure–driven mechanism remain elusive.

Department of Biochemistry and Molecular Genetics, University of Colorado at Denver and Health Sciences Center, Mail Stop 8101, Post Office Box 6511, Aurora, CO 80045, USA.

*To whom correspondence should be addressed. E-mail: Jeffrey.Kieft@uchsc.edu

Ideal model systems for understanding IRES RNA-driven translation are the mechanistically streamlined intergenic region (IGR) IRESs of the virus family Dicistroviridae (*4*). The IGR IRESs drive the association of the ribosomal subunits without any of the protein factors that comprise the canonical translation initiation apparatus (Fig. 1A) (*5*). Hence, this one structured RNA (molecular size ~66 kD) supplants over 1000 kD of structured initiation factor proteins, operating as an all-RNA translation initiation apparatus (*6–9*). The full-length IGR IRES folds in solution into two structurally independent domains (*10–13*). The larger domain (regions 1 and 2, Fig. 1A and fig. S1) is the ribosome-binding domain. It folds into a compact structure (*10*) that binds directly to the 40*S* subunit (*10*, *12*, *13*). Cryo–electron microscopy (cryo-EM) reconstructions of an IGR IRES bound to the ribosome reveal that the IGR IRES binds over the mRNA-binding groove, making contact to and changing the structure of both ribosomal subunits (40*S* and 60*S*) (*14*). However, these cryo-EM structures do not reveal the structure of the IRES, how the IRES structure creates a ribosome-binding site, or which IRES structural features specifically contact and manipulate the ribosome.

To address these questions and develop a model for the structural basis of IGR IRES-driven translation, we have solved the structure of the ribosome-binding domain of the *Plautia stali* intestine virus (PSIV) IGR IRES

RNA using x-ray crystallography to a resolution of 3.1 Å with R_{work} = 25.3% and R_{free} = 29.4% (Fig. 1B). In the structure, regions 1 and 2 pack side-by-side with stem-loop IV (SL IV) and SL V emerging from the same side of the structure (Fig. 1B). Both stem-loops have been shown through mutagenesis and footprinting experiments to make functionally critical direct contact to the 40*S* subunit (*10*, *12*, *13*), and isolated region 2 has been shown to bind to the 40*S* subunit (*12*). Thus, the position of SL IV and SL V identifies the side of the structure that is the 40*S* subunit–binding interface ("top" of the structure in Fig. 1B) and indicates that the 40*S* subunit recognition surface prefolds before subunit binding. The foundation of this prefolded IRES architecture is helix P2.2 (red, Fig. 1B), which is contacted by bases from multiple IRES elements (J2.3, J2.2, L1.2A, and L1.2B, cyan and green, Fig. 1B). This folded core corresponds to areas of strong protection in hydroxyl-radical probing experiments (fig. S2), providing additional evidence that we have captured the authentic prefolded, unbound form of the IRES RNA (*10*). Many of the most-conserved bases in the IGR IRESs cluster in this highly structured core region. Our structure suggests that these bases are kept invariant to maintain the specific intramolecular contacts that knit the structure together.

The two stem-loops are positioned together to contact a relatively small area on the ribosome by a set of specific intramolecular contacts involving pseudoknot III (PK III) and helix P2.2, which form a continuous helical stack that extends into PK II (Fig. 1B). The placement of SL IV is facilitated by underwinding of helix P2.2, which opens the normally deep and narrow major groove (Fig. 2A). The degree of underwinding is such that a single turn of helix covers a total rise of ~42 Å, as compared to ~34 Å for canonical A-form RNA. This feature is induced by four key bases that stack into the helix, forming two noncanonical base pairs and anchoring the 3′ end of SL IV (J2.3, Fig. 2A). The 5′ end of SL IV is anchored by a G-U wobble pair (G6110-U6082, Fig. 2B) (*12*). From these anchors in the P2.2 major groove, the stem of SL IV is closed with a U•U pair, the bases of which are flipped out from the P2.2 major groove (U6083-U6096, Fig. 2B). Whereas SL IV nestles in the major groove, SL V is positioned by several conserved bases that force the stem of SL V to emerge from the minor groove, placing it at nearly a right angle to P2.2 and adjacent to SL IV (Fig. 2C). Classic pseudoknot folding is characterized by two stacked helices and two single-stranded loops; the 5′-most loop crosses the major groove, whereas the other crosses the minor groove (*15*). Hence, in the IGR IRES, this classic pseudoknot architecture is maintained, despite the fact that both loops contain a large amount of embedded structured RNA (fig. S3).

Region 1 does not participate directly in the interactions that create the 40*S* subunit–binding site; rather, it packs against region 2 in position to contact the 60*S* subunit (vide infra). Regions 1 and 2 pack in an interaction in which the large L1.2 loop (green, Fig. 2D) cradles one strand of helix P2.2 (red, Fig. 2D). One strand of this loop (L1.2A) lies along the minor groove of P2.2, forming stabilizing A-minor interactions [for discussions of A-minor interactions, see (*16*)]. The other strand of the loop (L1.2B) forms the other half of the cradle; apparently poised to enter the major groove, it loops back to the minor groove to form more stabilizing A-minor interactions. The tight, complex packing of RNA that is essential for function is especially evident in this region, where five strands of RNA trace in close proximity. The

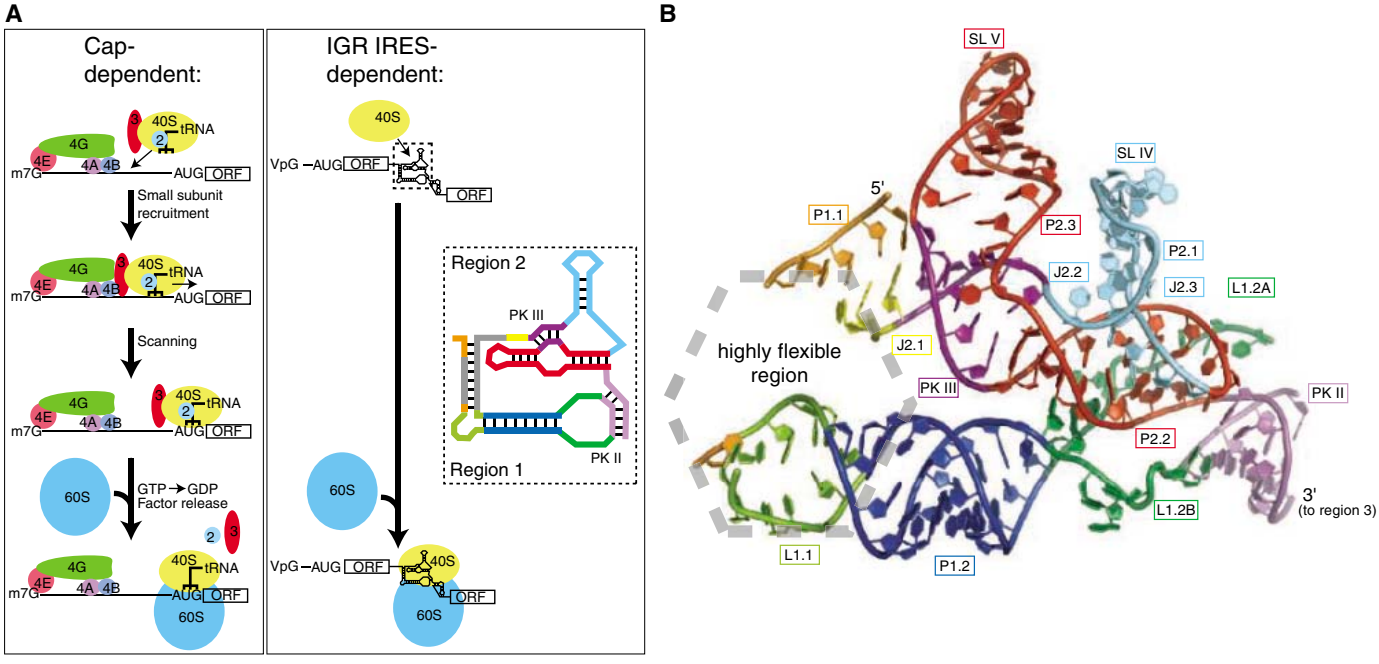

Fig. 1. IRES-driven initiation and the structure of the PSIV IGR IRES. (**A**) Ribosome recruitment strategies used in cap-dependent and IGR-IRES–dependent translation initiation. ORF, open reading frame; GTP, guanosine triphosphate; GDP, guanosine diphosphate. At right is the protein-independent pathway used by this IRES RNA. The inset is a cartoon of the secondary structure of the ribosome-binding domain, colored to match the structure of (B). Parts colored gray did not appear in the crystal structure and were not built into the final model. The secondary structure consists of two regions (regions 1 and 2), which contain two functionally critical pseudoknots (*10*, *12*, *13*). Because PK III is nested inside PK II, this forms an RNA tertiary structure called a double-nested pseudoknot (*15*). Figure S1 contains a detailed secondary structure with sequence information. (**B**) Structure of the ribosome-binding domain, colored to match the inset in (A). J, junction; P, paired/helix; L, loop. The gray hexagon shows structure that was weakly visible and hence conformationally flexible. The RNA crystallized in a domain-swapped dimer (fig. S4) in which the functionally essential structural features are preserved.

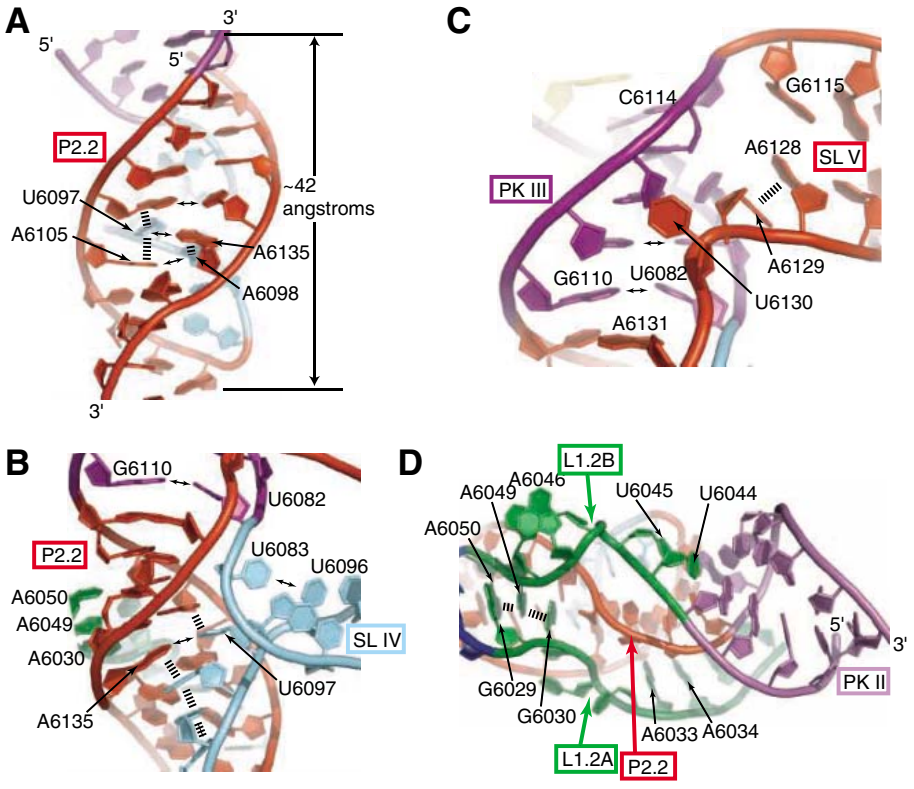

Fig. 2. Structural details of the IRES. (**A**) Underwound helix P2.2 (red) is shown from the minor groove side. A6105 (red) stacks into the helix, forming a noncanonical A•A N7-amino base pair with A6098 of J2.3 (cyan). A6135 (red) stacks on A6098 and forms a reverse (parallel) Watson-Crick A-U pair with conserved base U6097 of J2.3 (cyan). In this and subsequent panels, base pairing is indicated with double-ended arrows and stacking with a thick dashed line. (**B**) Within the P2.2 major groove, both U6097 (cyan) and U6082 (purple) pair with bases in P2.2 (red), whereas U6083 and U6096 pair with each other at the end of SL IV (cyan). Region 1 bases (green) buttress this structure through A-minor interactions. (**C**) The U6082-G6110 pairing extrudes U6130 from the helix and induces a sharp turn in the backbone. Bases A6129 and A6128 stack on the minor groove of the PK III helix, starting the base stacking that extends into SL V. (**D**) The two strands of L1.2 splay apart, with L1.2A lying in the minor groove of P2.2, stabilizing the inter-region packing through A-minor interactions (e.g., A6033 and A6034). Bases U6044 and U6045 of L1.2B continue to stack on the PK II stack, whereas A6046-A6048 form a u-turn–like structure (*27*), allowing A6049 and A6050 to reach the minor groove of P2.2.

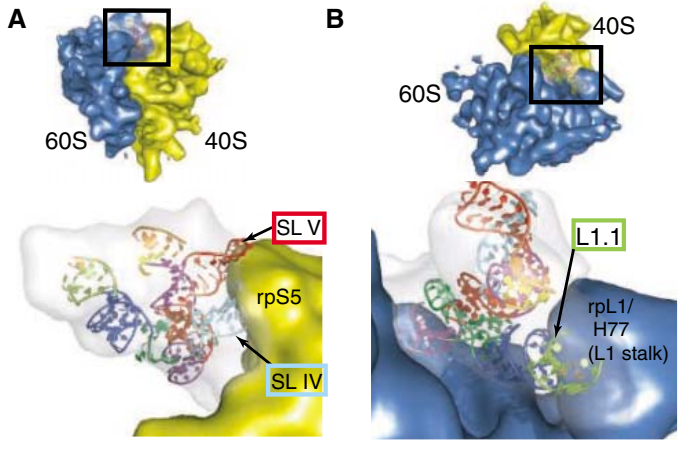

Fig. 3. Interaction of the IGR IRES RNA with the ribosome. (**A**) The PSIV IGR IRES ribosome affinity domain structure docked into the cryo-EM representation of the IRES bound to the 80*S* ribosome, with the 60*S* ribosome density computationally removed. The 40*S* subunit is in yellow, the cryo-EM density of the IRES is in gray, and the IRES crystal structure is colored as in Fig. 1. The positions of rpS5 (40*S* subunit) and SL IV and SL V (IGR IRES) are shown. (**B**) Detailed view of the interaction of the IGR IRES to the 60*S* subunit within the 80*S* ribosome–IRES complex, with the 40*S* subunit density computationally removed. The L1 stalk of the 60*S* subunit contacts IRES loop L1.1 and perhaps P1.1. For both (A) and (B), the orientation is indicated in the insets.

other parts of regions 1 and 2 (helix P1.1 and loop L1.1) are only weakly visible in the electron density. We built RNA structure into this weak density, but the structure is poorly defined in these regions, indicating conformational flexibility. Hence, although we can clearly see where L1.1 lies in relation to the rest of the structure, we cannot report its high-resolution structure. This flexibility corresponds to the fact that the RNA crystallized as a domain-swapped dimer in which the native interactions between regions 1 and 2 are preserved (for a detailed discussion, see fig. S4). Hence, the IRES contains regions of stable, highly structured RNA and other regions of flexible, less stable structure. We examined the functional significance of this observation by combining our structure with existing cryo-EM reconstruction data (*14*).

To identify the specific IGR IRES RNA structures that contact the ribosome, we docked the crystal structure into published cryo-EM reconstructions (Fig. 3). To generate a model for docking, we returned the SL IV and SL V stems to their wild-type lengths [these were changed to induce crystallization (*17*)]. With the use of the location of the 3′ end of the IRES RNA, assignments of region 3 and regions 1 and 2 into the cryo-EM maps (*14*), footprinting and directed hydroxyl-radical probing data (*12*, *18*), and the overall agreement of the crystal structure with the shape of the cryo-EM density, the docking orientation was unambiguous (fig. S5) (*12*, *14*, *18*). Based on the good, but not perfect, match of the structure to the cryo-EM density, we conclude that the IRES does not need to undergo a global structural rearrangement to match our structure. Rather, local structural shifts (such as a change in the relative angle of helices or a shift of region 1 relative to region 2) occur upon binding. The docking and fit are robust enough to identify the IRES RNA structural domains that contact the 40*S* and 60*S* subunits and to suggest a dynamic mechanism of IRES action.

Cryo-EM showed that small ribosomal protein S5 (rpS5) makes contact with the IGR IRES (*14*), and our docked structure reveals that SL IV and SL V are the features that interact with rpS5 (Fig. 3A). These are the only IRES contacts to rpS5, indicating that this is the keystone interaction that drives 40*S* subunit binding, induces conformational change, and begins the translation initiation process. This observation is supported by data showing that mutation of these loops abrogates 40*S* subunit binding and translation initiation activity (*10*, *12*, *13*). The apical loop sequences of SL IV and SL V are conserved almost universally among the IGR IRESs, underscoring that their specific interaction with rpS5 is critical for function (fig. S6). The HCV IRES also contacts rpS5, and the HCV IRES domain that contacts rpS5 also

changes the conformation of the 40*S* subunit (*19*–*21*), suggesting that this interaction is central to this mode of IRES RNA-driven translation.

In the docked structure, IRES loop L1.1 (and perhaps adjacent helices) is positioned to make direct contact with the large subunit's L1 stalk, which contains rpL1 and ribosomal RNA helix H77 (Fig. 3B) (*14*). That L1.1 and the adjacent P1.1 helix are poorly ordered suggests this part of the IRES is not stably folded until it interacts with the 60*S* subunit. During translation, the L1 stalk interacts with the T loop of E site–bound tRNA (*22*, *23*), which suggests that IGR IRES loop L1.1, when bound in the 80*S* ribosome, adopts a structure that mimics this portion of tRNA structure. Like the 40*S* subunit–binding stem-loops, IRES loop L1.1 is highly conserved, demonstrating the importance and specificity of its interactions with the L1 stalk (fig. S6) (*4*, *11*). Our observation that L1.1 makes an important contact to the 60*S* subunit predicts that mutating L1.1 will block translation initiation after 40*S* subunit binding. To test this prediction, we constructed two mutants and used them in preinitiation complex assays analyzed on sucrose gradients (Fig. 4, A to C). Both mutants produce IRES–40*S* subunit complexes but fail to progress to 80*S* ribosomes, demonstrating that L1.1 is critical for recruitment of the 60*S* subunit. Neither of these mutations globally misfold the RNA (Fig. 4B), which suggests that the effect is due to the loss of the direct L1.1 interaction with the 60*S* subunit.

The IRES interactions with rpS5 and the L1 stalk are the only intimate contacts to regions 1 and 2 in our docked structure. This does not preclude that other interactions may occur, especially upon proposed subtle conformational changes to the IRES. However, the fact that the conservation of nucleotides in regions 1 and 2 of the IRES is fully accounted for by the folded core and contacts with rpS5 and the L1 stalk suggests that other contacts may be nonspecific in nature (fig. S6).

Our structure of the PSIV IGR IRES ribosome-binding domain, combined with a wealth of published biochemical, functional, and low-resolution structural data, suggests a mechanistic model for the structural basis of IGR IRES-driven initiation that involves programmed regions of stable and flexible structure (Fig. 4D). We propose that P1.1 and L1.1 remain flexible when the IRES binds to the 40*S* subunit through structured SL IV and SL V (Fig. 4D, step 1). Support for this idea comes from a close examination of the IRES structure docked into the cryo-EM density of the 40*S* subunit–bound IRES. The part of the density that corresponds to L1.1 and P1.1 is weak or missing (*14*) (red oval, Fig. 4D). In the 40*S*-bound form, IRES region 3 overlaps with the P and A sites (*14*). 60*S* subunit binding (Fig. 4D, step 2) results in structural changes in the IRES and a shift that withdraws region 3 from the A and P sites, as well as a change in the structure of the ribosome's L1 stalk that is similar to changes associated with elongation factor binding (*14*, *24*, *25*). These IRES structural changes are explained by a 60*S* subunit binding–induced organization of L1.1 and perhaps P1.1, evident in the appearance of additional cryo-EM density around L1.1 and P1.1 upon 60*S* subunit binding (Fig. 4D) (*14*). Furthermore, the fact that regions 1 and 2 of the IRES make relatively few inter-region contacts suggests that the two regions can shift relative to one another. Change in the L1.1 and P1.1 structure thus could be linked to PK II and domain 3 through the P2.1 helix. Other ribosome features positioned near the IRES may also be part of this overall mechanism (*14*). Pestova *et al*. have reported that the IGR IRES RNAs also can recruit 80*S* ribosomes directly (*18*) in what must be a coupled series of events within the context of the assembled 80*S* ribosome.

Although there is great diversity in IRES structure, combining stable and flexible regions may be a strategy used by other IRESs. This structural characteristic is observed in the HCV IRES despite a very different overall RNA architecture (*26*). Thus, the structure presented here provides the basis for experiments aimed at understanding the basic tenets of RNA-based translation initiation.

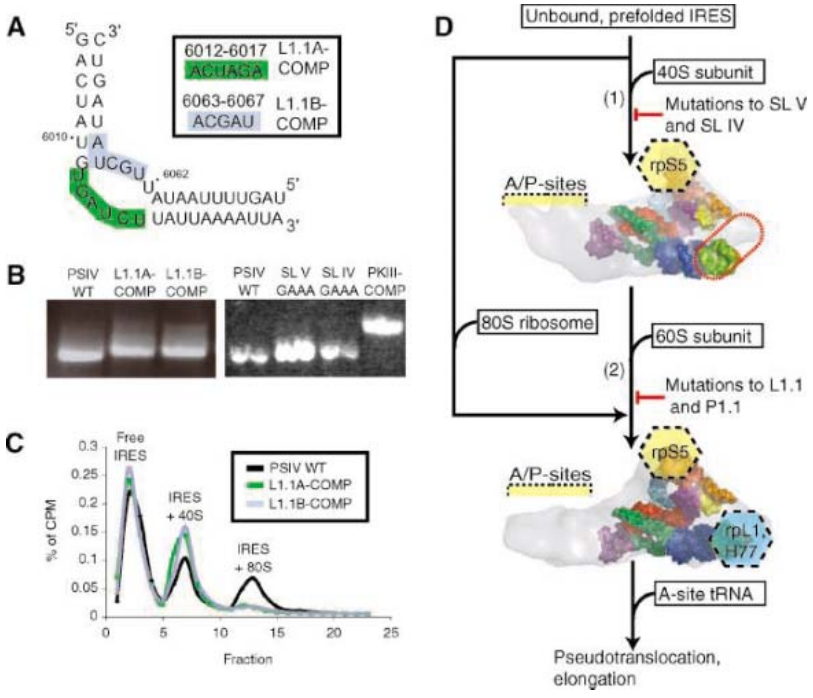

Fig. 4. IRES structural changes and a proposed mechanism of ribosome recruitment. (**A**) Sequences of two L1.1/P1.1 mutants. COMP, Watson-Crick complement. (**B**) Native gel analysis of these mutants shows that they do not globally misfold, because they run very close to wild-type (WT) RNA. Previously published (*10*) native gel analysis of mutants, in which SL IV and V were changed to GAAA tetraloops (which does not change the fold) and in which PK II was altered (which causes global misfolding), is shown for comparison at right. (**C**) Assembly assays of L1.1/P1.1 mutants analyzed on a sucrose gradient. The locations of 40*S*- and 80*S*-bound IRESs are indicated. CPM, counts per minute. (**D**) Interactions with the 40*S* subunit are shown in yellow, and those with the 60*S* subunit are shown in blue. The IRES is shown as a space-filling representation inside the corresponding gray cryo-EM density, colored as in previous figures. The folded, unbound IRES binds to the 40*S* subunit through SL IV and SL V interacting with rpS5, inducing a conformational change in the subunit and docking region 3 into the P site (step 1). Subsequent 60*S* subunit binding induces a series of conformational changes in both the IRES and the ribosome, including a putative organization of IRES structures L1.1 and P1.1 (step 2). The appearance of additional IRES density in the cryo-EM map of the 80*S* ribosome–bound IRES (indicated with the red oval) supports the existence of this structural switch.

References and Notes

1. J. W. B. Hershey, W. C. Merrick, in *Translational Control of Gene Expression*, N. Sonenberg, J. W. B. Hershey, M. B. Mathews, Eds. (Cold Spring Harbor Laboratory Press, Cold Spring Harbor, NY, 2000), pp. 33–88.
2. C. U. Hellen, P. Sarnow, *Genes Dev.* **15**, 1593 (2001).
3. S. Bonnal, C. Boutonnet, L. Prado-Lourenco, S. Vagner, *Nucleic Acids Res.* **31**, 427 (2003).

4. E. Jan, *Virus Res.* **119**, 16 (2005).
5. T. V. Pestova, C. U. Hellen, *Genes Dev.* **17**, 181 (2003).
6. J. Sasaki, N. Nakashima, *J. Virol.* **73**, 1219 (1999).
7. J. Sasaki, N. Nakashima, *Proc. Natl. Acad. Sci. U.S.A.* **97**, 1512 (2000).
8. E. Jan *et al.*, *Cold Spring Harbor Symp. Quant. Biol.* **66**, 285 (2001).
9. J. E. Wilson, T. V. Pestova, C. U. Hellen, P. Sarnow, *Cell* **102**, 511 (2000).
10. D. Costantino, J. S. Kieft, *RNA* **11**, 332 (2005).
11. Y. Kanamori, N. Nakashima, *RNA* **7**, 266 (2001).
12. T. Nishiyama *et al.*, *Nucleic Acids Res.* **31**, 2434 (2003).
13. E. Jan, P. Sarnow, *J. Mol. Biol.* **324**, 889 (2002).
14. C. M. Spahn *et al.*, *Cell* **118**, 465 (2004).
15. C. W. Hilbers, P. J. Michiels, H. A. Heus, *Biopolymers* **48**, 137 (1998).
16. P. Nissen, J. A. Ippolito, N. Ban, P. B. Moore, T. A. Steitz, *Proc. Natl. Acad. Sci. U.S.A.* **98**, 4899 (2001).
17. Materials and methods are available as supporting material on *Science* Online.
18. T. V. Pestova, I. B. Lomakin, C. U. Hellen, *EMBO Rep.* **5**, 906 (2004).
19. S. Fukushi *et al.*, *J. Biol. Chem.* **276**, 20824 (2001).
20. C. M. Spahn *et al.*, *Science* **291**, 1959 (2001).
21. J. S. Kieft, K. Zhou, R. Jubin, J. A. Doudna, *RNA* **7**, 194 (2001).
22. R. K. Agrawal *et al.*, *J. Cell Biol.* **150**, 447 (2000).
23. M. M. Yusupov *et al.*, *Science* **292**, 883 (2001).
24. M. G. Gomez-Lorenzo *et al.*, *EMBO J.* **19**, 2710 (2000).
25. R. K. Agrawal, A. B. Heagle, P. Penczek, R. A. Grassucci, J. Frank, *Nat. Struct. Biol.* **6**, 643 (1999).
26. J. S. Kieft *et al.*, *J. Mol. Biol.* **292**, 513 (1999).
27. F. M. Jucker, A. Pardi, *RNA* **1**, 219 (1995).
28. We acknowledge the staff at beamline ALS 8.2.1 for assistance, R. Zhao for managing the University of Colorado (UC) at Denver and Health Sciences Center x-ray facility, D. Farrell for computer administration, and M. Churchill, R. Bately, and A. Ferré-D'Amaré for useful discussions and advice. We especially thank C. Spahn for supplying various cryo-EM density files and R. Batey for the iridium (III) hexammine. R. Batey, M. Churchill, D. Bentley, L. Krushel, and R. Zhao provided a critical reading of this manuscript. This work was supported by a grant from NIH and funding from the UC Cancer Center in support of the x-ray facility. Structure factors and coordinates have been deposited in the Protein Data Bank under accession code 2IL9.

Supporting Online Material

www.sciencemag.org/cgi/content/full/1133281/DC1
Materials and Methods
Figs. S1 to S7
Table S1
References

1 August 2006; accepted 30 October 2006
Published online 23 November 2006;
10.1126/science.1133281
Include this information when citing this paper.

Rapid Chemically Induced Changes of PtdIns(4,5)P_2 Gate KCNQ Ion Channels

Byung-Chang Suh,[1]* Takanari Inoue,[2]* Tobias Meyer,[2] Bertil Hille[1]†

To resolve the controversy about messengers regulating KCNQ ion channels during phospholipase C–mediated suppression of current, we designed translocatable enzymes that quickly alter the phosphoinositide composition of the plasma membrane after application of a chemical cue. The KCNQ current falls rapidly to zero when phosphatidylinositol 4,5-bisphosphate [PtdIns(4,5)P_2 or PI(4,5)P_2] is depleted without changing Ca^{2+}, diacylglycerol, or inositol 1,4,5-trisphosphate. Current rises by 30% when PI(4,5)P_2 is overproduced and does not change when phosphatidylinositol 3,4,5-trisphosphate is raised. Hence, the depletion of PI(4,5)P_2 suffices to suppress current fully, and other second messengers are not needed. Our approach is ideally suited to study biological signaling networks involving membrane phosphoinositides.

Phosphoinositide phospholipids are major signaling molecules of cell membranes. Many cellular proteins are inhibited when phosphatidylinositol 4,5-bisphosphate [PI(4,5)P_2] is hydrolyzed by phospholipase C (PLC) and reactivated when phosphatidylinositol 4-phosphate [PI(4)P] 5-kinase restores PI(4,5)P_2 (*1*, *2*). For example, KCNQ K^+ channels are closed by muscarinic-receptor–triggered PLC activation (*3*, *4*). Closure of KCNQ2/KCNQ3 channels increases the excitability of central and peripheral neurons, and hypomorphic mutations in KCNQ subunits underlie familial epilepsies, deafness, and arrhythmias (*5*). Whether the depletion of PI(4,5)P_2 suffices to close KCNQ channels upon receptor activation remains controversial because much of the supporting experimental evidence is indirect. Can we rule out that increases of the many signaling molecules downstream of PLC or other changes in phosphoinositides are essential for closing channels instead of or together with the loss of PI(4,5)P_2? We used a new method to deplete plasma membrane–associated PI(4,5)P_2 in living cells within seconds without activating PLC. Upon addition of a dimerizing drug, PI(4,5)P_2 was selectively depleted in living cells without the production of diacylglycerol (DAG), inositol 1,4,5-trisphosphate (IP_3), or calcium signals.

The chemical dimerizer strategy uses heterodimerization of protein domains from FK506 binding protein (FKBP) and from mTOR (FRB) by the immunosuppressant rapamycin (*6*) or an analog called iRap (*7*). This approach has previously permitted us to develop a high-speed membrane translocation of Rho guanosine triphosphatases (GTPases) (*7*). Now we depleted PI(4,5)P_2 by inducible membrane translocation of Inp54p, a yeast inositol polyphosphate 5-phosphatase that specifically cleaves the phosphate at the 5 position of PI(4,5)P_2 (*8*) (Fig. 1A). Constitutively membrane-targeted Inp54p has been used to assess the roles of PI(4,5)P_2 in cytoskeleton–plasma membrane adhesion (*8*). We fused a truncated Inp54p to FKBP already tagged with cyan fluorescent protein (CFP)–FKBP (CF) (*9*, *10*). The CFP label of the resulting fusion protein CF-Inp54p (CF-Inp) exhibited good cytosolic localization in NIH3T3 cells. CF-Inp was then cotransfected along with Lyn_{11}-FRB (LDR), a membrane-anchored FRB (*7*), and YFP-PH(PLC-δ), a yellow fluorescent protein (YFP)–tagged pleckstrin homology (PH) domain from phospholipase C–δ1 (PLC-δ1) serving as a PI(4,5)P_2/IP_3 biosensor (*11*, *12*). The addition of iRap led to the translocation of the fluorescent CF-Inp from the cytosol to the plasma membrane and a reciprocal translocation of YFP-PH(PLC-δ) from the plasma membrane to the cytosol (Fig. 1, B and H), demonstrating inducible accumulation of the Inp54p enzyme at the plasma membrane and in situ PI(4,5)P_2 depletion. To analyze the kinetics, we measured the fluorescence intensities of CF-Inp and YFP-PH(PLC-δ) in a cytosolic region (Fig. 1C), which revealed quick translocation of both probes [half-time ($t_{1/2}$) = 12.3 ± 1.2 s and 14.7 ± 2.5 s; n = 12 cells from four experiments]. Control experiments with either a phosphatase-dead mutant of Inp54p [CF-Inp Asp^{281}→Ala^{281} (D281A)] (*13*) or a fusion protein lacking the phosphatase (CF) showed no translocation of YFP-PH(PLC-δ), although iRap did induce translocation of the two CFP constructs to the plasma membrane (Fig. 1, D to H).

We then studied whether PI(4,5)P_2 depletion suppresses currents in KCNQ K^+ channels in human embryonic kidney tsA-201 (tsA) cells. As controls, iRap alone had only minor, reversible effects on current amplitude and no effect on the voltage dependence of activation of KCNQ current (iRap, –24.2 ± 1.2 mV; controls, –23.9 ± 0.7 mV; n = 6 cells). Furthermore, in cells expressing the full Inp54p translocation system together with the M_1

[1]Department of Physiology and Biophysics, University of Washington School of Medicine, Seattle, WA 98195, USA. [2]Department of Molecular Pharmacology, Stanford University, Clark Center, 318 Campus Drive, Stanford, CA 94305, USA.

*These authors contributed equally to this work.
†To whom correspondence should be addressed. E-mail: hille@u.washington.edu

subtype of muscarinic receptors (M_1R) and the red fluorescent protein (RFP)–PH(PLC-δ) probe, only iRap and not the muscarinic agonist oxotremorine-M (Oxo-M) translocated the CF-Inp enzyme to the plasma membrane (Fig. 2A). The fast, irreversible translocation of CF-Inp reached half-maximal rate at 1.2 ± 0.1 μM iRap (n = 5 to 7 cells) (fig. S1). Both Oxo-M and iRap caused translocation of RFP-PH(PLC-δ), reflecting rapid depletion of $PI(4,5)P_2$, by PLC in one case and by the phosphatase in the other (Fig. 2A). Only the effect of Oxo-M was reversible. We were now ready to test our hypothesis. The application of iRap to cells expressing channels and the full Inp54p translocation system suppressed KCNQ current rapidly, fully, and irreversibly (Fig. 2, B and C). Suppression was not seen when the Inp54p enzyme or the membrane anchor was omitted, although Oxo-M acting via transfected M_1Rs was still effective at suppressing current reversibly. The saturated rate constant for suppression of KCNQ current by iRap was the same as for Oxo-M, equivalent to a 5-s $t_{1/2}$, and reached half-maximal at 0.6 ± 0.1 μM iRap (n = 5 to 9 cells) (Fig. 2D).

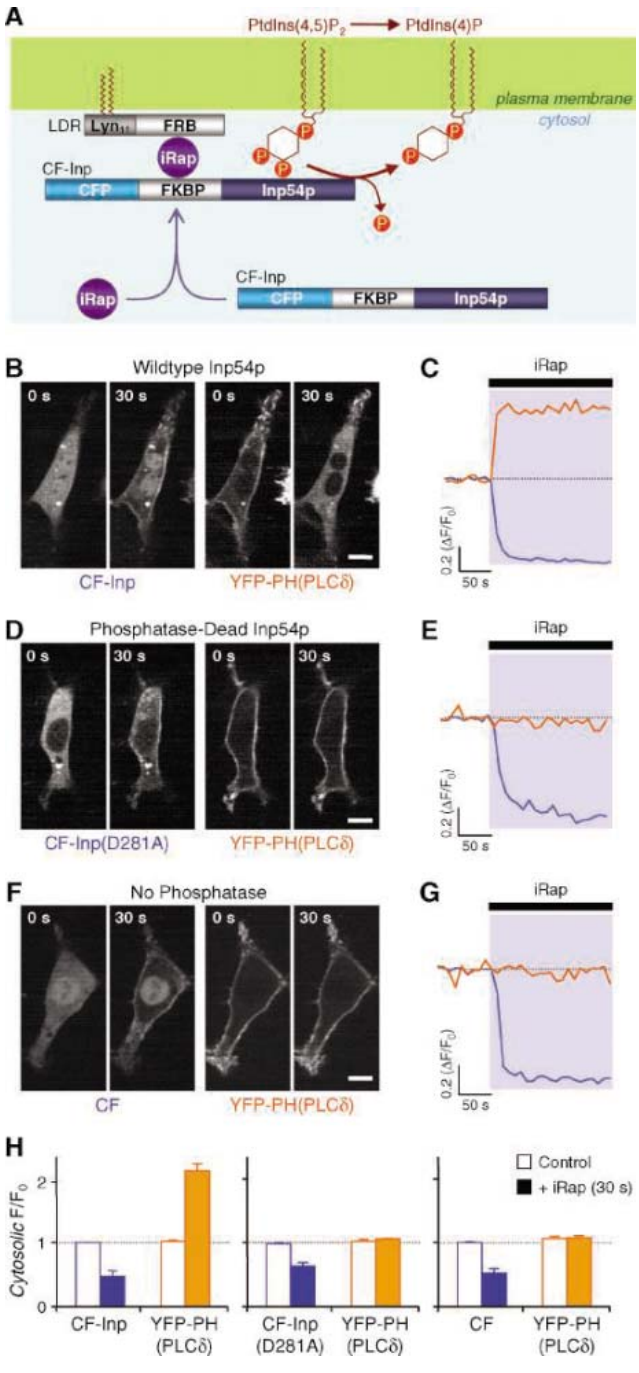

Fig. 1. In situ $PI(4,5)P_2$ hydrolysis induced by iRap heterodimerization in NIH3T3 cells. (**A**) FRB is anchored to plasma membrane via myristoylation and palmitoylation modification sequence Lyn_{11}. Inp54p is recruited from the cytosol upon addition of iRap, forming the tripartite complex FRB-iRap-FKBP. Membrane recruitment of Inp54p rapidly induces specific dephosphorylation at the 5 position of $PI(4,5)P_2$ [PtdIns(4,5)P_2]. PtdIns(4)P, PI(4)P. (**B**, **D**, and **F**) Time-series confocal fluorescent images of cells expressing LDR, YFP-PH(PLC-δ) and either CF-Inp (B), CF-Inp(D281A) (D), or CF (F). Images before and after the 30-s addition of iRap (5 μM). Scale bar, 10 μm. (**C**, **E**, and **G**) Cytosolic fluorescence intensities of CFP (blue) and YFP (yellow) for the cells shown in B (C), D (E), or F (G). Normalized fluorescence intensities are shown as a function of time. $\Delta F/F_0$, fluorescence change divided by initial fluorescence. (**H**) Normalized fluorescence intensity of CFP and YFP in the cytosol from more than four independent experiments with the same conditions as [(B) to (G)] before (white bars) and after (colored bars) 30-s iRap treatment. The black box refers to both the solid orange and solid blue bars, and the white box refers to the white bars, whether outlined with orange or blue. Mean values are shown and error bars indicate SEM.

The goal of our study was to use an enzyme distinct from PLC to determine whether depletion of $PI(4,5)P_2$ suffices to turn off KCNQ channels. Therefore, we had to rule out the alternative possibility that some essential downstream products of PLC, such as IP_3, DAG, or calcium transients, might also be generated by membrane translocation of Inp54p. In tsA cells where PLC was blocked with the inhibitor U73122 or where IP_3 accumulation was prevented by overexpressing IP_3 5-phosphatase (*14*), the iRap-induced translocation of CF-Inp, the depletion of $PI(4,5)P_2$ (fig. S2, A and B), and the suppression of KCNQ current were unaltered (Fig. 2, E and F). Further, in tsA cells expressing the YFP-labeled C1 domain of protein kinase C–γ, a DAG indicator (*15*), iRap induced no translocation of the indicator, but Oxo-M did (fig. S2C). Hence, CF-Inp/iRap does not induce DAG production. Finally, we measured intracellular calcium using fura-2 as a calcium indicator in tsA cells expressing M_1Rs. Application of Oxo-M led to a transient calcium rise that was abolished by overexpressing IP_3 5-phosphatase (fig. S2D). On the other hand, the application of iRap led to no calcium elevation. Analogous experiments in NIH3T3 cells also showed neither DAG production nor calcium elevation with CF-Inp/iRap.

As a further test of the phosphoinositide hypothesis, we used a similar strategy to increase $PI(4,5)P_2$ in the plasma membrane with a lipid kinase. We made a translocatable construct CF-PIPK by combining most of the enzyme PI(4)P 5-kinase type I–γ (PIPKI-γ) (*16*) with CFP-FKBP. In NIH3T3 cells and tsA cells, CF-PIPK fluorescence was largely in the cytosol at rest and moved to the plasma membrane irreversibly upon addition of iRap (fig. S3). In tsA cells also expressing KCNQ subunits, the KCNQ current was slowly augmented after the addition of iRap (exponential time constant τ = 138 ± 23 s; n = 4 cells), as might be predicted if there is a slow increase of membrane $PI(4,5)P_2$ (Fig. 3A). The midpoint of channel activation did not change (iRap, –28.5 ± 2.0 mV; controls, –27.3 ± 1.8 mV; n = 5 cells). However, current suppression by subsequent addition of Oxo-M was greatly slowed and incomplete after only 20 s of application (Fig. 3B), as if accumulation and speeded synthesis of $PI(4,5)P_2$ decreased the depletion by PLC. The effects of the translocated CF-PIPK enzyme were paralleled in cells overexpressing the non-translocating full-length original enzyme PIPKI-γ (fig. S4). Again, in those cells, the current suppression by Oxo-M was slowed and only partial [compare to similar experiments with PIPKI-β (*17*)]; current suppression by the coexpressed CF-Inp/iRap system was also slowed but remained nearly complete. A kinase-dead version of the kinase construct

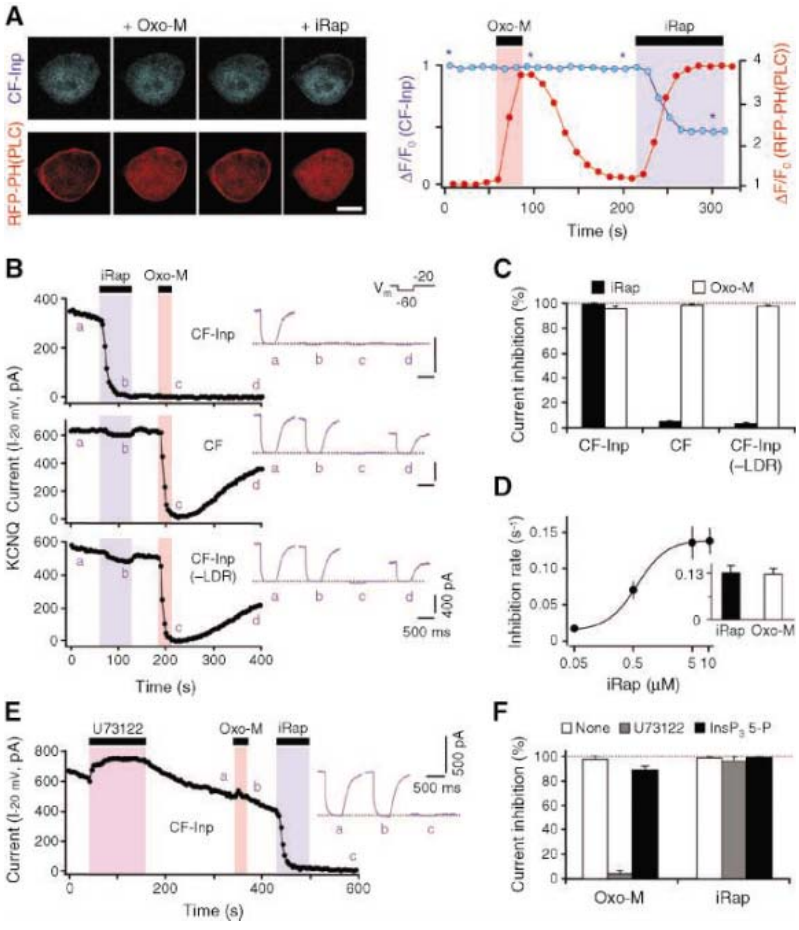

Fig. 2. Modulation of KCNQ current induced by CF-Inp and iRap in tsA cells. (**A**) Translocation of CF-Inp (blue) and RFP-PH(PLC-δ) (red) upon addition of Oxo-M (10 μM) or iRap (5 μM) to cells cotransfected with M_1R. Scale bar, 10 μm. Asterisks indicate times of the four images shown. (**B**) Channel modulation by iRap (5 μM) or Oxo-M (10 μM) in cells expressing CF constructs with LDR or CF-Inp alone. Insets show the current waveforms at indicated times a to d; the dotted line indicates zero current. V_m, membrane voltage protocol; $I_{-20\ mV}$, KCNQ current recorded at −20 mV. (**C**) Current inhibition by iRap and Oxo-M in cells expressing combinations of LDR and CF constructs. (**D**) Rate constants of current inhibition with various iRap concentrations. Inset shows the rate constants (s^{-1}) for inhibition by iRap (5 μM) or Oxo-M (10 μM) in CF-Inp–expressing cells (n = 3 to 10 cells). (**E**) Effect of Oxo-M and iRap on KCNQ channel in a cell treated with the PLC inhibitor U73122 (3 μM). (**F**) Current inhibition by Oxo-M and iRap in cells treated with U73122 or overexpressing IP_3 5-phosphatase (n = 3 to 7 cells). Error bars in (C), (D), and (F) indicate SEM.

(Asp^{253}→Ala^{253}, CF-PIPKi) (*18*) increased KCNQ current little and had almost no effect on subsequent suppression by muscarinic agonist (Fig. 3, A and B).

The ability of translocated CF-PIPK to augment KCNQ current suggests that KCNQ channels are not fully saturated by resting levels of plasma membrane–associated $PI(4,5)P_2$. We tested this further by taking advantage of a reported difference in $PI(4,5)P_2$ affinities for different KCNQ subunit isoforms: Increasing concentrations of short-chain $PI(4,5)P_2$ are reportedly needed to activate channels expressed from KCNQ3 alone, KCNQ2 and KCNQ3 together, and KCNQ2 alone, respectively (*19*). When we compared these channel types for responses to CF-PIPK/iRap, KCNQ2 current was augmented by 54 ± 12% (n = 5 cells), KCNQ2/KCNQ3 current by 27 ± 8% (n = 10 cells), and KCNQ3 channels by only 5 ± 2% (n = 5 cells) (Fig. 3C). Augmentation of current after iRap addition must be due to accumulation of extra $PI(4,5)P_2$. The experiments of Fig. 3C with KCNQ2/KCNQ3 heteromers suggest, therefore, that the degree of saturation by resting $PI(4,5)P_2$ is about 70%, which is in good agreement with preliminary published estimates of 72% (*20*) and 81% (*17*). KCNQ2 channels are even less saturated, and KCNQ3 channels are more saturated.

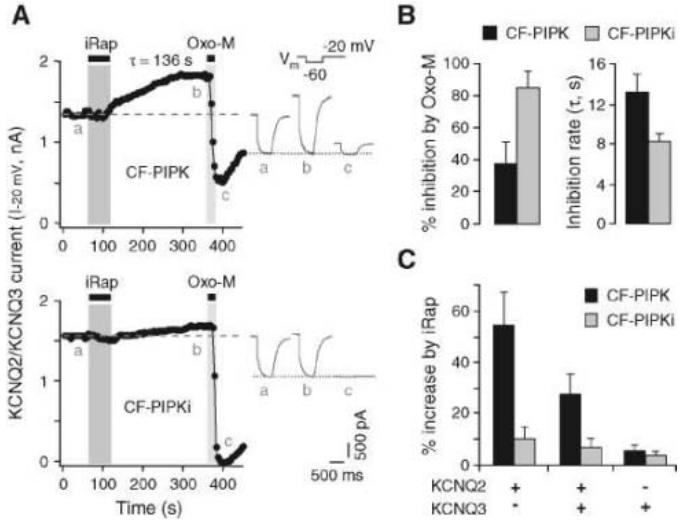

Fig. 3. Increase of KCNQ current by activation of PI(4)P 5-kinase. (**A**) Modulation of KCNQ2/KCNQ3 channels in tsA cells expressing CF-PIPK (top) or CF-PIPKi (bottom) constructs by application of iRap (5 μM) for 1 min. The dashed line indicates current amplitude before iRap. Insets show the current waveforms at indicated times a to c. (**B**) Percent inhibition by Oxo-M and time constant of inhibition after previous iRap translocation of CF-PIPK or CF-PIPKi. (**C**) Effects of CF-PIPK or CF-PIPKi on iRap-induced augmentation of current in homomeric KCNQ2, heteromeric KCNQ2/KCNQ3, or homomeric KCNQ3 channels (n = 4–10 cells). Error bars in (B) and (C) indicate SEM.

Triply phosphorylated $PI(3,4,5)P_3$ is a potent second messenger for growth factor signaling (*21*). Roles in ion channel regulation are less studied. Applied $PI(3,4,5)P_3$ restores the function of G protein–activated, inward rectifier Kir3.1/3.4 K^+ channels (but not constitutively active Kir2.1 channels) about as effectively as $PI(4,5)P_2$ in excised membrane patches (*22*). Therefore, we asked whether $PI(3,4,5)P_3$ affects KCNQ currents in intact cells. TsA cells grown in normal serum-containing medium have some plasma membrane–associated $PI(3,4,5)P_3$ as reported by the $PI(3,4,5)P_3$ indicator YFP-PH(Akt) (*23*),

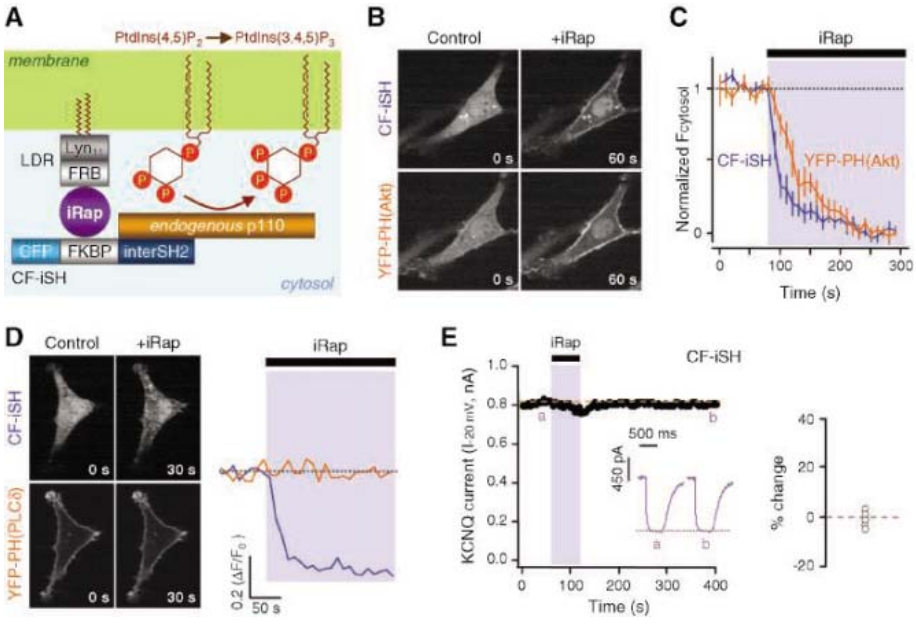

Fig. 4. Translocation of PI 3-kinase without change of KCNQ current amplitude. (**A**) The translocatable inter-SH2 domain of p85 and its complexation with endogenous p110 PI 3-kinase. PtdIns(3,4,5)P_3, PI(3,4,5)P_3. (**B**) Translocation of CF-iSH and YFP-PH(Akt) in NIH3T3 cells after a 1-min addition of iRap (5 μM). (**C**) Time course of translocation of CF-iSH and YFP-PH(Akt) by iRap. Error bars indicate SEM. (**D**) Translocation in cells coexpressing CF-iSH and YFP-PH(PLC-δ). (**E**) Modulation of KCNQ2/KCNQ3 channel activity by iRap in a tsA cell expressing LDR plus CF-iSH in serum-free conditions. Inset shows the current change after 4 min of iRap; mean, −0.4 ± 2.0% (n = 5 cells).

which is derived from the PH domain of Akt (fig. S5A). This resting PI(3,4,5)P_3 disappears if phosphatidylinositol 3-kinase (PI 3-kinase) activity is lowered by growth in serum-free conditions, by treatment with 0.5 to 1 μM of the inhibitor wortmannin, or by overexpression of the dominant-negative PI 3-kinase regulatory subunit Δp85 (fig. S5, A to C) (*24*). Still, the current and its suppression by Oxo-M remained normal (fig. S5, B and D) (*3*). To raise PI(3,4,5)P_3, we made CF-iSH, a translocatable construct combining CFP-FKBP with the inter–Src homology 2 (iSH2) domain from p85, which complexes in cells with endogenous PI 3-kinase p110 (Fig. 4A) (*25*). In NIH3T3 cells and tsA cells, the CF-iSH construct translocated rapidly to the plasma membrane ($t_{1/2}$ = 14.4 ± 3.6 s, n = 8 cells) upon addition of iRap and induced membrane translocation of YFP-PH(Akt) ($t_{1/2}$ = 36.5 ± 7.6 s) (Fig. 4, B and C). Nevertheless, the PI(4,5)P_2 indicator YFP-PH(PLC-δ) was not translocated (Fig. 4D), indicating that CF-iSH initiates synthesis of PI(3,4,5)P_3 at the plasma membrane with little depletion of PI(4,5)P_2. This agrees with reports that the amount of PI(3,4,5)P_3 made by receptor activation of endogenous 3-kinases is only a few percent of the available PI(4,5)P_2 (*26*). Adding iRap to tsA cells expressing CF-iSH and grown in serum-free conditions had little effect on the amplitude of KCNQ2/KCNQ3 current (Fig. 4E). It did reduce the subsequent suppression by Oxo-M slightly so that suppression was not complete in 20 s (fig. S6).

With intact cells, we have shown that decreases of PI(4,5)P_2 quickly turn off current in KCNQ2/KCNQ3 channels by more than 95% in the complete absence of the cascade of IP_3, calcium, and DAG signals normally generated by the activation of PLC. Conversely, an increase of PI(4,5)P_2 augments the current, whereas synthesis of PI(3,4,5)P_3 does not change the amplitude. During the activation of CF-Inp, rapid dephosphorylation of the PI(4,5)P_2 pool would generate a bolus of additional PI(4)P. Modeling shows that this dephosphorylation will produce a large transient elevation of PI(4)P, followed by a maintained plateau of extra PI(4)P. Nevertheless, our experiments show that this elevated PI(4)P is not able to sustain KCNQ current when PI(4,5)P_2 is depleted. These results give clarity to our hypothesis that the function of KCNQ channels is dependent on plasma membrane–associated PI(4,5)P_2. Our study also shows the utility of the iRap translocation strategy for perturbing the lipid composition of the plasma membrane. This method is noninvasive, inducible, rapid, and specific, a combination not found when using RNA interference, antibodies, or pharmacology. We have used this strategy in an accompanying paper studying the plasma membrane targeting of small GTPases (*27*). The phosphoinositide dependence of many cellular functions is now directly testable.

References and Notes

1. D. W. Hilgemann, S. Feng, C. Nasuhoglu, *Sci. STKE* **2001**, re19 (2001).
2. B. C. Suh, B. Hille, *Curr. Opin. Neurobiol.* **15**, 370 (2005).
3. B. C. Suh, B. Hille, *Neuron* **35**, 507 (2002).
4. P. Delmas, D. A. Brown, *Nat. Rev. Neurosci.* **6**, 850 (2005).
5. H. Lerche, Y. G. Weber, K. Jurkat-Rott, F. Lehmann-Horn, *Curr. Pharm. Des.* **11**, 2737 (2005).
6. D. M. Spencer, T. J. Wandless, S. L. Schreiber, G. R. Crabtree, *Science* **262**, 1019 (1993).
7. T. Inoue, W. D. Heo, J. S. Grimley, T. J. Wandless, T. Meyer, *Nat. Methods* **2**, 415 (2005).
8. D. Raucher *et al.*, *Cell* **100**, 221 (2000).
9. Materials and methods are available as supporting material on *Science* Online.
10. Correspondence about the iRap-inducible enzyme systems should be directed to T.I. (e-mail: jctinoue@stanford.edu).
11. T. P. Stauffer, S. Ahn, T. Meyer, *Curr. Biol.* **8**, 343 (1998).
12. K. Hirose, S. Kadowaki, M. Tanabe, H. Takeshima, M. Iino, *Science* **284**, 1527 (1999).
13. Y. Tsujishita, S. Guo, L. E. Stolz, J. D. York, J. H. Hurley, *Cell* **105**, 379 (2001).
14. L. F. Horowitz *et al.*, *J. Gen. Physiol.* **126**, 243 (2005).
15. E. Oancea, T. Meyer, *Cell* **95**, 307 (1998).
16. H. Ishihara *et al.*, *J. Biol. Chem.* **273**, 8741 (1998).
17. J. S. Winks *et al.*, *J. Neurosci.* **25**, 3400 (2005).
18. K. Ling, R. L. Doughman, A. J. Firestone, M. W. Bunce, R. A. Anderson, *Nature* **420**, 89 (2002).
19. Y. Li, N. Gamper, D. W. Hilgemann, M. S. Shapiro, *J. Neurosci.* **25**, 9825 (2005).
20. B. C. Suh, L. F. Horowitz, W. Hirdes, K. Mackie, B. Hille, *J. Gen. Physiol.* **123**, 663 (2004).
21. L. C. Cantley, *Science* **296**, 1655 (2002).
22. T. Rohacs, J. Chen, G. D. Prestwich, D. E. Logothetis, *J. Biol. Chem.* **274**, 36065 (1999).
23. C. D. Kontos *et al.*, *Mol. Cell. Biol.* **18**, 4131 (1998).
24. K. Hara *et al.*, *Proc. Natl. Acad. Sci. U.S.A.* **91**, 7415 (1994).
25. Q. Hu, A. Klippel, A. J. Muslin, W. J. Fantl, L. T. Williams, *Science* **268**, 100 (1995).
26. K. R. Auger, L. A. Serunian, S. P. Soltoff, P. Libby, L. C. Cantley, *Cell* **57**, 167 (1989).
27. W. D. Heo *et al.*, *Science* **314**, 1458 (2006).

28. Supported by NIH grants NS08174 and AR17803 (B.H.) and MH64801 and GM63702 (T.M.). T.I. is a recipient of a fellowship from the Quantitative Chemical Biology Program. We thank J. York for the Inp54p plasmid and advice on construction of CF-Inp, Alliance for Cellular Signaling for the p85 plasmid, T. Martin and Y. Aikawa (University of Wisconsin) for the PIPKI-γ plasmid and advice on construction of CF-PIPK, T. Wandless and J. Grimley for the iRap compound, J. Duman for help with calcium measurements, and K. Mackie for advice and discussion. Some images used the University of Washington Keck Imaging Center.

Supporting Online Material

www.sciencemag.org/cgi/content/full/1131163/DC1
Materials and Methods
Figs. S1 to S6
References

12 June 2006; accepted 25 August 2006
Published online 21 September 2006;
10.1126/science.1131163
Include this information when citing this paper.

$PI(3,4,5)P_3$ and $PI(4,5)P_2$ Lipids Target Proteins with Polybasic Clusters to the Plasma Membrane

Won Do Heo,[1] Takanari Inoue,[1] Wei Sun Park,[1] Man Lyang Kim,[1] Byung Ouk Park,[2] Thomas J. Wandless,[1] Tobias Meyer[1]*

Many signaling, cytoskeletal, and transport proteins have to be localized to the plasma membrane (PM) in order to carry out their function. We surveyed PM-targeting mechanisms by imaging the subcellular localization of 125 fluorescent protein–conjugated Ras, Rab, Arf, and Rho proteins. Out of 48 proteins that were PM-localized, 37 contained clusters of positively charged amino acids. To test whether these polybasic clusters bind negatively charged phosphatidylinositol 4,5-bisphosphate [$PI(4,5)P_2$] lipids, we developed a chemical phosphatase activation method to deplete PM $PI(4,5)P_2$. Unexpectedly, proteins with polybasic clusters dissociated from the PM only when both $PI(4,5)P_2$ and phosphatidylinositol 3,4,5-trisphosphate [$PI(3,4,5)P_3$] were depleted, arguing that both lipid second messengers jointly regulate PM targeting.

Small guanosine triphosphatases (GTPases) from the Ras, Rho, Arf, and Rab subfamilies often exert their role at the PM where they control diverse signaling, cytoskeletal, and transport processes (*1*–*3*). KRas, CDC42, and other family members require a cluster of positively charged amino acids for PM localization and activity (*2*, *4*). In vitro studies indicate that the physiological PM binding partner of such polybasic clusters could be phosphatidylserine, which has one negative charge, or the less abundant lipid second messenger $PI(4,5)P_2$, which has four negative charges (*5*–*7*). We took a genomic survey approach and investigated PM-targeting mechanisms by confocal imaging of 125 cyan fluorescent protein (CFP)–tagged constitutively active small GTPases (*8*). Expression in NIH3T3 and HeLa cells showed that 48 small GTPases were fully or partially localized to the PM (Fig. 1A and fig. S1).

Thirty-seven of these PM-localized small GTPases had C-terminal polybasic clusters consisting of four or more Lys or Arg residues at positions 5 to 20 from the C terminus (Fig. 1B and fig. S1). Polybasic clusters were found in three forms: They were present together with N-terminal myristoylation consensus sequences (as in Arl4) (*9*) or with C-terminal prenylation consensus sequences (as in KRas) (*5*, *6*, *10*), or they lacked lipid modifications (as in Rit) (*11*). We called these three combinations polybasic-myristoyl, polybasic-prenyl, and polybasic-nonlipid PM-targeting motifs, respectively. A number of remaining PM-targeted small GTPases had a combined prenylation and palmitoylation consensus sequence that mediated PM targeting without requiring polybasic amino acids (as does that of HRas) (Fig. 1, A and C) (*5*, *12*). Arf6 lacked a specific targeting motif and was only localized to the PM in its guanosine triphosphate (GTP)–bound form (fig. S2) (*13*). The sequence homology comparison of PM-localized small GTPases in Fig. 1C shows that closely homologous small GTPases can have different targeting motifs. We also confirmed, for the examples of Rit and KRas, that polybasic targeting motifs alone can be sufficient for PM targeting (Fig. 1D).

To test whether polybasic clusters are anchored to the PM by binding to $PI(4,5)P_2$ (*14*), we hydrolyzed PM $PI(4,5)P_2$ by rapid targeting of Inp54p, a 5′ specific $PI(4,5)P_2$ phosphatase (*15*), to the PM. This method is based on a PM-localized FK506-binding protein (FKBP12)–rapamycin–binding (FRB) construct and a cytosolic Inp54p enzyme conjugated with FKBP12 (CF-Inp) that can be translocated to the PM by chemical heterodimerization by using a rapamycin analog, iRap (*16*).

In experiments where we monitored $PI(4,5)P_2$ using a yellow fluorescent protein (YFP)–conjugated pleckstrin homology (PH) domain from phospholipase Cδ (PLCδ) (*17*), PM translocation of CF-Inp triggered a rapid and near complete dissociation of the YFP-PLCδ-PH domain from the PM (Fig. 2A). Despite this marked reduction in $PI(4,5)P_2$ concentration, only a small fraction of the polybasic-nonlipid tail fragment of Rit dissociated from the PM (Fig. 2B), which suggests that $PI(4,5)P_2$ is not alone responsible for PM targeting. Parallel experiments suggested that phosphatidylinositol 3,4,5-trisphosphate [$PI(3,4,5)P_3$] might be involved, because stimulation of cells with platelet-derived growth factor

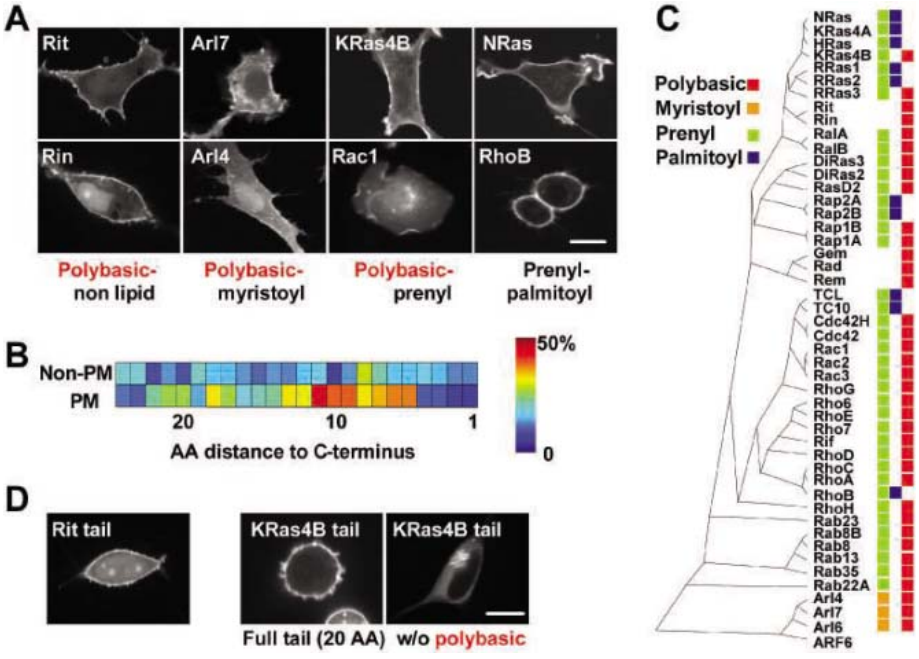

Fig. 1. A survey of the subcellular localization of 125 small GTPases shows that most PM-localized small GTPases have targeting motifs with clusters of polybasic amino acids. (**A**) Confocal images of the subcellular localization of CFP-conjugated small GTPases in NIH3T3 cells (full set of images in NIH3T3 and HeLa cells in fig. S1). The four main PM-targeting motifs are represented in the image panels. (**B**) Correlation between PM localization and the presence of lysine residues in a region 5 to 20 amino acids from the C terminus. (**C**) Phylogenetic tree of 48 small GTPases that were identified to be partially or fully localized to the PM. Individual membrane targeting elements are color coded: red for polybasic clusters and blue, green, and orange for palmitoyl, prenyl, and myristoyl consensus sequences, respectively. (**D**) Twenty-amino-acid-long C-terminal tail fragments of Rit and KRas are PM-localized. Lack of PM targeting of a KRas tail fragment without the polybasic region (right). Scale bars, 10 μm.

[1]Department of Molecular Pharmacology, 318 Campus Drive, Clark Building, Stanford University Medical School, Stanford, CA 94305, USA. [2]Division of Applied Life Science (BK21 Program) and Environmental Biotechnology National Core Research Center, Gyeongsang National University, Jinju 660-701, Korea.

*To whom correspondence should be addressed. E-mail: tobias1@stanford.edu

(PDGF) led to a small increase in PM localization of the Rit tail and this small effect could be reversed by addition of an inhibitor of phosphoinositide 3-kinase (PI 3-kinase), LY294002 (LY29) (Fig. 2C; control experiments in fig. S3). Strikingly, the combined reduction of both $PI(4,5)P_2$ and $PI(3,4,5)P_3$ concentration triggered a dissociation of most Rit tail protein from the PM (Fig. 2, D and E). The effect of reducing either $PI(4,5)P_2$ or $PI(3,4,5)P_3$ concentration alone on Rit tail localization was relatively small (Fig. 2E).

We also found that both $PI(4,5)P_2$ and $PI(3,4,5)P_3$ have to be lowered to significantly dissociate a tail fragment of Rin and a polybasic effector domain peptide from myristoylated alanine-rich C kinase substrate (MARCKS) protein (MARCKS ED) from the PM (Fig. 2, D and E). This MARCKS ED peptide was included because it has been extensively used for in vitro biochemical studies of the interaction between polybasic amino acids and phosphatidylserine and $PI(4,5)P_2$ (*7*, *14*, *18*, *19*). HRas, which has a prenyl-palmitoyl PM-targeting motif without a polybasic cluster, did not dissociate from the PM after depletion of $PI(4,5)P_2$ and $PI(3,4,5)P_3$ (Fig. 2E). Control experiments with the same constructs in HeLa cells showed similar results (fig. S4), and an analysis of the dissociation kinetics showed that PM dissociation occurs within minutes after CF-Inp activation and LY29 addition (fig. S5A). We also verified that PM dissociation of polybasic proteins occurred when we combined $PI(4,5)P_2$ depletion with addition of wortmannin, an alternative PI 3-kinase inhibitor, or with expression of a dominant negative PI 3-kinase inhibitory construct (*20*) (figs. S6 and S7). Additional control experiments are shown in figs. S8 to S12, including in vitro lipid-blot assays that showed enhanced affinity of proteins with polybasic clusters for $PI(3,4,5)P_3$ over $PI(4,5)P_2$. These control experiments strengthen the argument that $PI(4,5)P_2$ and the less abundant $PI(3,4,5)P_3$ both serve as PM anchors for proteins with polybasic clusters.

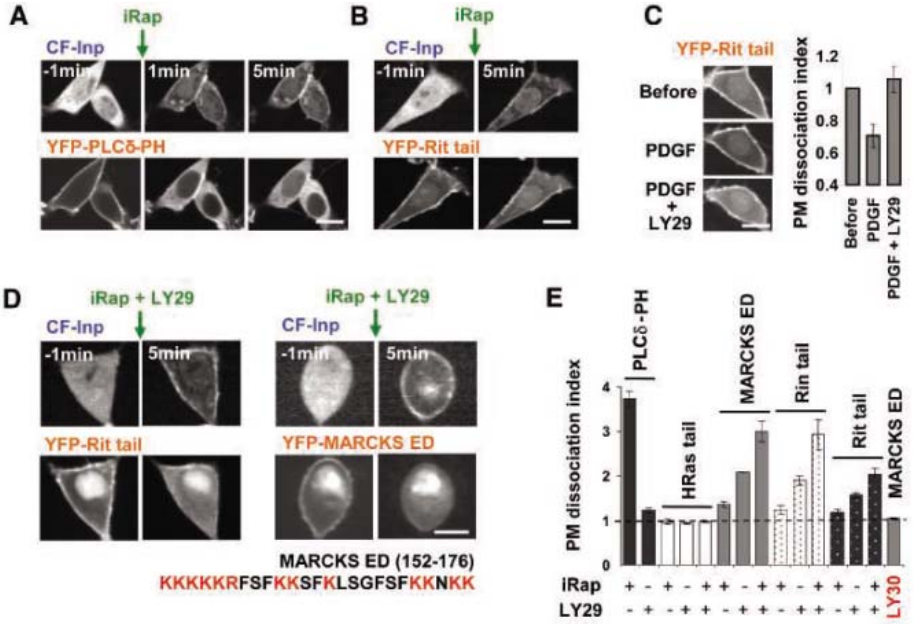

Fig. 2. Depletion of $PI(4,5)P_2$ and $PI(3,4,5)P_3$ dissociates Rit, Rin, and MARCKS ED with polybasic-nonlipid targeting motifs from the PM. (**A**) Development of a chemically inducible translocation method to deplete $PI(4,5)P_2$ from the inner leaflet of the PM (*22*, *23*). The $PI(4,5)P_2$ biosensor YFP-PLCδ-PH was cotransfected to monitor depletion of $PI(4,5)P_2$. (**B**) Depletion of $PI(4,5)P_2$ caused only a small reduction in the PM localization of YFP-conjugated Rit tail. (**C**) A small, but significant, PDGF receptor–mediated increase in Rit tail PM localization can be reversed by addition of the PI3-kinase inhibitor LY29 (before and 9 min after addition of 5 μM iRap). The bar graph shows a quantification of the same experiment. The PM dissociation index is the relative ratio of internal over PM fluorescence; that is, $F_{1cyt}/F_{1PM} * F_{0PM}/F_{0cyt}$, with F_0 and F_1 as the fluorescent intensities before and after $PI(4,5)P_2$ and $PI(3,4,5)P_3$ depletion. (**D**) Joint reduction in $PI(4,5)P_2$ and $PI(3,4,5)P_3$ triggered a near-complete dissociation of Rit tail and MARCKS ED from the PM. (**E**) Quantitative analysis of the CF-Inp and/or LY29-triggered PM dissociation of MARCKS ED, and Rit and Rin tails. PLCδ-PH and HRas tails are shown as controls. The inactive LY29 analog LY30 was used as a control (*24*). Scale bars, 10 μm.

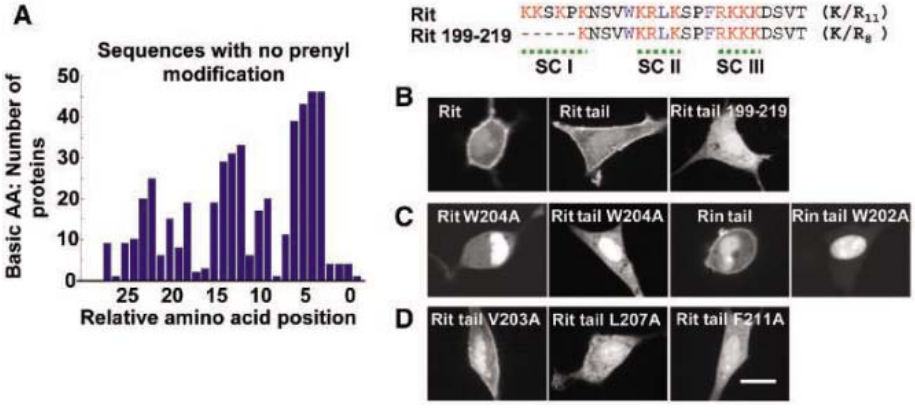

Fig. 3. Polybasic subclusters and hydrophobic amino acids are required for PM targeting by polybasic-nonlipid targeting motifs. (**A**) Statistical analysis of the relative sequence location of positively charged amino acids in nonprenylated small GTPases. (**B**) Loss of PM targeting of Rit tail fragment after removal of a single subcluster with positively charged amino acids. (**C**) Identification of a tryptophan residue in the polybasic regions of Rit and Rin that mediates PM over nuclear localization. Full-length small GTPases, as well as tail fragment mutants, are shown. (**D**) Identification of two additional hydrophobic amino acid residues that contribute to the PM targeting of Rit. Scale bars, 10 μm.

Insights into the electrostatic binding mechanism between positively charged polybasic clusters and negatively charged polyphosphoinositides came from a sequence comparison of nonprenylated PM-targeted small GTPases. Most of these proteins contain two or three subclusters of polybasic residues in the C-terminal tail. Each subcluster spans about four or five amino acids, and the mean distance between subclusters is nine amino acids (Fig. 3A). Consistent with a need for multiple subclusters, the removal of a flanking subcluster in the Rit tail was sufficient to abolish PM targeting (Rit tail 199 to 219) (Fig. 3B). This suggests that PM targeting results from additive binding energy of individual subclusters that each electrostatically interact with a $PI(4,5)P_2$ or $PI(3,4,5)P_3$ lipid. Selectivity for polyphosphoinositides over phosphatidylserine may occur because of opposing high relative-charge densities of polyphosphoinositides and polybasic subclusters (*7*).

We then investigated differences between the targeting mechanisms of the three polybasic-nonlipid, polybasic-myristoyl, and polybasic-prenyl PM-targeting motifs. A distinct feature of the polybasic-nonlipid targeting motifs is their similarity to nuclear localization sequences. We found hydrophobic amino acids to be im-

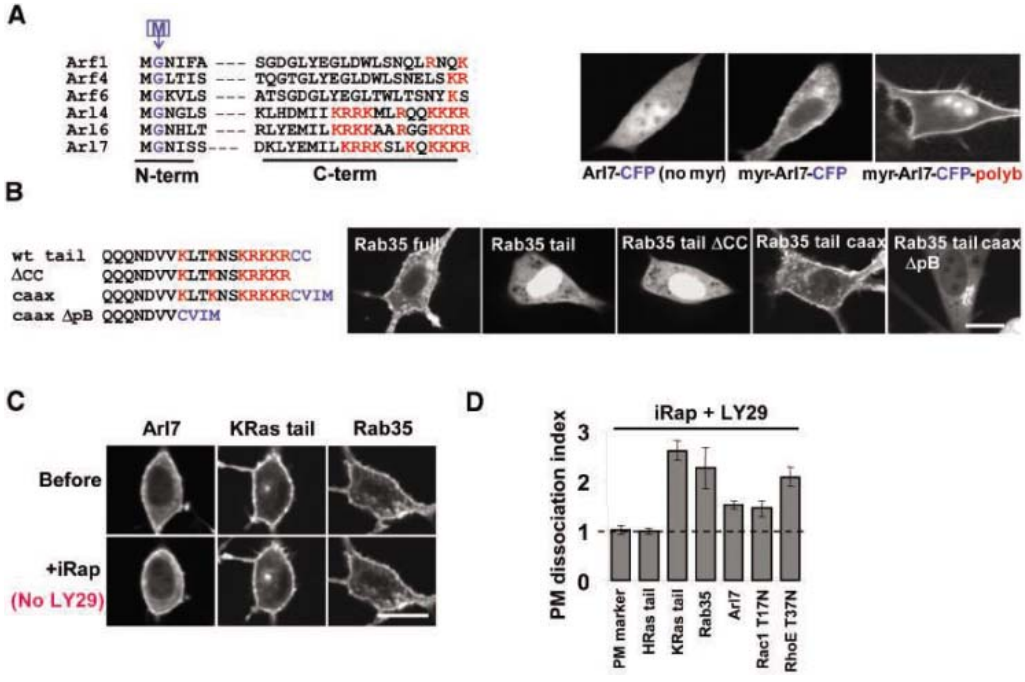

Fig. 4. Depletion of PI(4,5)P_2 and PI(3,4,5)P_3 dissociates proteins with polybasic-myristoyl and polybasic-prenyl targeting motifs from the PM. (**A**) Aligned sequences of the N terminus (6 amino acids) and C terminus (20 amino acids) of six ARF family members. Confocal images of an Arl7 mutant construct lacking the N-terminal myristoylation motif (left), a C-terminal tagged Arl7 control construct (middle), and a mutant construct with an internal CFP tag and a flexible C-terminal polybasic Arl7 tail (right). (**B**) PM localization motifs in geranylgeranylated Rab35. Confocal images from left to right: localization of wild-type Rab35, wild-type tail fragment, wild-type tail lacking geranylgeranylation motif (ΔCC), Rab35 tail ΔCC mutant with KRas caax (Rab35 tail caax), and Rab35 tail caax mutant lacking polybasic amino acids (Rab35 tail caax ΔpB). (**C**) Depletion of PI(4,5)P_2 by CF-Inp activation without L29 addition causes only a minimal PM dissociation of Arl7, KRas tail fragment, and Rab35. (**D**) Quantitative analysis of the much larger PM dissociation of polybasic-lipid modified proteins after depletion of PI(4,5)P_2 and PI(3,4,5)P_3 by CF-Inp activation and addition of LY29. Scale bars, 10 μm.

portant for selective PM localization, because site-directed mutagenesis of a single hydrophobic amino acid (Trp^{204}Ala in Rit or Trp^{202}Ala in Rin) led to a complete loss of PM targeting and a strong nuclear localization (Fig. 3C). A loss of PM targeting but with less nuclear targeting could also be observed for Leu^{207}Ala and Phe^{211}Ala Rit mutants (Fig. 3D) and for hydrophobic amino acid mutants of the small GTPases GEM and RAD (fig. S13). Thus, hydrophobic amino acids strengthen PM binding of polybasic-nonlipid motifs and prevent the polybasic cluster from functioning as a nuclear localization sequence.

The polybasic-myristoyl PM-targeting motifs have the distinct feature of a separated N-terminal myristoylation consensus sequence and a C-terminal polybasic cluster. Mutant constructs showed that effective PM targeting of Arl7 required an N-terminal myristoyl motif (left panel, Fig. 4A), as well as a flexible C-terminal polybasic tail (middle versus right panel, Fig. 4A), which suggests that the two ends of the protein synergistically support PM targeting.

The polybasic-prenyl PM-targeting motif includes proteins such as KRas for which a 20–amino acid tail sequence is sufficient for farnesylation and PM targeting (Fig. 1D), as well as Rab35 for which an intact GTPase domain is required for geranylgeranylation (*21*) and for PM targeting (second and third panels, Fig. 4B). We further compared the roles of farnesylation and geranylgeranylation by creating a Rab35 mutant with a consensus CAAX farnesylation sequence in place of the geranylgeranylation sequence. This mutant showed PM localization indistinguishable from that of the geranylgeranylated Rab35 (fourth panel, Fig. 4B). We also confirmed that the PM targeting of RAB35 requires a polybasic cluster (last panel, Fig. 4B). This shows that the polybasic-geranylgeranyl motifs of Rab35 can be equally effective in PM targeting as the polybasic-farnesyl motif of KRas, which supports the notion that both types of prenylation motifs can be grouped into a single polybasic-prenyl PM-targeting motif.

We then tested whether PI(4,5)P_2 and PI(3,4,5)P_3 also regulate polybasic-myristoyl and polybasic-prenyl targeting motifs. As for the polybasic-nonlipid targeting motif, depletion of PI(4,5)P_2 alone triggered only a minor reduction in PM localization of the Arl7 polybasic-myristoyl targeting motif and the KRas and Rab35 polybasic-prenyl motifs (Fig. 4C). Depletion of both PI(4,5)P_2 and PI(3,4,5)P_3 triggered significant PM dissociation of all polybasic-myristoyl and polybasic-prenyl constructs tested (Fig. 4D) with a kinetics similar to that of Rit (fig. S5), which suggests that PI(4,5)P_2 and PI(3,4,5)P_3 have the same role for PM localization for all three types of polybasic PM-targeting motifs. HRas was again included as a control protein without a polybasic cluster.

Our study shows that polybasic PM-targeting motifs are built from two parts, an unspecific membrane-targeting part that can be hydrophobic amino acids, myristoyl groups, or prenyl groups and a polybasic targeting part that provides PM specificity by binding of positively charged amino acid clusters to negatively charged PI(4,5)P_2 and PI(3,4,5)P_3 lipids in the PM. This gives PI(4,5)P_2 and PI(3,4,5)P_3 a ubiquitous role in regulating signaling, cytoskeletal, and transport proteins and argues that these lipid second messengers function as signaling hubs in cellular control systems.

References and Notes

1. M. Fivaz, T. Meyer, *Neuron* **40**, 319 (2003).
2. M. N. Teruel, T. Meyer, *Cell* **103**, 181 (2000).
3. J. L. Guan, *Science* **303**, 773 (2004).
4. D. Michaelson *et al.*, *J. Cell Biol.* **152**, 111 (2001).
5. K. A. Cadwallader, H. Paterson, S. G. Macdonald, J. F. Hancock, *Mol. Cell. Biol.* **14**, 4722 (1994).
6. F. Ghomashchi, X. Zhang, L. Liu, M. H. Gelb, *Biochemistry* **34**, 11910 (1995).
7. S. McLaughlin, D. Murray, *Nature* **438**, 605 (2005).
8. W. D. Heo, T. Meyer, *Cell* **113**, 315 (2003).
9. A. Schurmann *et al.*, *J. Biol. Chem.* **269**, 15683 (1994).
10. E. Choy *et al.*, *Cell* **98**, 69 (1999).
11. C. H. Lee, N. G. Della, C. E. Chew, D. J. Zack, *J. Neurosci.* **16**, 6784 (1996).
12. O. Rocks *et al.*, *Science* **307**, 1746 (2005).
13. H. Radhakrishna, J. G. Donaldson, *J. Cell Biol.* **139**, 49 (1997).
14. S. McLaughlin, J. Wang, A. Gambhir, D. Murray, *Annu. Rev. Biophys. Biomol. Struct.* **31**, 151 (2002).
15. T. Inoue, W. D. Heo, J. S. Grimley, T. J. Wandless, T. Meyer, *Nat. Methods* **2**, 415 (2005).
16. D. Raucher *et al.*, *Cell* **100**, 221 (2000).
17. T. P. Stauffer, S. Ahn, T. Meyer, *Curr. Biol.* **8**, 343 (1998).
18. J. Wang, A. Arbuzova, G. Hangyas-Mihalyne, S. McLaughlin, *J. Biol. Chem.* **276**, 5012 (2001).
19. C. Chapline, K. Ramsay, T. Klauck, S. Jaken, *J. Biol. Chem.* **268**, 6858 (1993).
20. S. Poser, S. Impey, K. Trinh, Z. Xia, D. R. Storm, *EMBO J.* **19**, 4955 (2000).
21. M. C. Seabra, C. Wasmeier, *Curr. Opin. Cell Biol.* **16**, 451 (2004).
22. B.-C. Suh, T. Inoue, T. Meyer, B. Hille, *Science* **314**, 1454 (2006); published online 21 September 2006; 10.1126/science.1131163.
23. Correspondence about the iRap inducible enzyme systems should be directed to T. Inoue (e-mail: jctinoue@stanford.edu).
24. T. W. Poh, S. Pervaiz, *Cancer Res.* **65**, 6264 (2005).

25. We thank A. Salmeen, M. F. Teruel, M. Fivaz, and other members of the Meyer laboratory for support; A. R. Koh and S. H. Ryu (POSTECH) for critical reading the

manuscript; S. McLaughlin (SUNY Stonybrook) and B. Hille (U. Washington) for discussions; and James Whalen for assisting with the in vitro lipid-binding assays. T.I. is a recipient of a fellowship from the Quantitative Chemical Biology Program. B.O.P. was supported by a grant from KOSEF/MOST EB-NCRC (grant no. R15-2003-012-01001-0) and by scholarships from the Brain Korea 21 program.

This work was supported by grants from National Institute of Mental Health and National Institute of General Medical Sciences, NIH, to T.M.

Supporting Online Material
www.sciencemag.org/cgi/content/full/1134389/DC1
Materials and Methods
Figs. S1 to S13
References

28 August 2006; accepted 11 October 2006
Published online 9 November 2006;
10.1126/science.1134389
Include this information when citing this paper.

A Genome-Wide Association Study Identifies *IL23R* as an Inflammatory Bowel Disease Gene

Richard H. Duerr,[1,2] Kent D. Taylor,[3,4] Steven R. Brant,[5,6] John D. Rioux,[7,8] Mark S. Silverberg,[9] Mark J. Daly,[8,10] A. Hillary Steinhart,[9] Clara Abraham,[11] Miguel Regueiro,[1] Anne Griffiths,[12] Themistocles Dassopoulos,[5] Alain Bitton,[13] Huiying Yang,[3,4] Stephan Targan,[4,14] Lisa Wu Datta,[5] Emily O. Kistner,[15] L. Philip Schumm,[15] Annette T. Lee,[16] Peter K. Gregersen,[16] M. Michael Barmada,[2] Jerome I. Rotter,[3,4] Dan L. Nicolae,[11,17] Judy H. Cho[18]*

The inflammatory bowel diseases Crohn's disease and ulcerative colitis are common, chronic disorders that cause abdominal pain, diarrhea, and gastrointestinal bleeding. To identify genetic factors that might contribute to these disorders, we performed a genome-wide association study. We found a highly significant association between Crohn's disease and the *IL23R* gene on chromosome 1p31, which encodes a subunit of the receptor for the proinflammatory cytokine interleukin-23. An uncommon coding variant (rs11209026, c.1142G>A, p.Arg381Gln) confers strong protection against Crohn's disease, and additional noncoding *IL23R* variants are independently associated. Replication studies confirmed *IL23R* associations in independent cohorts of patients with Crohn's disease or ulcerative colitis. These results and previous studies on the proinflammatory role of IL-23 prioritize this signaling pathway as a therapeutic target in inflammatory bowel disease.

Crohn's disease (CD) and ulcerative colitis (UC), the two common forms of idiopathic inflammatory bowel disease (IBD), are chronic, relapsing inflammatory disorders of the gastrointestinal tract. Each has a peak age of onset in the second to fourth decades of life and prevalences in European ancestry populations that average about 100 to 150 per 100,000 (*1*, *2*). Although the precise etiology of IBD remains to be elucidated, a widely accepted hypothesis is that ubiquitous, commensal intestinal bacteria trigger an inappropriate, overactive, and ongoing mucosal immune response that mediates intestinal tissue damage in genetically susceptible individuals (*1*). Genetic factors play an important role in IBD pathogenesis, as evidenced by the increased rates of IBD in Ashkenazi Jews, familial aggregation of IBD, and increased concordance for IBD in monozygotic compared to dizygotic twin pairs (*3*). Moreover, genetic analyses have linked IBD to specific genetic variants, especially *CARD15* variants on chromosome 16q12 and the *IBD5* haplotype (spanning the organic cation transporters, *SLC22A4* and *SLC22A5*, and other genes) on chromosome 5q31 (*3*–*7*). CD and UC are thought to be related disorders that share some genetic susceptibility loci but differ at others.

The replicated associations between CD and variants in *CARD15* and the *IBD5* haplotype do not fully explain the genetic risk for CD, so we performed a genome-wide association study testing 308,332 autosomal single nucleotide polymorphisms (SNPs) on the Illumina HumanHap300 Genotyping BeadChip (*8*). Our study population consisted of 567 non-Jewish, European ancestry patients with ileal CD and 571 non-Jewish controls. We initially focused on ileal CD, the most common location of CD, to minimize pathogenic heterogeneity. After exclusion of study subjects with genotype completion rates less than 94%, we included 547 cases and 548 controls in subsequent analyses (*8*). Single-marker allelic tests were performed using χ^2 statistics for all autosomal markers. Three SNPs had nearly two orders of magnitude greater significance compared to the next most significant markers, and they are the only markers that remain significant at the 0.05 level after Bonferroni correction. Two of the three markers, rs2066843 ($P = 2.86 \times 10^{-9}$, corrected $P = 8.82 \times 10^{-4}$) and rs2076756 ($P = 5.12 \times 10^{-10}$, corrected $P = 1.58 \times 10^{-4}$), are in the known CD susceptibility gene, *CARD15* (*4*, *5*). The third marker, rs11209026 ($P = 5.05 \times 10^{-9}$, corrected $P = 1.56 \times 10^{-3}$), is a nonsynonymous SNP (c.1142G>A, p.Arg381Gln) in the *IL23R* gene (GenBank accession: NM_144701, GeneID: 149233) on chromosome 1p31. This gene encodes a subunit of the receptor for the proinflammatory cytokine, interleukin-23 (IL-23), and is therefore an intriguing functional candidate. In addition to Arg381Gln, nine other markers in *IL23R* and in the intergenic region between *IL23R* and the adjacent IL-12 receptor, beta-2 gene (*IL12RB2*), had association *P*-values < 0.0001 in the non-Jewish, ileal CD case-control cohort (Table 1 and table S1a).

We next tested for association of *IL23R* markers in an independent ileal CD case-control cohort, consisting of 401 patients and 433 controls, all of Jewish ancestry (*8*). Significant associations were observed for several of the same markers that were associated in the non-Jewish cohort (Table 1 and table S1b). In a combined analysis of the data from the two ileal CD case-control cohorts (*8*), nine markers had highly significant association *P*-values ranging from 1.60×10^{-9} to 3.36×10^{-13} (Table 1 and table S1b).

We then extended the replication study by performing family-based association testing of 27 *IL23R* region markers in an independent cohort of 883 nuclear families in which both par-

[1]Division of Gastroenterology, Hepatology and Nutrition, Department of Medicine, School of Medicine, University of Pittsburgh, University of Pittsburgh Medical Center Presbyterian, Mezzanine Level, C-Wing, 200 Lothrop Street, Pittsburgh, PA 15213, USA. [2]Department of Human Genetics, Graduate School of Public Health, University of Pittsburgh, Crabtree A300, 130 Desoto Street, Pittsburgh, PA 15261, USA. [3]Medical Genetics Institute, Cedars-Sinai Medical Center, 8700 Beverly Boulevard, Los Angeles, CA 90048, USA. [4]IBD Center, Division of Gastroenterology, Cedars-Sinai Medical Center, 8700 Beverly Boulevard, Los Angeles, CA 90048, USA. [5]Harvey M. and Lyn P. Meyerhoff Inflammatory Bowel Disease Center, Department of Medicine, Johns Hopkins University School of Medicine, B136, 1503 East Jefferson Street, Baltimore, MD 21231, USA. [6]Department of Epidemiology, Bloomberg School of Public Health, Johns Hopkins University, 615 North Wolfe Street, Baltimore, MD 21205, USA. [7]Université de Montréal and the Montreal Heart Institute, S-6400, 5000 Belanger Street, Montreal, Quebec H1T 1C8, Canada. [8]Medical and Population Genetics Program, Broad Institute of MIT and Harvard, 7 Cambridge Center, Cambridge, MA 02142, USA. [9]Mount Sinai Hospital IBD Centre, University of Toronto, 441–600 University Avenue, Toronto, Ontario M5G 1X5, Canada. [10]Massachusetts General Hospital, Harvard Medical School, 185 Cambridge Street, Boston, MA 02114, USA. [11]Department of Medicine, University of Chicago, 5841 South Maryland Avenue, Chicago, IL 60637, USA. [12]Department of Pediatrics, The Hospital for Sick Children, 555 University Avenue, Toronto, Ontario M5G 1X8, Canada. [13]Royal Victoria Hospital, McGill University Health Centre, 687 Pine Avenue West, Montreal, Quebec H3A 1A1, Canada. [14]Immunobiology Research Institute, Cedars-Sinai Medical Center, Davis 4063, 8700 Beverly Boulevard, Los Angeles, CA 90048, USA. [15]Department of Health Studies, University of Chicago, 5841 South Maryland Avenue, Chicago, IL 60637, USA. [16]The Feinstein Institute for Medical Research, 350 Community Drive, Manhasset, NY 11030, USA. [17]Department of Statistics, University of Chicago, 5734 South University Avenue, Chicago, IL 60637, USA. [18]IBD Center, Section of Digestive Diseases, Departments of Medicine and Genetics, Yale University, S155A, 300 Cedar Street, New Haven, CT 06519, USA.

*To whom correspondence should be addressed. E-mail: judy.cho@yale.edu

ents and their IBD (CD, UC, or indeterminate IBD)–affected offspring were available for genotyping (Table 2 and table S2) (*8*). For Arg381Gln and other *IL23R* markers, we observed significant departure from random allele transmission to CD-affected offspring in both non-Jewish and Jewish families, providing further evidence for association between CD and *IL23R*. We also observed distortion of allele transmission to non-Jewish, UC-affected offspring, providing evidence for association of *IL23R* with non-Jewish UC. There was no evidence for association of Arg381Gln or other *IL23R* region markers in the Jewish UC families. In a combined analysis of the data from all 883 nuclear families and both case-control cohorts (*8*), all 10 *IL23R* markers in Table 2 showed highly significant association with IBD, with *P*-values ranging from 3.55×10^{-9} to 6.62×10^{-19}.

The *IL23R* gene is contained within two large blocks of linkage disequilibrium, and markers in the centromeric block containing exons 5 to 11 and part of the intergenic region between *IL23R* and *IL12RB2* have the strongest association signals (Fig. 1). There is no significant association within *IL12RB2* (Fig. 1), and we did not identify a *IL12RB2* SNP in the International HapMap CEU data that is correlated with an IBD-associated, *IL23R* region variant (*8*).

The IL23R protein contains an extracellular domain (composed of a signal sequence, an N-terminal immunoglobulin-like domain, and two cytokine receptor domains), a single transmembrane domain, and a 252–amino acid cytoplasmic domain (*9*). Arg-381, in the cytoplasmic domain, is the fifth amino acid internal to the transmembrane domain and is highly conserved between species (fig. S1). In contrast, two other nonsynonymous *IL23R* SNPs, rs1884444 (His3Gln) and rs7530511 (Pro310Leu), which are located within the extracellular domain, show no evidence for disease association (table S1, a and b).

The glutamine allele of Arg381Gln is much less common than the arginine allele, with an allelic frequency of 1.9% in the non-Jewish patients with ileal CD and 7.0% in non-Jewish controls. The glutamine allele appears to protect against development of CD in both non-Jewish [odds ratio (OR) = 0.26, 95% confidence interval (CI) (0.15 to 0.43)] and Jewish [OR = 0.45, 95% CI (0.27 to 0.73)] case-control cohorts. The glutamine allele is also significantly undertransmitted from heterozygous parents to non-Jewish and Jewish CD-affected offspring, non-Jewish UC-affected offspring, and all IBD-affected offspring (transmitted:nontransmitted = 45:130, $P = 1.32 \times 10^{-10}$ for the IBD phenotype in all 883 families) (Table 2 and table S2). Our discovery of an uncommon protective allele, or conversely, a very common predisposing allele, reflects a major theme in complex genetics; namely, that functional genetic variation exerts a continuum of susceptibility, neutral, and protective effects. Furthermore, alleles conferring protection against one disease may result in increased risk for another (*10*).

Table 1. Non-Jewish and Jewish ileal Crohn's disease (CD) case-control association study results for IL23R region markers with *P*-values < 0.0001 in the non-Jewish cohort. Minor allele frequencies (MAF), allelic test *P*-values, and odds ratios (OR) with 95% confidence intervals (CI) are shown for each case-control cohort (*8*). The ORs shown are for the minor allele. Combined Cochran-Mantel-Haenszel *P*-values are also shown (*8*). UTR, untranslated region.

Marker	Location	Non-Jewish case-control cohort				Jewish case-control cohort				Combined *P*-value
		CD (*n* = 547) MAF	Control (*n* = 548) MAF	*P*-value	OR [95% CI]	CD (*n* = 401) MAF	Control (*n* = 433) MAF	*P*-value	OR [95% CI]	
rs1004819	Intron	0.374	0.280	3.79×10^{-6}	1.53 [1.27,1.84]	0.426	0.334	1.00×10^{-4}	1.48 [1.21,1.82]	1.54×10^{-9}
rs7517847	Intron	0.331	0.443	1.09×10^{-7}	0.62 [0.52,0.74]	0.240	0.352	5.84×10^{-7}	0.58 [0.47,0.72]	3.36×10^{-13}
rs10489629	Intron	0.378	0.475	4.27×10^{-6}	0.67 [0.56,0.80]	0.355	0.465	5.79×10^{-6}	0.63 [0.52,0.77]	1.14×10^{-10}
rs2201841	Intron	0.385	0.291	4.57×10^{-6}	1.52 [1.27,1.83]	0.414	0.315	2.92×10^{-5}	1.53 [1.25,1.89]	5.46×10^{-10}
rs11465804	Intron	0.020	0.063	7.52×10^{-7}	0.30 [0.18,0.51]	0.048	0.096	1.39×10^{-4}	0.47 [0.31,0.71]	5.97×10^{-10}
rs11209026	Arg381Gln	0.019	0.070	5.05×10^{-9}	0.26 [0.15,0.43]	0.033	0.070	7.95×10^{-4}	0.45 [0.27,0.73]	3.55×10^{-11}
rs1343151	Intron	0.275	0.370	2.26×10^{-6}	0.65 [0.54,0.78]	0.229	0.336	1.69×10^{-6}	0.59 [0.47,0.73]	1.64×10^{-11}
rs10889677	Exon-3'UTR	0.385	0.288	1.82×10^{-6}	1.55 [1.29,1.86]	0.419	0.316	1.51×10^{-5}	1.56 [1.27,1.91]	9.58×10^{-11}
rs11209032	Intergenic	0.393	0.293	1.03×10^{-6}	1.56 [1.30,1.87]	0.382	0.298	3.49×10^{-4}	1.45 [1.18,1.79]	1.60×10^{-9}
rs1495965	Intergenic	0.498	0.412	2.93×10^{-5}	1.44 [1.21,1.71]	0.469	0.412	2.04×10^{-2}	1.26 [1.03,1.53]	2.55×10^{-6}

Table 2. Family-based and combined (case-control and family-based) association results. Family-based association *P*-values were computed using the empirical variance estimator implemented in the FBAT software package (*8*). Combined Fisher *P*-values for all case-control (Table 1) and nuclear family cohorts are also shown (*8*). UTR, untranslated region.

Marker	Location	Non-Jewish CD (518 families, 651 affected offspring)	Non-Jewish UC (215 families, 251 affected offspring)	Jewish CD (77 families, 99 affected offspring)	Jewish UC (80 families, 91 affected offspring)	All IBD (883 families, 1,119 affected offspring)	Combined (family-based and case-control) *P*-value
		P-value	*P*-value	*P*-value	*P*-value	*P*-value	
rs1004819	Intron	3.60×10^{-5}	1.20×10^{-3}	1.24×10^{-2}	5.47×10^{-1}	6.06×10^{-8}	1.78×10^{-14}
rs7517847	Intron	2.30×10^{-5}	2.71×10^{-1}	3.50×10^{-2}	5.00×10^{-1}	1.80×10^{-5}	9.99×10^{-16}
rs10489629	Intron	1.87×10^{-3}	2.70×10^{-1}	4.33×10^{-1}	8.21×10^{-1}	1.27×10^{-3}	1.62×10^{-11}
rs2201841	Intron	5.80×10^{-4}	3.21×10^{-4}	3.50×10^{-2}	5.69×10^{-1}	1.04×10^{-7}	1.10×10^{-14}
rs11465804	Intron	1.32×10^{-4}	2.70×10^{-3}	8.90×10^{-5}	3.71×10^{-1}	3.46×10^{-9}	3.33×10^{-16}
rs11209026	Arg381Gln	8.00×10^{-6}	2.97×10^{-4}	9.41×10^{-4}	4.91×10^{-1}	1.32×10^{-10}	6.62×10^{-19}
rs1343151	Intron	9.63×10^{-2}	8.51×10^{-2}	3.30×10^{-2}	1.89×10^{-1}	1.24×10^{-3}	2.74×10^{-12}
rs10889677	Exon-3'UTR	2.60×10^{-3}	3.35×10^{-4}	5.88×10^{-2}	7.32×10^{-1}	1.65×10^{-6}	3.40×10^{-14}
rs11209032	Intergenic	2.68×10^{-3}	3.57×10^{-4}	3.48×10^{-2}	7.50×10^{-1}	2.41×10^{-6}	5.50×10^{-13}
rs1495965	Intergenic	4.07×10^{-4}	1.74×10^{-2}	3.93×10^{-2}	9.21×10^{-1}	1.72×10^{-5}	3.55×10^{-9}

In addition to Arg381Gln, we found several other variants within the *IL23R* gene that are also associated with IBD (Tables 1 and 2 and tables S1 and S2). Marker rs11465804 is an intronic variant in a nonconserved region and is in significant linkage disequilibrium with Arg381Gln (correlation coefficient $r^2 = 0.84$ in the case-control data) and therefore is unlikely to confer disease risk independent of the latter. However, other markers show evidence for association that appears to be independent of Arg381Gln. For example, rs7517847, which has the most significant association *P*-value (3.36×10^{-13}) in the combined analysis of both ileal CD case-control cohorts (Table 1), is not in significant linkage disequilibrium with Arg381Gln ($r^2 = 0.03$ in the case-control data). To identify variants that are independent of the Arg381Gln signal, we performed conditional association testing of the combined case-control data by stratifying on the Arg381Gln genotypes. The *P*-values for these conditional tests (table S3) demonstrate multiple residual association signals throughout *IL23R*, indicating that there are multiple risk variants in the region. The *IL23R* gene is expressed as at least six alternatively spliced mRNAs, which generate diverse isoforms of the receptor protein (*11*). The most common splice variants result in the deletion of exons 7 and/or 10. We therefore speculate that the multiple genetic association signals detected in the centromeric portion of *IL23R* (Fig. 1) could exert their influence via differential splicing.

Notably, we found no evidence for association in our non-Jewish, ileal CD case-control cohort (table S4) with the *IL12RB1* gene, which encodes the second subunit of the IL-23 receptor (*9*), or the *IL23A* and *IL12B* genes, which encode the p19 and p40 subunits, respectively, of the heterodimeric IL-23 cytokine (*12*).

Previous work with mouse models has documented a requirement for IL-23 in murine colitis (*13*), experimental autoimmune encephalitis (*14*), and collagen-induced arthritis (*15*). IL-23 activity is present in the terminal ileum (*16*) and colon (*17*), and the present study demonstrates that *IL23R* variants are associated with both small intestinal (ileal CD) and large intestinal (UC) inflammation. Furthermore, transgenic expression of IL-23 subunit p19 results in severe systemic inflammation, including in the small and large intestine (*18*), highlighting this pathway's particular role in promoting strong activation of effector T cells and perpetuation of organ-specific inflammatory responses. At least part of this effect is likely mediated via inflammatory, IL-17–producing T cells (*19*–*23*), and elevated IL-17 levels have been observed in the colonic mucosa of both CD and UC patients (*24*).

Taken together, these findings suggest that blockade of the IL-23 signaling pathway would be a rational therapeutic strategy for IBD. In support of this, a monoclonal antibody directed against the p40 subunit of the receptor, which blocks both IL-23 and IL-12 proinflammatory activities, has produced promising results in a clinical trial of Crohn's disease (*25*). It has been postulated that specific targeting of the IL23p19/IL23R pathway may be particularly effective in blocking organ-specific inflammation, with less compromise of protective responses (*26*). However, at least one model of murine colitis is worsened in the absence of IL-23, implicating a role for IL-23 in the down-regulation of IL-12 (*27*). In addition, IL-23 function may be important for proper responses to mycobacterial (*28*, *29*) and intestinal infections (*22*). In assessing therapeutic approaches, the strong protective effect of the Arg381Gln allele could potentially be exploited to define desired functional outcomes (*10*). The contribution of the *IL23R* pathway to IBD will likely involve more than simple gain- or loss-of-function *IL23R* variants, and therapeutic interventions will be improved by a better understanding of the context and tissue-specific events associated with functional *IL23R* polymorphisms.

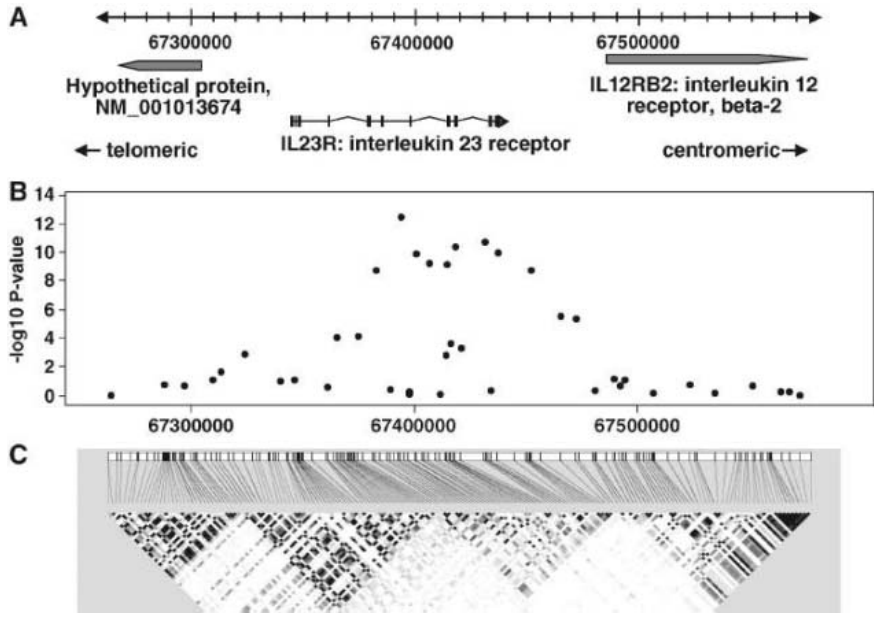

Fig. 1. Association signals in the *IL23R* gene region on chromosome 1p31. (**A**) Genomic locations of genes on chromosome 1p31 between 67,260,000 and 67,580,000 base pairs (Build 35). (**B**) The negative $\log_{10}$ association *P*-values (Cochran-Mantel-Haenszel chi-square test) from the combined Jewish and non-Jewish case-control cohorts are plotted for genotyped markers in the region. (**C**) Pairwise r^2 plot for International HapMap CEU data. The intensity of the shading is proportional to r^2. The *IL23R* gene is contained within two blocks of linkage disequilibrium, and the association signals are strongest in the centromeric block, which contains exons 5 to 11 and extends into the intergenic region between *IL23R* and *IL12RB2*. Note that markers in the block encompassing the *IL12RB2* gene do not demonstrate significant association.

References and Notes

1. D. K. Podolsky, *N. Engl. J. Med.* **347**, 417 (2002).
2. E. V. Loftus Jr., *Gastroenterology* **126**, 1504 (2004).
3. S. Vermeire, P. Rutgeerts, *Genes Immun.* **6**, 637 (2005).
4. J.-P. Hugot *et al.*, *Nature* **411**, 599 (2001).
5. Y. Ogura *et al.*, *Nature* **411**, 603 (2001).
6. J. D. Rioux *et al.*, *Nat. Genet.* **29**, 223 (2001).
7. V. D. Peltekova *et al.*, *Nat. Genet.* **36**, 471 (2004).
8. Materials and methods are available as supporting material on *Science* Online.
9. C. Parham *et al.*, *J. Immunol.* **168**, 5699 (2002).
10. J. H. Nadeau, E. J. Topol, *Nat. Genet.* **38**, 1095 (2006).
11. X. Y. Zhang *et al.*, *Immunogenetics* **57**, 934 (2006).
12. B. Oppmann *et al.*, *Immunity* **13**, 715 (2000).
13. D. Yen *et al.*, *J. Clin. Invest.* **116**, 1310 (2006).
14. D. J. Cua *et al.*, *Nature* **421**, 744 (2003).
15. C. A. Murphy *et al.*, *J. Exp. Med.* **198**, 1951 (2003).
16. C. Becker *et al.*, *J. Clin. Invest.* **112**, 693 (2003).
17. I. J. Fuss *et al.*, *Inflamm. Bowel Dis.* **12**, 9 (2006).
18. M. T. Wiekowski *et al.*, *J. Immunol.* **166**, 7563 (2001).
19. S. Aggarwal, N. Ghilardi, M. H. Xie, F. J. de Sauvage, A. L. Gurney, *J. Biol. Chem.* **278**, 1910 (2003).
20. C. L. Langrish *et al.*, *J. Exp. Med.* **201**, 233 (2005).
21. E. Bettelli *et al.*, *Nature* **441**, 235 (2006).
22. P. R. Mangan *et al.*, *Nature* **441**, 231 (2006).
23. M. Veldhoen, R. J. Hocking, C. J. Atkins, R. M. Locksley, B. Stockinger, *Immunity* **24**, 179 (2006).
24. S. Fujino *et al.*, *Gut* **52**, 65 (2003).
25. P. J. Mannon *et al.*, *N. Engl. J. Med.* **351**, 2069 (2004).
26. B. S. McKenzie, R. A. Kastelein, D. J. Cua, *Trends Immunol.* **27**, 17 (2006).
27. C. Becker *et al.*, *J. Immunol.* **177**, 2760 (2006).
28. F. A. Verreck *et al.*, *Proc. Natl. Acad. Sci. U.S.A.* **101**, 4560 (2004).
29. A. M. Cooper *et al.*, *J. Immunol.* **168**, 1322 (2002).

30. We thank the patients and their families for participating in the studies. The National Institute of Diabetes and Digestive and Kidney Diseases IBD Genetics Consortium is funded by the following grants: DK62431 (S.R.B.), DK62422 (J.H.C.), DK62420 (R.H.D.), DK62432 (J.D.R.), DK62423 (M.S.S.), DK62413 (K.D.T.), and DK62429 (J.H.C.). A.H.S. is on the Scientific Advisory Boards of Shire Pharmaceuticals, Schering (Canada), and Procter & Gamble Pharmaceuticals.

Supporting Online Material

www.sciencemag.org/cgi/content/full/1135245/DC1
Materials and Methods
Fig. S1
Tables S1 to S4
References and Notes

18 September 2006; accepted 18 October 2006
Published online 26 October 2006;
10.1126/science.1135245
Include this information when citing this paper.

Microfluidic Digital PCR Enables Multigene Analysis of Individual Environmental Bacteria

Elizabeth A. Ottesen,[1] Jong Wook Hong,[2] Stephen R. Quake,[3] Jared R. Leadbetter[4]*

Gene inventory and metagenomic techniques have allowed rapid exploration of bacterial diversity and the potential physiologies present within microbial communities. However, it remains nontrivial to discover the identities of environmental bacteria carrying two or more genes of interest. We have used microfluidic digital polymerase chain reaction (PCR) to amplify and analyze multiple, different genes obtained from single bacterial cells harvested from nature. A gene encoding a key enzyme involved in the mutualistic symbiosis occurring between termites and their gut microbiota was used as an experimental hook to discover the previously unknown ribosomal RNA–based species identity of several symbionts. The ability to systematically identify bacteria carrying a particular gene and to link any two or more genes of interest to single species residing in complex ecosystems opens up new opportunities for research on the environment.

A major challenge of environmental science is the identification of microbial species capable of catalyzing important activities in situ (*1*). PCR-based techniques that use single genes as proxies for organisms or key microbial activities continue to provide valuable insights into microbial community diversity (*2*–*4*). However, it has been difficult to interrelate gene inventories to derive correspondences between any two or more specific genes of interest, or to determine the phylogenetic species identity of organisms carrying particular genetic capabilities. Metagenomic (*5*) analyses of complex communities are dominated by genome "shrapnel"; unless the microbial community is dominated by one or a few species (*6*, *7*), resident genomes are not reliably reconstructed via computation (*8*, *9*). A gene of interest can be attributed to a specific organism only if it is linked to an unambiguous phylogenetic marker (i.e., on the same genome fragment) (*5*, *10*). Both PCR and metagenomic studies are typically carried out on homogenized, whole-community genomic DNA preparations. Thus, the cell as a distinct informational entity is almost entirely lost.

Outside of traditional culture-based isolation, few approaches can attribute multiple genes to a single species or cell type. Microautoradiography (*11*) and stable isotope probing (*12*) allow detection of cells or retrieval of genetic material from organisms that use a substrate of interest, but these techniques require active cellular incorporation of that substrate. Microscopy-based in situ hybridization techniques [fluorescence in situ hybridization (FISH) and variants (*13*, *14*)] allow colocalization of sequences through probe hybridization, but these methods require that both genes be actively transcribed, that their sequences be known in advance, and that their difference from related, nontarget genes is sufficient to enable effective probe design and implementation. Single-cell whole-genome amplification has recently been reported for a highly abundant, culturable marine microbial species, but has not yet been shown to be scalable to interrogating multitudes of diverse, co-resident microbes (*15*). Here, we applied commercially available microfluidic devices to perform a variant of "digital PCR" (*16*), separating and interrogating hundreds of individual environmental bacteria in parallel.

Microfluidic devices allow control and manipulation of small volumes of liquid (*17*, *18*), in this case allowing for rapid separation and partitioning of single cells from a complex parent sample. Single, partitioned cells served as templates for individual multiplex PCR reactions using primers and probes for simultaneous amplification of both small-subunit ribosomal RNA (rRNA) and metabolic genes of interest. Primers and probes with broad target specificities were used, with subsequent resolution of exact gene sequences after successful amplification and retrieval. This technique operates independent of gene expression, position on the genome, or physiological state of the cell at the time of harvest. The result was rapid colocalization of two genes (encoding 16*S* rRNA and a key metabolic enzyme) to single-genome templates, along with the determination of the fraction of cells within the community that encoded them. Subsequent retrieval of PCR products from individual chambers allowed sequence analysis of both genes.

Phylogenetic analysis of the rRNA gene allows classification of the host bacterium, and the metabolic gene is sequenced to confirm that the cell carried the genotype of interest. Additionally, because microfluidic digital PCR yields fluorescent signal upon amplification of a gene regardless of the number of copies present in the cell, this approach can yield estimates of the fraction represented by a given species within the general microbial community. The number of *rrn* operons present in a genome can vary widely, ranging from 1 [e.g., *Rickettsia prowazekii* (*19*)] to 15 [e.g., *Clostridium paradoxum* (*20*)], confounding the interpretation of traditional environmental gene inventories. Moreover, the use of single-cell PCR to prepare clone libraries avoids complications and PCR artifacts such as amplification biases and unresolvable chimeric products (*21*).

We used this technique to examine a complex, species-rich environment: the lignocellulose-decomposing microbial community resident in the hindguts of wood-feeding termites. Therein, the bacterial metabolism known as CO_2-reductive homoacetogenesis is one of the major sources of the bacterial fermentation product acetate (*22*). Acetogenic bacteria must compete for hydrogen with *Archaea* that generate methane, a potent greenhouse gas for which termites are considered a small yet significant source. Because of their high rates of bacterially mediated homoacetogenesis, many termites contribute less to the global methane budget than they might otherwise (*23*). Additionally, acetate serves as the insect host's major carbon and energy source, literally fueling a large proportion of this mutualistic symbiosis (*22*, *24*, *25*). A key gene of the homoacetogenesis pathway encodes formyl-tetrahydrofolate synthetase (FTHFS) (*26*). Although a diverse inventory of termite hindgut community FTHFS variants already existed (*27*), the identities of the organisms dominating homoacetogenesis in termites had remained uncertain. Here, with the use of microfluidics, we discovered the identities of a multitude of FTHFS-encoding organisms by determining their specific 16*S* rRNA gene sequences.

The "clone H group" of FTHFS genotypes corresponds to a large fraction of the sequences collected during an inventory of FTHFS genes present in the termite hindgut environment (*27*). We designed a specific primer set and a fluorescein-labeled probe capable of on-chip detection and amplification of the genotypes comprising this FTHFS group. We also redesigned broad-specificity "all-bacterial" 16*S* rRNA gene primers and used a previously published probe (*28*) to amplify and detect bacterial rRNA genes. Both the all-bacterial 16*S* rRNA gene and clone H group FTHFS primer-probe sets showed single-molecule sensitivity in multiplex on-chip reactions using purified plasmid or termite gut community DNA. The observed success rate for the amplification of individual genes from single-molecule templates was 48% (fig. S1) (*29*); thus, the success rate for coamplification of two genes from single-molecule templates is estimated to be about 1 in 5.

[1]Division of Biology, California Institute of Technology, Pasadena, CA 91125, USA. [2]Materials Research and Education Center, Samuel Ginn College of Engineering, Auburn University, Auburn, AL 36849, USA. [3]Department of Bioengineering and Howard Hughes Medical Institute, Stanford University, Stanford, CA 94305, USA. [4]Environmental Science and Engineering Program, California Institute of Technology, Pasadena, CA 91125, USA.

*To whom correspondence should be addressed. E-mail: jleadbetter@caltech.edu

Freshly collected termite hindgut luminal contents were suspended in a PCR reaction buffer and loaded into a microfluidic device (*29*). Each microfluidic panel uses micromechanical valves to randomly partition a single PCR mixture into 1176 independent 6.25-nl reaction chambers (Fig. 1). We considered single-cell separation to be achieved when fewer than one-third of chambers showed rRNA gene amplification. Assuming a Poisson distribution of cells, under such conditions 6% of chambers should have contained multiple cells or cell aggregates (*30*). PCR was carried out on a conventional flat-block thermocycler. Amplification was monitored using 5′ nuclease probes to generate a fluorescent signal detected with a modified microarray scanner.

Multiplex PCR amplifications from single cells or cell aggregates were successfully performed using diluted gut contents that had been partitioned on-chip (Fig. 2, left). We found global averages of 1.2 (±0.8) × 10^8 total bacterial 16*S* rRNA gene encoding units and 1.5 (±1.0) × 10^6 total clone H group FTHFS gene encoding units per *Zootermopsis nevadensis* termite (*31*). This suggests that, in *Z. nevadensis*, these particular FTHFS genes are carried by a minority population representing ~1% of gut symbionts. The observed variability of these measurements was not surprising, as the *Z. nevadensis* specimens examined were collected from different colonies and locations and had been maintained in captivity for varying periods of time.

Amplification products were retrieved from reaction chambers via syringe needle and were reamplified, cloned, sequenced, and analyzed using standard methods. Twenty randomly selected chambers that had amplified only a 16*S* rRNA gene (and not FTHFS) yielded a diversity of *Endomicrobia*, *Firmicutes*, *Bacteroidetes*, *Proteobacteria*, and *Spirochaetes* ribotypes, as expected on the basis of prior 16*S* rRNA gene clone libraries (*32*) (figs. S2 and S3). Two-thirds of chambers positive for FTHFS genes did not amplify 16*S* rRNA genes when either all-bacterial or termite treponeme–specific rRNA gene primers were used. This amplification success rate is comparable to that observed when purified, single-molecule templates were used (e.g., fig. S1) and remains a target for refinement and improvement in the future.

PCR products were retrieved and analyzed from 28 reaction chambers that coamplified both FTHFS and 16*S* rRNA genes. In 10 of those reactions, sequence analyses revealed that the FTHFS gene had coamplified with a clade of closely related 16*S* rRNA gene sequences affiliating with the "termite spirochete cluster" (*33*) of the genus *Treponema*. Members of this novel clade were never observed in chambers that lacked FTHFS gene amplification. An additional three chambers contained a single FTHFS type and multiple 16*S* rRNA genotypes, one of which in each affiliated with the above-mentioned group [*Zootermopsis* environmental genomovar (ZEG) 11.4, 10.2, and 10.1]. These latter reactions also contained two additional other *Spirochaetes* (Zn-FG7A and B in Fig. 3) in one chamber, a single γ-*Proteobacterium*

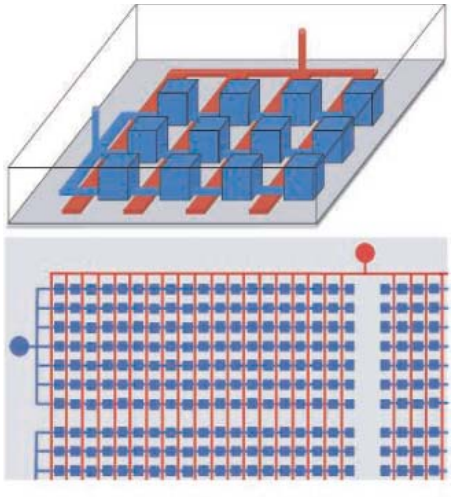

Fig. 1. Microfluidic digital PCR chip. Top: Schematic diagram showing many parallel chambers (blue) connected by channels to a single input. When pneumatic or hydraulic pressure is applied to the control channel network (red), the membranes between the red and blue channels are deflected upward, creating micromechanical valves. When the valves are closed, the continuous blue network is partitioned into independent PCR reactors. Bottom: Schematic showing how a single valve connection can be used to partition thousands of chambers. In the device used, each experimental sample could be partitioned into 1176 chambers, and each device contained 12 such sample panels.

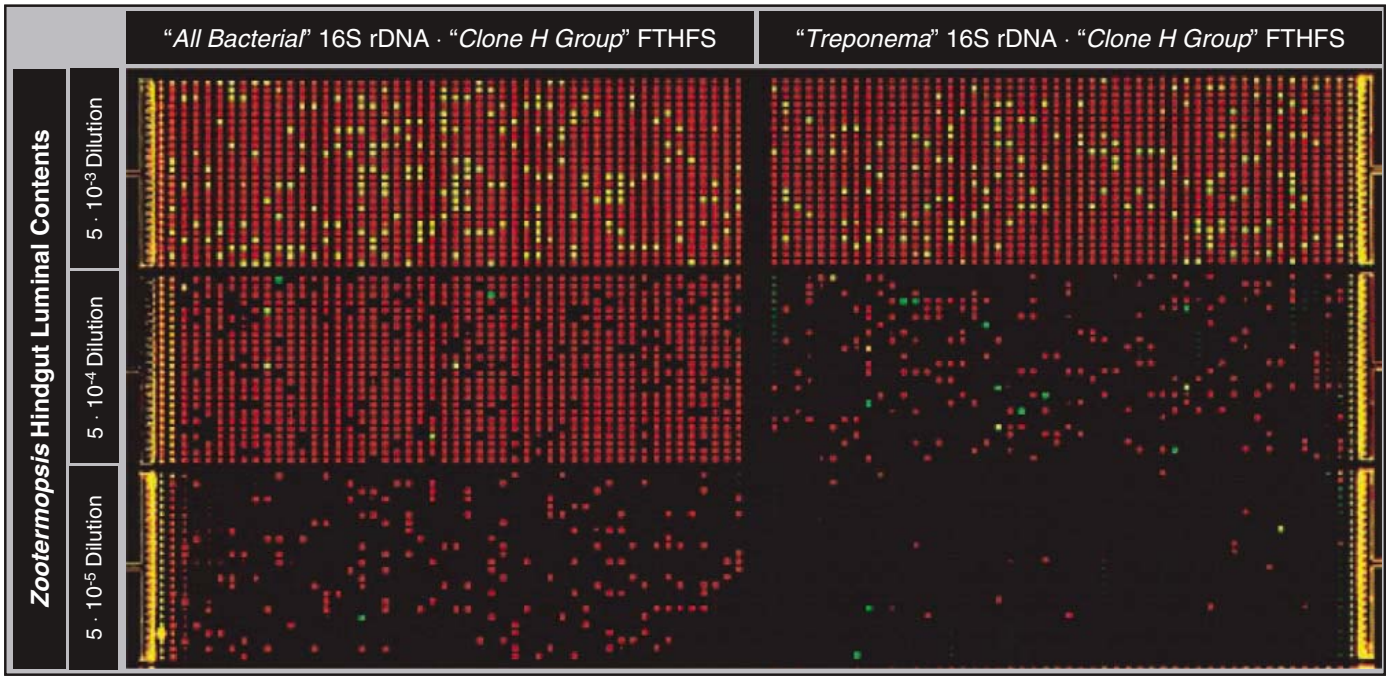

Fig. 2. Multiplex microfluidic digital PCR of single cells in environmental samples. Six panels from a representative experiment show microfluidic digital PCR on diluted hindgut contents harvested from a single *Z. nevadensis* individual. Left: Multiplex PCR using "all-bacterial" 16*S* rRNA gene (red fluorescence) and "clone H group" (*27*) FTHFS gene (green fluorescence) primers and probes. Reaction chambers that contained both genes in 1/500,000 dilutions from this and other on-chip experiments were sampled and the PCR products were analyzed (see Fig. 3). Right: The same, except that 16*S* rRNA primers specifically targeted members of the "termite cluster" (*33*) of the spirochetal genus *Treponema.*

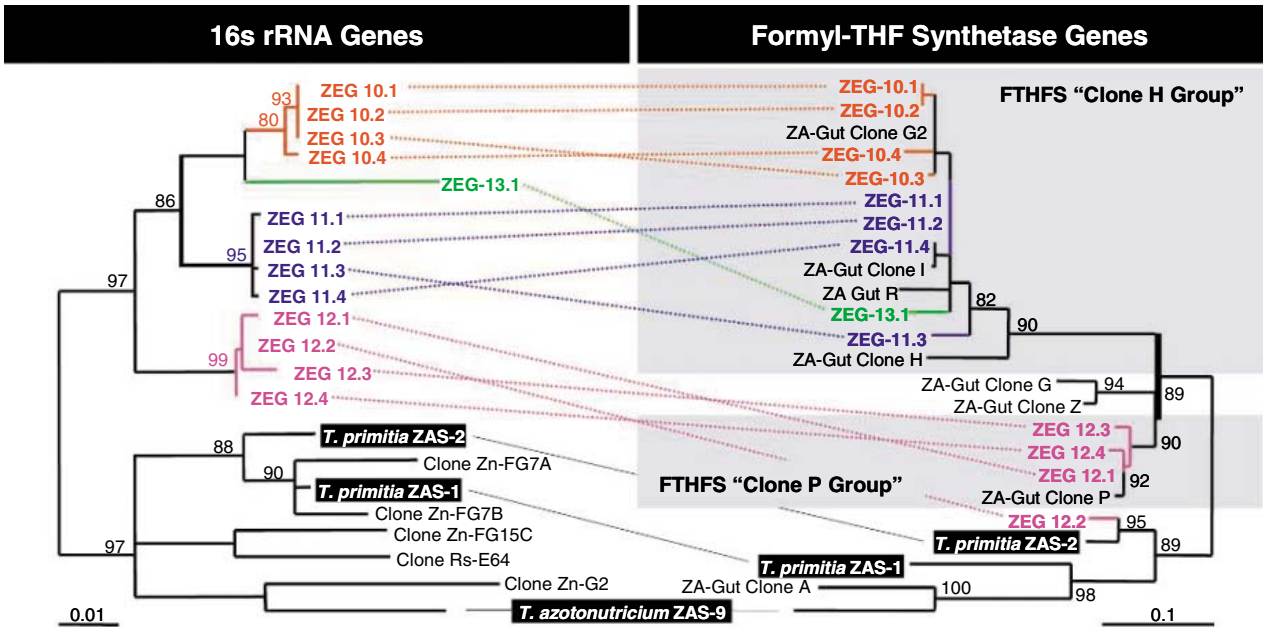

Fig. 3. "Clone H group" and "clone P group" FTHFS genes are encoded by not yet cultivated termite gut treponemes. Left: Phylogenetic tree of 16*S* rRNA genes cloned from cultivated strain isolates (orange) and from hindgut community microbiota. Right: Phylogenetic tree of FTHFS genes from the termite hindgut. Dotted lines connect genes believed to originate from the same genome. Incongruent gene phylogenies implicate acquisition of FTHFS genes via lateral gene transfer and can be observed in both isolated species (*Treponema primitia* ZAS-1) and proposed "environmental genomovars" (ZEG 12.2). Scale bars represent substitutions per alignment position. The trees were constructed using TreePuzzle (*39*); 630 (16*S* rDNA) and 249 (FTHFS) nucleotide positions were used. Citations for all sequences are listed in table S1.

sequence (Zn-FG12) in the second, and a *Firmicutes* sequence (Zn-FG1) in the third. The remaining 15 chambers analyzed (which coamplified FTHFS and rRNA genes) yielded 16*S* rDNA sequences in proportions that corresponded well with the ribotype diversity encountered in the general non-FTHFS encoding population. On the basis of this evidence, we conclude that the unique cluster of termite gut treponeme rRNA gene sequences that were repeatedly identified in FTHFS-containing chambers represents the ribotype of the FTHFS-encoding cells. We attribute the instances of FTHFS colocalization with other rRNA gene sequences to cell-cell aggregations. The latter is not to be unexpected in a complex, wood particle–filled, sticky environment such as the termite hindgut (*34*, *35*). Such aggregations appear to be largely random, although there may be a slight enrichment of proteobacterial sequences relative to the general population (figs. S2 and S3). Our results show that FTHFS sequences present in ~1% of bacterial cells were, in 13 of 28 trials, found in association with a 16*S* rRNA sequence type not identified in 20 random samplings of the bacterial population (16*S* rRNA–only chambers) at large. The probability of a 16*S* rRNA gene sequence type that is present in less than 5% of the population randomly colocalizing with FTHFS in 13 of 28 trials is low, on the order of 10^{-10} (*36*).

Refined phylogenetic analysis of 16*S* rRNA gene sequences that were repeatedly isolated from FTHFS-containing reaction chambers revealed that all such 16*S* rRNA gene sequences affiliated within the termite gut treponeme cluster of *Spirochaetes*. These 16*S* rRNA genes group into four distinct ribotype clusters (Fig. 3). These four sequence types share within-group sequence identity of >99% and between-group identities of 95 to 99%. We propose the term "environmental genomovar" (genome variant) to describe not-yet-cultivated organisms shown to encode two or more known genes of interest. Here, we label the four 16*S* ribotypes identified as ZEG 10 through 13; three genomovars (ZEG 10, 11, and 13) encode clone H group FTHFS sequences, whereas one genomovar (ZEG 12) encodes a clone P group FTHFS sequence. Previously, nine termite gut treponemes had been isolated and assigned the strain epithet ZAS (*Zootermopsis* acetogenic spirochete) 1 through 9 (*37*, *38*).

To build additional support for a spirochetal origin of clone H group FTHFS genotypes, we designed and used a termite treponeme–specific 16*S* rRNA gene primer set and gene probe, with the aim of reducing nonspirochetal background (Fig. 2, right). The frequency with which clone H group FTHFS genes were recovered increased from 1 in 175 cells of the general bacterial population, to 1 in 16 treponemal cells [several termite gut treponemes are already known or suspected to encode FTHFS genotypic variants that would not amplify with the clone H group FTHFS primer and probe set (*27*) (fig. S1)]. Similar to the amplification success rates observed in experiments using the "all-bacterial" 16*S* rRNA gene primers (Fig. 2, left) and those using the clone H primers against purified single-molecule templates (fig. S1), about one-third of FTHFS-positive reaction chambers also amplified detectable levels of 16*S* rRNA genes. Treponemal cells were deduced to constitute 10 to 12% of the bacterial community of *Z. nevadensis* (comparing amplification frequencies in the left and right panels of Fig. 3).

Our results show that specific, not yet cultivated *Treponema* species encode variants of a key gene underlying the dominant bacterial metabolism known to affect the energy needs of their termite hosts. The microfluidic, multiplex digital PCR approach taken here can be extended to expand our understanding of the genetic capacities of not-yet-cultivated species, and to collect and collate genetic information in a manner that builds conceptual genomovars that directly represent the organisms catalyzing important activities in various environments of global relevance.

References and Notes

1. N. D. Gray, I. M. Head, *Environ. Microbiol.* **3**, 481 (2001).
2. E. Zuckerkandl, L. Pauling, *J. Theor. Biol.* **8**, 357 (1965).
3. P. Hugenholtz, B. M. Goebel, N. R. Pace, *J. Bacteriol.* **180**, 4765 (1998).
4. S. J. Sogin, M. L. Sogin, C. R. Woese, *J. Mol. Evol.* **1**, 173 (1971).
5. C. S. Riesenfeld, P. D. Schloss, J. Handelsman, *Annu. Rev. Genet.* **38**, 525 (2004).
6. G. W. Tyson *et al.*, *Nature* **428**, 37 (2004).
7. M. Strous *et al.*, *Nature* **440**, 790 (2006).
8. S. G. Tringe *et al.*, *Science* **308**, 554 (2005).

9. J. C. Venter *et al.*, *Science* **304**, 66 (2004); published online 4 March 2004 (10.1126/science.1093857).
10. O. Béjà *et al.*, *Science* **289**, 1902 (2000).
11. J. L. Nielsen, D. Christensen, M. Kloppenborg, P. H. Nielsen, *Environ. Microbiol.* **5**, 202 (2003).
12. M. Manefield, A. S. Whiteley, R. I. Griffiths, M. J. Bailey, *Appl. Environ. Microbiol.* **68**, 2002 (2002).
13. R. I. Amann, W. Ludwig, K. H. Schleifer, *Microbiol. Rev.* **59**, 143 (1995).
14. K. Zwirglmaier, W. Ludwig, K. H. Schleifer, *Mol. Microbiol.* **51**, 89 (2004).
15. K. Zhang *et al.*, *Nat. Biotechnol.* **24**, 680 (2006).
16. B. Vogelstein, K. W. Kinzler, *Proc. Natl. Acad. Sci. U.S.A.* **96**, 9236 (1999).
17. T. Thorsen, S. J. Maerkl, S. R. Quake, *Science* **298**, 580 (2002); published online 26 September 2002 (10.1126/science.1076996).
18. J. W. Hong, S. R. Quake, *Nat. Biotechnol.* **21**, 1179 (2003).
19. H. Pang, H. H. Winkler, *J. Bacteriol.* **175**, 3893 (1993).
20. F. A. Rainey, N. L. Ward-Rainey, P. H. Janssen, H. Hippe, E. Stackebrandt, *Microbiology* **142**, 2087 (1996).
21. S. G. Acinas, R. Sarma-Rupavtarm, V. Klepac-Ceraj, M. F. Polz, *Appl. Environ. Microbiol.* **71**, 8966 (2005).
22. J. A. Breznak, J. M. Switzer, *Appl. Environ. Microbiol.* **52**, 623 (1986).
23. A. Brauman, M. D. Kane, M. Labat, J. A. Breznak, *Science* **257**, 1384 (1992).
24. D. A. Odelson, J. A. Breznak, *Appl. Environ. Microbiol.* **45**, 1602 (1983).
25. A. Tholen, A. Brune, *Environ. Microbiol.* **2**, 436 (2000).
26. L. G. Ljungdahl, *Annu. Rev. Microbiol.* **40**, 415 (1986).
27. T. M. Salmassi, J. R. Leadbetter, *Microbiology* **149**, 2529 (2003).
28. M. T. Suzuki, L. T. Taylor, E. F. DeLong, *Appl. Environ. Microbiol.* **66**, 4605 (2000).
29. See supporting material on *Science* Online.
30. Assuming a Poisson distribution, if 67% of chambers are empty, then the expected number of cells per chamber is –ln 0.67 or 0.40. The probability that a chamber contains more than one cell is $1 - 0.67 - ((e^{-0.40})*(0.40^1))/(1!)$ or 6.2%.
31. Value ± 1 standard deviation; 13 termites served as source of cells for $n = 32$ sample panels. All sample panels that met our conditions for single-cell separation and contained at least one FTHFS-positive chamber were used in calculation of gut bacterial loads.
32. M. Ohkuma, T. Kudo, *Appl. Environ. Microbiol.* **62**, 461 (1996).
33. T. G. Lilburn, T. M. Schmidt, J. A. Breznak, *Environ. Microbiol.* **1**, 331 (1999).
34. J. A. Breznak, H. S. Pankratz, *Appl. Environ. Microbiol.* **33**, 406 (1977).
35. J. R. Leadbetter, J. A. Breznak, *Appl. Environ. Microbiol.* **62**, 3620 (1996).
36. The binomial distribution function was used to calculate the probability that, in 13 of 28 trials, a sequence that is present in 5% of chambers (0 of 20 16*S*-only chambers) would randomly colocalize with clone H group FTHFS sequences.
37. J. R. Leadbetter, T. M. Schmidt, J. R. Graber, J. A. Breznak, *Science* **283**, 686 (1999).
38. T. G. Lilburn *et al.*, *Science* **292**, 2495 (2001).
39. H. A. Schmidt, K. Strimmer, M. Vingron, A. von Haeseler, *Bioinformatics* **18**, 502 (2002).

40. We thank M. Unger, A. Daridon, and L. Warren for advice and discussions. Supported by NIH grant 1RO1 HG002644-01A1, NIH National Research Service Award grant 5 T32 GM07616, an NIH Director's Pioneer Award, and NSF grant DEB-0321753. S.R.Q. is a founder, shareholder, and consultant for Fluidigm Corporation.

16 June 2006; accepted 30 October 2006
10.1126/science.1131370

Prevention of *Brca1*-Mediated Mammary Tumorigenesis in Mice by a Progesterone Antagonist

Aleksandra Jovanovic Poole,[1,2]* Ying Li,[1,2]* Yoon Kim,[1,2] Suh-Chin J. Lin,[1,2]† Wen-Hwa Lee,[1] Eva Y.-H. P. Lee[1,2]‡

Women with mutations in the breast cancer susceptibility gene *BRCA1* are predisposed to breast and ovarian cancers. Why the BRCA1 protein suppresses tumor development specifically in ovarian hormone–sensitive tissues remains unclear. We demonstrate that mammary glands of nulliparous *Brca1*/*p53*-deficient mice accumulate lateral branches and undergo extensive alveologenesis, a phenotype that occurs only during pregnancy in wild-type mice. Progesterone receptors, but not estrogen receptors, are overexpressed in the mutant mammary epithelial cells because of a defect in their degradation by the proteasome pathway. Treatment of *Brca1*/*p53*-deficient mice with the progesterone antagonist mifepristone (RU 486) prevented mammary tumorigenesis. These findings reveal a tissue-specific function for the BRCA1 protein and raise the possibility that antiprogesterone treatment may be useful for breast cancer prevention in individuals with *BRCA1* mutations.

Mutations in the breast cancer susceptibility gene *BRCA1* are associated with an increased risk of breast and ovarian cancers (*1*). Reduced *BRCA1* expression due to promoter methylation may contribute to breast cancer progression (*2*). The BRCA1 protein has been implicated in DNA damage repair, cell cycle checkpoint control, and transcriptional regulation [reviewed in (*3*, *4*)]. The specific suppression of breast and ovarian carcinogenesis by the pleiotropic BRCA1 tumor suppressor has been attributed to its regulation of estrogen receptor α (ERα) and two progesterone receptor isoforms (PRs) (*5*–*8*), which play important roles in breast development (*9*–*15*). BRCA1 interacts with ER and PRs directly and modulates ligand-dependent and -independent transcription activities of ERα and PR, as well as nongenomic functions of ERα (*5*–*8*). However, the mechanisms by which the ER and PRs contribute to BRCA1-mediated carcinogenesis remain unclear.

Hormone replacement therapy with progesterone and estrogen, but not estrogen alone, has been associated with an elevation in breast cancer risk in postmenopausal women (*16*–*18*). In mice, the long isoform of PR, PR-B, is required for full development of mammary gland (*15*, *19*), and overexpression of the short isoform, PR-A, leads to abnormal mammary gland development and ductal hyperplasia (*20*). These results are consistent with the hypothesis that PRs play a role in breast carcinogenesis.

To address the specific roles of ER and PRs in *Brca1*-mediated tumorigenesis, we studied $p53^{f5\&6/f5\&6}Cre^{c}$ and $Brca1^{f11/f11}p53^{f5\&6/f5\&6}Cre^{c}$ mice (fig. S1A) (*21*, *22*). Inactivation of both *Brca1* and *p53* genes in the mouse mammary gland mimics the majority of human *BRCA1*-associated tumors, which also harbor *p53* mutations (*3*, *4*). $Brca1^{f11/f11}p53^{f5\&6/f5\&6}Cre^{c}$ mammary glands from nulliparous mice at 2.5 months of age showed about 4.5-fold more branching points compared with wild-type or $p53^{f5\&6/f5\&6}Cre^{c}$ glands (Fig. 1A and fig. S1B). By 4 months of age, the nulliparous $Brca1^{f11/f11}p53^{f5\&6/f5\&6}Cre^{c}$ mammary gland showed further accumulation of side branches and extensive alveolar formation (Fig. 1B). The mammary gland morphology of mature, nulliparous $Brca1^{f11/f11}p53^{f5\&6/f5\&6}Cre^{c}$ was similar to that of wild-type pregnant mice, suggesting that proliferation of mammary epithelial cells (MECs) was altered. Proliferation of MECs is regulated by ovarian hormones (*23*). In the estrous phase, MEC proliferation as measured by 5-bromo-2-deoxyuridine (BrdU) incorporation was about five times higher in the $Brca1^{f11/f11}p53^{f5\&6/f5\&6}Cre^{c}$ mice than it was in wild-type or $p53^{f5\&6/f5\&6}Cre^{c}$ mice (Fig. 1C and fig. S1C). Increased MEC proliferation in $Brca1^{f11/f11}p53^{f5\&6/f5\&6}Cre^{c}$ mice was also seen in the diestrous phase (Fig. 1C and fig. S1C). Previous studies have shown that progesterone exerts its functional effects through paracrine action (*24*). Indeed, BrdU-positive MECs were found adjacent to PR-positive cells; there were also BrdU and PR double-positive MECs in the hyperplastic $Brca1^{f11/f11}p53^{f5\&6/f5\&6}Cre^{c}$ mammary gland (fig. S2), indicating that the paracrine action of PR was maintained, at least in most cases.

To assess the contribution of circulating estrogen and progesterone on MEC proliferation,

[1]Department of Biological Chemistry, University of California, Irvine, CA 92697–4037, USA. [2]Department of Developmental and Cell Biology, University of California, Irvine, CA 92697–4037, USA.

*These authors contributed equally to this work.
†Current address: Division of Developmental Biology, Cincinnati Children's Hospital Research Foundation, Cincinnati, OH 45229, USA.
‡To whom correspondence should be addressed. E-mail: elee@uci.edu

we treated ovariectomized mice with progesterone daily for 3 days, followed by BrdU pulse-labeling 2 weeks after surgery. In vehicle-treated mice, no BrdU-positive MECs were found in wild-type and $p53^{f5\&6/f5\&6}Cre^{c}$ mammary glands, but ducts containing one or two BrdU-positive cells were detected in $Brca1^{f11/f11}p53^{f5\&6/f5\&6}Cre^{c}$ mammary glands (Fig. 2A and fig. S3A). Importantly, the number of BrdU-positive MECs in $Brca1^{f11/f11}p53^{f5\&6/f5\&6}Cre^{c}$ mammary glands increased significantly upon exposure either to estradiol or progesterone alone or to a combination of both hormones (Fig. 2A and fig. S3A). The strong mitogenic effect of estradiol and progesterone on $Brca1^{f11/f11}p53^{f5\&6/f5\&6}Cre^{c}$ MECs prompted us to examine the expression of ER and PRs by immunostaining. No difference in ER expression was detected during diestrous or estrous phase.

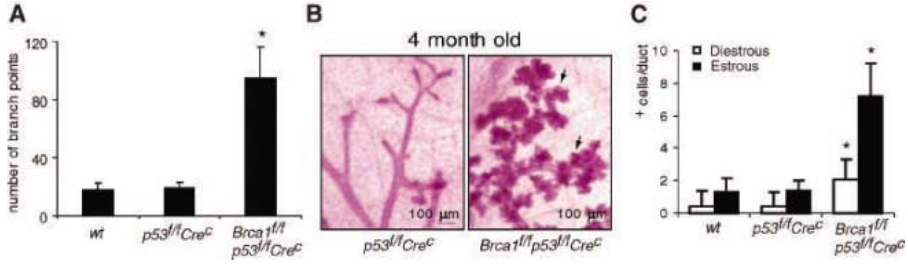

Fig. 1. Mutation in *Brca1/p53* leads to increased mammary ductal branching, alveologenesis, and proliferation. (**A**) Number of branching points in mammary glands of 2.5-month-old wild-type (wt), $p53^{f5\&6/f5\&6}Cre^{c}$, and $Brca1^{f11/f11}p53^{f5\&6/f5\&6}Cre^{c}$ mice was determined. The data represent averages of branch points in five randomly selected areas ± SD. (*$P \leq 0.05$) (**B**) Alveolar development in 4-month-old $p53^{f5\&6/f5\&6}Cre^{c}$ and $Brca1^{f11/f11}p53^{f5\&6/f5\&6}Cre^{c}$ mice. Arrows indicate alveoli. (**C**) Proliferation of mammary epithelial cells was determined at different estrous phases in wt, $p53^{f5\&6/f5\&6}Cre^{c}$, and $Brca1^{f11/f11}p53^{f5\&6/f5\&6}Cre^{c}$ mice by BrdU incorporation. Histogram shows the average number of BrdU-labeled cells per duct ± SD (*$P \leq 0.05$). At least 15 mammary ducts per animal were evaluated (a minimum of three mice per genotype).

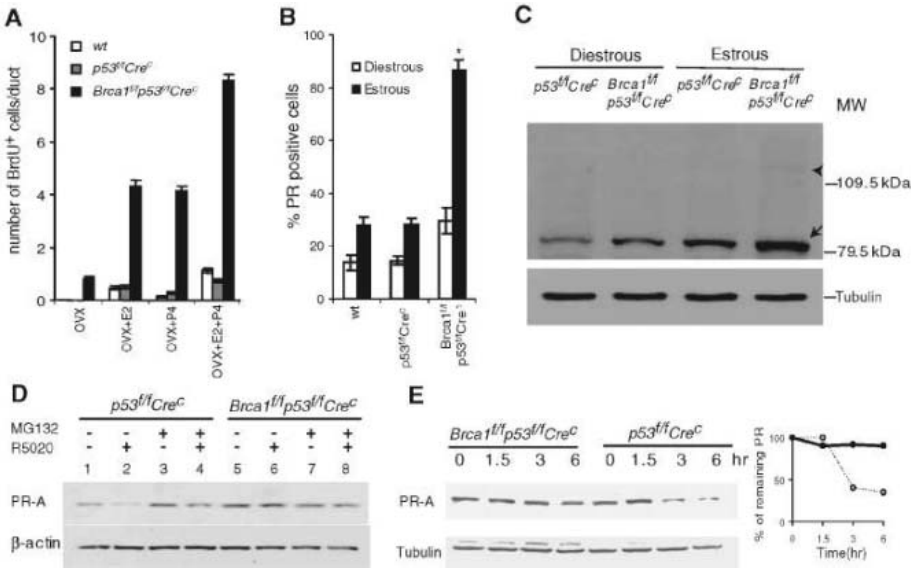

Fig. 2. Mitogenic effect of progesterone on $Brca1^{f11/f11}p53^{f5\&6/f5\&6}Cre^{c}$ mammary gland and stabilization of progesterone receptor in $Brca1^{f11/f11}p53^{f5\&6/f5\&6}Cre^{c}$ mammary epithelial cells. (**A**) Ovariectomized mice (14 to 20 weeks old) were treated with vehicle and 1 μg of E2, 1 mg of P4, or E2 and P4 (E2+P4) for 3 days, and BrdU was injected 2 hours before sacrifice. BrdU-positive MECs were detected by immunostaining and quantified in 15 mammary ducts. Average number of BrdU-positive cells in ovariectomized, E2-, P4-, and E2+P4-treated mice is shown in the histogram (error bars indicate SE,*$P \leq 0.05$). (**B** and **C**) Expression of PR protein in wt, $p53^{f5\&6/f5\&6}Cre^{c}$, and $Brca1^{f11/f11}p53^{f5\&6/f5\&6}Cre^{c}$ mice. Mammary gland tissues harvested at the diestrous or estrous phase were subjected to immunohistochemical staining by using PR antibody (anti-PR). Histogram represents the average percentage of PR-expressing cells per duct (error bars indicate SD). A minimum of five ducts per animal was evaluated (B). Whole-cell extracts from the mammary gland tissues as in (B) were used for immunoprecipitation by using PR antibody followed by Western blotting analyses (C). Arrow indicates PR-A; arrowhead indicates PR-B. (**D**) Effect of proteasome inhibitor, MG132, on PR protein quantities in $p53^{f5\&6/f5\&6}Cre^{c}$ and $Brca1^{f11/f11}p53^{f5\&6/f5\&6}Cre^{c}$ MECs. Cells were starved for 4 hours and then treated with or without MG132 (10 μM) and R5020 (10 nM) for 6 hours as indicated. Western blotting for PR was performed. β-actin served as a loading control. (**E**) Half-life of PR. MECs were treated with 100 μg/ml cyclohexamide and 10 nM R5020. Cells were harvested at the indicated time points. $p53^{f5\&6/f5\&6}Cre^{c}$ MECs, open circles; $Brca1^{f11/f11}p53^{f5\&6/f5\&6}Cre^{c}$ MECs, solid circles.

To explore this possibility, we established MEC cultures from the mammary glands of $Brca1^{f11/f11}p53^{f5\&6/f5\&6}Cre^{c}$ and $p53^{f5\&6/f5\&6}Cre^{c}$ mice at 2 months of age. Ligand treatment induced pronounced degradation of PR-A in $p53^{f5\&6/f5\&6}Cre^{c}$ MECs (Fig. 2D, lanes 1 and 2) compared with $Brca1^{f11/f11}p53^{f5\&6/f5\&6}Cre^{c}$ MECs (Fig. 2D, lanes 5 and 6). PR becomes polyubiquitinated upon exposure to progesterone and is subsequently degraded by the proteasome (*27*). Thus, we found that treatment with the proteasome inhibitor, MG132, led to accumulation of PR-A in $p53^{f5\&6/f5\&6}Cre^{c}$ MECs (Fig. 2D, lanes 2 and 4) but not in $Brca1^{f11/f11}p53^{f5\&6/f5\&6}Cre^{c}$ MECs (Fig. 2D, lanes 6 and 8). In the presence of cyclohexamide, 90% of PR-A remained in $Brca1^{f11/f11}p53^{f5\&6/f5\&6}Cre^{c}$ MECs, whereas only 40% of PR-A was detected in $p53^{f5\&6/f5\&6}Cre^{c}$ MECs 6 hours after the addition of the synthetic progesterone R5020 (Fig. 2E). These data suggest that Brca1 regulates PR stability.

To confirm that BRCA1 exerts a similar regulatory role in human breast cancer cells, we depleted BRCA1 with small interfering RNA

(siRNA) in T47D cells. This treatment led to a 3.5-fold increase in PR-A protein as well as an increase in PR-B, but it did not affect the ERα protein concentration (Fig. 3A, lanes 1 and 2). Treatment with MG132 stabilized both PR isoforms (PR-A and PR-B) in control cells but not in siBRCA1-treated cells (Fig. 3A, lanes 1 and 3 versus 2 and 4). In the absence of ligand, PR-A and PR-B were stable, and only a slight increase was detected in siBRCA1-treated cells (Fig. 3A, lanes 5 and 6). Ligand-induced phosphorylation of PR-B and PR-A, as demonstrated by the mobility shift, was not affected by BRCA1 suppression (Fig. 3A). Previous studies have shown that phosphorylation of Ser^{294} of PR-B is required for ligand-dependent proteasome degradation (*27*). However, BRCA1 suppression did not decrease PR-B phosphorylation at Ser^{294} (Fig. 3A).

We next evaluated ligand-induced polyubiquitination of PR in control and BRCA1-depleted normal human MCF10A MECs. PR ubiquitination was reduced in BRCA1-depleted cells. Conversely, overexpression of wild-type BRCA1 increased the amount of ubiquitinated PR (Fig. 3B). A protein complex consisting of BRCA1 and BARD1 displays E3 ubiquitin ligase activity (*28*). To test whether E3 ligase activity of BRCA1 is required for PR polyubiquitination, we introduced wild-type, ubiquitin ligase–defective ring-domain mutant BRCA1^{C61G} (*28*), and ZBRK1 interaction–defective mutant BRCA1^{Q356R} (*29*, *30*) into MCF10A cells. PR-A

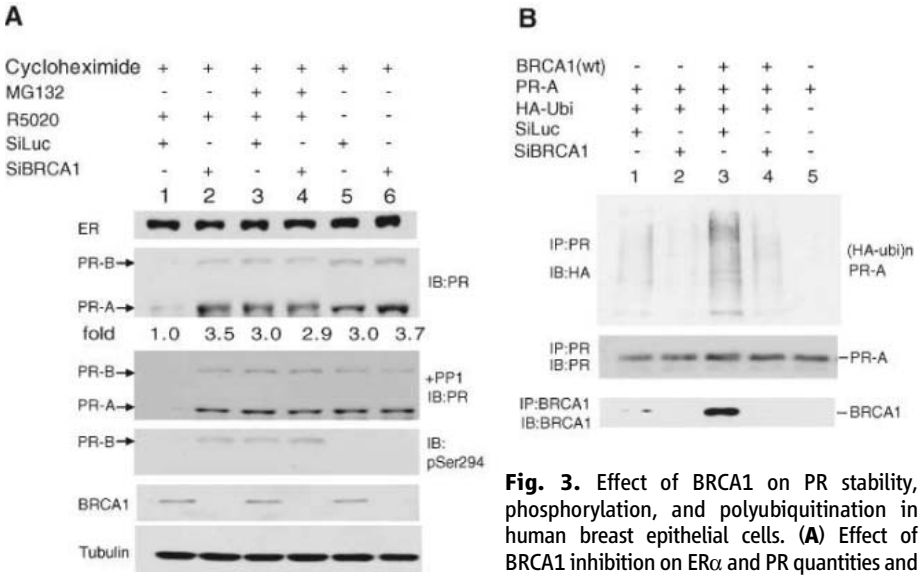

Fig. 3. Effect of BRCA1 on PR stability, phosphorylation, and polyubiquitination in human breast epithelial cells. (**A**) Effect of BRCA1 inhibition on ERα and PR quantities and PR phosphorylation. Human breast cancer T47D cells were infected with SiLuc or SiBRCA1 adenovirus. After being starved overnight, cells were treated with cycloheximide (80 μg/ml), R5020 (10 nM), and/or MG132 (10 μM) for 6 hours as indicated. Quantities of ERα and PR protein were compared by using Western blotting. Phosphorylation of PR-A and PR-B upon R5020 treatment was determined by mobility shift and change of protein mobility upon phosphatase treatment. PR phosphorylation at Ser^{294} was evaluated with Ser^{294}-phospho-specific antibody. α-tubulin served as a loading control. (**B**) BRCA1 regulates PR ubiquitination. MCF10A cells were transiently co-transfected with hemagluttinin (HA)-tagged ubiquitin, PR-A, and BRCA1 constructs (wt or mutants) as indicated, followed by infection with adenovirus expressing siRNA targeting BRCA1 or luciferase. Before harvest, cells were treated with 10 μM MG132 for 2 hours, followed by incubation with 10 nM R5020 for 2 hours. Anti-PR immunoprecipitates (IP) were analyzed by immunoblotting (IB) by using HA (top) and PR (middle) antibodies. Anti-BRCA1 immunoblotting shows efficiency of siBRCA1 (bottom). PP1, protein phosphatase 1.

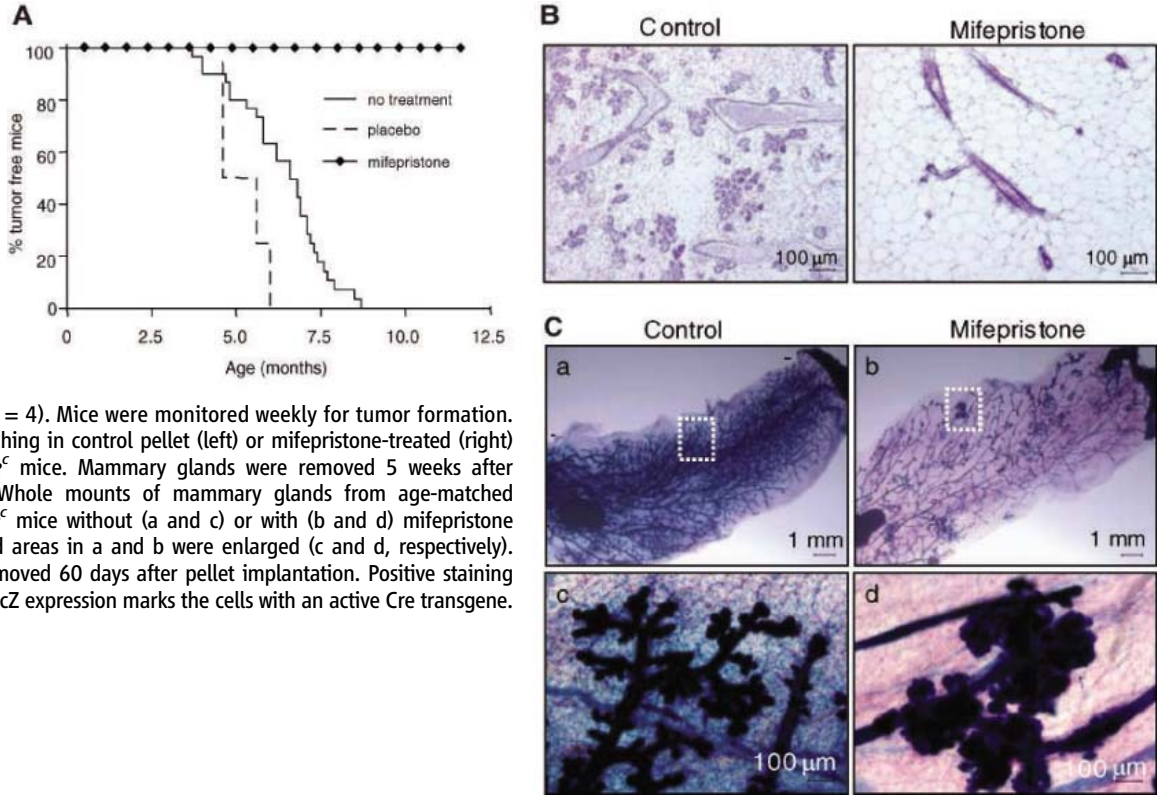

Fig. 4. Antiprogesterone treatment inhibits mammary tumorigenesis by decreasing ductal branching and alveolar proliferation in *Brca1*$^{f11/f11}$ *p53*$^{f5\&6/f5\&6}$*Cre*^{c} mice. (**A**) Nulliparous adult female *Brca1*$^{f11/f11}$ *p53*$^{f5\&6/f5\&6}$*Cre*^{c} mice, ages 3 to 4 months, were implanted with either a pellet containing 35 mg/60 day constant-release mifepristone (n = 14) or a placebo pellet (n = 4). Mice were monitored weekly for tumor formation. (**B**) Mammary gland branching in control pellet (left) or mifepristone-treated (right) *Brca1*$^{f11/f11}$*p53*$^{f5\&6/f5\&6}$*Cre*^{c} mice. Mammary glands were removed 5 weeks after pellet implantation. (**C**) Whole mounts of mammary glands from age-matched *Brca1*$^{f11/f11}$*p53*$^{f5\&6/f5\&6}$*Cre*^{c} mice without (a and c) or with (b and d) mifepristone pellet implantation. Boxed areas in a and b were enlarged (c and d, respectively). Mammary glands were removed 60 days after pellet implantation. Positive staining with X-galactosidase for LacZ expression marks the cells with an active Cre transgene.

ubiquitination increased in cells overexpressing wild type and $BRCA1^{Q356R}$, but not $BRCA1^{C61G}$ (fig. S5), indicating that E3 ligase activity of BRCA1 is required for PR polyubiquitination. However, PR failed to be ubiquitinated by BRCA1 and its interacting protein, BARD1, as assessed by an in vitro assay (fig. S6).

Because progesterone is a potent mitogen for $Brca1^{f11/f11}p53^{f5\&6/f5\&6}Cre^{c}$ MECs, we next tested whether blockade of PR activity by a progesterone antagonist could prevent or delay mammary carcinogenesis in $Brca1^{f11/f11}p53^{f5\&6/f5\&6}Cre^{c}$ conditional knockout mice. Mice were treated with a placebo pellet or with a pellet containing the antiprogesterone mifepristone (RU 486). The pellet released the drug over a 60-day period, and the mice were monitored weekly for tumor formation. The median tumor latency of $Brca1^{f11/f11}p53^{f5\&6/f5\&6}Cre^{c}$ mice was 6.6 months ($n = 25$) with complete penetrance (Fig. 4A). All the control untreated mice as well as the placebo-treated mice ($n = 4$) developed palpable tumors by 8.7 and 5.2 months of age, respectively. In contrast, no palpable tumors were detected in the mifepristone-treated mice ($n = 14$) at 12 months of age. Five weeks of mifepristone treatment substantially reduced branching and suppressed alveologenesis in the mammary glands of $Brca1^{f11/f11}p53^{f5\&6/f5\&6}Cre^{c}$ mice (Fig. 4B). By using R26R reporter mice to monitor Cre activity (*31*), we found LacZ-positive normal $Brca1^{f11/f11}p53^{f5\&6/f5\&6}$ MECs as well as hyperplastic foci in the mifepristone-treated mice (Fig. 4C). These foci did not progress to tumors, however. These results suggest that PR function is critical for *Brca1*-mediated mammary carcinogenesis and that antiprogesterone treatment can prevent or delay mammary carcinogenesis in *Brca1/p53* conditional knockout mice. In contrast, previous work has shown that treatment of $Brca1^{f11/f11}p53^{f5\&6/f5\&6}$ *MMTV-Cre* mice with the selective estrogen receptor modifier, tamoxifen, can increase mammary tumor incidence, an effect attributed to the estrogenic activities of tamoxifen in *Brca1*-deficient cells (*32*).

In a recent study, exposure to a progesterone pellet was found to dramatically increase mammary gland volume in *Brca1* conditional knockout mice but had little effect in wild-type mice (*8*). Our findings of deregulated PR turnover and mitogenic effect of progesterone in *Brca1*-deficient MECs are consistent with these results (*8*). Importantly, the mifepristone-mediated inhibition of mammary tumorigenesis in our *Brca1/p53*-deficient model provides a molecular framework for future clinical evaluation of antiprogesterones as a potential chemopreventive strategy in women who carry *BRCA1* mutations.

References and Notes

1. Y. Miki *et al.*, *Science* **266**, 66 (1994).
2. M. E. Thompson, R. A. Jensen, P. S. Obermiller, D. L. Page, J. T. Holt, *Nat. Genet.* **9**, 444 (1995).
3. N. S. Ting, W. H. Lee, *DNA Repair (Amsterdam)* **3**, 935 (2004).
4. N. Turner, A. Tutt, A. Ashworth, *Nat. Rev. Cancer* **4**, 814 (2004).
5. S. Fan *et al.*, *Science* **284**, 1354 (1999).
6. L. Zheng, L. A. Annab, C. A. Afshari, W. H. Lee, T. G. Boyer, *Proc. Natl. Acad. Sci. U.S.A.* **98**, 9587 (2001).
7. M. Razandi, A. Pedram, E. M. Rosen, E. R. Levin *Mol. Cell. Biol.* **24**, 5900 (2004).
8. Y. Ma *et al.*, *Mol. Endocrinol.* **20**, 14 (2006).
9. S. Nandi, *J. Natl. Cancer Inst.* **21**, 1039 (1958).
10. L. Hennighausen, G. W. Robinson, *Nat. Rev. Mol. Cell Biol.* **6**, 715 (2005).
11. X. Li, D. M. Lonard, B. W. O'Malley, *Mech. Ageing Dev.* **125**, 669 (2004).
12. K. S. Korach, *Science* **266**, 1524 (1994).
13. S. Mallepell, A. Krust, P. Chambon, C. Brisken, *Proc. Natl. Acad. Sci. U.S.A.* **103**, 2196 (2006).
14. W. P. Bocchinfuso *et al.*, *Endocrinology* **141**, 2982 (2000).
15. B. Mulac-Jericevic, J. P. Lydon, F. J. DeMayo, O. M. Conneely, *Proc. Natl. Acad. Sci. U.S.A.* **100**, 9744 (2003).
16. J. E. Rossouw *et al.*, *JAMA* **288**, 321 (2002).
17. V. Beral, E. Banks, G. Reeves, *Lancet* **360**, 942 (2002).
18. S. Lee *et al.*, *Int. J. Cancer* **118**, 1285 (2006).
19. J. P. Lydon *et al.*, *Genes Dev.* **9**, 2266 (1995).
20. G. Shyamala, X. Yang, G. Silberstein, M. H. Barcellos-Hoff, E. Dale, *Proc. Natl. Acad. Sci. U.S.A.* **95**, 696 (1998).
21. X. Xu *et al.*, *Nat. Genet.* **22**, 37 (1999).
22. S. C. Lin *et al.*, *Cancer Res.* **64**, 3525 (2004).
23. F. Bresciani, *Science* **146**, 653 (1964).
24. C. Brisken *et al.*, *Proc. Natl. Acad. Sci. U.S.A.* **95**, 5076 (1998).
25. M. D. Aupperlee, K. T. Smith, A. Kariagina, S. Z. Haslam, *Endocrinology* **146**, 3577 (2005).
26. T. A. King *et al.*, *Cancer Res.* **64**, 5051 (2004).
27. C. A. Lange, T. Shen, K. B. Horwitz, *Proc. Natl. Acad. Sci. U.S.A.* **97**, 1032 (2000).
28. R. Hashizume *et al.*, *J. Biol. Chem.* **276**, 14537 (2001).
29. L. Zheng *et al.*, *Mol. Cell* **6**, 757 (2000).
30. S. Furuta *et al.*, *Proc. Natl. Acad. Sci. U.S.A.* **102**, 9176 (2005).
31. P. Soriano, *Nat. Genet.* **21**, 70 (1999).
32. L. P. Jones *et al.*, *Oncogene* **24**, 3554 (2005).

33. The authors thank Baylor College of Medicine Core Facility for providing extracts of insect cells overexpressing PR-A and PR-B, C. X. Deng for *Brca1* floxed mice, P.-L. Chen for siRNA adenoviruses, S. Furuta and C. Smith for technical advice, and the R. Sprague family for their generosity. This study was supported by National Cancer Institute (NCI) grant CA049649, BCRF-35127 fund, U.S. Department of Defense grant DAMD17-02-1-0694 (E.L.), and NCI postdoc training fellowship (A.J.P.).

Supporting Online Material

www.sciencemag.org/cgi/content/full/314/5804/1467/DC1
Materials and Methods
Figs. S1 to S6
References

25 May 2006; accepted 20 October 2006
10.1126/science.1130471

Raman Workstation

The Raman Workstations are complete systems optimized for a given application and wavelength range. Systems are available for popular laser lines from 325 nm to 830 nm. For short ultraviolet wavelengths (such as 244 nm), the novel McPherson prism predisperser is used as a sharp cut-off filter. The systems include a solid-state laser, specialty filter(s), sample chambers with laser focusing, and signal collection optics. They are also available with a sample chamber compatible with cryogenic sample holders for photoluminescence work. The workstation provides high throughput and low scatter. Open architecture leaves room to grow. If the need arises to modify operating conditions, system elements can be specially modified or replaced.

McPherson For information 978-256-4512 www.mcphersoninc.com

Reverse Transcriptase

MonsterScript Reverse Transcriptase is a highly processive, thermostable enzyme that completely lacks ribonuclease H activity. The enzyme retains high activity at temperatures greater than 50°C and produces full-length complementary DNA greater than 15 kb from picogram amounts of RNA. The MonsterScript cDNA Synthesis Kit also includes betaine to enable improved reverse transcription through regions of difficult secondary structure.

Epicentre Biotechnologies For information 800-284-8474 www.EpiBio.com/MonsterScript.asp

Gene Expression Sample Preparation

The Biomek 3000 GeXP Methods for automated gene expression sample preparation is a software plug-in that provides methods to prepare samples for the GenomeLab GeXP Genetic Analysis system on the Biomek 3000 Liquid Handling Workstation. The suite includes fully validated methods for RNA sample prep, quantitation and normalization, and reaction setup. These methods deliver a complete solution for gene expression analysis from sample to answer.

Beckman Coulter For information 714-993-8955 www.beckmancoulter.com

Biomolecular Interaction Analysis

The RAP♦*id* 4 biomolecular interactions analysis system is based on resonant acoustic profiling (RAP) technology. The instrument enables real-time label-free measurement and analysis of biomolecular interactions with a high level of accuracy, reproducibility, and sensitivity. The instrument is a flow-based system that reduces the need to purify samples and generates accurate kinetics, affinity, and concentration measurements from complex mixtures, such as cell culture supernatants and periplasmic extracts. A standalone, fully automated platform, it requires minimal user intervention and is controlled via user-friendly software, typically processing an average of 400 samples per day. RAP measures the oscillation of a resonating quartz crystal, which decreases in proportion to the mass of the molecules binding to its surface. The system has been optimized for protein–protein interaction analysis and the manufacturer's scientists continue to broaden its applications.

Akubio For information +44 1223 225335 www.akubio.com

Amplification Kit

The TargetAmp 1-Round Biotin-aRNA Amplification Kit 104 produces microgram amounts of biotin-antisense RNA (aRNA) from as little as 25 ng of total RNA for use on Affymetrix GeneChip arrays, Illumina BeadChips, and other microarray platforms. The reaction can be completed in just one day.

Epicentre Biotechnologies For information 800-284-8474 www.EpiBio.com

Carbon Grid

The C-flat is an ultra-flat, holey carbon-coated support grid for transmission electron microscopy (TEM). Unlike competing holey carbon films, C-flat is manufactured without plastics, so it is clean upon arrival and the user has no residue to contend with. Made with patent-pending technology, C-flat provides an ultra-flat surface that results in better particle dispersion and more uniform ice thickness, leading to higher-quality data and higher resolution.

Electron Microscopy Sciences For information 215-412-8400 www.emsdiasum.com

Ventilators

The MiniVent and the MicroVent are part of a new line of compact, quiet, lightweight, and virtually vibrationless ventilators. The MiniVent can be used for mice or any other animals with tidal volumes between 30 to 350 μl. The Microvent can be used with very small animals such as perinatal mice with tidal volumes up to 130 μl. Large ventilators introduce system compliance issues from large amounts of dead space, but the MiniVent and MicroVent are sized to reduce the volume error to 3 μl or less. A rotary plunger performs a synchronized forward and rotating movement, eliminating the need for valves. Uniquely arranged bores and channels in the cylinder and plunger control inspiration and expiration during each stroke of the plunger. The MiniVent and MicroVent can use room air or any nonexplosive gas mixture to feed the pump intake. Multi-gas inlet adapters are also available for use with selectable gas mixtures.

Stoelting For information 630-860-9700 www.stoeltingco.com/physio

Newly offered instrumentation, apparatus, and laboratory materials of interest to researchers in all disciplines in academic, industrial, and government organizations are featured in this space. Emphasis is given to purpose, chief characteristics, and availability of products and materials. Endorsement by *Science* or AAAS of any products or materials mentioned is not implied. Additional information may be obtained from the manufacturer or supplier by visiting www.science.labvelocity.com on the Web, where you can request that the information be sent to you by e-mail, fax, mail, or telephone.

POSITIONS OPEN

SWARTHMORE

The Department of Biology at Swarthmore College invites applications for two different one-year faculty leave replacement positions at the **ASSISTANT PROFESSOR** level, each beginning September 2007. Applicants should have a Ph.D., teaching experience, and a strong commitment to undergraduate education. All application materials should be received by January 10, 2007.

Evolutionary biology: Teaching responsibilities include a broadly based, intermediate-level course in evolution with weekly laboratories, an advanced seminar with laboratory in some area within evolutionary biology, and participation in the Department's team-taught introductory course in organismal and population biology. Applicants should submit curriculum vitae, three letters of recommendation, and a statement of teaching and research interests to: **Dr. Colin Purrington, Evolutionary Biology Search, Department of Biology, Swarthmore College, Swarthmore, PA 19081-1390.**

Developmental biology: Teaching is expected to include an intermediate-level laboratory course in developmental biology as well as an intermediate level course in one's area of special interest. Such a course would be expected to complement the Department's offerings during the fall semester in areas such as genomics, immunology, or stem cell biology. Interested persons should submit curriculum vitae, three letters of recommendation, and a statement of teaching and research interests to: **Dr. Scott Gilbert, Developmental Biology Search, Department of Biology, Swarthmore College, Swarthmore, PA 19081-1390.**

Swarthmore College is an Equal Opportunity Educator and Employer and specifically invites and encourages applications from women and minorities.

PITHELIAL BIOLOGY RESEARCH POSITIONS
University of Chicago

Positions are available beginning February 2007 in a new multi-investigator, interactive Laboratory of Epithelial Pathobiology focused on mechanisms of adhesion and signaling related to epithelial morphogenesis, wound healing, and carcinogenesis; regulation of ion transport; and polarized membrane trafficking and targeting.

Positions are available both for new Ph.D. recipients at the **POSTDOCTORAL FELLOW** level and for more experienced individuals wishing to transition to independence. Appointment of the latter will be as **RESEARCH ASSOCIATE (ASSISTANT PROFESSOR)** with the potential for consideration of subsequent appointment to the faculty tenure-track at a later date.

Minimum requirements are a Ph.D.degree, two to three significant publications, and excellent communication skills. Candidates with an M.D. and prior research experience in epithelial pathobiology are also encouraged to apply.

Interested candidates should submit a letter of interest and current curriculum vitae to: **Karl Matlin, Ph.D.** at **e-mail: kmatlin@surgery.bsd.uchicago.edu.** *The University of Chicago and its Medical Center are Affirmative Action/Equal Opportunity Employers.*

The Department of Pediatrics at the University of Illinois at Chicago (UIC) is seeking a full-time, nontenure-track **RESEARCH ASSISTANT PROFESSOR** to conduct research concerning hematopoietic differentiation of human embryonic stem cells and bone marrow transplantation in mice. Required: Ph.D. and substantial experience related to these areas of research. To apply, submit letter of interest, curriculum vitae and three references by December 26, 2006, to **e-mail: pedsjobs@uic.edu,** or **fax: 312-413-8535,** or mail to: **Human Resources Office, Department of Pediatrics at University of Illinois at Chicago (M/C 856), 840 S. Wood Street, Chicago, IL 60612.** *UIC is an Affirmative Action/Equal Opportunity Employer.*

POSITIONS OPEN

World Agroforestry Centre
TRANSFORMING LIVES AND LANDSCAPES

The World Agroforestry Centre (ICRAF) invites applications for the position of a **LANDSCAPE ECOLOGIST** to undertake agro-ecosystem analysis and characterization studies as part of its ongoing research on natural resources management. Applications must be received by 2 January 2007.

For more information on the position, please visit our **website: http://www.worldagroforestrycentre.org.**

RADIOBIOLOGIST

FACULTY POSITION. The successful individual will develop an externally funded research program in the basic sciences that addresses the University of California, Davis (UCD) and Veterans Affairs (VA) core missions of patient care, education, and research. Such work will be carried out within the context of a joint appointment with the UCD, Department of Radiation Oncology and the VA. The holder of this post will be expected to utilize the scientific and intellectual resources available at UCD and VA Mather and Martinez in creation of a program that has the potential to either directly or indirectly impact the care of the UCD and VA patient population. In consideration of the UCD joint appointment, individuals that have a cancer biology focus are encouraged to apply. The series offered will be **ASSISTANT or ASSOCIATE PROFESSOR, REGULAR SERIES** at UCD, and VA **HEALTH SCIENTIST** at the VA.

Qualifications: A Ph.D, M.D., or equivalent degree is required as well as the capacity to initiate and complete a research project as demonstrated by a strong publication record as well as success in applying for and obtaining national-level grant funding. Strong communication skills and the desire to work in a collaborative research environment are essential.

Salary/rank: Commensurate with experience

Please apply to: **June M. Parker, Chief Administrative Officer, Department of Radiation Oncology, 4501 X Street, G-140, Sacramento, CA 95817.** Send a complete curriculum vitae and a letter outlining teaching, service activities, and the key elements of a research program that is linked to the needs of the VA population. Candidates should describe any previous activities mentoring women, minorities, students with disabilities, or other underrepresented groups. To be fully considered, please apply on or before January 31, 2007. *University of California, Davis, is responsive to the needs of dual-career couples.*

ASSISTANT OR ASSOCIATE PROFESSORSHIP
Whitney Laboratory for Marine Bioscience
University of Florida

The Whitney Laboratory for Marine Bioscience, a research center of the University of Florida, is offering a full-time research position that will be tenure-accruing in an appropriate department of the University. We are seeking a creative and innovative individual who will bring an interdisciplinary approach to studies of fundamental biological problems using marine models. Exceptional candidates in all fields of molecular, cell and systems biology, particularly in neuroscience, are strongly encouraged to apply. Full details of the position are available at **website: http//www.whitney.ufl.edu/facultysearch.htm.** Excellent state-of-the-art research facilities and a competitive startup package are available. Applicants should submit current curriculum vitae, a statement of research interests, and three letters of recommendation to: **Chair of the Search Committee, Whitney Laboratory for Marine Bioscience, 9505 Ocean Shore Boulevard, Saint Augustine, FL 32080.** Completed applications should be received by December 15, 2006.

Cold Spring Harbor 2007 Meetings & Courses

Meetings

Computational Cell Biology
March 6 - 9

Plant Genomes
March 15 - 18

Imaging Neurons & Neural Activity
March 22 - 25

Systems Biology: Global Regulation of Gene Expression
March 29 - April 1

Receptors, Channels & Synapses
April 18 - 22

The Ubiquitin Family
April 25 - 29

Telomeres & Telomerase
May 2 - 6

Workshop on Honey Bee Genomics & Biology
May 6 - 8

The Biology of Genomes
May 8 - 12

Phosphorylation, Signaling & Disease
May 16 - 20

Retroviruses
May 22 - 27

72nd Symposium: Clocks & Rhythms
May 30 - June 4

Yeast Cell Biology
August 15 - 19

Eukaryotic mRNA Processing
August 22 - 26

Mechanisms of Eukaryotic Transcription
August 29 - September 2

Eukaryotic DNA Replication
September 5 - 9

Microbial Pathogenesis and Host Response
September 15 - 19

Cell Death
September 26 - 30

Neurobiology of *Drosophila*
October 3 - 7

Clinical Cardiovascular Genomics
October 10 - 14

Genome Informatics
November 1 - 5

In Vivo Barriers to Gene Delivery
November 15 - 18

Molecular & Immunological Approaches to Vaccine Design
November 29 - December 2

Rat Genomics & Models
December 6 - 9

http://meetings.cshl.edu

Courses

Protein Purification & Characterization
April 11 - 24

Cell & Developmental Biology of *Xenopus*
April 14 - 24

Molecular Neurology & Neuropathology
June 6 - 12

Advanced Bacterial Genetics
June 6 - 26

Ion Channel Physiology
June 6 - 26

Molecular Embryology of the Mouse
June 6 - 26

Integrated Data Analysis for High Throughput Biology
June 13 - 26

Workshop on Autism Spectrum Disorders
June 14 - 21

Workshop on Mechanisms of Arousal, Alertness and Attention
June 23 - 29

Advanced Techniques in Molecular Neuroscience
June 29 - July 15

Molecular Techniques in Plant Science
June 29 - July 19

Neurobiology of *Drosophila*
June 29 - July 19

Structure, Function & Development of the Visual System
July 6 - 19

Eukaryotic Gene Expression
July 18 - August 7

Biology of Memory
July 22 - August 4

Imaging Structure & Function in the Nervous System
July 24 - August 13

Yeast Genetics & Genomics
July 24 - August 13

Cellular Biology of Drug Addiction
August 7 - 13

C. elegans
August 11 - 26

X-ray Methods in Structural Biology
October 15 - 30

Programming for Biologists
October 17 - 30

Immunocytochemistry, In Situ Hybridization & Live Cell Imaging
October 18 - 31

Phage Display of Proteins & Peptides
November 6 - 19

Proteomics
November 6 - 19

Computational & Comparative Genomics
November 7 - 12

The Genome Access Course
April 24 - 25
August 28 - 29
November 28 - 29

Lilly-Asian Scientific Excellence Awards Presented to Chinese Biologists

Lilly honored eight Chinese scientists with the 2006 Lilly-Asian Scientific Excellence Awards (LASEA) in biology on October 19 in Shanghai, China. These highly competitive awards for young Asian biomedical scientists recognize outstanding research creativity and impact. Recipients were selected by an international panel of scientists.

2006 award winners have made fundamental discoveries in genetics, infectious disease, neuroscience, oncology, and endocrinology:

Ling Chen, Ph.D., Guangzhou Institute of Biomedicine and Health, Chinese Academy of Sciences
Saijuan Chen, Ph.D., Shanghai Jiao Tong University
Hongkui Deng, Ph.D., Peking University
Xiang Gao, Ph.D., Nanjing University
Yongfeng Shang, Ph.D., Peking University Health Science Center
Hong Zhang, Ph.D., National Institute of Biological Sciences, Beijing
Xu Zhang, Ph.D., Institute of Neuroscience, Chinese Academy of Sciences
Guoping Zhao, Ph.D., Fudan University

Eli Lilly and Company is a leading, innovation-driven corporation committed to developing a growing portfolio of best-in-class and first-in-class pharmaceutical products that help people live longer, healthier, and more active lives. Groundbreaking science underlies the discovery and development of our medical solutions. Consistent with our mission to deliver breakthrough pharmaceutical products, Lilly has a long history of supporting basic scientific research, especially in the fields of chemistry and biology. We are proud to inaugurate the LASEA program in biology.

Lilly

Answers That Matter.

www.lilly.com

Federal Ministry of Education and Research

bccn

"Bernstein Award" 2007

Young Scientists Research Award in Computational Neuroscience

The German Federal Ministry of Education and Research (BMBF) has established the "National Network for Computational Neuroscience" with four high-performing "Bernstein Centers for Computational Neuroscience" as the major structural elements.

The "Bernstein Award" is equipped with up to 1.25 Mio Euros in the form of a grant over a period of five years. It will be awarded to a highly qualified young researcher, considering the candidates' verifiable research profile in the field of Computational Neuroscience and the scientific concept for a future young research group. Young researchers can apply for their own position and group. The group funded by the "Bernstein Award" will become an integral part of the National Network for Computational Neuroscience. Future announcements of the "Bernstein-Award" are in the scope of the Ministry's planning.

The grant is provided for a scientific project of a young research group headed by a postdoc regardless of nationality. The project will be conducted at a German university or research institution – within or outside the Bernstein Centers. It is a prerequisite for funding that the university or research institution concerned employs the young researcher during the funding period and supports him/her with the basic equipment in terms of laboratory space and other infrastructure. A statement made to that effect by the receiving institution must be included with the project outline to be submitted.

Deadline for applications is **May 31st, 2007**.

For more detailed information about the "Bernstein Award" including application conditions please visit:

www.bernstein-centers.de/en

SCIENTIFIC CONFERENCES
HINXTON CAMBRIDGE UK

wellcome trust

SCIENTIFIC CONFERENCE PROGRAMME

The Wellcome Trust Scientific Conference Programme is hosted at the dedicated conference facilities on the Wellcome Trust Genome Campus – home to one of the world's largest concentrations of expertise in genomics and bioinformatics, including the Wellcome Trust Sanger Institute and the European Bioinformatics Institute.

Winter 2006–07

Animal Health Research: Recent development and future directions

24–26 January

The first conference focusing on livestock diseases in developing countries, and the impact of those diseases on human health and wellbeing.

Spring 2007

Genomic Disorders

20–24 March

This meeting aims to present and discuss the latest findings relating to the genomic basis of human variation, congenital disorders and acquired diseases.

Microbial Genomes 2007

11–14 April

The second conference at Hinxton on genome analysis, microbial genome diversity and evolution, computational and functional microbial genomics, and host–pathogen interactions.

Humanising Model Organisms to Understand the Pathogenesis of Human Disease*

1–4 May

The first conference on understanding how the model system works for human disease, including cardiovascular, metabolic, infectious, neuromuscular, neurological and cancer diseases.

Summer 2007

Biotechnology: In relation to human and animal health*

13–17 June

This meeting will cover: the use of molecular tools in biomedical applications, including animal health and breeding, cloning and stem cells; and genetic modification, ethics and regulatory issues.

Vaccine Development Technologies

4–7 July

This series of conferences is aimed at accelerating vaccine availability, particularly for diseases against which we do not yet have vaccines or for which available vaccines are inadequate.

Genomics of Common Diseases

8–10 July

The availability of whole-genome association studies has started to redefine the genetic architecture of genetically complex disorders, and over the next few years will reveal new susceptibility genes for a wide range of common human diseases.

Molecular Biology of Hearing and Deafness

11–14 July

The first conference at Hinxton addressing the genetics of deafness, developmental biology, molecular basis of sensory function, cochlear damage, repair and regeneration, expression analysis, molecular diagnostics, otologic disease and approaches to treatments.

Interactome Networks†

29 August–2 September

The third genomes to systems conference with topics including ORFeome, binary interaction maps, DNA/protein networks, assembly, annotation, visualisation, data integrations and interactome modelling.

Autumn 2007

Mouse Molecular Genetics

5–9 September

New to Hinxton, this conference brings together researchers of multiple disciplines studying various molecular and genetic aspects of mammalian development and disease, primarily using the mouse model.

Evolution of Brain and Behaviour

12–16 September

Integrated Approaches to Brain Complexity†

26–28 September

The third conference on understanding the structural and functional complexity of the vertebrate nervous system.

Pharmacogenomics†

18–21 October

Focusing on the opportunities of emerging genomic information and technologies to interdisciplinary approaches in the study of variable responses of humans to drugs and toxic agents and how research may benefit the individual.

* Joint conference with European Science Foundation † Joint conference with Cold Spring Harbor Laboratory

More information and registration details will be available at **www.wellcome.ac.uk/conferences** or contact the Wellcome Trust Meetings Programme team at **wtmeetings@wtconference.org.uk**

Venue
Wellcome Trust Conference Centre, Wellcome Trust Genome Campus, Hinxton, Cambridgeshire, CB10 1RQ, UK

www.wtconference.org.uk

AWARDS

UNCF • MERCK SCIENCE INITIATIVE

"A mind is a terrible thing to waste"

MERCK

UNDERGRADUATE SCIENCE RESEARCH SCHOLARSHIP AWARDS

- 15 Awards Annually
- Scholarships up to $25,000
- Two Summer Internships at a Merck Research Facility

An applicant must:

- Be a full-time student at any four-year college or university
- Have junior year academic status
- Major in a life or physical science (first professional degrees excluded)
- Have a minimum cumulative GPA of 3.3 (4.0 point scale)

GRADUATE SCIENCE RESEARCH DISSERTATION FELLOWSHIPS

- 12 Fellowships Annually
- Fellowship Stipends up to $42,000
- Department Grants of $10,000
- Support for 12-24 months

An applicant must:

- Be enrolled full-time in a Ph.D. or equivalent doctoral program in a biomedical life or physical science
- Be engaged in and within 1-3 years of completing dissertation research

POSTDOCTORAL SCIENCE RESEARCH FELLOWSHIPS

- 10 Fellowships Annually
- Fellowship Stipends up to $70,000
- Department Grants of $15,000
- Support for 12-24 months

An applicant must:

- Hold a Ph.D. or equivalent degree in a biomedical life or physical science
- Be appointed as a new or continuing postdoctoral fellow by the end of 2007 at an academic or non-academic research institution (private industrial laboratories are excluded)

Applicants must be African American (Black), U.S. citizens or permanent residents, and attending an institution in the U.S.A. Applications must be submitted online at www.uncf.org/merck/ or postmarked by December 15, 2006

For more information, please contact your department chairperson or Jerry L. Bryant, Ph.D., at the **United Negro College Fund**, Inc., 8260 Willow Oaks Corporate Drive, P.O. Box 10444, Fairfax, VA 22031-4511, by fax (703) 205-3574, by e-mail at ***uncfmerck@uncf.org***.

COURSES

MBL Biological Discovery in Woods Hole

Founded in 1888 as the Marine Biological Laboratory

2007 Courses in Cell Biology

Physiology: Cell & Computational Biology
June 9 - July 27, 2007

Embryology: Concepts & Techniques in Modern Developmental Biology
June 9 - July 22, 2007

Biology of Parasitism: Modern Approaches
June 7 - August 4, 2007

Frontiers in Reproduction: Molecular & Cellular Concepts & Applications
May 5 - June 17, 2007

Molecular Biology of Aging
July 29 - August 18, 2007

Generous financial assistance is available!

For information on these and other courses visit:
www.MBL.edu/education or contact:
Admissions Coordinator, admissions@mbl.edu,
(508) 289-7401, 7 MBL Street, Woods Hole, MA 02543.

Applications are encouraged from women and members of underrepresented minorities. The MBL is an Equal Opportunity/Affirmative Action Institution.

DREW UNIVERSITY

RESIDENTIAL SCHOOL ON MEDICINAL CHEMISTRY: CHEMISTRY AND BIOLOGY IN DRUG DISCOVERY

Madison, New Jersey - June 11-15, 2007

The Residential School on Medicinal Chemistry is a weeklong graduate level course organized to provide an accelerated program for medicinal chemists and biologists who wish to broaden their knowledge of small molecule drug discovery and development. Attendance is limited to 200 selected participants with preference given to applicants having five years or less of drug discovery experience. The School's aim is to concentrate on the fundamentals that are useful in drug discovery spanning initial target validation through clinical development. Several case histories of recent successful drug development programs will also be presented.

The five-day program consists of lectures, seminars, case histories and discussions covering the following topics:

Strategic issues in drug discovery	**Structure-based drug design**
Target validation	**Drug-like properties**
Receptor binding	**Patents**
Enzyme inhibition	**Plasma protein binding**
Ion channels	**Pharmacokinetics & ADME**
High throughput screening	**Drug metabolism**
Hit to lead progression	**Preclinical toxicology**
Lead discovery & modification	**Clinical development**

More information and application forms can be obtained at **www.depts.drew.edu/resmed** or by contacting the School's office at Drew University, Hall of Sciences, Room 317A, Madison, NJ 07949, USA; Phone: 973/408-3787; Fax: 973/408-3504 or E-mail: resmed@drew.edu

MBL

Biological Discovery in Woods Hole

Founded in 1888 as the Marine Biological Laboratory

2007 Courses

Substantial financial assistance is available for many of our courses!

Analytical & Quantitative Light Microscopy
May 9 - May 18

Biology of Parasitism: Modern Approaches
June 7 - August 4

BioMedical Informatics
1st Session: May 27 - June 3
2nd Session: September 23 - September 30

Embryology: Concepts & Techniques in Modern Developmental Biology
June 9 - July 22

Frontiers in Reproduction: Molecular & Cellular Concepts & Applications
May 5 - June 17

Pathogenesis of Neuroimmunologic Diseases
August 12 - August 25

Methods in Computational Neuroscience
July 29 - August 26

Microbial Diversity
June 16 - August 2

Molecular Biology of Aging
July 29- August 18

Molecular Mycology: Current Approaches to Fungal Pathogenesis
August 7 - August 23

Neural Development & Genetics of Zebrafish
August 9 - August 22

Neural Systems & Behavior
June 9 - August 5

Neurobiology
June 2 - July 29

Neuroinformatics
August 11 - August 26

Optical Microscopy & Imaging in the Biomedical Sciences
October 9 - October 18

Physiology: Cell and Computational Biology
June 9 - July 29

Summer Program in Neuroscience, Ethics, & Survival (SPINES)
June 16 - July 14

Workshop on Molecular Evolution
July 22 - August 3

FOR MORE INFORMATION CONTACT: Admissions Coordinator, admissions@mbl.edu, (508) 289-7401, MBL, 7 MBL Street, Woods Hole, MA 02543

Applications are encouraged from women and members of underrepresented minorities.
The MBL is an Equal Opportunity/Affirmative Action Employer.

www.MBL.edu/education

WWW.NIH.GOV
Positions @ NIH
THE NATIONAL INSTITUTES OF HEALTH

Department of Health and Human Services
National Institutes of Health
Director, National Center for Research Resources and
Associate Director for Clinical Research (Extramural)

The Office of the Director, National Institutes of Health (NIH) in Bethesda, Maryland, is seeking applications from exceptional candidates for the position of Director, National Center for Research Resources (NCRR). The Director, NCRR, will also serve as the NIH Associate Director for Clinical Research (Extramural). NCRR, with a staff of approximately 100 employees and a $1 billion budget, is the focal point at NIH for biomedical, clinical and translational research resources. The incumbent serves as a principal advisor to the Director, NIH; participates in discussions relative to the development of major policy decisions affecting biomedical, clinical and translational research resources; provides advice and consultation to NIH components, advisory councils and grantee organizations and institutions; and assures that effective administrative procedures are established so that program operations and obligations of government funds and other resources are rendered consistent with statutory and regulatory requirements and within limitations imposed by the Department of Health and Human Services (DHHS) and Executive Branch policies. As Associate Director for Clinical Research (Extramural), the incumbent is expected to provide leadership for clinical research activities across the NIH. This leadership will involve the coordination of clinical research activities to enhance the integration of basic and clinical research. The Associate Director for Clinical Research will work closely with the other Institute and Center Directors to enhance the efficiency and effectiveness of clinical research supported by the NIH. Applicants must possess a Ph.D., M.D., or a comparable doctorate degree in the health sciences field plus senior level scientific experience and knowledge of biomedical, clinical and/or translational research programs in one or more health science areas. Salary is commensurate with experience and a full package of benefits (including retirement, health, life, long term care insurance, Thrift Savings Plan participation, etc.) is available. A detailed vacancy announcement, along with mandatory qualifications and application procedures, can be obtained via the NIH Home Page at: **http://www.jobs.nih.gov** under the Senior Job Openings section. Dr. Stephen Katz, Director, National Institute of Arthritis and Musculoskeletal and Skin Diseases, and Dr. David Schwartz, Director, National Institute of Environmental Health Sciences, will be serving as co-chairs of the search committee. Questions on application procedures may be addressed to **Ms. Regina Reiter at ReiterR@od.nih.gov or discussed with Ms. Reiter by calling 301-402-1130**. Applications **must** be received by **November 27, 2006**.

Department of Health and Human Services
National Institutes of Health
Tenure-Track Position

The Division of Intramural Research, National Institute on Deafness and Other Communication Disorders (NIDCD), located in Bethesda, MD, is seeking a tenure-track scientist to establish an independent research program to study molecular and/or cellular mechanisms of hearing and balance. We welcome applications from candidates with a wide range of expertise. Preference will be given to candidates whose experimental approaches complement those of our existing strong programs in the genetics, development and cell biology of hearing. The successful candidate will join a dynamic group of scientists in a growing intramural program that is at the forefront of research on communication disorders.

The NIDCD offers an exceptional working environment including well-equipped research laboratories and numerous opportunities for collaboration. Candidates for this position must possess a Ph.D. and/or M.D., post-doctoral experience, and an outstanding publication record. Salary is commensurate with education and experience.

Please submit a curriculum vitae including bibliography, three reprints of recent relevant publications, statement of research interests, an outline of your proposed research, and the names and addresses of three references to: **Ms. Trudy Joiner, Office of the Scientific Director, NIDCD, 5 Research Court, Room 2B28, Rockville, MD 20850 (joinert@nidcd.nih.gov)**. Applications will be accepted until **December 15, 2006**.

Department of Health and Human Services
National Institutes of Health
Clinical Center

Tenure-track Physician
Clinical Center/Nuclear Medicine Department

This position is located in The Warren G. Magnuson Clinical Center, Nuclear Medicine Department (NMD).

We are seeking a research-oriented physician for a possible tenure-track position. An M.D. or M.D. /PhD with U.S. Nuclear Medicine Board certification and CT training is needed to provide diagnostic and therapeutic nuclear medicine procedures as well as to participate in clinical research protocols of the NIH Intramural Program. U.S. citizenship or permanent residency status is required.

Please submit your curriculum vitae, bibliography, and a letter describing your clinical, research, and management experience to: **Mrs. Veronica Olaaje, HR Specialist, DHHS, NIH, OD/CSD-E, 2115 E. Jefferson Street, Rm. 2B209 MSC-8503, Bethesda, MD 20892-8503. Phone: 301-435-4748. Email: volaaje@mail.nih.gov**.

Salary is commensurate with experience. This appointment offers a full benefits package (including retirement, health, life and long term care insurance, Thrift Savings Plan participation, etc.). Application packages should be submitted as early as possible, but no later than **December 31, 2006**.

Selection for this position will be based solely on merit, without discrimination for non-merit reasons such as race, color, religion, sex, national origin, politics, marital status, sexual orientation, physical or mental handicap, age or membership or non-membership in an employee organization.

DEAN, College of Natural and Agricultural Sciences

A unique opportunity for decanal leadership exists at The University of California, Riverside in the College of Natural and Agricultural Sciences.

A doubling of faculty positions is projected over the next decade, adding to a rich infusion of new appointments over the past decade. This opportunity for growth occurs in the context of our distinctive, internationally renowned base of physical, biological, biomedical and agricultural sciences, combined with a new Health Sciences Research Initiative. An individual who can recognize the value of this existing diversity will find unparalleled opportunities to exercise a vision for its future. In undergraduate diversity, UC Riverside is the flagship campus of the UC system.

UCR seeks a distinguished scientist and leader for this position. The Dean is expected to provide the strong leadership and administrative direction in research, curriculum, fundraising and outreach — necessary to carry the College to preeminence.

The College has 237 permanent, ladder-rank faculty positions in thirteen departments and nine centers, with doctoral programs in a full array of scientific disciplines, as well as interdisciplinary programs. Research funding in the College for fiscal 2006 was over 53 million dollars. The campus anticipates growth in enrollment from the present 17,000 students to 25,000 by 2015.

The Dean is responsible for faculty appointments and promotions, developing public and private funding sources, fiscal management, allocation of resources, and coordination of College programs within the overall campus academic plan. The Dean reports to the Executive Vice Chancellor/Provost. Salary is commensurate with experience and qualifications. The appointment will be effective July 1, 2007 or whenever a suitable candidate is identified.

A comprehensive, land-grant research institution, UC Riverside is a vibrant, expanding campus, located in inland Southern California, 60 miles southeast of Los Angeles. It lies within an hour's drive of Palm Springs, the San Gabriel and San Bernardino Mountains, the Mojave and Coachella Deserts and Pacific Ocean beaches.

Nomination and Application Procedures: Candidates should include a letter of application with statement of interests, a current CV, and contact information for at least five references. All inquiries, nominations and applications will be held in confidence. Review of applications will begin January 2, 2007 and continue until the position is filled. Inquiries and questions should be directed to Professor Christopher Reed (chris.reed@ucr.edu), Chair of Search Committee, Department of Chemistry, UC Riverside, CA 92521; phone (951) 827 5197. Nominations and applications should be sent by E-mail to: Professor Raymond L. Williams (raymond.williams@ucr.edu), Director of Executive Searches, 3144 Hinderaker Hall, University of California, Riverside, CA 92521. UCR is an affirmative action/equal opportunity employer.

UNIVERSITY OF CALIFORNIA
UCRIVERSIDE

What will I find in a career at Lilly?

Answers.

For more than 130 years, Eli Lilly and Company has been dedicated to meeting the health care needs of people around the world. We address these needs primarily by developing innovative medicines—investing a higher percentage of our sales in research and development than any other major pharmaceutical company.

BIOMEDICAL INFORMATICS

The advent of post-genomic technologies such as gene expression, proteomics, functional genomics, genetic association studies, etc., and their application towards the goal of personalized medicine requires development of new informatics methods for integration and analysis of preclinical and clinical data. The applications developed by the candidate will provide decision enabling data and analyses in support of Lilly's pharmacogenomics and tailored therapeutics programs. The candidate will develop software to support discovery, translation, validation of clinical diagnostics and biomarkers, and enable integrative analysis of genomic, proteomic and clinical phenotypic data. The developed systems will be utilized by both Biological Research Scientists and Clinical Research Physicians. This position will directly support clinical trial research performed by the Diagnostics and Exploratory Medicine group at Lilly.

Candidates must have a Ph.D. in biomedical informatics, bioinformatics, computer science, computational biology, or a related field; or M.S. in biomedical informatics, bioinformatics, computer science, computational biology, or a related field, and 2 or more years of work experience.

For more information or to apply, visit **www.lilly.com/careers**. Eli Lilly and Company is an equal opportunity employer.

www.lilly.com/careers

Lilly
Answers That Matter.

Assistant/Associate Professor of Bioinformatics

Computational Biology Department of Biostatistics

Harvard School of Public Health

The Department of Biostatistics at Harvard School of Public Health (HSPH) is seeking an outstanding candidate for a tenure-track faculty position in Bioinformatics/Computational Biology at the level of Assistant or Associate Professor. The successful candidate would join an active group at HSPH developing novel computational and statistical methods, and conduct collaborative research with clinical and basic scientists at Harvard University and its affiliated medical centers. She/he is expected to play a vital leadership role in expanding the quantitative science research and educational programs at HSPH in bioinformatics and computational biology and its related fields. Candidates should have doctoral degree and a demonstrated record of achievement; candidates in all areas of computational biology, bioinformatics and statistical science are encouraged to apply.

Please send a letter of application, including a statement of current and future research interests, a curriculum vitae, sample publications, and the names of three referees to the address below. Applicants should ask their three referees to write independently to this address:

Computational Biology Junior Faculty Search Committee
Department of Biostatistics
Harvard School of Public Health
655 Huntington Avenue, 4th Floor
Boston, MA 02115

Harvard School of Public Health is strongly committed to increasing the representation of women and minority members among its faculty and particularly encourages applications from such candidates.

the future ocean
CHANGES, RESOURCES AND RISKS

The Christian-Albrechts University in Kiel invites applications for the positions of
14 Professorships (W1 and W2)
as part of the Excellence Cluster „The Future Ocean".

The Christian-Albrechts University in Kiel (CAU) jointly with the Leibniz-Institute of Marine Sciences (IFM-GEOMAR) is establishing a cross-faculty, multi-disciplinary research focus with the title "The Future Ocean" for the multi-facetted study of human-induced ocean change, marine hazards and marine resources (**www.uni-kiel.de/future-ocean/**). As part of this initiative, 14 new Professorships (W1 and W2) are being established which we wish to fill with exceptional young researchers from the fields of natural sciences, law, economics and medicine. Salary will normally be at grade W1, salary at grade W2 is however possible dependent on fulfilling legal and personal qualification requirements.

The W2-Professorships are initially for 5 years. The W1 Junior Professors will initially be appointed for 3 years („Beamtenverhältnis auf Zeit"); dependent on performance of the Junior Professor after these three years, the position can be extended by up to 3 additional years. The willingness to learn German is expected. The positions also bring with them funding for additional personnel and research materials so that the new Professors should quickly be able to set up excellent research groups. Multidisciplinary marine research is an important focus of the CAU. As a consequence we wish to open up long-term career opportunities at the University for successful junior faculty. Based upon performance of the individual appointees, a proportion of these initially non-tenured positions will be changed into tenured W2/W3-positions. We are seeking for each post an exceptional scientist.

Mathematics-Natural Sciences Faculty

Ocean acidification (www.uni-kiel.de/future-ocean/a1): to study the influence of ocean acidification on marine organisms. Research foci could range from the cellular to the ecosystem level and from molecular studies to field experiments. The position will be hosted at IFM-GEOMAR.
Seafloor warming (www.uni-kiel.de/future-ocean/a2): to study the influence of seafloor warming on sedimentary gas hydrates and/or benthic fauna with the help of a variety of methods (e.g. field studies and experiments, laboratory studies, numerical models). The position will be hosted at IFM-GEOMAR.
Ocean circulation (www.uni-kiel.de/future-ocean/a4): to study the relationships between changes in ocean circulation and the hydrological cycle with the use of Earth System models and their further development by implementation of palaeoenvironmental parameters. The candidate should have experience in the transient climate modelling of long time periods.
CO_2-Sequestration (www.uni-kiel.de/future-ocean/a5): to study various scenarios of CO_2-sequestration from an integrative stand-point, using molecular dynamics modelling, advanced spectroscopic methods and experimental high-pressure simulations of oceanic in-situ conditions. The candidate should be a demonstrated expert in one of these fields and build a group to cover the other fields, working closely with experts in adjacent fields already present in the Cluster in Kiel.
Chemistry of the ocean surface (www.uni-kiel.de/future-ocean/a6): to study the chemical structures and heterogeneous reactions on aerosols, in clusters or on air/ice or air/water interfaces with modern methods. The candidate should have demonstrated experience in the fields of reaction kinetics and/or spectroscopy.
Seafloor resources (www.uni-kiel.de/future-ocean/b3): to study the temporal and spatial influence of fluid movement on the formation of seafloor resources using a combination of numerical modelling with field information on physical and chemical boundary conditions. The position will be hosted at IFM-GEOMAR.
Natural hazards (www.uni-kiel.de/future-ocean/b4): to study geological hazards at plate boundaries, particularly earthquakes and slope instabilities. The position will be hosted at IFM-GEOMAR.
Sea level rise and coastal erosion (www.uni-kiel.de/future-ocean/b5): to study processes of hydrodynamics and sediment dynamics in the coastal zone. The candidate should have demonstrated experience in marine geophysics, especially in the field of high resolution hydro-acoustics at the sediment-water interface.
Risk management in the coastal zone (www.uni-kiel.de/future-ocean/b5): with demonstrated experience in geographic hazard research, preferably in coastal regions. The work should focus on the (further) development of qualitative and quantitative methods of risk assessment (particularly remote sensing) as well as the development of decision support systems for risk management.

Economics and Social Sciences Faculty

Living resources and overfishing (www.uni-kiel.de/future-ocean/b1): with demonstrated experience in economics, especially resource economics, property rights and decisions under uncertainty. The appointee will be expected to work in the area of "Living Resources and Overfishing" and if possible also "Coasts at Risks". This implies a willingness to carry out interdisciplinary research with other Cluster disciplines (esp. Marine Biology, Geography, Law). The appointee should also teach courses in the Bachelor/Master of Science in Economics and supervise doctoral students.
Ocean economics (www.uni-kiel.de/future-ocean/a7): with specialization in environmental and resource economics to work on the subject "Valuing the Oceans" within the Excellence-Cluster, investigating economic aspects of the role of the oceans in the global carbon cycle. We expect a willingness to carry out interdisciplinary studies both within the subject area and within the Cluster as a whole. The appointee should also teach courses in the Bachelor/Master of Science in Economics and supervise doctoral students.

Technical Faculty

CO_2-take-up in the ocean (www.uni-kiel.de/future-ocean/a3): with expertise in computer science, particularly algorithm design, numerical mathematics or optimization. The appointee is expected to study the optimization of the modeling of oceanic CO_2-uptake through the assimilation of both physical and biogeochemical data. Participation in the teaching programs in computer science (Diplom, Bachelor/Master of Science) is expected.

Medical Faculty

W2 - Molecular marine medicine (www.uni-kiel.de/future-ocean/b2): with experience in molecular and cell biology, in comparative genetics/genomics, in *in silico* analysis and in the molecular pathophysiology of human diseases. This position forms part of the molecular medicine focus of the CAU. Central to the work will be an evolutionary understanding of complex barrier break-downs in humans, a presently unsolved medical problem. Marine organisms with simple barrier functions should be used as models.

Faculty of Law

W2 - Law of the Sea (www.uni-kiel.de/future-ocean/b6): for research and teaching in the law of the sea, ideally in combination with both, domestic and international environmental and economic law. Additionally, participation in the teaching of public law would be welcome. Applicants must possess a "Habilitation" or demonstrate equivalent scientific achievements.

In addition to the necessary formal qualifications (as set out in §99 of the University Law of Schleswig-Holstein), a pre-requisite for a Junior Professorship is an excellent dissertation. The CAU would like to fill at least 50% of these new positions with female applicants. Peer-Monitoring, career counselling and special support will be provided if requested. The CAU offers a family-friendly working environment and is pro-active with respect to double-career families (**www.uni-kiel.de/audit-fgh**). The State Government and the University support the employment of disabled persons. Persons with disabilities will, with appropriate qualifications and aptitudes, be employed preferentially.

Selection will take place according to the normal procedure for university Professors. Applications, including a curriculum vitae, qualifying documentation (publications, evidence of external funding, teaching experience) and a research and financial plan for the establishment of the research group can be submitted until **8 January 2007** to: **The Rector, Prof. Dr. Thomas Bauer, Rektor der CAU, Christian-Albrechts-Platz 4, D-24118 Kiel, Germany.**

C A U
Christian-Albrechts-Universität zu Kiel

IFM-GEOMAR
Leibniz-Institut für Meereswissenschaften an der Universität Kiel

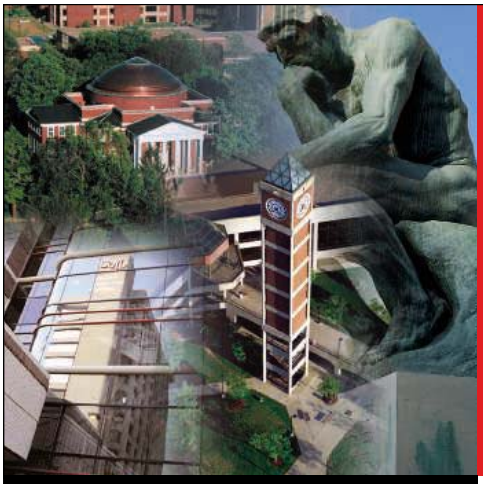

Bioinformatics Faculty Positions

The University of Louisville is seeking applicants to fill 10 new tenure-track faculty positions as part of a major multidisciplinary expansion of the university's Bioinformatics and Computational Biology infrastructure.

Excellence in Research and Education

The Departments of Biochemistry and Molecular Biology (School of Medicine), Bioinformatics and Biostatistics (School of Public Health and Information Sciences), Computer Engineering and Computer Science (J.B. Speed School of Engineering), Mathematics (College of Arts and Sciences) and basic science departments within the School of Dentistry have partnered to coordinate efforts to bring bioinformatics to the forefront in shaping the future of research at the University of Louisville. Come join our team!
bioinformatics.louisville.edu

The University of Louisville is an exciting academic community of people whose ideas and work make outstanding contributions to Kentucky and the nation. For more information, go to:

www.louisville.edu

The University of Louisville is an Equal Opportunity Employer.

Position Description

The University of Louisville Bioinformatics Task Force invites applications for five tenure-track positions scheduled to begin in fall 2007. The remaining five positions will be filled in fall 2009.

Depending on the experience of the applicant, available positions are at the assistant, associate or full professor level. Responsibilities will include research and teaching with high levels of collaborative and interdisciplinary activities.

Ideal candidates will be highly motivated scientists with excellent communication, presentation and interpersonal skills and a bioinformatics research focus to complement the expansion of biomedical research programs. Research experience may include structural bioinformatics, metabolomics, proteomics and genetic data analyses, high-throughput analyses, systems biology, visualization techniques and algorithms development.

Candidate Requirements

The positions require a Ph.D. in biochemistry, computer science, engineering or bioinformatics. Strong English language skills and a willingness to collaborate with researchers with diverse backgrounds are also necessary. In addition, applicants should have a demonstrated record of excellence in collaborative research activity and teaching, including experience with extramural funding agencies.

To Apply

For an application and additional information go to:
bioinformatics.louisville.edu/jobs.html

UNIVERSITY of LOUISVILLE

National Exposure Research Laboratory Post-Doctoral Program

- The National Exposure Research Laboratory (NERL) of the United States Environmental Protection Agency is accepting applications beginning November 20, 2006 through January 31, 2007 for approximately 16 federal, three-year post-doctoral research positions.
- Candidates will engage in research in areas such as environmental monitoring and characterization; computer modeling of the transport, transformation, and fate of pollutants in multiple media and at multiple scales; human and ecological exposure analysis; remote sensing applications; and landscape ecology.
- Specific research opportunities are posted on the NERL website at **http://www.epa.gov/nerl**.
- Post-doctoral positions will be in one or more of the following locations: Research Triangle Park, North Carolina; Cincinnati, Ohio; Las Vegas, Nevada; Athens, Georgia; or Washington DC metropolitan area.

FULL FEDERAL EMPLOYMENT BENEFITS:

- Full three-year appointments
- Paid relocation to EPA duty location
- Travel to professional and scientific meetings
- Vacation and sick leave
- Federal health benefits, life insurance, and retirement program
- Salary range of $51,972 - $84,559 (subject to increase in January 2007)
- Flexible start date beginning in March and no later than September 2007

APPLICATION PROCESS – Consult the NERL website at **http://www.epa.gov/nerl** for instructions on how to apply. Note – online applications from journal websites are not accepted. Applicants must provide:

- Up-to-date Curriculum Vitae
- Letter of recommendation from your research advisor or comparable official
- Cover letter indicating: positions and locations of interest, your email address, U.S. Citizenship status, AND How you learned of this program
- DD-214, if claiming veteran's preference

Applicants must be United States citizens or permanent residents. Only in the absence of qualified U.S. citizens will permanent residents who are citizens of countries specified as exceptions to the appropriations act ban on paying non-U.S. citizens be considered.

Specific job information is posted on the NERL Internet site at **http://www.epa.gov/nerl**. EPA provides reasonable accommodations to applicants with disabilities. If you need a reasonable accommodation for any part of the application and hiring process, please notify the Agency. The decision on granting reasonable accommodation will be on a case-by-case basis.

The U.S. EPA is an Equal Opportunity Employer.

UT SOUTHWESTERN MEDICAL CENTER
UNIVERSITY HOSPITALS & CLINICS

Cancer Immunobiology Center Research Non-Tenure Track Faculty Member

The Cancer Immunobiology Center at the University of Texas Southwestern Medical Center at **Dallas, TX** is seeking a Research Non-Tenure Track Faculty Member with a strong background in biochemistry and experience in running a GMP laboratory. The faculty candidate will both supervise and work in this facility. The applicant will interact with a research team, a clinical trials director and a technical group. Experience in producing proteins in mammalian cells or bacteria, monoclonal antibodies and immunconjugates is desirable. The reagents generated in this facility will be used in Phase I and II clinical trials. Salary and start-up packages are highly competitive. All applicants must have a PhD with minimum of 3 years of biotech experience in a GMP facility. Applicants must have experience in writing protocols, data sheets, batch records and oversight of FDA compliance.

Please send cover letter, letters of reference, curriculum vitae, and summary of professional goals to:

Cancer Immunobiology Center
c/o Linda Berry
UT Southwestern Medical Center
5323 Harry Hines Blvd.
Dallas, Texas 75390-8576
Email: linda.berry@utsouthwestern.edu

EOE

OTOLARYNGOLOGIST

The Section of Otolaryngology - Head and Neck Surgery at Dartmouth-Hitchcock Medical Center seeks a board certified or board eligible Otolaryngologist for a full-time faculty position.The candidate should possess an interest in an academic career and in the education of medical students and residents.This position will combine a general otolaryngology with a subspecialty practice in otology or pediatric otolaryngology. Fellowship training in otology/ neurotology or pediatric otolaryngology is desirable. Research interests will be encouraged. Academic rank will be commensurate with qualifications and experience.

Interested applicants are encourage to send letters of inquiry and CV to:

Daniel Morrison, MD, Chairman
Section of Otolaryngology - Head & Neck Surgery
Dartmouth-Hitchcock Medical Center
One Medical Center Drive
Lebanon, NH 03756
Telephone: 603-650-8123

DARTMOUTH–HITCHCOCK MEDICAL CENTER

Dartmouth-Hitchcock Medical Center is an affirmative action/equal opportunity employer and is especially interested in identifying female and minority candidates.

www.DHMC.org

Tulane University Health Sciences Center
TULANE CANCER CENTER

Louisiana Cancer Research Consortium
IN NEW ORLEANS

Endowed Eminent Scholar in Molecular Cancer Pharmacology

Tulane Cancer Center and the Louisiana Cancer Research Consortium (LCRC) seek an outstanding cancer scientist to become an Endowed Eminent Scholar, **The *Joe W. and Dorothy Dorsett Brown Foundation Distinguished Chair in Molecular Cancer Pharmacology***. The eminent scholar holding this tenure track position will be responsible for coordinating basic research leading to the discovery and pre-clinical development of cancer therapeutics. Tulane University Health Sciences Center and Louisiana State University Health Sciences Center in New Orleans have joined together to develop the LCRC, with the goal of achieving NCI designation as a Comprehensive Cancer Center. Continuing funding from a new state tax on cigarettes and significant financial commitment by both Tulane and LSU provide **generous resources for the successful candidate to recruit additional faculty members in both basic and clinical sciences. The goal is to establish a world-class program bringing basic research toward clinical testing. The successful candidate will enjoy modern laboratory space, access to shared core resources, and the opportunity to develop further the LCRC Cores.**

Qualified candidates should forward CV and three letters of reference to: Roy S. Weiner, M.D., Director, Tulane Cancer Center, Tulane University Health Sciences Center, 1430 Tulane Ave., SL-68, New Orleans, LA 70112, rweiner@tulane.edu or Krishna C. Agrawal, Ph.D.,Chairman, Department of Pharmacology, Tulane University Health Sciences Center, 1430 Tulane Ave., SL-83, New Orleans, LA 70112, agrawal@tulane.edu.

The position will remain open until a suitable / qualified applicant has been identified.

An affirmative action / equal opportunity employer.

MBL

Biological Discovery in Woods Hole

Founded in 1888 as the Marine Biological Laboratory

2007 Summer Research Fellowships

• Funding Available for Summer Research

APPLICATION DEADLINE: JANUARY 16, 2007

The MBL is pleased to announce the availability of funding for the following summer research programs in 2007 for junior or senior investigators holding a Ph.D., M.D., or equivalent degree. These prestigious awards provide funds for research and housing. Proposals for fellowship support will be considered in, but are not limited to, the following fields of investigation:

Cellular & Molecular Physiology
Molecular Biology
Developmental Biology
Neurobiology
Innate Immunity
Ecology
Parasitology
Microbiology

• Funding Available for Summer Research in Neuroscience

APPLICATION DEADLINE: JANUARY 16, 2007

The MBL is pleased to announce the availability of funding for the following summer research programs in Neuroscience in 2007. These programs will provide up to $50,000/year/award with a possibility for renewal for 3 years. As participants in the MBL's new Neuroscience Institute, scholars in these programs will benefit from the rich intellectual and interactive environment of the scientific community at the MBL.

ALBERT AND ELLEN GRASS FACULTY GRANTS PROGRAM

Proposals must describe collaborative research in any area of neuroscience by teams of two or more investigators, with a minimum stay of six weeks at the MBL in Woods Hole. The intent of the program is to attract new investigators to the MBL at the assistant, associate, or full professor levels. The collaborative research can be between new teams of investigators or between new investigators who wish to collaborate with a more established investigator.

Requests will also be considered for collaborative research projects at the MBL during the off-season period. Funds may be used for laboratory and equipment rentals, supplies, and incidental expenses, housing and travel costs.

DART FOUNDATION SCHOLARS PROGRAM IN LEARNING & MEMORY

Proposals must be targeted to the study of learning and memory with a minimum stay of six weeks at the MBL. Applications are encouraged from junior- or senior-level neuroscientists holding a Ph.D., M.D. or equivalent degree. Awards provide funds for research and laboratory rental, and cover the costs of housing and travel.

For application forms and information, contact: Fellowships Coordinator: fellows@mbl.edu or call Lenny Dawidowicz, 508.289.7268, MBL, 7 MBL Street, Woods Hole, MA 02543.

Applications are encouraged from women and members of underrepresented minorities. The MBL is an Equal Opportunity/ Affirmative Action Employer.

www.MBL.edu/fellowships

University of Michigan

Computational Biology of Complex Systems

University of Michigan
Medical School

The Center for Computational Medicine and Biology (CCMB) seeks to hire several Assistant/Associate Professors to develop independent research programs involving the modeling of complex biological systems. This work should address multiple levels of organization that connect molecules to function. We are interested in multi-scale, integrative analyses of metabolic pathways, regulatory networks, signal transduction cascades, and physiological systems. Research may be strictly computational or involve a wet lab component. Candidates should have an earned doctoral degree, at least two years post-doctoral experience, and a passion for teaching graduate and/or professional students. Successful candidates will have a tenure-track appointment in a Medical School Basic Science department and a research appointment in the CCMB, with its Bioinformatics Graduate Program and NIH National Center for Integrative Biomedical Informatics. You will have a generous start-up package, access to our extensive campus-wide computational environment, and encouragement to collaborate with colleagues in interdisciplinary Centers on Type 1 and Type 2 Diabetes, Metabolomics and Obesity, Neurosciences, Organogenesis, Infectious Diseases, Cardiovascular Disorders, Genetics, Cancer Biology, and Complex Systems.

The postings and application process can be viewed at **http://www.umich.edu/~jobs/**. Please refer to posting numbers **4504**, **4506**, and **4507**. You need apply for only one position; the screening committee will direct your materials to the most appropriate basic science department. Please submit electronically a cover letter, your research plans, curriculum vitae, any current grant support, and contact information for four references.

Please contact **Gil Omenn** or **Violet Elder** (**violet@umich.edu**) at the Center for Computational Medicine and Biology if you have questions; feel free to submit a second set of materials to this e-mail address if you so desire.

www.ccmb.med.umich.edu/jobs/EBS

The University of Michigan is an Equal Opportunity/Affirmative Action Employer.

CARDIOLOGIST
TRANSLATIONAL RESEARCH SCIENTIST

The Section of Cardiology at Dartmouth-Hitchcock Medical Center/Dartmouth Medical School is seeking to recruit two new faculty members (M.D or M.D./Ph.D.) board certified/eligible in Cardiovascular Disease with a strong interest in basic or translational research. The appointments will be made at the Assistant Professor/Associate Professor/Professor level depending on qualifications and experience. A position in the Angiogenesis Research Center is available to the qualified candidate. We seek individuals with a strong record of academic productivity and the potential to establish or bring an independent research program focusing on vascular biology and development, genetics, molecular imaging or myocardial biology. An expertise in zebrafish or Xenopus research is particularly welcome. The successful candidate will be expected to participate in clinical activities of the Section of Cardiology and to engage in teaching in the Experimental Molecular Medicine graduate program and in the Angiogenesis Research Center. State-of-the-art facilities in the Section of Cardiology and Angiogenesis Research Center include 3D echo, MR and CT imaging, an advance microscopy core, and a mouse physiology and imaging cores. Additionally, Dartmouth Medical School offers many facilities that include micro-CT and micro-PET imaging, transgenics/knockout core and genomics and proteomics cores.

Please e-mail your curriculum vitae, a description of your research program, career goals and the names of three references to: michael.simons@dartmouth.edu, Dr. Michael Simons, Director, Angiogenesis Research Center, Dartmouth Medical School, Lebanon, NH 03756.

DARTMOUTH–HITCHCOCK
MEDICAL CENTER
www.dhmc.org

Dartmouth College is an Equal Opportunity/Affirmative Action employer and encourages applications from women and members of minority groups.

LANCASTER UNIVERSITY

Department of Environmental Science

Professor/ Reader of Environmental Science

Reader
£41,133 - £46,295 p.a.

Professor by negotiation
min £50,064 p.a.

Lancaster University is a dynamic institution committed to building on the reputation it has developed during its first forty years for pioneering innovation and excellence in teaching and research.

To apply or receive further information online, please visit http://www.personnel.lancs.ac.uk/ or, telephone Personnel Services, **quoting reference A763**, on answerphone (01524) 846549.

Closing date: 12 January 2007.

In pursuance of the strategic growth of this research-led Department (which is an integral part of the Lancaster Environment Centre) we invite applications for the post of Reader or Professor in either:

- **Earth System Atmospheric Science** or
- **Environmental Radionuclide Management**

The anticipated start date for both posts is 1 June 2007.

Informal enquiries may be addressed to n.hewitt@lancaster.ac.uk or a.binley@lancaster.ac.uk

Aiming for Greater Diversity

HOWARD HUGHES MEDICAL INSTITUTE

HHMI Investigator Competition in Patient-Oriented Research

We invite applications from physician-scientists who have demonstrated originality and productivity as patient-oriented researchers and who show exceptional promise for future contributions to the understanding and treatment of human disease.

Eligibility

- M.D. or M.D./Ph.D. (or the equivalent)
- Licensed to practice medicine in the United States
- Tenured or tenure-track position (or the equivalent) at one of 121 eligible institutions
- Four to 16 years of experience as an independent investigator
- Principal investigator on an active NIH R01 grant or project leader on an active NIH P01 grant
- Outstanding patient-oriented research program

Application deadline: January 18, 2007

Application information:
www.hhmi.org/investigator_por/sci

Highly creative researchers who bridge the gap between clinical medicine and basic science are in a unique position to exploit our knowledge of the human genome and other recent advances to make discoveries that will improve human health.

The Howard Hughes Medical Institute seeks to appoint approximately 15 outstanding physician-scientists as HHMI investigators. This competition is open to researchers with faculty appointments at 121 leading institutions in the United States. Candidates should apply directly to HHMI; prior institutional approval is not required.

The Howard Hughes Medical Institute, a nonprofit medical research organization, plays a powerful role in advancing biomedical research and education in the United States. HHMI's investigator program rests on the conviction that scientists of exceptional talent, commitment, and imagination will make fundamental biological discoveries for the betterment of human health if they receive the resources, time, and freedom to pursue challenging questions. The Institute's investigators, selected through rigorous national competitions, include 11 Nobel Prize winners and 115 members of the National Academy of Sciences.

The Howard Hughes Medical Institute is an equal opportunity employer. Women and members of racial and ethnic groups traditionally underrepresented in the biomedical sciences are encouraged to apply.

HHMI
HOWARD HUGHES MEDICAL INSTITUTE

VASCULAR BIOLOGIST
DEPARTMENT OF PATHOLOGY
BETH ISRAEL DEACONESS MEDICAL CENTER
HARVARD MEDICAL SCHOOL

The Department of Pathology at Beth Israel Deaconess Medical Center is seeking a full-time biomedical scientist at the Assistant Professor level in the area of vascular biology and angiogenesis. The Medical Center is a tertiary care facility and a major teaching hospital of Harvard Medical School. The Department of Pathology is embarking on the most ambitious program of growth in its history and is now actively expanding the strength and depth of both its clinical and research faculty. Ground has been broken for a new, state-of-the-art research building that will accommodate most of the research scientists within the Medical Center and all of the scientists within the Pathology Department.

We are seeking candidates of exceptional promise who have strong records of research creativity and productivity in basic or translational research in vascular biology and angiogenesis. The research should involve fundamental mechanisms for the regulation of angiogenesis. It may also involve the use of model organisms or the development of new technologies and strategies for the study of tumor angiogenesis.

The successful candidate will receive a highly competitive start-up package, appointment to the faculty of Harvard Medical School and full membership in the Beth Israel Deaconess Vascular Biology Research Center. The Department of Pathology strongly encourages interactions among research and clinical faculty and provides opportunities to access an extraordinary human tissue resource through its Divisions of Anatomic Pathology and Laboratory Medicine. We also provide unparalleled opportunities for collaborative interactions within the basic and applied vascular biology research community at Harvard Medical School and its affiliated teaching hospitals.

Applicants must hold a PhD and/or MD degree. Beth Israel Deaconess Medical Center is committed to increasing the representation of women and members of minority groups on its faculty, and we particularly encourage applications from such candidates. Interested applicants should submit curriculum vitae, a statement outlining existing and planned research activities and career goals, and the names of three professional references to: **Dr. Jack Lawler, Director, Division of Cancer Biology and Angiogenesis, Beth Israel Deaconess Medical Center, Research North Room 270C, 99 Brookline Avenue, Boston, MA 02215.**

NIST

National Institute of Standards and Technology
Technology Administration, U.S. Department of Commerce

NANOPHOTONICS/NANOPLASMONICS
ATOMIC FORCE MICROSCOPY

The Center for Nanoscale Science and Technology at NIST in Gaithersburg, MD is seeking two exceptional experimentalists with strong records of creativity and achievement in the fields of (a) nanophotonics and/or nanoplasmonics, and (b) atomic force microscopy. The applicants should possess the leadership abilities necessary to build a thriving research program, and should have a strong interest in development of new instrumentation and measurement methods. It is important that the applicants be able to interact with multiple disciplines and present effectively their programs to a variety of audiences. The new research programs will interface with and build upon extensive NIST programs for electrical, magnetic, chemical, physical, optical, and biological nanoscale measurements and standards. For additional information about the Center for Nanoscale Science and Technology please visit **http://cnst.nist.gov**.

We will consider filling these positions at any appropriate level (payband III-V, salary $54,272-$139,774). Candidates must have a PhD degree in physical science or engineering. Experience in nanophotonics and/or nanoplasmonics is required for one position, and in atomic force microscopy for the other. CVs will be accepted on a continuing basis and should be sent by e-mail to **CNSTjobs@nist.gov**.

The Department of Commerce is an Equal Opportunity Employer. US citizenship is required.

Faculty Position in Comparative Genetics/Complex Traits - 06271

College of Veterinary Medicine

Located in Ithaca, N.Y., Cornell University is a bold, innovative, inclusive and dynamic teaching and research university where staff, faculty, and students alike are challenged to make an enduring contribution to the betterment of humanity.

Applications are invited for a tenure track position at the College of Veterinary Medicine (**www.vet.cornell.edu**), from individuals using comparative genetic approaches to the understanding of complex traits. Targeted areas of research include disease resistance/susceptibility, gene-environment interactions, behavior and development. Individuals interested in using genome-wide strategies to exploit the potential of dog and other domestic animal populations in genetic studies are particularly encouraged to apply.

Candidates should have a Ph.D., MD, and/or DVM or equivalent degrees, be committed to developing a state-of-the-art, externally funded research program, and be motivated to participate in the university's teaching and public service missions. The position includes a competitive start-up package and is offered at the Assistant Professor level, with revision appropriate to the successful applicant's qualifications. Emphasis will be placed on identifying an exceptionally talented and promising individual who can build on the existing and ongoing expansions of programs in computational genomics, comparative medicine (including a new genetic archive), and molecular genetics that are part of Cornell University's Life Sciences Initiative (**lifesciences.cornell.edu**). Departmental affiliation within the College will be determined based on the successful applicant's background and expertise.

Please send a curriculum vitae, three letters of reference, and a research statement in a PDF format to: **Professor John Schimenti, Chair, Comparative Genetics Search Committee, c/o: mcb75@cornell.edu**

Review of applications will begin immediately and will continue until the position is filled. Women and under-represented minorities are strongly encouraged to apply.

Cornell University

Cornell University is an Affirmative Action, Equal Opportunity Employer and Educator.

http://chronicle.com/jobs/profiles/2377.htm

Tenure Track Position in Nanotechnology
University of California San Francisco

The Department of Pharmaceutical Chemistry and the California Institute for Quantitative Biomedical Research, QB3, seek highly qualified applicants for a faculty position at the Assistant/Associate Professor level who have strong research interests in nanotechnology. This position is part of a major initiative at the Mission Bay/China Basin Landing campus of UCSF and will build on the University's strengths in Chemistry and Quantitative Biology. Of particular interest are applicants developing nanotechnology in areas that include diagnostics, molecular imaging, targeted therapeutics and basic biological discovery.

Applicants should have a Ph.D., M.D. or advanced degree with considerable research experience and are expected to establish a dynamic research program. Applicants are also expected to actively participate in graduate training in the Chemistry and Chemical Biology Program and in other Programs in Quantitative Biology, Biophysics or Bioengineering and in professional school teaching. Applicants will be eligible for membership in the Comprehensive Cancer Center, the Program in Biological Sciences (PIBS) and other graduate training programs including the UCSF/UCB joint Program in Bioengineering.

UCSF seeks candidates whose experience, teaching, research, or community service has prepared them to contribute to our commitment to diversity and excellence.

Please send a *curriculum vitae,* three letters of reference, a summary of current research (up to 3 pages), and a concise outline of future research (up to 3 pages) by **January 31, 2007**, to the address below.

Barbara Raymond
Nanotechnology Search Committee
Department of Pharmaceutical Chemistry
University of California, San Francisco
600 16th Street, MC 2280
Genentech Hall, Room 518
San Francisco, CA 94158-2517

UCSF is an Affirmative Action/Equal Opportunity Employer. The University undertakes affirmative action to assure equal employment opportunity for underutilized minorities and women, for persons with disabilities and for covered veterans.

eawag
aquatic research

Eawag is the Swiss Federal Institute of Aquatic Science and Technology, a Swiss-based and internationally active research institute within the ETH domain, committed to an ecological, economical and socially responsible management of water (Eawag; http://www.eawag.ch). We have an open position for an outstanding individual as

Head of the Department of Systems Analysis, Integrated Assessment, and Modelling

The mission of the department is to develop and apply models of natural, technical and social systems to improve our understanding of these systems, of the consequences of environmental policies, and to support environmental decision making.

The department supports 6 research groups with research topics in systems analysis and surface water modelling; modelling of soil, groundwater and watersheds; material flows in the anthroposphere; modelling of social systems; water environment and food security; and integrative modelling and decision analysis. The researchers in the department strongly collaborate with other departments of Eawag and internationally. Many of them teach at ETH Zürich or the University of Zürich and are involved in continuing education programs for water managers.

The successful candidate is expected to head the department and establish a research group on integrative modelling and decision analysis. She or he should have

- An excellent scientific record in environmental systems analysis and modelling.
- Capability and willingness to lead a multidisciplinary research department in a stimulating environment of water research.
- A sound knowledge of decision analysis and statistics.
- Experience in leading a research group in these fields and potential to attract external funding from competitive sources.
- Experience in management of significant research- and consulting projects.
- Willingness to cooperate in inter- and multidisciplinary projects.
- Experience in academic teaching and continuing education.
- Strong and integrative organizational and communication skills.

As a top research institute in aquatic sciences, Eawag provides excellent facilities for high quality research, provides a stimulating interdisciplinary research environment, and operates a child care centre. It hosts over 100 PhD students (mainly from ETH Zurich) which conduct research under the direction of Eawag faculty. Strong collaboration with ETH Zurich, which is one of the leading European universities, contributes to the attractive work environment. Zurich ranks among the cities with the highest quality of life worldwide.

For questions please contact Prof. Peter Reichert (reichert@eawag.ch). Your application letter, including CV, publication list, research interests as well as names and addresses of 5 referees, should be sent to:
Jadranka Vögelin, Human Resources, Eawag,
CH-8600, Dübendorf, Switzerland, or per e-mail (jadranka.voegelin@eawag.ch). Applications should be submitted by Jan. 31 2007,
interviews are planned for early March 2007.

Eawag: Das Wasserforschungs-Institut des ETH-Bereichs

FACULTY POSITIONS IN CELLULAR AND MOLECULAR IMMUNOLOGY

The Immunology Program at the H. Lee Moffitt Cancer Center & Research Institute and the University of South Florida's College of Medicine, Department of Interdisciplinary Oncology, are seeking highly qualified (PhD or MD) applicants for tenure track positions in Cellular and Molecular Immunology at Assistant, Associate and Full Professor levels. While applicants in all areas of Cellular and Molecular Immunology may apply, we are especially interested in individuals with molecular approaches and signal transduction mechanisms related to studies of T cells, chemokines, and the tumor microenvironment. Successful applicants will be expected to develop an outstanding research program in their area of interest.

Assistant Professor must have at least four years of postdoctoral experience in tumor immunology and high quality publications in peer-reviewed journals. The Associate/Full Professor must have a proven track record of independent research and demonstrated sustained extramural funding. In addition, the Associate Professor rank requires at least five years of experience with continuing and productive service as an Assistant Professor. The Professor rank requires documentation of national recognition, leadership ability and at least five years of experience with continuing and productive service as an Associate Professor. Salary is negotiable.

The Moffitt Cancer Center and Research Institute provides an exceptional environment for basic and translational research in Immunology, Molecular Oncology and Drug Discoveries. Extensive state-of-the-art core facilities are available for flow cytometry, gene profiling, proteomics, mouse model development, high throughput screening/chemistry, and drug discovery. Successful applicants will be provided generous laboratory and office space in the new Vincent A. Stabile Research Building.

Please reference position 11851. Send curriculum vitae and a brief statement of major academic interests in one single pdf document to The Immunology Search Committee at koransky@moffitt.usf.edu. Application review begins December 1, 2006. Applications will be accepted and continuously reviewed until the position is filled.

USF Health is committed to increasing its diversity and will give individual consideration to qualified applicants for this position with experience in ethnically diverse settings, who possess varied language skills, or who have a record of research that supports/benefits diverse communities or teaching a diverse student population.

H. LEE MOFFITT Cancer Center & Research Institute
The End Of Cancer Begins Here.
A National Cancer Institute Comprehensive Cancer Center
At the University of South Florida

USF University of South Florida
College of Medicine

The University of South Florida is an EO/EA/AA Employer. For disability accommodations, contact Kathy Jordan at (813) 632-1451 a minimum of five working days in advance. According to FL law, applications and meetings regarding them are open to the public.

www.moffitt.usf.edu

POSITIONS OPEN

FACULTY POSITION IN BIOCHEMISTRY AND MOLECULAR BIOLOGY
University of Nebraska Medical Center

The Department of Biochemistry and Molecular Biology invites applications for two tenure-leading positions at the rank of **ASSISTANT/ASSOCIATE PROFESSOR.** Qualifications include a Ph.D. or M.D. degree and relevant postdoctoral experience. Preference for both positions will be given to outstanding candidates who can utilize state-of-the-art biochemical and molecular approaches to cancer research, proteomics, and chromatin remodeling. The ideal candidates will have research interests and experience that will supplement ongoing research in the Department **(website: http://www.unmc.edu/Biochemistry/).**

The successful applicant will be expected to have or develop a funded, independent research program and to contribute significantly to the teaching programs of the Department. Submit your curriculum vitae, a description of research interests and teaching experience, and three letters of reference to: **Surinder K. Batra, Ph.D. Chair, BMB Search Committee, Department of Biochemistry/Molecular Biology, 985870 Nebraska Medical Center, Omaha, NE 68198-5870.** Also e-mail a PDF or MSWord file of the above documents to **e-mail: biochem@unmc.edu.** *University of Nebraska Medical Center is an Equal Opportunity/Affirmative Action Employer. Minorities and women are encouraged to apply.*

FACULTY POSITION
Department of Applied Science
College of William and Mary

The Department of Applied Science at the College of William and Mary, an interdisciplinary Ph.D.-focused Department established in 1995, invites applications for a tenure-track position at the **ASSISTANT PROFESSOR** level in biophysics, neurophysiology, biomedical engineering, biomaterials, or a related field, emphasizing either computational or experimental approaches. The new faculty member will be expected to establish a vigorous, independent, and well-funded graduate research program at the interface of the physical, mathematical, and biological sciences. Excellence and high commitment to the teaching of graduate and undergraduate students is expected of all faculty at the College. Located two hours south of Washington, D.C. in Williamsburg, Virginia, the College of William and Mary is the second oldest University in the United States and was recently named by the editors of Newsweek as the "hottest small state school" in the nation. Candidates should submit complete curriculum vitae, research statement, and copies of no more than five refereed publications to: **Faculty Search Committee, Department of Applied Science, The College of William and Mary, P.O. Box 8795, Williamsburg, VA 23187-8795,** and arrange to have three letters of recommendation mailed to the same address. Review of materials is expected to begin January 1, 2007, and continue until the position is filled. For more information see **website: http://as.wm.edu.**

The College is an Equal Employment Opportunity/Affirmative Action Employer.

POSTDOCTORAL RESEARCHER POSITION to study *E. coli* AraC family transcription activators, including development of antibacterial agents against AraC family virulence activators. Ph.D. required. Review of applications begins December 10, 2006, and continues until position filled. For more information and to apply go to **website: https://jobs.ku.edu** and search for position 00206132. Inquiries to: **Dr. Susan Egan, Department of Molecular Biosciences, University Kansas, Lawrence, Kansas,** at **e-mail: sme@ku.edu.** *University of Kansas is an Equal Opportunity/Affirmative Action Employer.*

POSITIONS OPEN

ENDOWED CHAIR/HISTORY OF SCIENCE
Thomas Hart and Mary Jones Horning Professorship

Oregon State University (OSU) invites nominations and applications for appointment to the Thomas Hart and Mary Jones Horning Professorship in the Humanities. This endowed Chair is in the Department of History and will be filled by an Historian of Science in any specialty. The holder of the Chair is expected to be a senior scholar with a distinguished record of publication and teaching in the history of science. Appointment to the Chair will carry tenure and a position of Professor in the Department of History. The estate of the late **Benjamin Horning** established an endowment at Oregon State University for the purpose of supporting the Humanities. Dr. Horning's intent was to improve and extend the teaching of humanities to students in the sciences and technical areas offered by Oregon State University. Visit our **website: http://oregonstate.edu/cla/history/.**

Nominations and applications should be sent to the: **Chair of the Horning Search Committee, Paul Farber, Oregon State University, Department of History, 306 Milam Hall, Corvallis OR 97331-5104.** Nominations and application should consist of a letter of interest (or a letter describing the nominee), curriculum vitae, and the names of three to five references. References will not be contacted until the Horning Search Committee has confirmed interest from the nominee. To ensure full consideration, applications (or nominations) must be received by January 31, 2007. *OSU is an Affirmative Action/Equal Opportunity Employer.*

TWO FACULTY POSITIONS
Dartmouth Medical School

The Angiogenesis Research Center at Dartmouth Medical School is seeking to recruit two new tenure-track faculty members (M.D., Ph.D., or M.D./Ph.D.) The appointments will be made at the **ASSISTANT PROFESSOR/ASSOCIATE PROFESSOR/PROFESSOR** level depending on qualifications and experience. We seek individuals with a strong record of academic productivity and the potential to establish or bring an independent research program focusing on vascular development, immunology, genetics, or signaling. An expertise in zebrafish or *Xenopus* research is particularly welcome. The successful candidate will be expected to actively engage in teaching in both the Experimental Molecular Medicine (PEMM) graduate program and within the Angiogenesis Research Center. State-of-the-art facilities within the Angiogenesis Research Center include an advance microscopy core and a core for the generation and analysis of new mouse models and mouse imaging. Additionally, Dartmouth Medical School offers many facilities that include micro-CT and micro-PET imaging, and genomics and proteomics cores. Please e-mail your curriculum vitae, a description of your research program, career goals, and the names of two to three references to **e-mail: tabatha.l.richardson@dartmouth.edu** or mail to: **Dr. Michael Simons, Director, Angiogenesis Research Center, Dartmouth Medical School, Lebanon, NH 03756.** *Dartmouth College is an Equal Opportunity/Affirmative Action Employer and is especially interested in identifying female and minority candidates.*

UNIVERSIDAD DE LOS ANDES
Faculty Positions

The Department of Chemistry at the Universidad de Los Andes in Bogotá D.C., Colombia, invites applications for full-time **PROFESSORAL POSITIONS** and **VISITING PROFESSOR** in the areas of biochemistry, organic chemistry, and geochemistry. Applicants should have a Ph.D. degree in the area of interest. Candidates must be committed to excellence in teaching and research. Applicants should submit detailed curriculum vitae and make arrangements to have recommendation letters sent to **e-mail: jumoreno@uniandes.edu.co.**

POSITIONS OPEN

The Yale University School of Medicine is seeking faculty at the **ASSISTANT or ASSOCIATE PROFESSOR** level with independent research programs in basic research pertinent to all areas of kidney biology or disease. Research interest in glomerular disease, kidney development, or translational science are encouraged. Laboratory space, startup package, and protected time commensurate with needs are available in the newly opened Anlyan Center. Successful applicants should be Board-certified/Board-eligible in nephrology. Demonstrated success in competing for extramural funding is desirable. Please reply with curriculum vitae, a description of the research program, and the names of three references by February 1, 2007, to:

Stefan Somlo, M.D.
Chief, Section of Nephrology
Yale University School of Medicine
P.O. Box 208029
333 Cedar Street
New Haven, CT 06520-8029
E-mail: denise.krause@yale.edu.

Yale University is an Affirmative Action/Equal Opportunity Employer.

ASSISTANT or ASSOCIATE PROFESSOR of HORTICULTURE

The Department of Horticulture at the University of Kentucky is seeking a creative and talented individual to fill a 12-month, Tenure-Track position in research (80 percent) and teaching (20 percent). The Department is interested in filling the position with an individual with demonstrated potential to establish a nationally recognized research program in horticulture. The person in this position will be expected to secure extramural funding to support research, to mentor graduate students, and to foster research collaboration. This position will contribute to undergraduate education through academic student advising and teaching a formal horticulture course. Individuals with diverse horticulture and/or plant science-related backgrounds are encouraged to apply. A Ph.D. in horticulture or related plant science is required. Candidates must be able to demonstrate evidence of research excellence and the ability to communicate effectively. Apply online at **website: http://www.uky.edu/HR/UKjobs/,** using the position title above. Review of applications will begin January 31, 2007, and continue until a suitable applicant is identified. For more information contact **Dr. Dewayne Ingram** at **telephone: 859-257-1758** or **e-mail: dingram@uky.edu.**

FACULTY POSITION
Cognitive Psychology

The Department of Psychology at Columbia University seeks an **ASSISTANT PROFESSOR** in the area of cognitive psychology to begin July 1, 2007. Candidates should provide evidence of excellence in research and a strong commitment to both graduate and undergraduate education. Ph.D. in psychology or related field required at the time of appointment. Applicants should submit their curriculum vitae, including e-mail address, copies of relevant papers, and arrange to have three letters of reference sent to the: **Cognitive Psychology Search Committee, Department of Psychology, Columbia University, 1190 Amsterdam Avenue, MC 5501, 406 Schermerhorn Hall, New York, NY 10027.** We will begin reviewing applications on December 1, 2006, and will continue until the position is filled. For more information see **website: http://www.columbia.edu/cu/psychology.**

Applications from minorities and women are encouraged. Columbia University is an Affirmative Action/Equal Opportunity Employer.

PROJECT MANAGEMENT AGENCY FOR THE

Federal Ministry of Education and Research

Call for Proposals

BMBF Competition „GO-Bio"

Group Leaders Biotechnology

The German Federal Ministry of Education and Research (BMBF) provides the opportunity to build up independent research groups for outstanding scientists from Germany and abroad. The main objective is to work on innovative, applied research oriented topics in the biosciences fields and to translate the inventive research activities into new entrepreneurial initiatives .

Besides a convincing scientific concept for new approaches to biosciences, candidates must present a promising strategy for application and commercialization of the outcomes. Additionally applicants need a German research institution to host and support their independent research group. Depending on the proposed concept the research group may consist of 1 group leader, 6 scientific members and 2 technical assistants .

Funded Projects are identified in a two-step procedure by a jury. Successful candidates and their teams will be funded by grants for an initial period of up to 3 years. Depending on a successful progress, the project can be extended for a maximum of 3 years.

The closing date for project outlines is January 15, 2007

Contact:
Dr. Ralf Jossek, e-mail: ptj-gobio@fz-juelich.de

www.fz-juelich.de/ptj/go-bio

RESEARCH Igniting ideas!

[redacted]

WORKING AT THE UNIVERSITY OF GENEVA

The **FACULTY OF SCIENCE** seeks a

FULL or ASSOCIATE PROFESSOR in Molecular Biology

(Professeur-e ordinaire ou Professeur-e adjoint-e)

POST: Full-time research and teaching position in the general area of molecular biology. Special consideration given to scientists studying important biological problems using novel chemical, genetic or biophysical approaches.

REQUIREMENTS: Ph.D. degree or equivalent. Experience in teaching and leading an independent research project.

STARTING DATE: 1er July 2007/at the earliest.

Candidates files must be addressed before **February 1st, 2007** (extension of the previous deadline) to : Décanat de la Faculté des sciences, 30, Quai Ernest-Ansermet, CH-1211 Genève 4, from whom additional information can be obtained regarding the responsibilities of the post and other conditions.

The University of Geneva is an equal opportunity employer and encourages applications from female candidates.

UNIVERSITÉ DE GENÈVE

[redacted]

Max-Planck-Gesellschaft
Max Planck Society

Selbstständige Nachwuchsgruppen

Independent Junior Research Groups

The Max Planck Society invites applications from outstanding young scientists in all fields of research pursued by the Max Planck Society (Biology and Medicine; Chemistry, Physics and Technology; Human Sciences).

Successful applicants will have demonstrated the ability to perform excellent research. They will be offered an

Independent Junior Research Group Leader position

(W2; equivalent to associate professor level without tenure) including a five-year grant (research positions, budget, investments) at a

Max Planck Institute of their choice.

Applications should include a CV, a list of publications, copies of three publications, a one-page summary of scientific achievements, and a two-page research plan. For further information and detailed application instructions see

http://www.snwg.mpg.de

The Max Planck Society is committed to equal opportunities and to employing disabled persons.

The deadline for application is **January 10, 2007.**

POSITIONS OPEN

FACULTY POSITIONS IN ATMOSPHERIC SCIENCE

The MIT Department of Earth, Atmospheric and Planetary Sciences seeks applicants for two faculty positions in atmospheric science. One position is in atmospheric chemistry, the second is in other areas of atmospheric science.

Atmospheric Chemistry: Areas of specific interest include multiphase (gas, aerosol, cloud) chemical and physical processes, and the multiple roles of atmospheric chemistry in climate. Our preference is for a scientist with strong laboratory and/or field measurement experience but scientists with outstanding theoretical and modeling experience applied to field measurements are also encouraged to apply. Depending on accomplishments and experience, the appointment can be at **ANY LEVEL**, including **FULL PROFESSOR.** The successful candidate will have an outstanding record of accomplishment in their discipline, a strong commitment to teaching and student advising, and an abiding interest in relating their work to complementary work in the atmospheric and climate sciences at MIT. Joint appointments with other MIT departments are also potentially negotiable where appropriate.

Atmospheric Science: We seek individuals with a strong background and interest in atmospheric physics, dynamics, synoptic meteorology, and/or climate science. Candidates should have a thorough understanding of theory and a desire to build a top-quality research program which can link to ongoing projects in the Department. We are particularly interested in individuals with a strong commitment to research, teaching, and graduate advising. Strong preference will be given to candidates at the junior faculty level.

To apply to either of these positions, please send your curriculum vitae, a statement of your research and teaching objectives, and the names of five potential references to: **Professor Maria Zuber, Head, Department of Earth, Atmospheric and Planetary Sciences, MIT, Cambridge, MA 02139;** and to **e-mail: mjr@mit.edu.** *MIT is an Equal Opportunity/Affirmative Action Employer. Applications from women, minorities, veterans, older workers, and individuals with disabilities are strongly encouraged.*

FACULTY POSITIONS IN BIOLOGICAL SCIENCES

The Department of Biological Sciences at Mississippi State University **(website: http://www.msstate.edu/dept/biosciences)** invites applications for **ASSISTANT PROFESSOR** tenure-track positions that begin August 16, 2007. These faculty members will contribute to one of three focus areas: cell biology/genetics, ecology/evolution or microbiology/immunology. The scientific infrastructure at Mississippi State University includes focus areas in proteomics, genomics and digital biology, along with these supporting facilities: the Life Sciences and Biotechnology Institute **(website: http://www.mafes.msstate.edu/biotech),** the Electron Microscope Center **(website: http://www.msstate.edu/dept/emc)** and the GeoResources Institute **(website: http://www.gri.msstate.edu).** Successful candidates will develop externally funded research programs in any of the above-mentioned areas, direct graduate students, and contribute to the teaching mission of the Department. Minimum requirements include a Ph.D. in a related biological sciences field, but all-but-dissertation candidates will be considered. To apply, send curriculum vitae, reprints of three representative publications, a concise statement of current and future research interests (one page), and identify the position/area you are applying for, plus relevant areas of teaching competence. Applicants should also arrange for at least three letters of reference to be submitted on their behalf. Screening will begin January 15, 2007, and will continue until the positions are filled. Send application packets to: **Dr. Nancy Reichert, Interim Head, Department of Biological Sciences, P.O. Box GY, Mississippi State University, Mississippi State, MS 39762 (e-mail: facultysearch@biology.msstate.edu).** *Mississippi State University is an Affirmative Action/Equal Opportunity Employer.*

POSITIONS OPEN

INSTITUT PASTEUR

POSTDOCTORAL FELLOWSHIPS
Institut Pasteur, Paris, France

Founded in 1887 by Louis Pasteur and located in the heart of Paris, the Institut Pasteur is a world-renowned private research organization. The Pasteur Foundation is seeking outstanding Fellowship Applicants. Candidates may apply to any laboratory within 10 departments: cell biology and infection; developmental biology; genomes and genetics; immunology; infection and epidemiology; microbiology; neuroscience; parasitology and mycology; structural biology and chemistry; and virology. See website for details.

Fellowships are $60,000 per year for three years ($45,000 stipend plus $15,000). *U.S. citizenship required.* Deadline: February 2, 2007.

E-mail: pasteurus@aol.com.

Website: http://www.pasteurfoundation.org.

NEW FACULTY POSITIONS
Department of Pharmacology, Toxicology, and Therapeutics
University of Kansas Medical Center (KUMC)

The Department of Pharmacology, Toxicology, and Therapeutics under the direction of **Curtis Klaassen, Professor and Chair (website: http://www.kumc.edu/pharmacology/),** is continuing its expansion by inviting applications for two **ASSISTANT PROFESSORS,** tenure-track faculty positions to augment the strength of our eight recent hires. Preference will be given to candidates in areas such as nuclear receptors, toxicology, or xenobiotic disposition (absorption, distribution, metabolism, excretion) that complement existing strengths in the Department and the Medical Center. This expansion is supported by a new Centers of Biomedical Research Excellence (COBRE) grant entitled Nuclear Receptors in Liver Function and Dysfunction, a recently renewed training grant in environmental sciences, and a new research building. Broad areas of strength at the Medical Center include cancer, neuroscience, reproductive biology, renal pathophysiology, and growing efforts in liver biology. A competitive startup package and appropriate space will be offered. Standard support facilities are present, including biotechnology, transgenics, proteomics, and a state-of-the-art imaging center. The Department also has excellent molecular biology (robot, real time PCR, sequencer), and liquid chromatography/mass spectrometry facilities. Applications will be reviewed as they are received until the positions are filled. Anticipated appointment date is as early as July 1, 2007. Applicants must be proficient in the use of the English language. Applicants should provide curriculum vitae, statement of research interests, and names of three references. To review the position description and apply online go to **website: http://jobs.kumc.edu** and search for position J0020073. Paid for by KUMC. *The University of Kansas Medical Center is proud to be an Equal Opportunity/Affirmative Action Employer.*

POSTDOCTORAL FELLOW to work on a palate development. Expertise in cell signaling, tissue culture, biochemical, molecular biological, and morphological techniques required. Submit curriculum vitae, current research activities, and career goals in electronic format to: **Human Resources, The Texas A&M University System Health Science Center, 3302 Gaston Avenue, Dallas, TX 75246; e-mail: jobs@tambcd.edu.** *Baylor College of Dentistry is an Equal Opportunity Employer.*

POSITIONS OPEN

The Biological Sciences Department at California State Polytechnic University, Pomona, invites applications for a tenure-track, **ASSISTANT or ASSOCIATE PROFESSOR** position, in cell and molecular biology, beginning September 2007. Candidates are required to have research and development experience in biotechnology or the pharmaceutical industry and will be expected to participate in the undergraduate biotechnology major program. A Ph.D. in biology, molecular biology, or related fields is required and postdoctoral experience is preferred. We will consider cell and molecular biology candidates with a broad range of interests, but applicants with stem cell research are especially encouraged to apply. The successful candidate will combine excellence in teaching with an externally funded research program that will involve undergraduate and Master's students. Teaching responsibilities will include courses in cell and molecular biology, and development of a graduate-level course related to the individual's area of expertise. Cal Poly Pomona is a comprehensive Master's level University with a diverse student body. The successful candidate will have demonstrated ability to be responsive to the educational equity goals of the University and its increasing ethnic diversity and international character. Applicants should forward (1) curriculum vitae, (2) statement of teaching philosophy, (3) proposed plan of research, (4) reprints of three representative publications, and (5) the names and contact information of three references to: **Chair, Cell and Molecular Biology Search Committee, Biological Sciences Department, California State Polytechnic University, 3801 West Temple Avenue, Pomona, CA 91768-4132.** Review of applications will begin on January 22, 2007. Official transcripts and three letters of reference will be required of all finalists. For further information, visit the Department **website: http://www.csupomona.edu/~biology.** As required by the Clery Disclosure Act, the University's annual security report is available at **website: http://www.csupomona.edu/~public_safety.**

California State Polytechnic University, Pomona, is an Equal Opportunity, Affirmative Action Employer. Cal Poly Pomona subscribes to all state and federal regulations and prohibits discrimination based on gender, race, sexual orientation, national origin, disability, marital status, age, religion, or veteran status. The University hires only individuals lawfully authorized to work in the United States.

ENVIRONMENTAL GEOPHYSICS

The Vancouver Campus of Washington State University (WSU) invites applications for a full-time, tenure-track **ASSISTANT PROFESSOR** in environmental geophysics. Area of emphasis is open, but candidates with expertise in surface or shallow subsurface processes, and who complement the strengths of existing science faculty, are strongly encouraged to apply. Successful applicant will teach two courses per year, advise both graduate and undergraduate students, and establish a productive, externally funded research program. Excellence in research and instruction are the main criteria for selection. Minimum qualifications: Ph.D. in geophysics-related discipline by date of hire. Preferred candidates will demonstrate a commitment to working with diverse student and community populations. WSU Vancouver is located across the Columbia River from Portland, Oregon, and offers significant opportunities for research and an excellent quality of life. Additional information is available at **website: http://www.vancouver.wsu.edu/programs/sci/.** Applicants should submit a cover letter, curriculum vitae, statement of research interests and accomplishments, statement of teaching philosophy and interests, copies of two publications, and three letters of reference to: **Environmental Geophysics Search, Washington State University Vancouver, 14204 N.E. Salmon Creek Avenue, Vancouver, WA 98686-9600.** Review of completed applications will begin on January 2, 2007. *Washington State University is an Equal Opportunity/Affirmative Action Educator and Employer. Members of groups historically underrepresented in science are strongly encouraged to apply.*

School of Computational Science at Florida State University

Faculty Position in Computational Evolutionary Biology

The Computational Evolutionary Biology (CEB) group at the School of Computational Science (**http://www.scs.fsu.edu**) at Florida State University seeks candidates for a faculty position in computational evolutionary biology starting in Fall 2007. The successful applicant will have joint appointments in the School of Computational Science and a secondary department best suited to their research interests.

We seek candidates at the Assistant Professor level but exceptional candidates at more senior levels will also be considered. We are especially interested in applicants who are applying computational phylogenetics to model evolutionary processes. This includes those developing algorithms to estimate ancestral values for molecular/morphological traits, population parameters, and selection/mutation models, and those working to elucidate the evolution of protein structure/function, gene-networks and morphological development. We will also consider exceptional applicants whose research centers around algorithm development for phylogenomics.

This hire builds on existing strengths in theoretical phylogenetics and population genetics at FSU and comes at a time when the university is expanding research in the life sciences through its Pathways of Excellence Cluster hiring initiatives. The department of Biological Science is currently recruiting a new cluster of faculty to explore the mappings between molecular processes and resulting phenotypes (**http://pathways.fsu.edu/faculty/igp/**). This expansion will provide excellent opportunities for new collaborations between the Computational Evolutionary Biology group and members of the Department of Biological Science.

A Ph.D. in one of the sciences is required. Postdoctoral experience is highly desired. The new faculty member will be expected to participate in MS/PhD degree programs in both Computational Science and their secondary department, to have an active research program and to be involved in teaching in both departments.

Those interested in being considered for the position should apply electronically to **http://www.scs.fsu.edu/jobs.php**. Applications received by **January 1, 2007** are assured of full consideration.

Applications require electronic submission of a Curriculum Vitae, research and teaching statements (PDF files preferred) and the names of four references. Inquiries concerning the position should be sent to: **cebhire@scs.fsu.edu**.

FSU is an EO/AA Employer committed to diversity in hiring.

University of California, Irvine
DEAN, SCHOOL OF BIOLOGICAL SCIENCES

The University of California, Irvine invites applications and nominations for the position of Dean, School of Biological Sciences. The university seeks an independent thinker with skills to navigate within a complex/multi-constituent organization and who is decisive while fair and strategically focused. The successful candidate has a keen intellectual capacity and creativity, and is an open and persuasive communicator who leads from values; a candidate with energy and vision to head and continue the mission of the school. Key selection criteria will include:

- Demonstrated leadership in promoting the latest intellectual advances in the Biological Sciences
- Experience and demonstrated success with external relations/development - Demonstrated skill/ability to work effectively with the business community and other constituents in resource development and advancement of the School
- Faculty leadership and team building - Proven ability to inspire consensus and develop a culture that is mutually supportive, goal-directed and ambitious. Ability to attract and recruit world-class faculty
- Administrative management - Demonstrated success as an administrator, including staff development, facility/resource management and fiscal leadership

Celebrating 40 years of innovation, the University of California, Irvine is a top-ranked public university dedicated to teaching, scholarship and community service. Founded in 1965, UCI is among the fastest-growing campuses in the University of California system, with more than 24,000 students, 1,400 faculty members and 8,300 staff. The second-largest employer in dynamic Orange County, UCI contributes an annual economic impact estimated at $3.3 billion. It is located on a 1500-acre site three miles from the ocean in the community of Orange County. The School of Biological Sciences, one of ten schools at the University of California, Irvine, currently has an operating budget of $27.5 million, and extramural grant funds of $38.8 million. The School has an enrollment of approximately 3500 undergraduate students and 400 graduate students, 105 full time faculty and over 250 additional academic researchers, and 149 staff members. The School represents a premier center for biological education and research with four solid departments: Developmental and Cell Biology, Ecology and Evolutionary Biology, Molecular Biology and Biochemistry, and Neurobiology and Behavior.

Candidates for this position should have a strong academic record that would justify a senior rank appointment in one of the four departments with a sustained record of peer reviewed extramural funding and an international reputation in a biological sciences discipline. Review of applications will begin on **February 1, 2007** and the position will remain open until filled. We encourage electronic application submission; please click the online application link to begin the submission process: **http://www.evc.uci.edu/searches/index.html**. Paper applications and nominations may be sent to the address below: **School of Biological Sciences Dean Search Committee, C/O Heike Rau, 509 Administration, University of California, Irvine, Irvine, CA 92697-1000;** OR email: **biosrch@uci.edu.**

UCI is an Equal Opportunity Employer committed to excellence through diversity and strongly encourages applications from all qualified applicants, including women and minorities.

CHAIRMAN,
Department of Cell Biology
University of Oklahoma Health Sciences Center

Applications/nominations are invited for Chair of the Department of Cell Biology at the University of Oklahoma Health Sciences Center. This individual must be committed to the Department's mission of biomedical research in cellular, developmental, and molecular biology, as well as medical education. The successful candidate will have an M.D., Ph.D., or equivalent doctoral degree, qualify for tenured appointment as Professor, and be an internationally recognized leader in his/her area of research. Candidates with interests in cancer biology and diabetes are particularly sought, given the Department's participation in the ongoing expansion of the OU Cancer Institute and the Oklahoma Diabetes Center. Leadership positions in the OUCI are available for qualified applicants. With over $180 million in public and private support, OUCI represents the largest investment in biomedical research in the state's history. Please send a letter of application, curriculum vitae, the names and contact information for five references, plus a one-page summary that includes teaching philosophy and goals for maintaining and expanding the Department to: **Dr. Robert Foreman, Chair, Cell Biology Chair Search Committee, The University of Oklahoma, BMSB 653, 940 Stanton L. Young Blvd., Oklahoma City, OK, 73104 (http://w3.ouhsc.edu/cell%5Fbiology/)**. The review of applications will begin immediately and continue until the position is filled.

The University of Oklahoma is an Equal Opportunity Institution.

ASSISTANT/ASSOCIATE PROFESSOR BIOLOGY

the City College of New York

Compensation: $38,001 - $79,220 Commensurate with qualifications and experience

College Web Site: www.ccny.cuny.edu

Notice Number: FY12577

Closing Date: 12/27/06

POSITION DESCRIPTION AND DUTIES

The Biology Department at City College invites applications for a tenure track position in Neuroscience. The candidate must use molecular, genetic or cellular approaches to problems in neurobiology. The candidates' research should complement the research interests of existing faculty; these include cellular and molecular aspects of development and behavior, bird-song development, sensory motor integration and plasticity, neurophysiology and anatomy of the visual cortex, and visual control of eye growth. City College has an active and expanding neuroscience community, which include the departments of Biomedical Engineering, Psychology and Physiology/Pharmacology.

QUALIFICATION REQUIREMENTS

Doctorate required. Candidate must demonstrate a strong interest and commitment to undergraduate teaching and the capability of developing and maintaining an active research program supported by external funding.

TO APPLY: PLEASE SEND COVER LETTER, CURRICULUM VITAE, NAMES OF THREE PROFESSIONAL REFERENCES, TO: **Ofer Tchernichovski, Chairman, Neuroscience Search, Biology Dept., Room J526, The City College of New York, 160 Convent Avenue, New York, NY 10031**

The City University of New York is an Equal Employment Opportunity/Affirmative Action/Immigration Reform and Control Act/ Americans with Disabilities Act Employer

CITY COLLEGE IS CUNY

POSITIONS OPEN

MILLER SCHOOL OF MEDICINE
UNIVERSITY OF MIAMI

PROFESSOR, PHARMACOGENOMICS

The University of Miami Miller School of Medicine is fostering major expansion of its genetics research program. The Department of Psychiatry and Behavioral Sciences is under new leadership **(Julio Licinio, M.D., Chairman)** and it is undergoing significant growth and is opening a new Center on Pharmacogenomics. The Center is focused on understanding pharmacogenomics mechanisms underlying clinical response and identifying new targets for drug development. We are recruiting for a new faculty member at the **PROFESSOR** level with the ability to develop research programs in molecular genetics, genomics, and in genetics related to antidepressant response. Outstanding background with publications, grant track record, and mentoring experience is required. We seek a Senior Investigator with a documented track record who can develop new and independent funded lines of research in pharmacogenomics applied to depression and antidepressants. Competitive startup package available with excellent benefitsSend curriculum vitae, contact information for three references to: **Julio Licinio, M.D., Chairman, Department of Psychiatry and Behavioral Sciences, University of Miami Miller School of Medicine, e-mail: licinio@miami.edu.** *The University of Miami is an Equal Opportunity/Affirmative Action Employer.*

ASSISTANT PROFESSOR
Molecular Microbiology/Immunology

The Department of Biological Sciences at Purdue University Calumet invites applications for a tenure-track position to begin in August 2007. A Ph.D. degree, postdoctoral experience, and excellent verbal/written communication skills are required. Responsibilities will include (1) teaching undergraduate and graduate courses, which may include introductory biology, microbiology, immunology, and upper-division courses in areas of expertise, (2) establishing a vigorous extramurally funded research program, involving graduate/undergraduate students, that will complement and enhance current departmental strengths in molecular biology and biotechnology, and (3) service to the University. Purdue University Calumet, the Chicago-area campus of the Purdue University system, is a M.S. Comprehensive University with over 9,300 students, of which approximately 425 undergraduate majors and 25 graduate students are enrolled in the Department of Biological Sciences **(website: http://www.calumet.purdue.edu/biology/).** Review of applications will begin January 15, 2007, and continue until the position is filled. Inquiries or letters of application stating teaching philosophy and research interests, curriculum vitae, copies of graduate/undergraduate transcripts, and three original letters of recommendation with contact information should be sent to: **Dr. W-T Evert Ting, Chair of Search Committee, Department of Biological Sciences, Purdue University Calumet, 2200 169th Street, Hammond, IN 46323-2094; e-mail: biosearch@calumet.purdue.edu.** *Purdue University Calumet is an Equal Access/Equal Opportunity/Affirmative Action Employer.*

ASSISTANT PROFESSOR, BIOLOGY
Saint Francis University

Reach higher and go farther with the Department of Biology at Saint Francis University, tenure-track, Assistant Professor position opportunity in neurobiology to begin August 2007. For a complete job description, application information, and University facts please visit our **website: http://www.francis.edu** or refer to **website: http://www.sciencemag.org/.** *Saint Francis University is committed to diversity, and we encourage candidates who will contribute to meeting that goal to apply. Applications and nominations of women and minorities are strongly encouraged. Affirmative Action/Equal Opportunity Employer.*

POSITIONS OPEN

DIRECTOR
Stanley S. Scott Cancer Center
Louisiana State University Health Sciences Center
New Orleans

The Louisiana State University Health Sciences Center (LSUHSC), School of Medicine in New Orleans, Stanley S. Scott Cancer Center, is accepting applications for the Director of the Cancer Center. The position requires an M.D., Ph.D., or both, with combined M.D., Ph.D. degrees preferred. Preference will be given to candidates with experience in working within or in developing a successful plan for an NCI designated cancer center. The ideal incumbent must demonstrate scholarly experience as evidenced by academic accomplishments, publications, service on national study sections, service on editorial boards, and a track record of extramural research funded through NCI or other NIH funding mechanisms. Administrative experience with building either cancer research programs or cores in an academic setting is preferred. The incumbent should qualify for appointment at the level of Professor. A track record in basic, translational, epidemiological, and/or clinical research is required. Knowledge of current clinical oncology operations in relation to academic medicine will be viewed positively. The ideal candidate should have demonstrated ability in developing translational research from the basic scientific observations to clinical trials or clinically relevant research.

The incumbent will be appointed to the appropriate clinical department and will be a member of the Stanley S. Scott Cancer Center. Also the incumbent will be Co-Director of the Louisiana Cancer Research Consortium of LSU and Tulane. Please send curriculum vitae including current grant funding, a brief cover application letter detailing professional interests and goals, and the names of three references to: **Bernard Wan, Dean's Office, School of Medicine, 533 Bolivar Street, New Orleans, LA 70112** with an **e-mail: bwan@lsuhsc.edu.**

LSUHSC is an Affirmative Action/Equal Opportunity Employer.

DEAN, DIVISION OF NATURAL SCIENCES AND MATHEMATICS
University of Denver

Applications and nominations are invited for the position of Dean of Natural Sciences and Mathematics at the University of Denver (DU). The Dean is the chief academic, administrative and budgetary officer of the Division, is responsible for leadership of all internal programs, as well as external relationships and constituencies, and reports to the Provost. The Division **(website: http://www.nsm.du.edu)** consists of the Departments of Biological Sciences, Chemistry and Biochemistry, Geography, Mathematics, Physics and Astronomy, the Eleanor Roosevelt Institute, and the Denver Research Institute. The successful candidate should have: proven administrative experience; strong organizational, communication, leadership and interpersonal skills; the ability to interact effectively with all levels of academic administration, faculty, students, and the external community; experience in promoting grant-funded research and fundraising; a doctoral degree in a relevant field; a record of accomplishment in both teaching and research to merit appointment as a tenured full Professor in one of the departments of the Division. For a detailed description of the position, and the application process see **website: http://portfolio.du.edu/NSMSearch.** *The University of Denver is strongly committed to enhancing diversity. It encourages applications from women, minorities, people with disabilities, and veterans. DU is an Equal Employment Opportunity/Affirmative Action Employer.*

The Institute of Technology of the University of Minnesota, Twin Cities, invites nominations and applications for **HEAD OF THE DEPARTMENT OF MECHANICAL ENGINEERING.** Complete job description and application instructions can be found at **website: http://www.me.umn.edu/.** *The University of Minnesota is an Equal Opportunity Educator and Employer.*

POSITIONS OPEN

MILLER SCHOOL OF MEDICINE
UNIVERSITY OF MIAMI

FACULTY POSITION
Molecular and Cellular Pharmacology

The Department of Molecular and Cellular Pharmacology at the University of Miami, Miller School of Medicine is seeking applications for a **TENURE-TRACK FACULTY POSITION** (rank open). Candidates must have a Ph.D. and/or M.D. degree and have an established record of research excellence. Applicants from all areas of molecular/cellular biology and biomedical research are welcome. The new faculty member will complement existing research efforts in the Department. Rank and salary will be commensurate with experience. Generous laboratory space and startup funds are available.

Applicants should send electronic and hard copies of their curriculum vitae, statement of research interests and direction, and contact information for three references, to **e-mail: elalor@med.miami.edu** (e-copies) and **Dr. James D. Potter, Search Committee Chair, Department of Molecular and Cellular Pharmacology, University of Miami Miller School of Medicine, P.O. Box 016189, Miami, FL 33101.** *An Equal Opportunity/Affirmative Action Employer.*

The Office of Science, Department of Energy is seeking a motivated and highly qualified individual to serve as the **ASSOCIATE DIRECTOR,** Office of Biological and Environmental Research. As such, you will provide leadership and direction in establishing vision, strategic plans, goals, and objectives for the research activities supported. You may apply through two different methods, one is for a **SENIOR EXECUTIVE SERVICE** appointment and the second is for an **INTERGOVERNMENTAL PERSONNEL ACT** appointment. The announcement number is SES-SC-HQ-005. The announcement opens on November 6, 2006, and closes on December 21, 2006. Visit **website: http://www.usajobs.opm.gov/** for more information and for instructions concerning application procedures.

TWO FACULTY POSITIONS IN MICROBIAL PATHOGENESIS
University of Kansas Medical Center

The Department of Microbiology, Molecular Genetics and Immunology at the University of Kansas Medical Center (KUMC) invites applications for two tenure-track faculty positions: one at the **ASSISTANT PROFESSOR** level and one at the **ASSOCIATE PROFESSOR** level. We seek exceptional candidates (Ph.D., M.D., or M.D./Ph.D. degree), with documented evidence of quality research and a commitment to research and teaching at a major research University medical center.

The successful candidates will be expected to establish extramurally funded (Assistant Professor) or have extramurally funded (Associate Professor) independent research programs focused on bacterial or viral pathogenesis. Competitive salaries, startup packages, state of the art BSL-3 laboratories, animal care facilities, and excellent core facilities are available.

Applicants apply online for Assistant Professor position J0087656, or Associate Professor J0083042, and attach a letter of interest, curriculum vitae, description of research plans and contact information for at least three references at **website: http://jobs.kumc.edu.** Additional information describing the Department can be found at **website: http://www.kumc.edu/microbiology.** To ensure full consideration, applications should be received by January 15, 2007, but applications will be accepted until the positions are filled. Paid for by KUMC.

The University of Kansas Medical Center is an Equal Employment Opportunity/Affirmative Action Employer.

POSITIONS OPEN

The laboratory of **Dr. Katherine Ferrara** at University of California, Davis, and the Center for Molecular and Genomic Imaging are seeking a highly motivated **POSTDOCTORAL FELLOW or PROJECT SCIENTIST** to develop radiochemical methods to characterize the biodistribution of lipid and polymer-shelled nanoparticles. Research in our laboratory involves the development of methods to enhance local drug delivery and imaging methods for the assessment of drug and vehicle biodistribution and cell trafficking. Ideal candidates will have a Ph.D. in organic chemistry or radiochemistry and experience in synthesizing, designing, and validating probes for nuclear medicine. Experience with positron emission tomography (PET) probe synthesis is particularly desirable. Development of independent research program and funding will be encouraged and assistance provided. To apply, please send your curriculum vitae, a brief statement of research interests, and contact information for five references to: **Katherine W. Ferrara, Biomedical Engineering, University of California, Davis, 451 E. Health Sciences Drive, GBSF 2303, Davis, CA 95616,** or to **e-mail: kwferrara@ucdavis.edu.**

FACULTY POSITION IN THE BIOLOGY OF HEPATITIS C VIRUSES
Department of Microbiology-Immunology
Northwestern University
Feinberg School of Medicine

A tenure-track position is open for a full-time faculty researcher (Ph.D., M.D./Ph.D. or M.D.) studying hepatitis C viruses.

Rank is open, and salary is negotiable. All applicants should have substantial peer-reviewed publications that demonstrate research productivity and the ability to perform cutting-edge research. Candidates for an **ASSISTANT PROFESSOR** position should have postdoctoral research experience. Persons seeking appointment as **ASSOCIATE PROFESSOR** should have substantial research productivity and a history of grant support and academic service. Candidates should have an interest in teaching graduate and medical students. Starting date is negotiable after September 1, 2007. Application materials will be reviewed as received but, to receive full consideration, should be received by February 1, 2007. Please send complete curriculum vitae and the name and contact information of at least three references by **e-mail: virosearch@northwestern.edu.** *Northwestern University is an Affirmative Action, Equal Opportunity Employer. Women and minorities are encouraged to apply. Hiring is contingent upon eligibility to work in the United States.*

DIRECTOR, MARINE SCIENCE PROGRAM

The Marine Science Program at Florida International University (FIU) is seeking applicants for a newly created position of **DIRECTOR** (rank commensurate with experience). The Marine Science Program is a new and growing interdisciplinary initiative emphasizing research and teaching in coastal marine science (visit our webpage at **website: http://www.fiu.edu/~marine/** for information about our Program). In addition to continuing his/her own research, the Director's responsibilities include leading growth and operations of the Marine Science Program. To ensure full consideration, applications should be received by January 19, 2007. Screening of applications will begin on that date, and continue until a suitable candidate is selected. Applicants should send a cover letter, curriculum vitae, a summary of their professional interests, and contact information for three to five references to: **Joel Trexler, Search Committee Chair, Department of Biological Sciences, Florida International University, Miami, FL 33199; e-mail: trexlerj@fiu.edu; telephone: 305-348-1966.** *FIU is an Affirmative Action/Equal Opportunity Institution.*

TWO POSTDOCTORAL RESEARCH ASSOCIATE POSITIONS IN ENVIRONMENTAL NEUROTOXICOLOGY

Two Postdoctoral Research Associate positions are available beginning December 1, 2006, in the Insecticide Toxicology Research Laboratory at Cornell University's New York State Agricultural Experiment Station campus in Geneva, New York. Successful applicants will participate in NIEHS-funded research to define the mechanisms of insecticide action on rat and human voltage-sensitive sodium channels, map the binding sites for insecticides in relation to sites of action of other toxicants and drugs, and identify the molecular basis of the differences in sensitivity to insecticides between mammalian sodium channel isoforms and between mammalian and insect sodium channels. A Ph.D. degree in an appropriate biological discipline is required. Preference will be given to applicants with prior training and experience in at least one of the following areas: the development and use of transfected mammalian cell lines for the expression and assay of receptors and ion channels; voltage or patch-clamp analysis of ion currents; or, the development and validation of ligand-receptor docking models. Salary will be based on NIH postdoctoral compensation guidelines; an attractive fringe benefits package is included. Send a letter of application with curriculum vitae and the names of three professional references to: **Professor David M. Soderlund, Department of Entomology, New York State Agricultural Experiment Station, Cornell University, 630 West North Street, Geneva, NY 14456 (e-mail: dms6@cornell.edu).** *Cornell University is an Equal Opportunity, Affirmative Action Educator and Employer.*

POSTDOCTORAL FELLOWSHIPS AVAILABLE

The Lombardi Comprehensive Cancer Center at Georgetown University, a multidisciplinary NCI-designated cancer research center with $70 million in grant support, is currently recruiting **POSTDOCTORAL FELLOWS** into positions funded by an NCI training grant. The goal is to develop strong basic and translational scientists with an interest in cancer research. Successful applicants will choose a mentor from an interdisciplinary group of investigators who are committed to cancer research. Research programs include: Development of novel anticancer therapies; the genetic and molecular mechanisms of malignant progression; the role of growth factor signal pathways; invasion and metastasis; the development of hormone and drug insensitivity; the etiology of cancer, biomarkers, and molecular epidemiology.

Go to **website: http://lombardi.georgetown.edu/education/index.htm** for further information.

Salary is competitive and commensurate with qualifications and experience. *U.S. citizenship or permanent residency is required.*

Applicants should send curriculum vitae, a short statement of research interests and career goals, and the names and addresses of three references to **Erin Warnock** at **e-mail: ebw27@georgetown.edu.** *Minorities and women are strongly encouraged to apply.*

POSTDOCTORAL RESEARCH POSITION

The Laboratory of Cellular and Molecular Cerebral Ischemia is offering outstanding candidates the opportunity to study novel neuronal, vascular, and inflammatory mediators of oxidative stress and cellular plasticity (*Journal of the American Medical Association*, **293**: 90, 2005; *Histology Histopathology*, **21:** 103, 2006). Expertise in molecular biology with in vitro and in vivo experimental models is required. Please forward curriculum vitae and three references to: **Kenneth Maiese, M.D., Neurology, 8C-1 UHC, Wayne State University, 4201 Saint Antoine, Detroit, MI 48201, fax: 313-966-0486, e-mail: kmaiese@med.wayne.edu.** *Wayne State University is an Equal Opportunity/Affirmative Action Employer.*

POSITIONS OPEN

PENNSTATE University Park

POSTDOCTORAL POSITIONS
The Center for Infectious Disease Dynamics (CIDD)
The Pennsylvania State University

The Center for Infectious Disease Dynamics provides a highly collaborative, interdisciplinary environment to address challenges in infectious disease research. There are immediate openings available for applicants with expertise in the following areas: molecular virology; innate immunity; genomics; protein structure/function; mathematical biology.

Please see **website: http://www.cidd.psu.edu** for detailed descriptions of these positions and application procedures.

Pennsylvania State is committed to Affirmative Action, Equal Opportunity, and the diversity of its workforce.

GRANTS

BRAIN TUMOR SOCIETY RESEARCH GRANTS
One-Year $100,000 grants
Two-Year $200,000 grants
Available in the United States and Canada
Letter of Intent Deadline: January 16, 2007

The Brain Tumor Society (BTS) is awarding grants to fund basic scientific and translational research directed at finding a cure for brain tumors. Grants are awarded annually at a maximum of $100,000 per year. Grants may be used for startup projects or supplementary funding. Funds cannot be used for indirect costs. Clinical projects will not be funded. Letter of intent packets available on **website: http://www.tbts.org.**

MARKETPLACE

The Protein People™

biotinylation

Small sample. Big recovery. Free T-shirt!

EZ-Link® Sulfo-NHS and Sulfo-NHS-LC† Biotinylation Kits from Pierce are the most highly referenced kits for facilitating the biotinylation of many hundreds of antibodies and other proteins. Now this superior technology is available to label microgram quantities of antibody/protein samples in microliter volume.

The improved speed and recovery of these kits comes from our exclusive Zeba™ Spin Desalting Columns. Spin desalting greatly shortens sample preparation time and allows multiple samples to be processed at once.

Highlights:

- Biotinylate 50-200 µg of protein in 200-700 µl total volume per reaction
- Zeba™ Desalting Columns deliver > 85% protein recovery, a more concentrated sample and substantially shorter processing time
- Water-soluble reagents link biotin to protein via a stable amide bond
- Reagents do not penetrate cell membranes
- Deliver antibody/protein recoveries typically > 70%

FREE T-shirt! Order a new microbiotinylation kit (Product # 21925, 21935, 21945 or 21955) by Dec. 31, 2006, and receive a FREE protein-patterned T-shirt. After receiving your qualifying order, visit www.piercenet.com/offers to request your free T-shirt.

When you visit that site, you will need to submit information included in your qualifying order as well as your contact information. One free T-shirt per order. Void where prohibited and outside the U.S.

www.piercenet.com/microbiotin

PIERCE

Tel: 815-968-0747 or 800-874-3723 • Fax: 815-968-7316
Customer Assistance E-mail: CS@piercenet.com

For distributors outside the U.S. and Europe, visit www.piercenet.com

For European offices and distributors, visit www.perbio.com

E-Notebook 10.0

Desktop to Enterprise Knowledge Management

New **CombiChem · RXN Planning · E-Signatures · 21CFR11 · SQL Server · Oracle Cartridge**

Research Notebooks at your *fingertips*

E-Notebook Ultra is the efficient, accurate way to write lab notebooks entries as you work. It stores MS Office documents, *ChemDraw* structures and reaction drawings, and related data in an electronic notebook you can search by text or chemical structure. Organize pages by project, experiment or customize with MSDE database. *CombiChem/Excel* builds combinatorial libraries.

E-Notebook Workgroup, intended for use with a medium number of users, offers much of the functionality delivered in *E-Notebook Enterprise* while using SQL Server as the database. Learning to use and administer the application is quick and straightforward. *E-Notebook* applies various data types to suit different disciplines with an unlimited number of workflows.

E-Notebook Enterprise edition integrates notebook keeping at group and enterprise levels to promote lab productivity and information sharing. *Oracle Cartridge* manages chemical structures in a common data repository with detailed security and *21CFR11 Compliance*. The enterprise edition also works with procurement and inventory management systems to save time locating chemicals and entering structures.

E-Notebook Ultra $590
Workgroup $2,300
Enterprise $8,600

▸ **Knowledge Management**

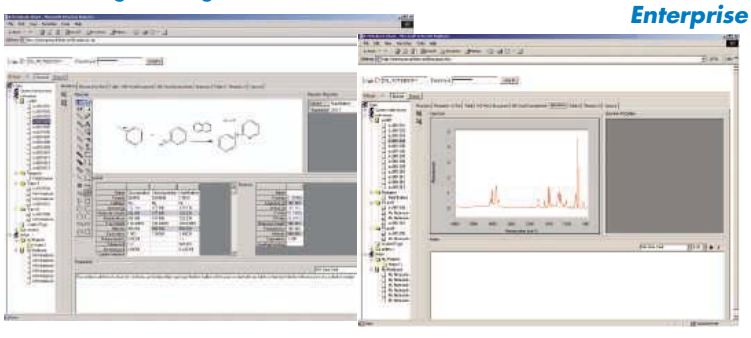

▸ **Galactic Spectral Controls**

Also Available:

ChemOffice Ultra 06 **$1,290**
A fully integrated suite of drawing, chemistry, biology and knowledge software for scientists. Includes *ChemDraw, Chem3D, CombiChem, BioOffice, Inventory, E-Notebook & ChemACX.*

ChemDraw Ultra 10.0 **$890**
With 500,000 users worldwide, *ChemDraw* is the standard structure drawing software. *Ultra* includes *ChemNMR, Struct<=>Name, ChemDraw/Excel & ChemFinder/Office.*

Chem3D Ultra 06 **$590**
Molecular modeling with MOPAC & GAMESS and interfaces to Gaussian & Jaguar.

BioOffice Ultra 06 **$890**
Integrated suite of biology and knowledge software. Includes *BioDraw, BioAssay, BioViz, Bio3D, Inventory & E-Notebook.*

BioDraw Ultra 10.0 **$290**
Draw your biological pathways with membranes, enzymes, receptors & DNA.

BioAssay Ultra 10.0 **$590**
Manage high and low throughput biological screening data, set-up models, automated calculations and curve-fitting.

Inventory Ultra 10.0 **$890**
Manage your compounds and reagents. *ChemACX* database includes 400 catalogs. *Ultra* includes *Inventory & ChemACX.*

ChemACX Ultra 10.0 **$590**
Over 400 catalogs, 690,000 products & one million skus from leading chemical suppliers.

All prices suggested U.S. annual subscription.

Buy & Save Online!

www.CambridgeSoft.com
Europe 00 800 875–20000
Germany 49 69 2222 2280
America 1 800 315–7300
France 33 1 70 71 98 80
Japan 0120 731 800

☑ Download **Free Software** http://FreeSW.SciStore.com
☑ Request a **Free DVD** http://FreeDVD.SciStore.com

You may also request a Free DVD by mailing this coupon

Name _____
Company _____
Street _____
City _____ State _____
Country _____ Zip _____
Phone, Fax _____ Email _____

Free DVD
$49 value

US 1 800 315–7300 **INT'L** 1 617 588–9300 **FAX** 1 617 588–9390 **EMAIL** info@cambridgesoft.com
EU 00 800 875 20000 **UK** +44 1223 464900 **JP** 0120 146 700 **WWW** www.cambridgesoft.com
MAIL CambridgeSoft Corporation 100 CambridgePark Drive Cambridge, Massachusetts 02140 USA

CambridgeSoft®
www.cambridgesoft.com